Technical Report
**TR-23-18**
December 2024

# Cementitious materials and components in SFR

## Synthesis report

**Per Mårtensson**

SVENSK KÄRNBRÄNSLEHANTERING AB

SWEDISH NUCLEAR FUEL
AND WASTE MANAGEMENT CO

Box 3091, SE-169 03 Solna
Phone +46 8 459 84 00
skb.se

SVENSK KÄRNBRÄNSLEHANTERING

ISSN 1404-0344
**SKB TR-23-18**
ID 1933345
December 2024

# Cementitious materials and components in SFR

## Synthesis report

Per Mårtensson, Svensk Kärnbränslehantering AB

*Key Words:* Cement, Cementitious, Concrete, Grout, SFR, Barriers.

This report is published on www.skb.se

© 2024 Svensk Kärnbränslehantering AB

# Summary

This report compiles SKB's current understanding on the evolution of the properties of the cementitious materials and components used in the final repository for short-lived radioactive waste, SFR, during the first 100 000 years post-closure. The presented information is mainly based on research and development that has been carried out under SKB's own auspices.

The report begins with a description of the SFR repository and the cementitious components to be covered in this report. This is followed by a compilation of the different types of cements and cementitious materials used in the construction of SFR1 and the materials foreseen for use in the construction of SFR3 as well as cementitious materials for backfilling, sealing and closure of the repository. In addition, also concrete waste packaging such as concrete tanks and moulds are included. The final part of the background chapters comprises a brief summary of the processes that can affect the properties of the materials during construction, operation and post-closure.

Against this background, the properties of the cementitious components at closure as well as the expected evolution of the properties during the first 100 000 years post-closure are described in separate chapters for each individual waste vault. Based on these descriptions, the report recommends material property data for the cementitious components in SFR for selected periods up to 100 000 years post-closure.

The report thus links together the information obtained from reports where materials and methods used in the construction of the facility are reported with reports related to the assessment of post-closure safety of SFR. In addition, this report also includes information from SKB's responses to injunctions and supplementary data produced within the safety assessment work. In this way, a coherent picture of the expected evolution of the cementitious materials and components in SFR during the first 100 000 years post-closure can be presented.

# Sammanfattning

Denna rapport sammanställer SKB:s samlade kunskap rörande utvecklingen av egenskaperna hos cementbaserade material och komponenter i Slutförvaret för kortlivat radioaktivt avfall, SFR, under de första 100 000 åren efter förslutning. Kunskapen baseras på forskning och utveckling som till största delen har utförts i SKB:s egen regi.

Rapporten inleds med en beskrivning av anläggningen och de cementbaserade komponenter som inkluderas i denna rapport. Detta följs av en sammanställning av de olika typer av cement och cementbaserade material som förekommer i SFR1 och som förväntas förekomma i SFR3 liksom vid återfyllnad och förslutning av anläggningen. Utöver detta inkluderas även avfallsbehållare såsom betongkokiller och betongtankar. Som en sista del i bakgrundskapitlen redovisas en kortfattad sammanfattning av de olika processer som kan påverka materialens egenskaper under såväl uppförande som drift och efter förslutning.

Med utgångspunkt i denna beskrivning redovisas de olika komponenternas förväntade egenskaper vid förslutning samt den förväntade utvecklingen av egenskaperna under de första 100 000 åren efter förslutning i separata kapitel för de olika bergssalarna. Slutligen redovisar rapporten föreslagna materialdata för de olika komponenterna under hela den omfattade tidsperioden.

Rapporten knyter på detta sätt samman information som inhämtats från rapporter där material och metoder för uppförande av anläggningen redovisas med rapporter framtagna inom säkerhetsanalysarbetet för SFR. Utöver detta inkluderar den sammanställning som redovisas i denna rapport även underlag i form av svar på förelägganden och kompletterande underlag framtagna inom säkerhetsanalysarbetet. På så sätt kan en sammanhållen bild av den förväntade utvecklingen av de cementbaserade komponenterna i SFR under de första 100 000 åren efter förslutning presenteras.

# Contents

# 1 Introduction

## 1.1 Background

### 1.1.1 The final repository for short-lived radioactive waste, SFR

The final repository for short-lived radioactive waste (SFR) located in Forsmark, Sweden, receives low- and intermediate-level waste from Swedish nuclear facilities. SKB plans to extend SFR to host also waste from the decommissioning of the nuclear power plants and other nuclear facilities. Additional disposal capacity is also needed for operational waste, since the operational life-times of some nuclear facilities have been extended.

SFR includes underground waste vaults together with above-ground buildings that house the technical installations. The underground part is located below the Baltic Sea. The existing facility (SFR1) comprises five waste vaults, including a silo, with a total disposal capacity of approximately 63 000 $m^3$. The extension (SFR3) will have a disposal capacity of 180 000 $m^3$ in six new waste vaults.

SFR1 was taken into operation in 1988 (the silo in 1991) and according to current plans operation of SFR3 will start around 2029. Closure of SFR is currently planned for 2075 which gives an operational period of close to 90 years for SFR1 and about 45 years for SFR3.

The different waste vaults are described in detail in Chapter 2.

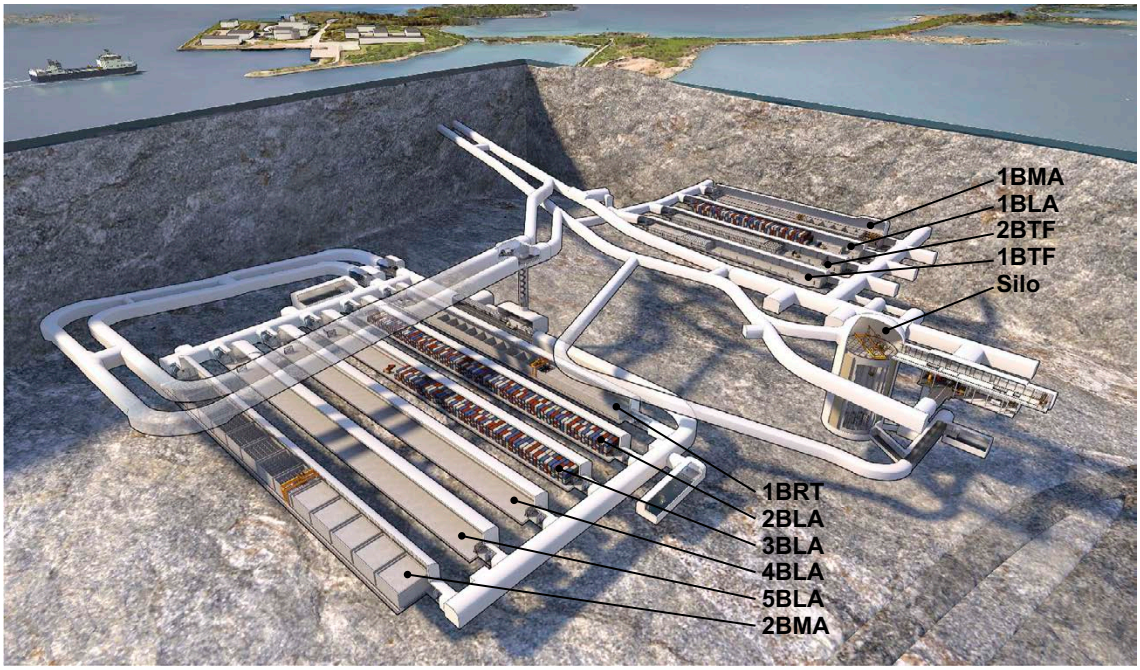


***Figure 1-1.*** *View of SFR with SFR1 in the upper right part of the illustration and SFR3 in the lower left. The waste vaults in the figure are the silo for intermediate-level waste, 1–2BMA: Waste vaults for intermediate-level waste, 1–2BTF: Waste vaults for concrete tanks, 1BRT: Waste vault for segmented reactor pressure vessels and 1–5BLA: Waste vaults for low-level waste.*

### 1.1.2 The role of cementitious materials and components in SFR

In SFR, vast amounts of concrete and other cementitious materials are used. Many of the structures in which cementitious materials are used in SFR constitute parts of the engineered barrier system that aim to retard the radionuclide release from the repository. Other structures comprise different types of buildings or other components such as parts of the drainage system etc. Cementitious materials are also used for grouting of waste, as rock reinforcement as well as in rock injection grouts used to reduce the inflow of water into the repository during the operational period.

The following types of cementitious materials are used:

- **Structural concrete** is used in structures in which strength and durability are required such as the engineered barrier structures in e.g. 1–2BMA and the silo as well as in the plugs that will be constructed at closure but also in other types of structures which do not constitute parts of the engineered barrier system.
- **Grout** is used to fill voids between waste packages in the silo and 1–2BTF with the main purpose of providing additional stability to the stack of waste packages and/or to reduce the total void volume inside the waste domain. Grouts also provide additional sorption capacity for radionuclides.
- **Shotcrete** is sprayed onto the rock walls in the repository in order to provide additional stability and reduce the risk for rock fall-out.
- **Injection grouts** are injected into fractures in the bedrock in order to reduce the inflow of groundwater into the repository.
- **Grout for rock bolts** is used to secure the rock bolts in the bedrock but also to create a favourable chemical environment around the rock bolts in order to reduce the corrosion rate.

### 1.1.3 Post-closure evolution of the properties of the cementitious components

During construction, operation and post-closure, the properties of the cementitious components will slowly change due to both short- and long-term processes.

Detailed understanding of the influence of these processes on the post-closure evolution of the properties of the cementitious components in the repository is an important part of the analysis of the post-closure safety of SFR. Of particular importance has been the task of motivating the data used to describe the evolution of properties such as pH, hydraulic conductivity and diffusivity of the materials but also correctly determining the sorption capacity for different radionuclides for cementitious materials in various degradation states.

In order to provide the required data, the evolution of the properties of the cementitious materials and components in SFR has been studied by SKB or by researchers contracted by SKB during several decades, starting already during the 1980's and still continuing today. However, in order to further improve the basis for the selected data, also information reported in the common scientific literature has been used.

## 1.2 Purpose of the work presented in this report

The purpose of this report is to recommend non-pessimistic material property data for all cementitious components in SFR for selected time periods up to 100 000 years post-closure. To this end, the following aims are set for this report:

- Present a detailed description of all types of cementitious materials used in SFR today and planned for future use, including mixing proportions and properties of these materials.
- Present a detailed description of all existing and future cementitious components in SFR1 and SFR3, including type of cementitious material, dimensions and construction method (if possible).
- Describe relevant processes which are active during construction, operation and post-closure and which could influence the status of the cementitious components at closure and up to 100 000 years post-closure.

- Present a detailed and well-motivated description of the status of all cementitious components in SFR at closure, also including recommended material property data.
- Present a detailed and well-motivated description of the expected evolution of the properties of the cementitious components in SFR for selected time periods up to 100 000 years post-closure.
- Recommend material property-data for all cementitious components for selected time periods up to 100 000 years post-closure.
- Form a basis for identification of needs for future work regarding the cementitious components in SFR and construction methods.

## 1.3 Not included in this report

The following is not included in this report:

- The report only covers cementitious materials used in the repository itself as well as the waste packaging (concrete moulds and -tanks) and does not include cementitious materials inside the waste packages.
- This report presents a compilation of information from reports regarding the evolution of the properties of the cementitious components carried out by SKB or organisations contracted by SKB. However, this report does not present the complete scientific background to cementitious materials and degradation processes as this has already been covered in the reports referred to within this report.

## 1.4 Relation to other reports

The following relations with other reports are made:

- **The initial state report** (SKB TR-23-02) provides details on the lay-out of the repository as well as the dimensions of the different cementitious components.
- **The waste process report** (SKB TR-23-03) provides details on the processes in the waste that could affect the evolution of the properties of the cementitious components.
- **The barrier process report** (SKB TR-23-04) provides the detailed scientific background to the processes that could affect the properties of the cementitious components.
- **The climate report** (SKB TR-23-05) presents the expected climate evolution in the vicinity of the repository.
- **The data report** (SKB TR-23-10) provides a compilation of data currently used to describe the material properties of the different cementitious components in SFR for the different time periods.
- **The closure plan for SFR** (Mårtensson et al. 2022) presents the plan for closure of SFR.
- **Other SKB reports** referred-to in this report provide details on the expected evolution of the properties of the cementitious components.
- **Other internal SKB documents and reports from consultants or external laboratories** referred-to in this report provide additional information on specific details on the evolution of the properties of cementitious materials.

## 1.5 Structure of this report

This report comprises in total 15 chapters with the following content:

**Chapter 1** gives a background and a general introduction to the report.

**Chapter 2** describes the design of the SFR repository systems and cementitious components in the waste vaults.

**Chapter 3** presents the different types of cement and cementitious materials used in SFR1 or planned for use in SFR1 and SFR3.

**Chapter 4** gives a brief presentation of the processes that may affect the properties of the cementitious components in SFR during construction, the operational period and post-closure.

**Chapter 5** provides a general description of relevant properties of cementitious materials and conditions in SFR over time.

**Chapter 6** presents the expected status of the cementitious components at closure of the repository.

**Chapter 7** presents the expected evolution of the cementitious components in the silo until 100 000 years post-closure.

**Chapter 8** presents the expected evolution of the cementitious components in 1BMA until 100 000 years post-closure.

**Chapter 9** presents the expected evolution of the cementitious components in 2BMA until 100 000 years post-closure.

**Chapter 10** presents the expected evolution of the cementitious components in 1BRT until 100 000 years post-closure.

**Chapter 11** presents the expected evolution of the cementitious components in 1–2BTF until 100 000 years post-closure.

**Chapter 12** presents the expected evolution of the cementitious components in 1BLA until 100 000 years post-closure.

**Chapter 13** presents the expected evolution of the cementitious components in 2–5BLA until 100 000 years post-closure.

**Chapter 14** presents the expected evolution of the cementitious components which are common for all parts of the repository until 100 000 years post-closure.

**Chapter 15** presents a short summary as well as a compilation of remaining uncertainties and identified future work needed to close the uncertainty gaps.

# 2 Design of SFR

## 2.1 Overview

The current SFR facility (SFR1) comprises five waste vaults for different waste categories located in the bedrock at a depth between about 60 (top of silo top) and 130 meters (bottom of silo) beneath the surface of the Baltic Sea and is reached via access tunnels from a surface facility. The planned extension (SFR3) will comprise six additional waste vaults and will be located at between about 120 and 140 meters beneath the surface of the Baltic Sea, Figure 2-1.

In Sections 2.5 to 2.11, detailed information on the cementitious components in the individual waste vaults are given. More information on the design of the vaults can be found in the initial state report (SKB TR-23-02). For details concerning the various types of waste and conditioning methods, please refer to the inventory report (SKB R-18-07).

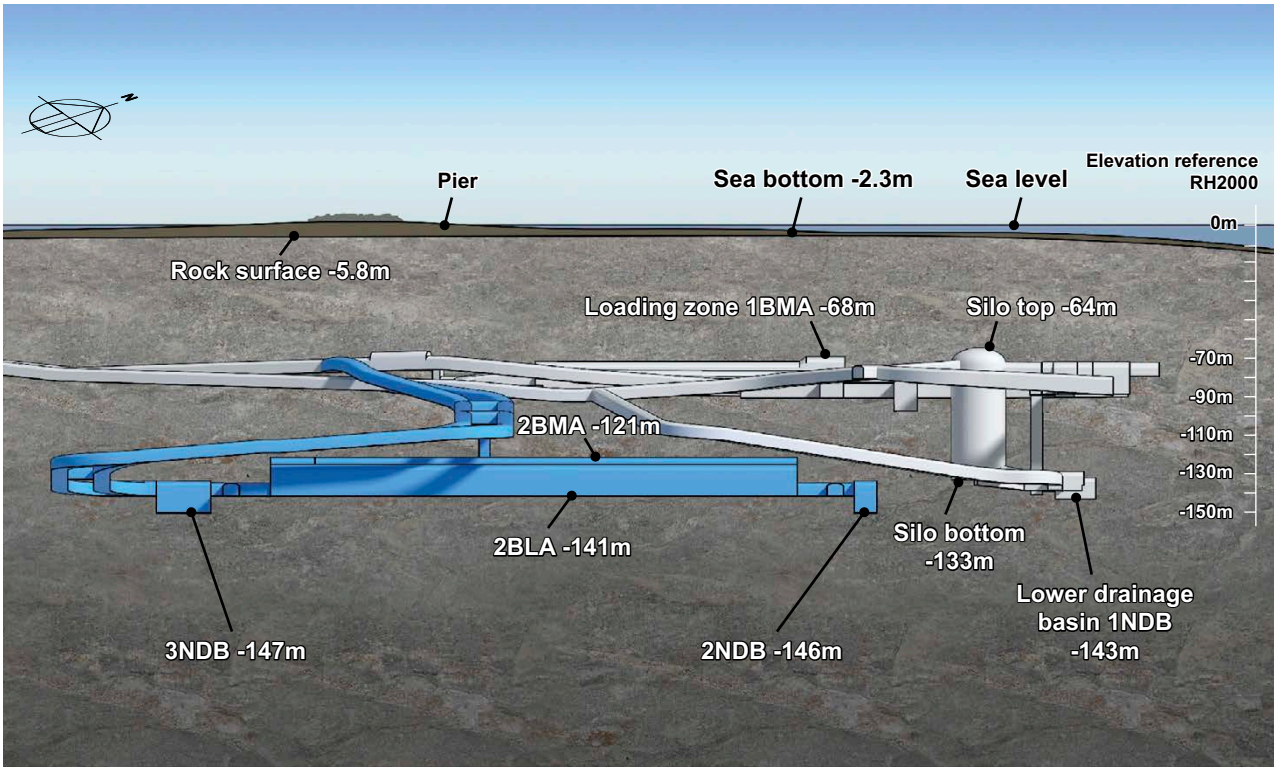


***Figure 2-1.*** *View of SFR with designated levels in RHB 2000 (RHB 2000 is the Swedish geographical height system). View is towards the NW, approximately perpendicular to the waste vaults. Note that stipulated elevations for the top surface of the rock and the sea floor are to be regarded as approximate since they are point data and vary in the plane above SFR. The grey part is SFR1 and the blue part is SFR3 (SKB TR-23-02).*

## 2.2 System components

The repository system is divided into a number of system components i.e. physical components of the repository system each of which contains one or more components. As an example, the system component *silo barriers* contain the components *concrete barriers*, *bentonite barriers* and *vault and backfill.*

SFR comprises the following system components (SKB TR-23-01, Section 3.5.4):

- Waste form,
- concrete and steel packaging,
- silo barriers,
- BMA barriers,
- BRT barriers,
- BTF barriers,
- BLA barriers,
- plugs and other closure components and
- geosphere.

In the following sections an overview of the different system components and their respective cementitious components is presented. Further details regarding the dimensions of the waste vaults and the concrete structures with references are found in the initial state report (SKB TR-23-02).

## 2.3 Cementitious components in SFR

In this report, the post-closure evolution of all types of cementitious materials and structures (in this report denominated *cementitious components*) which are left in SFR post-closure is described regardless of whether they constitute engineered barriers or not.

The motivation for this approach is the need for a detailed understanding of the evolution of the properties of materials that could influence the evolution of the properties of the engineered barriers. As an example, severe leaching of grout for rock bolts or shotcrete during the operational period could increase the risk of rock fall-out which could induce cracks in the engineered barriers in e.g. 1–2BTF (concrete tanks) or pose a threat to the staff operating the facility.

The cementitious components of the engineered barriers are described in Section 2.3.1 and the others which do not constitute parts of the engineered barrier system in Section 2.3.2.

### 2.3.1 Engineered barriers in SFR

#### *Safety functions of the engineered barriers in SFR*

The post-closure safety of SFR is achieved by limiting the activity of long-lived radionuclides disposed in the repository and ensuring that the transport of radionuclides from the waste, through the engineered barriers and through the geosphere and biosphere is sufficiently retarded. The overall post-closure safety principles for SFR are therefore formulated as *limitation of the activity of long-lived radionuclides* and *retention of radionuclides*.

The content of long-lived radionuclides in the waste is limited by only accepting for disposal certain kinds of waste. Slow outward transport of radionuclides is achieved by ensuring a low water flow rate through the waste and the engineered barriers, through each waste vault and through the repository, and by retarding radionuclide transport relative to this water flow. This retardation is achieved mainly by ensuring effective sorption in the cementitious materials.

Post-closure safety assessment relies on understanding of the future evolution of the repository and its environs and is described in the following three areas; 1) Initial state, 2) Internal processes, and 3) External conditions. From these areas of knowledge, a set of safety functions can be defined and they describe how any repository component contributes to the post-closure safety.

The evolution of the safety functions over time is evaluated with the aid of a set of safety function indicators. These consist of measurable or calculable properties of respective repository system component. For these properties qualitative criteria are given that are coupled to the specified function. An example of a safety function is *limit advective transport* through relevant engineered barriers. The related indicator is *hydraulic conductivity* of bentonite in the silo and plugs as well as outer concrete structures in 1–2BMA. The qualitative criterion specified is that the hydraulic conductivity shall be low.

The following definitions are used (SKB TR-23-01, Section 5.5):

- A safety function is defined as a role by means of which a repository component contributes to safety.
- A safety function indicator is a measurable or calculable property of a repository component that is used to indicate the extent to which the safety function is upheld.

The safety functions and safety function indicators for the engineered barriers in the different waste vaults are summarised in Table 2-1. The safety functions and safety function indicators of the waste form is not included in Table 2-1 as the waste is not within the scope of this report.

However, the reader will notice that the waste packaging (concrete tanks and moulds) are included in this report. Of these, only the concrete tanks have a safety function and are therefore included in Table 2-1. In 1BRT, 1–2BMA, 1–5BLA and the silo, low groundwater flow through the waste packaging is not relied upon in the safety assessment and therefore no safety functions are defined for the concrete moulds. For details concerning the waste form and waste packaging, see the post-closure safety report for PSAR (SKB TR-23-01, Section 5.4.1).

**Table 2-1. Safety functions and safety function indicators of the engineered barriers in SFR (SKB TR-23-01, Table 5-1).**

| Safety function | Safety function indicator | Part of component |
|---|---|---|
| Limit advective transport | Hydraulic conductivity in concrete and bentonite: low | Bentonite in silo and plugs<br>Outer concrete structures in 1–2BMA, concrete tanks** in 1–2BTF |
| | Hydraulic conductivity in backfill (including crushed rock foundation): high | Backfill (including crushed rock foundation) in 1–2BMA and 1–2BTF |
| Sorb radionuclides | Amount of cementitious material: high<br>pH in porewater: high<br>Redox potential: low (reducing)<br>Concentration of complexing agents: low | Cementitious materials in silo, 1–2BMA, 1BRT and 1–2BTF |
| Allow gas passage* | Permeability: sufficient to allow gas passage | Gas evacuation system in silo and 2BMA, Cementitious materials in 1BMA and 1–2BTF |

* An analysis on the need for a gas evacuation system also in 1BMA is currently undertaken but a final decision has not yet been made.
** Formally, the concrete tanks in 1–2BTF are defined as a part of the waste form and waste packaging.

### *Cementitious components of the engineered barrier system in SFR*

Table 2-1 shows that the engineered barrier system in SFR comprises different types of materials. However, as this report only covers the evolution of the cementitious components in SFR, other types of materials are excluded hereon. SKB (TR-23-01, Table 4-1) compiles all barriers essential for the post-closure safety of SFR.

It should be noted though that this report includes among the engineered barriers also concrete moulds and tanks, formally included as a part of the waste form and packaging (SKB TR-23-01, Table 5-1). The motivation for this is – among others – the impact of the load-bearing capacity of the concrete tanks and moulds on the load-bearing capacity of the concrete lids in the different waste vaults as discussed in the relevant sections in Chapter 7-13.

For the descriptions in this report, the engineered barrier system is defined as:

- **Silo**: The cementitious components of the engineered barriers in the silo comprise the concrete structure, the gas permeable grout and the concrete moulds.
- **1BMA and 2BMA**: The cementitious components of the engineered barriers in 1BMA and 2BMA comprise the concrete caissons and the concrete moulds.
- **1BRT**: The cementitious components of the engineered barriers in 1BRT comprise the concrete structure.
- **1BTF and 2BTF**: The cementitious components of the engineered barriers in 1BTF and 2BTF comprise the concrete structures, grout, cementitious backfill and concrete tanks and moulds.
- **1BLA, 2BLA, 3BLA, 4BLA, 5BLA**: No engineered barriers comprising cementitious components are present in 1BLA, 2BLA, 3BLA, 4BLA or 5BLA.

### 2.3.2 Other cementitious components

The following cementitious components are also included in this report:

- Concrete plugs in tunnels.
- Concrete plugs in boreholes.
- Shotcrete on rock walls.
- Grout for rock bolts.
- Injection grouts.
- Concrete slabs in waste vaults without engineered barriers.

## 2.4 Closure of SFR

SFR will be decommissioned and closed when all waste has been disposed, currently planned around the year 2075. After decommissioning and closure, the repository is a passive system that can be left without having to take any further measures to maintain proper function. Facilities above ground will be demolished during clearance of the site.

Closure of the waste vaults and tunnels at repository level includes installation of backfill material as well as construction of plugs at selected locations. The ramp will be filled with crushed rock and sealed with plugs. Finally, the ground surface will be restored to blend in with the surrounding landscape. In addition, all boreholes in the SFR area which were not sealed prior to construction of SFR3 will be sealed. An illustration of the closed repository is shown in Figure 2-2.

The planned closure measures are shortly described for each waste vault in the following sections and described in detail in the closure plan (Mårtensson et al. 2022).

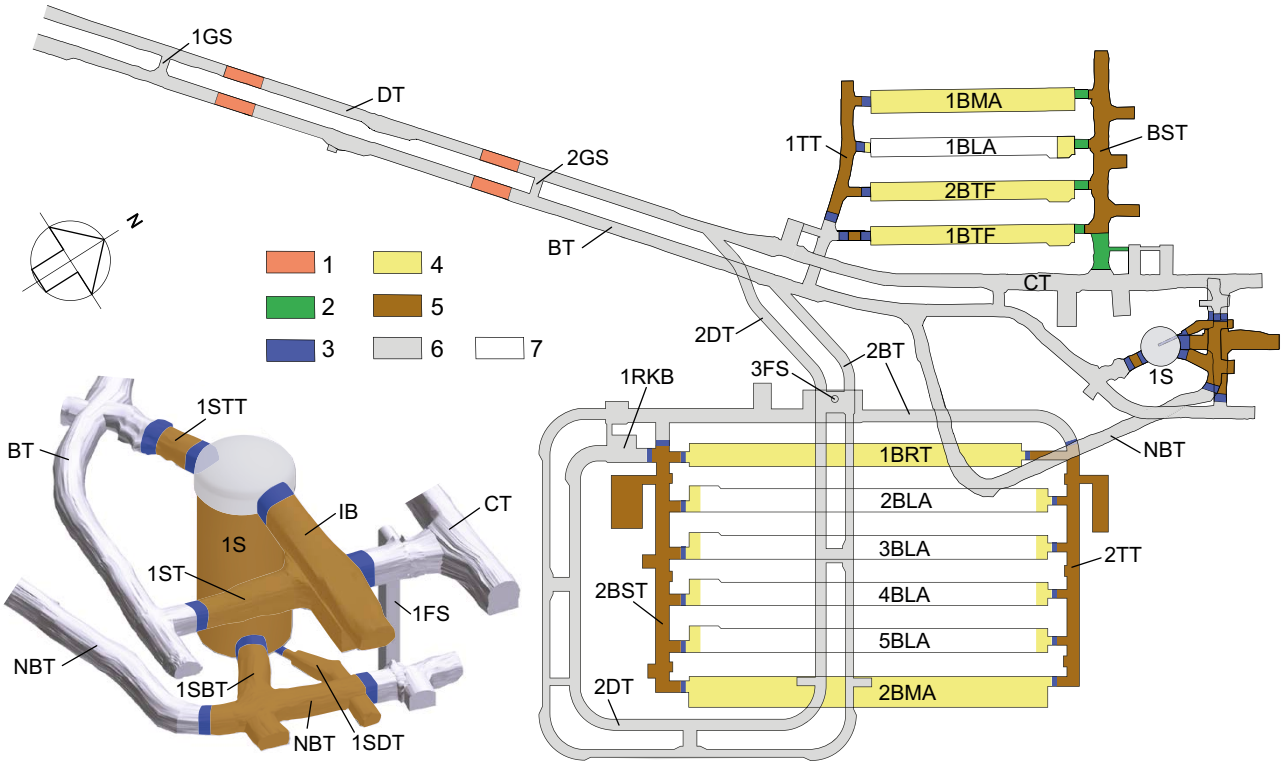


***Figure 2-2.*** *Schematic plan of SFR post-closure, with a detailed view of the silo. Key to numbering: 1) Plugs in access tunnels 2) Transition material 3) Mechanical support of concrete 4) Backfill material of macadam 5) Hydraulically tight section of bentonite 6) Backfill material in the silo top, access tunnels and the central area of the tunnel system 7) Non-backfilled parts.*

## 2.5 Silo

### 2.5.1 Overview

The silo is a 68.7 meters high cylindrical vault with a diameter of 29.4 to 31.0 meters (SKB TR-23-02) in which a free-standing cylinder made from reinforced *Silo concrete* (Section 3.3.1) is erected. In the interior of the concrete silo, inner walls create a number of vertical shafts in which the waste is disposed as shown in Figure 2-3.

The concrete silo is founded on a bed of a mixture of 90 % sand and 10 % bentonite by weight and the gap between the concrete cylinder wall and the rock is filled with bentonite. During the operational period, the bentonite in the gap is protected by a concrete lid which will be removed prior to backfilling of the silo top.

### 2.5.2 Cementitious components in the silo

The cementitious components in the silo comprise the following components which are described in more detail below:

- Slab.
- Outer wall.
- Lid.
- Inner walls.
- Permeable grout between waste packages and inner walls.
- Concrete moulds.

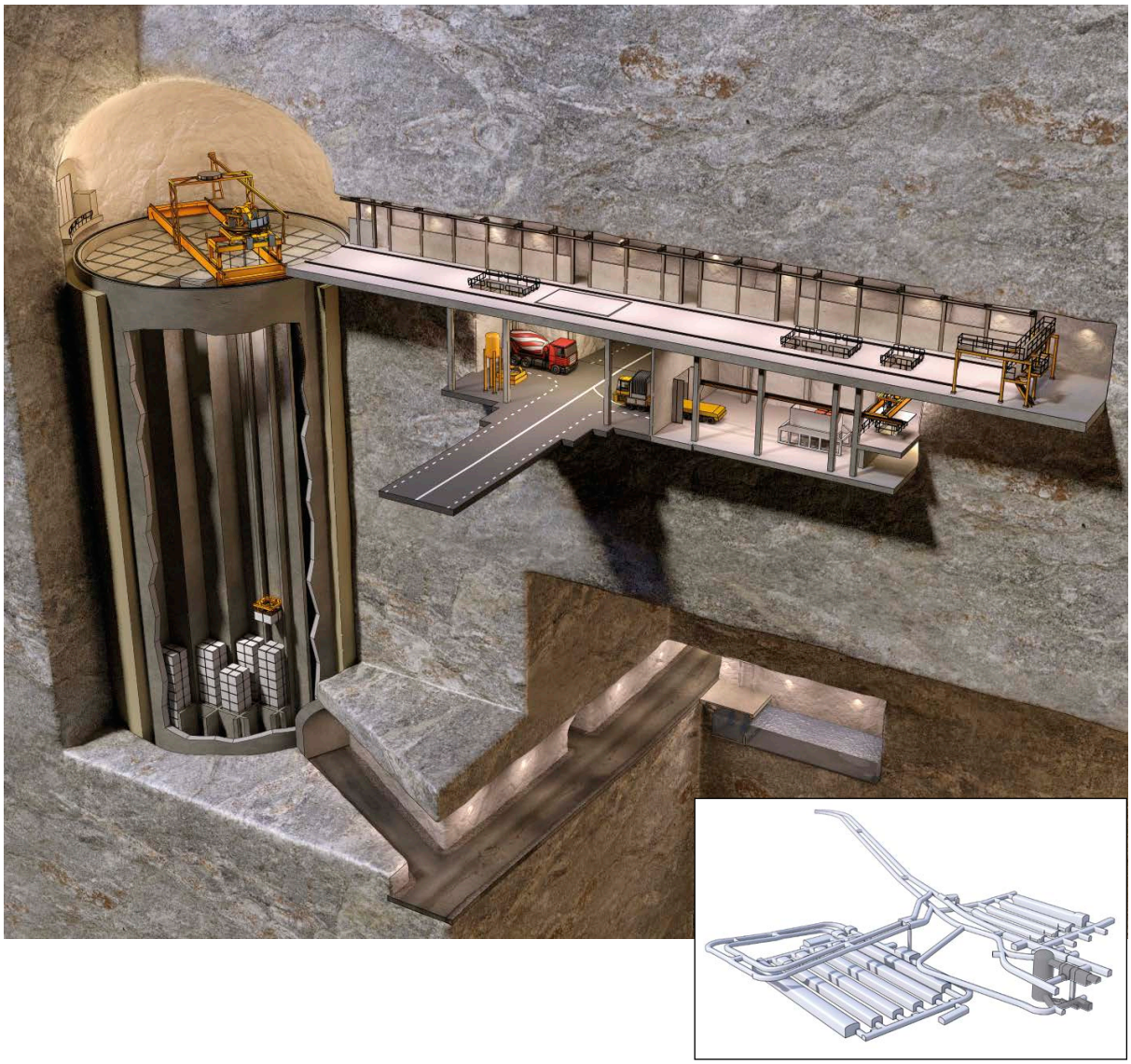

***Figure 2-3.*** *Illustration of the silo during the operational period. The inset shows a view of SFR with the position of the silo in darker grey.*

The prefabricated concrete elements, visible in Figures 2-3 and 2-8, that provide radiation shielding during the operational period will be removed prior to closure and are not included in this report.

In order to avoid repetition, the following cementitious components which are common for all waste vaults will be described in Section 2.12:

- Concrete plugs in tunnels.
- Concrete plugs in investigation boreholes.
- Shotcrete on the rock walls (not present in the silo).
- Grout for rock bolts.
- Injection grout in the surrounding bedrock.

### *Slab, inner and outer walls*

The concrete cylinder is made of reinforced *Silo concrete* (Section 3.3.1) and has the dimensions 27.6 m × 52.6 m (∅ × h) (SKB TR-23-02). The thickness of the slab and outer wall is 900 mm and 800 mm, respectively.

The interior of the concrete silo is divided into vertical shafts by 200 mm thick inner walls also made from reinforced *Silo concrete*. The dimensions of the largest shafts are 2.55 m × 2.55 m but also smaller shafts exist as shown by the horizontal cross section of the interior of the silo in Figure 2-4.

The construction of the concrete silo comprised two steps. As a first step, the slab was cast on top of the foundation layers (Figure 2-5) which includes the following components[1]: Butyl liner (1.5 mm), plastic foil (0.1 mm) and concrete (50 mm)). This was followed by casting of the outer and inner walls by means of slip-forming (Figure 2-6). This method ensured that no casting joints were formed in the outer and inner walls but also excluded the use of tie rods which probably would have been left in the concrete structure if traditional formwork had been used.

However, there are some concerns regarding the amount of reinforcement used in the slab, outer and inner walls. According to Cronstrand et al. (SKBdoc 1326418 ver 0.1, internal document, in Swedish) the amount of reinforcement in these parts is not sufficient to ensure sufficient crack width distribution and the risk for cracking already during construction must therefore be considered.

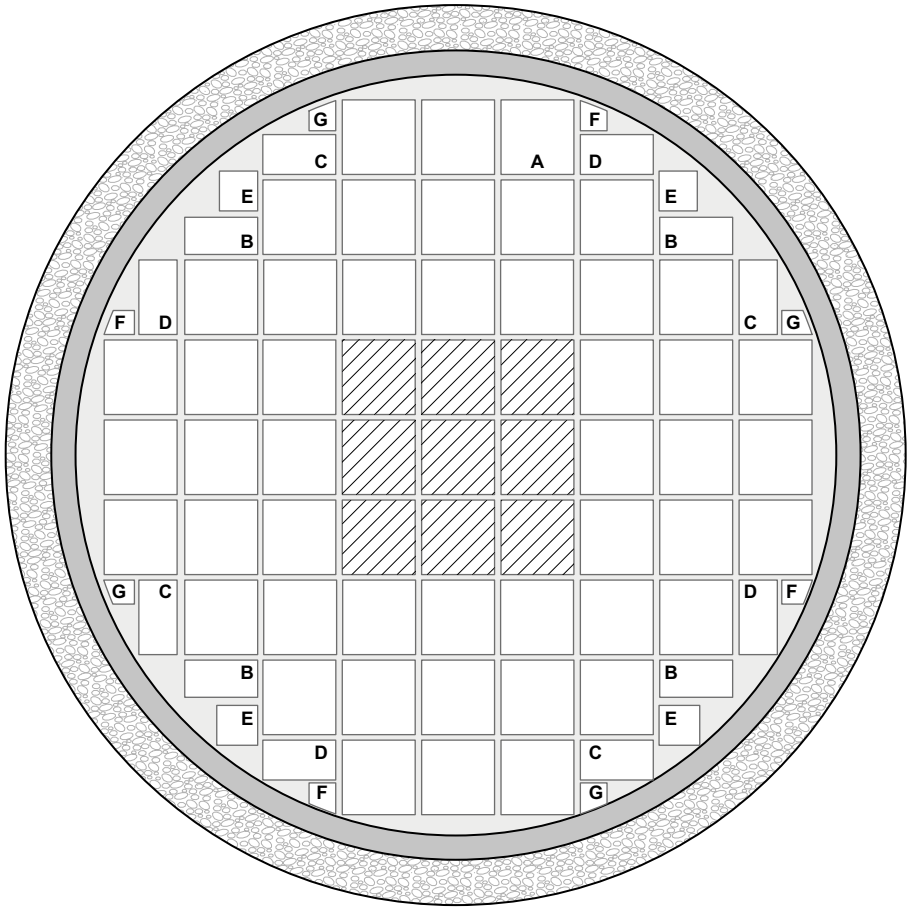


***Figure 2-4.*** *Schematic illustration from above of the division of the silo in shafts, indicating the location of the bituminised wastes in the central shafts. A denotes full-size shafts; B, C and D half-size shafts; E quarter-size shafts; F and G small shafts. There are also small shafts in the periphery that are assumed to be backfilled with grout and hence they are not shown in the figure (SKB TR-23-02).*

[1] Ritning 1-1010031 gruppnummer 117-1581, See also SKBdoc 1326418 ver 0.1. (Internal document, in Swedish.)

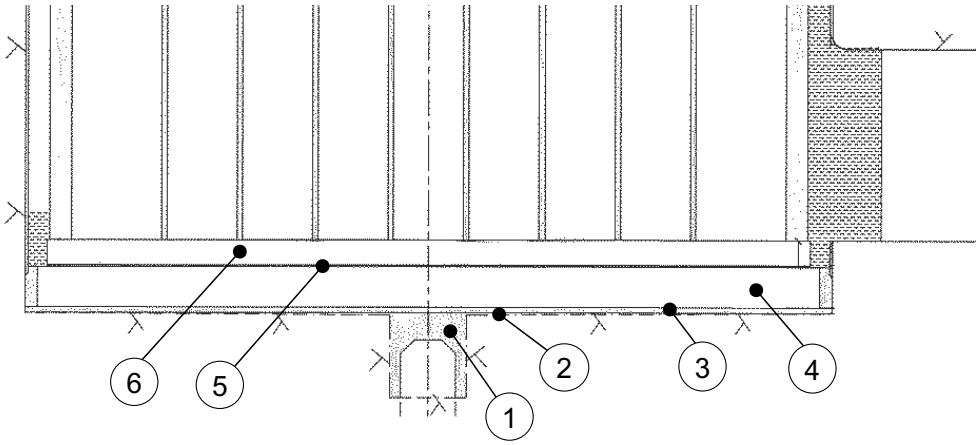


***Figure 2-5.*** *The foundation of the silo. Key to numbering: 1) Silo drainage tunnel, 2) Blinding for levelling, 3) Bottom drainage system, 4) Bottom bed 90/10 sand bentonite, 5) Sealing layer, 6) Slab of concrete silo (Börgesson et al. 2015).*

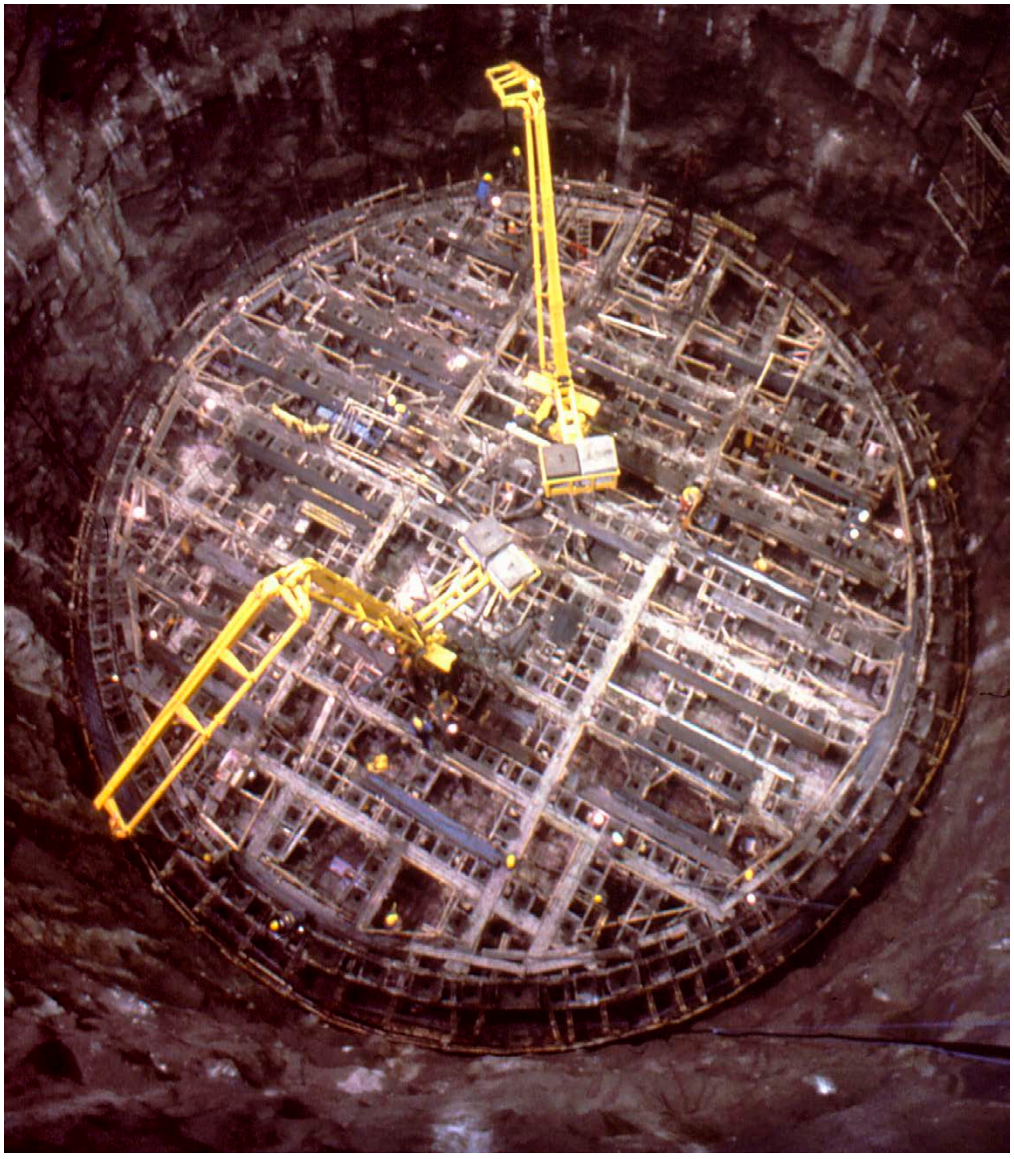

***Figure 2-6.*** *The silo during construction.*

#### *Lid*

The lid of the silo will be constructed at closure of the repository and will have an estimated thickness of 1 000 mm and be made from reinforced concrete. The lid will be perforated by a number of sand-filled holes with a diameter of about 100 mm that constitute a part of the gas evacuation system. The concrete mixing proportions for the lid have not yet been decided but at present it is assumed to be *2BMA concrete* (Section 3.3.3).

#### *Permeable grout between the waste packages and inner walls*

From the start of operation of the silo until June 2022, the *Original silo grout* (Section 3.4.1) was used for grouting of the waste packages in the silo. However, from June 2022 this was replaced by the *New silo grout* (Section 3.4.2). The thickness of the layer of grout between the steel/concrete moulds and the inner walls is 50 to 100 mm. The thickness is given by the dimensions of the moulds (1.2 m × 1.2 m × 1.2 m and four moulds in each layer) and the dimensions of the shafts (2.55 m × 2.55 m) with the variations mainly being due to variations in the positions of the waste packages inside the shaft. However, because of the small distance between the individual moulds, only minor amounts of grout are expected in these parts. For the steel drums the amount of grout surrounding the drums is significantly larger.

#### *Concrete moulds*

The concrete moulds (Figure 2-7) have the dimensions 1.2 m × 1.2 m × 1.2 m and are made from reinforced *SFR mould concrete* (Section 3.3.7). The thickness of the walls and bottom of the concrete moulds is 100–350 mm with a vast majority having a thickness of 100 mm. The lid is normally at least 100 mm thick (SKB R-18-07).

### 2.5.3 Activities in the silo during the operational period

#### *Disposal and grouting of waste packages*

During the operational period, concrete and steel moulds as well as steel drums containing radioactive waste conditioned in cement grout or bitumen are disposed in the silo. At present, waste is only disposed in the full-size shafts (Type A in Figure 2-4).

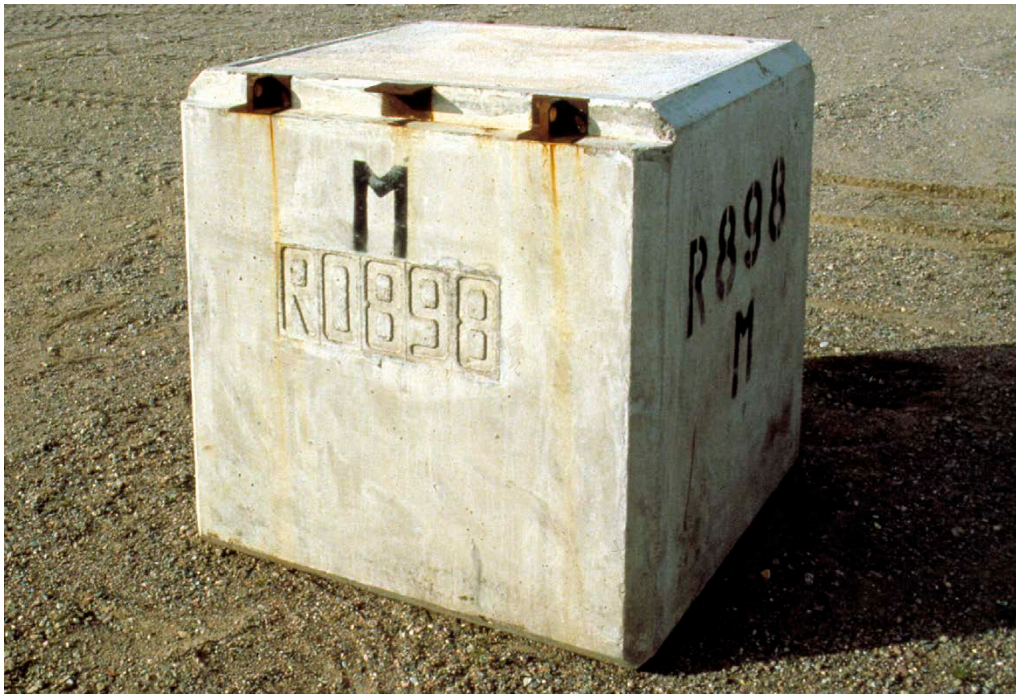


***Figure 2-7.*** *A concrete mould.*

After disposal of five or six layers of waste packages, the waste packages are grouted to provide additional stability to the stack. The grout does not formally constitute a hydraulic barrier but provides additional sorption capacity for radionuclides. During the operational period, all shafts are covered with prefabricated concrete elements for radiation shielding except for during disposal of waste as shown in Figure 2-8. These elements will be removed prior to closure (Mårtensson et al. 2022) and are therefore not included among the cementitious components covered in this report.

### *Work related to the presence of groundwater in some of the shafts in the silo*

During the period 2010 to 2013 groundwater was observed in shafts number 41, 42, 48, 52, 53, 62, 76, 86, 95 and 96 during preparations prior to grouting of waste.[2] In all, a total of 10 shafts were found to contain between 0.1m$^3$ and 12 m$^3$ groundwater giving a total of 36.1 m$^3$. Because of this, an extensive investigation programme was carried out to clarify the many possible consequences of the observed groundwater and the following conclusions were made:

- The presence of groundwater in these shafts had a negligible impact on the average chemical properties of the inner walls.[3]
- The level of radioactivity in the groundwater that was pumped out of the shafts was very low.[4]
- Grouting had not been carried out during the period during which the groundwater could have intruded into the silo.[5]
- No water was found in the nine central shafts which contain the bituminised waste.[6]
- Three of the shafts (41, 95, 96) in which water was found are in contact with the outer wall.

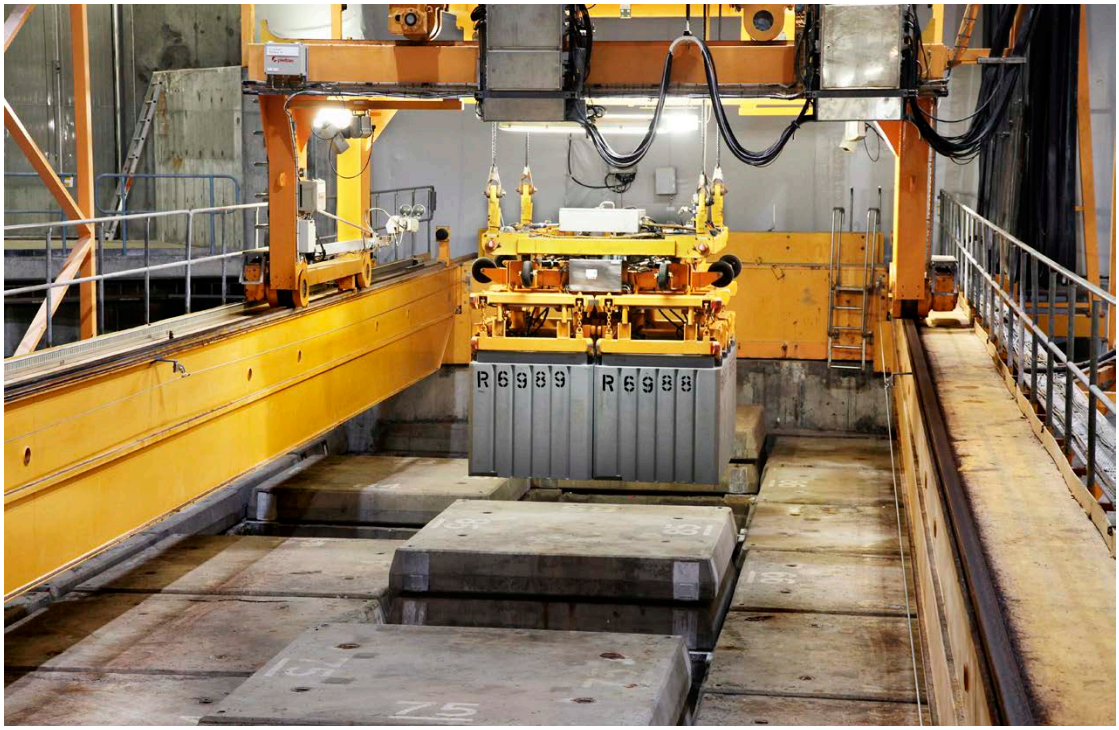


***Figure 2-8.*** *Disposal of waste packages (steel moulds) in the silo.*

[2] SKBdoc 1320850 ver 3.0. (Internal document, in Swedish.)

[3] SKBdoc 1327780 ver 3.0. (Internal document, in Swedish.)

[4] SKBdoc 1320850 ver 3.0. (Internal document, in Swedish.)

[5] SKBdoc 1327780 ver 3.0. (Internal document, in Swedish.)

[6] SKBdoc 1320850 ver 3.0. (Internal document, in Swedish.)

### 2.5.4 Closure of the silo

At closure, the shafts are first filled with the permeable grout up to the rim of the concrete silo. This provides a radiation shield which simplifies the work of reinforcing and casting the concrete lid which will be cast on a thin layer of sand placed on top of the grouted waste. The concrete lid will also contain a number of fully penetrating sand-filled holes that constitute one part of the gas evacuation system, Figure 2-9.

The concrete lid covering the bentonite in the gap between the concrete silo and the rock wall will be demolished and removed to allow for replacement of the uppermost part of the bentonite layer which may have been affected during the operational period.

The silo top above the concrete lid will be backfilled with several layers of various types of backfill materials as illustrated in Figure 2-9. Once backfilling is completed, plugs will be installed to hydraulically separate the silo from the other parts of the repository in order to limit groundwater flow through the silo, Figure 2-2.

The planned measures for closure of the silo are described in more detail in the closure plan for SFR (Mårtensson et al. 2022).

### 2.5.5 Functions of the cementitious components in the silo

#### *Operational period, sealing and closure*

During the operational period, the main functions of the cementitious components in the silo are to enable emplacement and grouting of waste as well as to enclose the waste packages and provide radiation shielding.

Table 2-2 compiles the functions of the cementitious components of the silo which are related to the load-bearing capacity and risk for cracking and – in this work – identified significant loads experienced by each individual component during the operational period, sealing and closure. The identified loads form the basis for the assessment of the risk for cracking during these periods and in a following step the assessment of recommended hydraulic conductivity and diffusivity data presented in Table 6-1. See also the initial state report for PSAR (SKB TR-23-02, Section 4.2) for additional information.

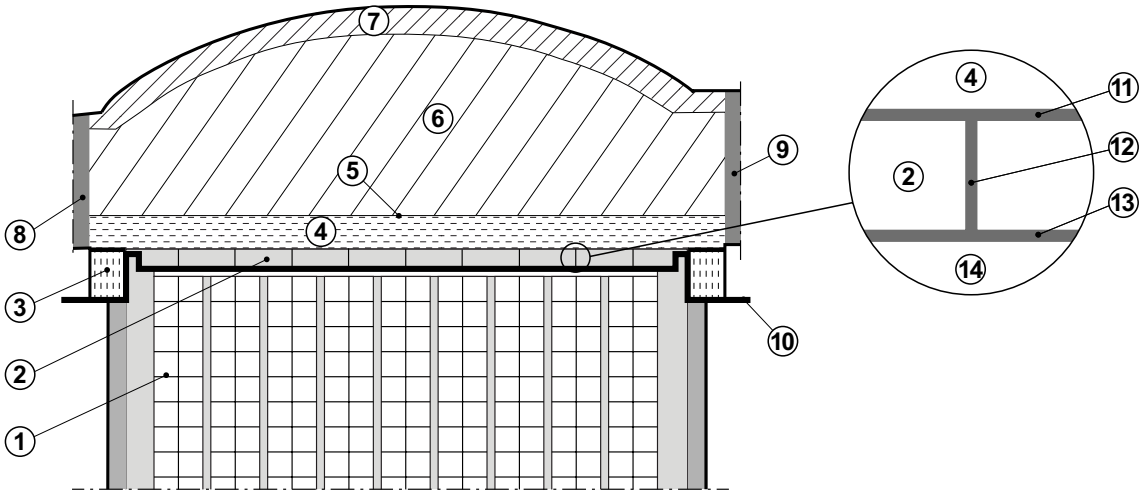


***Figure 2-9.*** *Schematic cross-section of silo top after closure. Key to numbering: 1) Waste 2) Reinforced concrete slab with sand layer and gas evacuation channels 3) Compacted fill of 30/70 bentonite/sand mixture 4) Compacted fill of 10/90 bentonite/sand mixture 5) Unreinforced concrete slab 6) Compacted fill of friction material 7) Cement-stabilised sand 8) Constraining wall of concrete against the silo roof tunnel (1STT) 9) Constraining wall of concrete against loading-in building (IB) 10) Boundary between works associated with grouting and backfilling 11) Sand layer 100 mm 12) Gas evacuation channels ∅ 0.1 m 13) Sand layer 50 mm 14) Grout (permeable).*

**Table 2-2. Functions of the cementitious components in the silo and identified significant loads during the operational period, sealing and closure.**

| Cementitious component | Function | Identified significant load |
|---|---|---|
| **Slab** | Provide a stable foundation for the concrete structure and the grouted waste. | Weight of concrete structure and grouted waste packages. |
| **Outer wall** | Enclose the waste packages and prevent bentonite expansion. | Pressure from packed bentonite (no swelling pressure foreseen). |
| **Lid** | No function: constructed at closure. | |
| **Inner walls** | Enable grouting of waste packages. Provide mechanical support to the outer walls. | Hydrostatic pressure from wet grout during grouting of waste packages. |
| **Permeable grout** | Stabilise the stack of waste packages. | No significant loads identified |
| **Concrete moulds** | Enclose and enable handling of the waste. | Weight of stack of waste packages, hydrostatic load from wet grout. |

### *Post-closure*

The entire concrete silo and its interior including inner walls, grout, and waste packages serve as mechanical elements that withstand the swelling pressure from the bentonite, the internal pressure caused by gas formation and the load from self-weight. All these cementitious components also have chemical barrier functions by sorption of radionuclides. Cementitious materials also set a high pH, which limits corrosion of steel and gas production caused by microbial activity.

Concrete moulds, concrete structures and grout also contribute to limit the groundwater flow through the waste and thus the release of radionuclides.

Table 2-3 compiles the functions (not including the safety functions, see below) of the cementitious components of the silo which are related to the load-bearing capacity and risk for cracking and – in this work – identified significant loads experienced by each individual component post-closure. The identified loads form the basis for the assessment of the risk for cracking post-closure and in a following step the assessment of recommended hydraulic conductivity and diffusivity data presented in Chapter 7.

The safety functions and safety function indicators for the engineered barriers in the silo are compiled in Table 2-1. See also the post-closure safety report for PSAR (SKB TR-23-01, Section 4.4.1) for additional information.

**Table 2-3. Functions of the cementitious components in the silo and origin of the significant loads post-closure.**

| Cementitious component | Function | Origin of significant load |
|---|---|---|
| **Slab** | Provide a stable foundation for the concrete structure and the grouted waste. | Compressive load from the concrete structure and grouted waste packages. |
| **Outer wall** | Enclose the waste packages and prevent bentonite expansion. | External load from the bentonite swelling pressure, internal load from swelling waste and gas. |
| **Lid** | Carry the load of the backfill material in the silo top. | Weight of backfill material in the silo top. |
| **Inner walls** | Provide mechanical support to the outer walls and lid. | Pressure from swelling waste and gas. |
| **Permeable grout** | Stabilise the stack of waste packages. | Pressure from swelling waste and gas. |
| **Concrete moulds** | Enclose and enable handling of the waste. | Internal loads from swelling waste and gas, compressive loads from stack of waste packages. |

## 2.6 1BMA, vault for intermediate-level waste

### 2.6.1 Overview

The vault for intermediate-level waste, 1BMA has the dimensions 19.6 m × 16.5 m × 160 m (w × h × l) (SKB TR-23-02) with walls and roof lined with shotcrete. In the waste vault, a concrete structure with the dimensions 15.6 m × 8.2 m × 140 m (w × h × l) made from reinforced *1BMA concrete* (Section 3.3.2) and comprising 13 larger compartments and 2 smaller ones is erected, Figure 2-10. For a detailed description of the design of the existing concrete structure; see Elfwing et al. (2015).

As a complement to the existing concrete structure in 1BMA, new outer walls will be cast outside the existing ones at closure. This is discussed further in Section 2.6.4.

### 2.6.2 Cementitious components in 1BMA

The cementitious components of 1BMA comprise the following components which are described in more detail below.

- Slab.
- Existing outer walls.
- New outer walls.
- Lid.
- Inner walls.
- Prefabricated concrete elements.
- Gas evacuation system.
- Concrete moulds.

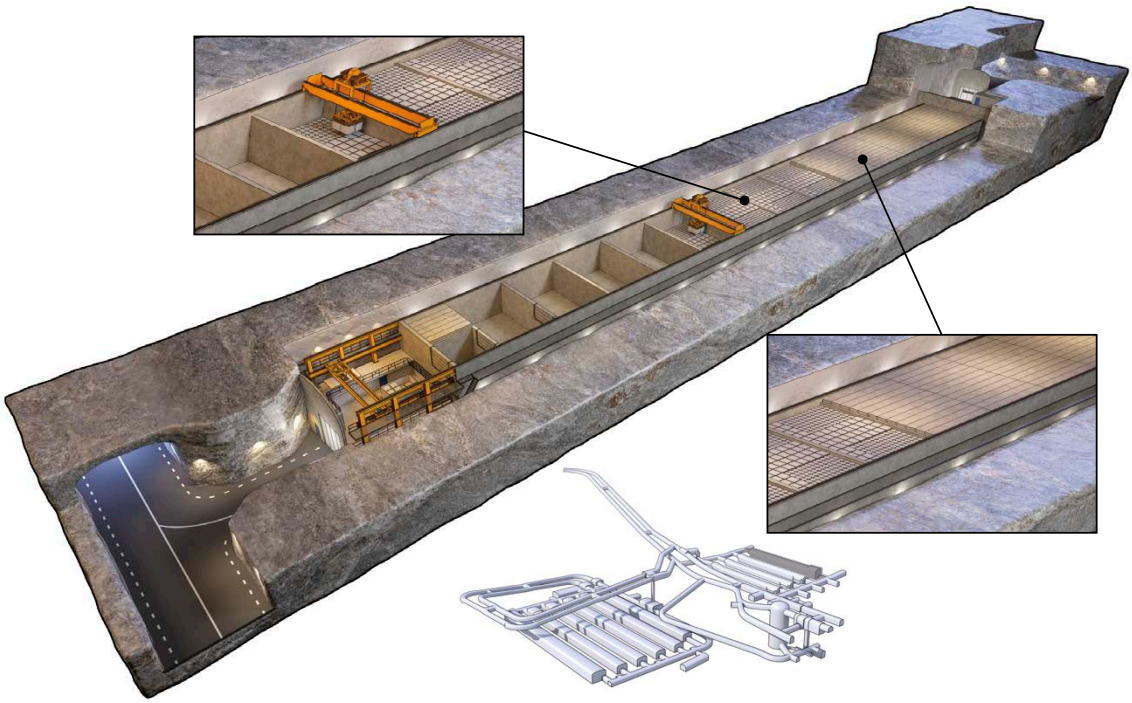

***Figure 2-10.*** *Illustration of 1BMA during the operational period. The upper detail shows the emplacement of waste packages, the lower detail shows the concrete lid. In addition, there is a view of SFR with the position of 1BMA in darker grey.*

### *Slab*

The slab has the dimensions 15.6 m × 140 m with a thickness of 250–300 mm and is made from reinforced *1BMA concrete*, Section 3.3.2. The loadbearing parts of the concrete structure (concrete beams) are founded on solid rock whereas the slab is founded on a bed of crushed rock levelled with gravel.

Casting of the concrete structure in 1BMA was done section-wise as indicated in Figure 2-11 where each individual section is marked with a number using standard methods for casting of slab on ground. Note that Figure 2-11 is only indicative and that the actual positions of the casting joints in the concrete structure differ somewhat from the positions shown in this figure. The dashed lines indicate the position of the load-bearing concrete beams beneath the slab, see Figure 2-17.

### *Existing outer walls*

The existing outer walls of the concrete structure in 1BMA are 8.2 meters high and are made from reinforced *1BMA concrete* (Section 3.3.2) (SKB TR-23-02). The nominal thickness of the walls is 400 mm except for the wall facing the reloading zone and the upper part of the long walls on which the overhead crane rests which are 600 mm and 700 mm thick, respectively.

As shown in Figure 2-12, the existing outer walls contain a number of holes, the purpose of which was to enable the previously planned grouting of the waste packages. Each compartment has a total of 12 holes – 6 in each existing outer wall – at three different levels. Figure 2-12, also shows dark spots caused by corrosion products from the tie rods used to keep the formwork together during casting.

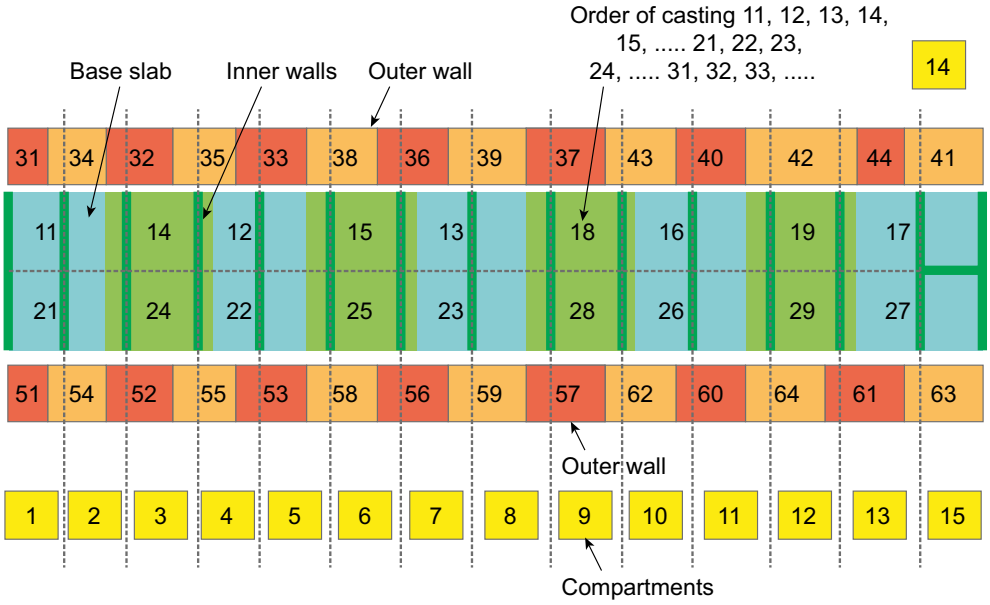


***Figure 2-11.*** *Casting sections in the main concrete structure in 1BMA. Order of casting: 11, 12, 13... –21, 22, 23… etc. Light green and blue sections represent the slab whereas the red and orange sections represent the two long outer walls. Dark green represents inner walls. Dashed lines indicate the position of the load-bearing concrete beams beneath the slab. Yellow indicates the compartments.*


***Figure 2-12.*** *The interior of one of the compartments in 1BMA showing the holes in the existing outer walls which were planned to be used for grouting of the waste packages at closure of the repository. The dark spots show the position of the tie rods used to keep the formwork together during casting.*

### *New outer walls*

The new outer walls (see Figure 2-17) will be cast outside of the existing outer walls at closure using *2BMA concrete*. The thickness of the walls will be about 900 mm (Figure 2-17) and contain steel reinforcement. The new outer walls will be cast using the methods described by Wimelius (2021). A traditional formwork which is supported against the adjacent bedrock will be used and the use of tie rods will therefore not be required.

### *Prefabricated concrete elements*

In order to provide radiation shielding during the operational period, each compartment is covered by prefabricated concrete elements that rests on top of the edges of the inner walls as well as on concrete moulds placed in two rows in the centre of each compartment. As mentioned in the following section (Lid), the lid does not require mechanical support from the prefabricated concrete elements and concrete moulds post-closure.

The thickness of the concrete elements is about 400 mm (Figure 2-17) but the lateral dimensions vary as shown in Figure 2-14. The concrete elements are made locally using standard concrete from a local production plant. The mixing proportions have varied over the years but the most recent elements were made from concrete based on *Anläggningscement Slite Standard P*. Presumably, the properties of the concrete for these elements resemble those of the *1BMA concrete*, Section 3.3.2.

### *Lid*

The reinforced concrete lid will presumably be made from *2BMA concrete* (Section 3.3.3) and be cast on top of the prefabricated concrete elements at closure of 1BMA. Calculations performed by Westerberg – assuming concrete class C30/37 – conclude that the lid needs to be at least 800 mm thick and contain steel reinforcement to resist the pressure from the intruding groundwater during saturation without relying on the mechanical support from the prefabricated concrete elements and waste packages.[7] Alternatively, less reinforcement can be used but in that case the thickness of the lid needs to be increased.

### *Inner walls*

The concrete structure is divided into 13 larger compartments with the nominal lateral dimensions 9.9 m × 14.8 m (volume 1 070 $m^3$) and two smaller ones with the nominal lateral dimensions 4.9 m × 7.2 m by 400 mm thick inner walls made from reinforced *1BMA concrete* (Section 3.3.2). However, recent measurements have shown that compartments 12 and 13 were somewhat smaller than nominal with a volume of 1 062.58 $m^3$ (compartment 12) and 1 055.89 $m^3$ (compartment 13) respectively.[8] This may influence the risks associated with swelling of waste, e.g. bituminised ion-exchange resins.

In each inner wall there is a doorway which is left open until start of disposal of waste in the compartment when it is closed by means of concrete blocks, Figure 2-13.

***Figure 2-13.*** *Sealed doorway in the inner wall separating two adjacent waste compartments.*

[7] SKBdoc 1583182 ver 1.0. (Internal document, in Swedish.)

[8] SKBdoc 1935977 ver 2.0. (Internal document, in Swedish.)

#### *Gas evacuation system*

The gas evacuation system constitutes a number of channels in the lid which are filled with a permeable grout, e.g. the *New silo grout*. The need for a gas evacuation system in 1BMA is currently being analysed and a final decision concerning the installation of such a system has not yet been made. However, for the sake of completeness, the gas evacuation system is included in this report.

#### *Concrete moulds*

A large number of concrete moulds are disposed in 1BMA (SKB R-18-07). The concrete moulds are of the same type as those used for the waste in the silo but moulds with thick walls (above 100 mm) are not used in 1BMA. See Section 2.5.2 for details.

### 2.6.3 Activities in 1BMA during the operational period

#### *Disposal of waste packages*

During the operational period, concrete and steel moulds, as well steel drums (on a drum tray or in a drum box) are disposed in the compartments by a remote-controlled overhead crane that runs on the top edge of the walls of the concrete structure, Figure 2-10. The waste is disposed as it arrives at SFR; moulds are stacked six in height and drums eight in height. At least two rows of concrete moulds are disposed in each compartment to support the prefabricated concrete elements which are installed as the compartments are filled, Figure 2-14.

Prior to installation of the waterproofing membrane in the roof of the waste vault, Figure 2-14, a thin layer of concrete was cast on top of the concrete elements in order to prevent the intrusion of groundwater into the waste compartments. However, after installation of the waterproofing membrane this is no longer done.

***Figure 2-14.*** *Waste vault for intermediate-level waste, 1BMA, during the operational period. Note the different states of the different compartments. Those in the farthest part have been entirely filled with waste and provided with concrete elements for radiation shielding and a thin layer of concrete. The compartments in the middle have been filled with waste and covered with radiation shielding concrete elements while no waste has yet been disposed in the nearest compartments.*

### *Investigations of the status of the concrete structure*

The used design and method for construction of the concrete structure in 1BMA described in Section 2.6.2 have caused the following four types of damages of importance for the post-closure safety of 1BMA, the causes and effects of which have been extensively studied and described by Elfwing et al. (2015):

- Corrosion of the steel tie rods which may cause the formation of permeable zones in the vicinity of the tie rods, Figure 2-15 left image.
- Spalling of the concrete covering layer due to corrosion of the steel reinforcement bars, Figure 2-15 right image.
- Formation of permeable joints due to poor preparation of the surface of the previously cast section of the concrete structure, Figure 2-16 left image.
- Formation of cracks due to restrained shrinkage during cooling of the hardening concrete during the construction period, Figure 2-16 right image.

***Figure 2-15.*** *Corrosion of a steel tie rod (left image) and spalling of the concrete covering layer due to corrosion of the reinforcement bars (right image).*

***Figure 2-16.*** *Example of a poorly prepared joint between two adjacent sections (left image) and a crack formed in the centre of a section of the existing outer wall of the concrete structure (right image).*

As a part of this investigation programme, several cores were extracted from different parts of the concrete structure. The length of these cores corresponds to about half of the thickness of the concrete structure in question in order not to penetrate the barriers. After coring, the holes were filled with a cement grout.

The conclusions from this investigation programme were that the operational safety of the concrete structure was not impaired by the detected damages. However, the presence of cracks did not comply with the description of the assumed initial state of 1BMA (SKB TR-14-02) and that repair measures to the concrete structure were required; see also Section 2.6.4.

The investigation programme was followed by a programme in which different repair methods were described and evaluated (SKBdoc 1467828 ver 2.0, internal document, in Swedish, Elfwing et al. 2016). The report recommends that new walls should be cast outside the original ones and that the thickness of the lid should be increased in order to withstand the combined load from the weight of the backfill material on top of the concrete structure and the groundwater pressure during saturation post-closure.

The report also recommends that all repair measures should be carried out at closure of SFR. This was because the observed damages was found not to impair the operational safety of 1BMA and that carrying out the repair measures during the operational period would affect the operation of the facility.

The impact of the suggested measures on radionuclide release was investigated by von Schenck et al. (2015) as well as by Elfwing et al. (2018) who concluded that the suggested measures can ensure that the post-closure safety of the repository can be upheld. This was also confirmed in a recent safety assessment for SFR (SKB TR-23-01).

### 2.6.4 Closure of 1BMA

#### *Repair measures of the walls of the concrete structure*

As obvious from the findings presented in Section 2.6.3 and references therein, the presence of cracks and joints in the slab and existing outer walls will have a negative impact on the transport properties of these components. For this reason, new walls with improved transport properties and load-bearing capacity will be cast outside the existing ones at closure of SFR.

Two main alternatives have been studied, the main difference being the degree of adhesion between the existing and the new outer walls. Of these, Westerberg (SKBdoc 1583182 ver 1.0, internal document, in Swedish) evaluated the load-bearing capacity of new outer walls without considering any mechanical support from the existing outer walls whereas Eriksson (2021) investigated a system with a strong adhesion between the new and the existing outer walls.

Based on the findings in these studies Wimelius (2021) recommend that new walls should be cast outside the existing outer walls and that means to minimise the adhesion between existing and new walls should be utilised. Wimelius (2021) therefore suggest a procedure for the construction of the new walls including the following steps:

- Cleaning of the surface of the existing concrete structure.
- Repairing the surface damages caused by e.g. spalling due to rebar corrosion.
- Covering the existing outer walls with e.g. a bitumen sheet, a tarpaulin or a plastic sheet to prevent adhesion between the new and existing outer walls
- Mounting of new reinforcement.
- Construction of formwork.
- Casting.

For the slab, several methods for mitigating the effect of the cracks and thus limiting the flow of groundwater into the waste compartments from beneath have been evaluated.[9] However, as none of these methods have been found suitable it has been decided to leave the slab in its current condition (SKB TR-23-02).

### *Casting of lid, backfilling and closure*

Following the construction of new outer walls, a reinforced concrete lid with a thickness of at least 800 mm is cast on top of the prefabricated concrete elements.[10]

In the following steps installations and equipment in the waste vault are dismantled after which the vault is backfilled with macadam. At the end of the waste vault that connects to the adjacent tunnels; plugs will be installed to hydraulically separate the waste vault from the other parts of the repository in order to limit groundwater flow along the waste vault. A cross-section of the backfilled 1BMA with new outer walls is shown in Figure 2-17.

The closure plan for SFR (Mårtensson et al. 2022) describes the planned measures for closure of 1BMA in more detail.

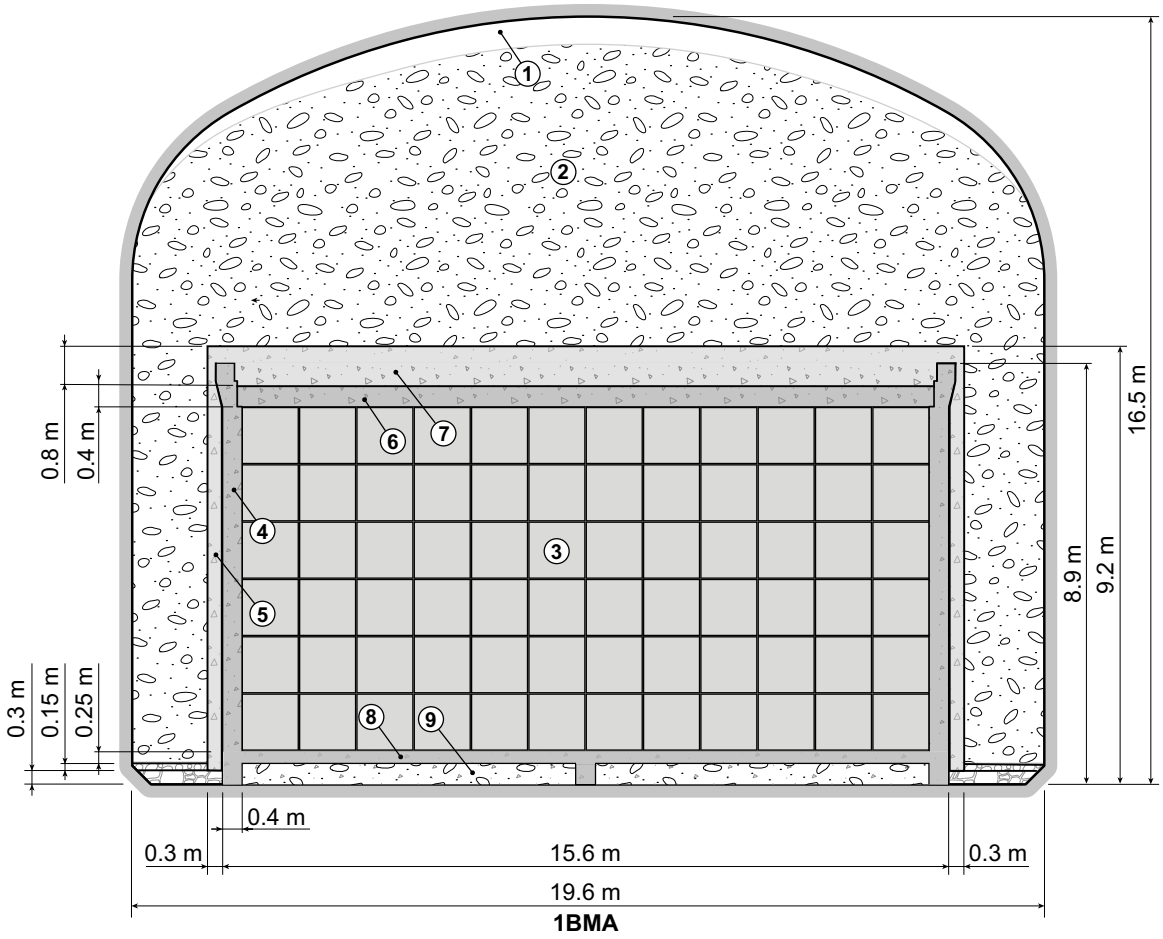


***Figure 2-17.*** *Schematic cross-section of 1BMA after restoration of the walls and closure. Key to numbering: 1) Void 2) Macadam backfill 3) Waste domain 4) Existing outer wall 5) New outer wall 6) Pre-fabricated concrete element 7) New concrete lid 8) Slab 9) Crushed rock.*

[9] SKBdoc 1467828 ver 2.0. (Internal document, in Swedish.)

[10] SKBdoc 1583182 ver 1.0. (Internal document, in Swedish.)

### 2.6.5 Functions of the cementitious components in 1BMA

#### *Operational period, sealing and closure*

During the operational period, the main functions of the cementitious components in 1BMA are to enable transport and emplacement of waste as well as to enclose the waste packages and provide radiation shielding.

Table 2-4 compiles the functions of the cementitious components of 1BMA which are related to the load-bearing capacity and risk for cracking and – in this work – identified significant loads experienced by each individual component during the operational period, sealing and closure. The identified loads form the basis for the assessment of the risk for cracking during these periods and in a following step the assessment of recommended hydraulic conductivity and diffusivity data presented in Table 6-2. See also the initial state report for PSAR (SKB TR-23-02, Section 5.2 for additional information).

**Table 2-4. Functions of the cementitious components in 1BMA and identified significant loads during the operational period, sealing and closure.**

| Cementitious component | Function | Origin of significant load |
|---|---|---|
| **Slab** | Provide a stable base for the waste packages. | Weight of stack of waste packages. |
| **Existing outer walls** | Provide radiation shielding, provide a stable base for the overhead crane during emplacement of waste. | Dynamic load from moving overhead crane during transport of waste packages. |
| **New outer walls** | No function: constructed at closure. | N/A |
| **Lid** | No function: constructed at closure. | N/A |
| **Inner walls** | Enable emplacement of waste packages. Provide radiation shielding and support the prefabricated concrete elements. | Weight of prefabricated concrete elements |
| **Prefabricated concrete elements** | Provide radiation shielding. | Weight of wet concrete during casting of the lid. |
| **Gas evacuation system** | No function: constructed at closure. | N/A |
| **Concrete moulds** | Enclose and enable handling of the waste. Mechanical support for the prefabricated concrete elements. | Weight of stack of waste packages, prefabricated concrete elements and weight of wet concrete during casting of the lid. |

#### *Post-closure*

The new outer walls and lid constitute the main hydraulic barriers, limiting the groundwater flow through the waste but also other parts of the concrete structure and the concrete moulds contribute to this function. Further, the new outer walls and lid maintain the structural integrity of the concrete structure and must therefore resist the load from the backfill material and groundwater pressure during saturation of the repository.

In addition, all cementitious materials (waste form, concrete moulds and concrete structures) have chemical barrier functions. The use of cementitious materials ensures good sorption properties for many radionuclides. Cementitious materials also set a high pH value, which limits corrosion of steel and gas production caused by microbial activity.

Table 2-5 compiles the functions (not including the safety functions, see below) of the cementitious components in 1BMA which are related to the load-bearing capacity and risk for cracking and – in this work – identified significant loads experienced by each individual component post-closure. The identified loads form the basis for the assessment of the risk for cracking post-closure and in a following step the assessment of recommended hydraulic conductivity and diffusivity data presented in Chapter 8.

The safety functions and safety function indicators for the engineered barriers in 1BMA are compiled in Table 2-1. See also the post-closure safety report for PSAR (SKB TR-23-01, Section 4.4.2) for additional information.

**Table 2-5. Functions of the cementitious components in 1BMA and origin of the significant loads post-closure.**

| Cementitious component | Function | Origin of significant load |
|---|---|---|
| **Slab** | Provide a stable base for the waste packages. | Weight of stack of waste packages and later also from weight of lid and backfill material. Groundwater pressure during saturation. |
| **Existing outer walls** | No function. | N/A |
| **New outer walls** | Provide support to the lid and backfill material | Groundwater pressure during saturation and pressure from backfill material. |
| **Lid** | Carry the weight of the backfill material on top of the concrete structure | Groundwater pressure during saturation and weight of backfill material. |
| **Inner walls** | Carry the weight of the lid and backfill material on top of the concrete structure during later periods | Pressure from the outer walls, lid and backfill material during saturation. Later, weight of lid, outer walls and backfill material. |
| **Prefabricated concrete elements** | No function. | Weight of lid and backfill material during later periods. |
| **Gas evacuation system** | Ensure that gas can be transported out of the concrete structure at a low pressure. | The load-bearing capacity of the gas evacuation system is insignificant and therefore disregarded. |
| **Concrete moulds** | Enclose the waste. Provide mechanical support to the lid. | Weight of lid and backfill material during later periods. Internal pressure from swelling of waste and gas*. |

*It should be noted that most of the potentially swelling waste are disposed in steel moulds or steel drums and not in concrete moulds.

## 2.7 2BMA, vault for intermediate-level waste

### 2.7.1 Overview

The vault for intermediate-level waste, 2BMA will have the dimensions 23.5 m ×18.6 m × 275 m (w × h × l) (SKB TR-23-02). The walls and roof of the waste vault will be lined with shotcrete and rock bolts will be used to further reduce the risk of rock fall-out.

In 2BMA, a total of 13 free-standing caissons with a base of 18.1 m × 18.1 m and a height of 9 m made from unreinforced *2BMA concrete* (Section 3.3.3) will be constructed. The caissons will be provided with concrete inner walls to create separated shafts with the dimensions about 2.6 m × 2.6 m within which the waste will be emplaced, Figure 2-18.

The caissons will be founded on a thick reinforced concrete slab, the main function of which is to ensure that e.g. uneven settlements in the crushed rock foundation or uneven distribution of the waste packages during emplacement do not cause cracking of the caisson.

A waterproofing membrane will be installed in the roof and along the walls of the waste vault to collect and divert any intruding groundwater and prevent corrosion of the waste packages during the operational period.

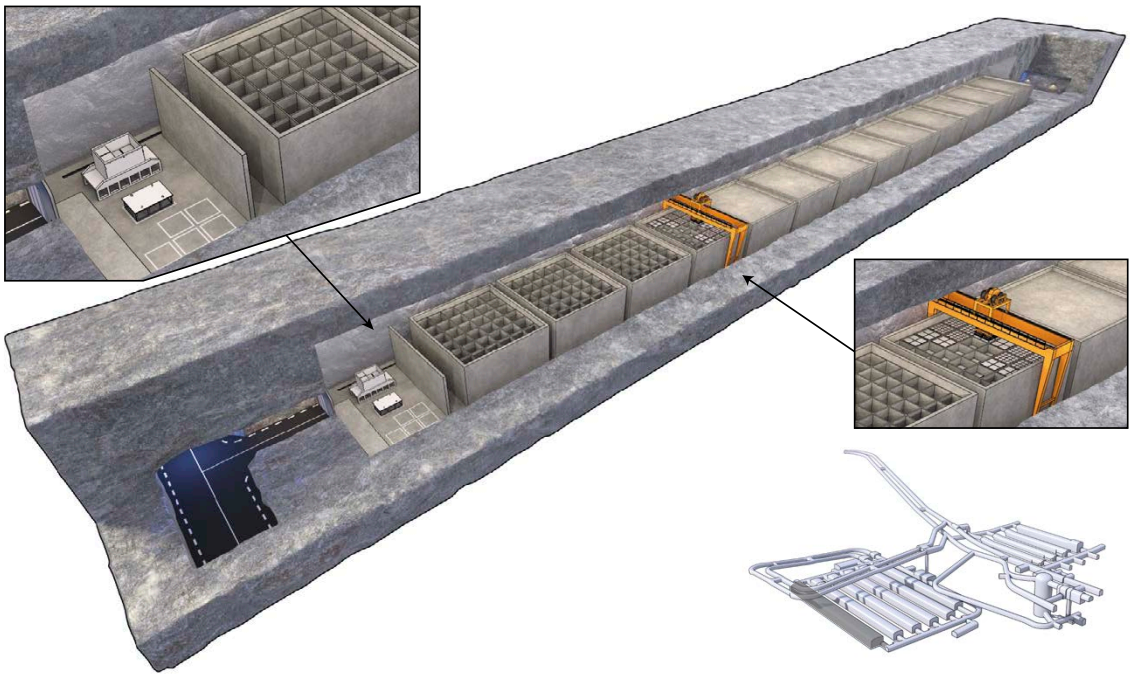

***Figure 2-18.*** *Illustration of 2BMA during the operational period. The lower detail shows a view of SFR with the position of 2BMA in darker grey.*

### 2.7.2 Cementitious components in 2BMA

The cementitious components of 2BMA comprise the following components which are described in more detail below.

- Reinforced concrete slab.
- Slabs (bottom of concrete caissons).
- Outer walls.
- Lids.
- Inner walls.
- Prefabricated concrete elements.
- Gas evacuation system.
- Concrete moulds.

#### *Reinforced concrete slab*

The reinforced concrete slab, which constitutes the foundation of the concrete caissons, will have a thickness of about 500 mm (Figure 2-22), a length of about 275 m and be made from *2BMA concrete* (Section 3.3.3) or similar. The slab is expected to be cast in sections – compare Figure 2-11 – with the consequence that a number of joints will form along and across the slab. However, the distance between these joints is uncertain.

The reinforced concrete slab will be founded on a layer of crushed rock/macadam and be covered with a foil of a material that prevents adhesion between the reinforced concrete slab and the slabs of the concrete caissons. This is expected to enable unrestrained shrinkage and expansion of the caissons caused by temperature and humidity variations during construction and the operational period and reduce the risk of cracking; see Sections 4.2 and 4.4.

### *Slabs*

The slabs of the concrete caissons will have the dimensions 18.1 m × 18.1 m × 0.6 m and be made from *2BMA concrete* (Section 3.3.3) or similar.

The slabs will be constructed using traditional formwork for casting of slab on ground by means of the methods tested and evaluated by Mårtensson and Vogt (2020). In order to improve the strength and reduce the hydraulic conductivity of the construction joints between the slabs and the outer walls, the slabs will be provided with a recess and optional joint seals as shown in Figure 2-19.

### *Outer walls*

The outer walls will be 680 millimetres thick and be made from *2BMA concrete* (Section 3.3.3) or similar. The walls will be cast using a traditional formwork for walls which is held together by tie rods as shown in Figure 2-20, right image. In order to keep the formwork in position during casting it will be supported against the adjacent rock wall and rock floor as shown in Figure 2-20, left image.

During casting, the tie rods will be separated from the wet concrete by the use of protective concrete tubes in order to enable removal of the tie rods during dismantling of the formwork.

Tests carried out by Mårtensson (2021a) have shown that concrete tubes can be successfully used to protect the tie rods from the wet concrete but also that the tubes can be filled with a cementitious grout in such a way that the transport properties of the materials and interfaces be representative of the bulk concrete, Figure 2-21.

Prior to casting of the walls, the recess in the slab will be thoroughly cleansed in order to ensure strong adhesion between these two parts as well as a low hydraulic conductivity of the joint.

As a further measure to reduce the risk of crack formation in the walls due to temperature shrinkage during construction, the slab of the concrete caisson will be heated to about the expected maximum temperature of the concrete walls caused by the concrete's heat of hydration prior to casting of the outer walls. This strategy was successfully tested by Mårtensson and Vogt (2020).

***Figure 2-19.*** *The image shows the recess in the peripheral part of the slab (i.e. the future position of the outer walls) of the concrete caisson that constituted the final part of the development programme and which was constructed at the Äspö Hard Rock Laboratory (Mårtensson and Vogt 2020). The recess improves the mechanical strength of this joint and the visible copper joint seal in the left part of the recess contributes to a low hydraulic conductivity of the joint.*

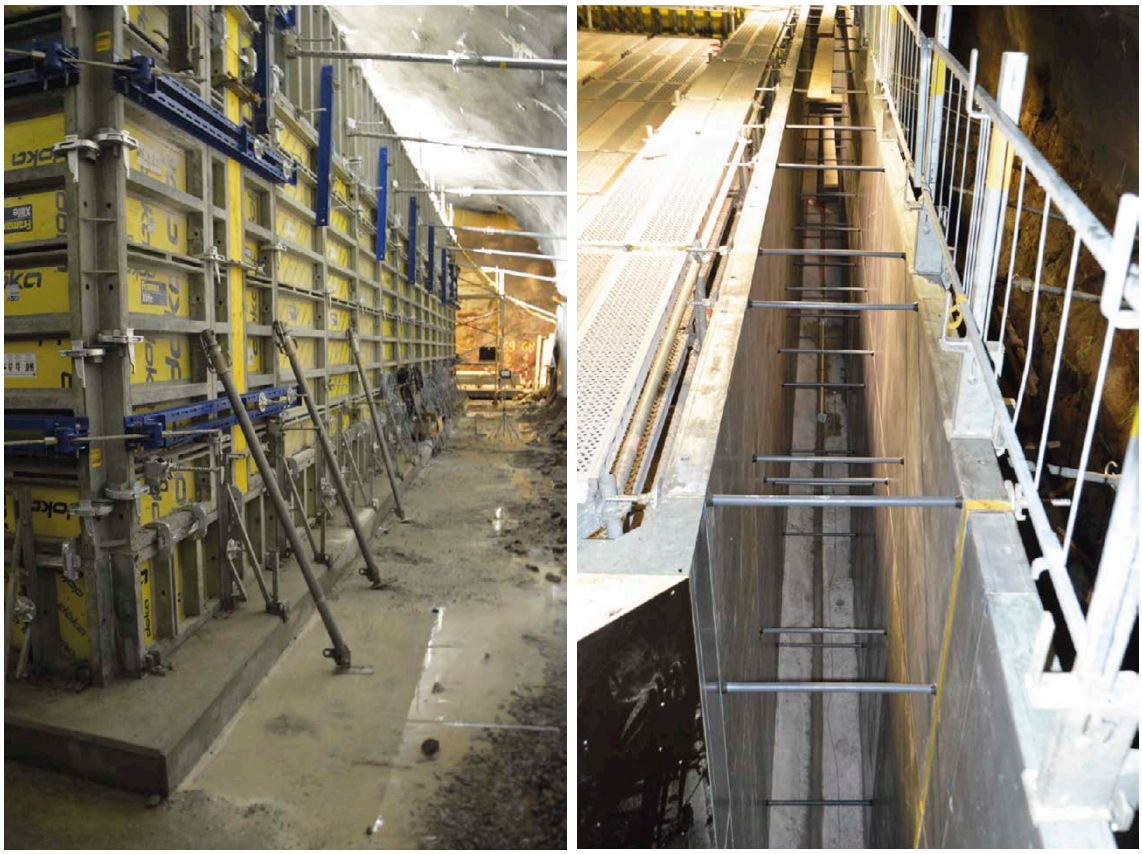

***Figure 2-20.*** *Outside (left image) with supports against adjacent rock wall and rock floor and inside of a traditional formwork utilising tie rods in order to keep the formwork together during casting. The images show the concrete caisson that constituted the final part of the development programme and which was constructed at the Äspö Hard Rock Laboratory (Mårtensson and Vogt 2020).*

***Figure 2-21.*** *Test casting performed in order to evaluate different combinations of tie rods and protective tubes (left image) and a core extracted from this test (right image). In the right image, the filling material in the centre is surrounded by the concrete tube and the concrete used for casting of the test structure (Mårtensson 2021a).*

### *Lids*

The concrete lids will be cast on top of corrugated steel sheets which rest on the prefabricated concrete elements and be made from unreinforced *2BMA concrete* (Section 3.3.3) or similar. From calculations performed by Westerberg (2017) the lids will have a preliminary thickness of only 600 mm because of the support from the inner walls.

The lid will also be provided with a gas evacuation system, see Section Gas evacuation system below.

### *Inner walls*

The purpose of the inner walls is to provide mechanical support to the outer walls and lid against external loads from e.g. the groundwater pressure during saturation and the backfill material. According to calculations performed by Könönen and Olsson (2018) the thickness of the inner walls will be 330 and 200 mm respectively. The thicker walls will constitute the row of inner walls closest to the outer walls whereas the thinner walls will constitute all other parts of the inner walls. The inner walls will be provided with holes in order to ensure that any intruding groundwater is evenly distributed within the entire caisson during saturation of the vault post-closure.

According to Könönen and Olsson (2018), concrete of class C50/60 should be used to ensure sufficient compressive strength. In the case a weaker concrete is used, the thickness of the inner walls must be increased. The different concrete classes with details of compressive strength and w/c ratio are described in Svensk Byggtjänst (2017, Table 12.4:4)

At the time of writing, the construction method for the inner walls remains to be tested and evaluated. Possible methods are e.g. traditional casting, installation of prefabricated concrete elements and slip forming.

### *Prefabricated concrete elements*

In order to provide radiation shielding during the operational period, each shaft will be covered by a prefabricated concrete element that rests on top of the edges of the inner and outer walls as shown in SKB (TR-23-02, Figure 6-5) The dimensions of the concrete elements will be on the order of 2.8 m × 2.8 m with a thickness of about 500 mm. The concrete elements can be manufactured at the local concrete production plant using e.g. *2BMA concrete* or purchased from any available manufacturer of this type of components. In the latter case it can be expected that a different type of concrete than the *2BMA concrete* will be used.

### *Gas evacuation system*

According to Elfwing et al. (2017), the gas evacuation system constitutes a total of 6 holes in the lid of each caisson, each with the lateral dimensions 250 mm × 200 mm and each filled with a permeable grout, e.g. the *2BMA grout,* Section 3.4.4.

This choice is motivated by the findings by Elfwing et al. (2017) who showed that the use of a material with the same properties as the *2BMA grout* did not affect the total flow of groundwater through the waste. If instead sand was used, an increased flow during the first 20 000 years post-closure was observed. However, in the study by Elfwing et al. (2017) a hydraulic conductivity of $8.5 \times 10^{-10}$ m/s was used for the concrete in the lid, instead of $(1–5) \times 10^{-12}$ m/s suggested for the lid at closure in this report, Table 6-3. The impact of this is probably that the influence of the grout-filled holes on groundwater flow will increase compared to the case studied by Elfwing et al. (2017).

### *Concrete moulds*

Only a few concrete moulds with waste will be disposed in 2BMA (SKB R-18-07). The concrete moulds are of the same type as those used for the waste in the silo but moulds with thick walls (above 100 mm) are not expected in 2BMA. See Section 2.5.2 for details.

### 2.7.3 Activities in 2BMA during the operational period

During the operational period, waste packages comprising steel and/or concrete moulds are emplaced in the caissons by a remote-controlled overhead crane which is separated from the caissons, Figure 2-18. After emplacement of the waste packages, prefabricated concrete elements are placed on top of the caissons to provide radiation shielding during the operational period.

### 2.7.4 Closure of 2BMA

At closure, corrugated steel sheets which will serve as one part of the gas evacuation system are placed on top of the prefabricated concrete elements. This is followed by casting of the concrete lid, which is provided with holes filled with a permeable material for efficient gas transport.

Installations and equipment in the vault are then removed and the vault is backfilled with macadam. Finally, plugs are installed to hydraulically separate the waste vault from the other parts of the repository in order to limit groundwater flow along the waste vault.

Figure 2-22 shows a schematic illustration of 2BMA post-closure. The closure plan for SFR (Mårtensson et al. 2022) describes the planned measures for closure of 2BMA in more detail.

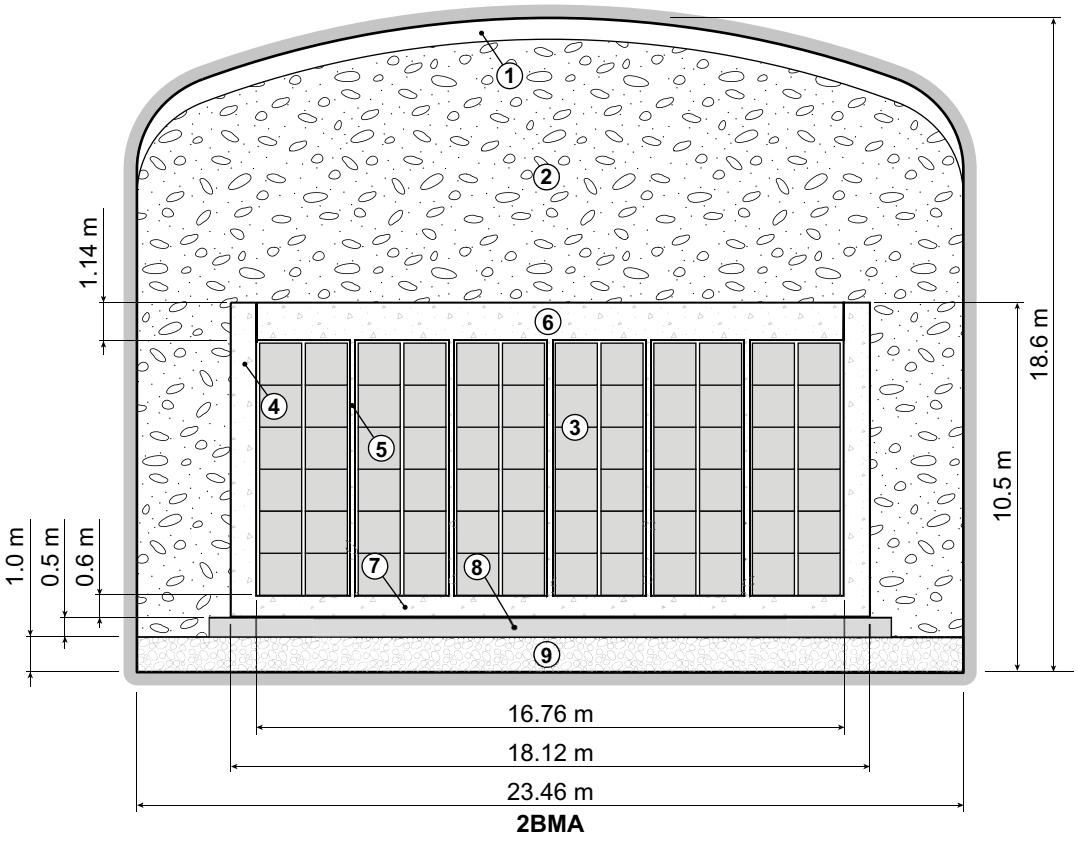


***Figure 2-22.*** *Schematic cross-section of 2BMA post-closure. Key to numbering: 1) Void 2) Macadam backfill 3) Waste domain 4) Outer wall 5) Inner wall 6) Lid 7) Caisson slab 8) Slab 9) Crushed rock.*

### 2.7.5 Functions of the cementitious components in 2BMA

#### *Operational period, sealing and closure*

During the operational period, the main functions of the cementitious components in 2BMA are to enable transport and emplacement of the waste packages as well as to enclose the waste packages and provide radiation shielding.

Table 2-6 compiles the functions of the cementitious components of 2BMA which are related to the load-bearing capacity and risk for cracking and – in this work – identified significant loads experienced by each individual component during the operational period, sealing and closure. The identified loads form the basis for the assessment of the risk for cracking during these periods and in a following step the assessment of recommended hydraulic conductivity and diffusivity data presented in Table 6-3. See also the initial state report for PSAR (SKB TR-23-02, Section 6.2) for additional information.

**Table 2-6. Functions of the cementitious components in 2BMA and identified significant loads during the operational period, sealing and closure.**

| Cementitious component | Function | Origin of significant load |
|---|---|---|
| **Reinforced concrete slab** | Enable construction and provide a stable base for the caissons. | Weight of the concrete caissons, waste packages and backfill material. |
| **Slabs** | Provide mechanical support to the outer and inner walls and waste packages. | Weight of the concrete caisson and waste packages. |
| **Outer walls** | Provide radiation shielding and carry the load from the prefabricated concrete elements. | The outer walls of the concrete caissons do not experience any loads during the operational period. |
| **Lids** | No function: constructed at closure. | N/A |
| **Inner walls** | Provide mechanical support to the prefabricated concrete elements. | Weight of prefabricated concrete elements |
| **Prefabricated concrete elements** | Provide radiation shielding. | Weight of wet concrete during casting of the lid. |
| **Gas evacuation system** | No function: constructed at closure. | N/A |
| **Concrete moulds** | Enclose and enable handling of the waste packages. | Weight of stack of waste packages. |

#### *Post-closure*

Post-closure, the outer walls and lid constitute the main hydraulic barriers, limiting the groundwater flow through the waste but also other parts of the concrete structure and the concrete moulds contribute to this function. In addition, the concrete structures maintain the structural integrity of the whole structure against the load from the backfill and groundwater pressure during saturation post-closure.

Further, all the cementitious components (waste form, concrete moulds and concrete structures) have chemical barrier functions. The use of cementitious materials ensures good sorption properties for many radionuclides. Cementitious materials also set a high pH value, which limits corrosion of steel and gas production caused by microbial activity.

The gas evacuation system has a barrier function to allow gas transport at a low pressure. The gas evacuation system thus prevents a high gas pressure inside the concrete caisson and reduces the risk for cracking of the concrete caissons

Table 2-7 compiles the functions (not including the safety functions, see below) of the cementitious components in 2BMA which are related to the load-bearing capacity and risk for cracking and – in this work – identified significant loads experienced by each individual component post-closure. The identified loads form the basis for the assessment of the risk for cracking post-closure and in a following step the assessment of recommended hydraulic conductivity and diffusivity data presented in Chapter 9.

The safety functions and safety function indicators for the engineered barriers in 2BMA are compiled in Table 2-1. See also the post-closure safety report for PSAR (SKB TR-23-01, Section 4.4.3) for additional information.

**Table 2-7. Functions of the cementitious components in 2BMA and origin of the significant loads post-closure.**

| Cementitious component | Function | Origin of significant load |
|---|---|---|
| **Reinforced concrete slab** | Provide a stable base for the caissons. | Weight of the concrete caissons, waste packages and backfill material. |
| **Slabs** | Provide mechanical support to the outer and inner walls and waste packages. | Weight of the concrete caisson and waste packages. Groundwater pressure during saturation. |
| **Outer wall** | Provide support for the prefabricated concrete elements, lid and backfill material. | Groundwater pressure during saturation and weight of backfill material. |
| **Lids** | Carry the weight of the backfill material on top of the concrete caisson | Groundwater pressure during saturation and weight of backfill material. |
| **Inner walls** | Provide mechanical support to the prefabricated concrete elements. | Groundwater pressure during saturation and weight of lid and backfill material. |
| **Prefabricated concrete elements** | No function | Weight of lid and backfill material during later periods. |
| **Gas evacuation system** | Ensure that gas can be transported out of the concrete structure at a low pressure. | The load-bearing capacity of the gas evacuation system is insignificant and therefore disregarded. |
| **Concrete moulds** | Enclose the waste. | Weight of lid and backfill material during later periods. Internal pressure from swelling of waste and gas*. |

* It should be noted that most of the potentially swelling waste are disposed in steel moulds or steel drums and not in concrete moulds.

## 2.8 1BRT, vault for reactor pressure vessels

### 2.8.1 Overview

The vault for reactor pressure vessels, 1BRT, will have the dimensions 17.3 m × 15.2 m × 255 m (w × h × l) (SKB TR-23-02). The walls and roof of the waste vault will be lined with shotcrete and rock bolts will be used to further reduce the risk of rock fall-out.

In 1BRT, a concrete structure will be cast on a bed of crushed rock in which the waste packages will be emplaced. The parts of the concrete structure farthest from the reloading zone will be divided into a number of compartments by inner walls whereas the part nearest to the reloading zone will be without inner walls and used for emplacement of waste with non-standard dimensions, Figure 2-23.

According to present plans, slab and walls will be cast separately using standard methods for construction of reinforced concrete structures. For that reason, the risk for formation of cracks in the concrete structure due to temperature shrinkage in the end of the cement hydration process cannot be neglected. It is also anticipated that tie rods will be used and left in the outer walls after dismantling of the formwork. The tie rods can be made of e.g. steel or glass fibres but no decision has yet been made. However, in order to avoid the formation of cracks or permeable zones around the tie rods due to corrosion of the tie rods, the use of the same type of concrete protective tubes as evaluated for 2BMA (Section 2.7.2) can be considered.

A waterproofing membrane will be installed in the roof and along the walls of the waste vault to collect and divert any intruding groundwater and prevent corrosion of the waste packaging and steel reinforcement during the operational period.

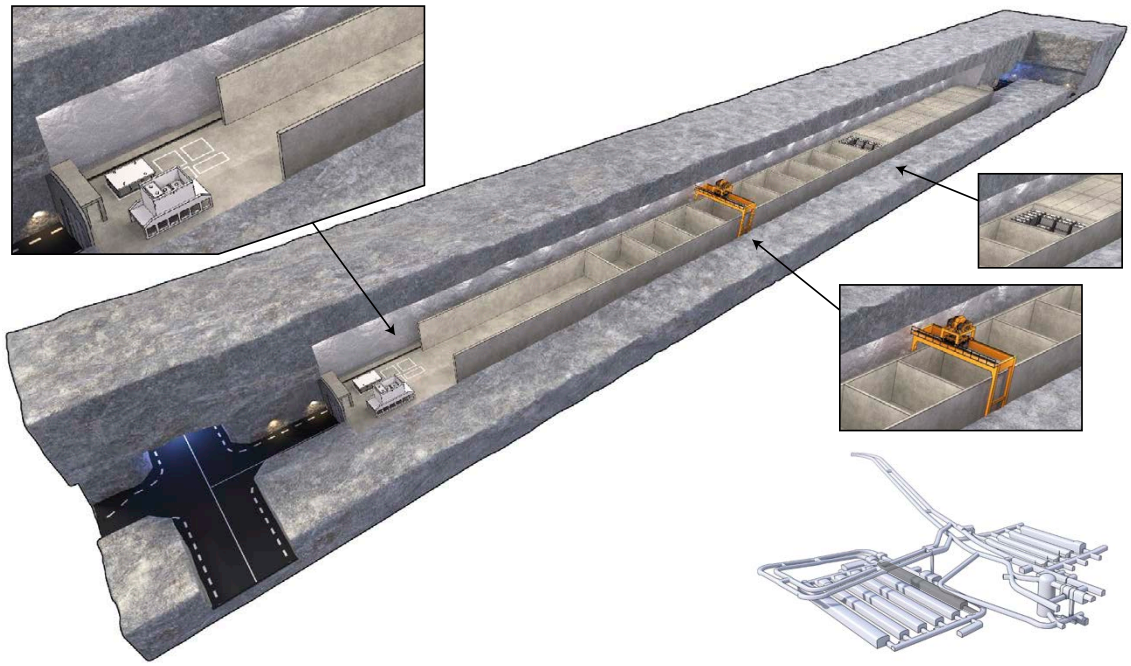

***Figure 2-23.*** *Illustration of 1BRT during the operational period. The lower detail shows SFR with the position of 1BRT in darker grey.*

### 2.8.2 Cementitious components in 1BRT

The cementitious components of 1BRT comprise the following components which are described in more detail below.

- Slab.
- Outer walls.
- Lid.
- Inner walls between waste compartments.
- Inner walls between waste packages.
- Prefabricated concrete elements.

#### *Slab*

The slab will be founded on a layer of crushed rock/macadam and have the dimensions 254.4 m × 12.3 m with a nominal thickness of about 700 mm, (SKB TR-23-02). Presumably the slab will be made from *2BMA concrete* (Section 3.3.3).

The slab will be constructed using standard methods for casting of slab on ground. Because the slab does not formally constitute a hydraulic barrier (SKB TR-23-10), no precautions to avoid the formation of cracks during casting have been prescribed. For that reason, it is expected that cracks will form in the slab due to temperature shrinkage towards the end of the cement hydration process.

#### *Outer walls*

The long outer walls of the concrete structure will presumably be made from reinforced *2BMA concrete* or similar and have the dimensions 224 m × 5.7 m (l × h). The short walls facing the reloading zone at tunnel 2BST and the inner zone at tunnel 2TT (see Figure 2-2) will each be 11.5 meters long. All walls will have a thickness of 500 mm (SKB TR-23-02) and standard methods for casting of reinforced concrete walls will be used.

As the walls do not formally constitute a hydraulic barrier (Table 2-1), tie rods can be used during construction. However, in order to improve the hydraulic properties of the concrete walls, the same type of concrete protective tubes as described for 2BMA (Section 2.7.2) can be used also here.

#### *Lid*

At closure, a 500 mm thick concrete lid (SKB TR-23-02) made from either *2BMA concrete* (Section 3.3.3) or *1BRT self-compacting concrete* (Section 3.3.5) will be cast. The use of reinforcement in this lid or not has yet to be decided upon. As the lid will rest upon the waste packages and inner walls, tensile stresses due to external loads are not expected and the use of reinforcement therefore not required.

#### *Inner walls between waste compartments*

The inner walls between the waste compartments – lateral dimensions 10.5 m × 10.5 m and a height of 5.2 m – will have a thickness of 500 mm (SKB TR-23-02) and be made from reinforced *2BMA concrete* (Section 3.3.3) or similar.

Construction of the inner walls can be done using standard methods for casting of reinforced concrete walls. For that reason, some cracks may form in the walls during construction, the width of which is dependent on the amount of reinforcement used. Also, tie rods are expected to remain in the inner walls after dismantling of the formwork.

#### *Inner walls between waste packages*

The inner walls between the waste packages will be constructed once the compartments have been filled with waste through filling of the space between the waste packages with *1BRT self-compacting concrete* (Section 3.3.5). The waste packages in the inner part of the concrete structure are placed with a spacing of about 200 mm in order to ensure sufficient thickness and load-bearing capacity of the inner walls between the waste packages (Pettersson 2017).

At present, the use of reinforcement bars is not planned for use in the inner walls between the waste packages. However, as the final mixing proportions of the *1BRT self-compacting concrete* has not been decided, the option of using reinforcing fibres is still open.

#### *Prefabricated concrete elements*

After emplacement of the waste packages, the compartments are covered with prefabricated concrete elements for radiation shielding.

Due to possible uncertainties regarding contamination of the prefabricated elements, the most feasible solution is to leave them in their current position when casting the main lid at closure. Even though the fate of these elements is not discussed in the closure plan for SFR (Mårtensson et al. 2022) and Figure 2-24 indicates that they will be removed, this report assumes that these elements will be re-placed after casting of inner walls between the waste packages.

### 2.8.3 Activities in 1BRT during the operational period

#### *Disposal of waste packages*

During the operational period, waste packages will be placed in the inner compartments by means of an overhead crane. Waste packages with non-standard dimensions will be placed in the outer parts by means of a suitable lifting and transport device. The waste packages in the inner parts are emplaced with a spacing of about 200 mm (Pettersson 2017) in order to ensure sufficient thickness and load-bearing capacity of the inner walls between the waste packages.

#### *Casting of inner walls between the waste packages*

Casting of the inner walls between the waste packages in the compartments farthest to the reloading zone, (nominal thickness 200 mm, (Pettersson 2017)) is done through filling the slits between the waste packages with *1BRT self-compacting concrete* either successively during the operational period or at closure. *1BRT self-compacting concrete* (Section 3.3.5) is used because the presence of radioactive waste restricts the presence of staff for concrete poking during casting. The inner walls will provide additional support for the external concrete structure by creating an internal concrete monolith.

### 2.8.4 Closure of 1BRT

In the case grouting of the waste packages has not been done during the operational period, this is done at closure.

A concrete lid is cast on top of the grouted waste packages and prefabricated concrete elements. During this work, standard methods for casting of concrete slabs can be used. This is because the lid does not formally constitute a hydraulic barrier (see Table 2-1) and there are therefore currently no restrictions on the number and width of the cracks formed in the lid.

It must be noted that the number and width of cracks formed in a concrete structure are dependent on the amount and distribution of the reinforcement but also on the adhesion between different construction parts. For the lid in 1BRT, a strong adhesion between the lid and the prefabricated elements is expected and the width of the cracks in the lid will therefore be restricted even if reinforcement is not used. From the investigation of 1BMA by Elfwing et al. (2015), a reasonable estimate is that then maximum width of any cracks formed in the lid is unlikely to exceed 0.5 mm.

Casting of the lid is followed by filling of the space around and above the concrete structure with crushed rock backfill material. Concrete plugs are finally installed at the ends towards the waste vault tunnel (2BST) and the transverse tunnel (2TT) to prevent transport of groundwater along the axis of the waste vault, Figure 2-2.

Figure 2-24 shows a schematic illustration of 1BRT post-closure. The closure plan for SFR (Mårtensson et al. 2022) describes the planned measures for closure of 1BRT in more detail.

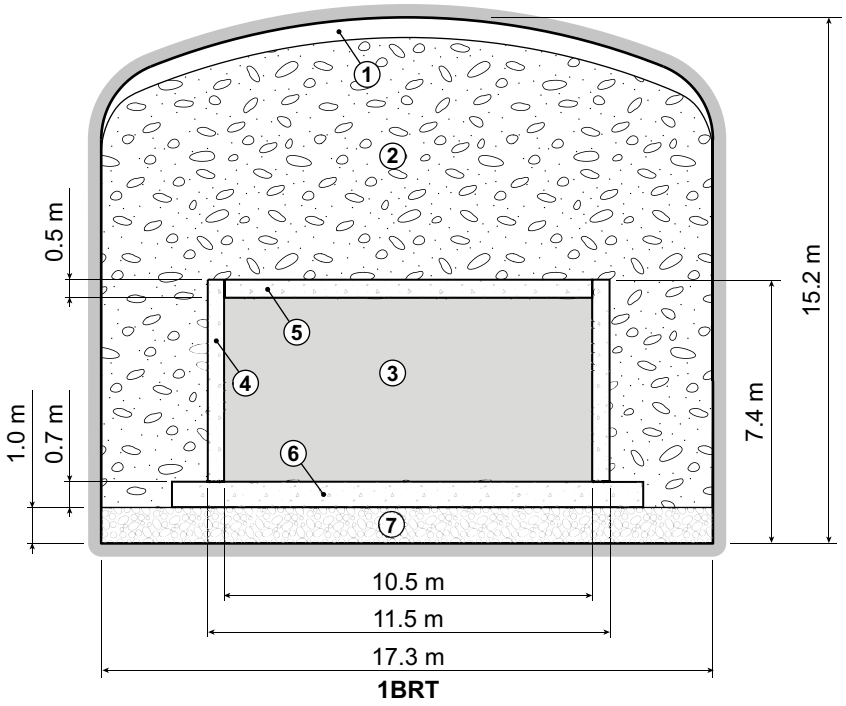


***Figure 2-24.*** *Schematic cross-section of 1BRT post-closure. Key to numbering: 1) Void 2) Macadam backfill 3) Waste domain 4) Outer wall 5) Lid 6) Slab 7) Crushed rock.*

### 2.8.5 Functions of the cementitious components in 1BRT

#### *Operational period, sealing and closure*

During the operational period, the main functions of the cementitious components in 1BRT are to enable transport and emplacement of the waste packages as well as to enclose the waste packages and provide radiation shielding.

Table 2-8 compiles the functions of the cementitious components of 1BRT which are related to the load-bearing capacity and risk for cracking and – in this work – identified significant loads experienced by each individual component during the operational period, sealing and closure. The identified loads form the basis for the assessment of the risk for cracking during these periods and in a following step the assessment of recommended hydraulic conductivity and diffusivity data presented in Table 6-4. See also the initial state report for PSAR (SKB TR-23-02, Section 7.2) for additional information.

**Table 2-8. Functions of the cementitious components in 1BRT and identified significant loads during the operational period, sealing and closure.**

| Cementitious component | Function | Origin of significant load |
|---|---|---|
| **Slab** | Enable transport and emplacement of the waste packages. | Weight of stack of waste packages, inner walls and prefabricated concrete elements. Dynamic load from moving transport vehicle during transport of waste |
| **Outer walls** | Enclose the waste packages and provide radiation shielding. | Pressure from wet concrete during construction of inner walls between the waste packages |
| **Lid** | No function: constructed at closure. | N/A |
| **Inner walls between waste compartments** | Enable emplacement and grouting of the waste packages and provide radiation shielding. | Pressure from wet concrete during construction of inner walls between the waste packages, weight of prefabricated concrete elements |
| **Inner walls between waste packages** | No function: constructed at closure. | Possibly weight of prefabricated concrete elements or no loads. |
| **Prefabricated concrete elements** | Provide radiation shielding. | Weight of wet concrete during casting of the lid. |

#### *Post-closure*

All cementitious components (waste form and concrete structures) have chemical barrier functions. The use of cementitious materials set a high pH which limits corrosion of steel and thus the release of induced radioactivity. Further, a high pH also limits gas production through microbial activity and ensures good sorption properties for many radionuclides, thus limiting their release.

The concrete structures contribute to limit the groundwater flow through the waste. In addition, the concrete structures maintain the structural integrity of the whole structure against the load from the backfill and groundwater pressure during saturation at repository closure.

Table 2-9 compiles the functions (not including the safety functions, see below) of the cementitious components in 1BRT which are related to the load-bearing capacity and risk for cracking and – in this work – identified significant loads experienced by each individual component post-closure. The identified loads form the basis for the assessment of the risk for cracking post-closure and in a following step the assessment of recommended hydraulic conductivity and diffusivity data presented in Chapter 10.

The safety functions and safety function indicators for the engineered barriers in 1BRT are compiled in Table 2-1. See also the post-closure safety report for PSAR (SKB TR-23-01, Section 4.4.4) for additional information.

**Table 2-9. Functions of the cementitious components in 1BRT and origin of the significant loads post-closure.**

| Cementitious component | Function | Origin of significant load |
|---|---|---|
| **Slab** | Provide a stable foundation for the waste packages and concrete structure | Groundwater pressure during saturation and weight from waste packages, concrete structure and backfill material after saturation. |
| **Outer walls** | Provide support for the prefabricated concrete elements, lid and backfill material. | Groundwater pressure during saturation and weight of backfill material and lid. |
| **Lid** | Carry the weight of the backfill material on top of the concrete caisson | Groundwater pressure during saturation and later only weight of backfill material. |
| **Inner walls between waste compartments** | Carry the weight of the lid and backfill material on top of the concrete structure during later periods | Pressure from the outer walls, lid and backfill material during saturation. Later, weight of lid, outer walls and backfill material. |
| **Inner walls between waste packages** | Provide mechanical support to the prefabricated concrete elements. | Groundwater pressure during saturation and weight of lid and backfill material. Internal pressure from swelling waste and gas. |
| **Prefabricated concrete elements** | No function | Weight of lid and backfill material during later periods. |

## 2.9 1BTF and 2BTF, vaults for concrete tanks

### 2.9.1 Overview

The two waste vaults for concrete tanks, 1BTF and 2BTF, each have the dimensions 14.7 m × 160 m × 9.5 m (w × l × h) (SKB TR-23-02). The walls and roof of the vaults are lined with shotcrete and rock bolts are used for additional protection against rock fall-out.

The concrete slabs rest on a draining foundation of crushed rock and are surrounded by a one meter high skirting along the rock wall. On the skirting, a number of concrete pillars are constructed to enable the planned backfilling of the vaults at closure; see detail in the lower right part of Figures 2-25 and 2-26.

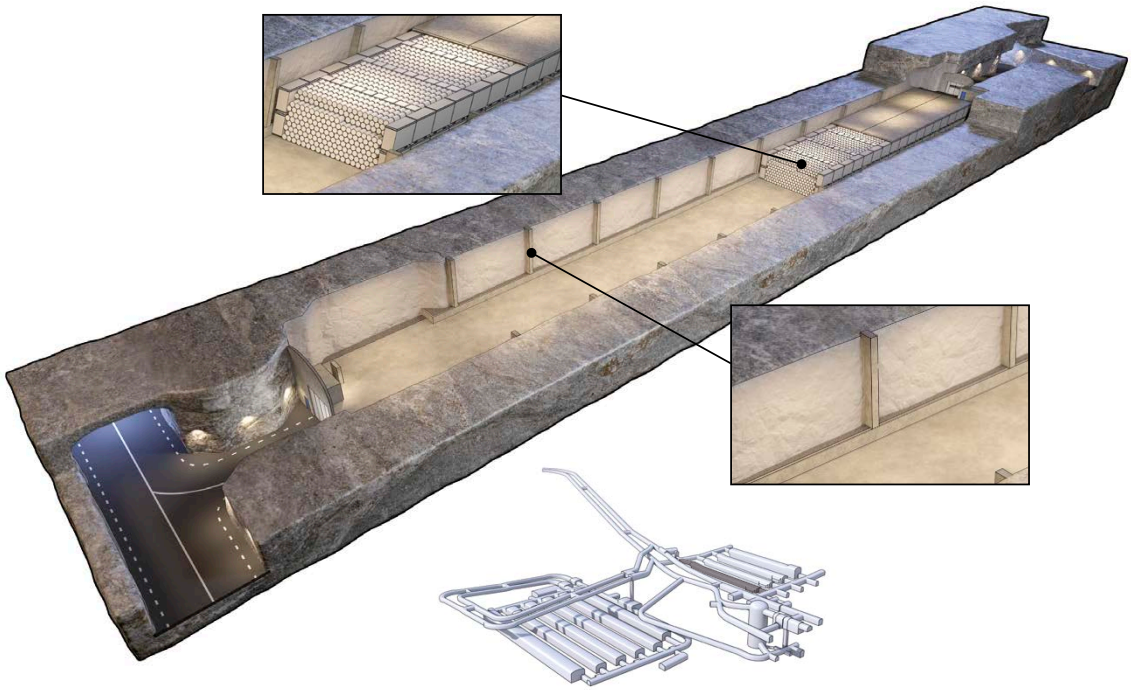

***Figure 2-25.*** *Illustration of 1BTF during the operational period. The upper detail shows the emplacement of ash-filled drums, the lower detail shows the skirting and concrete pillars. In addition, there is a view of SFR with the position of 1BTF in darker grey.*

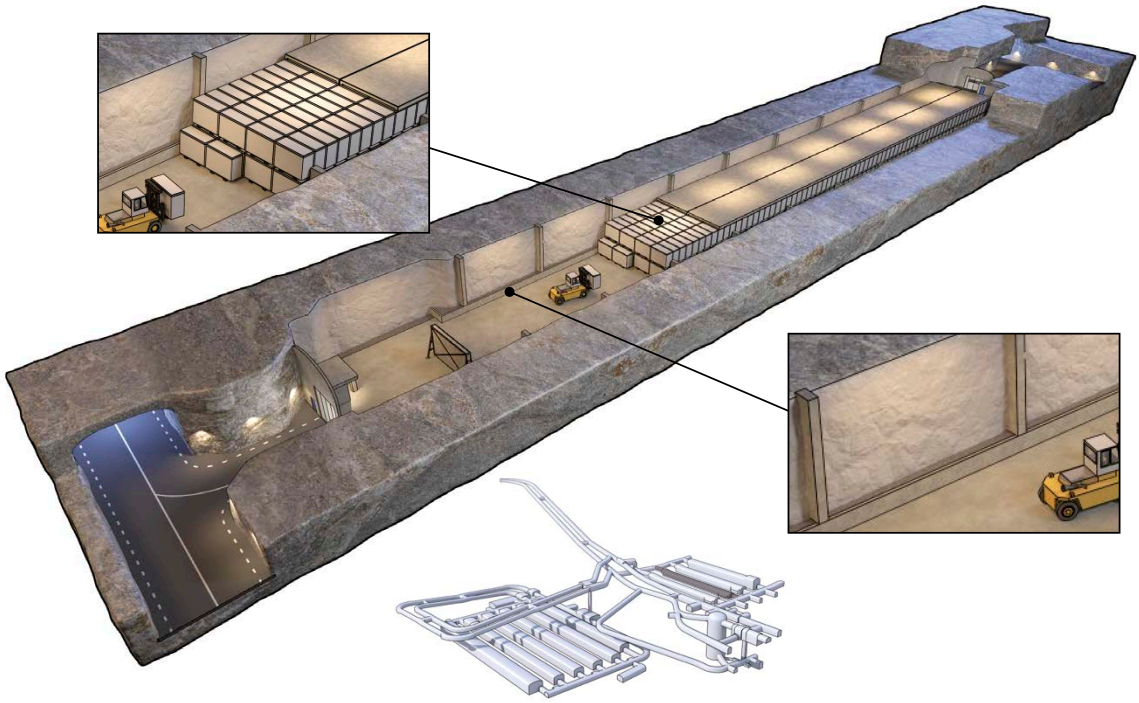

***Figure 2-26.*** *Illustration of 2BTF during the operational period. The upper detail shows the emplacement of concrete tanks, the lower detail shows the skirting and concrete pillars. In addition, there is a view of SFR with the position of 2BTF in darker grey.*

### 2.9.2 Cementitious components in 1–2BTF

The cementitious components of 1–2BTF comprise the following components which are described in more detail below.

- Slabs.
- Lids.
- Prefabricated concrete elements.
- Grout between waste packages.
- Cementitious backfill.
- Concrete tanks.
- Concrete moulds.

#### *Slabs*

The slabs in 1–2BTF each have the dimensions 160 m × 14.6 m × 0.25 m and are founded on a 450 mm thick layer of crushed rock (SKB TR-23-02). No documentation concerning the mixing proportions of the concrete used in these slabs has been found. For that reason, it is assumed that *1BMA concrete* (Section 3.3.2) was used also here.

#### *Lids*

At closure, a reinforced concrete lid will be cast on top of the prefabricated concrete elements that rests on top of the concrete tanks and the cementitious backfill covering the steel drums. The final dimensions of the lid have not yet been decided even though Figure 2-29 suggests a thickness of 400 mm. Presumably *BTF backfill concrete* (Section 3.3.8) will be used but also *2BMA concrete* can be used.

### *Prefabricated concrete elements*

In order to provide radiation shielding during the operational period and protect the concrete tanks from intruding groundwater, prefabricated concrete elements are placed on top of the concrete tanks. The thickness of the concrete elements is 400 mm, Figure 2-29. The length of the elements corresponds to half of the waste emplacement zones and the elements are somewhat inclined to allow for any water to be drained towards the sides of the waste vault. The concrete elements are made locally using standard concrete from a local production plant. The mixing proportions have varied over the years but the most recent elements were made from concrete based on *Anläggningscement Slite Standard P*. Presumably, the properties of the concrete for these elements resemble those of the *1BMA concrete*, Section 3.3.2.

### *Grout between waste packages*

During the operational period, the steel drums are grouted with *BTF grout* (Section 3.4.3) in order to stabilise the stack of drums. As shown in Figure 2-28, the distance between the steel drums is small which means that only a small amount of grout surrounds each drum.

At closure of 1–2BTF, also the concrete tanks will be grouted using *BTF grout.* The horizontal distance between the concrete tanks is estimated to between 10 and 100 mm whereas the vertical distance is 200 mm as determined by the height of the steel pallets on which the tanks are placed.

As a consequence of the methods used for grouting of the waste packages, it is uncertain if the voids between the waste packages – and in particular between the steel drums – is entirely filled with grout. The most likely scenario is that there will remain some voids which have not been filled but the number, distribution and dimensions of these voids are difficult to estimate. However, as no controls aimed at checking the degree of filling are carried out during or after grouting, this remains uncertain.

### *Cementitious backfill*

The cementitious backfill constitutes the section between the stack of waste packages and the rock wall which at closure is filled with *BTF backfill concrete* (Section 3.3.8). As shown in Figure 2-29, the width of this section is 500 mm whereas the height corresponds to that of the stack of waste packages and the prefabricated concrete elements, i.e. about 5 meters in all.

### *Concrete tanks*

The concrete tanks (Figure 2-27, left image) are made from reinforced *BTF tank concrete* (Section 3.3.6) and have the dimensions 1.3 m × 3.3 m × 2.3 m (w × l × h) with thickness of walls and bottom of 150 mm (SKB R-18-07). The lid, which is also made from reinforced *BTF tank concrete,* has a thickness of 150 mm and is bolted to the body of the concrete tank by means of eight steel bolts. In the lid, a steel hatch (Figure 2-27, right image) seals a 600 mm × 600 mm large opening which is used during filling of the tank with ion-exchange resins. Between the steel hatch and the steel frame in the lid of the concrete tank, a 10 mm thick rubber seal is placed. The steel hatch is secured by means of three sprints also shown in Figure 2-27.

All parts of the concrete tanks are painted with a water-repellent epoxy paint. The joint between the lid and the body of the concrete tank is sealed with a combination of different materials. According to information from the manufacturer, the tightness of the tanks is controlled by means of vacuum testing prior to shipment.

### *Concrete moulds*

Concrete moulds with waste are emplaced in 1BTF to provide support for the steel drums and the level of radioactivity in these moulds is low (SKB R-18-07). No concrete moulds are emplaced in 2BTF. The concrete moulds are of the same type as those in the silo (see Section 2.5.2 for details) but moulds with thick walls (above 100 mm) are not emplaced in 1BTF.

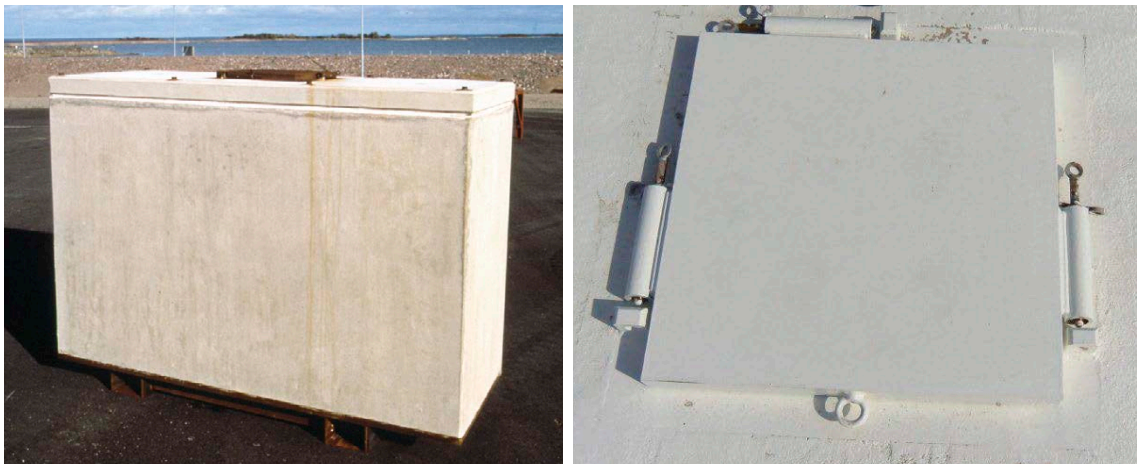

***Figure 2-27.*** *A concrete tank (left) and a close-up of the steel hatch in the lid used for filling of the tanks with ion-exchange resins.*

### 2.9.3 Activities in 1–2BTF during the operational period

#### *Disposal and grouting of steel drums*

In 1BTF, steel drums containing ashes have been disposed in the inner part of the waste vault. As shown in Figure 2-28 left image, the drums are supported by concrete tanks on each side of the stack. After disposal of a number of rows of steel drums, a wall made of concrete moulds is emplaced across the waste vault after which the steel drums are grouted with *BTF-grout*.

#### *Disposal of concrete tanks*

In 2BTF and in the outer part of 1BTF, concrete tanks containing dewatered ion-exchange resins are emplaced (4 abreast and 2 in height) by means of a forklift truck. After emplacement, prefabricated concrete elements are placed on top of the tanks for radiation shielding and to protect the concrete tanks from groundwater dripping from the roof of the rock vault, Figure 2-28 right image. As a further means of protection of the concrete tanks, the joints between the prefabricated concrete elements are covered with steel sheets. The concrete tanks are not grouted during the operational period.

***Figure 2-28.*** *1BTF (left) and 2BTF (right) during the operational period.*

### 2.9.4 Closure of 1–2BTF

At closure, the gap between the concrete tanks and rock walls in 1–2BTF are filled with *BTF backfill concrete*, Section 3.3.8. This is followed by grouting of the voids between the concrete tanks with *BTF grout* and casting of a reinforced concrete lid on top of the prefabricated concrete elements.

It should be noted that the current version of the closure plan for SFR (Mårtensson et al. 2022) does not include a cementitious backfill on the short-sides of the stacks of waste packages in 1–2BTF, i.e. towards the reloading zones and the inner zones towards the transverse tunnel. However, in this report, cementitious backfilling is assumed also in these parts.

As a final step, the spaces above the concrete lids are filled with crushed rock backfill and plugs are installed in the entrance tunnels in order to seal of the vaults from the adjacent parts of the repository, see Figure 2.2.

Figure 2-29 shows a schematic illustration of 1BTF and 2BTF post-closure. The closure plan for SFR (Mårtensson et al. 2022) describes the planned measures for closure of 1–2BTF in more detail.

### 2.9.5 Functions of the cementitious components in 1–2BTF

#### *Operational period, sealing and closure*

During the operational period, the main functions of the cementitious components in 1–2BTF are to enable transport and emplacement of the waste packages as well as to provide radiation shielding.

Table 2-10 compiles the functions of the cementitious components of 1–2BTF which are related to the load-bearing capacity and risk for cracking and – in this work -identified significant loads experienced by each individual component during the operational period, sealing and closure. The identified loads form the basis for the assessment of the risk for cracking during these periods and in a following step the assessment of recommended hydraulic conductivity and diffusivity data presented in Table 6-5. See also the initial state report for PSAR (SKB TR-23-02, Section 8.2) for additional information.

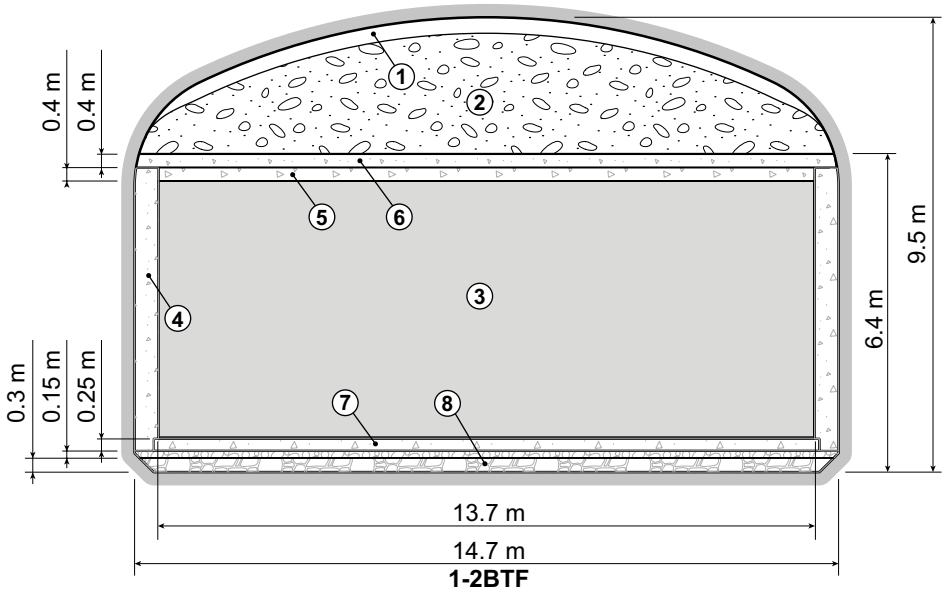


***Figure 2-29.*** *Schematic cross-section of 1BTF and 2BTF post-closure. Key to numbering: 1) Void 2) Macadam backfill 3) Waste domain 4) Cementitious backfill 5) Pre-fabricated concrete elements 6) Cast concrete lid 7) Slab 8) Crushed rock (0.3 m + 0.15 m).*

**Table 2-10. Functions of the cementitious components in 1–2BTF and identified significant loads during the operational period, sealing and closure.**

| Cementitious component | Function | Origin of significant load |
|---|---|---|
| **Slabs** | Enable transport and emplacement of the waste packages. | Dynamic load from forklift truck with waste packages during transport and weight of the stack of waste packages and prefabricated concrete elements. |
| **Lids** | No function: constructed at closure. | N/A |
| **Prefabricated concrete elements** | Provide radiation shielding and protect the concrete tanks from intruding groundwater. | Weight of wet concrete during casting of lid. |
| **Grout between waste packages** | Stabilise the stack of steel drums. Concrete tanks are grouted at closure. | The grout between the waste packages does not experience any loads during this period. |
| **Cementitious backfill** | No function: constructed at closure. | N/A |
| **Concrete tanks** | Enclose and enable handling of the waste. Provide mechanical support for the prefabricated concrete elements. | Weight from upper tank and prefabricated concrete elements. Some tanks experience the pressure from the wet grout during grouting of the steel drums, Figure 2-28, left image. |
| **Concrete moulds** | Enclose and enable handling of the waste. Provide mechanical support for the prefabricated concrete elements and enable sequential grouting of the steel drums. | Pressure from wet grout during grouting of the steel drums. |

### *Post-closure*

For the concrete tank section, the concrete tanks are the main hydraulic barriers. For the sections containing the ash-filled drums, the concrete between inner and outer steel drums, the grout and the concrete packaging surrounding them contribute to limit the groundwater flow through the waste.

All the cementitious materials (waste form, waste packaging, grout, cementitious backfill and concrete structures) have chemical barrier functions. The use of cementitious materials ensures good sorption properties for many radionuclides. Cementitious materials also set a high pH value, which limits corrosion of steel and gas production caused by microbial activity.

Table 2-11 compiles the functions (not including the safety functions, see below) of the cementitious components in 1–2BTF which are related to the load-bearing capacity and risk for cracking and – in this work – identified significant loads experienced by each individual component post-closure. The identified loads form the basis for the assessment of the risk for cracking post-closure and in a following step the assessment of recommended hydraulic conductivity and diffusivity data presented in Chapter 11.

The safety functions and safety function indicators for the engineered barriers in 1–2BTF are compiled in Table 2-1. See also the post-closure safety report for PSAR (SKB TR-23-01, Section 4.4.5) for additional information.

**Table 2-11. Functions of the cementitious components in 1–2BTF and origin of the significant loads post-closure.**

| Cementitious component | Function | Origin of significant load |
|---|---|---|
| **Slabs** | Provide a stable foundation for the stack of waste packages. | Weight of stack of concrete tanks and moulds, later also from lid and backfill material. |
| **Lids** | Protect the waste packages from the weight of the backfill material. | Groundwater pressure during saturation. Later weight of backfill material. |
| **Prefabricated concrete elements** | No function. | Weight of lid and backfill material |
| **Grout between waste packages** | Stabilise the stack of waste packages. | The load-bearing capacity of the grout between the waste packages is insignificant and therefore not considered. |
| **Cementitious backfill** | Enclose and stabilise the stack of waste packages and provide support for the lid and the backfill material. | Groundwater pressure during saturation. Later weight of lid and backfill material. |
| **Concrete tanks** | Enclose the waste. Provide mechanical support for the prefabricated concrete elements. | Groundwater pressure during saturation. Later weight of concrete tank, lid and backfill material. |
| **Concrete moulds** | Enclose the waste. Provide mechanical support for the prefabricated concrete elements. | Groundwater pressure during saturation. Weight of stack of waste packages, lid and backfill material. |

## 2.10 1BLA, vault for low-level waste

### 2.10.1 Overview

The vault for low-level waste, 1BLA (Figure 2-30) has the dimensions 14.7 m × 160 m × 12.7 m (w × l × h) (SKB TR-23-02). The walls and roof are lined with shotcrete which in combination with the use of rock bolts reduces the risk for rock fall-out during the operational period. The vault has a reinforced concrete slab with a thickness of 250 mm on top of a draining layer of crushed rock. Up until 2021, the waste packages were protected from groundwater dripping from the roof of the rock vault by means corrugated steel sheets mounted in the roof of the waste vault as shown in Figure 2-31. In 2022, a waterproofing membrane was installed in the roof, replacing the corrugated steel sheets and providing the same function.

### 2.10.2 Cementitious components in 1BLA

The cementitious components of 1BLA comprise the following component which is described in more detail below.

- Slab.

#### *Slab*

The slab is founded on a draining layer of crushed rock and has the dimensions 160 m × 13.7 m × 0.25 m (SKB TR-23-02). It is assumed that *1BMA concrete* was used for casting the slab in 1BLA but no documentation that verifies this assumption has been found.

### 2.10.3 Activities in 1BLA during the operational period

During the operational period, ISO-containers containing short-lived, low-level radioactive waste are stacked (assuming 20-foot full-height containers) two abreast and three in height by means of a forklift truck, Figure 2-31. The image shows 1BLA prior to installation of the waterproofing membrane which was conducted in 2022.

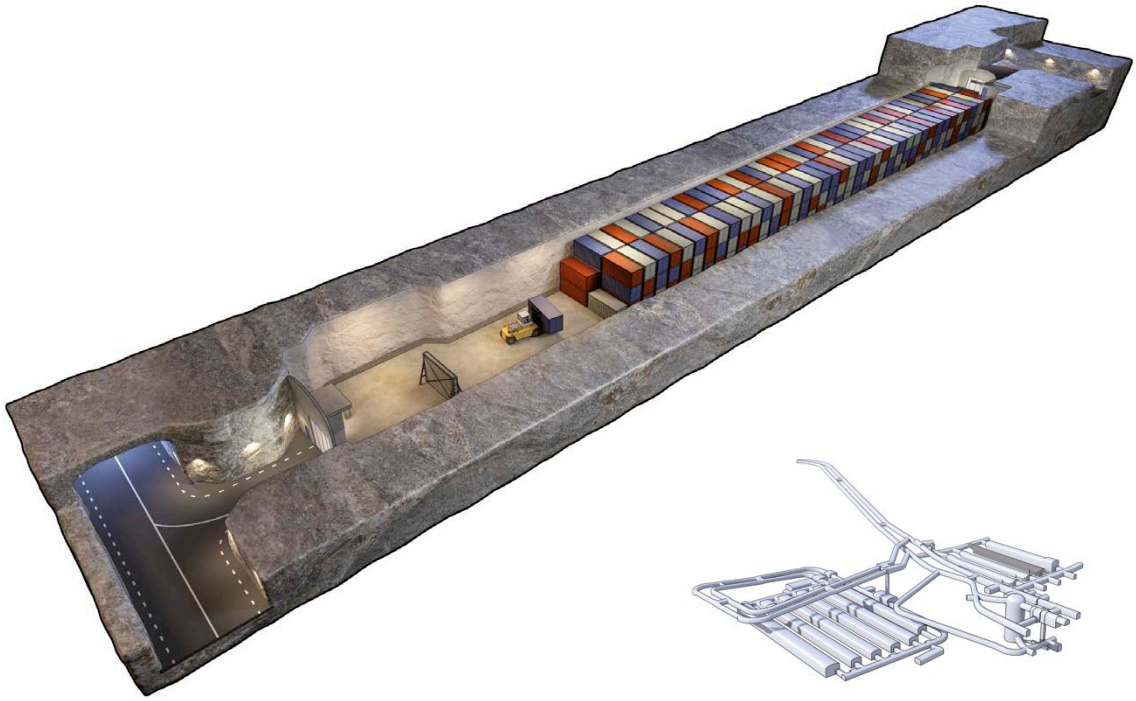

***Figure 2-30.*** *A schematic illustration of 1BLA during the operational period. The lower detail shows a view of SFR with the position of 1BLA in darker grey.*

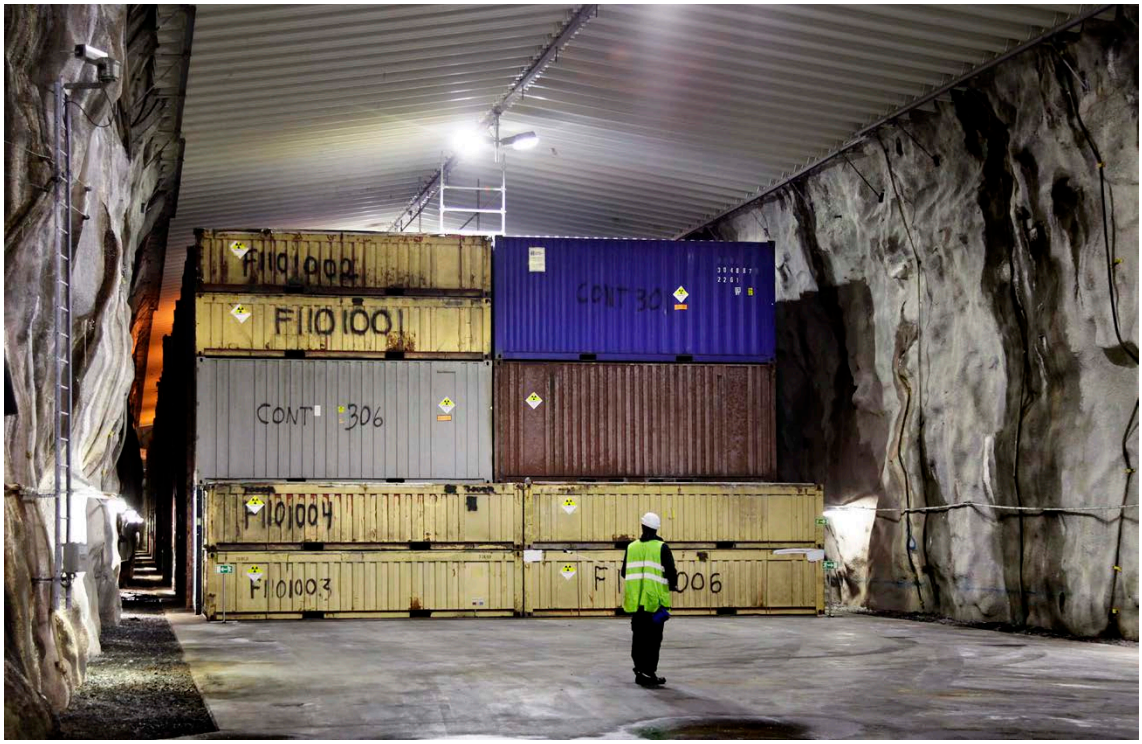


***Figure 2-31.*** *1BLA during the operational period.*

### 2.10.4 Closure of 1BLA

At closure, technical installations in the waste vault will be dismantled and plugs installed in the entrance tunnels between 1BLA and other parts of the repository in order to limit groundwater flow along the waste vault.

Figure 2-32 shows a schematic illustration of 1BLA post-closure. The closure plan for SFR (Mårtensson et al. 2022) describes the planned measures for closure of 1BLA in more detail.

### 2.10.5 Functions of the slab in 1BLA

#### *Operational period, sealing and closure*

During the operational period, the slab is used for transport and emplacement of ISO-containers.

Table 2-12 compiles the functions of the slab in 1BLA which are related to the load-bearing capacity and risk for cracking and – in this work – identified significant loads experienced by the slab during the operational period, sealing and closure. The identified loads form the basis for the assessment of the risk for cracking during these periods and in a following step the assessment of recommended hydraulic conductivity and diffusivity data presented in Table 6-6. See also the initial state report for PSAR (SKB TR-23-02, Section 9.2) for additional information.

**Table 2-12. Functions of the slab in 1BLA and identified significant loads during the operational period, sealing and closure.**

| Cementitious component | Function during the operational period | Dimensioning loads |
|---|---|---|
| Slab | Enable transport and emplacement of the ISO-containers. | Dynamic load from moving forklift truck with ISO-container and weight of stack of ISO-containers. |

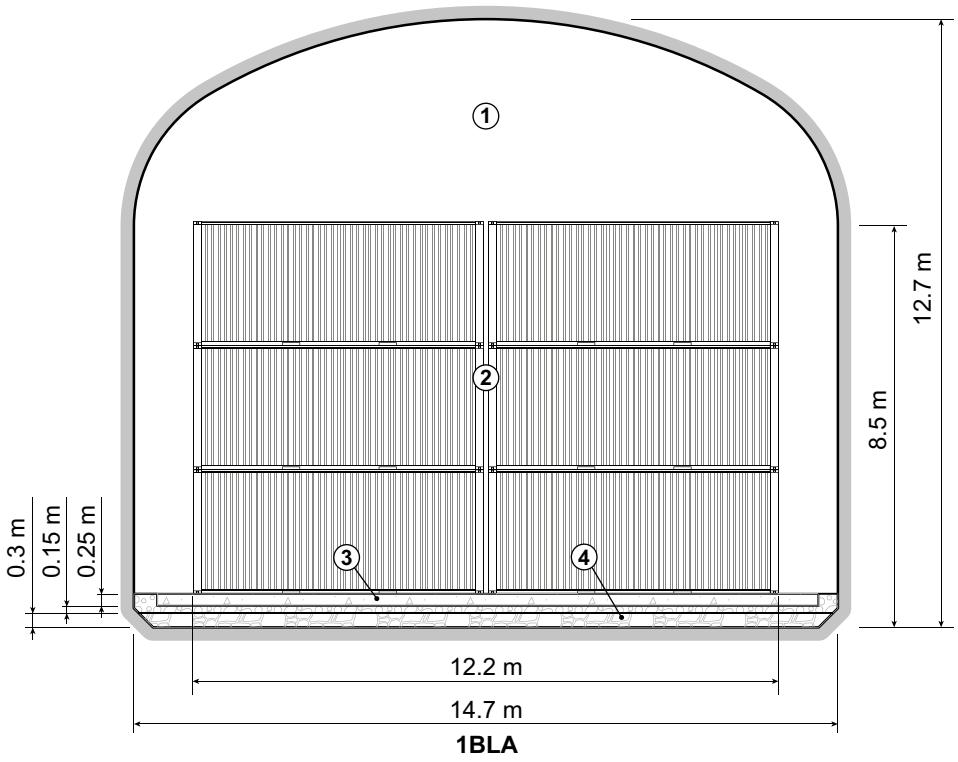


***Figure 2-32.*** *Schematic cross-section of 1BLA post-closure, exemplified with full-height containers. Key to numbering: 1) Void 2) Waste domain 3) Slab 4) Crushed rock.*

### *Post-closure*

The slab in 1BLA does not constitute a part of the engineered barrier system. Instead, the only function post-closure is to carry the load from the stack of ISO-containers.

Table 2-13 compiles the functions (not including the safety functions, see below) of the slab in 1BLA which are related to the load-bearing capacity and risk for cracking and – in this work – identified significant loads experienced by the slab post-closure. The identified loads form the basis for the assessment of the risk for cracking post-closure and in a following step the assessment of recommended hydraulic conductivity and diffusivity data presented in Chapter 12.

See also the post-closure safety report for PSAR (SKB TR-23-01, Section 4.4.6) for additional information.

**Table 2-13. Functions of the slab in 1BLA and origin of the significant loads post-closure.**

| Cementitious component | Function | Origin of significant load |
|---|---|---|
| **Slab** | Provide a stable foundation for the stack of ISO-containers. | Weight of stack of ISO-containers. |

## 2.11 2–5BLA vaults for low-level waste

### 2.11.1 Overview

The vaults for low-level waste, 2–5BLA, (Figure 2-33) will each have the dimensions 17.5 m × 275 m × 12.4 m (w × l × h) (SKB TR-23-02). The walls and roof will be lined with shotcrete which, in combination with the use of rock bolts, will reduce the risk for rock fall-out during the operational period. The vaults will all have a concrete slab on top of a draining foundation on which the waste packages (mainly ISO-containers) will be placed. A waterproofing membrane will be installed in the roof and along the walls of each of the 2–5BLA vaults to collect and divert any intruding groundwater and prevent corrosion of the waste packages during the operational period.

***Figure 2-33.*** *Illustration of 2–5BLA during the operational period. The lower detail shows a view of SFR with the position of the four waste vaults in darker grey.*

### 2.11.2 Cementitious components in 2–5BLA

The cementitious components of 2–5BLA comprise the following components which are described in more detail below.

- Slabs.

#### *Slabs*

The slabs in 2–5BLA will be founded on a layer of crushed rock and each have the dimensions 275 m × 15.9 m with a thickness of 400 mm. The slabs will presumably be made from *2BMA concrete* (Section 3.3.3) or similar but the mixing proportions of the concrete have not yet been decided.

### 2.11.3 Activities in 2–5BLA during the operational period

During the operational period, ISO-containers containing short-lived, low-level radioactive waste are stacked (assuming 20-foot half-height containers) two abreast and six in height by means of a forklift truck as illustrated in Figure 2-33.

### 2.11.4 Closure of 2–5BLA

At closure, technical installations in the waste vaults will be dismantled and plugs installed in the entrance tunnels between 2–5BLA and other parts of the repository to limit water flow along the waste vaults. Figure 2-34 shows a schematic illustration of 2–5BLA post-closure.

The closure plan for SFR (Mårtensson et al. 2022) describes the planned measures for closure of 2–5BLA in more detail.

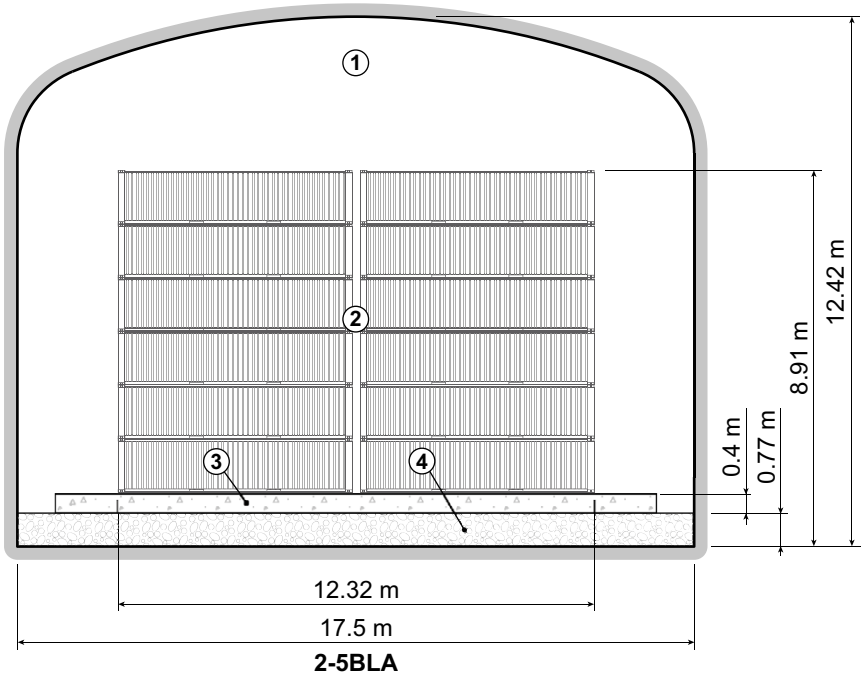


***Figure 2-34.*** *Schematic cross-section of 2–5BLA post-closure, exemplified with half-height containers. Key to numbering: 1) Void 2) Waste domain 3) Slab 4) Crushed rock.*

### 2.11.5 Functions of the slabs in 2–5BLA

#### *Operational period, sealing and closure*

During the operational period, the slabs are used for transport and emplacement of ISO-containers.

Table 2-14 compiles the functions of the slabs in 2–5BLA which are related to the load-bearing capacity and risk for cracking and – in this work – identified significant loads experienced by the slabs during the operational period, sealing and closure. The identified loads form the basis for the assessment of the risk for cracking during these periods and in a following step the assessment of recommended hydraulic conductivity and diffusivity data presented in Table 6-7. See also the initial state report for PSAR SKB TR-23-02, Section 10.2 for additional information.

**Table 2-14. Functions of the slabs in 2–5BLA and identified significant loads during the operational period, sealing and closure.**

| Cementitious component | Function | Origin of significant load |
|---|---|---|
| **Slabs** | Enable transport and emplacement of the ISO-containers. | Dynamic load from moving forklift truck with ISO-container and weight of stack of ISO-containers. |

#### *Post-closure*

The slabs in 2–5BLA do not constitute parts of the engineered barrier system. Instead, the only function post-closure is to carry the load from the stack of ISO-containers.

Table 2-15 compiles the functions (not including the safety functions, see below) of the slabs in 2–5BLA which are related to the load-bearing capacity and risk for cracking and – in this work – identified significant loads experienced by the slabs post-closure. The identified loads form the basis for the assessment of the risk for cracking post-closure and in a following step the assessment of recommended hydraulic conductivity and diffusivity data presented in Chapter 13.

See also the post-closure safety report for PSAR (SKB TR-23-01, Section 4.4.7) for additional information.

**Table 2-15. Functions of the slabs in 2–5BLA and identified significant loads post-closure.**

| Cementitious component | Function | Origin of significant load |
|---|---|---|
| **Slabs** | Provide a stable foundation for the stack of ISO-containers. | Weight of stack of ISO-containers. |

## 2.12 Plugs, other closure components and common cementitious components

### 2.12.1 Overview

At closure of the repository, plugs and other closure components will be installed in the waste vaults and tunnel system of SFR whereas sealing of boreholes can be done at any suitable point in time.

In Section 2.12.2, a brief description of the plugs used to seal the different parts of the repository will first be presented. This is followed by descriptions of the cementitious components of the plugs and other closure components and other cementitious components which are common for all waste vaults in SFR, Section 2.12.3.

### 2.12.2 Plugs

#### *Plugs to waste vaults (except the silo)*

A total of five plugs (P1TT, P1BTF, P1BST, P2TT and P2BST) will be installed to seal the waste vaults in SFR, see Figure 2-35. All plugs consist of a hydraulically tight bentonite section and at least two mechanical supports that hold the hydraulically tight bentonite section in place as illustrated in Figure 2-37. In all plugs except the plug for the waste vault tunnel in SFR1 (P1BST), the mechanical supports are made of concrete (concrete plug). Since the geometry of the tunnels make it unsuitable to install concrete plugs to isolate the bentonite section in P1BST, mechanical supports comprising a transition material are expected to be used instead.

#### *Plugs to silo*

Three plugs: lower silo plug (NSP), upper silo plug (ÖSP) and silo roof plug (STP) are installed to seal the silo, see Figure 2-36. As with the plugs to the waste vaults, these plugs comprise a central bentonite section which is sandwiched between two or several mechanical supports as shown in the schematic illustration in Figure 2-37.

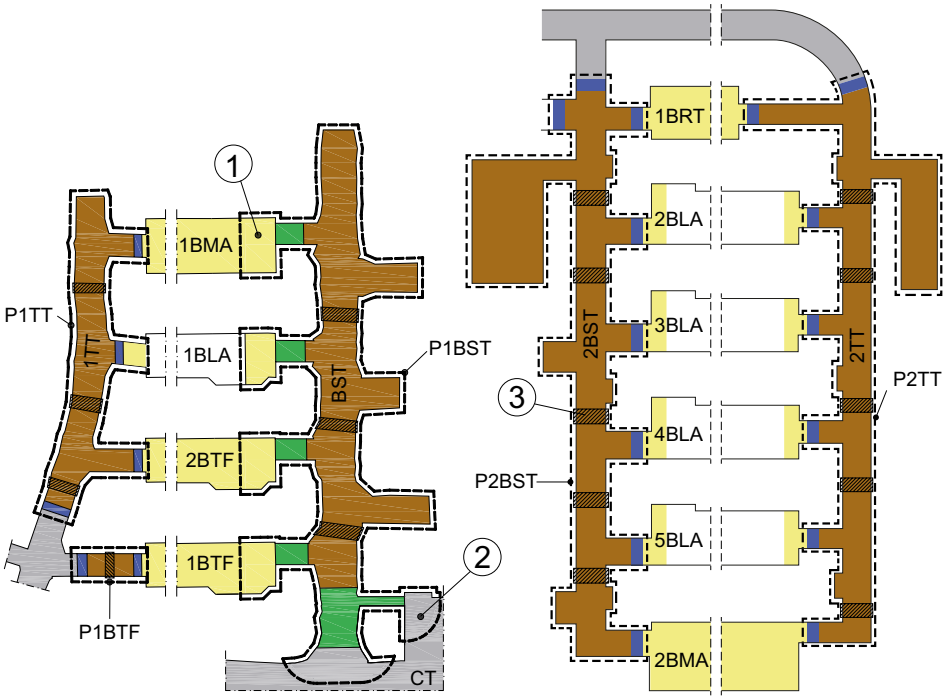


***Figure 2-35.*** *Plugs adjacent to waste vaults are marked with a dashed line. Key to numbering: 1) Yellow colour within borderline for plugs shows parts of backfill in rock that are active parts of the earth dam plug, green colour shows transition material and brown colour shows hydraulically tight material 2) Grey colour within borderline for plug shows parts of backfill in tunnel system that are active parts of the earth dam plug 3) Hatched areas indicate where damaged zone should be removed by controlled methods. Blue and green sections represent mechanical constraints made from concrete and a transition material respectively.*

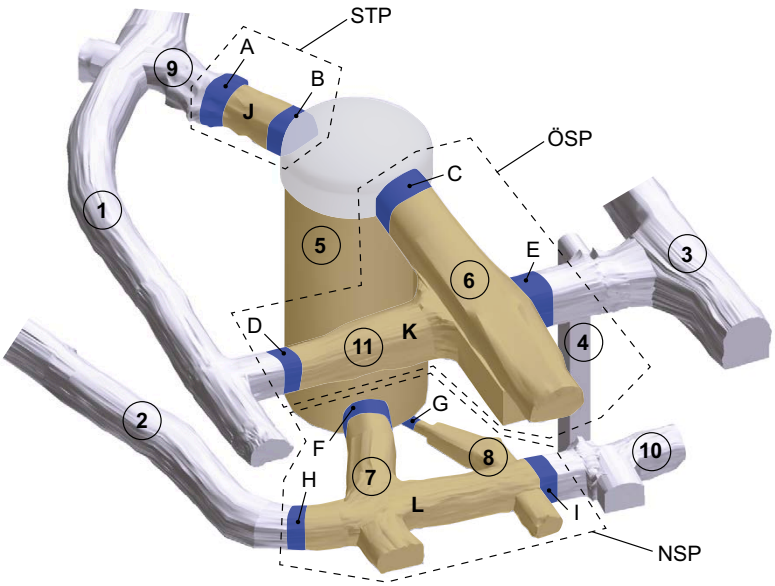


***Figure 2-36.*** *Illustration of closed silo with three plug sections (NSP, ÖSP and STP). Blue colour shows concrete plugs (A-I) and brown colour shows hydraulic tight sections (J, K, L). Key to numbering: 1) Construction tunnel, BT 2) Lower construction tunnel, NBT 3) Central tunnel, CT 4) Connecting shaft, 5) Silo, 6) Loading-in building, IB 7) Silo bottom tunnel, 8) Drainage tunnel, 9) Silo roof tunnel, 1STT, 10) Terminal part of lower construction tunnel, 11) Silo tunnel. Tunnel parts 1, 2, 3, 4 and 10 belong to the tunnel system.*

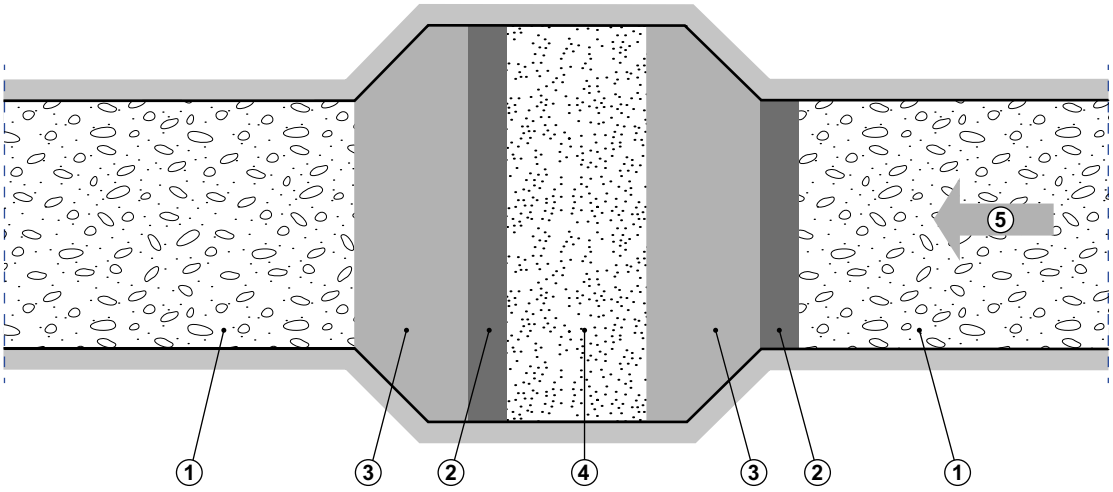


***Figure 2-37.*** *Schematic illustration of the reference design of a plug. Key to numbering: 1) Crushed rock backfill 2) Supporting wall 3) Concrete 4) Bentonite 5) Working direction.*

### *Plugs for access tunnels and tunnel system*

At closure, plugs will be installed in the access tunnels to minimise the water flow in these tunnels (see Figure 2-2). A schematic illustration of the reference design of the plugs in the tunnels is shown in Figure 2-37. The remaining part of the access tunnels and tunnel system will be backfilled with crushed rock backfill material with a high hydraulic conductivity.

### *Plugs for sealing of investigation boreholes*

The investigation boreholes that were included in the early investigations and those that intersect or are located very close to the underground facility have been or will be sealed prior to the start of construction of SFR3. The remaining investigation boreholes will be sealed when suitable.

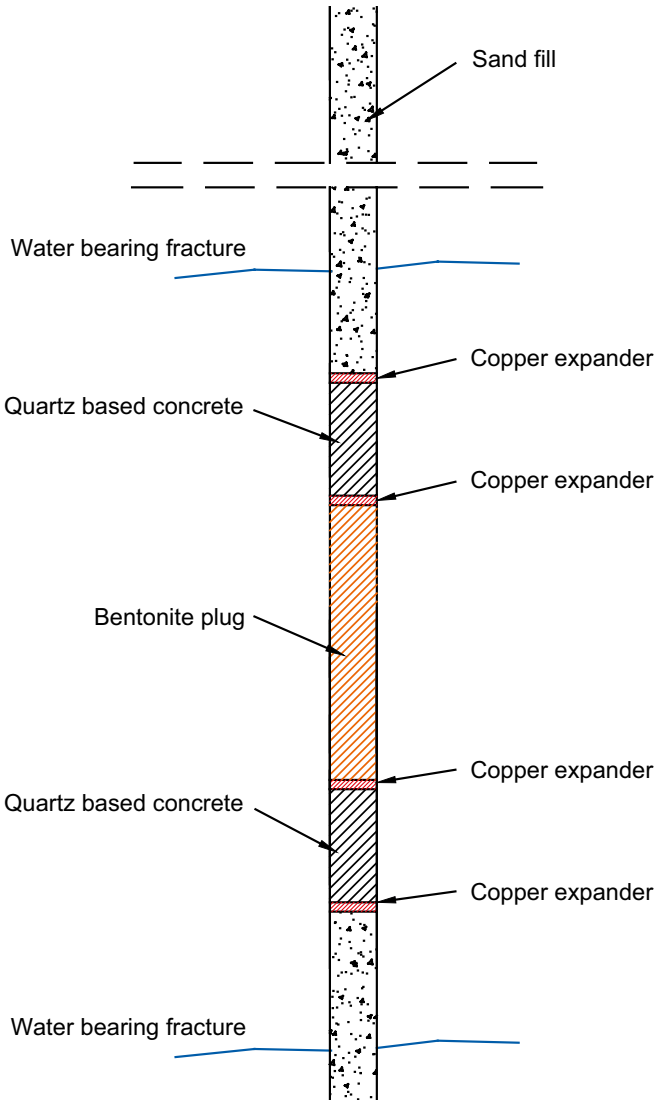


***Figure 2-38.*** *A representative section of a borehole including all types of sealing components (Sandén et al. 2018).*

The current reference design for sealing of investigation boreholes comprises a combination of various components such as sand-filled sections, hydraulically tight bentonite sections, concrete plugs and other components which will be utilised in different sections of the different boreholes depending on the hydraulic and mechanical properties of the surrounding bedrock as well as the distance to the repository. The current designs for borehole sealing are described by Johannesson et al. (SKBdoc 1550055 ver 2.0, internal document, in Swedish) and further information is provided by Sandén et al. (2017, 2018) and Pusch and Ramqvist (2004, 2007). An illustration of a representative section of a sealed borehole of class BHC3 is shown in Figure 2-38.

### 2.12.3 Cementitious components of the Plugs and other closure components and common cementitious components

The plugs and other closure components and common cementitious components comprise the following components which are described in more detail below.

- Concrete plugs in tunnels.
- Concrete plugs in boreholes.
- Shotcrete on the rock walls.
- Grout for rock bolts.
- Injection grout in the surrounding bedrock.

### *Concrete plugs in tunnels*

As indicated in Section 2.12.1, a number of plugs will be installed in the tunnel system at closure, most of which will comprise at least two concrete plugs made from *SFR plug concrete* (Section 3.3.10) or similar as mechanical supports.

As shown by Eriksson and Malm (2013) the volume of the largest of the unreinforced concrete plugs, which has a diameter of about 14 meters, will be about 400 $m^3$. However, as shown by Eriksson et al. (2012) also other design options with even larger concrete plugs have been considered. Regardless of design, the vast volumes of concrete will put strict requirements on the choice of concrete mixing proportions and construction method to avoid extensive temperature increase during construction.

As a means to reduce the volume of the concrete plugs, reinforcement can be used. A study by Enzell and Malm concerning plugs for closure of the repository for spent fuel showed that thickness of a concrete plug can be reduced from about 4.5 to 2.5 meters by the use of sufficient amounts of reinforcement.[11] At present, the dimensions, amount of reinforcement and concrete mixing proportions for the concrete plugs in SFR remain to be decided.

### *Concrete plugs in investigation boreholes*

Similar to the plugs in the tunnel system, concrete plugs in the boreholes are used as mechanical supports to enclose the hydraulically tight bentonite sections.[12] The volume of these plugs is very small with a maximum of a few tens or perhaps a hundred $dm^3$ depending on borehole diameter and length of the concrete plug.

Up until the year 2020, the intention was to use *SFR borehole concrete* (Section 3.3.11) for the concrete plugs in the boreholes. However, a production test in a water-filled borehole indicated an unexpected high risk for concrete separation (Mårtensson 2019). For that reason – and also considering other tests presented by Mårtensson (2019) – it was instead concluded that standard concrete for underwater casting is a more suitable choice in this application, Section 3.3.12.

### *Shotcrete on rock walls*

In SFR1, *SFR shotcrete* (Section 3.3.9) was used to prevent rock fall-out from the roof and walls of tunnels and waste vaults. In SFR3 a similar material based on currently available cement types and admixtures will be used instead. Measurements in both waste vaults and tunnels in SFR1 (Lundin 2011) showed that the thickness of the layer of shotcrete varied between 51–130 mm with a calculated mean value of 82 mm. This agrees with the information provided by Gaucher et al. (2005) also mentioned in Section 3.3.9.

Recent measurements in similar positions confirmed these findings.[13] For SFR3, the thickness of the layers of shotcrete is uncertain but according to SKB (TR-23-02, Appendix A) up to 300 mm thick layers can be foreseen.

### *Grout for rock bolts*

During construction of the facility, rock bolts secure the bedrock in order to prevent rock fall-out. The holes in which the rock bolts are installed are filled with *SFR grout for rock bolts* (Section 3.4.6) in order to secure the rock bolts and to create an environment that limits corrosion of the bolts.

### *Injection grout in the fractures in the surrounding bedrock*

During construction of the facility, the fractures in the surrounding bedrock are injected with *SFR injection grouts* (Section 3.4.5) in order to reduce the inflow of groundwater into the repository. The amount and properties of the various injection grouts are dependent on the structure of and groundwater flow in the fracture network.

---

[11] SKBdoc 1681017 ver 1.0. (Internal document)

[12] SKBdoc 1550055 ver 2.0. (Internal document, in Swedish.)

[13] SKBdoc 1991682 ver 0.1. (Internal document, in Swedish.)

### 2.12.4 Functions of the plugs, other closure components and common cementitious components

#### *Operational period, sealing and closure*

Table 2-16 compiles the functions of the plugs, other closure components and common cementitious components during the operational period, sealing and closure which are related to the load-bearing capacity and risk for cracking and – in this work – identified significant loads that each component experiences during these periods. The identified loads form the basis for the assessment of the risk for cracking during these periods and in a following step the assessment of recommended hydraulic conductivity and diffusivity data presented in Table 6-8. See also the initial state report for PSAR (SKB TR-23-02, Section 11.2) for additional information.

**Table 2-16. Functions of the plugs, other closure components and common cementitious components and identified significant loads during the operational period, sealing and closure.**

| Cementitious component | Function | Origin of significant load |
|---|---|---|
| **Concrete plugs in tunnels** | No function: constructed at closure. | N/A |
| **Concrete plugs in boreholes** | Enclose the bentonite sections | Bentonite swelling pressure and groundwater pressure. |
| **Shotcrete on rock walls** | Prevent rock fall-out | Weight of a large rock piece. |
| **Grout for rock bolts** | Prevent rock fall-out | Weight of a large rock piece. |
| **Injection grout in the surrounding bedrock** | Reduce groundwater inflow | Not relevant. The function of injection grouts is only to limit groundwater intrusion. |

#### *Post-closure*

Table 2-17 compiles the functions (not including the safety functions, see below) of the plugs and other closure components and other cementitious components in SFR which are related to the load-bearing capacity and risk for cracking and – in this work – identified significant loads experienced by each individual component post-closure. The identified loads form the basis for the assessment of the risk for cracking post-closure and in a following step the assessment of recommended hydraulic conductivity and diffusivity data presented in Chapter 14.

The safety functions and safety function indicators for the plugs and other closure components and other cementitious components in SFR are compiled in Table 2-1. See also the post-closure safety report for PSAR (SKB TR-23-01, Section 4.4.8) for additional information.

**Table 2-17. Functions of plugs, other closure components and common cementitious components and origin of the significant loads post-closure.**

| Cementitious component | Function | Origin of significant load |
|---|---|---|
| **Concrete plugs in tunnels** | Enclose the bentonite sections | Bentonite swelling pressure and groundwater pressure. |
| **Concrete plugs in boreholes** | Enclose the bentonite sections | Bentonite swelling pressure and groundwater pressure. |
| **Shotcrete on rock walls** | Prevent rock fall-out | Weight of a large rock piece. |
| **Grout for rock bolts** | Prevent rock fall-out | Weight of a large rock piece. |
| **Injection grout in the surrounding bedrock** | No function | Not relevant. The function of injection grouts is only to limit groundwater intrusion during the operational period. |

# 3 Cementitious materials in SFR

In SFR several different types of cementitious materials are used or will be used in the concrete structures as well as for grouting of waste packages and backfilling of waste vaults. Cementitious materials are also found in the injection grouts, shotcrete and grout for rock bolts.

The use of cementitious materials ensures the post-closure safety of the repository through their chemical, mechanical and transport properties. This is provided by the structural stability of the structures in the repository, the favourable chemical environment and the low hydraulic conductivity of these materials. In addition, the cementitious materials and the structures in which they are used provide radiation shielding as well as a safe and healthy working environment during the operational period.

In this chapter the mixing proportions of the different types of cementitious materials that have been used or are expected to be used in SFR are presented, thus providing detailed information on the properties of the different materials discussed in the following chapters.

The chapter begins with a description of the different cement types used and expected for future use in the various cementitious materials (Section 3.2). This is followed by descriptions of the various types of concretes (Section 3.3) and grouts (Section 3.4) used and expected for use. However, for several of the future materials, only indicative mixing proportions based on current understanding of the required properties are given. This is because the final mixing proportions of some of the materials aimed for use have not yet been decided.

This chapter also includes an introduction to the minerals and nomenclature involved in cement chemistry, Section 3.1. For an introduction to the cement reactions and basic cement chemistry, the reader is referred to standard textbooks on this subject.

## 3.1 Classification of cements

### 3.1.1 Cement nomenclature

Cementitious materials constitute a complex mixture of different cement minerals, amorphous phases and minerals originating from the aggregate material. In the literature, these compounds can be described by their chemical formula, by their name or by the short form used in cement terminology. Table 3-1 presents names in full and short form as well and the chemical formula for several important cement minerals.

**Table 3-1. Short form, trivial name, chemical name and chemical formula of some important minerals in cement chemistry.**

| Short form in cement nomenclature | Trivial name | Chemical name | Chemical formula |
|---|---|---|---|
| | **Clinker Oxides** | | |
| C | Quick lime, burnt lime | Calcium oxide | $CaO$ |
| S | Quartz | Silicon dioxide | $SiO_2$ |
| A | Alumina | Aluminium oxide | $Al_2O_3$ |
| F | Hematite | Iron oxide | $Fe_2O_3$ |
| M | Magnesia | Magnesium oxide | $MgO$ |
| N | | Sodium oxide | $Na_2O$ |
| T | | Titanium oxide | $TiO_2$ |
| K | | Potassium oxide | $K_2O$ |
| $\bar{S}$ | | Sulphur trioxide | $SO_3$ |
| $\bar{C}$ | | Carbon dioxide | $CO_2$ |
| | **Clinker minerals** | | |
| $C_2S$ | Belite | Dicalcium silicate | $2CaO \cdot SiO_3$ |
| $C_3S$ | Alite | Tricalcium silicate | $3CaO \cdot SiO_3$ |
| $C_3A$ | | Tricalcium aluminate | $3CaO \cdot Al_2O_3$ |
| $C_4AF$ | | Tetracalcium aluminoferrite | $4CaO \cdot Al_2O_3 \cdot Fe_2O_3$ |
| | **Hydroxides** | | |
| NH | Caustic soda, lye | Sodium hydroxide | $NaOH$ |
| KH | Caustic potash | Potassium hydroxide | $KOH$ |
| MH | Brucite | Magnesium hydroxide | $Mg(OH)_2$ |
| CH | Portlandite | Calcium hydroxide | $Ca(OH)_2$ |
| | **Other important minerals** | | |
| $C_6A\tilde{S}_3H_{32}$ | Ettringite | Calcium trisulfato aluminate hydrate | $Ca_6[Al(OH)_6]_2(SO_4)_3 \cdot 26H_2O$ |
| $C_3S\tilde{C}\tilde{S}H_{15}$ | Thaumasite | | $CaSi(OH)_6CaCO_3CaSO_4 \cdot 12H_2O$ |
| $C_4(A, F)\tilde{S}H_n$ | Monosulphate | | $(CaO)_3(Al,Fe)_2O_3CaSO_4 \cdot nH_2O$ |
| CSH | | Calcium silicate hydrate | |
| | Hydrotalcite | | $(Mg_6Al_2(OH)16CO_3 \cdot 4H_2O)$ |
| $C_3AH_6$ | Hydrogarnet | | $3CaO \cdot Al_2O_3 \cdot 6\ H_2O$ |
| CASH | | Calcium aluminate silicate hydrate | |
| $C_3FH_6$ | Fe-katoite | | |
| $C_3AS_{3-x}H_{2x}$ | Katoite | | $Ca_3Al_2(SiO_4)_{3-x}(OH)_{4x}$ |
| $C\tilde{C}$ | Calcite | Calcium carbonate | $CaCO_3$ |
| $C\tilde{S}H_2$ | Gypsum | Calcium sulphate | $CaSO_4 \cdot 2H_2O$ |

### 3.1.2 Cement classes

The Swedish cement standard (SIS 2011a) defines five main cement classes, CEMI, CEMII, CEMIII, CEMIV and CEMV with varying amount of Portland clinker and other constituents such as fly ash, blast furnace slag or limestone. Of these, CEMI contains 95–100 % clinker and the other types increasing and varying amounts of other constituents. A detailed description of the different cement classes is beyond the scope of this report and the reader is therefore referred to SIS (2011a) or Svensk Byggtjänst (2017, Section 12.3 and 12.4) for further reading.

## 3.2 Cement types used in the cementitious materials in SFR

In SFR, different types of cement have been used and are planned for use in the various cementitious materials. The choice of cement type is based on availability which has varied over time as well as on the required properties of the material in question.

According to available information, *Anläggningscement Degerhamn* (Section 3.2.1) was used in all concrete structures in SFR1. This cement has also been used in the *Original silo grout* from the start of operation of SFR1.

During 2019 the Degerhamn plant was closed and for SFR3 other types of cement will have to be used instead. At present, the most similar product is *Anläggningscement Slite std P* (Section 3.2.2) which has a similar composition and properties. However, also other options exist such as products in which the cement clinker is partially replaced by supplementary cementitious materials such as fly ash or blast furnace slag.

Unexpectedly, during the early summer 2021 information was obtained that permission for continued quarrying of limestone for cement production in Slite was not granted and that production was not allowed to proceed beyond October 2021. At present (December 2023), production in Slite has been resumed but the long-term production of cement in Slite using locally quarried limestone is uncertain.

### 3.2.1 Anläggningscement Degerhamn

#### *Composition and properties*

*Anläggningscement Degerhamn* was produced in Degerhamn on the island of Öland in the Baltic Sea until 2019. *Anläggningscement Degerhamn* is a CEMI cement (Section 3.1.2) with a low $C_3A$ content and a moderate heat development. The moderate heat development makes it suitable for use in construction of concrete structures where a low maximum temperature and low temperature shrinkage are required. The low $C_3A$ content makes it less sensitive to sulphate attack.[14]

As shown in Table 3-2, the chemical composition of *Anläggningscement Degerhamn* reported in different studies has varied somewhat, probably caused by variations in the composition of the rock material used in cement production.

**Table 3-2. Composition of *Anläggningscement Degerhamn*.**

| Reference | Höglund and Bengtsson 1991 | Gaucher et al. 2005 | Wiborgh and Lindgren (1987)* |
|---|---|---|---|
| **Component** | **Content (% by weight)** | | |
| CaO | 64 | 65.5 | 64.4 |
| $SiO_2$ | 21 | 22.7 | 19.7 |
| $Al_2O_3$ | 3.5 | 3.56 | 4.8 |
| $Fe_2O_3$ | 4.6 | 4.32 | 2.9 |
| MgO | 0.7 | 0.45 | 1.2 |
| $K_2O$ | 0.62 | 0.57 | 1.2 |
| $Na_2O$ | 0.07 | 0.05 | 0.1 |
| $SO_3$ | 2.2 | 2.07 | 3.2 |
| Cl | < 0.1 | Not reported | < 0.01 |
| $CaCO_3$ | 0.9 | Not reported | 1.1 |
| **Corresponding clinker components** | **Content (% by weight)** | | |
| $C_3S$ | 64.4 | Not reported | Not reported |
| $C_2S$ | 10.9 | Not reported | Not reported |
| $C_3A$ | 2.0 | Not reported | Not reported |
| $C_4AF$ | 13.9 | Not reported | Not reported |
| Gypsum | 3.7 | Not reported | Not reported |
| Alkali hydroxides, *NH + KH* | 0.7 | Not reported | Not reported |

* The values are reported by Wiborgh and Lindgren (1987) but the original reference has not been found.

[14] Sulphate attack is a term used to describe the detrimental effects of chemical reactions between $C_3A$ and sulphate. Sulphate attack is commonly known to cause the formation of ettringite, an expansive mineral, the formation of which is claimed to cause cracking of cementitious materials. See for example Skalny et al. (2002) for further details. See also Section 4.14.

#### *Use in SFR*

*Anläggningscement Degerhamn* was used in all concrete structures in SFR1 for which information on concrete mixing proportions has been found. *Anläggningscement Degerhamn* has also been used in the *Original silo grout* (Section 3.4.1) since start of disposal as well as in the shotcrete used in SFR1.

### 3.2.2 Anläggningscement Slite Standard P

#### *Composition and properties*

*Anläggningscement Slite Standard P* is produced in Slite on the island of Gotland in the Baltic Sea. *Anläggningscement Slite Standard P* is a CEMI cement (Section 3.1.2) with a low $C_3A$ content and a moderate heat development. The moderate heat development makes it suitable for construction of concrete structures where low maximum temperature and low temperature shrinkage are required whereas the low $C_3A$ content makes it less sensitive to sulphate attack.

The chemical composition of *Anläggningscement Slite standard P* was provided by the manufacturer (Cementa AB 2021a)[15] and Table 3-3 shows average values from production control during 2019 and 2020. As a comparison, the composition of *Anläggningscement Degerhamn* previously reported by Höglund and Bengtsson (1991) is also shown here.

**Table 3-3. Composition of *Anläggningscement Slite standard P* (Cementa AB 2021a)[16] and *Anläggningscement Degerhamn* (Höglund and Bengtsson 1991).**

| Cement type | Anläggningscement Slite Standard P | Anläggningscement Degerhamn |
|---|---|---|
| **Component** | **Content (% by weight)** | |
| CaO | 62.9 | 64 |
| $SiO_2$ | 20.9 | 21 |
| $Al_2O_3$ | 3.2 | 3.5 |
| $Fe_2O_3$ | 4.0 | 4.6 |
| MgO | 2.5 | 0.7 |
| $K_2O$ | 0.55 | 0.62 |
| $Na_2O$ | 0.19 | 0.07 |
| $SO_3$ | 2.8 | 2.2 |
| Cl | < 0.01 | < 0.1 |
| $CaCO_3$ | Not reported | 0.9 |
| Loss on ignition | 2.6 | Not reported |
| **Corresponding clinker components** | **Content (% by weight)** | |
| $C_3S$ | 60.1 | 64.4 |
| $C_2S$ | 14.7 | 10.9 |
| $C_3A$ | 1.9 | 2.0 |
| $C_4AF$ | 12.1 | 13.9 |
| Gypsum | Not reported | 3.7 |

As shown in Table 3-3, the clinker composition of *Anläggningscement Slite standard P* is similar to that of *Anläggningscement Degerhamn*, both containing low levels of alkalis ($K_2O$ and $Na_2O$) as well as a low amount of $C_3A$. *Anläggningscement Slite Standard P* is therefore a suitable alternative to replace *Anläggningscement Degerhamn*.

[15] Cementa AB 2021a. Anläggningscement Std P Slite, Typanalys 2020. Dated 2021-02-24. (Internal document, in Swedish.)

[16] Cementa AB 2021a. Anläggningscement Std P Slite, Typanalys 2020. Dated 2021-02-24. (Internal document, in Swedish.)

#### *Use in SFR*

*Anläggningscement Slite standard P* was used during a short period of time for the production of the *Original silo grout*, Section 3.4.1. *Anläggningscement Slite standard P* is also considered a suitable candidate for use during construction of SFR3 if permission for continued quarrying and production in Slite is granted.

### 3.2.3 Slite Standard P

#### *Composition and properties*

*Slite standard P* is a CEMI cement (Section 3.1.2) from Slite on the island of Gotland in the Baltic Sea which was produced until about 1999. The chemical composition of *Slite standard P* has been reported by Malmström (1990) and is presented in Table 3-4.

From Table 3-4, the most important difference between *Anläggningscement Slite Standard P* and *Slite Standard P* is the higher content of $C_3A$ in *Slite Standard P*. The impact of this is a reduced resistance to sulphate attack and *Slite Standard P* is therefore not classified as sulphate resistant.

**Table 3-4. Composition of *Slite standard P* (Malmström 1990) and *Anläggningscement Slite Standard P* (Cementa AB 2021a).[17]**

| Cement type | Slite Standard P | Anläggningscement Slite Standard P |
|---|---|---|
| **Component** | **Content (% by weight)** | |
| CaO | 63.9 | 62.9 |
| $SiO_2$ | 20.4 | 20.9 |
| $Al_2O_3$ | 4.58 | 3.2 |
| $Fe_2O_3$ | 2.16 | 4.0 |
| $TiO_2$ | 0.24 | Not reported |
| MgO | 3.16 | 2.5 |
| $K_2O$ | 1.28 | 0.55 |
| $Na_2O$ | 0.25 | 0.19 |
| MnO | 0.06 | Not reported |
| $SO_3$ | 3.4 | 2.8 |
| Cl | < 0.01 | < 0.01 |
| **Corresponding clinker components** | **Content (% by weight)** | |
| $C_3S$ | 61.2 | 60.1 |
| $C_2S$ | 12.3 | 14.7 |
| $C_3A$ | 8.5 | 1.9 |
| $C_4AF$ | 6.6 | 12.1 |
| Alkali hydroxides, *N* + *K* | 0.7 | |

#### *Use in SFR*

*Slite standard P* was originally used for production of the *BTF grout* (Section 3.4.3). However, production of *Slite Standard P* was phased out during 1999 and the recommendation was to replace *Slite Standard P* with *Slite Byggcement* which was later replaced by *Bascement Slite* (Section 3.2.5). It is, however, unclear if this recommendation was followed in the production of the *BTF grout* or if other types of cement were used instead.

[17] Cementa AB 2021a. Anläggningscement Std P Slite, Typanalys 2020. Dated 2021-02-24. (Internal document, in Swedish.)

### 3.2.4 Velox Slite

#### *Composition and properties*

*Velox Slite* is a CEMI cement (Section 3.1.2) from Slite on the island of Gotland in the Baltic Sea. The chemical composition of *Velox Slite* was provided by the manufacturer (Cementa AB 2021b)[18] and Table 3-5 shows average values from production control during 2019 and 2020. As a comparison, the composition of *Anläggningscement Slite standard* P is also shown here.

The most striking difference between these two cement types is the considerably higher $C_3A$ content in *Velox Slite* compared to *Anläggningscement Slite Standard P*. The impact of this is a reduced resistance to sulphate attack and *Velox Slite* is therefore not classified as sulphate resistant.

**Table 3-5. Composition of *Velox Slite* (Cementa AB 2021b)[19] and *Anläggningscement Slite Standard P* (Cementa AB 2021a).[20]**

| Cement type | Velox Slite | Anläggningscement Slite Standard P |
|---|---|---|
| **Component** | **Content (% by weight)** | |
| CaO | 62.2 | 62.9 |
| $SiO_2$ | 19.2 | 20.9 |
| $Al_2O_3$ | 4.7 | 3.2 |
| $Fe_2O_3$ | 3.0 | 4.0 |
| MgO | 3.3 | 2.5 |
| $K_2O$ | 1.0 | 0.55 |
| $Na_2O$ | 0.28 | 0.19 |
| $SO_3$ | 3.3 | 2.8 |
| Cl | 0.05 | < 0.01 |
| Loss on ignition | 2.8 | 2.6 |
| **Corresponding clinker components** | **Content (% by weight)** | |
| $C_3S$ | 60.6 | 60.1 |
| $C_2S$ | 9.3 | 14.7 |
| $C_3A$ | 7.3 | 1.9 |
| $C_4AF$ | 9.2 | 12.1 |
| Gypsum | Not reported | Not reported |

#### *Use in SFR*

No application has been identified where *Velox Slite* is currently or historically used in SFR. However, having a composition similar to that of *Slite standard P* it is not unlikely that it has been used for production of the *BTF grout* during some part of the period between the years 2000 and 2020, i.e. the period from which no information regarding choice of cement type in the *BTF grout* is available.

### 3.2.5 Bascement Slite

#### *Composition and properties*

*Bascement Slite* is a CEM II cement (Section 3.1.2) which is produced in Slite on the island of Gotland in the Baltic Sea. As shown in Table 3-6, the composition of *Bascement Slite* has varied since start of production.

[18] Cementa AB 2021b. Velox Slite, Typanalys 2020. Dated 2021-02-24. (Internal document, in Swedish.)

[19] Cementa AB 2021b. Velox Slite, Typanalys 2020. Dated 2021-02-24. (Internal document, in Swedish.)

[20] Cementa AB 2021a. Anläggningscement Std P Slite, Typanalys 2020. Dated 2021-02-24. (Internal document, in Swedish.)

The composition of *Generation 1* was reported by and used in a modelling exercise performed by Idiart et al. (2019a) but the original reference (most likely data from production control at Cementa AB) has not been obtained. In this material, the fly ash content was about 12.3 % with an estimated composition shown in Table 3-6. In *Generation 2*, fly ash was to a large extent replaced by limestone. According to information from the manufacturer (Cementa AB 2021c)[21] *Generation 2* contains 12.6 % limestone (including gypsum) and only 2.6 % fly ash.

**Table 3-6. Composition of *Bascement Slite*.**

| Component | Generation 1<br>Idiart et al. (2019a) | Generation 2<br>Cementa AB (2021c)[22] |
|---|---|---|
| | Content (% by weight) | |
| CaO | 56.3 | 58.7 |
| $SiO_2$ | 23.5 | 18.5 |
| $Al_2O_3$ | 6.4 | 5.1 |
| $Fe_2O_3$ | 3.4 | 2.9 |
| MgO | 2.6 | 3.2 |
| $K_2O$ | 1.2 | 1.0 |
| $Na_2O$ | 0.3 | 0.27 |
| $SO_3$ | 3.5 | 3.3 |
| Cl | < 0.1 | 0.07 |
| **Additional information** | **Content (% by weight)** | |
| $C_3A$ | 5.4 | 6.4 |
| $CaCO_3$+$C\hat{S}H_2$ | 4.8 | 12.6 |
| Fly Ash | 12.3 | 2.6 |

### *Use in SFR*

*Bascement Slite* is currently used only in the *BTF tank concrete* (Section 3.3.6) for production of concrete tanks but probably also for production of concrete moulds. *Bascement Slite* is currently not planned for use in other applications in SFR.

## 3.2.6 Aalborg White cement

### *Composition and properties*

*Aalborg White cement* is a CEMI cement (Section 3.1.2) produced in Aalborg in Denmark. The composition of *Aalborg White cement* (Table 3-7) is reported by Pusch and Ramqvist (2004, Appendix 1) with reference to "company declared compositions".

**Table 3-7. Composition of *Aalborg White cement* (Pusch and Ramqvist 2004, Appendix 1).**

| Component | Content (% by weight) |
|---|---|
| CaO | 69.28 |
| $SiO_2$ | 24.9 |
| $Al_2O_3$ | 1.91 |
| $TiO_2$ | - |
| $Fe_2O_3$ | 0.33 |
| $Na_2O$ | 0.15 |
| $K_2O$ | - |
| MgO | 0.58 |
| $SO_3$ | 2.11 |
| Loss On Ignition | 0.7 |

[21] Cementa AB 2021c. Bascement Slite, Quality certificate 2021. Dated 2022-02-07. (Internal document.)

[22] Cementa AB 2021c. Bascement Slite, Quality certificate 2021. Dated 2022-02-07. (Internal document.)

### *Use in SFR*

*Aalborg White cement* is currently only planned for use in the *SFR borehole concrete*, Section 3.3.11, even though the use of this concrete at present is somewhat uncertain.

## 3.2.7 Anläggningscement FA Slite

### *Composition and properties*

*Anläggningscement FA Slite* is a Portland fly ash cement of type CEM II / A-V 42.5 N MH/LA/NSR which is manufactured in Slite. It is adapted for use in medium-coarse to coarse constructions with requirements for cement with moderate heat generation. *Anläggningscement FA Slite* has a low $C_3A$ content and therefore less sensitive to sulphate attack, i.e. chemical processes caused by high sulphate concentrations in soil and water. The low alkali content contributes to an increased resistance against alkali silica reactions.

The chemical composition of *Anläggningscement FA Slite* was provided by the manufacturer (Cementa AB 2022)[23] and Table 3-8 shows average values from production control during 2021 and 2022.

**Table 3-8 Composition of *Anläggningscement FA Slite* (Cementa AB 2022).[24]**

| Component | Content (% by weight) |
|---|---|
| CaO | 56.0 |
| $SiO_2$ | 23.9 |
| $Al_2O_3$ | 5.9 |
| $Fe_2O_3$ | 4.3 |
| MgO | 2.6 |
| $K_2O$ | 0.78 |
| $Na_2O$ | 0.23 |
| SO3 | 2.8 |
| Cl | < 0.01 |
| Free $CaCO_3$ | - |
| Loss on ignition | 2.8 |
| **Additional information** | **Content (% by weight)** |
| $C_3A$ | 1.6 |
| $CaCO_3$+$C\hat{S}H_2$ | 4.7 |
| Alkalis, N+K | 0.74 |
| Fly Ash | 12.2 |

### *Use in SFR*

*Anläggningscement FA Slite* has been used in the production of the *New silo grout* (Section 3.4.2) since June 2022 when this grout replaced the *Original silo grout*. The reason for using this cement is the simple fact that the concrete production plant where the *New silo grout* is mixed switched to this cement in April 2022.

[23] Cementa AB 2022. Anläggningscement FA Slite. Typanalys 2021. Dated 2022-02-07. (Internal document, in Swedish.)

[24] Cementa AB 2022. Anläggningscement FA Slite. Typanalys 2021. Dated 2022-02-07. (Internal document, in Swedish.)

### 3.2.8 Cement types in SFR: Summary

In Table 3-9 a comparison of the composition of the different types of cement currently or historically used in SFR or identified as suitable for use in SFR3 is presented. However, it should be recognised that the composition of the cements may vary over time as a function of the composition of the raw materials which are not always the same in an entire quarry. For other cements like *Bascement Slite* and *Anläggningscement FA Slite* additional compositional variations may be caused by variations in the compositions of the supplementary cementitious materials added. For those reasons the compositions presented in Table 3-9 should be regarded as an indication of the composition of the cements rather than exact and invariable values.

From Table 3-9, the amounts of the main constituents such as $C_3S$ and $C_2S$ are rather similar in most types of the cements shown here whereas instead significant variations in the amount of $C_3A$ are observed. As the amount of $C_3A$ has a significant influence on the sensitivity of the cementitious materials towards sulphate attack, cements with a low amount of $C_3A$ should be chosen for SFR3 as well as the remaining cementitious components in SFR1. However, as previously noted in this report, future cement production in Sweden is currently uncertain and the properties of the future cements available for SFR therefore difficult to predict.

**Table 3-9. A comparison of the composition of the different types of cements used or planned for use in SFR1 and identified as suitable for use in SFR3.**

| Cement type | Degerhamn Anläggnings-cement | Anläggnings-cement Slite std P | Velox Slite | Slite std P | Bas-cement Slite, Gen 1. | Aalborg white cement | Anläggnings-cement FA Slite |
|---|---|---|---|---|---|---|---|
| **Reference** | **Höglund and Bengtsson (1991)** | **Cementa AB (2021a)[25]** | **Cementa AB (2021b)[26]** | **Malmström (1990)** | **Idiart et al. (2019a)** | **Pusch and Ramqvist (2004)** | **Cementa AB (2022)[27]** |
| **Component** | **Content (% by weight)** | | | | | | |
| CaO | 64 | 62.9 | 62.2 | 63.9 | 56.3 | 69.28 | 56.0 |
| $SiO_2$ | 21 | 20.9 | 19.2 | 20.4 | 23.5 | 24.9 | 23.9 |
| $Al_2O_3$ | 3.5 | 3.2 | 4.7 | 4.58 | 6.4 | 1.91 | 5.9 |
| $Fe_2O_3$ | 4.6 | 4.0 | 3.0 | 2.16 | 3.4 | 0.33 | 4.3 |
| $TiO_2$ | | | | 0.24 | | | |
| MgO | 0.7 | 2.5 | 3.3 | 3.16 | 2.6 | 0.58 | 2.6 |
| $K_2O$ | 0.62 | 0.55 | 1.0 | 1.28 | 1.2 | - | 0.78 |
| $Na_2O$ | 0.07 | 0.19 | 0.28 | 0.25 | 0.3 | 0.15 | 0.23 |
| MnO | | | | 0.06 | | | |
| $SO_3$ | 2.2 | 2.8 | 3.3 | 3.4 | 3.5 | 2.11 | 2.8 |
| Cl | < 0.1 | < 0.01 | 0.05 | < 0.01 | < 0.1 | NR | < 0.01 |
| **Corresponding clinker components** | **Content (% by weight)** | | | | | | |
| $C_3S$ | 64.4 | 60.1 | 60.6 | 61.2 | NR | NR | NR |
| $C_2S$ | 10.9 | 14.7 | 9.3 | 12.3 | NR | NR | NR |
| $C_3A$ | 2.0 | 1.9 | 7.3 | 8.5 | 5.4 | NR | 1.6 |
| $C_4AF$ | 13.9 | 12.1 | 9.2 | 6.6 | NR | NR | NR |
| Gypsum | 3.7 | NR | NR | NR | NR | NR | NR |

NR: Not reported

[25] Cementa AB 2021a. Anläggningscement Std P Slite, Typanalys 2020. Dated 2021-02-24. (Internal document, in Swedish.)

[26] Cementa AB 2021b. Velox Slite, Typanalys 2020. Dated 2021-02-24. (Internal document, in Swedish.)

[27] Cementa AB 2022. Anläggningscement FA Slite. Typanalys 2021. Dated 2022-02-07. (Internal document, in Swedish.)

## 3.3 Concrete and shotcrete in SFR

In SFR, large amounts of different types of concrete and shotcrete with varying mixing proportions and properties have been used, are used and will be used. The mixing proportions of some of these materials used in the construction of SFR1 or designed for use in the construction of SFR3 are known whereas the mixing proportions of others are yet not known. This is because information from construction of SFR1 has been lost or the requirements for future materials have yet not been specified and the mixing proportions therefore not yet decided.

In this section the mixing proportions and properties of all types of concrete and shotcrete used or planned for use in SFR are presented. For the types of concrete for which the mixing proportions are not known, the presented mixing proportions are based on the predicted requirements which in turn are based on the application in which the material is planned for use.

As a background, the different concrete classes with details of compressive strength and w/c ratio are described in Svensk Byggtjänst (2017, Table 12.4:4).

### 3.3.1 Silo concrete

#### *Function and requirements*

The *Silo concrete* was used for construction of the slab, outer and inner walls of the concrete silo in SFR1 in the 1980's. The main requirements of the *Silo concrete* include high strength, low hydraulic conductivity and effective diffusivity but the concrete should also set a high pH value, which limits corrosion of steel and gas production caused by microbial activity and provide good sorption capacity for radionuclides.

#### *Mixing proportions*

The mixing proportions of the *Silo concrete* is shown in Table 3-10 (Jacobsen and Gjörv 1987). According to Wiborgh and Lindgren (1987, Table 4.1) this corresponds to class K400 at the time of construction. From the w/c ratio given in Table 3-10, this corresponds to current-day class C40/50.

**Table 3-10. Mixing proportions of the *Silo concrete*. (Jacobsen and Gjörv 1987)**

| Component | Amount (kg/m$^3$) |
|---|---|
| Cement (Anläggningscement Degerhamn) | 350 |
| Water | 164.5 |
| Aggregates (Total) | 1 829 |
| Aggregates (16–32 mm) | 535 |
| Aggregates (8–16 mm) | 374 |
| Aggregates (0–8 mm) | 920 |
| Admixtures | 0.5% Sika Plastiment BV-40<br>0.05–0.2% Sika Retarder |
| W/c ratio | 0.47 (0.46–0.49) |

#### *Mineral composition of the hardened concrete*

The mineral composition of the hardened *Silo concrete* (including cement minerals and aggregates) has been modelled by e.g. Gaucher et al. (2005) and the results were also later used in the work by Cronstrand (2007). Table 3-11 shows the results presented by Cronstrand (2007).

**Table 3-11. Calculated mineral composition of the *Silo concrete* at the time of closure including the hydrated cement and aggregates (Cronstrand 2007).**

| Mineral phases | Amount (mol/dm$^3$)* | Amount (Volume %) |
|---|---|---|
| Quartz | 15.096 | 40.62 |
| K-feldspar | 1.307 | 16.69 |
| CSH_1.8 | 0.847 | 13.61 |
| Albite | 1.067 | 12.56 |
| Portlandite | 0.811 | 3.14 |
| Ettringite | 0.022 | 1.85 |
| Biotite | 0.083 | 1.36 |
| Hydrogarnet | 0.050 | 0.87 |
| Hydrotalcite | 0.008 | 0.27 |
| Magnetite | 0.040 | 0.21 |

* The data presented in this column has been obtained by Cronstrand (2007) by recalculating mineral volume data presented by Gaucher et al. (2005). The total volume of the minerals in Gaucher et al. (2005, Table 2-8) is 852 cm$^3$. In addition, Gaucher et al. (2005) assumes a total porosity of 15 %.

The mineral composition of the hardened *Silo concrete* – excluding the unreactive aggregate materials – has also been modelled by Idiart et al. (2019a) as well as by Höglund (2001, 2014) and Höglund and Bengtsson (1991). Table 3-12 presents a compilation of the main minerals identified by Idiart et al. (2019a) and Höglund (2014). The complete list of minerals is found in Idiart et al. (2019a, Table 5-2) and Höglund (2014, Table 2-7).

As shown in Table 3-12, there are significant differences in the reported mineral composition between the two studies. Since both studies have used the same starting composition for the concrete, these differences can only be explained by differences in the set-up of the calculations and cement mineral database used. It is, however, not within the scope of this study to further discuss possible explanations for these differences.

**Table 3-12. Calculated mineral composition and porosity of the *Silo concrete* calculated by Idiart et al. (2019a) and Höglund (2014)**

| Mineral phases | Amount (mol/dm$^3$) | |
|---|---|---|
| | Idiart et al. (2019a) | Höglund (2014) |
| Portlandite | 1.422 | 1.036 |
| Hydrotalcite OH | 0.016 | - |
| Calcite | 0 | 0.063 |
| Monocarboaluminate | 0.033 | - |
| Ettringite | 0 | 0 |
| Monosulfoaluminate | 0.081 | - |
| Monosulphate | - | 0.096 |
| Hydrogarnet OH | 0.111 | 0.34 (Total $C_3FH_6$ + $C_3AH_6$) |
| C-S-H Jennite | 1.100 | 1.225 (Total CSH-gel) |
| C-S-H Tobermorite | 0.161 | - |
| Porosity | 0.110 | 0.099 |

### *Properties of the hardened concrete*

Unfortunately, no test protocols from the construction of the concrete silo or documents in which data from such protocols have been compiled have been found. Instead, data obtained from other sources describing similar types of concrete have been used to obtain reasonable data for the hardened *Silo concrete*.

Wiborgh and Lindgren (1987) presents an early compilation of transport data available in the literature for different types of concrete and cement paste.[28] Based on this compilation, the data shown in Table 3-13 were selected for the hardened *Silo concrete*. According to Wiborgh and Lindgren (1987), the same data were selected for all concrete barriers in SFR. It should be noted the suggested bulk density in Table 3-13 differs from that calculated from Table 3-10 which is 2 345 kg/m$^3$. The reason for the rather low estimate in Table 3-10 is not known.

Using the concrete classes of today, the w/c ratio of the *Silo concrete* corresponds to class C40/50 (Svensk byggtjänst 2017, Table 12.4:4) with an estimated 28 days compressive strength (cube) of 57 MPa.

The porosity of the *Silo concrete* has been estimated by Idiart et al. (2019a) who reported a value of 11 %. This can be compared with 10 % reported by Höglund (2014) and 15 % reported by Gaucher et al. (2005). Finally, Table 5-4 reports total porosity values for standard concrete with varying w/c ratios. From this table, the porosity of the *Silo concrete* is expected to be about 13 %.

**Table 3-13. Assumed properties of the hardened *Silo concrete* (Wiborgh and Lindgren 1987, Table 4.18)**

| Property | Unit | Value |
|---|---|---|
| Density (solid) | kg/m$^3$ | 2600 |
| Density (bulk) | kg/m$^3$ | 2210*** |
| Compressive strength* | MPa | 55–60 |
| Average porosity | % | 15** |
| Specific surface | m$^2$/g | 200 |
| Hydraulic conductivity | m/s | $10^{-11}$ |
| Effective diffusivity | m$^2$/s | $3 \times 10^{-12}$ |
| Pore diffusivity | m$^2$/s | $2 \times 10^{-11}$ |

* The compressive strength is not reported by Wiborgh and Lindgren (1987) and has instead been estimated from the w/c ratio of the *Silo concrete*.

** Idiart et al. (2019a) reported a porosity of 11 % for the Silo concrete.

*** The calculated bulk density of the silo concrete (Table 3-10) is 2345 kg/m$^3$.

## 3.3.2 1BMA concrete

### *Function and requirements*

The *1BMA concrete* was used for construction of the slab, existing outer and inner walls of the concrete structure in 1BMA. It is also expected that the *1BMA concrete* was used also in the slabs in 1BLA and 1–2BTF even though no documentation that confirms this assumption has been found. The main requirements of the *1BMA concrete* include high strength, low hydraulic conductivity and effective diffusivity but the concrete should also set a high pH value, which limits corrosion of steel and gas production caused by microbial activity and provide good sorption capacity for radionuclides.

[28] The cement paste is typically made up of cement and water but can also contain additional fine-grained materials such as silica, fly ash and limestone. The maximum grain size of the materials in the paste is in the range of 100 μm.

### *Mixing proportions*

Information on the mixing proportions of the 1BMA concrete is scarce. Information found in protocols from the time of casting state that the *1BMA concrete* contained about 280 kg cement/$m^3$ and that the w/c ratio varied between 0.59 and 0.65, (Elfwing et al. 2015). However, no further details on concrete mixing proportions and properties were included in these protocols.

However, because the existence of these protocols was unknown during many years it has been a general assumption that the *Silo concrete* was used also for the construction of 1BMA as well as in all other concrete structures in SFR1. For that reason, all modelling of the post-closure evolution of the properties of the concrete barriers in 1BMA carried out up to about the year 2015 when these documents were discovered have been carried out using the mixing proportions of the *Silo concrete*: see e.g. (Cronstrand 2007, Gaucher et al. 2005, Höglund 2001, 2014).

### *Mineral composition of the hardened concrete*

The mineral composition of the hardened *1BMA concrete* is reported by Idiart et al. (2019a) and a compilation of the main minerals is presented in Table 3-14. The complete list of minerals is found in Idiart et al. (2019a, Table 5-2).

**Table 3-14. Calculated concentration of the main mineral phases and porosity in the *1BMA concrete* (Idiart et al. 2019a).**

| Mineral phases | Amount (mol/$dm^3$) |
|---|---|
| **Cement minerals** | |
| Portlandite | 1.198 |
| Hydrotalcite OH | 0.014 |
| Calcite | 0 |
| Monocarboaluminate | 0.028 |
| Ettringite | 0 |
| Monosulfoaluminate | 0.068 |
| Hydrogarnet OH | 0.098 |
| C-S-H Jennite | 0.930 |
| C-S-H Tobermorite | 0.137 |
| Porosity | 0.13 |
| **Aggregates** | |
| Inert fraction | 0.704 |

### *Properties of the hardened concrete*

The protocols from construction of the concrete structure in 1BMA did not contain any information on the properties of the fresh and hardened concrete. Because of this, these properties have instead been estimated from literature data for concrete with a similar w/c ratio as the *1BMA concrete* as well as from studies of new samples prepared with the same w/c ratio as the *1BMA concrete* (Villar et al. 2019).

An estimate of the compressive strength of the *1BMA concrete* is obtained from Svensk Byggtjänst (2017). Here, a w/c ratio of 0.59 to 0.65 corresponds to current concrete classes C30/37 and C28/35 respectively with an expected 28 days compressive strength of about 44 and 42 MPa respectively for cube-shaped specimens.

Information concerning the transport properties of the *1BMA concrete* was obtained from Villar et al. (2019) who studied the properties of newly prepared specimens of concrete similar to the *1BMA concrete*, Table 3-15. Note that the maximum aggregate size in the concrete tested by Villar et al. (2019) was only 8 mm whereas the maximum size in the *1BMA concrete* was probably 32 mm. The use of small aggregates only was because the use of larger aggregates could impair the quality of the results from the measurements on the small specimens used.

**Table 3-15. Mixing proportions of the concrete used in the tests carried out by Villar et al. (2019).**

| Component | Product | Amount (kg/m$^3$) |
|---|---|---|
| Cement | Anläggningscement Degerhamn | 280 |
| Water | | 176.4 |
| Aggregates | Crushed granite | |
| 0–4 mm | | 1 361 |
| 4–8 mm | | 544 |
| Super plasticiser | Master Glenium Sky 823 | 3.1 |

Unfortunately, during specimen preparation, Villar et al. (2019) realised that the first specimen (denoted *OPC micro concrete* in Table 3-16) contained a larger number of air voids than expected and the sample was therefore not considered representative for the *1BMA concrete*. For that reason, it was decided to prepare a new block (denoted *BMA concrete* in Table 3-16). However, also this block contained more pores than expected (Figure 3-1) but in spite of this it was decided to proceed with the material investigations.

Table 3-16 presents a summary of the results from the different tests. For more details, please refer to Villar et al. (2019).

**Table 3-16. Summary of the properties of concrete specimens tested by Villar et al. (2019).**

| | OPC micro concrete | Source* | BMA concrete | Source* |
|---|---|---|---|---|
| Bulk density | 2 350 kg/m$^3$ | Table 4-4 | 2 375 kg/m$^3$ | Table 4-3 |
| Dry density | 2 110 kg/m$^3$ | Table 4-4 | 2 255 kg/m$^3$ | Table 4-4 |
| Particle density (water) | 2 750 kg/m$^3$ | Table 4-6 | 2 730 kg/m$^3$ | Table 4-6 |
| Particle density (He) | 2 600 kg/m$^3$ | Table 4-6 | 2 556 kg/m$^3$ | Table 4-6 |
| Average porosity (MIP) | 0.092 | Table 4-8 | 0.118 | Table 4-8 |
| Average porosity (From densities) | 0.168 | Table 4-8 | 0.172 | Table 4-8 |
| Gas permeability (Average) | $3.22 \times 10^{-14}$ m/s | Table 5-6 | $1.27 \times 10^{-11}$ m/s | Table 5-6 |
| Hydraulic conductivity (Permeameter) | $2 \times 10^{-11}$ m/s | | | |
| Hydraulic conductivity (P/V controller) | $1.3 \times 10^{-11}$ m/s | Table 6-4 | $1.9 \times 10^{-11}$ m/s | Table 6-4 |
| Effective diffusivity | $7.9 \times 10^{-12}$ m$^2$/s | Table 7-7 | $9.3 \times 10^{-12}$ m$^2$/s | Table 7-7 |

* Refers to tables in Villar et al. (2019)

The results presented in Table 3-16 can be compared with the results from the modelling study carried out by Idiart et al. (2019a) in which the average porosity of the *1BMA concrete* is estimated to 13 %. This indicates that the specimens tested by Villar et al. (2019) contain additional pores compared to the ideal specimens in the modelling study. This is probably also reflected in the density of the specimens which is a little lower than expected. Also, the hydraulic conductivity obtained by Villar et al. (2019) is a little higher than what could be expected from a "perfect" specimen.


***Figure 3-1.*** *Core from the block denoted "BMA concrete".*

### 3.3.3 2BMA concrete

#### *Function and requirements*

Primarily, the *2BMA concrete* was designed for use for construction of the concrete caissons in 2BMA. However, it is expected that the *2BMA concrete* will also be used for other concrete structures in SFR3 such as the concrete structure in 1BRT and the slabs in 2–5BLA. The main requirements of the *2BMA concrete* include high strength, low hydraulic conductivity and effective diffusivity but the concrete should also set a high pH value, which limits corrosion of steel and gas production caused by microbial activity and provide good sorption capacity for radionuclides.

#### *Mixing proportions*

The mixing proportions for the *2BMA concrete*, Table 3-17, was designed by Lagerblad et al. (2017) and has been tested with only slight modifications in two large scale experiments by Mårtensson and Vogt (2019, 2020).

For the development work, the requirements stated that only aggregates obtained from crushed rock obtained from the excavation of SFR3, a low cement content and low amounts of admixtures should be used but also a 90 days compressive strength of at least 50 MPa. With this background, the use of rather large amounts of limestone filler as an additive was necessary to ensure sufficient workability, Table 3-17. For all requirements, see Mårtensson and Vogt (2020).

However, a few months after the finalisation of the work by Mårtensson and Vogt (2020) it was informed that the production of *Anläggningscement Degerhamn* would cease. Because of this, the final mixing proportions for the *2BMA concrete* will need to include cement from another plant. Presumably *Anläggningscement Slite Standard P* (Section 3.2.2), which has a similar composition as *Anläggningscement Degerhamn* (Table 3-3) will be used but this requires that permission for continued quarrying and production in Slite is granted.

**Table 3-17. Mixing proportions for the *2BMA concrete* (Mårtensson and Vogt 2019, 2020)**

| Component | Product/ Manufacturer | Amount (kg/m$^3$) |
|---|---|---|
| Cement | (Anläggningscement Degerhamn) | 320 |
| Limestone filler | OMYACARB 2GU | 130 |
| Limestone filler | Myanit 10 | 34.3 |
| Water* | Tap water | 169.4 |
| Aggregates 16–22 mm | (Crushed rock) | 383.5 |
| Aggregates 8–16 mm | (Crushed rock) | 415.1 |
| Aggregates 4–8 mm | (Crushed rock) | 89.7 |
| Aggregates 0–4 mm | (Crushed rock) | 819.9 |
| Superplasticiser | MasterGlenium Sky 558 | 1.60 |
| Superplasticiser | Master Sure 910 | 1.70 |
| Retarder | Master Set RT 401 | 0–3.0** |

* Water in admixtures not included

** The amount of retarder is strongly depended on the transport time and temperature of the concrete components during mixing and transport of the concrete.

#### *Mineral composition of the hardened concrete*

The mineral composition of the hardened *2BMA concrete* has been modelled by Idiart et al. (2019a) and a compilation of the main minerals identified by Idiart et al. (2019a) is presented in Table 3-18. The complete list of minerals is found in Idiart et al. (2019a, Table 5-2).

**Table 3-18. Calculated mineral composition and porosity of the *2BMA concrete* (Idiart et al. 2019a).**

| Mineral phases | Amount (mol/dm$^3$) |
|---|---|
| **Cement minerals** | |
| Portlandite | 1.205 |
| Hydrotalcite OH | 0.059 |
| Calcite | 1.591 |
| Monocarboaluminate | 0.013 |
| Ettringite | 0.024 |
| C-S-H Jennite | 0.964 |
| C-S-H Tobermorite | 0.141 |
| Porosity | 0.077 |
| **Aggregates** | |
| Inert fraction | 0.708 |

From Table 3-18, the mineral composition of the *2BMA concrete* reveals the presence of comparatively large amounts of calcite. The origin of this is the limestone filler that was included in the concrete mix in order to increase the volume of paste and thus to improve the workability of the fresh concrete.

### *Properties of the hardened concrete*

The properties of the hardened *2BMA concrete* have been studied both during the design of the concrete mixing proportions (Lagerblad et al. 2017) as well as during the large-scale tests (Mårtensson and Vogt 2019, 2020).

The average 28 days and 6 months compressive strength were measured by Mårtensson and Vogt (2019, 2020), Table 3-19. Also, splitting tensile strength and tensile strength were measured on some samples but for these tests the statistical basis was considerably smaller than for the measurements of the compressive strength. During measurements of the tensile strength, for some samples rupture occurred at or very close to the interface between the material sample and the steel plate to which it was glued and these results are therefore uncertain.

Finally, measurements of drying shrinkage and hydraulic conductivity were carried out for a few specimens. However, because of the very low hydraulic conductivity of the specimens, the measurements were very time consuming and for some specimens a stable flow was never achieved. For that reason, some measurements were interrupted after a couple of weeks and a maximum hydraulic conductivity was calculated from the assumption that water would have penetrated the specimen at the same time as the measurement was interrupted.

A compilation of the results from all measurements carried out during the development and testing program is presented in Table 3-19.

**Table 3-19. A compilation of the properties of the *2BMA concrete* measured during development and large-scale tests. (References: see table)**

| Property | Method | Lagerblad et al. (2017) | Mårtensson and Vogt (2019) | Mårtensson and Vogt (2020) |
|---|---|---|---|---|
| Compressive strength (28 days) | (SIS 2012a, SIS 2012b) | 70.8 MPa | 45–55 MPa | 41–53 MPa |
| Compressive strength (6 months) | (SIS 2012a, SIS 2012b) | - | 66–71 MPa | 49–69 MPa |
| Tensile strength (6 months) | Not stated. | | 1.4–3.2 MPa | |
| Splitting tensile strength | SIS (2011b) | 5.43 MPa | - | 2.8–5.3 MPa |
| Shrinkage (228 days) | SIS (2000) | 0.4 ‰ | 0.3–0.4 ‰ | 0.37 ‰ |
| Shrinkage (228 days) | Sealed specimens | 0.14 ‰ | 0.04 ‰ | 0.02–0.12 ‰ |
| Hydraulic conductivity | | | $< 1 \times 10^{-11}$ m/s | $\leq 1 \times 10^{-11}$ m/s |

In addition to the measurements undertaken during development and testing, also a dedicated investigation programme with focus on the transport properties of the *2BMA concrete* was carried out by Villar et al. (2019). In these tests, ∅ 100 mm cores extracted from two small cubes (denoted ETAPP 1 and ETAPP 2) manufactured in conjunction with and using the same concrete as used in the two parts of the experiments reported by Mårtensson and Vogt (2019) (Figure 3-2) as well as a core from the wall in the second part of the experiment (denoted TAS05_09) were used (Figure 3-3).

***Figure 3-2.*** *The small cubes manufactured just after finishing of the two castings performed by Mårtensson and Vogt (2019) from which cores used by Villar et al. (2019) were extracted.*


***Figure 3-3.*** *Positions in the wall of the second part of the casting carried out by Mårtensson and Vogt (2019) in which cores were extracted for studies of the material properties by Villar et al. (2019).*

Table 3-20 presents a summary of the results from the different tests. All details on how the measurements were performed are presented in Villar et al. (2019).

**Table 3-20. Summary of the properties of the *2BMA concrete* (Villar et al. 2019).**

| | ETAPP 1 and 2 (Average) | Source* | TAS05_09 | Source* |
|---|---|---|---|---|
| Bulk density | 2390 kg/m$^3$ | Table 4-1 | 2420kg/m$^3$ | Table 4-2 |
| Dry density | 2275 kg/m$^3$ | Table 4-1 | 2330 kg/m$^3$ | Table 4-2 |
| Particle density (water) | 2750 kg/m$^3$ | Table 4-6 | 2720 kg/m$^3$ | Table 4-6 |
| Particle density (He) | 2600 kg/m$^3$ | Table 4-6 | 2592 kg/m$^3$ | Table 4-6 |
| Average porosity (MIP) | 0.138 | Table 4-8 | 0.153 | Table 4-8 |
| Average porosity (From densities) | 0.162 | Table 4-8 | 0.133 | Table 4-8 |
| Gas permeability (Average) | $3 \times 10^{-13}$ m/s ** | Table 5-6 | $1.1 \times 10^{-11}$ m/s | Table 5-6 |
| Hydraulic conductivity (Permeameter) | $1.9 \times 10^{-10}$ m/s | Table 6-2 | | |
| Hydraulic conductivity (P/V controller) | $8.7 \times 10^{-13}$ m/s | Table 6-2 | $1.3 \times 10^{-11}$ m/s | Table 6-2 |
| Effective diffusivity | $4.9 \times 10^{-12}$ m$^2$/s | Table 7-7 | $4.8 \times 10^{-12}$ m$^2$/s | Table 7-7 |

* Refers to tables in Villar et al. (2019)

** Note that for some of the samples no flow was detected. These samples were not included in the calculation of the average gas permeability.

A comparison between the values reported by Mårtensson and Vogt (2019, 2020) and those reported by Villar et al. (2019) shows that the values differ both between the two studies carried out by Mårtensson and Vogt (2019, 2020) but also between these two studies and the study carried out by Villar et al. (2019).

The most plausible explanation for these differences is the small size of the specimens used in particular by Villar et al. (2019). This is because, for small specimens, any inhomogeneities will have a larger impact on the average properties of the specimen than for larger specimens. For the specimens studied by Villar et al. (2019), the observed voids have probably had a significant impact on the transport properties of the materials and both the hydraulic conductivity and effective diffusivity for specimens without voids are probably lower than what was observed by Villar et al. (2019). For this reason, in the selection of hydraulic conductivity and diffusivity data for undegraded concrete presented in Table 5-6 and 5-8 the values obtained by Villar et al. (2019) are not fully considered.

The observed variations also remind on the fact that care must be taken when using material data obtained from small samples (sometimes also with poor statistics) when assigning material property data for cementitious materials.

The porosity values presented in Table 3-20 can be compared with the results from modelling of concrete hydration (Idiart et al. 2019a, Table 5-2) which reports a total porosity of only 7.7 % for the *2BMA concrete*. As a comparison, Höglund (2019) assumed a porosity of 11 % for the *2BMA concrete*. Finally, Table 5-4 reports total porosity values for standard concrete with varying w/c ratios. From this table, the porosity of standard concrete with the same w/c ratio as the *2BMA concrete* is about 14 %. However, this value is probably too high since the presence of large amounts of limestone filler is not considered. See also Section 5.1.3 for more information on porosity for the different types of concrete.

### 3.3.4 2BMA concrete for inner walls

#### *Function and requirements*

The *2BMA concrete for inner walls* will be used for construction of the inner walls of the concrete caissons in 2BMA. The main requirements of the *2BMA concrete for inner walls* include high strength, setting a high pH value, which limits corrosion of steel and gas production caused by microbial activity and provide good sorption capacity for radionuclides.

#### *Mixing proportions*

The mixing proportions of the *2BMA concrete for inner walls* will be dependent on the choice of construction method for the inner walls. As an example, the use of prefabricated elements will require different mixing proportions than if the walls are constructed by means of traditional casting of slip forming. It is however, expected that granitic aggregates and a cement with a low $C_3A$ content will be used in order to provide sufficient sulphate resistance.

#### *Mineral composition of the hardened concrete*

The mineral composition of the *2BMA concrete for inner walls* will resemble that of the *2BMA concrete* or the *Silo concrete* depending on whether filler materials are used or not. See Sections 3.3.1 and 3.3.3 for details.

#### *Properties of the hardened concrete*

The properties of the hardened *2BMA concrete for inner walls* will be similar to those of the *Silo concrete* or the *2BMA concrete*. See Sections 3.3.1 and 3.3.3 for details.

### 3.3.5 1BRT self-compacting concrete

#### *Function and requirements*

The *1BRT self-compacting concrete* will be used for construction of the inner walls between the waste packages in 1BRT. These walls will be constructed after emplacement of the waste by means of filling the slits between the waste packages.

The main requirements of the *1BRT self-compacting concrete* include high strength, low hydraulic conductivity and effective diffusivity but the concrete should also set a high pH value, which limits corrosion of steel and gas production caused by microbial activity and provide good sorption capacity for radionuclides. In addition, self-compacting properties concrete ensure that the slits between the waste packages will be entirely filled with concrete without the need for concrete poking. This reduces the radiological consequences for the staff performing this task.

#### *Mixing proportions*

The mixing proportions of the *1BRT self-compacting concrete* have not yet been decided. However, it is expected that granitic aggregates and a cement with a low $C_3A$ content will be used in order to provide sufficient sulphate resistance.

Pettersson (2017) discusses the requirements for the *1BRT self-compacting concrete* and suggests the following mixing proportions, Table 3-21.

**Table 3-21. Suggested mixing proportions for the *1BRT self-compacting concrete* (Pettersson 2017).**

| Component | Product/ Manufacturer | Amount (kg/m$^3$) |
|---|---|---|
| Cement | | 350 |
| Filler | Limestone, fly ash, slag. | Not specified |
| w/c | | 0.5 |
| Water/ powder* | | 0.3 |
| Aggregates 8–12/16 mm | Crushed rock | 30–40 % of total aggregates |
| Aggregates 0–8 mm | Crushed rock or sand | 60–70 % of total aggregates |
| Superplasticiser | | Accepted |

* Powder also includes the filler material and not only the cement.

#### *Mineral composition of the hardened concrete*

The mineral composition of the *1BRT self-compacting concrete* is uncertain. However, it is expected that the mineral composition of the *1BRT self-compacting concrete* will be similar to that of the *Silo concrete* or the *2BMA concrete* depending on if large amounts of limestone fillers are used or not.

#### *Properties of the hardened concrete*

According to Pettersson (2017), the mixing proportions recommended in Table 3-21 corresponds to class C32/40 with an expected 28 days compressive strength of about 47 MPa. However, from Svensk Byggtjänst (2017, Table 12.4:4) a w/c ratio of 0.5 corresponds to class C35/45 with an expected 28 days compressive strength of 52 MPa. Finally, from the similar mixing proportions, the properties of the *1BRT self-compacting concrete* should be similar to those of the *2BMA concrete*, Tables 3-19 and 3-20.

### 3.3.6 BTF tank concrete

#### *Function and requirements*

The *BTF tank concrete* is used for manufacturing of the concrete tanks.

The main requirements of the *BTF tank concrete* include high strength, low hydraulic conductivity and effective diffusivity but the concrete should also set a high pH value, which limits corrosion of steel and gas production caused by microbial activity and provide good sorption capacity for radionuclides.

#### *Mixing proportions*

The requirements in the drawings of the tank state that the *BTF tank concrete* should correspond to class C30/37.[29] According to Svensk Byggtjänst (2017) this would require a w/c ratio of 0.59. However, according to information obtained from the manufacturer of the concrete tanks (Norvatek), the maximum w/c for the concrete used is 0.55 (Class C32/40) but the information also shows that the concrete actually used has a w/c ratio of about 0.42 corresponding to class C45/55.

The present mixing proportions of the *BTF tank concrete* are shown in Table 3-22. However, because the concrete tanks have been produced over a period of at least 30 years, it is expected that different concrete mixing proportions have been used for the tanks currently in storage in 1–2BTF due to the varying availability of cement types and admixtures. However, no information on previously used concrete mixing proportions has been obtained.

**Table 3-22. Mixing proportions for the *BTF tank concrete* provided by the manufacturer of the concrete (St. Eriks 2021).[30]**

| Component | Product/manufacturer | Amount (kg/1 000 kg) |
|---|---|---|
| Cement | Bascement Slite | 202 |
| Water | Tap water | 85.0 |
| w/c | | 0.421 |
| Aggregates 0–2 mm | | 50 |
| Aggregates 0–8 mm | | 300 |
| Aggregates 8–16 mm | | 360 |
| Superplasticiser | Sika VS-1 | 1.20 |
| Air entraining agent | Sika Aer-s | 0.40 |

[29] SKBdoc 1569083, ver 0.1. (Internal document, in Swedish.)

[30] St. Eriks 2021. Recept nr 51, halvflyt lagringstank. (Internal document, in Swedish.)

### *Mineral composition of the hardened concrete*

The mineral composition of concrete based on *Bascement Slite* has been reported by Idiart et al. (2019a). The results presented in Table 3-23 are based on the use of the first generation of *Bascement Slite* (Table 3-6) and a w/c ratio of 0.47. The complete list of minerals is found in Idiart et al. (2019a, Table 5-2).

**Table 3-23. Calculated mineral composition and porosity of the *BTF tank concrete* (Idiart et al. 2019a).**

| Mineral phases | Amount (mol/dm$^3$) |
|---|---|
| **Cement minerals** | |
| Portlandite | 0.826 |
| Hydrotalcite OH | 0.059 |
| Calcite | 0 |
| Monocarboaluminate | 0.063 |
| Ettringite | 0.013 |
| C-S-H Jennite | 1.000 |
| C-S-H Tobermorite | 0.142 |
| C-A-S-H 1.25 | 0.194 |
| Porosity | 0.088 |
| **Aggregates** | |
| Inert fraction | 0.714 |

### *Properties of the hardened concrete*

Even though no data on the properties of the *BTF tank concrete* have been obtained, reasonable estimates of the porosity, pH and mechanical strength can be obtained from the mixing proportions presented in Table 3-22.

According to Svensk Byggtjänst (2017, Table 12.4:4) the 28 days compressive strength of concrete with a w/c ratio of 0.59 and 0.42 (corresponding to classes C30/37 and C45/55) is about 44 and 62 MPa respectively.

Considering the transport properties, Idiart et al. (2019a) show that the porosity of cement paste based on *Bascement Slite* is somewhat lower than that of cement paste based on *Anläggningscement Degerhamn* for a similar w/c ratio.

For standard concrete without cracks and other hydraulically permeable zones, the transport properties will be controlled by the total porosity, the pore size distribution and the connectivity of the pore system in the cement paste and the interface between the cement paste and the aggregates. For concrete based on *Bascement Slite* and *Anläggningscement Degerhamn*, these properties are expected to be similar enough to assess that also the transport properties will be within the same range even though the mineral distribution differs somewhat.

The chemical properties of the concrete pore water will be affected by the presence of portlandite (Table 3-23) which will set pH to 12.5 once the alkali hydroxides have been leached. A summary of the mineral composition of different cement types after hydration showing the influence of fly ash addition can be found in Idiart et al. (2019a, Table 4-14).

Based on the discussion above, Table 3-24 summarises the expected properties of the *BTF tank concrete*.

**Table 3-24. Expected properties of the hardened *BTF tank concrete*.**

| Property | Unit | Value |
|---|---|---|
| Bulk density | kg/m$^3$ | 2 500 |
| Compressive strength | MPa | 45–60 |
| Average porosity | % | 10–11 |
| Hydraulic conductivity | m/s | $10^{-12}$–$10^{-11}$ |
| Effective diffusivity | m$^2$/s | $(1–5) \times 10^{-12}$ |

### 3.3.7 SFR mould concrete

#### *Function and requirements*

The *SFR mould concrete* is used for manufacturing of the concrete moulds. The main requirements of the *SFR mould concrete* include high strength, low hydraulic conductivity and effective diffusivity but the concrete should also set a high pH value, which limits corrosion of steel and gas production caused by microbial activity and provide good sorption capacity for radionuclides.

#### *Mixing proportions*

The detailed mixing proportions of the *SFR mould concrete* are not known. Information on drawings indicates concrete class C30/37 or similar with a w/c ratio of about 0.5.[31] Older drawings indicate concrete class K40 T. It should be noted that at least some of the concrete moulds are manufactured by the same company that manufactures the concrete tanks.

Based on this, it is assumed that the mixing proportions for the *SFR mould concrete* are similar to those of the *BTF tank concrete*, Section 3.3.6. However, because the concrete moulds have been produced over a period of more than 30 years, the mixing proportions of the *SFR mould concrete* will have varied over time as a consequence of availability of cement types and admixtures.

#### *Mineral composition of the hardened concrete*

From the previous section, the mineral composition of the *SFR mould concrete* have probably varied in accordance with that of the *BTF tank concrete* over the more than 30 years of production. See Section 3.3.6 for details.

#### *Properties of the hardened concrete*

Also the properties of the hardened *SFR mould concrete* have probably varied in accordance with those of the *BTF tank concrete* over the more than 30 years of production. See Section 3.3.6 for details.

### 3.3.8 BTF backfill concrete

#### *Function and requirements*

The *BTF backfill concrete* will be used to fill the gap between the waste packages and the rock walls in 1–2BTF at closure.

The main requirements of the *BTF backfill concrete* include high strength, low hydraulic conductivity and effective diffusivity but the concrete should also set a high pH value, which limits corrosion of steel and gas production caused by microbial activity and provide good sorption capacity for radionuclides. Finally, self-compacting properties will be beneficial in order to ensure a high degree of filling of this volume without the need for concrete poking during casting.

[31] SKBdoc 1671610, ver 0.1. (Internal document, in Swedish.)

#### *Mixing proportions*

The mixing proportions of the *BTF backfill concrete* have not yet been decided. However, from the similar requirements, it is expected that the mixing proportions of the *BTF backfill concrete* will be similar to those of the *1BRT self-compacting concrete* (Section 3.3.5).

#### *Mineral composition of the hardened concrete*

Based on the expected similar mixing proportions for this material and the *1BRT self-compacting concrete* it is expected that the mineral composition of these two materials will also be similar.

#### *Properties of the hardened concrete*

The most important properties of the hardened *BTF backfill concrete* are high strength, high pH, low hydraulic conductivity and low effective diffusivity. A detailed specification has not yet been formulated but it is assumed that the properties of the *BTF backfill concrete* will be similar to those of the *1BRT self-compacting concrete* (Section 3.3.5) even though the final mixing proportions may differ somewhat.

### 3.3.9 SFR shotcrete

#### *Function and requirements*

The *SFR shotcrete* is used to provide additional stability to the rock walls and roof in the tunnels and waste vaults and to prevent rock fall-out during the operational period.

#### *Mixing proportions*

No information on the mixing proportions of the shotcrete used in SFR1 has been found. However, Gaucher et al. (2005) presents the following details with reference to Anders Carlsson at Swedpower but it is unclear if this is written or oral information.

- Cement type: Anläggningscement with similar composition as *Anläggningscement Degerhamn.*
- Total porosity: 15 %.
- Fibres: 18 mm and 30 mm steel fibres, in total 1 % by shotcrete volume.
- Thickness: 80–120 mm in the roof and 50 mm on the walls.

Due to current lack of information, it is in this report assumed that the mixing proportions of the shotcrete in SFR3 will be similar to those of the shotcrete used in SFR1.

#### *Mineral composition of the hardened shotcrete*

Based on the information above, Gaucher et al. (2005) calculated the mineral composition of the *SFR shotcrete* at the time of closure of the repository, Table 3-25. Note that the majority of the mineral volume constitutes the inert aggregate materials and unreactive fibres.

**Table 3-25. Mineral composition of the *SFR shotcrete* at the time of closure (Gaucher et al. 2005).**

| Mineral | Amount ($cm^3$) | Amount (Volume %) |
|---|---|---|
| Quartz | 380.78 | 41.3 |
| Albite | 177.78 | 19.3 |
| K-feldspar | 156.50 | 17.0 |
| CSH_1.8 | 127.57 | 13.9 |
| Portlandite | 29.70 | 3.22 |
| Ettringite | 15.24 | 1.65 |
| Biotite | 12.80 | 1.39 |
| Hydrogarnet | 8.4 | 0.91 |
| Unreactive fibres | 8.00 | 0.87 |
| Hydrotalcite | 2.13 | 0.23 |
| Magnetite | 1.97 | 0.21 |
| Friedel's salt | 0.35 | 0.04 |

### *Properties of the hardened shotcrete*

No protocols including material investigations of the hardened *SFR shotcrete* have been found and data from the time of construction of SFR1 is therefore not available. However, from controls carried out since the start of operation of SFR, detailed information on the current status of the shotcrete can be obtained.

During 2011 and 2021–2022, Lundin (SKBdoc 1390675 ver 1.0, internal document, in Swedish) and Holmberg (SKBdoc 1991682 ver 0.1, internal document, in Swedish) investigated the status of the shotcrete in tunnels and waste vaults in SFR and the results are summarised in Table 3-26. Results from previous investigations are summarised in Holmberg (SKBdoc 1991682 ver 0.1, internal document, in Swedish) and not included in this report.

**Table 3-26. Properties of the *SFR shotcrete*.**

| | Minimum value | | Maximum value | |
|---|---|---|---|---|
| **Property** | **Lundin 2011[32]** | **Holmberg 2022[33]** | **Lundin 2011[34]** | **Holmberg 2022[35]** |
| Density (kg/m$^3$) | 2 161 | 2 150 | 2 251 | 2 265 |
| Compressive strength (MPa) | 47.5 | 42.8 | 69.6 | 72.6 |
| Fibre content (% by volume) | 0 | 0 | 0.78 | 0.63 |
| Carbonation depth (mm) | 0 | 3 | 52 | 60 |
| Sulphate content (%) | 0.17 | 0.37 | 0.59 | 1.7 |
| Chlorine content (% of cement weight) | 0.07 | < 0.01 | 2.99 | 2.8 |
| Water intrusion (mm) | 3 | 20 | 35 | 47 |
| Adhesion (MPa) | 0.1 | 0.26 | 1.24 | 2.15 |
| Thickness (mm) | 51 | 18 | 130 | 108 |

## 3.3.10 SFR plug concrete

### *Function and requirements*

The *SFR plug concrete* will be used for construction of the concrete plugs that constitute the mechanical constraints for the bentonite sections of the plugs that will be constructed in SFR at closure, Figures 2-35 and 2-36. The *SFR plug concrete* must have a high mechanical strength to withstand the swelling pressure from the adjacent bentonite sections. The chemical properties include the conflicting requirements of high pH in order to prevent corrosion of reinforcement bars (if such are used) and low pH to avoid undesired interactions with the adjacent bentonite sections.

From a construction point of view, the *SFR plug concrete* should be self-compacting because of the expected poor accessibility for concrete poking during pouring. Finally, the maximum temperature during concrete hydration should be as low as possible to prevent cracking due to temperature shrinkage during hydration.

### *Mixing proportions*

The mixing proportions for the *SFR plug concrete* have not yet been decided. However, in order to reduce the risk for cracking during construction, the thermal output during hydration and thus the maximum temperature in the plug must be low. For this reason, it will be preferred to use a concrete with a low cement content. In addition, a cement with coarser grains is preferred over a more fine-grained cement as this reduces the rate of the chemical reactions and thus also the emitted energy per time unit. Finally, granitic aggregates are expected to be used. As examples, Table 3-27 presents two

[32] SKBdoc 1390675 ver 1.0. (Internal documant, in Swedish.)

[33] SKBdoc 1991682 ver 0.1. (Internal document, in Swedish.)

[34] SKBdoc 1390675 ver 1.0. (Internal documant, in Swedish.)

[35] SKBdoc 1991682 ver 0.1, (Internal document, in Swedish.)

representative examples used for the construction of concrete plugs in large-scale experiments in the Äspö hard rock laboratory.

Of the two types of concrete presented in Table 3-27, the concrete for the DOMPLU experiment was a so-called low-pH concrete whereas the concrete for the PROTOTYPE-experiment was a standard concrete without pH-reducing additives. Both these types of concrete are self-compacting.

**Table 3-27. Mixing proportions of two different types of concrete used for the construction of concrete plugs related to the repository for spent nuclear fuel.**

| Component | Amount (Kg/m$^3$) | |
|---|---|---|
| | DOMPLU (Vogt et al. 2009) | PROTOTYPE, Plug II (Dahlström 2009, Table 5-2) |
| Cement | 120 (Anläggningscement Degerhamn) | 400 (Portland cement) |
| Silica fume | 80 (Elkem, Fesil) | - |
| Water | 165 | 192 |
| Filler | 369 (Limus 25, Nordkalk) | 289 (Not specified) |
| Filler | | 100 (Limus 40) |
| Aggregates 0–8 mm | 1 037 (Natural sand) | 746 |
| Aggregates 8–16 mm | 558 (Natural or crushed) | 668 |
| Superplasticiser | 6.38 (Glenium 51, BASF) | Not specified |
| Total | 2 335 | 2 395 |

### *Mineral composition of the hardened concrete*

The mineral composition of the hydrated cement paste of the concrete for DOMPLU (Table 3-27) has been reported by Grandia et al. (2010b), Table 3-28.

**Table 3-28. Calculated volume fractions (%) for the hydrated cement paste of the DOMPLU concrete. (Grandia et al. 2010b)**

| Component | Amount (Volume %) |
|---|---|
| Porosity | 30.167 |
| Silica fume | 8.790 |
| CH | 0.013 |
| CSH | 0.045 |
| $C_3AH_6$ | 4.425 |
| $FH_3$ | 0.429 |
| PozzCSH | 45.208 |
| Aggregate | 10.000 |

For the PROTOTYPE concrete, the mixing proportions show significant similarities with the *2BMA concrete* which implies that the mineral composition should also be similar; see Table 3-18.

### *Properties of the hardened concrete*

Table 3-29 presents the properties of the materials specified in Table 3-27 as examples of concrete for large concrete plugs. It is expected that the properties of the *SFR plug concrete* will be similar to these two materials.

**Table 3-29. Properties of two different types of concrete used for the construction of concrete plugs related to the repository for spent nuclear fuel. The values presented here are average values of the results presented in the references.**

| Property | Unit | DOMPLU | Reference | PROTOTYPE | Reference |
|---|---|---|---|---|---|
| Density | Kg/m$^3$ | 2 356 | Magnusson and Mathern (2015) | 2 400 | Dahlström (2009) |
| Compressive strength (28 days) | MPa | 64.3 | Magnusson and Mathern (2015) | 75.3 | Dahlström (2009) |
| Compressive strength (90 days) | MPa | 86.5 | Magnusson and Mathern (2015) | Not specified | |
| Tensile splitting strength (28 days) | MPa | 5.8 | Magnusson and Mathern (2015) | Not specified | |
| Tensile splitting strength (90 days) | MPa | 6.4 | Magnusson and Mathern (2015) | Not specified | |
| pH in porewater | | < 11 | Vogt (2019) | ≥ 13 | Known for standard concrete |

### 3.3.11 SFR borehole concrete

#### *Function and requirements*

The *SFR borehole concrete* is used in the concrete plugs that constitutes one of the components in the concept for borehole sealing (Figure 2-38) using e.g. the equipment shown in Figure 3-4. The main function of the concrete plugs in boreholes is to prevent erosion or expansion of the hydraulically tight bentonite sections. The *SFR borehole concrete* must therefore have a reasonably high compressive strength and a low shrinkage to ensure good adhesion and a tight interface towards the adjacent borehole wall. Also, the pH in the porewater must be low to prevent undesired interactions with the adjacent bentonite. Finally, the fresh concrete must be rather flowable with a high stability to prevent separation if in contact with water in the borehole during pouring and hydration.

***Figure 3-4.*** *The drill-rig used when sealing an investigation bore-hole at the Äspö hard rock laboratory. For further details, see Sandén et al. (2018).*

### *Mixing proportions*

The mixing proportions of the *SFR borehole concrete,* Table 3-30, is reported in Pusch and Ramqvist (2004, Appendix 1). The low cement content ensures that a sufficiently large part of the material will remain after leaching of the cement minerals and the addition of silica ensures a low pH in the porewater.

**Table 3-30. Mixing proportions of the SFR borehole concrete (Pusch and Ramqvist 2004, Appendix 1).**

| Component | Amount (kg/m$^3$) |
|---|---|
| Cement (Aalborg White cement) | 60 |
| Water | 150 |
| Silica Fume (Elkem) | 60 |
| Finely ground $\alpha$-quartz (Sibelco) | 200 |
| Finely ground cristobalite quartz (Sibelco) | 150 |
| Superplasticiser (Glenium 51) | 4.38 (dry weight) |
| Aggregates (Underås, natural sand) | 1679 |

As shown in Figure 3-5 the *SFR borehole concrete* is highly flowable with the properties of self-compacting concrete.

### *Mineral composition of the hardened concrete*

No information of the mineral composition of the hardened *SFR borehole concrete* using the mixing proportions shown in Table 3-30 has been found. However, because of the low cement content, only 60 kg/m$^3$, the majority of the minerals will be inert minerals such as quartz and other granitic aggregate minerals whereas the amount of cement minerals will be low.

***Figure 3-5.*** *Measurement of the flowability of the* ***SFR borehole concrete*** *(left image) and testing of concrete pouring using the drill tube (right image).*

#### *Properties of the hardened concrete*

The following properties of the hardened *SFR borehole concrete* is reported in Pusch and Ramqvist (2004, Appendix 1).

- Strength: For one day curing, the cube strength is on the order of 1 MPa at 10–20 °C and for two days curing time it is 1.9 MPa at 5 °C and 4.5 MPa at 20 °C.
- Shrinkage/expansion: Shrinkage will take place in the first month yielding a gap between rock and concrete of less than 10 μm, but it is followed by expansion that will eventually almost close the gap.
- Pore size: The porosity is about 0.6 and the maximum void size less than a few tens of micro meters, which ensures that clay particles cannot penetrate the concrete.

From Pusch and Ramqvist (2004, Appendix 1) the following information is obtained, Table 3-31.

**Table 3-31. Evolution of compressive strength for *SFR borehole concrete* (Pusch and Ramqvist 2004, Appendix 1).**

| Curing time in days | 5 °C Cube strength (MPa) | 20 °C Cube strength (MPa) |
|---|---|---|
| 2 | 1.9 | 4.5 |
| 3 | 4 | 6.6 |
| 7 | 7.5 | 10.6 |
| 28 | 14 | 40 |
| 72 | 32 | 55.2 |
| 91 | 35.4 | 57.4 |

Leaching experiments reported in Pusch and Ramqvist (2004, Appendix 1) showed that pH in the leachate varied between 8.98 and 10.38.

### 3.3.12 Alternative SFR borehole concrete

As an alternative to the *SFR borehole concrete*, the use of a commercial ready-made concrete for casting under-water is currently being discussed. A few different alternatives from different manufacturers are available but no details can be presented at this stage. Also, information concerning the detailed mixing proportions of such products are difficult to obtain due to company secrets.

In tests reported by Mårtensson (2019) standard concrete for under-water casting was successfully used for casting a concrete plug at a depth of about 200 meters in a water-filled borehole.

## 3.4 Grouts

In SFR, different types of cementitious grouts have been used, are used and will be used in the future. The mixing proportions of the materials previously used or used today are reasonably well known but some information is missing. This is either because information has been lost since the time of use or that information has not been provided by the manufacturer when e.g. type of cement used in the production plant has been changed.

Regarding materials for future use, requirements have in some cases not yet been specified and the mixing proportions therefore not yet decided.

In this section, the mixing proportions and properties of all types of grout used or planned for use in SFR are presented. For the types of grout for which the mixing proportions are not known, the presented mixing proportions are based on the predicted requirements which in turn are based on the application in which the material in question is planned for use.

### 3.4.1 Original silo grout

#### *Function and requirements*

The primary function of the *Original silo grout* is to stabilise the stack of waste packages in the silo. The grout also has to be sufficiently permeable in order to permit the transport of any gases formed through the different degradation processes occurring inside the concrete silo.

#### *Mixing proportions*

The *Original silo grout* was designed by Björkenstam (1997), Table 3-32. However, grouting of waste packages in the silo was carried out also earlier using a grout (here denominated *Reference grout*) with significantly different mixing proportions, in particular a much lower cement content. The mixing proportions of this grout are shown in the rightmost column in Table 3-32. However, as this grout was used during only a short period of time and also because the number of waste packages grouted with this grout is unknown it is not discussed further in this report. It must also be stated that the very high w/c ratio of the *Reference grout* and the low amount of cellulose added implies that the *Reference grout* must have been very sensitive to separation and therefore less suitable in this application. No reports on this issue have though been found.

Initially, the *Original silo grout* was based on the use of *Anläggningscement Degerhamn* but since the closing of the Degerhamn plant in 2019, *Anläggningscement Slite Standard* P has been used instead.

In order to obtain a high hydraulic conductivity, a high w/c is required. However, this introduces stability issues of the grout with a risk of separation and bleeding. In order to mitigate these risks, a cellulose derivative is added in order to improve the stability of the fresh grout. However, the addition of cellulose also requires that an anti-foaming agent is added in order to prevent extensive foaming.

During the first 25 years of operation, the *Original silo grout* was mixed locally in SFR from its components. However, from about 2014 and onward it has been produced at a local concrete production plant.

**Table 3-32. Mixing proportions of the *Original silo grout* and the *Reference grout* used as a starting point in the development of the *Original silo grout*. (Björkenstam 1997).**

| Component | Product | Original silo grout (kg/m$^3$) | Reference grout (kg/1 000 kg dry material) |
|---|---|---|---|
| Cement | Anläggningscement Degerhamn | 325 | 170 |
| Aggregates | Baskarp B70 (Natural sand) | 1 302 | 830 |
| Anti-foaming agent | Foamaster PD-1 | 2 kg/ton dry material | 2 kg |
| Cellulose | Methocel ME 0975 | 2 kg/ton dry material | 2 kg |
| Water | Tap water | 366 | 228,5 |
| w/c | | 1.125 | 1,34 |

#### *Mineral composition of the hardened grout*

Gaucher et al. (2005) have modelled the mineral composition of the *Original silo grout*, also including the aggregates, at the time of closure of the repository, Table 3-33. Note that most of the mineral volume comprises inert aggregate minerals with Quartz, K-feldspar and Albite being the dominant.

**Table 3-33. Calculated mineral composition of the *Original silo grout* at the time of closure of the repository (Gaucher et al. 2005).**

| Mineral | Amount ($cm^3$) | Amount (Volume %) |
|---|---|---|
| Quartz | 316.75 | 44.44 |
| K-feldspar | 130.18 | 18.26 |
| CSH_1.8 | 106.11 | 14.89 |
| Albite | 97.98 | 13.75 |
| Portlandite | 24.80 | 3.48 |
| Ettringite | 15.58 | 2.19 |
| Biotite | 10.65 | 1.49 |
| Hydrogarnet | 7.02 | 0.98 |
| Hydrotalcite | 2.09 | 0.29 |
| Magnetite | 1.64 | 0.23 |

### *Properties of the hardened Original silo grout*

The required properties of the hardened *Original silo grout* are shown in Table 3-34 (Björkenstam 1997) together with average values from statistics from grout production control. Table 3-34 shows that the 28 days compressive strength varies between 6–12 MPa. The variations of the hydraulic conductivity are large and the compilation shows values from just above the requirement ($0.5 \times 10^{-8}$ m/s) to close to $2\,500 \times 10^{-8}$ m/s, i.e. 5 000 times larger.

No measurements of the total porosity of the *Original silo grout* have been found. Instead, the value of 30 % suggested by Höglund (2001) will be used in this work.

**Table 3-34. Properties of the hardened *Original silo grout.***

| Property | Requirement | Production control[36] |
|---|---|---|
| Compressive strength | ≥4.5 MPa | 6–12 MPa |
| Hydraulic conductivity | $\geq 5 \times 10^{-9}$ m/s | $(5–25\,000) \times 10^{-9}$ m/s |

The following comment on the large variations of the hydraulic conductivity can be made. The hydraulic conductivity is measured on samples that have been cast separately in plastic tubes and that sample preparation can have a significant impact on the results. As an example, Thorsell (SKBdoc 1336225 ver 1.0, internal document, in Swedish) showed that some of the specimens shown in Figure 3-6 (left image) contain channels and voids and therefore these specimens have a high hydraulic conductivity whereas other specimens are more homogeneous with a lower hydraulic conductivity. As the specimens have been wetted to illustrate their different porosities, a darker part of the specimen illustrates an area with a higher porosity than the brighter parts.

As a comparison, Figure 3-6 (right image)[37] shows a slit with the same dimensions as the slits in the silo formed between the moulds and the inner walls (width 2.55 m and thickness 75 mm) which has been filled with the *Original silo grout* using a similar method as when the waste is grouted in the silo. The experiment was conducted in order to investigate whether the grout can be released seven meters above the surface of the hardened grout from a previous grouting campaign without separating. The results showed that the grout was free from voids, channels or other imperfections but also that the properties varied somewhat within the slit. Also, measurements of the hydraulic conductivity of specimens from this slit varied in the range $(16–2\,560) \times 10^{-9}$ m/s. However, for a total of 18 specimens 15 had a hydraulic conductivity below $360 \times 10^{-9}$ m/s with only three outliers with a hydraulic conductivity above $1\,500 \times 10^{-9}$ m/s. This shows that the homogeneity of the grout in the slit is considerably better than indicated in production control.

[36] SKBdoc 1400966 ver 1.0. (Internal document, in Swedish.)

[37] SKBdoc 1614170 ver 1.0. (Internal document, in Swedish.)

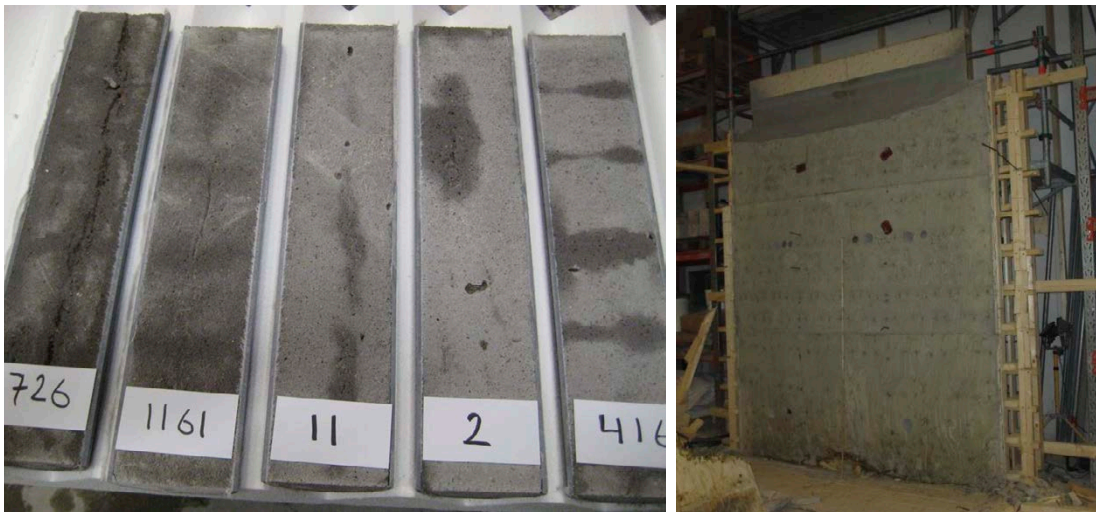


***Figure 3-6.*** *Specimens used to measure the hydraulic conductivity of the* ***Original silo grout*** *which have been cut in half in order to permit the study of the structure of the material (left image). The surfaces of the samples have been wetted and dried shortly in order to more clearly expose areas with higher porosity, thus the colour difference in the samples.*[1] *The right image shows a slit with the same dimensions as the slit between the waste packages and the inner walls in the silo which has been filled with the* ***Original silo grout****.*[2]

### 3.4.2 New silo grout

#### *Function and requirements*

The function and requirements of the *New silo grout* are the same as those of the *Original silo grout* described in the previous section with the addition that the *New silo grout* should not contain any organic additives such as cellulose or cellulose derivatives.

#### *Mixing proportions*

The mixing proportions of the *New silo grout*, Table 3-35, were designed by Lagerlund and Holmberg (2021) and up-scaled to production scale by Holmberg and Lagerlund (2021). As a final test, the grout was used in a simulated production environment also including sampling and evaluation of grout stability under the conditions prevailing in the silo during grouting (Holmberg 2021).

**Table 3-35. Mixing proportions of the *New silo grout*. (Holmberg and Lagerlund 2021).**

| Component | Product | Amount (kg/m$^3$) |
|---|---|---|
| Aggregates | Natural sand 0–4 mm | 1 303.7 |
| Cement | Anläggningscement Slite standard P | 319.7 |
| Bentonite | DantoCon Pure C | 17.9 |
| Water | Tap water | 398.2 |
| w/c | | 1.25 |

[1] SKBdoc 1336225 ver 1.0. (Internal document, in Swedish.)

[2] SKBdoc 1614170 ver 1.0. (Internal document, in Swedish.)

### *Mineral composition of the hardened grout*

The mineral composition of the *New silo grout* has not been studied. During the design work, *Anläggningscement Slite Standard P* was used and during that stage it was therefore assumed that the mineral composition of the *New silo grout* will resemble that of the *Original Silo grout*. This is because the mineral composition of *Anläggningscement Degerhamn* and *Anläggningscement Slite Standard P* are similar.

However, in May 2022 when the *New silo grout* was first used for grouting of the waste packages in the silo, the concrete production plant informed SKB that they were now instead using *Anläggningscement FA Slite*.

An indication of the impact of this can be obtained by comparing the mineral composition of the *1BMA concrete* and the *BTF tank concrete* in which *Bascement Slite* which has a similar composition as *Anläggningscement FA Slite* are used respectively. See Sections 3.2.8, 3.3.2 and 3.3.6 for details.

### *Properties of the hardened grout*

The required properties of the hardened *New silo grout* are the same as those of the *Original Silo grout*.

Statistics from the development work compiled by Holmberg (2021) show that the average compressive strength of the *New silo grout* varied between 6.2 and 9.3 MPa whereas the average hydraulic conductivity varied between $13.3 \times 10^{-9}$ and $361 \times 10^{-9}$ m/s, Table 3-36. Some of the variations can be explained by minor differences in the mixing proportions and methods used for mixing but all results were within the requirements. Figure 3-7 also shows that the *New silo grout* was stable and no separation or other inhomogeneities were observed after pouring the grout into a slit in which the grout was allowed to fall a maximum of seven meters.

***Figure 3-7.*** *The photograph shows the* ***New silo grout*** *after pouring the grout into a slit with the same dimensions as the slit between the waste packages and the inner walls in the concrete silo. The distance between the container from which the grout was released and the floor shown in this picture was seven meters. (Holmberg 2021).*

**Table 3-36. Properties of the *New silo grout*.**

| Property | Requirement | Data from the development work | Data from production control |
|---|---|---|---|
| **Reference** | | **(Holmberg 2021)** | **See footnote[38]** |
| Compressive strength | >4.5 MPa | 6.2–9.3 MPa | 4.5–6.4 |
| Hydraulic conductivity | $>5\times10^{-9}$ m/s | $(13.3–361)\times10^{-9}$ m/s | $(9.84–449)\times10^{-9}$ m/s |

## 3.4.3 BTF grout

### *Function and requirements*

The *BTF grout* is used for grouting of the steel drums in 1BTF during operation in order to improve the stability of the stack. It may be used also for grouting of the concrete tanks in both 1BTF and 2BTF at closure of the repository but the material in that application has yet to be decided.

The requirements of the *BTF grout* are unknown. This is because no documents have been found in which the requirements of the *BTF grout* are described but also because no tests are carried out during grout production or grouting.

### *Mixing proportions*

The mixing proportions of the *BTF grout* (Table 3-37) were probably developed by Vattenfall R&D during the late 1980's or early 1990's but no documentation from the development work has been found. As mentioned in Section 3.2.3, *Slite standard P* has not been produced since about the year 1999. For that reason, other types of cement must have been used during the period 1999 to 2021 when Ingvarsson (2021, personal communication) informed that *Anläggningscement Slite Standard P* was used for production of the *BTF grout* that was used in the 2021 grouting campaign.

**Table 3-37. Mixing proportions for the *BTF grout*.[39]**

| Component | Product | Amount (kg/m$^3$) |
|---|---|---|
| Aggregates | Tierp (Natural sand) | 1001 |
| Cement | Slite Std P. or similar | 523 |
| Silica | Elkem Materials | 21 |
| Bentonite | Brebent | 25 |
| Water | Tap water | 424 |
| w/c | | 0.81 |

### *Mineral composition of the hardened grout*

No studies have been found that presents the mineral composition of the hardened *BTF grout*. However, as the type of cement used during about 20 years of grouting is unknown, any modelling or experimental studies would be rather uncertain.

### *Properties of the hardened BTF grout*

As mentioned above, no documentation from the development of the *BTF grout* has been found and for that reason the original requirements are unknown. Also, because no material testing is carried out during grouting, no data on the properties of the hardened *BTF grout* are available.

However, based on the mixing proportions presented in Table 3-37 it can be assumed that the *BTF grout* will have a pH of about 13 at closure of the repository due to the presence of the alkali hydroxides in the cement paste. Also, the amount of portlandite should be high as the amount of silica is not

[38] SKBdoc 1400966 ver 1.0. (Internal document, in Swedish.)

[39] SKBdoc 1211064 ver 2.0. (Internal document, in Swedish.)

sufficient to convert all portlandite to CSH. For that reason, pH can be expected to be about 12.5 over an extended period of time.

According to Svensk Byggtjänst (2017, Table 12.4:4) a w/c ratio of 0.8 corresponds to class C20/24 with a 28 days compressive strength of about 31 MPa.

The high w/c ratio will result in a reasonably high porosity whereas the effects on the hydraulic conductivity will be less pronounced. From Svensk Byggtjänst (2017, Table 10.5:1) the porosity of concrete with a w/c ratio of 0.85 is 0.155. From Table 5-6 a hydraulic conductivity in the range of $1–5 \times 10^{-12}$ m/s can therefore be expected.

### 3.4.4 2BMA grout

#### *Function and requirements*

The *2BMA grout* will be used to fill the channels in the lid of the concrete caissons that constitute parts of the gas evacuation system. The gas evacuation system should prevent the formation of a large gas bubble inside the caissons and gases should be transported out of the caissons at a low enough pressure to prevent cracking of the outer walls due to an elevated pressure inside the caissons. The *2BMA grout* should therefore have a high enough hydraulic conductivity for efficient transport of any gases formed inside the caissons.

#### *Mixing proportions*

At present, the detailed requirements for the *2BMA grout* have not been formulated. However, at this stage it is reasonable to assume similar mixing proportions as the *New silo grout*, Table 3-35.

#### *Mineral composition of the hardened grout*

The mineral composition of the *2BMA grout* is controlled by the chemical composition of the cement as well as the type of bedrock used to produce the aggregates. A reasonable assumption is that the aggregates will be produced from granitic bedrock or natural sand with a granitic origin and also that the aggregates will constitute 65–80 % of the solid minerals in the grout.

The remaining part of the solid minerals in the *2BMA grout* comprises the cement minerals whose detailed mineral composition is determined by the composition of the raw material used to produce the cement clinker as well as any additives such as gypsum, fly ash or other supplementary cementitious materials.

#### *Properties of the hardened grout*

The properties of the hardened *2BMA grout* are expected to be similar to those of the *New silo grout*, Section 3.4.2.

### 3.4.5 SFR injection grouts

#### *Function and requirements*

The *SFR injection grouts* are used for grouting of the fracture system in the bedrock during excavation of the facility in order to reduce the inflow of groundwater into the tunnels and waste vaults during the operational period.

The *SFR injection grouts* should have a high penetrability in even the smallest of fractures. The setting time should be short in order to prevent that the fresh grout is washed out of the fractures by the groundwater pressure. In order to ensure efficient grouting, various grouts with somewhat different properties and mixing proportions may be used.

### *Mixing proportions*

The mixing proportions of injection grouts mainly comprise fine-grained cement and water with optional admixtures where the required properties determine the w/c ratio as well as types and amounts of additives. Typically, the w/c ratio may vary between about 0.5 and 0.9 depending on application and properties of the fracture network in the bedrock. However, from Christiansson (1987) and Christiansson and Bolvede (1985)[40] detailed information from grouting in SFR1 show that many different grouts with a w/c ratio ranging from one (1) to five (5) were used during construction of SFR1 and that both *Anläggningscement Degerhamn* and fast setting cement were used.

Brantberger and Jansson (2009) suggests the use of three different low-pH injection grouts in the repository for spent fuel which could also be used during construction of SFR3, Table 3-38.

**Table 3-38. Suggested mixing proportions for three different low-pH grouts for grouting of fractures in the bedrock in the repository for spent nuclear fuel. (Brantberger and Jansson 2009, Appendix C)**

| Component | Relative amounts in fresh grout by weight | | |
|---|---|---|---|
| | Injection grout | Plug grout | Stop grout |
| Water | 1.68 | 0.8 | 0.64 |
| Cement | 1.0 | 1.0 | 1.0 |
| Silica | 1.37 | 1.38 | 1.37 |
| Superplasticiser | 0.07 | 0.07 | 0.07 |
| Water/ dry material | 1.4 | 0.9 | 0.82 |

Table 3-39 suggests mixing proportions for the corresponding materials without the low-pH requirement which could be used for grouting of the fractures in SFR3 during excavation of the facility.[41] These materials are considered a more likely choice for SFR than those presented in Table 3-38. This is because experiences from low-pH materials in a production environment are scarce compared to those from using standard materials.

**Table 3-39. Suggested mixing proportions for three different conventional grouts for grouting of fractures in the bedrock in SFR.[42]**

| Component | Relative amounts in fresh grout | | |
|---|---|---|---|
| | Injection grout | Plug grout | Stop grout |
| Water | 0.8 | 0.5 | 0.7 |
| Cement (Injektering 30)* | 1.0 | 1.0 | 1.0 |
| Accelerator | 0.04 | - | - |
| w/c | 0.8 | 0.5 | 0.7 |

* Injektering 30 is a fine grained cement manufactured in Degerhamn and has a similar composition as *Anläggningscement Degerhamn* (Cementa AB 2023).

### *Mineral composition of the hardened grout*

The mineral composition of the hardened *SFR injection grouts* is determined by the composition of the binder as no aggregates are used. Here, the mineral composition of a conventional grout is only dependent on the type of cement used in this application. For a compilation of the clinker composition of different types of cement, see Table 3-9.

[40] Christiansson R, Bolvede P, 1985. Byggnadsgeologisk uppföljning, slutrapport. SKB SFR 85-04, Svensk Kärnbränslehantering AB. (Internal document in Swedish.)

[41] SKBdoc 1716704 ver 1.0. (Internal document, in Swedish.)

[42] SKBdoc 1716704 ver 1.0. (Internal document, in Swedish.)

For the low-pH grouts suggested by Brantberger and Jansson (2009) the mineral composition will also be influenced by the addition of large amounts of silica. This addition will consume the portlandite and instead form additional amounts of CSH. This reduces the pH in the grout pore water to below 11 once the grout has been depleted from the alkali hydroxides.

#### *Properties of the hardened grout*

The properties of the hardened *SFR injection grouts* are controlled by the w/c ratio and by the type of cement used. The properties can be tested by means of casting of specimens for production control during the injection work but it will be impossible to determine the properties of the grout inside the fractures.

### 3.4.6 SFR grout for rock bolts

#### *Function and requirements*

The *SFR grout for rock bolts* is used to fill the holes in the bedrock in which the rock bolts are installed. The main functions of the *SFR grout for rock bolts* are to secure the rock bolts in the bedrock as well as to provide a favourable chemical environment that prevents corrosion of the rock bolts.

#### *Mixing proportions*

The grouts for rock bolts mainly comprise fine-grained cement and water with optional admixtures where the required properties determine the w/c ratio as well as types and amounts of admixtures.

Eriksson et al. (2009) suggest mixing proportions for a low-pH grout for rock bolts in the repository for spent fuel, Table 3-40, which could be used also in SFR in the case its properties are found to be better than the conventional grout. However, in order to ensure a high enough pH to protect the rock bolts from corrosion, a conventional grout without the addition of silica as shown in the right-most column in Table 3-40 should preferably be used. Also, the use of low-pH grout for rock bolts is hampered by the lack of experience from the use of such materials in tunnel production.

Bogdanoff (2013) reports with reference to Martna and Jansson[43] that the grout for rock bolts used during construction of SFR1 had a w/c ratio of 0.27–0.30 but no further information is provided. Unfortunately, the original reference has not been found and the information has therefore not been verified. It should be noted that Bogdanoff (2013) questions the low w/c ratio stipulated and claims that the grout will probably be too stiff for this application.

**Table 3-40. Mixing proportions for grouts for rock bolts.**

| Reference | Low-pH grout (Eriksson et al. 2009) | Conventional grout (Martna and Jansson 1986)[44] |
|---|---|---|
| Component | Amount (kg/m$^3$) | Amount (Relation) |
| Water | 266.6 | 27–30 |
| Cement | 340 | 100 |
| Silica | 226.7 | |
| Filler (Quartz) | 1 324 | |
| Superplasticiser (Glenium 51) | 4 | |

[43] Martna J, Jansson S, 1986. Bedömning och kontroll av bergförstärkningarnas beständighet i SFR. BKU 86:3 SFR 1, Forsmark. (Internal document, in Swedish.)

[44] Martna J, Jansson S, 1986. Bedömning och kontroll av bergförstärkningarnas beständighet i SFR. BKU 86:3 SFR 1, Forsmark. (Internal document, in Swedish.)

#### *Mineral composition of the hardened grout*

The mineral composition of the hardened *SFR grout for rock bolts* is determined by the composition of the binder as no aggregates are used. Here, the mineral composition of the conventional grout used in SFR is only dependent on the type of cement used in this application. However, for SFR1 no information on the type of cement used in the grout for rock bolts has been found.

For the low-pH grout for rock bolts suggested by Eriksson et al. (2009), the mineral composition will also be influenced by the addition of large amounts of silica. This addition will consume basically all portlandite and instead form additional amounts of CSH. In addition, the pH in the porewater will be reduced to about 11 once the material has been depleted from the alkali hydroxides.

#### *Properties of the hardened grout*

The properties of the hardened *SFR grout for rock bolts* are mainly controlled by the w/c ratio and the composition of the binder material. Nominally, standard concrete with a low w/c ratio should have a low hydraulic conductivity and a high compressive strength but this is not necessarily true also for grouts that do not contain any aggregate materials and therefore may be very brittle. However, for the purpose of this report, the properties of the *SFR grout for rock bolts* are estimated from the w/c ratio of the material. For the conventional grout (Martna and Jansson 1986)[45] the low w/c ratio will yield a high compressive strength, a low hydraulic conductivity and a low diffusivity.

### 3.4.7 Cement paste for boreholes

#### *Function and requirements*

The *Cement paste for boreholes* was used for sealing of about ten boreholes in the early 1980's (SKB 1983).

#### *Mixing proportions*

The mixing proportions of the cement paste for boreholes are presented in Table 3-41.

**Table 3-41. Mixing proportions of the *Cement paste for boreholes* (SKB 1983, underbilaga 4:2).**

| Component | Product | Amount |
|---|---|---|
| Cement | Slite standard | Not reported |
| Water | Not Sea water | Not reported |
| Plasticiser | Cementa flyttillsats V33 | 1.5% |
| w/c | | 0.25 |

#### *Mineral composition of the hardened grout*

The clinker composition of the cement (*Slite standard*) is unknown and hence no information about the mineral composition of the hardened *Cement paste for boreholes* is presented. However, it is reasonable to assume that the clinker composition of *Slite standard* resembles that of *Slite Standard P* whose estimated mineral composition is presented in Section 3.2.3.

#### *Properties of the hardened grout*

With a w/c ratio of only 0.25, the *Cement paste for boreholes* should have a low porosity and a high compressive strength. However, the important factors are the properties of the paste in the borehole which are also affected by the method used and the presence of water in the borehole. Both these factors are, however, unknown.

[45] Martna J, Jansson S, 1986**.** Bedömning och kontroll av bergförstärkningarnas beständighet i SFR. BKU 86:3 SFR 1, Forsmark. (Internal document, in Swedish.)

# 4 Processes

## 4.1 Overview

As a basis for the prediction of the post-closure evolution of the properties of the cementitious components, a detailed process understanding is required.

The processes that affect the properties of the cementitious components in SFR are categorised into five groups, i.e. thermal processes (Section 4.1.1), hydraulic processes (Section 4.1.2), mechanical processes (Section 4.1.3), chemical processes (Section 4.1.4), and radionuclide transport (Section 4.1.5).

Following the introduction in Sections 4.1.1 to 4.1.5, Sections 4.2 to 4.21 present the individual processes in more detail. However, a complete description of the scientific background of these processes is beyond the scope of this report. This is instead found in the Waste and Barrier process reports for PSAR (SKB TR-23-03, TR-23-04) and references therein as well as in other reports referred to under each separate heading.

### 4.1.1 Thermal processes

In low- and intermediate-level radioactive waste, heat generating processes, such as radioactive decay and radiation attenuation, are negligible (SKB TR-23-03, Section 3.1.2). The temperature of the cementitious components will therefore be determined by the temperature of the surrounding rock.

As long as the temperature at repository depth is above the freezing point of the porewater in the cementitious materials, the effect of the temperature is negligible. However, if freezing of the porewater occurs, cracks may form. Upon thawing, this may lead to increased groundwater flow in the cracks and reduced capability of the barriers to limit outward transport of radionuclides. This is because slow outward transport of radionuclides is achieved e.g. by ensuring a low flow of groundwater through the engineered barriers and by retarding radionuclide transport relative to this groundwater flow through sorption in the cement matrix.

Further, also thermal processes occurring during construction and the operational period must be considered as these will affect the status of the cementitious components at closure. Among these, the influence of the exothermal chemical reactions in the cement paste during hydration and the subsequent cooling presents the largest risk for cracking. This is discussed in more detail in Section 4.2.

The following thermal processes have been identified and will be discussed further in the indicated sections:

- Heat transport, Section 4.2.
- Phase changes/freezing, Section 4.3.

### 4.1.2 Hydraulic processes

The groundwater flow through the cementitious components is determined by the geometry and hydraulic conductivity of the various components as well as by the groundwater flow in the bedrock surrounding the repository which in turn is influenced by climate conditions and shoreline position.

If gas is also present, a two-phase flow occurs where both the groundwater flow and the gas flow are affected by the relative degree of saturation of the respective phases.

The following hydraulic processes have been identified and will be discussed further in the indicated sections:

- Water uptake and transport under unsaturated conditions, Section 4.4.
- Water transport under saturated conditions, Section 4.5.
- Gas transport/dissolution, Section 4.6.

### 4.1.3 Mechanical processes

Post-closure of the repository, the cementitious components will be subjected to both internal and external mechanical loads, which will give rise to mechanical stresses. As long as the load-bearing capacity of the cementitious components is sufficient, mechanical stresses will not adversely affect their properties. However, if the load-bearing capacity is insufficient, cracks can form with e.g. increased hydraulic conductivity of the cementitious components as a consequence.

The following processes which may cause mechanical stresses in the cementitious components have been identified and will be discussed further in the indicated sections:

- Heat transport, Section 4.2.
- Phase changes/freezing, Section 4.3.
- Pressure from swelling waste, Section 4.7.
- Rock fall-out, Section 4.9.
- Dissolution, precipitation and recrystallisation, Section 4.14.
- Metal corrosion, Section 4.17.
- Gas production, Section 4.18.

### 4.1.4 Chemical processes

Post-closure of the repository, the properties of the cementitious components will be affected by chemical interactions with surrounding groundwater or substances dissolved in the groundwater, either from the bedrock or from the dissolution/decomposition of materials in the waste.

Some processes such as metal corrosion and gas formation may cause cracking of the cementitious components while others mainly affect the mineral composition of the materials. Finally, some processes may affect radionuclide retention, by forming complexing agents or changing the pore-water composition in the materials.

The following chemical processes have been identified and will be discussed further in the indicated sections:

- Advection and dispersion, Section 4.10.
- Diffusion, Section 4.11.
- Sorption, Section 4.12.
- Colloid stability, transport and filtering, Section 4.13.
- Dissolution, precipitation and recrystallisation, Section 4.14.
- Aqueous speciation and reactions, Section 4.15.
- Microbial processes, Section 4.16.
- Metal corrosion, Section 4.17.
- Gas production, Section 4.18.

### 4.1.5 Radionuclide transport

The following processes related to radionuclide transport have been identified and will be discussed further in the indicated sections:

- Speciation of radionuclides, Section 4.19.
- Transport of radionuclides in the water phase, Section 4.20.
- Transport of radionuclides in the gas phase, Section 4.21.

## 4.2 Heat transport

### *Overview*

Heat transport affects the temperature of the cementitious components in the repository and therefore causes the structures to shrink upon cooling or expand due to heating. Under most conditions, shrinkage increases the tensile strain in the materials and thus the risk for formation of cracks, whereas heating normally leads to increased compressive strain and reduced risk of cracking.

Cementitious materials are known for their high compressive strength but instead their tensile strength is poor. In order to increase the tensile strength of concrete structures, significant amounts of reinforcement are used. The ability of a concrete structure to accommodate tensile strain will therefore be dependent on both the properties of the concrete itself, the dimensions of the concrete structure as well as of the amount of reinforcement. The ability to accommodate compressive strain is on the other hand mainly related to the compressive strength of the concrete itself.

Generally, heat transport is considered to mainly be of concern post-closure and particularly with respect to the risk for freezing of the porewater in the cementitious materials during a permafrost, Section 4.3. This is because temperature differences at repository depth are normally small during this period and mainly determined by the temperature of the surrounding rock while the impact of the low- and intermediate-level radioactive waste is considered negligible.

However, two specific cases exist that must be considered and which have been included in this section, namely temperature shrinkage during cement hydration and cooling of the concrete structures caused by the intruding groundwater during saturation of the repository.

Heat transport (cooling of the warm concrete) during cement hydration causes temperature shrinkage and is a well-known cause for the formation of cracks in concrete structures. The risk for severe cracking can be reduced through the use of reinforcement and concrete with a low thermal output. However, also cooling of the raw materials during mixing and/or cooling during and after casting can be utilised.

The importance of carefully considering this process during the construction work has been manifested for 1BMA where a large number of cracks have been observed in the concrete structure as discussed further in Chapter 8.

Cooling of the concrete structure due to intrusion of cooler groundwater during saturation of the repository has been suggested by Höglund (2014) as a possible cause for the formation of cracks in the concrete barriers in the repository. However, the risk for crack formation is dependent on e.g. the dimensions of the concrete structure, the amount of reinforcement and the design of the foundation and not only by the temperature differences involved in this process. For that reason, the impact of this process needs to be evaluated for each individual concrete structure; see also the following section.

### *Expected influence on the properties of the cementitious components*

Post-closure, heat transport is not expected to affect the properties of the cementitious components. The exception is freezing of the porewater if permafrost reaches repository depth. This is discussed in Section 4.3.

Heat transport during construction of the concrete structures is not expected to influence the properties of the structures as long as cracks are not formed. However, the formation of cracks will influence their transport properties as discussed in Section 4.8.

For smaller free-standing concrete structures, temperature shrinkage during construction is of little concern. This is because expansion and shrinkage in such structures are unrestrained and the risk for the build-up of large levels of strain is therefore low.

For larger concrete structures and for concrete structures which are attached to an adjacent component, restrained shrinkage may cause the build-up of large levels of tensile strain. In such cases, compensating methods need to be utilised in order to reduce the maximum temperature differences between adjacent parts and thus also the maximum levels of strain. Such methods involve cooling

of the fresh concrete during and after casting (Grahm et al. 2015) or heating of the previously cast part of the concrete structure as utilised by Mårtensson and Vogt (2020). See these reports for more details.

The influence of cooling of the concrete structure during saturation of the repository is more difficult to assess and is dependent on the detailed design of the concrete structure, the design of the foundation as well as whether shrinkage is restrained as in 1BMA or unrestrained as planned for 2BMA. Here, unrestrained shrinkage is not predicted to induce the formation of cracks whereas the risk for cracking is larger if shrinkage is restrained. However, the judgement also has to include evaluation of the influence of the temperature evolution of the bedrock and foundation on which the concrete structure is founded in order to make a well-justified assessment of the risk for crack formation. This is discussed further for the relevant cementitious components in Chapters 7–15.

## 4.3 Phase changes/freezing

### *Overview*

The resistance of a cementitious material to frost cracking depends on its pore structure and degree of water saturation. The gel pores and capillary pores are quickly filled with water under normal outdoor climate conditions while saturation of the air pores requires water exposure for a more extended period of time.

For the very long time-perspectives related to climate variations and predictions of future permafrost, the time to completely saturate the pore system of the cementitious materials in SFR can be neglected. For that reason, complete saturation of the pore system can be assumed at the time of first possible permafrost at repository depth.

When the porewater freezes to ice, it expands by about 9 % compared to the volume of liquid water. However, the freezing point of concrete porewater decreases with decreasing pore size, Table 4-1. This means that for a porous material such as a cementitious material, at a certain temperature the larger air pores will be filled with ice whereas the smaller capillary pores and gel pores will contain unfrozen water. The greater the proportion of the total amount of porewater that is frozen at a certain temperature, the greater the risk of the concrete being damaged.

**Table 4-1. Freezing point of water confined in pores of different diameter (Svensk Byggtjänst 2000).**

| Pore size (Ångström) | Freezing temperature (°C) |
|---|---|
| ∞ | 0 |
| 1 270 | −2 |
| 440 | −6 |
| 270 | −10 |
| 190 | −15 |
| 150 | −20 |
| 110 | −30 |
| 90 | −40 |

The exact temperature at which a sufficiently large amount of porewater has frozen to cause the formation of cracks in a cementitious material depends on the detailed pore structure of the material as well as – to a lesser extent – the composition of the porewater. The pore structure in turn, depends on the mixing proportions of the material as well as extent of degradation of the material.

### *Expected influence on the properties of the cementitious components in SFR*

A number of studies have been carried out in order to clarify the impact of permafrost on different concrete structures in SFR with particular emphasis on the *Silo concrete* and the *1BMA concrete*.

Emborg et al. (2007) investigated the influence of freezing of the concrete cylinder in the silo and concluded that a large enough part of the porewater would have frozen at a temperature between 0 and −5 °C to cause cracking of the concrete. However, the exact temperature at which cracking could occur was not given.

In a later modelling study, Tang and Bager (2013) concluded that the concrete used in the structures in SFR which are surrounded by a gravel backfill, (both *Silo concrete* and *1BMA concrete*) will not crack as described by Emborg et al. (2007). This conclusion was motivated by the fact that the concrete will be under an external pressure caused by the freezing of water in the gravel backfill outside the concrete structure (Tang 2014, personal communication). Being focused on structures surrounded by a gravel backfill, the conclusions from this study are not valid for the silo which is surrounded by bentonite.

In an experimental study performed by Thorsell (2013), cores extracted from the concrete structure in 1BMA were exposed to temperatures down to −10 °C. The experiments verified the conclusions made by Emborg et al. (2007) and cracking was observed in specimens exposed to temperatures between −3 and −7 °C. However, some concern was raised regarding the fact that the concrete specimens were dried at 105 °C prior to water saturation as this might have altered the pore structure of the specimens and thus affected the results of the experiments (Tang 2014, personal communication).

In an attempt to verify the conclusions drawn by Tang and Bager (2013), an experimental study of concrete that was allowed to freeze under the influence of an external pressure was conducted by Pålbrink and Rydman (2013). In this study, concrete specimens were enclosed in a thick steel cylinder and surrounded by water-saturated gravel in order to mimic the conditions in 1BMA post-closure, Figure 4-1. The w/c ratio of the concrete used in these experiments was 0.7 in order to obtain a somewhat more porous concrete with resemblance of leached concrete which would be more susceptible to cracking during freezing. The lowest temperature reached in all the experiment was below −10 °C but in none of the experiments were the structural collapse predicted by Emborg et al. (2007) or observed by Thorsell (2013) observed.

The findings presented above suggest that freezing of concrete which is confined in an ice-filled rock volume does not have the expected impact on the material in terms of cracking. For a full understanding of why the outcome differs in the different studies, further research is required.

To be able to assess the risk that the properties of the cementitious components will be seriously affected by freezing post-closure, not only understanding about the influence of sub-zero temperatures on the properties of the different types of cementitious materials is required but also a well-based assessment of the future climate evolution.


***Figure 4-1.*** *Experimental set-up for freezing of concrete samples under the influence of an external pressure. The picture on the left shows how the sample was placed in the container on a bed of gravel while the right one shows the container completely filled with water and gravel before the lid was attached.*

Here, early freezing will have a more profound effect on the properties of the materials than if freezing occurs far in the future. As an example, in the event that permafrost first occurs in 50 000 years post-closure, it can be expected that the properties of the cementitious materials will already have changed significantly and the additional impact of freezing will be of only minor importance. See also (Näslund et al. 2017).

## 4.4 Water uptake and transport under unsaturated conditions

### *Overview*

Water uptake and transport in the cementitious materials in the repository under unsaturated conditions will occur both during the operational period and post-closure.

During the operational period, the relative humidity in the cementitious materials will be controlled by the relative humidity in the waste vaults and/or whether they are in contact with groundwater in the draining layer beneath the concrete structure or not. Under dry conditions, cementitious materials will slowly dry whereas the pore system of a cementitious material will soon be saturated if in a moist environment or in contact with the groundwater.

Directly after sealing and the cessation of drainage pumping, groundwater will start to saturate the repository. Numerical calculations (Börgesson et al. 2015) have shown that it will take between 13 and 53 years for water to fully saturate the silo vault, which is surrounded by bentonite. Full resaturation of the other waste vaults has been calculated to take a few years (Holmén and Stigsson 2001). The cement-conditioned waste will become saturated shortly after repository closure, whereas the bituminised waste will take a considerably longer time due to the hydrophobic character of bitumen.

As a comparison, Emborg et al. (2007), calculated the time to fully saturate the outer wall of the silo alone to about 2 000 years if the water transport through the surrounding bentonite is sufficient. This shows the large uncertainties in such predictions.

### *Expected influence on the properties of the cementitious components*

The presence of water affects all chemical processes in cementitious materials, including alterations of the mineral composition, corrosion of metals and degradation of waste. However, the time to full saturation of the cementitious materials is considered too short for the process to affect the properties of the concrete barriers other than marginally.

Instead, water uptake and transport under unsaturated conditions is mainly of concern in the following two cases:

- Drying shrinkage during the operational period
- Water transport during the saturation of the repository.

Drying shrinkage during the operational period is not expected to influence the properties of the cementitious components as long as cracks are not formed. However, the formation of cracks will influence the hydraulic properties of these. This is further discussed in Section 4.8.

The relative air humidity in the repository is generally high during the moist summer periods and low during the drier winter months as shown in Figure 4-2. However, humidity variations in the concrete are much smaller since moisture transport in the concrete pore system is slow. Measurements of the relative humidity in the concrete in 1BMA carried out by Rosenqvist and Stojanović in January 2011 utilising sensors installed in the actual wall of the concrete structure showed that the relative humidity only a few centimetres from the surface of the concrete structure is between 84–96 % with the lowest value 20 mm from the surface and the highest value about 325 mm from the surface.[46] These values are significantly higher than those in the surrounding air during this period (RH only about 60–70 %), confirming the slow moisture transport in the concrete.

[46] SKBdoc 1314759 ver 1.0. (Internal document, in Swedish.)

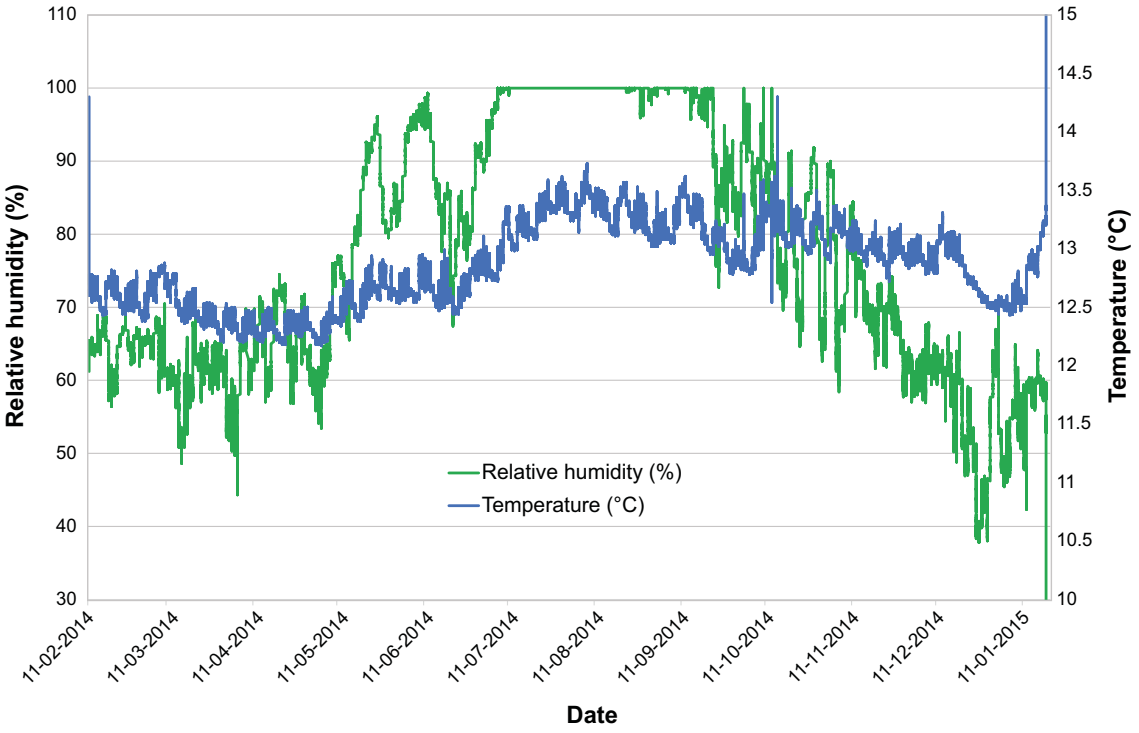


***Figure 4-2.*** *Temperature and relative humidity in the air in 1BMA from February 2014 to January 2015.*

Rosenqvist and Stojanović also found that the relative humidity in cores from the concrete structure which were extracted in October 2010 were about 92 %, i.e. higher than in the air in 1BMA during this period.[47]

Tests carried out by Mårtensson and Vogt (2019) showed that drying of the *2BMA concrete* is very slow even under dry conditions. This indicates that drying shrinkage and associated cracking of the cementitious components are expected to be insignificant during the operational period.

Groundwater transport through the cementitious components during the saturation of the repository is of vital importance as this is a prerequisite for filling of the interior of the concrete structures with groundwater. If groundwater transport through the concrete barriers is insufficient, a pressure difference between the outside and the interior of the concrete structures corresponding to the groundwater pressure will form with a risk for cracking. This is discussed in detail for the individual waste vaults in Chapter 7 to 11. See also Section 4.8.

The risk for cracking can be reduced by the use of e.g. large amounts of reinforcement, supporting inner walls or increased thickness of the outer structural components.

## 4.5 Water transport under saturated conditions

### *Overview*

The water flow through the cementitious components in the repository is determined by the groundwater pressure gradient and the hydraulic conductivity of the component. High-quality concrete has a very low hydraulic conductivity and serves as an effective flow barrier while a porous grout has a higher hydraulic conductivity.

However, even for high-quality concrete, leaching of the soluble cement minerals will eventually lead to an increase of the hydraulic conductivity of the materials over the long time-periods considered in a safety analysis. In addition, the formation of penetrating cracks creates local flow paths which will increase the hydraulic conductivity of the material significantly; see Section 4.8.

[47] SKBdoc 1314759 ver 1.0. (Internal document, in Swedish.)

#### *Expected influence on the properties of the cementitious components*

The water flow through the cementitious components has a major impact on several of the degradation processes such as mineral alterations and corrosion of metals. In addition, water transport under saturated conditions also affects the rate at which the waste is decomposed and the radionuclides are transported out of the repository. For information on the influence of concrete degradation on the flow of water through the waste, see e.g. (Abarca et al. 2013, 2020).

## 4.6 Gas transport/dissolution

#### *Overview*

Gas formed through various degradation processes in the repository will to some extent dissolve in the porewater of the cementitious materials and be transported out of the repository by advection or diffusion, see Sections 4.10 and 4.11. However, for some gases such as hydrogen gas, the solubility is very low and transport of dissolved gases is of minor importance.

If the rate of gas formation exceeds the solubility limit, a gas phase will be formed in the pore systems of the materials. If the gas pressure exceeds the gas entry pressure of the material, the gas will be transported through gas carrying passages. However, gas can also be transported in the form of a "bubble flow", that is, without the formation of a continuous gas phase (Neretnieks and Ernstson 1997).

#### *Expected influence on the properties of the cementitious components in SFR*

Gas transport/dissolution is not expected to affect the properties of the cementitious components in the long-term perspective as long as the pressure inside the structures does not exceed the load-bearing capacity of the structure. In such an event, cracks may be formed through which the gas and water can be expelled. See also Section 4.8.

## 4.7 Pressure from swelling waste

#### *Overview*

Water uptake in hygroscopic waste such as ion-exchange resins can cause swelling of the waste packages. If insufficient expansion volume is available, this process can generate an internal mechanical pressure and eventually lead to cracking of the waste packaging.

High internal pressures and crack formation may also be caused by corrosion of metallic waste, waste packages or reinforcement bars (Section 4.17) and gas production (Section 4.18).

#### *Expected influence on the properties of the cementitious components*

The main risk associated with pressure from swelling waste is the formation of cracks in the cementitious components, but the influence of this process is unique for each waste vault and for each cementitious component. This is because the risk of cracking is dependent on for example how the waste has been conditioned and whether the waste packages have been grouted or not but also on the mechanical strength of the cementitious component in question.

## 4.8 Crack formation

#### *Overview*

Crack formation is strictly speaking not a process on its own but rather the effect of a large number of different processes. However, as the formation of cracks has an important influence on the transport properties of the cementitious components in the repository it is here treated as a process. Please note that the influence of earth quakes is not considered in this report. This is because the prediction of the timing and magnitude of earth quakes are associated with considerable uncertainties and consequently also the assessment of the impact of earth quakes will be very uncertain.

See the following individual sections for more details concerning the processes that have been identified as possible causes of crack formation:

- Heat transport, Section 4.2.
- Phase changes/freezing, Section 4.3.
- Pressure from swelling waste, Section 4.7.
- Rock fall-out, Section 4.9.
- Dissolution, precipitation and recrystallisation, Section 4.14.
- Metal corrosion, Section 4.17.
- Gas production, Section 4.18.

A more extensive list of processes that could cause cracking of the cementitious components and including also those not considered in this work is found in Höglund (2014, Section 4.2). See also the Waste and Barrier process reports for PSAR (SKB TR-23-03, TR-23-04).

### *Expected influence on the properties of the cementitious components*

The main functions of many of the cementitious components are to limit advective and diffusive flow through the waste and to effectively delay the release of radionuclides through sorption on the cement minerals. In crack-free concrete, the flow will be diffusive and sorption of radionuclides efficient thanks to the large contact surface with the cement minerals. On the other hand, for cracked concrete, the advective flow can dominate and the sorption capacity will be lower due to the reduced contact surface between water and the cement minerals.

An important consequence of fully penetrating cracks in concrete structures is an increased hydraulic conductivity of the material as shown in Figure 4-3. The figure shows that already the formation of one crack with a width of only 0.1 mm every 10 meters will increase the hydraulic conductivity to about $10^{-7}$ m/s for a concrete for which the hydraulic conductivity without cracks is $10^{-11}$ m/s.

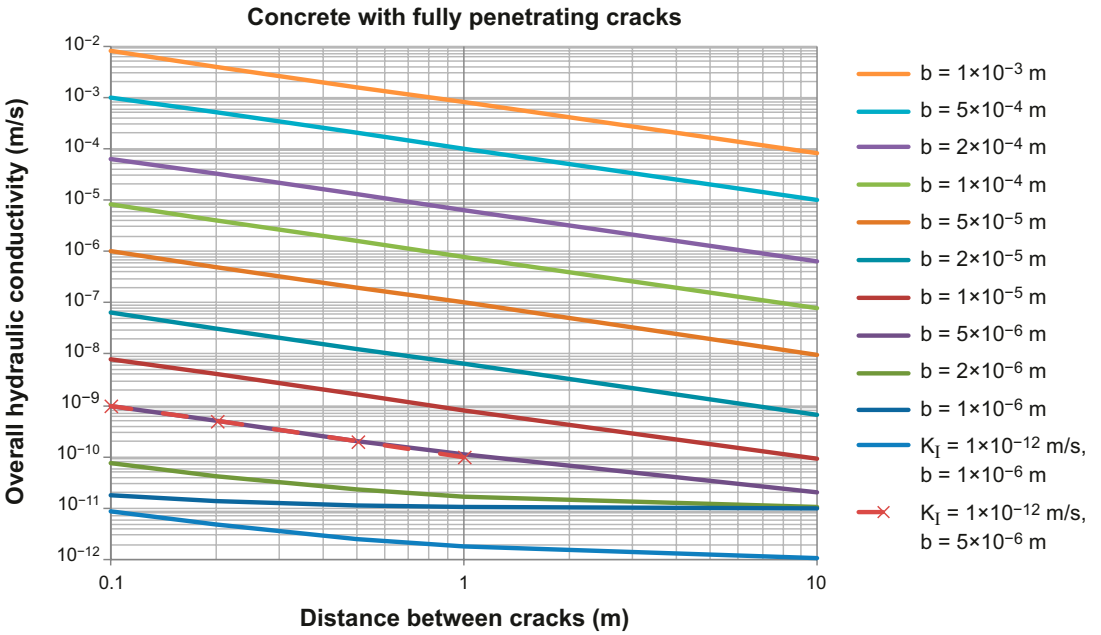


***Figure 4-3.*** *The impact of fully penetrating cracks on the hydraulic conductivity of a concrete structure. The curves show the influence of crack width (b) and distance between cracks (x-axis) on the hydraulic conductivity of a concrete structure made from concrete with an original hydraulic conductivity ($K_I$) of $1 \times 10^{-11}$ m/s. (Höglund 2014). In addition, the hydraulic conductivity of concrete with an initial hydraulic conductivity of $1 \times 10^{-12}$ m/s is shown for cases with cracks with a width of one (lowest blue line)) and five (Dashed red line) µm respectively.*

However, the investigation of the concrete structure in 1BMA carried out by Mårtensson et al. (2014) and using He-leak-detection showed that cracks with a width smaller than about 0.2 mm were not fully penetrating. This means that Figure 4-3 might overestimate the impact of narrow cracks on the hydraulic conductivity of thick concrete structures as such cracks – even though visible on the surface – might not be fully penetrating.

The increased hydraulic conductivity leads to increased water flows through the cementitious components (Section 4.5), which e.g. may increase the dissolution rate of the cement minerals in the vicinity of the crack (Section 4.14).

The impact of fully penetrating cracks on the diffusivity of the cementitious components is less dramatic but still not insignificant as shown in Figure 4-4.

## 4.9 Rock fall-out

### *Overview*

Rock fall-out i.e. large or small blocks falling from the roof or walls of the waste vault may – if large enough – cause the formation of cracks (Section 4.8) in the lids or upper parts of the outer walls of the concrete structures.

In order to reduce the impact force of the blocks, vaults that contain concrete structures with important barrier functions will be backfilled with crushed rock at closure. In addition to this, all vaults are provided with rock bolts and shotcrete to reduce the risk for rock fall-out during the operational period.

### *Expected influence on the properties of the cementitious components*

As discussed above, rock fall-out may cause cracking of the concrete structures. However, the consequences of rock fall-out are dependent on the design of the lid, the size of the block, the position of the impact site as well as on the amount of backfill material on top of the lid. The consequences of rock fall-out are also affected by the degradation state of the concrete structure. For these reasons, the consequences of rock fall-out will be unique for each individual concrete structure and when it occurs.

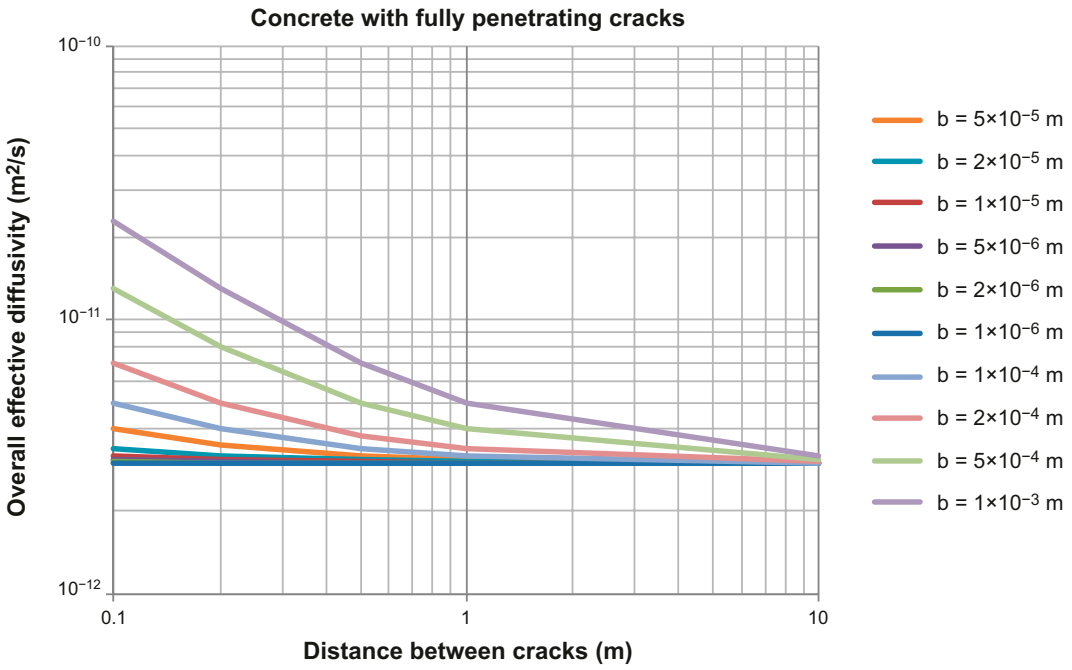


***Figure 4-4.*** *The impact of fully penetrating cracks on the effective diffusivity of a concrete structure. The curves show the influence of crack width (b) and distance between cracks (x-axis) on the effective diffusivity of a concrete structure made from concrete with an original diffusivity of* $3 \times 10^{-12}$ $m^2/s$. *(Höglund 2014).*

## 4.10 Advection and dispersion

### *Overview*

Dissolved substances can be transported through the cementitious components through advection, dispersion and diffusion. In this context, advection involves a transport process where a dissolved substance follows the water's bulk flow. Water flow through the cementitious materials is determined by the pressure gradient and by the hydraulic conductivity of the material.

In the concrete used in the engineered barriers, the hydraulic conductivity is so low that transport of solutes mainly takes place by diffusion while advection plays a minor role. However, a number of processes can directly or indirectly influence the transport properties of the concrete and thus affect the relationship between advective and diffusive transport; see the following sections:

- Heat transport, Section 4.2 (indirectly through e.g. thermal expansion).
- Phase changes/freezing, Section 4.3.
- Pressure from swelling waste, Section 4.7.
- Crack formation, Section 4.8.
- Rock fall-out, Section 4.9.
- Dissolution, precipitation and recrystallisation, Section 4.14.
- Aqueous speciation and reactions, Section 4.15 (indirectly through e.g. increased the rate of corrosion).
- Metal corrosion, Section 4.17.
- Gas production, Section 4.18 (indirectly through e.g. gas pressure to build up).

### *Expected influence on the properties of the cementitious components*

Advection and dispersion will only have a small effect on the properties of undegraded cementitious materials as diffusion is the dominant transport mechanism at this stage.

However, as the pore structure of the materials changes and cracks form, the advective flow will increase. This, in turn, will increase the dissolution rate further and the process will have an accelerating course leading to a further increase in the advective flow. For degraded materials, advection and dispersion will therefore have a more pronounced influence on the post-closure evolution of the properties of the material than during the early stages when the number and width of the penetrating cracks are small and permeable zones few.

## 4.11 Diffusion

### *Overview*

Diffusion will be the dominant transport mechanism for all types of ions in undegraded cementitious components with no or only a few narrow cracks and a pore system characterised by small and poorly connected pores.

Through diffusion in the porewater, soluble cement minerals will be dissolved and transported out of the repository. As degradation progresses, the porosity and number of cracks will increase and in the long term, the role of diffusion will diminish. Instead Advection and dispersion (Section 4.10) will be the dominant transport mechanism.

### *Expected influence on the properties of the cementitious components*

Initially, diffusion is the dominant transport mechanism in the cementitious components and therefore has an important, albeit slow, impact on the evolution of the properties of the cementitious components. However, as mentioned above, with increasing porosity and number of cracks, the role of diffusion is reduced and instead Advection and dispersion (Section 4.10) will be the dominant transport mechanism.

## 4.12 Sorption

### *Overview*

In the post-closure safety assessments, sorption has been identified as a process that needs to be considered (SKB TR-14-07). However, this process is mainly identified due to its impact on transport of radionuclides and not because of its effect on the post-closure evolution of the properties of the cementitious components in the repository.

The term sorption here mainly includes processes in which radionuclides bind to various minerals in the cementitious components via adsorption sites or are incorporated into precipitated minerals in the cementitious materials. However, the general meaning involves all types of chemical species in solution that binds to solid surfaces.

### *Expected influence on the properties of the cementitious components in SFR*

Sorption of dissolved species has a limited impact on the evolution of the properties of the cementitious components in SFR.

## 4.13 Colloid stability, transport and filtering

### *Overview*

In the post-closure safety assessments, colloid stability, transport and filtering has been identified as a process that needs to be considered (SKB TR-14-07). However, this process is mainly identified due to its impact on transport of radionuclides and not because of its effect on the post-closure evolution of the properties of the cementitious components in the repository.

The stability and transport of colloids are dependent on the chemical composition of the water, i.e. the ionic strength, redox potential and pH, but also on the type of colloids present in the solution and their properties.

In the cement porewater which is characterised by high pH and high ionic strength, the stability of colloids is low and the number of colloids in the porewater in the cementitious materials is therefore small (SKB TR-23-04).

### *Expected influence on the properties of the cementitious components in SFR*

The influence of colloid stability, transport and filtering on the post-closure evolution of the properties of the cementitious components in SFR is expected to be negligible. This is because the concentration of colloids in the porewater will be very low.

## 4.14 Dissolution, precipitation and recrystallisation

### *Overview*

Cement minerals can dissolve in the porewater or in the groundwater in direct contact with the surface of the cementitious materials. Cement minerals can also react with substances dissolved in the water to form new solid compounds in the pore system or on the surface of the cementitious components. The reactions that occur and the chemical equilibria depend both on the original mineral composition of the cementitious material and on the substances that are dissolved in the water.

Dissolution of cement minerals in the cementitious components can lead to increased porosity and thus increased transport rate of water and dissolved substances. Conversely, precipitation of secondary minerals in the pore system or on surfaces can cause cracks to be re-filled with decreased hydraulic conductivity of the material as a consequence. However, precipitation of potentially swelling minerals such as ettringite and thaumasite can on the other hand cause cracking of the material even though this is somewhat controversial (Neville 2014, Skalny et al. 2002).

Because of the long time-frames, the impact of dissolution, precipitation and recrystallisation has mainly been studied by modelling, see e.g. the studies by Höglund (2001, 2014, 2018, 2019) and Idiart et al. (2019a, 2019b). However, some experimental studies also exist. As examples, Lagerblad (2001) and Trägårdh and Lagerblad (1998) investigated the properties of old concrete samples which had been in contact with freshwater for up to 100 years. In addition, Babaahmadi (2015) investigated the properties of cement paste and concrete specimens which had undergone accelerated degradation through electrochemical leaching.

### *Expected influence on the properties of the cementitious components*

Dissolution, precipitation and recrystallisation of the cement minerals in the cementitious components have a significant impact on the post-closure evolution of the properties of the cementitious components. As an example of the general evolution of the mineral composition in a cementitious component, Figure 4-5 shows the evolution of the mineral composition in a certain point in the concrete structure in 2BMA over a period of 100 000 years. Please note that the detailed evolution of other concrete structures is dependent on material properties, groundwater composition and position in the concrete structure. For that reason, Figure 4-5 must only be regarded as an example that shows the general trend of concrete degradation and not the evolution of the mineral composition in all points in all concrete structures in SFR.

### *Influence of high concentrations of salts*

A special case that must be considered when discussing mineral alterations in cementitious materials is the influence of high concentrations of salts in the waste. The is because of the significant impact of high concentrations of – in particular – $SO_4^{2-}$ and $CO_3^{2-}$ on the formation of expanding minerals such as ettringite and thaumasite.

In SFR, salts from e.g. evaporator concentrates are disposed. These evaporator concentrates are conditioned in bitumen or cement and placed in different types of packaging, e.g. steel drums, and concrete or steel moulds before disposal.

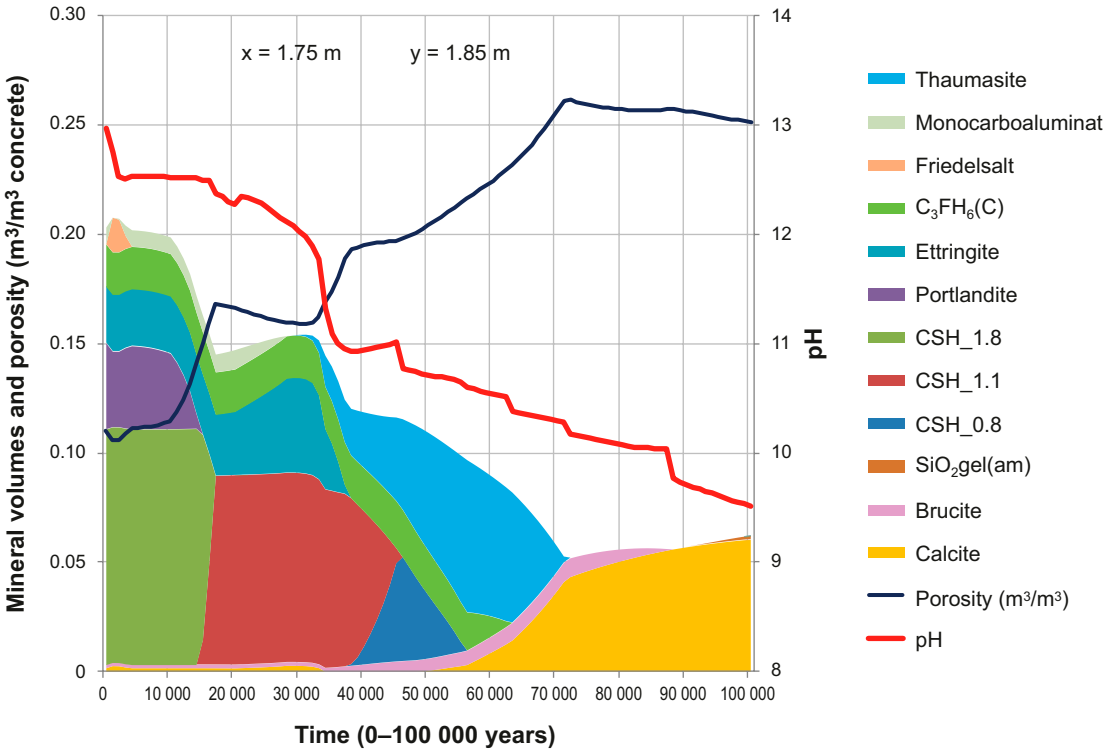


***Figure 4-5.*** *The image shows an example on the evolution of the mineral composition of a cementitious material in a specific point in the concrete structure in 2BMA over a period of up to 100 000 years (Höglund 2014, Figure 7-17).*

The current waste acceptance criteria impose limits to the amounts of sulphate and chloride salts, ensuring that materials in the waste will not increase the rate of concrete degradation in SFR. However, in older wastes, high concentrations of e.g. $SO_4^{2-}$ or $CO_3^{2-}$ from e.g. evaporator concentrates can influence the rate of concrete degradation and the type of secondary minerals formed. The consequences of this will be dependent on conditioning method and distance from the waste packages to other parts of the cementitious barrier system. As an example, the influence of conditioning method of salts with high concentrations of $CO_3^{2-}$ on the evolution of the mineral composition in the barriers in 1BMA is discussed below.

Because the possible impact of high concentrations of salt on the evolution of the properties of the cementitious components will be heterogeneous, any general description of the impact of salts will be highly uncertain. Instead, a general discussion concerning the possible impact of high concentrations of different types of salt on rate and mechanisms of concrete degradation is presented in the following sections.

**Influence of sulphates, $SO_4^{2-}$**

The impact of increased levels of sulphate on concrete degradation has been studied in great detail and the commonly accepted term “sulphate attack” often refers to the formation of ettringite, an expansive mineral. The term “sulphate attack” implies that ettringite formation with subsequent cracking will have a negative impact on the properties of the cementitious components. However, limited ettringite formation may cause porosity clogging in the affected regions with a reduced degradation rate of the interior parts as a consequence. For an extended introduction, the many aspects of sulphate attack are discussed by Skalny et al. (2002).

Ettringite formation is dependent on the presence of aluminates and in particular high levels of $C_3A$ in the cement renders the cementitious material sensitive to sulphate attack. This also means that sulphate attack and the effects thereof can be mitigated by choosing a cement with a low content of $C_3A$.

On behalf of SKB, the consequences of increased levels of sulphate have been studied by Höglund and Pers (2000) and Laviña and Idiart.[48]

Höglund and Pers (2000) investigated the consequences of introducing a new conditioning method for the evaporator concentrates from the Forsmark nuclear power plant. The method comprised drying the evaporator concentrates completely and placing the solid material in steel moulds. The method was never approved but the results from the study are of some relevance in this discussion.

The report concluded that the disposal of large amounts of solid salts in steel drums had the potential of causing significant concrete degradation inside the waste domain. The report also discussed the possible use of different pre-treatment methods for the salts, e.g. addition of large amounts of calcium but concluded that the most suitable solution was to not dispose solid salts in high concentrations in the repository. Höglund and Pers (2000) also concluded that grouting of the voids between the waste packages could have a detrimental effect on the other components of the concrete structure. This is because the formation of expansive minerals such as ettringite in the grout could induce a high internal pressure on the outer walls with possible cracking as a consequence.

In the more recent study, Laviña and Idiart investigated the impact of sulphates in the waste on the properties of the 1BMA concrete barriers.[49] The results showed (in agreement with many textbooks on the subject) that increased levels of sulphate can cause the formation of expansive minerals such as ettringite but also thaumasite can form under some conditions. A simple mechanical analysis showed that a volumetric expansion of up to 1.5 % can be expected. According to the model referred-to by Laviña and Idiart this exceeds the threshold for mechanical damage and cracking can therefore be expected in the affected parts of the concrete structure.[50] It should be noted that – in addition to the reference case – the study by Laviña and Idiart also included a number of sensitivity cases in which

[48] SKBdoc 1967610 ver 1.0. (Internal document.)

[49] SKBdoc 1967610 ver 1.0. (Internal document.)

[50] SKBdoc 1967610 ver 1.0. (Internal document.)

the impact of model alterations was investigated.[51] These sensitivity cases showed that the sensitivity of the model was significant for changes in temperature and the type of secondary minerals allowed to form in the calculations.

### Influence of carbonates, $CO_3^{2-}$

Also increased levels of carbonates may cause the formation of expansive minerals, mainly thaumasite. Thaumasite can form also in sulphate resistant cements through a reaction with CSH but requires also some sulphate to form. For this reason, carbonate is not limited in the current waste acceptance criteria; it is there judged that the rather strict limit for sulphate is sufficient to prevent significant thaumasite formation.

The impact of increased levels of carbonate in the waste in 1BMA has been studied by Cronstrand (2010). The study found a strong correlation between conditioning method for carbonate-containing waste and impact on the concrete barriers.

For waste packages containing sufficient amounts of cementitious materials, most of the carbonate reacted within the waste package and did not cause any major alterations with respect to the most important minerals – portlandite and CSH – in the concrete barriers compared to waste with low levels of carbonate. This is visible in a comparison between Figure 4-6 and 4-7 which show the volume of all respective minerals in 1 $dm^3$ assuming low or high amounts of carbonate in the waste, respectively.

In Figures 4-6 and 4-7, the part from 0–0.4 meters constitutes the concrete barrier wheras the remaining part constitutes the waste compartment. Figure 4-7, shows that the carbonate in the waste reacts within the waste compartment and forms large amounts of monocarboaluminate, not present in Figure 4-6.

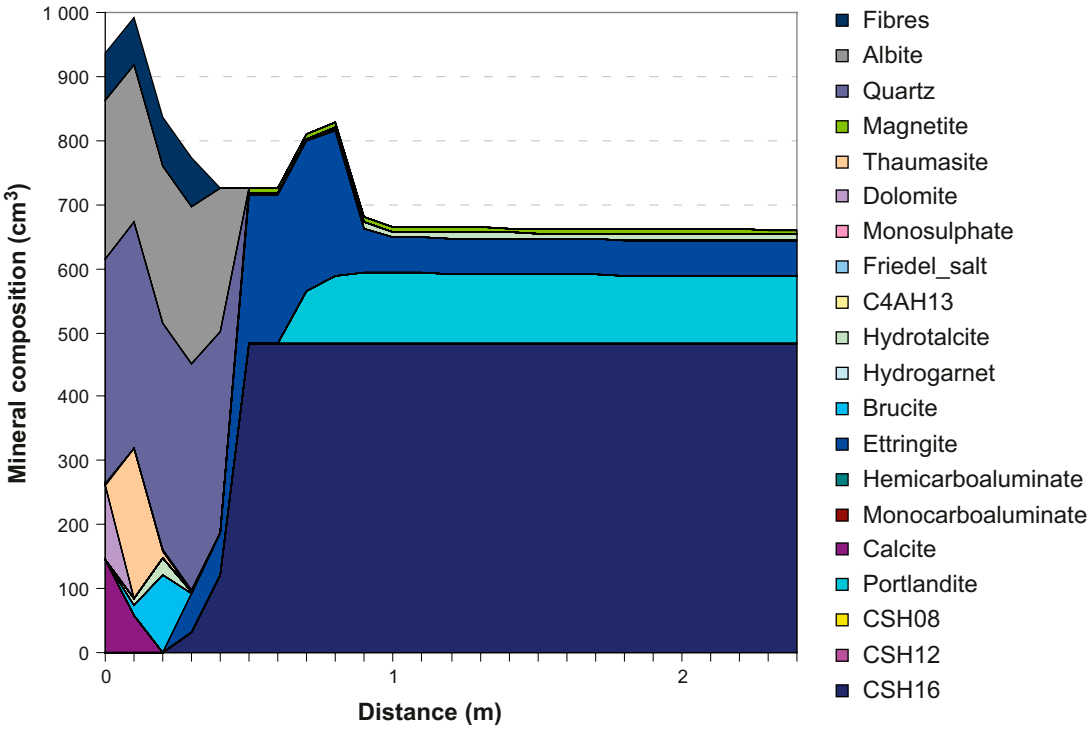


***Figure 4-6.*** *Mineral composition and total porosity (white area) in the structural concrete in 1BMA at 50 000 years post-closure, as a function of distance from the contact zone between the concrete structue and the groundwater saturated backfill material. Reference scenario for cement conditioned waste with low levels of carbonate (Cronstrand 2010, Figure B-31).*

[51] SKBdoc 1967610 ver 1.0. (Internal document.)

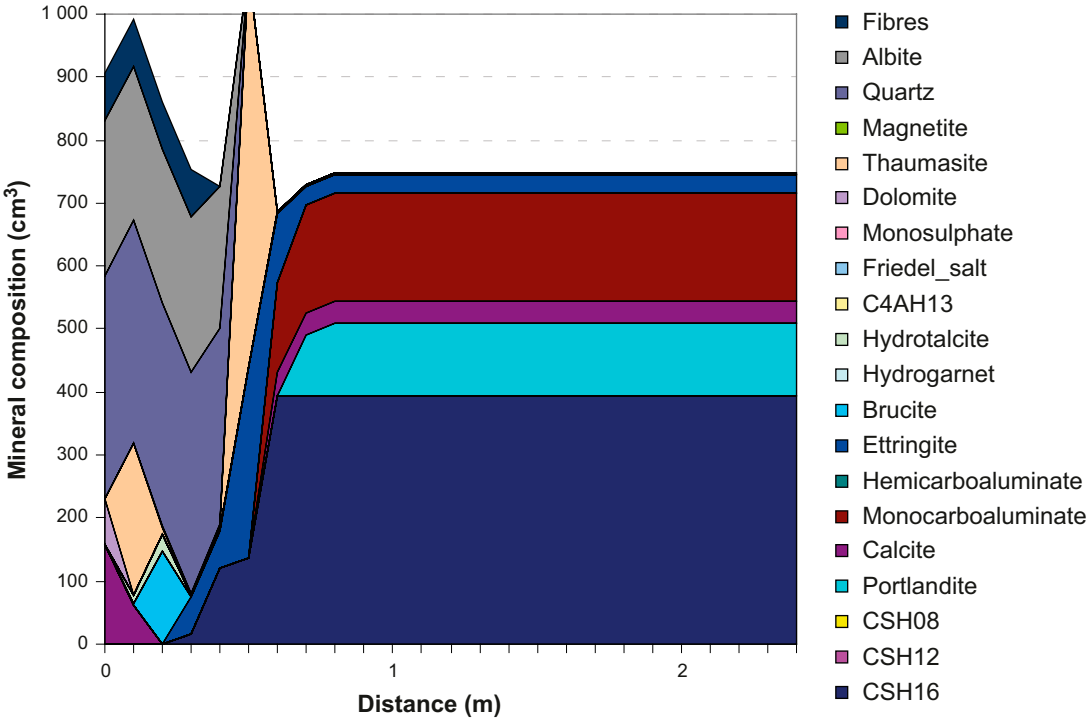


***Figure 4-7.*** *Mineral composition and total porosity (white area) in the structural concrete in 1BMA at 50 000 years post-closure as a function of distance from the contact zone between the concrete structue and the groundwater saturated backfill material. Scenario for a cement conditioned waste with high levels of carbonate (Cronstrand 2010, Figure B-35).*

From Figures 4-6 and 4-7 follows that most of the additional thaumasite is formed inside the waste compartment and not in the concrete barrier. This protects the concrete barrier from detrimental effects from the high carbonate content and mineral alterations in the barrier are therefore small.

Cronstrand (2010) concludes that the analysis only focused on local effects and stresses that "*a waste container situated in the centre of the repository will have a considerably lower influence on the degradation rate due to the redundancy of buffer material in terms of cementitious waste*".

This emphasises the difficulties in presenting a general description of the post-closure evolution for highly heterogeneous initial conditions in terms of carbonate content, waste form material, conditioning method, number of waste packages containing the waste material of interest and position of the waste packages inside the waste compartment.

However, for a theoretical case with a compartment filled with waste with high levels of carbonate conditioned with bitumen (so far, no compartment contains only bituminised waste, see SKB (TR-23-02), the situation becomes significantly different. Because of the absence of cementitious conditioning materials in the waste compartment, any carbonate will instead react with the cementitious materials in the concrete barriers. As shown in Figure 4-8, the consequence of this is the formation of thaumasite in a larger part of the barrier but also a redistribution of the portlandite and calcite.

### *Sealing of cracks in concrete structures*

A special case of precipitation relates to the sealing of cracks in concrete structures. This can occur either through late cement hydration in the interior of the concrete structure or through the precipitation of secondary minerals through a reaction between species in the groundwater and species in the cement pore water. However, the general processes are the same as those that cause precipitation of secondary minerals on e.g. the surface of a concrete structure or elsewhere where waters with different compositions are mixed.

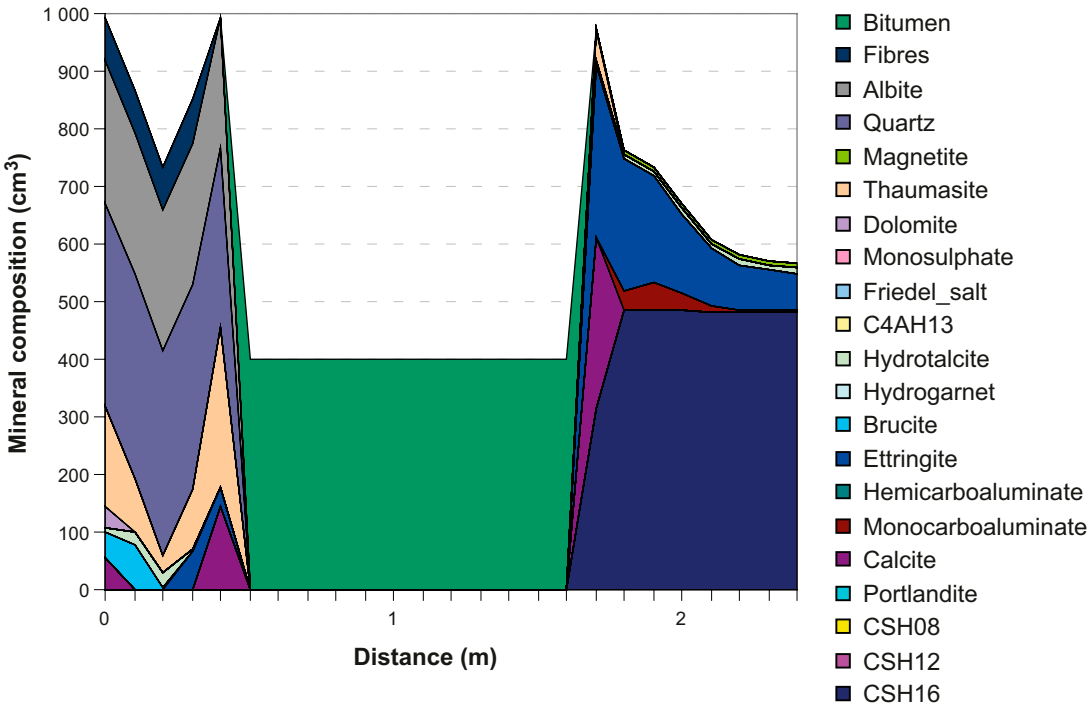


***Figure 4-8.*** *Mineral composition and total porosity (white area) in the structural concrete in 1BMA at 50 000 years post-closure as a function of distance from the contact zone between the concrete structure and the groundwater saturated backfill material. Scenario for a bituminised waste with high levels of carbonate (Cronstrand 2010, Figure B-43).*

Over the years, sealing of cracks has been rather extensively studied; see e.g. Neretnieks and Moreno (2013, Section 6.5 and Appendix) and Soler et al. (2020). However, even though the process is extensively studied there remains significant obstacles before this process can be credited for when material property data to be used in e.g. radionuclide transport calculations are selected for the different cementitious components. Because of this, the impact of sealing of cracks in the concrete structures in SFR is not considered when material property data are suggested in this report.

## 4.15 Aqueous speciation and reactions

### *Overview*

Aqueous speciation describes the chemical forms of dissolved elements under specific geochemical/physical conditions. Chemical reactions occur when a constraint is put on a system at equilibrium, i.e. any change due to migration or dissolution of chemical species may result in aqueous chemical reactions occurring.

In the cementitious materials, the porewater constituents reflect the barrier materials themselves and the aqueous inputs from the geosphere or waste form materials and packaging. The major factors affecting speciation are the pH, Eh, and the concentration and type of other chemicals in the system, including the presence of complexing agents. pH is fundamentally important as it defines the balance between protons and hydroxyl ions in the solution.

The concrete barriers will exert a very significant influence on the aqueous speciation and reactions in the porewater via the high pH and ionic strength generated through dissolution of the cement minerals as illustrated in Figure 4-5.

The Eh of the porewater is expected to become reducing soon post-closure, with consumption of oxygen introduced during the operational period through microbial processes and metal corrosion. The reducing character of the surrounding groundwater will also help maintain reducing conditions over time.

#### *Expected influence on the properties of the cementitious components*

The composition of the porewater may influence the properties of the cementitious materials. As examples, elevated levels of sulphate and carbonate may cause the formation of ettringtite or thaumasite whereas increased levels of chloride may lead to the formation of Friedel's salt. However, also other minerals may form through different chemical reactions, many of which may have an impact on e.g. the porosity and pH of the porewater.

However, the composition of the porewater may also influence other processes and e.g. increased levels of chloride ions or reduced pH may increase the rate of corrosion of reinforcement bars or other types of embedded metallic components, Section 4.17. If corrosion is extensive cracking of the concrete may occur.

## 4.16 Microbial processes

#### *Overview*

Microbial processes may occur in the repository during both the operational period and post-closure. Being very hardy species, microbes can thrive in environments where life would otherwise not be expected. However, in environments characterised by very high or low temperatures or very high or low pH, the microbial activity is low.

During the operational period, oxygen will be the main source of energy for the microbes whereas other species such as nitrate, Mn(IV), Fe(III), sulphate, sulphur and carbon dioxide will be the main sources of energy for the microbes post-closure once all oxygen has been consumed.

Many microorganisms attach and grow on surfaces of all types in aquatic systems. Attachment to a surface is commonly a more favourable state compared to being unattached; at least in a system with flowing water. Typically, microbial biofilms form where gradients of nutrients and sources of energy are present.

Microbial biofilms can reach a thickness of several centimetres when the availability of organic carbon is large. Under other conditions, biofilms can be as thin as a monolayer of bacteria in the range of some micrometres.

#### *Expected influence on the properties of the cementitious components*

Microbial activity in the cementitious components is limited by the high pH prevailing in the repository. The process will therefore only have a negligible impact on the post-closure evolution of the properties of cementitious components post-closure (SKB TR-23-04).

## 4.17 Metal corrosion

#### *Overview*

Metals embedded in cementitious components such as reinforcement bars, tie rods and other steel objects, as well as other metals in the waste such as zinc and aluminium, will corrode during both the operational period and post-closure. This can occur either in the presence of oxygen (aerobic corrosion) or in its absence (anaerobic corrosion). According to Duro et al. (2012), the time until all oxygen is SFR is exhausted is less than one year if only steel corrosion is considered. For that reason, corrosion in SFR will occur under anaerobic and alkaline conditions.

The effects of metal corrosion in cementitious materials depend on type of metal, type of corrosion process (aerobic or anaerobic), corrosion rate and whether soluble or insoluble corrosion products are formed. The molar volume of insoluble corrosion products is often significantly larger than that of the metal/alloy (SKB TR-23-03, Figure 3-7) and the cause of spalling of the covering layer of concrete discussed further below.

The often most visible effects of metal corrosion are discoloration of the concrete surface and spalling of the covering layer as shown in Figure 4-9. The process behind spalling is the formation of voluminous corrosion products on (in Figure 4-9) the reinforcement bars in the concrete structure. Once this layer of corrosion products is thick enough, the internal pressure will exceed the tensile strength of the concrete with spalling as a consequence. This will lead to loss of function of the reinforcement bars and affect the concrete structure's ability to accommodate tensile stresses. See (Höglund 2014) for more details.

If the corrosion products instead dissolve in the concrete porewater, voids may form between the metal and the concrete with the formation of a permeable zone and reduced load-bearing capacity of the structure as consequences. However, regardless of corrosion process, the consequence of rebar corrosion will be a reduction of the load-bearing capacity of the concrete structure.

The impact of metal corrosion on the properties of the concrete is not restricted to the direct effects discussed above. Through anaerobic metal corrosion, hydrogen gas is formed through the reaction exemplified by the anaerobic corrosion of iron, Equation 4-1.

$$3\ Fe(s) + 4\ H_2O \rightarrow Fe_3O_4(s) + 4\ H_2(g) \qquad \text{Equation 4-1}$$

The consequences of this reaction are dependent on the reaction rate and hence the rate of gas formation. For fast reactions, such as corrosion of aluminium and zinc in an alkaline environment, large amounts of gas can be formed in short time. Failure to release this gas may result in the evolution of a high gas pressure inside the concrete structures with a risk for cracking (Section 4.8) as a consequence.

For steel, the long-term corrosion rate under anoxic alkaline conditions is expected to be 0.001–0.1 µm/year (SKB TR-23-10) and hence the rate of gas formation is considerably lower than for corrosion of aluminium and zinc which has been assumed to be 1 mm/year (Moreno et al. 2001, Moreno and Neretnieks 2013, SKB TR-14-10).

***Figure 4-9.*** *Concrete spalling due to corrosion of reinforcement bars on the inside of the existing outer walls of the concrete structure in 1BMA..*

#### *Expected influence on the properties of the cementitious components*

The most significant impact of corrosion relates to corrosion of reinforcement bars which causes cracking and spalling of the concrete covering layer. Eventually rebar corrosion also leads to a loss of function of the reinforcement bars and reduced load-bearing capacity of the component.

In addition, through anaerobic corrosion (Eq. 4-1) hydrogen gas will form. If this gas cannot be transported out of the concrete structure, a high gas pressure may evolve. For very high pressures, cracking of the concrete structure may occur. However, this can be prevented by the installation of a gas evacuation system as planned for the silo and 2BMA.

Finally, corrosion of steel ensures that reducing condition are maintained within the repository over long periods. This is discussed extensively by Duro et al. (2012).

## 4.18 Gas production

#### *Overview*

The main source of gas production in the cementitious components post-closure is the anaerobic corrosion of metals, Section 4.17. Other potential sources of gas formation are microbial processes (Section 4.16) and radiolytic decomposition of organic materials.

#### *Expected influence on the properties of the cementitious components*

Gas formation can cause a gas pressure to build up inside the concrete structures. How this affects the concrete structure depends on the structure's ability to release the gas as well as on its mechanical strength and it will therefore be unique for each individual structural component.

In SFR, measures will be taken to ensure that gas production does not affect the functions of the concrete barriers and it is therefore expected that the influence of gas formation on the post-closure evolution of the properties of the cementitious components will be negligible.

## 4.19 Speciation of radionuclides

#### *Overview*

This process describes the speciation of radionuclides, i.e. the establishment of all chemical equilibria determining the thermodynamically (and kinetically) stable chemical forms of radionuclides in solutions.

In addition to typical reactions in solutions, these equilibria include redox reactions as well as the formation of radionuclide solid phases and sorbed species. The latter is addressed separately in Section 4.12. The process and its influence on the properties of the cementitious components is further described and evaluated in the Barrier process report (SKB TR-23-04) and references therein.

#### *Expected influence on the properties of the cementitious components in SFR*

The influence of speciation of radionuclides on the post-closure evolution of the properties of the cementitious components is judged to be negligible for all waste vaults.

## 4.20 Transport of radionuclides in the water phase

### *Overview*

Transport of radionuclides in the water phase involves mainly the processes advection and dispersion (Section 4.10), diffusion (Section 4.11) and sorption (Section 4.12) but also the process speciation of radionuclides (Section 4.19). See also the Barrier process report (SKB TR-23-04).

### *Expected influence on the properties of the cementitious components*

The influence of transport of radionuclides in the water phase on the post-closure evolution of the properties of the cementitious components is judged to be negligible for all waste vaults.

## 4.21 Transport of radionuclides in the gas phase

### *Overview*

This process relates to the transport of radionuclides, such as C-14, H-3 and Rn-222, in a gas phase.

### *Expected influence on the properties of the cementitious components in SFR*

The influence of transport of radionuclides in the gas phase on the post-closure evolution of the properties of the cementitious components is judged to be negligible for all waste vaults in SFR.

For an evaluation of the influence of gas production in general; see Section 4.18.

# 5 General description of relevant properties of the cementitious components and conditions over time

Section 5.1 presents a description of the chemical, mechanical and transport properties of the cementitious components in SFR. A general understanding of these properties is required to subsequently establish the status of the cementitious components at closure (Chapter 6) as well as their post-closure evolution (Chapters 7–14).

Further, the conditions that can affect the cementitious components are described in Section 5.2, including their evolution over time. Finally, Section 5.3 introduces the time periods which are used in the description of the evolution of the properties of the cementitious components over time.

## 5.1 Properties of the cementitious components

As a basis for the recommendation of material property data for the various cementitious components and time periods, detailed understanding of the evolution of the chemical properties, the load-bearing capacity and the transport properties are required.

In the following sections, a general introduction to these properties in the context of SFR is presented, which is subsequently applied in the description of the cementitious components in the subsequent chapters. First are the chemical properties described (Section 5.1.1), subsequently the load-bearing capacity (Section 5.1.2) and the transport properties (Section 5.1.3).

### 5.1.1 Chemical properties

#### *Overview*

The chemical properties of the cementitious components include the mineral composition of the material and porewater composition with mainly pH and Eh in the porewater being the measured properties. The chemical properties determine the speciation of the radionuclides and influence the materials' ability to retard the release of radionuclides by sorption.

The original mineral composition of a cementitious material is determined by the type of cement used but also by the type and amount of the different solid additives such as silica, limestone, fly ash etc. In the long term, the mineral composition is also influenced by interactions with water and with species dissolved in the water. Through dissolution of the original cement minerals and precipitation of secondary minerals (Section 4.14), the mineral composition of the cementitious components gradually changes as illustrated in Figure 4-5. In conjunction with this, also the porewater composition changes as dissolved species diffuse through the pore system and are transported out into the groundwater in the surrounding bedrock.

With time, these changes will gradually affect the pH and Eh of the porewater as well as the sorption capacity of the minerals present. Changes of the chemical properties will also lead to changes in the speciation of the radionuclides which in turn will affect their solubility and ability to sorb onto the cement minerals.

The descriptions of the evolution of the chemical properties of the cementitious components are mainly based on modelling studies but for material data, also experimental studies are considered. However, it is difficult to accurately describe the evolution of the chemical properties of the cementitious components based on experiments as all experiments have to be conducted under accelerated conditions as exemplified by e.g. the work by Babaahmadi (2015) and/or involve extrapolations over long time.

For selection of representative values for material property data for different time periods, also the spatial variability of the properties in different parts of the cementitious components has to be considered. Here, the material in the surface region may be significantly degraded whereas parts further inside will have the characteristics of the undegraded material.

To overcome the fact that the properties in a specific point will not be representative for the entire structure, a range of values is instead selected to describe the average chemical properties of the cementitious components for selected time periods. A further motivation to this approach is the temporal variability caused by the long periods for which the data are selected, Section 5.3.

Table 5-1 presents expected pH for the different chemical degradation states of a typical cementitious material, compare Figure 4-5. As illustrated in Figure 4-5, the transition between the different CSH-phases is gradual and proceeds over a range of years. Besides this, also the type and amount of other minerals are affected during this process. However, for the purpose of Table 5-1, pH in the cement pore water has been selected based on the Ca/Si ratio of the CSH phases. A brief description of the relation between concrete degradation states and porewater properties is also presented in (SKB TR-23-10, Section 7.4)

**Table 5-1. Approximate pH for the selected chemical degradation states for cementitious materials at 25 °C*.**

| pH | Material characteristics |
|---|---|
| ≥ 13 | Undegraded material. pH in the porewater controlled by NaOH and KOH |
| 12.5 | A relatively long and stable phase, where pH in the porewater is controlled by the dissolution of portlandite, $Ca(OH)_2$ |
| 12–12.5 | All portlandite has been dissolved and pH in the porewater is controlled by the dissolution of CSH_1.8 |
| 11 | Expected initial pH of a so-called “low-pH-concrete” which contains significant amounts of silica fume |
| 10.5–11 | pH in the porewater is controlled by the dissolution of CSH_1.1 |
| 10–10.5 | pH in the porewater is controlled by the dissolution of CSH_0.8 |
| ≤ 10 | All CSH-phases have been dissolved. $CaCO_3$ is the main remaining cement mineral. |

* Data estimated from Figure 4-5.

### *General uncertainties*

The prediction of the post-closure evolution of the chemical properties of the cementitious components relies on a detailed knowledge of their status at closure and on an understanding of the processes that influence these properties over time.

For SFR, information presented in Chapter 2 with references is judged to be sufficient for a reasonably accurate description of the chemical properties of the cementitious components at closure. Further, the general understanding of the influence of the different processes discussed in Chapter 4 on the post-closure evolution of the chemical properties of the cementitious materials is also judged satisfactory. See also Höglund (2014) and SKB (TR-23-04) for more details on the most important processes. However, there do exist some uncertainties associated with the combined effect of cracking and interactions with the groundwater and the impact of high concentrations of salts in the waste.

Of these processes, cracking is not expected to alter the general evolutionary trend of the chemical properties even though the rate of alteration will increase as cracking exposes a larger part of the concrete structure to the surrounding groundwater as shown by Cronstrand (2007).

The understanding of the future geochemical and hydrogeological conditions in the vicinity of the repository is somewhat uncertain given the uncertain future climate evolution. For SFR, Cronstrand (2007) has studied the impact of climate changes on the evolution of the engineered barriers in the silo and 1BMA. This study concludes that the degradation rate of the barriers in 1BMA and the silo is not significantly affected by temperature and salinity variations. The impact of high concentrations of salt in the waste is also discussed in Section 4.14.

In all, there do exist some uncertainties in the models used to predict the post-closure evolution of the chemical properties of the cementitious components. However, the impact of these uncertainties is judged to be limited and it is therefore assessed that the description of the post-closure evolution of the chemical properties of the cementitious components presented in this report is reasonably correct.

### 5.1.2 Load-bearing capacity

#### *Overview*

A sufficient load-bearing capacity of a cementitious component can be obtained through careful design, use of concrete with high strength and reinforcement.

During both the operational period and post-closure, the load-bearing capacity will not only be affected by concrete degradation and rebar corrosion but also by processes in the waste and degradation of adjacent supporting components. Eventually, through these processes, the load-bearing capacity of the component will be insufficient to withstand internal or external loads. The most important consequence of this is that cracks will start to form which in turn will affect the hydraulic conductivity and effective diffusivity of the components (Section 5.1.3). In addition, cracking reduces the area available for sorption of radionuclides. This is because the presence of cracks increases the ratio between advective and diffusive transport and sorption is less effective for advective transport than for diffusive transport of radionuclides. For this reason, the evolution of the load-bearing capacity will be a critical parameter in the safety assessment.

In Mårtensson (2017) the rate of loss of load-bearing capacity of a concrete structure through portlandite leaching is assumed to correspond to a reduction of the thickness of the concrete structure by 15 mm/1 000 years.

The assumed rate takes it starting point in Figure 8-6 which shows that the average rate of portlandite leaching over long periods is about 10 mm/1 000 years but also that the initial rate is faster. In addition, Mårtensson (2017) assumes that the load-bearing capacity of portlandite depleted concrete is completely lost. This does not agree with the findings by Babaahmadi (2015) who showed that also portlandite leached concrete has some remaining strength: see Table 5-2. Finally, the rate of loss of load-bearing capacity suggested by Mårtensson (2017) also considers the presence of a leaching front in the material. Also, this is based on the findings by Babaahmadi (2015) who showed that a Ca/Si gradient was developed in the material while leaching progressed. Mårtensson (2017) assumed that also the compressive strength of the material in a part of the gradient zone corresponding to 50 % of the completely portlandite leached part was lost.

In all, this means that Mårtensson (2017) overestimates the impact of concrete degradation both in terms of average rate over longer periods and consequence. This was, however, found to be justifiably considering the purpose of that report.

Table 5-2 presents the expected compressive and tensile strength for various cementitious materials and degradation states. The strength of a partially degraded material is difficult to determine because gradients are developed within the material. For that reason, measurements cannot accurately determine the mechanical strength of a partially leached sample.

**Table 5-2. Expected compressive and tensile strength for various cementitious materials and degradation states.**

| Compressive strength (MPa)* | Tensile strength (MPa) | Material characteristics |
|---|---|---|
| 60 | 6 | Undegraded standard concrete with a w/c ratio of about 0.45 |
| 50 | 5 | Undegraded standard concrete with a w/c ratio of about 0.55 |
| 40 | 4 | Undegraded standard concrete with a w/c ratio of about 0.65 |
| 30 | 3 | Undegraded standard concrete with a w/c ratio of about 0.80 |
| 20 | 2 | Undegraded standard concrete with a w/c ratio of about 1.15 |
| 5–10 | 1 | Cementitious grout with a w/c ratio above 1 |
| 12 | 2 | Portlandite depleted concrete (Babaahmadi 2015, Table 4-3) |

* The compressive strength has been obtained from Svensk Byggtjänst (2017, Table 12.4:4) unless other reference given.

In comparison with concrete degradation, both loss of function of the reinforcement bars and loss of support from adjacent structural components will have a more significant impact on the evolution of the load-bearing capacity of the cementitious components. Of these, rebar corrosion will affect the

load-bearing capacity already at an early stage, i.e. within the first 1 000 years post-closure whereas loss of support from adjacent structures will occur much later.

An important factor here is that the maximum load experienced by a specific cementitious component will vary over time. As an example, during the saturation period, the maximum load will be that of the groundwater pressure whereas the maximum load will only be that of the backfill material once the repository is fully saturated. This means that for some concrete structures, loss of function of the reinforcement bars may not be critical for its load-bearing capacity.

In all, this means that the assessment of the risk for the formation of cracks in a cementitious component or complete loss of structural integrity of a concrete structure has to consider the coupling between the processes that affect the load-bearing capacity of the component in question and those that affect the supporting components for the actual load at a certain period in time.

For this reason, the tables in Chapters 7-14 include a rating of the load-bearing capacity of the different construction parts on a scale from 5 to 1 as defined in Table 5-3. This rating will also form the basis for the recommendation of transport properties for the various periods.

**Table 5-3. Rating used in the assessment of the load-bearing capacity of the cementitious components – including support from adjacent structural components – in SFR.**

| Rating* | Structural characteristics of the component |
|---|---|
| 5 | The load-bearing capacity is sufficient to withstand any foreseeable load or combination of loads. |
| 4 | The load-bearing capacity is somewhat reduced due to reduced function of the reinforcement and/or some concrete degradation. Support from adjacent structures prevents cracking due to all but the largest loads. |
| 3 | The load-bearing capacity is significantly reduced due to reduced/lost function of the reinforcement, concrete degradation and reduced support from adjacent structural components. Support from adjacent structures still prevent extensive cracking. |
| 2 | The load-bearing capacity is insufficient and extensive cracking can be expected. Support from adjacent structural components prevents loss of structural integrity or collapse. |
| 1 | The load-bearing capacity is lost and no support from adjacent structural components can be accounted for. The structural integrity of the component is lost. |

* The colour coding is included in the tables in Chapter 7–14 to improve the clarity of the rating of the load-bearing capacity of the cementitious components.

#### *General uncertainties*

The main uncertainties associated with the prediction of the load-bearing capacity of the different structural components in SFR originates from the complexity of correctly determining the combined impact of concrete degradation, loss of function of the reinforcement bars (if any) and the loss of mechanical support from adjacent structural components, waste or backfill materials.

This means that even though the individual processes are reasonably well understood, the synergistic effect of these processes introduces a significant complexity with associated uncertainties.

### 5.1.3 Transport properties

#### *Overview*

The transport properties include the hydraulic conductivity and effective diffusivity, i.e. the ability of the components to restrict advective and diffusive transport of species dissolved in the groundwater.

The hydraulic conductivity and effective diffusivity of the cementitious components are affected by the initial porosity of the material as well as by the presence of penetrating cracks, joints or other permeable zones. Transport is also influenced by the groundwater pressure gradient over the material. At low gradients the groundwater becomes almost stagnant and diffusion will be the dominant transport mechanism whereas at larger gradients, advective transport will be increasingly influential.

Consequently, diffusion may be important also for severely degraded materials due to the low gradients in the fully saturated repository.

The initial porosity of cementitious materials is mainly controlled by the w/c ratio and includes mainly gel pores and capillary pores. Typically, the diameter of these pores is in the sub micrometre range. In addition, the cement paste also contains unconnected air pores with a diameter up to about one millimetre. From Svensk Byggtjänst (2017, Table 10.5:1) the porosity for different types of fully hydrated standard concrete is obtained, Table 5-4. The evolution of porosity as a consequence of concrete degradation is illustrated in Figure 4-5 and data given in Table 5-5. As shown in Table 5-5, the porosity of completely degraded concrete is about 0.25, i.e. considerably larger than that of any of the concretes in Table 5-4.

**Table 5-4. Porosity for selected types of standard concrete at full hydration.**

| Water/cement | 28 days compressive strength* (MPa) | Porosity** |
|---|---|---|
| 0.85 | 29 | 0.155 |
| 0.75 | 32 | 0.154 |
| 0.65 | 39 | 0.147 |
| 0.55 | 48 | 0.140 |
| 0.45 | 58 | 0.127 |
| 0.35 | 70 | 0.117 |

* The compressive strength has been obtained from Svensk Byggtjänst (2017, Figure 12.4:1)
** The porosity has been obtained from Svensk Byggtjänst (2017, Table 10.5:1)

**Table 5-5. Expected porosity for selected degradation states of standard concrete.**

| Porosity (%) * | Material characteristics |
|---|---|
| 11–13 | Undegraded concrete with a w/c ratio below 0.5 (From Table 5-4) |
| 13–15 | Undegraded concrete with a w/c ratio between 0.5 and 0.7 (From Table 5-4) |
| 14–16 | No portlandite left. CSH_1.8 is the dominant CSH-phase |
| 15–17 | CSH_1.1 is the dominant CSH-phase |
| 20 | CSH_0.8 is the dominant CSH-phase |
| 20–25 | All CSH-phases has been dissolved. $CaCO_3$ is the dominant remaining mineral. |

* Data estimated from Figure 4-5.

### *Hydraulic conductivity*

Höglund (2014) studied the influence of porosity on the hydraulic conductivity of standard concrete using two different calculation models, Figure 5-1. In this figure, both curves have been fitted to a hydraulic conductivity of $8.3 \times 10^{-10}$ m/s for concrete with a porosity of 11 %. However, it should be noted that this value corresponds to the initial state hydraulic conductivity for concrete structures recommended in the Data report for PSAR (SKB TR-23-10) and also considers the presence of a small number of cracks. As shown in e.g. Section 3.3.3, the hydraulic conductivity of uncracked specimens is about two orders of magnitude lower. The implication of this is that the results in Figure 5-1 are judged reasonably valid with respect to the porosity dependence of the conductivity but not its absolute magnitude.

An indication of the impact of cracking on the hydraulic conductivity of a concrete structure is given in Figure 4-3. This figure shows that only a few narrow cracks are allowed for the hydraulic conductivity not to exceed $8.3 \times 10^{-10}$ m/s if the hydraulic conductivity of the uncracked concrete is $10^{-11}$ m/s.

In Figure 5-1, the blue line (Kozeny-Carman) shows the calculated hydraulic conductivity as a function of porosity for a material which retains a “concrete-like” structure. As a comparison, the red line (modified Kozeny-Carman) shows the hydraulic conductivity as a function of porosity for concrete with a structure that gradually transforms from concrete-like to sand-like.

In this report, the Kozeny-Carman model is used for selection of hydraulic conductivity data. This is because the cementitious components are expected to – at least partly – retain a concrete-like structure even when severely degraded.

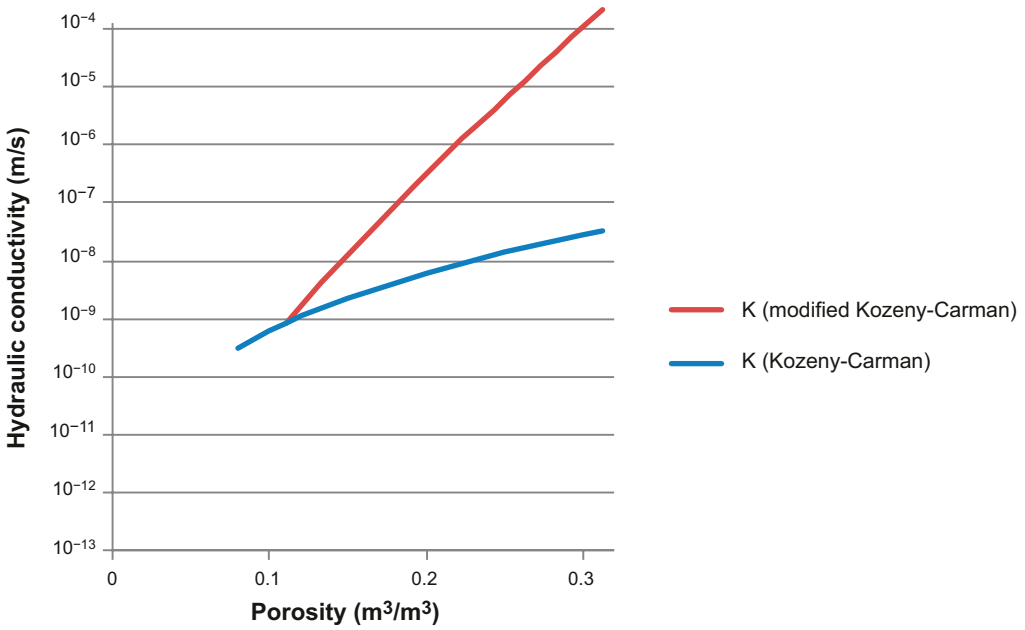


***Figure 5-1.*** *Hydraulic conductivity of a porous material calculated using Kozeny-Carman (blue line) and the modified Kozeny-Carman (red line) models 2014).*

The use of the modified Kozeny-Carman model can be motivated because the hydraulic conductivity is not only dependent on the total porosity of the material but also on the grain size distribution. Here, fine-grained materials normally have a lower hydraulic conductivity than coarser materials with the same total porosity. However, it can be disputed if alterations of the grain size distribution in concrete due to concrete degradation is significant enough to motivate the use of the modified Kozeny-Carman model. This is because concrete also contain inert fine-grained materials (aggregates, fillers) which will remain also in severely degraded concrete.

The hydraulic conductivity of concrete is also dependent on the presence of cracks and other permeable zones and a comparison between Figure 5-1 and Figure 4-3 shows that the impact of penetrating cracks is considerably larger than that of increased porosity. As an example, the hydraulic conductivity of concrete with a porosity of 0.25 corresponds to that of concrete with about one crack with a width of 0.5 mm per 10 meters. This means that the prevention of the formation of penetrating cracks will be crucial in order to prevent significant degradation of the transport properties of the cementitious components.

Table 5-6 and 5-7 present hydraulic conductivity data for the different degradation states for standard cementitious materials. Table 5-6 presents data for chemically degraded cementitious materials without cracks, while Table 5-7 presents data for undegraded cementitious materials with fully penetration cracks. In Table 5-6 the porosity has also been included to illustrate the correlation between the porosity and the hydraulic conductivity.

**Table 5-6. Expected hydraulic conductivity for selected degradation states for cementitious material without cracks.**

| Hydraulic conductivity (m/s)* | Porosity (%) | Material characteristics |
|---|---|---|
| $(1–5)\times10^{-12}$ | 11–13 | Undegraded concrete with a w/c ratio below 0.5 |
| $(1–5)\times10^{-12}$ | 13–15 | Undegraded concrete with a w/c ratio between 0.5 and 0.7 |
| $(5–9)\times10^{-12}$ | 14–16 | No portlandite left. CSH_1.8 is the dominant CSH-phase |
| $10^{-11}$–$10^{-9}$ | 15–17 | CSH_1.1 is the dominant CSH-phase |
| $10^{-9}$–$10^{-7}$ | 20 | CSH_0.8 is the dominant CSH-phase |
| $10^{-7}$–$10^{-5}$ | 20–25 | All CSH-phases has been dissolved. $CaCO_3$ is the principal remaining mineral. |

* Data estimated from Figure 5-1 (blue line) but with an adjustment of the hydraulic conductivity for undegraded concrete to $(1–5)\times10^{-12}$ m/s instead of $8.3\times10^{-10}$ m/s as used by Höglund (2014). The value $(1–5)\times10^{-12}$ m/s is selected from the measured data presented in Section 3.3.3.

**Table 5-7. Expected hydraulic conductivity for undegraded cementitious materials with fully penetrating cracks.**

| Hydraulic conductivity (m/s)* | Material characteristics |
|---|---|
| $(1–5)\times10^{-12}$ | Undegraded concrete without cracks |
| $10^{-11}$–$10^{-10}$ | Concrete with a few cracks in the µm range |
| $10^{-10}$–$10^{-8}$ | Concrete with a few cracks with a width below 0.1 mm |
| $10^{-9}$–$10^{-8}$ | Cementitious grout such as the *New silo grout* with a w/c ratio above 1 |
| $10^{-8}$–$10^{-5}$ | Concrete with a crack with a width not exceeding 0.5 mm or several cracks with widths below 0.05 mm. |
| $10^{-5}$–$10^{-3}$ | Concrete with a crack with a width not exceeding 1 mm or several cracks with widths below 0.1 mm to severely cracked concrete. |
| 0,01–0,1** | The component has completely lost its structural integrity |

* Data estimated from Figure 4-3 except for data for the *New silo grout*. The value $(1–5)\times10^{-12}$ m/s is selected from the measured data presented in Section 3.3.3.

** The values have been selected from Lagerlund (2022) who measured the hydraulic conductivity of coarse materials aimed for use in dams.

### *Effective diffusivity*

Höglund (2014) also modelled the influence of porosity on the effective diffusivity of standard concrete using several different calculation models, Figure 5-2. In this figure, the curves have been fitted to an effective diffusivity of $3\times10^{-12}$ m$^2$/s for concrete with a porosity of 11 %. For the different values of the exponent *n* illustrated in Figure 5-2, Idiart and Shafei (2019) suggest that the value of the exponent of 2.5 gives the best agreement. This value is therefore also used in this work and has been used to produce the values of effective diffusivity for concrete with varying porosity that are reported in Table 5-8.

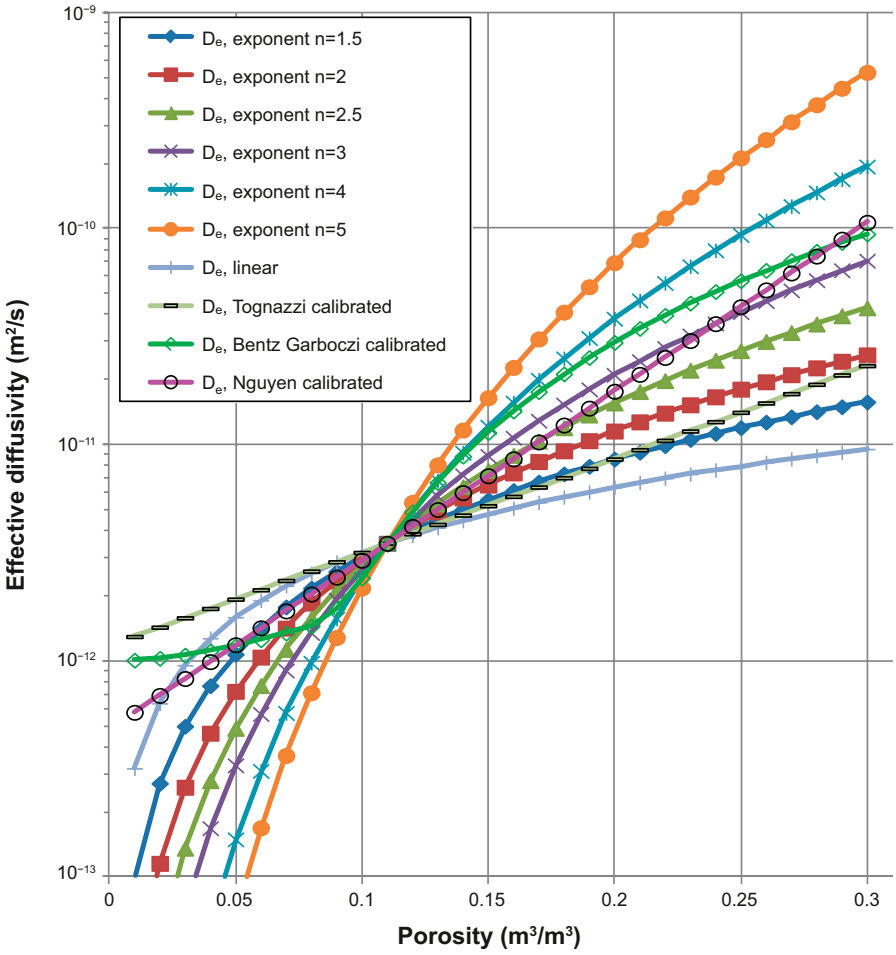


***Figure 5-2.*** *Effective diffusivity as a function of porosity for different calculation models (Höglund 2014).*

Table 5-4 shows that the expected porosity for the different types of concrete used or expected to be used in SFR is nominally 0.11–0.15, with some uncertainties regarding the porosity of the *2BMA concrete*. In Figure 5-2 this corresponds to an effective diffusivity in the range of $(2–8)\times10^{-12}$ m$^2$/s for $n = 2.5$. With increasing porosity, the effective diffusivity also increases and for fully degraded concrete with a porosity between 25 and 30 %, the effective diffusivity is $(2–5)\times10^{-11}$ m$^2$/s for $n = 2.5$.

Table 5-8 and 5-9 presents values of the effective diffusivity for the different degradation states for standard concrete or grout. The values represent average values calculated from data reported in Chapter 3, in this section and other reports, however excluding very high and very low values.

Table 5-8 presents data for concrete without cracks whereas Table 5-9 presents data for concrete with fully penetrating cracks. In Table 5-8 the porosity has also been included to illustrate the correlation between the porosity and the effective diffusivity.

**Table 5-8. Expected effective diffusivity for the selected degradation states for cementitious materials without cracks.**

| Effective diffusivity (m$^2$/s) | Porosity (%) | Material characteristics |
|---|---|---|
| $(2–5)\times10^{-12}$ | 11–13 | Undegraded concrete with a w/c ratio below 0.5 |
| $(5–9)\times10^{-12}$ | 13–15 | Undegraded concrete with a w/c ratio between 0.5 and 0.7 |
| $(5–9)\times10^{-12}$ | 14–16 | No portlandite left. CSH_1.8 is the dominant CSH-phase |
| $5\times10^{-12}–5\times10^{-11}$ | 15–17 | CSH_1.1 is the dominant CSH-phase |
| $(1–5)\times10^{-11}$ | 20 | CSH_0.8 is the dominant CSH-phase |
| $(3–8)\times10^{-11}$ | 25–30 | All CSH-phases has been dissolved. $CaCO_3$ is the main remaining mineral. |

**Table 5-9. Expected effective diffusivity for undegraded cementitious materials with fully penetrating cracks.**

| Effective diffusivity (m$^2$/s) * | Material characteristics |
|---|---|
| $(2–5)\times10^{-12}$ | Undegraded concrete without cracks |
| $(2–5)\times10^{-12}$ | Concrete with a few cracks with a width below 0.1 mm |
| $10^{-11}–10^{-10}$ | Cementitious grout such as the *New silo grout* with a w/c ratio above 1 without cracks |
| $(5–9)\times10^{-12}$ | Concrete with one crack with a width not exceeding 0.5 mm or several cracks with widths below 0.05 mm. |
| $10^{-11}$ | Concrete with one crack with a width not exceeding 1 mm or several cracks with widths below 0.1 mm. |
| $10^{-10}$ | Severely cracked concrete |
| $10^{-9}$ | The component has completely lost its structural integrity |

* Data estimated from Figure 4-4.

### *General uncertainties*

The general uncertainties associated with assessment of the transport properties of the cementitious components at closure are generally small for concrete structures. This is because the properties of the cementitious materials can be verified prior to construction and many of the concrete structures are inspected during the operational period and repaired if required.

For the different types of grout, non-destructive testing after grouting is not possible. This means that assessments of the initial state of e.g. grouts for grouting of waste packages, injection grouts and grout for rock bolts have to rely on tests carried out during the development work.

Predictions of the post-closure evolution of the transport properties are associated with greater uncertainties with the main concern being the increased hydraulic conductivity caused by the formation of cracks. As shown in Figure 4-3, the impact of penetrating cracks on the average hydraulic conductivity of a concrete wall is significant with roughly an increase of the hydraulic conductivity of about one order of magnitude with a doubled crack width. Because the width of a single crack will be dependent on several factors, predictions of crack widths will be difficult with significant uncertainties in the predictions of the hydraulic conductivity of cracked concrete structures as a consequence.

## 5.2 Expected evolution of the conditions in the repository

The evolution of the properties of the cementitious components in SFR is not only dependent on the properties of these components at closure but also on the geochemical, geothermal and hydrogeological properties in the bedrock around the repository. These properties will in turn, with some delay, vary with the surface climate and shoreline position. The following external factors of importance for the post-closure evolution of the properties of the cementitious components will be shortly discussed below:

- Temperature (Section 5.2.1)
- Groundwater flow rate and direction (Section 5.2.2)
- Groundwater composition (Section 5.2.3)

### 5.2.1 Temperature

#### *Overview*

The temperature at repository depth will with some delay follow the average surface temperature above the repository. However, as long as permafrost does not reach repository depth, the post-closure evolution of the properties of the cementitious components in SFR will not be sensitive to the small expected temperature variations in the surrounding bedrock

In recent predictions of the future climate evolution in the Forsmark region, temperate conditions are expected to prevail during up to about 100 000 years post-closure (SKB TR-23-05, Section 3.4). (SKB TR-23-05, Figure 3-27) shows that the predicted increase in annual mean surface air temperature (compared to the average of +6.1 °C for the period 1985–2006) during the first 10 000 years after closure as well as the uncertainties in these predictions vary significantly depending of the future $CO_2$ emissions. For low emissions an increase of only about 1 °C is predicted whereas for the high emissions scenario an increase of up to 8 °C is possible. The uncertainties are, however, large.

Finally, (SKB TR-23-05, Figure 3-28) shows that also the timing of glacial inception depends on the future evolution of the concentration of greenhouse gases in the atmosphere. However, this figure also shows that for a glacial inception to occur before 50 000 years after closure, low $CO_2$ emissions would be required. For that reason, in the description of the expected post-closure evolution of the properties of the cementitious components presented in Chapters 7–14, freezing of concrete is not considered.

#### *General uncertainties*

Given the current situation with increasing levels of $CO_2$ in the atmosphere, accurate predictions of the evolution of the temperature over the following 100 000 years are uncertain. However, as mentioned above, temperature has a minor influence on the evolution of the properties of the cementitious components as long as permafrost does not reach repository depth.

For this reason, the impact of uncertainties concerning future temperatures on the accuracy of predictions of the post-closure evolution of the cementitious components will be small.

### 5.2.2 Groundwater flow rate and direction

#### *Overview*

Groundwater flow and direction will affect the rate of processes occurring in the repository, including e.g. leaching of the cement minerals and radionuclide transport.

Groundwater flow and direction are dependent on the position of the repository in relation to the shoreline of the Baltic Sea. However, groundwater flow and direction are also influenced by the temperature, e.g. due to a permafrost or an extended period of global warming that influences the position of the shoreline.

During the initial period post-closure of the repository, groundwater flow will be very low in the repository due to the location of the repository beneath the Baltic Sea. However, due to shoreline regression, the position of the shoreline will shift and eventually terrestrial conditions will prevail above the repository. At this stage, the flow direction of the groundwater will change but more

importantly for degradation of the cementitious materials, the total groundwater flow rate through the waste vaults will increase (Öhman and Odén 2018, Section 6.2). Soon after the shoreline has passed the position of the repository, rather stationary conditions will prevail.

#### *General uncertainties*

The most important uncertainties associated with predictions of the future groundwater flow and direction are related to the future climate evolution with particular emphasis on future sea levels in relation to land rebound. As long as the repository is submerged beneath the Baltic Sea, groundwater flow in the repository will be low. However, once terrestrial conditions prevail above the repository, groundwater flow will increase and direction change.

However, with current climate changes, predictions of the future position of the shoreline will be increasingly uncertain, both in terms of position and timing. As a consequence, also predictions of groundwater flow and direction in the repository are becoming increasingly uncertain (SKB TR-23-05, Section 3.5).

### 5.2.3 Groundwater composition

#### *Overview*

The composition of the incoming groundwater is of major importance in the prediction of the evolution of the chemical properties of the cementitious components in the repository. This is because the composition of the groundwater influences the post-closure evolution of the mineral composition of the cementitious materials.

The composition of the groundwater in the Swedish bedrock depends on the depth and for shallower groundwaters also on the local surface environment. Typically, the ionic strength of the groundwater increases with increasing depth.

The groundwater at repository depth is initially brackish/saline (SKB TR-23-01, Table 6-1). During the period of terrestrial and temperate conditions, the groundwater changes from being brackish/saline to become slowly and increasingly influenced by meteoric water infiltrating. The timing of the transition to a complete dilute groundwater composition is however uncertain. When the area above the repository is terrestrial, meteoric water is expected to infiltrate, but this will likely occur relatively slowly (SKB-TR-23-01, Section 6.3.6).

#### *General uncertainties*

In analogy to groundwater flow rate and direction, predictions of the timing of events that may cause alterations of the composition of the groundwater at repository depth are associated with uncertainties related to the future climate evolution and shoreline position. See also Section 5.2.2.

## 5.3 Time periods

As shown in Chapter 4, the post-closure evolution of the properties of the cementitious components is influenced by several different processes. Due to changing conditions in the repository and concrete degradation, the influence of each process will vary over time. For this reason, the description of the properties of the cementitious components described in Chapters 6–14 will be divided into the following five different time periods, the characteristics of which will be described in more detail below:

- At closure (Section 5.3.1).
- The saturation period: 0–100 years post-closure (Section 5.3.2).
- The submerged period: 100–1 000 years post-closure (Section 5.3.3).
- 1 000–20 000 years post-closure (Section 5.3.4).
- 20 000–100 000 years post-closure (Section 5.3.5).

As a remark, for some easily degraded cementitious components, the duration of the final two periods will differ from that shown here with typically a shorter duration of the second last period and a very long final period.

### 5.3.1 At closure

The status of the cementitious components at closure – i.e. after backfilling of the waste vaults and construction of plugs but prior to saturation – is dependent on the materials and methods of construction as well as of processes that have affected the cementitious components during the operational period and backfilling.

The following processes assumed to take place during the operational period will be of importance for the status of the cementitious components at closure:

- Heat transport (Section 4.2).
- Water uptake and transport under unsaturated conditions (Section 4.4).
- Crack formation (Section 4.8).
- Metal corrosion (Section 4.17).

### 5.3.2 The saturation period: 0–100 years post-closure

During the first about 100 years post-closure, groundwater slowly fills the waste vaults and starts to saturate the pores and voids in the different cementitious components. At this stage, the main degradation mechanisms of the cementitious components are those caused by the mechanical load from the backfill materials, the waste packages and the groundwater pressure at repository depth prior to saturation of the interior of the concrete structures. Mechanical loads are also caused by the internal pressure from swelling of waste and gases formed through corrosion of primarily fast-corroding aluminium and to some extent also zinc, which has a somewhat slower corrosion rate.

However, during this period the influence of chemical degradation on the properties of the cementitious components is small, since this period is short and the chemical processes slow.

The following processes will be of importance for the evolution of the properties of the cementitious components during the saturation period, i.e. up to 100 years post-closure:

- Heat transport (Section 4.2).
- Water uptake and transport under unsaturated conditions (Section 4.4).
- Gas transport/dissolution (Section 4.6).
- Pressure from swelling of waste (Section 4.7).
- Crack formation (Section 4.8).
- Advection and dispersion (Section 4.10).
- Diffusion (Section 4.11).
- Metal corrosion (Section 4.17).
- Gas production (Section 4.18).

### 5.3.3 The submerged period: 100–1 000 years post-closure

During the submerged period about 100–1 000 years post-closure, the gradual change in shoreline position transforms the conditions above the repository from marine to terrestrial with a marked change in groundwater flow and direction in the bedrock surrounding the repository as a consequence.

At the beginning of this period, the waste vaults are saturated with groundwater which means that the external loads on the concrete structures are limited to the loads caused by the backfill materials whereas internal loads are expected to be mainly caused by swelling of waste, primarily bituminised

ion-exchange resins. Hydrogen gas formed mainly through anaerobic corrosion of steel and some remaining zinc in anti-corrosion paint may also add a small contribution but as long as the gas evacuation systems are in function, this can be neglected.

Due to the gradual shift of the shoreline position during this period, groundwater flow through the waste vaults will increase (Öhman and Odén 2018, Section 6.2). In this report, it is assumed that terrestrial conditions will prevail above the repository at the end of this period even though the exact timing of this event cannot be explicitly determined given the uncertainties related to the future climate evolution (SKB TR-23-05, Section 3.5). See also Section 5.2.2

The following processes will be of importance for the evolution of the properties of the cementitious components during the submerged period from 100 to 1 000 years post-closure:

- Water transport under saturated conditions (Section 4.5).
- Gas transport/dissolution (Section 4.6).
- Pressure from swelling of waste (Section 4.7).
- Crack formation (Section 4.8).
- Advection and dispersion (Section 4.10).
- Diffusion (Section 4.11).
- Dissolution, precipitation and recrystallisation (Section 4.14).
- Metal corrosion (Section 4.17).
- Gas production (Section 4.18).

### 5.3.4 1 000–20 000 years post-closure

Between 1 000 and 20 000 years post-closure, terrestrial conditions prevail above the repository. Shoreline regression continues to shift the position of the shoreline further away from the repository with a change in groundwater flow rate and direction in the bedrock surrounding the repository as a consequence.

External loads during this period are limited to the pressure from the backfill materials used in some of the waste vaults. However, as degradation of the concrete structures and corrosion of the reinforcement bars proceed, the ability of the structures to withstand these loads will be reduced compared to the preceding period with a possible formation of cracks as a consequence.

During this period, chemical processes occurring in the waste continue to produce gases but at a lower rate than during the previous periods. This is because of the formation of layers of corrosion products on the metal objects which affects the rate of transport of reactants and products, but also because of a reduced amount of metals in the repository. In addition, during this period, efficient gas transport is expected since gases can be transported through the gas evacuation system or cracks in the concrete structures.

The magnitude of internal forces caused by swelling of waste is probably similar to the preceding period unless significant degradation which has affected the swelling of the ion-exchange resins has occurred. In addition, as indicated by the study by Emborg et al. (2007), the time to reach full saturation of also the interior of the silo might be considerably longer than that suggested by Holmén and Stigsson (2001) and Börgesson et al. (2015), The consequence of this is that swelling may occur also during this period.

During this period, also interactions with the groundwater and species dissolved in the groundwater continues to alter the mineral composition of the cement minerals and composition of the porewater in these materials. For that reason, significant alterations of the properties of the cementitious components in which low-quality cementitious materials have been used and for thinner concrete structures can be expected at the end of this period. For thick concrete structures, degradation is expected to be less severe.

The following processes will be of importance for the evolution of the properties of the cementitious components during the period from 1 000 to 20 000 years post-closure:

- Water transport under saturated conditions (Section 4.5).
- Gas transport/dissolution (Section 4.6).
- Pressure from swelling of waste (Section 4.7).
- Crack formation (Section 4.8).
- Advection and dispersion (Section 4.10).
- Diffusion (Section 4.11).
- Dissolution, precipitation and recrystallisation (Section 4.14).
- Metal corrosion (Section 4.17).
- Gas production (Section 4.18).

### 5.3.5 20 000–100 000 years post-closure

During this period, the most important process will be dissolution, precipitation and recrystallisation of the cement minerals (Section 4.14) which in combination with the external load from the backfill materials can cause cracking or loss of structural integrity of the cementitious components.

The following processes will be of importance for the evolution of the properties of the cementitious components during the period from 20 000 to 100 000 years post-closure:

- Water transport under saturated conditions (Section 4.5).
- Crack formation (Section 4.8).
- Advection and dispersion (Section 4.10).
- Dissolution, precipitation and recrystallisation (Section 4.14).
- Metal corrosion (Section 4.17).

# 6 Expected status and recommended material property data for cementitious components at closure

In this chapter the expected status of the cementitious components at closure is described. The description is based on an evaluation of the expected influence of the processes (Chapter 4) acting during the operational period given the design (Chapter 2) and the materials (Chapter 3) used in the cementitious components. The description presented here thus constitutes the starting point for the prediction of the post-closure evolution of the properties of these components presented in Chapters 7–14.

With this background, material property data for the cementitious components at closure are recommended. The recommended data constitute a best estimate based on available information and current understanding of the construction process and the degradation processes during the operational period. For that reason, the recommended data are not meant to be uncritically used in radionuclide transport calculations as such intentionally are more cautiously chosen.

Following the table with recommended data, the uncertainties regarding the status of the cementitious components at closure are shortly discussed. Examples include the properties of the different types of grout which cannot be inspected as well as the status of concrete structures for which dimensions, amount of reinforcement and/or construction method have not yet been finally settled.

The status of the cementitious components are presented separately for each waste vault in Sections 6.1 to 6.7. In order to avoid repetition, the status of the properties of the following cementitious components which are common for all waste vaults and tunnels are described in Section 6.8 (at closure) and Chapter 14 (post-closure evolution) respectively:

- Concrete plugs in tunnels.
- Concrete plugs in investigation boreholes.
- Shotcrete on the rock walls.
- Grout for rock bolts.
- Injection grout in the surrounding bedrock.

## 6.1 Cementitious components in the silo

In this section, the expected status at closure of the cementitious components in the silo which were introduced in Section 2.5 is described, Section 6.1.1. This is followed by Section 6.1.2 which recommends material property data of the cementitious components at closure and Section 6.1.3 which summarises identified specific uncertainties in the descriptions.

### 6.1.1 Expected status at closure

#### *Slab*

**Chemical properties**

During the operational period, concrete degradation on the underside of the slab will be minute. This is because a sealing layer comprising a butyl liner and a thin layer of concrete which prevents any concrete/bentonite interactions during the operational period is placed between the sand/bentonite foundation and the slab, Figure 2-5.

Also, alterations of the mineral composition of the slab on the inside of the concrete cylinder will be minute because the slab is covered with grouted waste packages and inner walls.

**Load-bearing capacity**

During the operational period, the slab will only experience compressive loads from the concrete silo and the grouted waste packages whereas tensile loads caused by uneven settlements in the foundation layer are not expected. This statement is supported by the results from the control programme carried out during the operational period which have shown that settlements so far have been small (SKB TR-14-02, Table 7-1).

According to Cronstrand et al. (2011), the compressive strength of the undegraded concrete in the silo slab is significantly higher than the expected maximum compressive load. The limited access to groundwater in the slab will limit concrete degradation during the operational period. Some rebar corrosion may occur but this is not expected to affect the ability of the slab to resist the homogeneous compressive load from the grouted waste packages and inner walls. It is also reasonable to assume that the compressive strength of the concrete in the slab has increased thanks to continued hydration during the operational period compared to the 28 days compressive strength normally used as a dimensioning value. As an example Mårtensson and Vogt (2019, Tables 5-5 and 5-6) observed an increase of the compressive strength of the 2BMA concrete from an average of 49 MPa at 28 days to 67.7 MPa at six months.

The conclusion is therefore that the load-bearing capacity of the slab at closure will be sufficient to resist the combined compressive load from the grouted waste packages, inner walls, lid and backfill material during the operational period and cracking is therefore not expected to occur.

**Transport properties**

From the previous section, the load-bearing capacity of the slab of the silo is judged to be sufficient to prevent cracking during the operational period. Also, drying shrinkage or temperature variations during the operational period are not expected to cause cracking as the slab is sandwiched between the foundation layers and the grouted waste packages and such variations are therefore minute. The consequence of this is that the transport properties of the slab at closure be similar to those of the slab at the start of the operational period.

For the slab, which is cast on top of a thin layer of concrete (Section 2.5.2), the main risk for cracking is instead related to temperature shrinkage during construction. In case of a strong adhesion between the slab and the thin layer of concrete, there is a potential for restrained temperature shrinkage with a risk for cracking as a consequence. Currently, no information regarding the status of the slab at the start of the operational period has been found.

In all, the risk for formation of penetrating cracks in the slab during construction cannot be ignored. It is therefore expected that the slab of the concrete silo at closure of SFR will have the transport properties of undegraded concrete with a few penetrating cracks with a width below 0.5 mm.

### *Outer wall*

**Chemical properties**

Alterations of the mineral composition on the inside of the outer wall are expected to be minute during the operational period even though carbonation could occur on the inside of the outer wall in the small shafts where no waste packages have yet been emplaced, see Figure 2-4. In the large shafts adjacent to the outer wall, waste packages have been emplaced and grouted and carbonation is therefore limited to the upper parts where no waste packages have yet been emplaced.

Also, only minor alterations of chemical properties of the outer wall at the interface with the surrounding bentonite are expected during the operational period. Cement/bentonite interactions are inherently slow and the influence on the mineral composition within the cement part of this system is small as shown by e.g. Mårtensson and Kalinowski (2019). In addition to this, the draining system that is attached to the rock wall will prevent intrusion of groundwater and this further limits concrete/bentonite interactions during the operational period.

In all, the chemical properties of the outer wall of the concrete silo at closure are expected to correspond to those of the undegraded *Silo concrete*, Section 3.3.1.

Finally, as mentioned in Section 2.5.3, groundwater was found in three of the shafts that faces the outer wall and some leaching can therefore be expected. However, from the findings presented by Mårtensson the impact of this on the chemical properties of the outer wall is minute.[52]

**Load-bearing capacity**

The load-bearing capacity of the outer wall at the time of closure is expected to be equivalent to that of the outer wall at the end of the construction phase or better thanks to the continued hydration of the concrete during the operational period, see above.

This statement is supported by the fact that chemical degradation of the concrete during the operational period will be minute and not expected to affect the mechanical properties of the *Silo concrete*. It is also supported by the fact that corrosion of the reinforcement bars is expected to be slow due to the high pH in the concrete in combination with the slow saturation of the outer wall.

The load-bearing capacity of the outer wall is further improved by the mechanical support from the inner walls and grouted waste packages and the risk for formation of penetrating cracks due to external loads is therefore minute during the operational period.

No internal loads such as pressure from swelling waste are expected during the operational period due to the low access to groundwater in the waste compartment during this period. Also, gas formation is not expected during this period for the same reason and any gases formed should be transported out of the still open silo. The fact that groundwater was found in three of the shafts facing the outer wall (Section 2.5.3) is not expected to affect the load-bearing capacity of the outer wall as the investigation programme showed that the impact on the chemical properties of the concrete had been small and the time during which water had been present in the shafts comparatively short. The presence of water is not expected to affect the magnitude of internal loads as no bituminised waste was affected by the intruding groundwater.

Finally, the risk for cracking due to uneven and sudden settlements of the concrete silo due to uneven load distribution or rock movements is limited. This is supported by several consecutive measurements compiled in the initial state report for SR-PSU (SKB TR-14-02, Table 7-1) which have shown that settlements of the silo so far have been small.

In conclusion, the load-bearing capacity of the outer wall will be sufficient to prevent cracking during the operational period.

**Transport properties**

From the previous section, the load-bearing capacity of the outer wall is judged to be sufficient to prevent cracking during the operational period. Also, drying shrinkage or temperature variations during the operational period are not expected to cause cracking thanks to the humid conditions and small temperature variations in the silo during the operational period.

The consequence of this is that the transport properties of the outer wall at closure are expected to be the same as those of the outer walls at the start of the operational period.

For the outer walls, the main risk for cracking is instead related to the method of construction, i.e. slip forming. Here, there is a small possibility that horizontal cracks may have formed during the construction work in the case the still not yet completely hardened concrete attached to the formwork during slip-forming. However, no information that this occurred has been found. In addition, cracking due to temperature shrinkage during construction is also possible but no information on the properties of the concrete silo prior to installation of the bentonite has been found.

In all – and even though some uncertainties regarding the current status of the outer wall of the concrete silo remains to be resolved – it is predicted that the outer wall of the concrete silo will not contain any penetrating cracks at the time of closure and that the transport properties therefore will correspond to those of uncracked *Silo concrete,* Section 3.3.1.

[52] SKBdoc 1327780 ver 3.0. (Internal document, in Swedish.)

### *Lid*

#### Chemical properties

At closure, the lid will have the chemical properties of undegraded *2BMA concrete*, Section 3.3.3 or similar. This is because the lid will be constructed at closure of the repository.

#### Load-bearing capacity

The load-bearing capacity of the lid of the silo at the time of closure will be sufficient to carry the load from the backfill material without the risk for cracking. This is because the lid is constructed at closure which prevents degradation during the operational period but also because the lid is supported by the inner walls, the grouted waste packages and a layer of sand as shown in Figure 2-9.

#### Transport properties

At closure, the lid (not including the gas evacuation system) will have the transport properties of undegraded *Silo concrete*. Cracks in the lid at the time of closure are not anticipated as the dimensions, amount of reinforcement and method of construction can be optimised to prevent cracking.

### *Inner walls*

#### Chemical properties

At closure, the average chemical properties of the inner walls of the concrete silo are expected to correspond to those of up to 90 years-old *Silo concrete*, characterised by high pH and low porosity due to prolonged cement hydration in the humid environment in the waste vault during the operational period. Alterations of the mineral composition of the inner walls will be minute due to the restricted amount of groundwater in the interior of the silo. See also Section 2.5.3 concerning the impact of the presence of groundwater in some of the shafts on the properties of the inner walls.

#### Load-bearing capacity

From the previous section, alterations of the mineral composition of the inner walls during the operational period are expected to be negligible. Instead, it is a reasonable assumption that the compressive strength of the concrete itself will increase during the operational period thanks to continued cement hydration. Further, only limited corrosion of the reinforcement bars is expected during this period with the possible exception of the rebars in the shafts in which groundwater was detected.[53] Finally, the load-bearing capacity of the inner walls is further improved by the support from the grouted waste packages.

Therefore, the load-bearing capacity of the inner walls at closure will be sufficient to carry the vertical load from the lid and the backfill material as well as to provide support to the outer wall to withstand the horizontal load from the pressure from the surrounding bentonite.

However, the inner walls must also withstand the load from the wet grout during grouting of the waste packages, corresponding to a height of about 6 meters of grout with a density of about 2 000 kg/m$^3$. Currently, no information on the resistance of the inner walls towards the pressure from the wet grout has been found. However, for the purpose of this report, it is assumed that the load-bearing capacity of the inner walls towards the pressure from the wet grout is sufficient to prevent cracking during grouting. This statement is justified by the fact that grouting was already planned from the start of operation of the silo and this must therefore have been considered when designing the silo.

As a final remark, internal loads due to swelling of waste are not expected during the operational period because of the limited access to groundwater in the shafts during this period.

In all, this means that the formation of cracks in the inner walls due to insufficient load-bearing capacity during the operational period is not expected.

[53] SKBdoc 1327780 ver 3.0. (Internal document, in Swedish.)

**Transport properties**

As mentioned in the previous section, the load-bearing capacity of the inner walls of the silo is judged to be sufficient to prevent cracking during the operational period. Also, drying shrinkage or temperature variations during the operational period are not expected to cause cracking because of the humid conditions and small temperature variations in the silo during the operational period.

The consequence of this is that the transport properties of the inner walls at closure are expected to be the same as those of the inner walls at the start of the operational period.

For the inner walls, the main risk for cracking is instead related to the method of construction, i.e. slip forming. Here, there is a small possibility that horizontal cracks may have formed during construction in the case the still not yet completely hardened concrete attached to the formwork during slip-forming. In addition, cracking due to temperature shrinkage during construction is also possible. However, because no inspection protocols have been found, this can currently only be speculated upon.

In all – and even though some uncertainties regarding the current status of the inner walls of the concrete silo remains to be resolved – it is expected that the inner walls of the concrete silo will not contain any penetrating cracks at the time of closure and that the transport properties therefore will correspond to those of uncracked *Silo concrete,* Section 3.3.1.

### *Concrete moulds*

**Chemical properties**

At closure, the concrete moulds are expected to have the chemical properties of undegraded concrete. This is because the moulds are manufactured just prior to use and then grouted once emplaced in the silo. In addition, the amount of free water inside the moulds, i.e. water that is not fixed in the waste matrix (mainly cement solidified ion exchange resins and filter aid) is low. This means that even though some decomposition of the waste may occur during the operational period, interactions between the decomposition products and the interior of the concrete moulds will be limited. Interactions with the surrounding grout will be negligible during the operational period due to the low amount of available water in the shaft and the fact that the grout and the concrete moulds have similar chemical properties.

However, as discussed in Section 2.5.3, a total of 36 $m^3$ of groundwater – varying from 0.1 $m^3$ to 12 $m^3$ – was found in ten of the shafts in the silo during the period 2010 to 2013 and in several of these shafts concrete moulds had been emplaced but not yet grouted. Based on a series of investigations, Mårtensson concluded that the impact of this on the average chemical properties of the concrete moulds and inner walls was minute.[54] In this report, the impact of the intruding groundwater on the average chemical properties of the concrete moulds is therefore not considered.

**Load-bearing capacity**

The load-bearing capacity of the concrete moulds at closure is expected to be sufficient to ensure that even the concrete moulds furthest down in the stacks of moulds can carry the load from a stack of concrete moulds. This conclusion is supported by the study by Bultmark (2017a) who showed that a concrete mould can carry the weight of a stack of a material with a density of 2 500 kg/$m^3$ with a height of about 100 meters without the support from any grout. There is thus sufficient margin to prevent the risk for cracking of the concrete moulds due to the load from the stack of waste packages.

As a final remark, internal loads due to swelling of waste are not expected during the operational period because of the limited access to groundwater in the shafts during this period.

**Transport properties**

Based on the discussions above, the transport properties of the concrete moulds at closure are expected to correspond to those of undegraded *SFR mould concrete* without cracks or other permeable zones.

[54] SKBdoc 1327780 ver 3.0. (Internal document, in Swedish.)

### *Permeable grout between the waste packages and the inner walls*

#### Chemical properties

At closure, the permeable grout surrounding the waste packages are expected to have the chemical properties of undegraded *Original silo grout* (Section 3.4.1) or *New silo grout* (Section 3.4.2). This is because the grout has been enclosed in the silo with negligible contact with the groundwater or other components that could alter the chemical properties of the grout during the short operational period.

#### Load-bearing capacity

As described in Section 3.4.1 and 3.4.2, the compressive strength of the *Original silo grout* and *New silo grout* is low. Further, the capacity to withstand tensile loads is hampered by the lack of reinforcement. However, the load-bearing capacity of the grout at closure is expected to be sufficient to withstand the small compressive loads experienced during the operational period. Also, because swelling of waste is not expected during the operational period, tensile loads are not expected.

In all, this concludes that the load-bearing capacity of the permeable grout between the waste packages and the inner walls is expected to be sufficient to prevent cracking during the operational period.

#### Transport properties

From the previous section, cracking due to insufficient load-bearing capacity of the grout between the waste packages and the inner walls during the operational period is not expected. The consequence of this is that the transport properties of this grout at the time of closure will correspond to those of the undegraded hardened grout.

In addition to transport within the grout itself, gases and water can also be transported in empty voids and channels between the waste packages in the case that these parts are not entirely filled with grout. Pettersson and Thunberg (2012) showed that the flow of grout in narrow slits was very slow and inhomogeneities were also observed. This indicates that there is a potential risk that the narrow slits between the waste packages in the silo are not entirely filled with grout and permeable zones therefore formed in these parts of the stack of waste packages. However, the probability for the formation of a continuous permeable zone through the entire shaft is low. This is because grouting of the waste packages is done sequentially and permeable zones can be sealed in a subsequent grouting campaign.

In all, this concludes that the transport properties of the permeable grout between the waste packages and inner walls at the time of closure are expected to be similar to those of the undegraded *Original Silo grout* (Section 3.4.1) or *New silo grout* (Section 3.4.2).

## 6.1.2 Recommended material property data

In Table 6-1, recommended material property data for the cementitious components in the silo at closure are presented. The recommendations are based on the descriptions of the cementitious components presented in Section 2.5 with data for the undegraded cementitious materials taken from Chapter 3. In addition, the final selection of material property data also relies on the information presented in Section 6.1.1 and Section 5.1.

**Table 6-1. Recommended material property data for the cementitious components in the silo at closure.**

| | pH | Porosity | Hydraulic conductivity | Diffusivity | Compressive strength** | Tensile strength** |
|---|---|---|---|---|---|---|
| | - | % | m/s | $m^2/s$ | MPa | MPa |
| **Slab** | ≥ 13 | 11–13 | $10^{-8}$–$10^{-5}$ | $(5–9)\times10^{-12}$ | 55–60 | 4–5 |
| **Outer wall** | ≥ 13 | 11–13 | $(1–5)\times10^{-12}$ | $(2–5)\times10^{-12}$ | 55–60 | 4–5 |
| **Lid*** | ≥ 13 | 11–13 | $(1–5)\times10^{-12}$ | $(2–5)\times10^{-12}$ | 55–60 | 4–5 |
| **Inner walls** | ≥ 13 | 11–13 | $(1–5)\times10^{-8}$ | $(2–5)\times10^{-12}$ | 55–60 | 4–5 |
| **Permeable grout** | ≥ 13 | 30 | $(5–20)\times10^{-9}$ | $(1–5)\times10^{-11}$ | 5–9 | 0.5–1 |
| **Concrete moulds** | ≥ 13 | 10–12 | $(1–9)\times10^{-12}$ | $(2–5)\times10^{-12}$ | 40–50 | 4–5 |

* Not including the sand-filled gas evacuation channels.
** Refers to the cementitious material used in the various components.

### 6.1.3 Specific uncertainties

The following specific uncertainties concerning the properties of the cementitious components of the silo have been identified:

- There is a lack of information concerning the status of the slab, outer and inner walls at the start of the operational period with specific emphasis on the presence of cracks in these components.
- The outcome of the grouting of the waste packages is somewhat uncertain and in particular the presence of permeable zones between the waste packages caused by incomplete grouting of these sections is not known.
- The impact of the gas evacuation channels in the lid on the over-all transport properties of the lid is not fully known and therefore not considered in this report. The concrete will have a very low hydraulic conductivity (on the order of $10^{-11}$ to $10^{-12}$ m/s) compared to that of the sand planned for filling of the channels which will have a grain size of about 2 mm (Höglund and Bengtsson 1991) and a hydraulic conductivity of about $10^{-2}$ m/s (Kennedy et al. 1984). The influence of type of material in the channels in the lid that constitute one part of the gas evacuation system in 2BMA is discussed in Section 6.3.1.

## 6.2 Cementitious components in 1BMA

### 6.2.1 Expected status at closure

In this section the expected status at closure of the cementitious components in 1BMA which were introduced in Section 2.6 is described, Section 6.2.1. This is followed by Section 6.2.2 which recommends material property data for the cementitious components at closure and Section 6.2.3 which summarises identified specific uncertainties in the descriptions.

#### *Slab*

**Chemical properties**

The current status of the slab in 1BMA has been thoroughly investigated and the results from the reports generated within the investigation programme are compiled in Elfwing et al. (2015). From the findings presented in that report, it can be concluded that the chemical properties of the slab have been altered during the operational period.

The most important finding reported by Elfwing et al. (2015) is the increased levels of chlorine detected in several specimens taken from the slab with a highest value of above 3 % of the cement weight within the upper 50 mm of the slab in some positions. The levels decrease further into the slab but levels close to 1 % of the cement weight were found as deep into the slab as 150 mm in some positions.

However, restrictions on the number of cores that was permitted to be extracted from the slab motivated drilling in positions where high chlorine levels were anticipated and the statistical basis therefore both small and biased. The high chlorine levels are still of great concern as high chlorine levels are known to increase the corrosion rate for steel reinforcement embedded in the concrete.

With the installation of the waterproofing membrane in 1BMA in 2011, the concrete structure is now protected from the intruding groundwater and the levels of chlorine will not increase further. However, the chlorine currently within the concrete will not be removed during the operational period and continue to incur an increased rate of rebar corrosion.

The investigation programme (Elfwing et al. 2015) also revealed that carbonation had occurred in the upper parts of the slab, causing a transformation of the portlandite into calcite with a reduction in pH as a consequence, Figure 6-1 and Figure 6-2. However, as evident from these figures, carbonation only reaches a few mm into the concrete and hence not influencing the corrosion rate of the reinforcement bars which are mainly placed further into the slab where pH will still be controlled by the presence of portlandite and therefore remain at about 12.5.

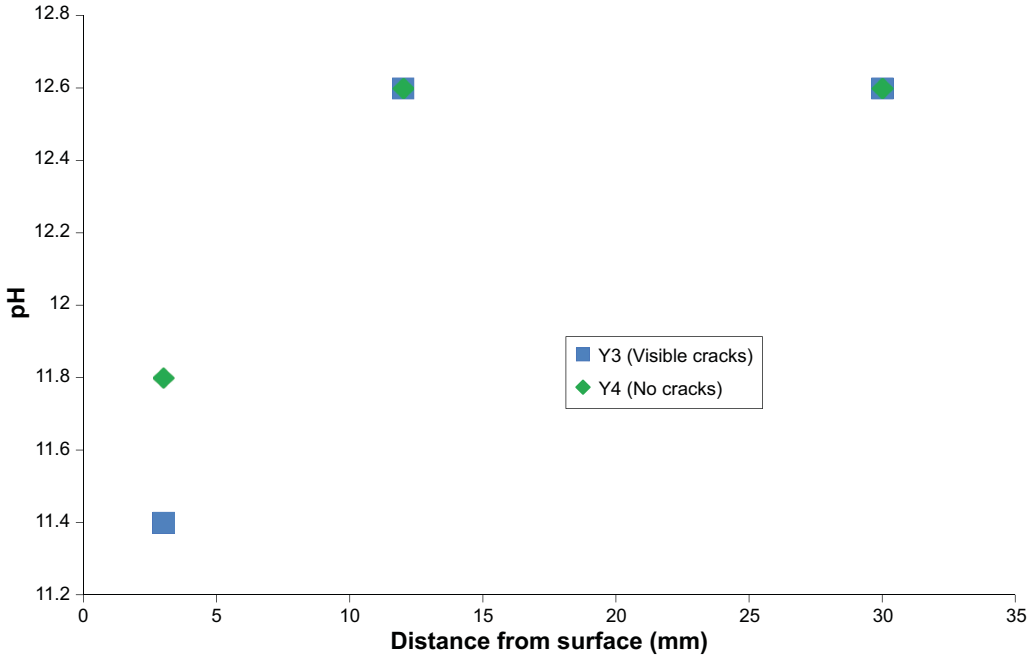


***Figure 6-1.*** *pH in cores from the slab in compartment 13 in 1BMA. Redrawn from (SKBdoc 1314759 ver 1.0, internal document, in Swedish, Figure 30).*

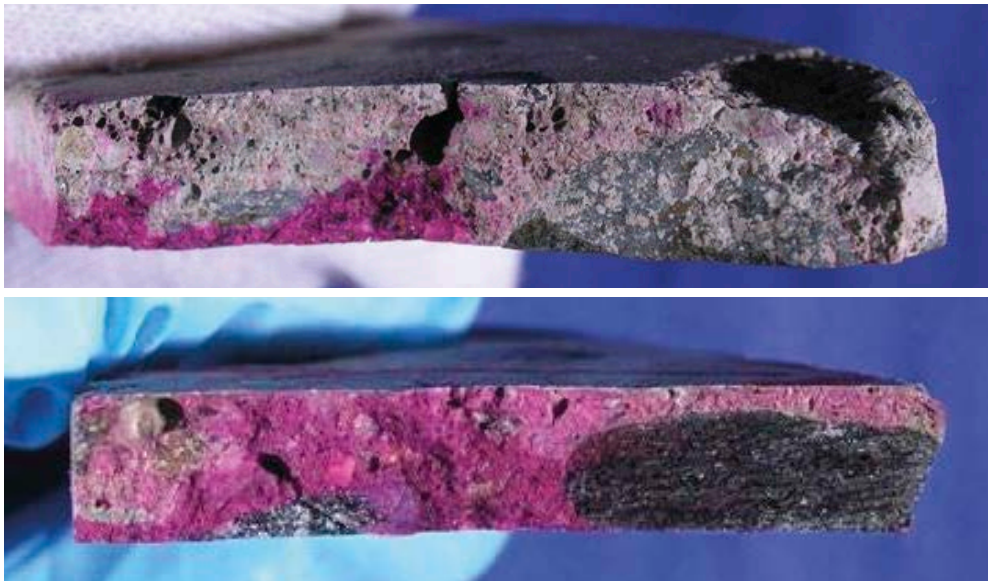

***Figure 6-2.*** *Concrete samples obtained from cores with a diameter of 100 mm and a thickness of about 15 mm sprayed with a phenolphthalein solution. Outside of concrete structure is facing upwards. Purple colour indicates that carbonation has not occurred. Note that the change in colour occurs at a pH of about 9.2 and that areas in which carbonation is not complete may pass undetected with this method. (Elfwing et al. 2015).*

In Figure 6-1, the highest observed pH is 12.6. This is a little lower than expected since leaching of the alkali hydroxides during the operational period is not expected and pH would therefore have been about 13. However, the method used for measuring the pH involved crushing of a piece of concrete followed by dissolution in water and determination of pH through titration with 0.01 M HCl using a phenolphthalein indicator.[55]

[55] SKBdoc 1314759 ver 1.0. (Internal document, in Swedish.)

With this method description as a background, it is possible to refer the lower than expected pH to losses during sample preparation caused by e.g. incomplete dissolution of the cement minerals and transfer of the alkali hydroxides to the titration solution. In addition, the laboratory was not accredited for this method and experience of the type of sample preparation and method of analysis used here possibly therefore limited and uncertainties larger.

In all, the chemical properties of the slab in 1BMA have been affected by carbonation and chlorine intrusion, the main effect of which is an increased corrosion rate of the reinforcement bars embedded in the concrete. Leaching of the concrete at the underside of the slab is prevented during the operational period by the design of the vault. Especially the layer of draining material beneath the concrete structure prevents leaching as shown by Elfwing et al. (2015).

#### Load-bearing capacity

Based on calculations performed by Westerberg (SKBdoc 1466364 ver 1.0, internal document, in Swedish), Elfwing et al. (2015) concludes that the load-bearing capacity of the slab is sufficient to carry the load from the stack of 6 concrete moulds, each with a weight of 5 metric tons.

The load-bearing capacity of the slab in 1BMA has also been calculated by Nytorp Jansson (2020a). The findings by Nytorp Jansson (2020a) showed that the load-bearing capacity of the slab and thus the risk for cracking was dependent on the stiffness of the foundation layer of the slab. However, the calculations also showed that only a rather low stiffness was required to prevent cracking. Nytorp Jansson (2020a) finally noted that the stiffness of the foundation layer in 1BMA should be considerably higher than that required as long as standard construction methods were used.

The conclusion is therefore that the load-bearing capacity of the slab is sufficient to prevent cracking during the operational period. For uncertainties, see Section 6.2.3.

#### Transport properties

From the previous section, cracking of the slab is not expected during the operational period. Instead, the transport properties of the slab at the time of closure will be controlled by the cracks formed during construction. This is because there are currently no plans of restoration of the slab prior to closure.

As shown in Figure 4-3, the average hydraulic conductivity of a concrete structure with penetrating cracks is dependent on the width and average distance between the individual cracks and therefore likely to be unique for each compartment of the concrete structure in 1BMA.

For the existing outer walls of the concrete structure in 1BMA, Höglund (2014, Section 6.15) calculated the hydraulic conductivity to about $1 \times 10^{-4}$ m/s and the effective diffusivity to just above $3 \times 10^{-12}$ m$^2$/s based on the description of the status of these walls presented in Elfwing et al. (2015).

Based on a comparison of the degree of cracking of the slab and the walls reported by Elfwing et al. (2015) it is concluded that the transport properties of the outer walls reported by Höglund (2014) provides a reasonable estimate of the transport properties of the slab of the concrete structure in 1BMA.

### *Existing outer walls*

#### Chemical properties

The current status of the existing outer walls in 1BMA has been thoroughly investigated and the results from the reports generated during the investigation programme are compiled by Elfwing et al. (2015). From the findings presented in that report, it can be concluded that the chemical properties of the existing outer walls have been slightly altered during the operational period.

In analogy with the slab, increased amounts of chlorine are found in the existing outer walls but the levels were lower and not exceeding 1 % of the cement weight. Also, some carbonation has occurred.

With the installation of the waterproofing membrane in 1BMA, the concrete structure will be protected from the intruding groundwater and the levels of chlorine will not increase further. However, the chlorine currently within the concrete will not be removed during the operational period and continue to incur an increased rate of rebar corrosion.

#### Load-bearing capacity

During the operational period, the dominant load is that from the overhead crane used for emplacement of the waste packages. Here, Elfwing et al. (2015) concludes that the load-bearing capacity of the existing outer walls is not compromised by the observed concrete degradation and rebar corrosion and extensive additional cracking is therefore not anticipated.

#### Transport properties

Höglund (2014) estimated the hydraulic conductivity of the existing outer walls of the concrete structure in 1BMA based on the description of the status of these walls presented in Elfwing et al. (2015). In this report Höglund (2014, Section 6.15) estimates the hydraulic conductivity of the existing outer walls to $2.6–5.3 \times 10^{-4}$ m/s and the effective diffusivity to $3.5 \times 10^{-12}$ m$^2$/s.

Since significant additional cracking is not expected during the operational period, these values will be representative for the existing outer walls also at closure of 1BMA.

### *New outer walls*

#### Chemical properties

At closure, the chemical properties of the new outer walls will be the same as those of the undegraded *2BMA concrete*. This is because the new outer walls will be cast outside the existing ones at closure of 1BMA and therefore no degradation will occur prior to closure.

#### Load-bearing capacity

As concluded by Westerberg, the load-bearing capacity of the outer walls at closure will be sufficient to withstand the combined load from the backfill material and the pressure from the intruding groundwater during saturation if constructed according to the information provided in Section 2.6.2.[56] Cracking of the new outer walls is therefore not expected during backfilling of the waste vault.

#### Transport properties

At closure, the transport properties of the new outer walls of 1BMA are expected to be the same as those of the *2BMA concrete*, Section 3.3.3. This is because the planned construction method for the new outer walls suggested by Wimelius (2021) will ensure that no cracks or other permeable zones will form during construction of these walls. See also Section 2.6.4.

### *Lid*

#### Chemical properties

The lid will be constructed at closure and the chemical properties of the lid at closure will therefore be the same as those of the undegraded *2BMA concrete* or a similar material.

#### Load-bearing capacity

From Section 2.6.2, the load-bearing capacity of the lid of the concrete structure in 1BMA will be sufficient to withstand the combined load from the backfill material and pressure from intruding groundwater during saturation of the repository. Cracking of the lid is therefore not expected during backfilling of the waste vault.

[56] SKBdoc 1583182 ver 1.0. (Internal document, in Swedish.)

**Transport properties**

The transport properties of the lid will be the same as those of undegraded *2BMA concrete* or a similar material. This is because the lid can be designed and constructed using such a material and according to such principles that cracking during construction and backfilling of the waste vault can be avoided, Section 2.6.2. However, the average transport properties of the lid are also dependent on the transport properties of the gas evacuation system, see below.

### *Inner walls*

**Chemical properties**

At closure, the chemical properties of the inner walls will be representative for those of up to 90 years old *1BMA concrete*.

From Section S*lab*, some carbonation has probably occurred in the surface regions of the inner walls with a reduced pH in these regions as a consequence. Also, chlorine intrusion in the inner walls is possible but the extent of this varies between the different compartments since some were closed already at an early stage whereas others are still open.

The right part of Figure 6-3 shows that discoloration of the inner walls due to corrosion of tie rods is small compared to that of the existing outer wall shown in the left part of the image. This implies that corrosion of the reinforcement bars and tie rods has been small during the first 30 years of operation and is an indication of low levels of chlorine in the inner walls. After the installation of the water-proofing membrane, no further intrusion of chlorine containing groundwater will occur during the remaining part of the operational period.


***Figure 6-3.*** *The interior of compartment 12 in 1BMA showing the inner wall to the right and the existing outer wall to the left as well as some concrete moulds. Note the holes in the existing outer walls in the left part of the image planned for use during the now abandoned grouting of the waste packages.*

**Load-bearing capacity**

The function of the inner walls during the operational period is to provide support for the prefabricated concrete elements, Table 2-4. The weight of these elements is low in comparison with the compressive strength of the concrete in the inner walls and the load-bearing capacity of the inner walls thus sufficient unless extensive degradation occurs.

In Figure 6-3, spalling is not observed in the inner walls and because of the installation of the water-proofing membrane only little corrosion is expected until closure. However, it must be remembered that Figure 6-3 only shows one of the 13 compartments. For the compartments which are filled with waste packages and closed, the status of the inner walls is not known.

**Transport properties**

Cracks have been found also in the inner walls between the waste compartments and in particular in the corners of the doorways between the individual compartments (Figure 6-4). However, because the inner walls do not formally constitute a hydraulic barrier they were not included in the inspection programme described by Elfwing et al. (2015). For that reason, detailed information on the presence of cracks in all parts of the inner walls is not available. Instead, the crack illustrated in Figure 6-4 is regarded as an assumed representative example for all inner walls.

Because these cracks will not be sealed prior to closure and a lack of detailed information on the width and distribution of cracks in the inner walls, the same transport properties are assigned to the inner walls as to the existing outer walls.

### *Prefabricated concrete elements*

**Chemical properties**

At closure of 1BMA, the chemical properties of the prefabricated concrete elements will vary between those of fairly young to up to 90 years old *1BMA concrete* with increased levels of chlorine caused by intruding groundwater during the period prior to the installation of the waterproofing membrane. Some carbonation may have occurred, but this will be limited to the outer few millimetres of the elements, Figure 6-2. Leaching is not expected and with the installation of the waterproofing membrane further interactions with the groundwater will not occur.

***Figure 6-4.*** *Penetrating crack in the upper corner of a doorway between two adjacent waste compartments.*

**Load-bearing capacity**

The prefabricated concrete elements do not experience any external loads during construction and the operational period. The load-bearing capacity is therefore not relevant during these stages.

During casting of the lid, the prefabricated elements must be able to carry the weight of the wet concrete, corresponding to about 2 000 kg/m$^2$ for an 800 mm thick lid. It is expected that the load-bearing capacity of the prefabricated elements will be sufficient but this must be clarified prior to casting of the lid.

**Transport properties**

From the previous section, the transport properties of the prefabricated elements will correspond to those of up to 90 years old *1BMA concrete*. However, in this report, the transport properties of the prefabricated elements are evaluated for the elements as a group. For that reason, the transport properties will be determined by the width of the slits between the individual elements, estimated to between 1 and 10 millimetres.

### *Gas evacuation system*

**Chemical properties**

From Section 3.4.4 the chemical properties of the permeable grout in the gas evacuation system (*2BMA grout*) in the lid at closure will be the same as those of the undegraded *New silo grout*, Section 3.4.2. No alterations are expected as the channels are filled just prior to backfilling and closure of the repository.

**Load-bearing capacity**

The load-bearing capacity of gas evacuation system is not relevant.

**Transport properties**

From Section 3.4.4, the transport properties of the permeable *2BMA grout* in the gas evacuation system in the lid at closure will be the same as those of the undegraded *New silo grout*, Section 3.4.2. No alterations are expected as the channels are filled just prior to closure of the repository.

### *Concrete moulds*

**Chemical properties**

First, the status of a majority of the concrete moulds in 1BMA is uncertain since they are stored in closed compartments and not easily available for inspections. Even though valid for a number of the concrete moulds; the text below is therefore associated with some uncertainties as discussed in Section 6.2.3.

At closure, the concrete moulds in 1BMA will have the chemical properties of up to 90 years-old reinforced *SFR mould concrete,* which is expected to have been at least partially exposed to ground-water with increased chlorine levels as a consequence. It is also likely that some carbonation of the parts closest to the surface may have occurred.

The extensive corrosion shown in Figure 6-5 indicates that the concrete moulds have been exposed to rather harsh conditions and their chemical properties are likely to have been affected. However, as shown in Figure 6-3, no signs of corrosion of the reinforcement bars in the concrete moulds are shown.

It must, however, be noted that the concrete moulds shown in Figure 6-5 have been stored in an open compartment since the 1990:ies. The status of the concrete moulds stored in the already closed compartments is unknown because of poor accessibility for inspection.

***Figure 6-5.*** *The lifting eye in the upper parts of a concrete mould with obvious signs of severe corrosion. The concrete mould has been stored in an open compartment for many years and is thus not representative for all concrete moulds in 1BMA.*

Several waste packages contain evaporator concentrates. However, according to SKB (R-18-07) no concrete moulds containing evaporator concentrates have yet been disposed in 1BMA. This means that the concrete moulds have not been exposed to internal chemical attacks from dissolved salts. Instead, external attacks may occur if salts are released from other waste packages but no such interactions are expected during the operational period.

**Load-bearing capacity**

The load-bearing capacity of concrete moulds has been calculated by Bultmark (2017a). The calculations showed that a concrete mould can carry the weight from a stack with a height of about 100 meters of a material with a density of 2 500 kg/m$^3$. There is thus sufficient margin to prevent cracking of the concrete moulds due to the load from the stack of waste packages.

**Transport properties**

Based on the findings presented in the previous sections, the transport properties of the concrete moulds at closure are expected to correspond to those of up to 90 years old *SFR mould concrete* without cracks. This conclusion is also based on the fact that no cracks are expected to form in the concrete moulds during manufacturing and that moulds in which cracks are identified in the production control are discarded.

### 6.2.2 Recommended material property data

In Table 6-2, recommended material property data for the cementitious components in 1BMA at closure are presented. The recommendations are based on the descriptions of the cementitious components in 1BMA presented in Section 2.6 with material property data for the undegraded cementitious materials taken from Chapter 3. In addition, the final selection of material property data also relies on the information presented in Section 6.2.1 and Section 5.1.

**Table 6-2. Recommended material property data for the cementitious components in 1BMA at closure.**

| | pH<br>- | Porosity<br>% | Hydraulic conductivity<br>m/s | Diffusivity<br>$m^2/s$ | Compressive strength***<br>MPa | Tensile strength***<br>MPa |
|---|---|---|---|---|---|---|
| **Slab** | ≥ 13 | 12–15 | $10^{-5}$–$10^{-4}$ | $(2–5)\times10^{-12}$ | 40–50 | 4–5 |
| **Existing outer walls** | ≥ 13 | 12–15 | $10^{-5}$–$10^{-4}$ | $(2–5)\times10^{-12}$ | 40–50 | 4–5 |
| **New Outer walls** | ≥ 13 | 11–13 | $(1–5)\times10^{-12}$ | $(2–5)\times10^{-12}$ | 55–60 | 4–5 |
| **Lid*** | ≥ 13 | 11–13 | $(1–5)\times10^{-12}$ | $(2–5)\times10^{-12}$ | 55–60 | 4–5 |
| **Inner walls** | ≥ 13 | 12–15 | $10^{-5}$–$10^{-4}$ | $(2–5)\times10^{-12}$ | 40–50 | 4–5 |
| **Prefabricated Concrete elements**** | ≥ 13 | 12–15 | $10^{-3}$ | $10^{-10}$ | 40–50 | 4–5 |
| **Gas evacuation system** | ≥ 13 | 30 | $(5–20)\times10^{-9}$ | $(1–5)\times10^{-11}$ | 5–9 | 0.5–1 |
| **Concrete moulds** | ≥ 13 | 10–12 | $(1–5)\times10^{-12}$ | $(2–5)\times10^{-12}$ | 40–50 | 4–5 |

* Not including the gas evacuation system.
** As a group and including the slits between the individual elements.
*** Refers to the cementitious material used in the respective components.

### 6.2.3 Specific uncertainties

The following specific uncertainties concerning the properties of the cementitious components in 1BMA have been identified:

- There are significant uncertainties concerning the status of the slab, concrete moulds and inner walls in closed compartments. For these components, inspections are not easily conducted because the compartments are filled with waste and covered by prefabricated concrete elements and a thin layer of concrete.
- The installation of a gas evacuation system in the lid and the design thereof have not yet been settled.
- There are some uncertainties concerning the detailed design of the foundation of the concrete structure and whether the concrete beams beneath the slab rests on solid rock or on crushed rock material. This has some impact on predictions on the influence of settlements in the foundation and the risk for cracking of the slab.
- There remain some uncertainties regarding the status of the reinforcement bars close to the underside of the slab as no cores from this part of the slab have been investigated.

## 6.3 Cementitious components in 2BMA

### 6.3.1 Expected status at closure

In this section, the expected status at closure of the cementitious components in 2BMA which were introduced in Section 2.7 is described, Section 6.3.1. This is followed by Section 6.3.2 in which material property data for the cementitious components at closure are recommended and Section 6.3.3 which summarises identified specific uncertainties in the descriptions.

#### *Reinforced concrete slab*

**Chemical properties**

At closure, the chemical properties of the reinforced concrete slab in 2BMA will correspond to those of 40–45 years old *2BMA concrete* that has been exposed to a humid environment.

Alterations of the chemical properties of the bulk and top of the concrete slab are not expected due to the short duration of the operational period but also because the upper part of the slab is protected by the concrete caisson.

Some leaching of the underside of the slab due to interactions with the groundwater in the draining layer could have occurred but this requires some clogging of the draining material. However, this is less likely during the short time-span of the operational period and leaching of the reinforced concrete slab is therefore not expected.

#### Load-bearing capacity

The load-bearing capacity of the reinforced concrete slab will be sufficient to carry the homogeneous compressive load from a full concrete caisson, Section 2.7. This statement is justified by that the dimensions and amount of reinforcement can be adjusted during the design work to ensure a sufficient load-bearing capacity. The risk for cracking can be further reduced by careful compaction of the foundation layer.

#### Transport properties

From the previous section, cracking due to insufficient load-bearing capacity is not expected during the operational period. Instead, temperature or drying shrinkage during construction and the operational period constitute the greatest risks for cracking. Of these, drying shrinkage is not expected because the concrete slab will be in close contact with the groundwater in the draining layer and also be covered by the concrete caisson.

Also cracking due to temperature shrinkage can be avoided by carefully selecting material, amount of reinforcement and construction method for the reinforced concrete slab. However, as this slab does not formally constitute a hydraulic barrier, avoiding cracking will probably not be a priority.

In all, the transport properties of the reinforced concrete slab in 2BMA at closure are expected to correspond to those of the *2BMA concrete* with a few small cracks.

### *Slabs*

#### Chemical properties

At closure, slabs of the concrete caissons will have the chemical properties of 40–45 years old *2BMA concrete*. Any interactions with the groundwater have been prevented by the draining layer and the reinforced concrete slab but also by the waterproofing membrane installed in the roof of the waste vault that diverts any intruding groundwater. Carbonation is also mitigated by the stack of waste packages which prevents gas exchange at the surface of the slabs.

#### Load-bearing capacity

The load-bearing capacity of the slabs will be sufficient to carry the compressive load from the waste packages during the entire operational period. Having a high compressive strength and with support from the reinforced concrete slab, uneven distribution of the waste packages will not cause the formation of any cracks in the slabs during the operational period.

#### Transport properties

From the previous section, cracking due to insufficient load-bearing capacity during the operational period is not expected.

Mårtensson and Vogt (2019, 2020) showed that that cracking of the slabs during construction can be prevented by the use of concrete with a low thermal output in combination with suitable choice of construction methods and design of foundation; see also Section 2.7.2.

Further, Mårtensson and Vogt (2019) also showed that cracking due to drying shrinkage during the operational period can be prevented and also that unrestrained shrinkage can be enabled by the use of an adhesion reducing foil between the reinforced concrete slab and the slab of the concrete caisson, Figure 6-6.

***Figure 6-6.*** *The concrete structure was covered with a tarpaulin to protect in from the wet atmosphere in the tunnel and dripping groundwater (left image) and dried for a few months using two dehumidifiers (right image). One of the dehumidifiers (orange box) is seen in the centre of the image. (Mårtensson and Vogt 2019).*

In all, these findings indicate that the slabs at closure will have the transport properties of 40–45 years old *2BMA concrete* without penetrating cracks.

### *Outer walls*

#### Chemical properties

The chemical properties of the outer walls of the concrete caisson at closure will correspond to those of 40–45 years old *2BMA concrete*. Any interactions with intruding groundwater are prevented by the waterproofing membrane and leaching or mineral alterations are therefore not expected. Some carbonation may occur but as shown for 1BMA (Section 6.2), this will be limited to the outer few millimetres of the walls.

#### Load-bearing capacity

The outer walls of the concrete caissons in 2BMA will not experience any external or internal loads during the operational period except for the load from the concrete elements. Penetrating cracks are therefore not expected to form during the operational period. During backfilling of the waste vault, the outer walls will experience also the load from the backfill material. However, because the outer walls can be designed to withstand the groundwater pressure at repository depth (Westerberg 2017), they are also expected to withstand the considerably lower pressure from the backfill material.

During construction of the inner walls, the outer walls may experience an internal hydrostatic pressure from the wet concrete. In addition, thermal expansion of the concrete during the hydration process may also result in an internal pressure. However, the magnitude of this pressure will be dependent on choice of construction method.

If the concrete mixing proportions and method for construction of the inner walls are not carefully controlled, the tensile strength of the concrete in the unreinforced outer walls may be exceeded with the formation of cracks as a consequence. This is because some thermal expansion of the inner walls must be expected due to the heat of cement hydration. However, as this is a well-known phenomenon it is expected that the concrete mixing proportions and method for construction of the inner walls will be carefully selected to avoid cracking of the outer walls during the construction of the inner walls.

In all, it is expected that the load-bearing capacity of the outer walls will be sufficient to prevent the formation of cracks during construction and the operational period.

**Transport properties**

From the previous sections it is expected that the transport properties of the outer walls of the concrete caissons at closure will correspond to those of 40–45 years old concrete without cracks or other permeable zones. This statement is supported by the following studies:

- Mårtensson and Vogt (2019, 2020) showed that the formation of cracks in large unreinforced concrete structures can be prevented by using concrete with a low thermal output during hydration in combination with carefully selected construction methods; see Section 2.7.2 for details.
- Mårtensson and Vogt (2019, 2020) also showed that the hydraulic properties of the joint between the slab and the outer walls will be on the same order of magnitude as the bulk concrete by careful cleansing of the casting joint between the slab and the walls of the concrete caisson prior to casting of the outer walls.
- Mårtensson (2021a) showed that the hydraulic conductivity of sealed concrete tubes (including interfaces with bulk concrete and sealing grout) used to protect the tie rods during casting of the walls is on the same order of magnitude as that of bulk concrete. See also Section 2.7.2.
- Cracking due to drying shrinkage or uneven settlements during the operational period is not expected as discussed in more detail in the previous section.
- Investigations in 1BMA (Elfwing et al. 2015) showed that the relative humidity in concrete which has been exposed to the underground climatic conditions of the waste vault in 1BMA for about 30 years was above 90 % except for in the outer 25–40 mm. This indicates that unless extensive measures are taken to reduce the RH in 2BMA, drying shrinkage will not cause the formation of penetrating cracks in the outer walls of the concrete caissons in 2BMA. The installation of the waterproofing membrane in 2BMA is not expected to alter this conclusion since local groundwater intrusion will have a minor impact on the overall relative humidity in the concrete.
- Mårtensson and Vogt (2019) showed that cracking due to drying shrinkage can be prevented by a suitable design of the foundation.

As a final remark, cracking of the outer walls of the caissons could occur during construction of the inner walls. However, as discussed above, it is assumed that careful choice of concrete mixing proportions and construction method for the inner walls will ensure that the pressure from the inner walls does not exceed the load-bearing capacity of the outer walls.

### *Lid*

**Chemical properties**

At closure, the chemical properties of the lid will be the same as those of undegraded *2BMA concrete*, Section 3.3.3. This is because the lid is constructed at the time of closure.

**Load-bearing capacity**

According to Westerberg (2017) a thickness of the lid of 600 mm is sufficient to resist the groundwater pressure at repository depth during saturation of the repository. From this follows that the thickness of the lid will also be sufficient to resist the pressure from the backfill material alone during backfilling of the waste vault and cracking is therefore not expected during this process.

**Transport properties**

From the previous sections, penetrating cracks are not expected to form in the lid prior to closure and the transport properties will therefore be the same as those of *2BMA concrete* without cracks.

However, the average transport properties of the lid are also dependent on the transport properties of the gas evacuation system. The average transport properties of the lid are discussed in more detail in the section about the gas evacuation system.

### *Prefabricated concrete elements*

#### Chemical properties

At closure, the chemical properties of the prefabricated concrete elements will correspond to those of up to 40–45 years old *2BMA concrete*. Any interactions with intruding groundwater are prevented by the waterproofing membrane in the roof of the waste vault and leaching or mineral alterations are therefore unlikely during the operational period. Some carbonation may occur but as shown for 1BMA (Section 6.2), this will be limited to the outer few millimetres of the elements.

#### Load-bearing capacity

The prefabricated concrete elements do not experience any external loads during construction and the operational period. The load-bearing capacity is therefore not relevant during these stages.

During casting of the lid, the prefabricated elements must be able to carry the weight from the wet concrete, corresponding to about 1 500 kg/m$^2$ for a 600 mm thick lid. This will not exceed the load-bearing capacity of the concrete elements and cracking of the prefabricated elements due to excessive loads prior to backfilling and closure is therefore not expected.

#### Transport properties

From the previous section, the transport properties of the prefabricated elements as such will correspond to those of up to 45 years old *2BMA concrete*. The transport properties of the prefabricated elements as a group are controlled by the width of the slits between the individual elements, estimated to between 1 and 10 millimetres.

### *Inner walls*

#### Chemical properties

Only minute alterations of the chemical properties of the inner walls are expected during the operational period. Any intruding groundwater is diverted by the waterproofing membrane and leaching or mineral alterations are therefore not expected during the operational period. Some carbonation may occur but as shown for 1BMA (Section 6.2), this will be limited to the outer few millimetres of the inner walls.

#### Load-bearing capacity

Könönen and Olsson (2018) and Westerberg (2017) have shown that the inner walls as described in Section 2.7.2 can resist the combined load from the backfill material and the groundwater pressure at repository depth during saturation of the repository. From this follows that the load-bearing capacity of the inner walls will be sufficient to carry the weight from the prefabricated concrete elements and the backfill material alone and the formation of penetrating cracks is therefore not expected.

#### Transport properties

The transport properties of the inner walls will be dominated by the presence of the holes that ensure that the intruding groundwater will be evenly distributed within the concrete caisson during the saturation period. For that reason, the concrete or construction method used will have a small influence on the transport properties of the inner walls of the concrete caissons at closure.

### *Gas evacuation system*

#### Chemical properties

According to the information in Section 2.7.2 the channels in the gas evacuation system will be filled with the *2BMA grout*. According to Section 3.4.4, the mixing proportions of the *2BMA grout* have yet not been decided but similar mixing proportions as those of the *New silo grout* were expected. For this reason, the chemical properties of the permeable grout in the gas evacuation system at closure are expected to be the same as those of the *New silo grout*, Section 3.4.2. No alterations are expected as the channels are filled at closure of the repository.

**Load-bearing capacity**

The load-bearing capacity of the gas evacuation system is not relevant.

**Transport properties**

From Section 3.4.4, the transport properties of the permeable grout in the gas evacuation system in the lid at closure will be the same as those of the undegraded *New silo grout*, Section 3.4.2. No alterations are expected as the channels are filled at closure of the repository.

However, the following remark can be made:

Elfwing et al. (2017) investigated the impact of the type of material used to fill these channels as well as their position in the lid on the transport properties of the lid. Elfwing et al. (2017) found that the influence of the gas evacuation system on the flow through the waste was negligible if the channels were filled with permeable *2BMA grout* (Section 3.4.4) and the hydraulic conductivity of the concrete in the lid was $8.3 \times 10^{-10}$ m/s. However, in the case that the channels were filled with sand, the flow of water through the waste increased by a factor of 3.47 compared to a lid without these channels during the initial period post-closure when the concrete in the lid was undegraded.

However, it should be noted that the hydraulic conductivity of the concrete used in the calculations presented by Elfwing et al. (2017) is two to three orders of magnitude higher than that expected for concrete without cracks. For that reason, the influence of the gas evacuation system on the flow of groundwater through the waste might have been somewhat underestimated by Elfwing et al. (2017).

### *Concrete moulds*

**Chemical properties**

At closure, the chemical properties of the concrete moulds in 2BMA will correspond to those of up to 40–45 years old reinforced *SFR mould concrete*, Section 3.3.7.

Any intruding groundwater is diverted by the waterproofing membrane and leaching or mineral alterations are therefore not expected. Some carbonation may occur but as shown for 1BMA (Section 6.2), this will be limited to the outer few millimetres of the elements. Any interactions with the waste are also prevented by the lack of water inside the concrete moulds prior to saturation of the waste vault.

(As a remark, final conditioning of waste for 2BMA is currently not permitted as the Waste Acceptance Criteria, WAC, for 2BMA have not yet been approved. This does not mean that waste currently in storage cannot be disposed in 2BMA but only that a decision has not yet been taken. The consequence of this is that some waste packages older than 45 years might be disposed in 2BMA but the number is expected to be low.)

**Load-bearing capacity**

The load-bearing capacity of the concrete moulds in 1BMA has been calculated by Bultmark (2017a) who showed that a concrete mould at closure can carry the weight from a 100-meter-tall stack of a material with a density of 2 500 kg/m$^3$. The load-bearing capacity of the concrete moulds is thus sufficient to carry the weight of the stack of waste packages during the operational period and cracking is therefore not expected.

No internal loads are expected during the operational period because the absence of water inside the concrete caissons prevents any chemical reactions with the waste.

**Transport properties**

From the findings presented in the previous sections, the transport properties of the concrete moulds at closure are expected to correspond to those of 40–45 years old *SFR mould concrete* without cracks. See above concerning older concrete moulds. This conclusion is also based on the assumption that no cracks will form in the concrete moulds during manufacturing and that moulds in which cracks are identified in the production control are discarded.

### 6.3.2 Recommended material property data

In Table 6-3, recommended material property data for the different cementitious components in 2BMA at closure are presented. The recommendations are based on the descriptions of the cementitious components presented in Section 2.7 with material property data for the undegraded cementitious materials taken from Chapter 3. In addition, the final selection of material property data also relies on the information presented in Section 6.3.1 and Section 5.1.

**Table 6-3. Recommended material property data for the cementitious components in 2BMA at closure.**

| | pH<br>- | Porosity<br>% | Hydraulic conductivity<br>m/s | Diffusivity<br>$m^2/s$ | Compressive strength****<br>MPa | Tensile strength****<br>MPa |
|---|---|---|---|---|---|---|
| **Reinforced concrete slab** | ≥13 | 11–13 | $10^{-9}$–$10^{-7}$ | (5–9)×$10^{-12}$ | 55–60 | 4–5 |
| **Slab** | ≥13 | 11–13 | (1–5)×$10^{-12}$ | (2–5)×$10^{-12}$ | 55–60 | 4–5 |
| **Outer walls** | ≥13 | 11–13 | (1–5)×$10^{-12}$ | (2–5)×$10^{-12}$ | 55–60 | 4–5 |
| **Lid*** | ≥13 | 11–13 | (1–5)×$10^{-12}$ | (2–5)×$10^{-12}$ | 55–60 | 4–5 |
| **Inner walls***** | ≥13 | 11–13 | (1–5)×$10^{-3}$ | $10^{-10}$ | 55–60 | 4–5 |
| **Concrete elements**** | ≥13 | 11–13 | $10^{-3}$ | $10^{-10}$ | 55–60 | 4–5 |
| **Gas evacuation system** | ≥13 | 30 | (5–20)×$10^{-9}$ | (1–5)×$10^{-11}$ | 5–9 | 0.5–1 |
| **Concrete moulds** | ≥13 | 10–12 | (5–9)×$10^{-12}$ | (2–5)×$10^{-12}$ | 40–50 | 4–5 |

* Not including the gas evacuation system.
** As a group and including the slits between the individual elements.
*** The transport properties will be controlled by the presence of the holes in the inner walls which ensure that intruding groundwater will be evenly distributed within the entire waste domain.
**** Refers to the cementitious material used in the respective components.

### 6.3.3 Specific uncertainties

The work carried out by Mårtensson and Vogt (2019, 2020) and Mårtensson (2021a) have considerably reduced the uncertainties regarding the properties of the different cementitious components in 2BMA. However, the following specific uncertainty has been identified:

- At present, the construction method for the inner walls has yet not been decided. For this reason, there remain some uncertainties regarding the impact of construction method on the properties of the outer walls of the concrete caisson.

## 6.4 Cementitious components in 1BRT

### 6.4.1 Expected status at closure

In this section, the expected status at closure of the cementitious components in 1BRT which were introduced in Section 2.8 is described, Section 6.4.1. This is followed by Section 6.4.2 which recommends material property data for the cementitious components at closure and Section 6.4.3 which summarises identified specific uncertainties in the descriptions.

#### *Slab*

**Chemical properties**

At closure, the chemical properties of the slab of the concrete structure in 1BRT will have the characteristics of 45–50 years old reinforced *2BMA concrete*. Alterations of the mineral composition are not expected during the operational period, apart from some carbonation of the upper few millimetres of the slab.

Chlorine intrusion is possible from the underside of the slab. However, as this requires extensive clogging of the draining layer beneath the slab it is not expected during the operational period. Chlorine intrusion in the top surface of the slab is not expected since the waste vault is provided with a waterproofing membrane that diverts any intruding groundwater to the drainage system.

#### Load-bearing capacity

During the operational period, the slab must withstand the compressive load from the stack of waste packages as well as from the dynamic load from the transport of waste packages in the outer parts of the structure by means of a fork-lift truck. With well-known loads, the dimensions and amount of reinforcement can be adjusted to ensure a sufficient load-bearing capacity. Cracking of the slab due to excessive loads during the operational period is therefore not expected.

#### Transport properties

From the previous section, the formation of penetrating cracks in the slab during the operational period due to insufficient load-bearing capacity is not expected.

However, at the time of writing of this report, it is not prescribed that such construction methods that prevents cracking or formation of casting joints during construction must be used for the slab in 1BRT. This is because the slab does not formally constitute a hydraulic barrier. For that reason, it cannot be ruled out that the slab will contain a few small cracks and/or permeable construction joints already at the start of the operational period.

### *Outer walls*

#### Chemical properties

At closure and in analogy with the slab, the chemical properties of the outer walls of the concrete structure in 1BRT will have the characteristics of 40–45 years old reinforced *2BMA concrete*. Alterations of the mineral composition are not expected during the operational period, apart from some carbonation in the surface region of the walls. Chlorine intrusion is not expected thanks to the waterproofing membrane that protects the concrete structure from intruding groundwater.

#### Load-bearing capacity

During the operational period, the load-bearing capacity of the outer walls must be sufficient to withstand the hydrostatic pressure from the *1BRT self-compacting concrete* (Section 3.3.5) during casting of the inner walls between the waste packages. However, the magnitude of the hydrostatic pressure can be controlled by careful implementation of the casting process and cracking thus prevented.

For this reason, it is expected that the load-bearing capacity of the outer walls of the concrete structure in 1BRT will be sufficient to prevent cracking during the operational period and backfilling.

#### Transport properties

The transport properties of the outer walls of the concrete structure at the time of closure are difficult to predict. This is because they are dependent on the detailed method of construction and the presence of cracks, tie rods, casting joints or other permeable zones.

At the time of writing of this report, the use of such construction methods that prevents cracking or formation of casting joints or other permeable zones in the outer walls are not prescribed. In addition, the use of tie rods to keep the formwork together during casting and which are left in the concrete walls after casting is completed is not restricted.

For those reasons, it cannot be ruled out that the outer walls may contain a few small cracks and/or permeable construction joints which may affect the transport properties of the outer walls at closure. However, revisions of the requirements may change this conclusion.

### *Lid*

#### Chemical properties

At the time of closure, the lid will have the chemical properties of undegraded *2BMA concrete* (Section 3.3.3) or similar. This is because the lid will be constructed at closure of the repository.

**Load-bearing capacity**

The load-bearing capacity of the lid will be sufficient to carry the load from the backfill material and cracking therefore not expected. This statement is justified by that the waste domain constitutes a cementitious monolith that will provide a significant mechanical support for the lid.

**Transport properties**

The transport properties of the lid of the concrete structure at closure are difficult to predict as they are dependent on the detailed method of construction and the presence of cracks, casting joints or other permeable zones.

At the time of writing of this report, the use of such construction methods that prevents cracking or formation of casting joints or other permeable zones in the lid are not prescribed. For that reason, it cannot be ruled out that the lid may contain a few small cracks and/or somewhat permeable construction joints at closure. However, revision of the requirements may change this conclusion.

### *Prefabricated concrete elements*

**Chemical properties**

At the time of closure, the prefabricated concrete elements will have the chemical properties of up to 40–45 years old *2BMA concrete*. Leaching or mineral alterations are unlikely because the water-proofing membrane will divert any intruding groundwater to the drainage system. Some carbonation may occur but as shown for 1BMA (Section 6.2), this will be limited to the outer few millimetres of the elements.

**Load-bearing capacity**

The load-bearing capacity of the prefabricated elements will be sufficient to carry the load from the lid and the backfill material and cracking is therefore not expected. This statement is justified by that the waste domain constitutes a cementitious monolith that will provide a significant mechanical support for the prefabricated elements.

During casting of the lid, the prefabricated elements must be able to carry the weight of the wet concrete, corresponding to about 1 250 kg/m$^2$ for the 500 mm thick lid of 1BRT (Figure 2-24). This is much lower than the compressive strength of the prefabricated elements and cracking/crushing therefore not expected.

**Transport properties**

From the previous sections, the transport properties of the prefabricated elements as such will correspond to those of up to 45 years old *2BMA concrete*. The transport properties of the prefabricated elements as a group are controlled by the width of the slits between the individual elements, estimated to between 1 and 10 millimetres.

### *Inner walls between the waste compartments*

**Chemical properties**

At closure, the inner walls between the waste compartments of the concrete structure in 1BRT will have the chemical properties of 40–45 years old reinforced *2BMA concrete*. Chlorine intrusion or leaching are not expected thanks to the waterproofing membrane that diverts intruding groundwater to the drainage system but some carbonation in the surface region may have occurred.

**Load-bearing capacity**

During the operational period, the load-bearing capacity of the inner walls between the waste compartments must be sufficient to withstand the hydrostatic pressure from the fresh *1BRT self-compacting concrete* used to construct the inner walls between the waste packages. However, as the magnitude

of the hydrostatic pressure can be controlled during casting of these walls, it is expected that the tensile strength of the inner walls between the compartments will not be exceeded and cracking thus prevented.

**Transport properties**

From the previous section, the load-bearing capacity of the inner walls between the waste compartments will be sufficient to prevent cracking during the operational period. However, from Section 2.8, some cracking or formation of construction joints which may affect the transport properties of the inner walls between the waste compartments may occur already during construction. This is because the inner walls between the waste compartments do not formally constitute a hydraulic barrier and the use of construction methods that prevents cracking or formation of casting joints or other permeable zones in these walls are not prescribed today.

For those reasons, it cannot be ruled out that the inner walls between the waste compartments may contain a few small cracks and/or permeable construction joints which may affect the transport properties of these walls already at closure. The transport properties of the inner walls between the waste compartments are therefore expected to correspond to those of *2BMA concrete* with a few cracks. However, revisions of the requirements may change this conclusion.

#### *Inner walls between waste packages*

**Chemical properties**

At closure, the inner walls between the waste packages will have the chemical properties of between one and 45 years old *1BRT self-compacting concrete* depending on if these walls are constructed during operation or at closure.

Chlorine intrusion or leaching are not expected thanks to the waterproofing membrane that diverts intruding groundwater to the drainage system. Carbonation is not expected because these walls will be in direct contact with the waste packages and inner walls between the waste compartments and hence the contact with $CO_2$ in the ambient atmosphere in the waste vault will be limited.

**Load-bearing capacity**

The load-bearing capacity of the inner walls between the waste packages will be sufficient to contribute to carry the weight of the lid and the backfill material and cracking is therefore not expected. This statement is justified by that the inner walls between the waste packages constitute parts of the stable cementitious monolith inside the waste compartment.

**Transport properties**

From the previous section, cracking of the inner walls between the waste packages due to insufficient load-bearing capacity during the operational period is not expected. However, cracks may instead form during construction as a consequence of restrained temperature shrinkage towards the end of the cement hydration process.

For that reason, the presence of cracks must be considered when assessing the transport properties of the inner walls between the waste packages. In addition, the absence of reinforcement increases the risk that a few larger cracks are formed rather than several small ones. However, the influence of the adjacent waste packages on the width and number of cracks cannot be determined with accuracy.

### 6.4.2 Recommended material property data

In Table 6-4, recommended material property data for the cementitious components in 1BRT at closure are presented. The recommendations are based on the descriptions of the cementitious components presented in Section 2.8 with material property data for the undegraded cementitious materials taken from Chapter 3. In addition, the final selection of material property data also relies on the information presented in Section 6.4.1 and Section 5.1.

**Table 6-4. Recommended material property data for the cementitious components in 1BRT at closure.**

| | pH<br>- | Porosity<br>% | Hydraulic conductivity<br>m/s | Diffusivity<br>$m^2/s$ | Compressive strength**<br>MPa | Tensile strength**<br>MPa |
|---|---|---|---|---|---|---|
| **Slab** | ≥13 | 11–13 | $10^{-11}$–$10^{-8}$ | $(2–5)\times10^{-12}$ | 55–60 | 4–5 |
| **Outer wall** | ≥13 | 11–13 | $10^{-11}$–$10^{-8}$ | $(2–5)\times10^{-12}$ | 55–60 | 4–5 |
| **Lid** | ≥13 | 11–13 | $10^{-11}$–$10^{-8}$ | $(2–5)\times10^{-12}$ | 55–60 | 4–5 |
| **Inner walls between the waste compartments** | ≥13 | 11–13 | $10^{-11}$–$10^{-8}$ | $(2–5)\times10^{-12}$ | 55–60 | 4–5 |
| **Inner walls between waste packages** | ≥13 | 11–13 | $10^{-8}$–$10^{-5}$ | $(5–9)\times10^{-12}$ | 55–60 | 4–5 |
| **Concrete elements*** | ≥13 | 11–13 | $10^{-3}$ | $10^{-10}$ | 55–60 | 4–5 |

* As a group and including the slits between the individual elements.
** Refers to the cementitious material used in the respective components.

### 6.4.3 Specific uncertainties

The following specific uncertainties concerning the properties of the cementitious components in 1BRT have been identified:

- The main uncertainties regarding the status of the cementitious components in 1BRT at closure emanates from the fact that the detailed construction methods for 1BRT have not yet been specified. Additionally, because the concrete structure in 1BRT does not formally constitute a hydraulic barrier the use of such construction methods that prevent the formation of cracks or other hydraulically conducting zones are not prescribed today.
- There also remains some uncertainties concerning the transport properties of the inner walls between the waste packages. This is because these walls are constructed by filling the space between the waste packages with concrete and no post-casting controls can therefore be carried out.

## 6.5 Cementitious components in 1BTF and 2BTF

### 6.5.1 Expected status at closure

In this section, the expected status at closure of the cementitious components in 1–2BTF which were introduced in Section 2.9 is described, Section 6.5.1. This is followed by Section 6.5.2 which recommends material property data for the cementitious components at closure and Section 6.5.3 which summarises identified specific uncertainties in the descriptions.

#### *Slabs*

**Chemical properties**

As shown in Figure 2-28, the slabs in 1–2BTF are at least periodically wet and the slabs have therefore likely been exposed to chlorine containing groundwater during an extended period of time. From the studies presented in Section 6.2.1 (1BMA) increased chlorine levels can therefore be expected to a depth of at least 100 mm.

With a thickness of only 250 mm and with possible contact also with the groundwater in the draining foundation, there is a potential that a large part of the slabs in 1–2BTF will be chlorine infected at closure. However, major alterations of the mineral composition through leaching are not expected during the comparatively short operational period.

**Load-bearing capacity**

The load-bearing capacity of the slabs in 1–2BTF has been calculated by Nytorp Jansson (2020b). The calculations showed that the load-bearing capacity was dependent on the stiffness of the foundation layer. For a poorly compacted foundation layer, the load-bearing capacity of the slab

was calculated to be insufficient to carry the load from the stack of waste packages. Nytorp Jansson (2020b) concludes that the stiffness modulus of the foundation layer has to be at least 105 MPa to avoid cracking of the slab. Nytorp Jansson (2020b) also states that this should be possible to achieve for the rather thin foundation layers in 1–2BTF as long as sufficient compaction has been carried out. However, information concerning the properties of the foundation layers in 1–2BTF has not been found.

From above, the available information is not sufficient to unambiguously determine if the load-bearing capacity of the slabs in 1–2BTF is sufficient to prevent the formation of cracks during the operational period and some cracking must therefore be anticipated. This conclusion is also supported by the fact that corrosion of the reinforcement bars during the up to 90 years of operation will reduce the load-bearing capacity of the slabs further.

#### Transport properties

As discussed above, the risk for formation of penetrating cracks in the slabs in 1–2BTF due to insufficient load-bearing capacity during the operational period cannot be ignored.

Also, because the slabs in 1–2BTF do not formally constitute hydraulic barriers (SKB TR-23-01) prevention of cracking or formation of casting joints or other permeable zones during construction were probably not prescribed. For that reason, the probability that the slabs contained a few small cracks and/or somewhat permeable construction joints already at the start of the operational period cannot be neglected. This is also supported by the findings in 1BMA where a number of permeable joints have been identified.

### *Lids*

#### Chemical properties

The lids in 1–2BTF will be constructed once the operational period has been concluded. For this reason, the lids will have the chemical properties of undegraded *2BMA concrete* or similar at closure of the repository.

#### Load-bearing capacity

The load-bearing capacity of the lids in 1–2BTF will be sufficient to carry the load from the backfill material. This is because the lid will rest on the prefabricated concrete elements which rests on the grouted concrete tanks as well as on the grouted steel drums and only experience a comparatively small compressive load. Tensile loads are not expected as the weight of the backfill material is homogeneously distributed.

#### Transport properties

From the previous section, cracking of the lids during the operational period due to insufficient load-bearing capacity is not expected.

However, because the lids in 1–2BTF do not formally constitute hydraulic barriers (SKB TR-23-01), the use of such construction methods to prevent cracking or formation of casting joints or other permeable zones during construction are not prescribed today. For that reason, the potential for the lids to contain a few small cracks and/or permeable construction joints which will affect the transport properties of the lids must be considered when recommending transport data for the lids.

### *Prefabricated concrete elements*

#### Chemical properties

At closure, the prefabricated concrete elements will have the average chemical properties of between a few years old and up to 90 years old concrete depending on the time at which the elements were manufactured and installed.

In analogy with the slabs shown in Figure 2-28, the prefabricated concrete elements will have been exposed to humid to wet and saline conditions during the operational period with increased chlorine levels in the concrete as a consequence. From the studies presented in Section 6.2.1 (1BMA), increased chlorine levels can probably be expected to a depth of at least 100 mm.

However, even though the prefabricated concrete elements are exposed to dripping groundwater, the amount of water is not expected to be sufficient for leaching of the cement minerals to occur other than locally. For that reason, the average chemical properties of the bulk of the concrete are expected to remain virtually unaffected at closure with the exception of enhanced levels of chlorine and some carbonation in the surface regions.

#### Load-bearing capacity

The load-bearing capacity of the prefabricated elements in 1–2BTF will be sufficient to carry the load from the lid and the backfill material. This is because the prefabricated elements will rest on the stack of concrete tanks and grouted steel drums and only experience comparatively small compressive and tensile loads.

During casting of the lid, the prefabricated concrete elements must be able to carry the weight from the fresh concrete, corresponding to about 1 000 kg/m$^2$ for a 400 mm thick lid, Figure 2-29. This will not exceed the load-bearing capacity of the prefabricated concrete elements and cracking is therefore not expected.

#### Transport properties

From the previous section, the prefabricated elements as such will have the transport properties of up to 90 years old concrete. The transport properties of the prefabricated elements as a group are controlled by the width of the slits between the individual elements, estimated to between 1 and 10 millimetres.

### *Grout between waste packages*

#### Chemical properties

At closure, the grout between the waste packages that are grouted during the operational period (steel drums and concrete moulds) are expected to have the chemical properties of up to 90 years old *BTF grout* (Section 3.4.3). Also, increased levels of chlorine can be expected in the upper parts of the grout. This is because these waste packages are not protected by prefabricated concrete elements during the operational period.

The chemical properties of the grout surrounding the concrete tanks will be representative of undegraded *BTF grout*. This is because the concrete tanks will be grouted once the operational period has been concluded.

#### Load-bearing capacity

The load-bearing capacity of the grout between the waste packages is poor. This is because the *BTF grout* has a rather low compressive strength (Section 3.4.3) but also because the method used for grouting does not ensure a complete fill and that voids resulting in a poor cohesion may have formed. However, the grout will not experience any loads during the operational period and backfilling and cracking due to insufficient load-bearing capacity is therefore not expected.

#### Transport properties

As indicated in Section 3.4.3, the transport properties of the *BTF grout* are not dramatically affected by the rather high w/c ratio. Instead, the presence of voids in the grout due to incomplete fill will be of greater importance. However, detailed information on the size and distribution of such voids cannot be obtained as inspections post-grouting are not possible.

### *Cementitious backfill*

#### Chemical properties

At closure, the cementitious backfill will have the chemical properties of undegraded *BTF backfill concrete* (Section 3.3.8). This is because backfilling will be done at the end of the operational period and no chemical degradation will occur prior to closure.

#### Load-bearing capacity

The cementitious backfill will carry the compressive load from the lid and the crushed rock backfill. The compressive strength of the *BTF backfill concrete* is significantly higher than the compressive load and cracking is therefore not expected.

#### Transport properties

The transport properties of the cementitious backfill in 1–2BTF at closure are dependent on the detailed method of construction and the presence of cracks or casting joints. At the time of writing of this report, the mixing proportions of the cementitious backfill and the method for backfilling have not been decided.

As an indication, the Data report for PSAR (SKB TR-23-10) recommends a hydraulic conductivity of $1.0 \times 10^{-8}$ m/s for the cementitious backfill. According to Figure 4-3, this value allows for only a few small cracks, each with a width of 10 to 50 μm.

### *Concrete tanks*

#### Chemical properties

At the time of closure, the concrete tanks will have the chemical properties of up to 90 years-old *BTF tank concrete*.

Interactions with the groundwater are negligible during the operational period. This is because the tanks are painted with a water-repellent paint and protected by the concrete elements that diverts the majority of the intruding groundwater to the drainage system. The paint also prevents extensive drying and carbonation. Interactions with any remaining water in the dewatered ion-exchange resins are prevented as the dewatered waste is placed in a rubber bag inside the concrete tank.

#### Load-bearing capacity

The load-bearing capacity of the concrete tanks has been studied by Bultmark (2017b). In this study, Bultmark (2017b) showed that the load-bearing capacity of the concrete tanks was sufficient to withstand any loads occurring during the operational period even in the unlikely event of loss of function of the reinforcement bars and spalling of the concrete covering layer.

From the previous section, concrete degradation is not expected during the operational period. Further, rebar corrosion is not expected because water and chlorine intrusion are prevented by the water-repellent paint. The load-bearing capacity of the concrete tanks is therefore expected to remain unaffected during the operational period and no cracks are expected to form prior to closure.

#### Transport properties

During the operational period, cracking of the concrete tanks due to insufficient load-bearing capacity is not expected. Further, no cracks are expected at the time of disposal. Also, the tightness of the seal is expected to be according to the requirements even though some uncertainties remain concerning the durability of the seal over long periods of time as also discussed in Section 6.5.3.

Based on this, the transport properties of the concrete tanks at the time of closure are expected to be the same as those of the *BTF tank concrete* without cracks or other permeable zones.

### *Concrete moulds*

#### Chemical properties

At closure, the concrete moulds in 1BTF will have the chemical properties of up to 90 years-old undegraded *SFR mould concrete*. This statement is justified by that the moulds are manufactured just prior to use and then grouted within a few years after emplacement. This prevents any interactions with the surroundings and alterations of the average chemical properties of the concrete moulds will therefore be limited.

#### Load-bearing capacity

The load-bearing capacity of the concrete moulds at closure will be sufficient to ensure that even the concrete mould furthest down in the stack of moulds can carry the weight of the stack of concrete moulds, lid and backfill material. This conclusion is supported by the study by Bultmark (2017a) who showed that a concrete mould can carry the weight from a 100 meter tall stack of a material with a density of 2 500 kg/m$^3$ without the support from any grout.

#### Transport properties

From the previous section, the concrete moulds at closure will have the transport properties of undegraded but up to 90 years-old concrete without cracks or other permeable zones.

## 6.5.2 Recommended material property data

In Table 6-5, recommended material property data for the cementitious components in 1–2BTF at closure are presented. The recommendations are based on the descriptions of the cementitious components presented in Section 2.9 with material property data for the undegraded cementitious materials taken from Chapter 3. In addition, the final selection of material property data also relies on the information presented in Section 6.5.1 and Section 5.1.

**Table 6-5. Recommended material property data for the cementitious components in 1–2BTF at closure.**

| Cementitious component | pH | Porosity | Hydraulic conductivity | Diffusivity | Compressive strength** | Tensile strength** |
|---|---|---|---|---|---|---|
| | - | % | m/s | m$^2$/s | MPa | MPa |
| **Slab** | ≥ 13 | 12–15 | $10^{-8}$–$10^{-5}$ | (2–5) × $10^{-12}$ | 40–50 | 4–5 |
| **Lid** | ≥ 13 | 11–13 | (1–5) × $10^{-12}$ | (2–5) × $10^{-12}$ | 55–60 | 4–5 |
| **Concrete elements*** | ≥ 13 | 12–15 | $10^{-3}$ | $10^{-10}$ | 40–50 | 4–5 |
| **Grout between waste packages** | ≥ 13 | 14–16 | $10^{-5}$–$10^{-3}$ | (1–5) × $10^{-11}$ | 25–35 | 2–3 |
| **Cementitious backfill** | ≥ 13 | 11–13 | (1–5) × $10^{-11}$ | (3–8) × $10^{-12}$ | 55–60 | 4–5 |
| **Concrete tanks** | ≥ 13 | 10–12 | (1–5) × $10^{-12}$ | (2–5) × $10^{-12}$ | 55–60 | 4–5 |
| **Concrete moulds** | ≥ 13 | 10–12 | (5–9) × $10^{-12}$ | (2–5) × $10^{-12}$ | 40–50 | 4–5 |

* As a group and including the slits between the individual elements.
** Refers to the cementitious material used in the respective components.

### 6.5.3 Specific uncertainties

The following specific uncertainties concerning the properties of the cementitious components in 1–2BTF have been identified:

- The detailed design of the lid has not yet been decided and the load-bearing capacity and transport properties of the lid at closure are therefore associated with some uncertainties.
- The properties of the grout between the waste packages at closure are uncertain. This applies both to the properties of the grout itself (Section 3.4.3) and the fact that it is not possible to control the degree of filling post-grouting and the dimensions and distribution of voids are therefore unknown. As a first task, the properties of the grout should be controlled during an upcoming grouting campaign.
- The detailed specifications of the materials that are used in the seal between the body and the lid of the concrete tanks are not known and hence it is uncertain how each of them is affected by the alkaline environment in the repository. In the case of fast degradation of the sealing materials, there is a potential for a significant increase of the hydraulic conductivity in this part already early post-closure.
- According to recent information, there is a hole with a diameter of 22 mm in some of the concrete tanks (Figure 6-7). This hole, which is situated in the upper part of one of the walls should be sealed with a bolt prior to disposal but it is unclear if this has been done for all tanks. The effect of this is that the tanks will be filled with intruding groundwater at closure and that the risk for cracking due to a high external pressure is therefore negligible. However, the open hole will also affect the transport properties of the tanks post-closure.

***Figure 6-7.*** *The hole in the concrete tank used in the tests reported by Lundqvist.*[1]

[1] SKBdoc 2000090, ver 1.0. (Internal document, in Swedish.)

## 6.6 Cementitious components in 1BLA

### 6.6.1 Expected status at closure

In this section the expected status at closure of the slab in 1BLA which was introduced in Section 2.10 is described, Section 6.6.1. This is followed by Section 6.6.2 which recommends data for the material properties of the slab at closure and Section 6.6.3 which summarises identified specific uncertainties in the descriptions.

#### *Slab*

**Chemical properties**

At closure, the slab will have the average chemical properties of up to 90 years old concrete which has been exposed to a marine environment.

As shown in Figure 2-31, the slab in 1BLA has been partly protected from contact with intruding groundwater by means of corrugated steel sheets. However, since the sheets did not extend all the way to the rock walls, and were also corroded in some places, the slab has been exposed to some chlorine-containing groundwater. However, during 2021 a waterproofing membrane which diverts the intruding groundwater was installed in 1BLA.

Further, some concrete/groundwater interactions may have occurred also on the underside of the slab. In case of clogging of the drainage layer, moisture transport through the slab may have occurred with chlorine enrichment and possibly also increased rebar corrosion as a consequence. Whether this has occurred or not is, however, uncertain as chlorine analysis has not been carried out.

**Load-bearing capacity**

The load-bearing capacity of the slab in 1BLA has been calculated by Nytorp Jansson (2020b). The calculations showed that the load-bearing capacity was dependent on the stiffness of the foundation layer. For a poorly compacted foundation layer, the load-bearing capacity of the slab was insufficient with respect to the load from the stack of waste packages (ISO-containers). Nytorp Jansson (2020b) concludes that the stiffness modulus of the foundation layer has to be at least 105 MPa to – with certainty – avoid cracking of the slab but states that this should be possible to achieve for the rather thin foundation layer in 1BLA as long as sufficient compaction has been carried out. At present, no documented information concerning the properties of the foundation layer in 1BLA has been found.

The load-bearing capacity of the slab in 1BLA has also been calculated by Könönen who studied the impact of alternative dimensions of the ISO-containers for different stacking alternatives.[57] Könönen showed that the extent of cracking and the width of the individual cracks will depend on the distribution of ISO-containers on the slab.[58] Könönen also showed that the load-bearing capacity of the slab will be sufficient to carry the load from the stack of ISO-containers, but that cracking must be anticipated for all stacking alternatives.[59]

In all, both of the referred-to studies indicate that cracks may have formed in the slab in 1BLA due to external loads from the stack of waste packages during the operational period. The risk for cracking is further increased since corrosion of the reinforcement bars during the up 90 years of operation will reduce the load-bearing capacity of the slab compared to at the time of construction.

[57] SKBdoc 1360313 ver 1.0. (Internal document, in Swedish.)

[58] SKBdoc 1360313 ver 1.0. (Internal document, in Swedish.)

[59] SKBdoc 1360313 ver 1.0. (Internal document, in Swedish.)

**Transport properties**

With reference to the previous section, formation of penetrating cracks in the slab in 1BLA due to insufficient load-bearing capacity during the operational period must be expected. Also, because the slab in 1BLA does not formally constitute a hydraulic barrier (Table 2-1) some cracking or formation of casting joints were probably accepted during construction. However, because no inspection protocols have been found, information on the current status of the slab is lacking.

In all, it is suggested that the slab at the time of closure will have the transport properties of *1BMA concrete* with a number of penetrating cracks, similar to those found in 1BMA, Section 6.2.1.

### 6.6.2 Recommended material property data

In Table 6-6, recommended material property data for the slab in 1BLA at closure are presented. The recommendations are based on the descriptions of the slab presented in Section 2.10 with material property data for the undegraded cementitious materials taken from Chapter 3. In addition, the final selection of material property data also relies on the information presented in Section 6.6.1 and Section 5.1.

**Table 6-6. Recommended material property data for the slab in 1BLA at closure.**

| | pH<br>- | Porosity<br>% | Hydraulic conductivity<br>m/s | Diffusivity<br>$m^2/s$ | Compressive strength*<br>MPa | Tensile strength*<br>MPa |
|---|---|---|---|---|---|---|
| **Slab** | ≥13 | 12–15 | $10^{-8}$–$10^{-5}$ | $(2–5)\times10^{-12}$ | 40–50 | 4–5 |

* Refers to the cementitious material used in the respective components

### 6.6.3 Specific uncertainties

The following specific uncertainty concerning the properties of the slab in 1BLA has been identified:

- There is a lack of detailed information concerning the number and widths of the cracks in the slab in 1BLA.

## 6.7 Cementitious components in 2–5BLA

### 6.7.1 Expected status at closure

In this section the expected status at closure of the slabs in 2–5BLA which were introduced in Section 2.11 is described, Section 6.7.1. This is followed by Section 6.7.2 which recommends material property data for the slabs at closure and Section 6.7.3 which summarises identified specific uncertainties in the descriptions.

#### *Slabs*

**Chemical properties**

At the time of closure, the slabs in 2–5BLA will have the chemical properties of 40–45 years old reinforced *2BMA concrete*. Alterations of the mineral composition are not expected during the operational period, although some carbonation of the upper few millimetres of the slabs could occur. This is because a waterproofing membrane will be installed in the waste vault that diverts intruding groundwater to the drainage system and prevents concrete/groundwater interactions.

However, in the case of (unexpected) clogging of the drainage system beneath the slab, groundwater may come in direct contact with the underside of the slab with leaching and chlorine intrusion as possible consequences.

**Load-bearing capacity**

During the operational period, the slabs must withstand the static load from the stack of waste packages (ISO-containers) as well as the dynamic load from the transport of waste packages which is carried out by means of a fork-lift truck.

Even though no reports have been found where the load-bearing capacity of the slabs in 2–5BLA has been evaluated, it is judged that the load-bearing capacity of the slabs will be sufficient to carry the identified loads and therefore cracking during the operational period is not expected. This is because the loads are well-known and the dimensions and amount of reinforcement in the slabs can be adjusted to accommodate these loads. Also, thanks to prolonged cement hydration, the compressive strength of the *2BMA concrete* at closure is likely to exceed the 28-days strength used in the dimensioning work.

**Transport properties**

From the previous section, crack formation of the slabs in 2–5BLA during the operational period is not expected.

However, because the slabs in 2–5BLA do not formally constitute hydraulic barriers (SKB TR-23-01), the use of such construction methods that prevent cracking or formation of joints or other permeable zones during construction are currently not prescribed. For that reason, it is expected that the slabs at closure will contain a few small cracks and/or somewhat permeable construction joints which may affect the transport properties of the slabs.

### 6.7.2 Recommended material property data

In Table 6-7, recommended material property data for the slabs in 2–5BLA at closure are presented. The recommendations are based on the descriptions of the slabs presented in Section 2.11 with material property data for the undegraded cementitious materials taken from Chapter 3. In addition, the final selection of material property data also relies on the information presented in Section 6.7.1 and Section 5.1.

**Table 6-7. Recommended material property data for the slabs in 2–5BLA at closure.**

| | pH<br>- | Porosity<br>% | Hydraulic conductivity<br>m/s | Diffusivity<br>$m^2/s$ | Compressive strength*<br>MPa | Tensile strength*<br>MPa |
|---|---|---|---|---|---|---|
| **Slabs** | ≥ 13 | 11–13 | $10^{-8}$–$10^{-5}$ | $(2–5) \times 10^{-12}$ | 55–60 | 4–5 |

* Refers to the cementitious material used in the respective components.

### 6.7.3 Specific uncertainties

The following specific uncertainty concerning the properties of the slabs in 2–5BLA has been identified:

- The main uncertainty relates to the fact that the dimensions, amount of reinforcement and method of construction of the slabs in 2–5BLA have not yet been specified and the risk for cracking due to temperature shrinkage or the formation of permeable casting joints during construction is therefore not fully known. This means that although cracking during the operational period can be prevented, cracking can still occur during construction unless specific measures are taken.

## 6.8 Plugs, other closure components and common cementitious components

### 6.8.1 Expected status at closure

In this section the expected status at closure of the plugs, other closure components and the other cementitious components which are common for all parts of the repository and which were introduced in Section 2.12 is described, Section 6.8.1. This is followed by Section 6.8.2 which recommends material property data for the cementitious components at closure and Section 6.8.3 which summarises identified specific uncertainties in the descriptions.

#### *Concrete plugs in tunnels*

**Chemical properties**

At closure, the concrete plugs in the tunnels will have the chemical properties of undegraded hardened *SFR plug concrete*, Section 3.3.10. This is because the concrete plugs are cast at closure of the repository and no degradation will therefore occur.

**Load-bearing capacity**

Prior to saturation of the repository, the concrete plugs will only experience the small loads from the backfill materials. The load-bearing capacity will be sufficient to resist these loads and cracking therefore not expected.

**Transport properties**

The transport properties of the concrete plugs in the tunnels at closure are mainly controlled by the presence of cracks or permeable zones at the rock/plug interface or by cracks in the plug itself.

The main concern relates to the risk for cracking caused by temperature shrinkage during construction. Here, a concrete plug whose entire circumference is in direct contact with and adhered to the surrounding bedrock is likely to crack in some places due to high levels of strain caused by temperature shrinkage towards the end of the cement hydration process. As means to prevent cracking, the concrete plug can be cooled during casting or large amounts of reinforcement used.

It is therefore expected that the transport properties of the concrete plugs in the tunnels at closure will correspond to those of undegraded *SFR plug concrete* with a few small penetrating cracks. However, for the thick concrete plugs, it is uncertain if all cracks will penetrate the entire plug.

#### *Concrete plugs in investigation boreholes*

**Chemical properties**

At closure, the concrete plugs in the investigation boreholes that were sealed prior to excavation of SFR1 will have the chemical properties of up to 90 years old *Cement paste for boreholes,* Section 3.4.7. For investigation boreholes that will be sealed prior to excavation of the extension of SFR, the chemical properties will be representative of up to 50 years old *Alternative borehole concrete* (See motivation in Section 2.12.2).

According to Grandia et al. (2010a) mineral transformation in boreholes are very slow and only minor/negligible alterations are expected during the operational period.

**Load-bearing capacity**

The load-bearing capacity of the concrete plugs in the investigation boreholes must be sufficient to withstand the swelling pressure of the bentonite section enclosed by them. Because this load is strictly compressive, cracking of the concrete plugs in the investigation boreholes is not expected during the operational period.

**Transport properties**

According to the previous section, cracking of the concrete plugs in the investigation boreholes is not expected during the operational period. However, in spite of this, the transport properties of the concrete plugs in the boreholes are difficult to predict. This is because on-site inspections in the investigation boreholes are not possible but also because experiments under representative conditions utilising destructive investigation methods are complicated and time consuming.

In the tests reported by Mårtensson (2019), significant separation of the *SFR borehole concrete* was observed for a concrete plug cast in a water-filled borehole at a depth of about 200 meters (Figure 6-8) whereas the *Alternative borehole concrete* (Standard concrete for casting under water) showed no signs of separation (Figure 6-9).

***Figure 6-8.*** *Two parts of the core made of* ***SFR borehole concrete*** *extracted from a depth of about 220 meters showing a zone which has been enriched in cement (upper picture) and a zone which has been depleted from cement (lower picture) (Mårtensson 2019).*

***Figure 6-9.*** *A part of the core, without signs of separation, made of standard concrete for casting under water extracted from a depth of about 220 meters (Mårtensson 2019).*

As shown in Figures 6-8 and 6-9 it is obvious that the transport properties at closure will be dependent on the success of the installation. Even though type of concrete for the concrete plugs in the investigation boreholes has not yet been selected, it must be assumed that type of concrete and installation method will be carefully tested and evaluated prior to the first installation in order to ensure the required properties of the concrete plug.

It is therefore expected that the concrete plugs in the investigation boreholes will have the transport properties of up to 50 years old *Alternative SFR borehole concrete* (Section 3.3.12) or up to 90 years old the *Cement paste for boreholes* (Section 3.4.7) which was used for sealing of a number of investigation boreholes in the 1980's (SKB 1983, underbilaga 4.1).

### *Shotcrete on the rock walls*

#### Chemical properties

Based on the findings by Lundin (SKBdoc 1390675 ver 1.0, internal documant, in Swedish) and Holmberg (SKBdoc 1991682 ver 0.1, internal document, in Swedish) presented in Section 3.3.9 it is expected that the shotcrete in SFR at the time of closure will have the chemical properties of up to 90 years old *SFR shotcrete* which has been exposed to a marine environment. This means that both leaching, carbonation and intrusion of species from the groundwater such as sulphate and chlorine must be expected.

#### Load-bearing capacity

The load-bearing capacity of the shotcrete on the rock walls relates to its ability to prevent the fall-out of small rock pieces, the function of which is ensured through addition of steel fibres and a sufficiently strong adhesion to the bedrock.

Lundin (SKBdoc 1390675 ver 1.0, internal documant, in Swedish) and Holmberg (SKBdoc 1991682 ver 0.1, internal document, in Swedish) showed that corrosion of the steel fibres in up to 30 years old shotcrete was limited and only the fibres in the surface region of the shotcrete showed signs of corrosion. They also showed that the adhesion of the shotcrete to the bedrock was within the requirements. From the reported observations, it is expected that the load-bearing capacity of the shotcrete in SFR will be sufficient also at closure and that extensive cracking due to insufficient load-bearing capacity will not occur during the operational period.

#### Transport properties

With an estimated porosity of about 15 % (Section 3.3.9) the transport properties of the *SFR shotcrete* at closure should be similar to those of the *BTF grout*. However, the compressive strength (Table 3-26) indicate that the transport properties would rather correspond to those of the *Silo concrete* or the *2BMA concrete*.

However, for shotcrete, the presence of inhomogeneities will have a larger influence on the transport properties than for cast concrete. Therefore, the transport properties of the shotcrete will not only depend on the mixing proportions of the material but also on the skill of the operator of the equipment.

For that reason, it is predicted that the transport properties of the shotcrete on the rock walls will have a larger variation than those of the concrete structures with values ranging from those of cast concrete to those of concrete with significant amounts of pores and voids.

### *Grout for rock bolts*

#### Chemical properties

At closure, the grout for rock bolts is expected to have the chemical properties of unaltered to slightly leached *SFR grout for rock bolts* (Section 3.4.6) with a pH of at least 12.5 and a high portlandite concentration.

However, the chemical properties of the grout for rock bolts will be dependent on the availability of groundwater in the borehole in which each individual rock bolt has been emplaced. As an example, Windelhed et al. (2002) suggest that aging of concrete in dry boreholes is extremely slow whereas degradation can be considerably faster if the borehole is intersected by a fracture with a high flow of groundwater. This means that leaching and mineral alterations could be more extensive in some holes.

**Load-bearing capacity**

The load-bearing capacity of the grout for rock bolts relates to its function of securing the bolt in the bedrock. With reference to the findings presented by Windelhed et al. (2002), loss of load-bearing capacity on a general scale is not expected during the operational period. Based on their conclusions, the load-bearing capacity of the *SFR grout for rock bolts* is expected to be sufficient to prevent the loss of function of the grout for rock bolts in all but possibly a few boreholes in SFR prior to closure. This also means that cracking due to insufficient load-bearing capacity is not expected during the operational period.

**Transport properties**

The transport properties of the grout for rock bolts are dependent on the properties of the material itself but probably more importantly also on the skill of the operator of the grouting equipment. Windelhed et al. (2002) shows a number of examples where grouting has failed and discusses the consequences thereof.

However, by careful control of grout preparation and grouting of the rock bolts, the number and size of voids and channels can be considerably reduced if not entirely prevented. For that reason, it is predicted that the transport properties of the grout for rock bolts at closure will have the characteristics of up to 90 years old *SFR grout for rock bolts* which has undergone only minor mineral alterations and which contains only a few smaller voids.

#### *Injection grouts in the fractures in the surrounding bedrock*

**Chemical properties**

The chemical properties of the injection grouts in the fractures in the surrounding bedrock will be dependent on the mixing proportions of the grout but also on the flow of groundwater at the interface between the grouted and un-grouted zones. The properties will also depend on the presence of voids or channels in the grout that could increase the rate of leaching.

Therefore, the chemical properties of the grout in different fracture systems in the bedrock in SFR will be unique for each system and vary from those of unaltered *SFR injection grout* in dry fractures to those of somewhat leached material in fractures with a high groundwater flow and also where grouting was less successfully carried out.

**Load-bearing capacity**

The load-bearing capacity of the injection grout is not relevant.

**Transport properties**

At closure, the transport properties of the injection grout in the fractures in the bedrock will show considerable variations between different fracture systems.

### 6.8.2 Recommended material property data

In Table 6-8, recommended material property data for the plugs and other closure components and common cementitious components at closure are presented. The recommendations are based on the descriptions of the cementitious components presented in Section 2.12 with material property data for the undegraded cementitious materials taken from Chapter 3. In addition, the final selection of material property data also relies on the information presented in Section 6.8.1 and Section 5.1.

**Table 6-8. Recommended material property data for the plugs and other closure components and common cementitious components at closure.**

| Cementitious component | pH<br>- | Porosity<br>% | Hydraulic conductivity<br>m/s | Diffusivity<br>$m^2/s$ | Compressive strength*<br>MPa | Tensile strength*<br>MPa |
|---|---|---|---|---|---|---|
| Concrete plugs in tunnels | ≥ 13 | 11–13 | $10^{-9}$ | $(2–5) \times 10^{-12}$ | 50–60 | 4–5 |
| Concrete plugs in boreholes | ≥ 13 | 11–13 | $10^{-12}$–$10^{-11}$ | $(2–5) \times 10^{-12}$ | 40–50 | 4–5 |
| Shotcrete on the rock walls | 12.5 | 12–15 | $10^{-12}$–$10^{-6}$ | $10^{-12}$–$10^{-11}$ | 45–70 | 4–5 |
| Grout for rock bolts | ≥ 13 | 10–15 | $10^{-8}$–$10^{-4}$ | $(1–5) \times 10^{-11}$ | 25–30 | 0.5–1 |
| Injection grout | 12.5 | 15–30 | $10^{-8}$–$10^{-4}$ | $10^{-12}$–$10^{-10}$ | 25–40 | 0.5–1 |

* Refers to the cementitious material used in the respective components

### 6.8.3 Specific uncertainties

The following specific uncertainties concerning the properties of the common cementitious components have been identified:

- The main uncertainties regarding the material property data presented in Table 6-8 are related to difficulties in performing on-site inspections of the components, e.g. the concrete plugs in investigation boreholes, grout for rock bolts and injection grout in the bedrock.
- The detailed design of the concrete plugs for tunnels has not been finally specified and the properties of these plugs at the time of closure are therefore somewhat uncertain.

# 7 The silo: post-closure evolution

In this chapter, the expected evolution of the properties of the cementitious components in the silo during the first 100 000 years post-closure is described. The starting point for the descriptions is the expected status of the cementitious components in the silo at closure presented in Section 6.1. The evolution of the properties of the cementitious components in the silo is then influenced by the processes presented in Chapter 4.

Detailed descriptions of the cementitious components of the silo are given in Section 2.5. In addition, Chapter 3 presents detailed specifications and properties of the cementitious materials in the various components of the silo.

## 7.1 Literature

The following reports form the basis for the description of the post-closure evolution of the properties of the cementitious components in the silo presented in this chapter:

- **Bultmark (2017a)** calculated the load-bearing capacity of concrete moulds.
- **Cronstrand (2007)** modelled the evolution of the mineral composition of the barrier system of the silo, including both the cementitious and bentonite components.
- **Cronstrand (2014)** modelled the evolution of pH in the waste vaults in SFR1.
- **Gaucher et al. (2005)** modelled the evolution of the mineral composition of the barrier system of the silo, including both the cementitious and bentonite components.
- **Idiart et al. (2020)** modelled concrete/ bentonite interactions in the bentonite barrier in the rock vault for legacy waste (BHA) in the repository for long-lived low- and intermediate level radioactive waste, SFL. Even though the focus of this study was on montmorillonite dissolution, some parts of the report also included concrete degradation.
- **Höglund (2014, Appendix B)** modelled the impact of the formation of cracks on the transport properties of the outer concrete structure of the silo.
- **Höglund and Bengtsson (1991)** studied the risk that the sand in the gas evacuation system in the lid of the concrete silo is blocked by the precipitation of secondary minerals.
- **Könönen and Olsson (2018)** modelled the impact of rock fall-out on the structural integrity of the lid of the concrete caissons in 2BMA which serve as a representative example in lack of specific studies on the impact of rock fall-out on the properties of the concrete lid of the silo.
- **Moreno et al. (2001)** and **Moreno and Neretinieks (2013)** studied gas flows in cracks in concrete.
- **Olsson (2016b)** studied the risk for cracking of the outer concrete structure due to internal loads from swelling waste and gas formation.
- **von Schenk and Bultmark (2014)** studied the effect of swelling of bituminised ion-exchange resins on the structural integrity of the concrete silo.
- **Wiborgh and Lindgren (1987)** compiled material data for different types of cementitious materials.

## 7.2 Slab

### 7.2.1 Chemical properties

The evolution of the mineral composition of the slab of the concrete silo is expected to follow the general trend outlined for the outer wall presented in Section 7.3. The detailed description of the different degradation steps is therefore not repeated here.

However, the rate of concrete degradation could proceed at a slightly higher rate in the slab than in the outer walls. This is because the slab is founded on a 90/10 sand/bentonite mixture with an expected higher hydraulic conductivity than that of the bentonite surrounding the outer walls (Abarca et al. 2020, Appendix A). However, the difference is probably insignificant to be relevant considering all other uncertainties associated with predictions of the properties of the slab for a period of up to 100 000 years. In addition, Figure 2-5 shows that the sand/bentonite mixture is covered with a sealing layer which prevents direct contact between the slab and the sand/bentonite and therefore limits interactions between these two components, as long as this layer is intact.

In spite of the somewhat uncertain description, it is expected that the evolution of the chemical properties of the slab of the concrete silo will follow that for the outer wall outlined in Section 7.3.1.

### 7.2.2 Load-bearing capacity

The load-bearing capacity of the slab mainly depends on the mineral composition of the concrete. This is because the slab experiences only compressive loads from the silo and the waste packages. The status of the reinforcement bars is therefore of lesser importance post-closure. However, in the unlikely event of significant uneven settlements in the sand/bentonite layer, reinforcement in the slab would be required to prevent cracking. As shown in Section 6.1.1, settlements of the concrete silo have so far been small and an increased rate post-closure is not expected even though the weight of the silo will increase further during the operational period as a consequence of the emplacement of additional number of waste packages and amounts of grout.

As shown in Figures 7-1 to 7-5, chemical degradation of the *Silo concrete* is very slow. Based on the conclusions made by Cronstrand (2007) (Section 7.3.2) it is expected that the slab will remain structurally intact during up to at least 50 000 years post-closure and the formation of additional penetrating cracks is therefore not expected during this time period.

Also, even though continued chemical degradation beyond this point in time will reduce the load-bearing capacity of the slab further, Figure 7-5 shows that CSH-gels is found in a majority of the cross section of the outer wall still at 100 000 years post-closure. The slab is therefore predicted to be able to carry the evenly distributed load from the completely filled and grouted silo but be sensitive to settlements in the sand/bentonite mixture. However, such settlements are not anticipated at this stage because the foundation layer has been compressed by the weight from the silo during several millennia.

### 7.2.3 Transport properties

According to Section 6.1.1, there remain some uncertainties regarding the status of the slab of the concrete silo at closure with respect to the presence of penetrating cracks formed during construction. Because of to these uncertainties, it was in Section 6.1.1 stated that the slab at closure is expected to have the transport properties of a concrete structure that contains one or a few cracks with a width below 0.5 mm.

From Section 7.2.2, the risk for formation of new penetrating cracks in the slab is low during at least up to 50 000 years post-closure. This is because the slab will only experience compressive loads and also because of the slow chemical degradation of the slab (Cronstrand 2007, Gaucher et al. 2005). In addition, cracking due to drying shrinkage is not expected since the slab is completely saturated.

Also, beyond this point in time, only minor alterations of the transport properties are expected. This is because the pore system of the concrete is slowly infilled with secondary minerals and eventually – when no porosity remains – any further interactions will be very slow or even completely halted. See Figure 7-7 and (Cronstrand 2007).

However, as shown in Figures 7-1 to 7-5, clogging of the concrete pore system is associated with the formation of significant amounts of ettringite, a mineral known to be able to cause the formation of cracks in concrete. This means that even though the original concrete pore system may be infilled with secondary minerals, additional porosity may form in the shape of micro cracks caused by expansive ettringite. Due to these uncertainties, porosity and transport properties recommended for the slab of the concrete silo, presented in Table 7-1, have a similar evolutionary trend as for e.g. 2BMA, even though porosity clogging is not expected there. See also Section 7.2.5.

In conclusion, the transport properties of the slab of the concrete silo is expected to be similar to those of the slab at closure during at least up to about 50 000 years post-closure. After that, the hydraulic conductivity and diffusivity could decrease due to the clogging of the pore system but also increase due to the formation of some new cracks. This prediction is, however associated with some uncertainties concerning the chemical and mechanical processes over such a long period of time.

### 7.2.4 Recommended material property data

Table 7-1 presents recommended material property data for the slab of the concrete silo for selected time periods up to 100 000 years post-closure. The recommendations are based on information regarding the status of the slab at closure presented in Section 6.1, the expected evolution of the properties of the slab described in the previous sections and the properties of degraded concrete given in Section 5.1.

**Table 7-1. Recommended material property data for the slab of the silo for selected time periods up to 100 000 years post-closure.**

| | | Time period (Years post-closure) | | | | |
|---|---|---|---|---|---|---|
| **Property** | **Unit** | **At closure** | **0–1 000** | **1 000–20 000** | **20 000–50 000** | **50 000–100 000** |
| **pH** | - | ≥ 13 | ≥ 13 | 12.5–13 | 12.5–12 | 11–12 |
| **Porosity** | % | 11–13 | 11–13 | 11–14 | 12–15 | 14–16 |
| **Load-bearing capacity** | Rating (5–1) | 5 | 5 | 4–5 | 4 | 3–4 |
| **Hydraulic conductivity** | m/s | $10^{-8}$–$10^{-5}$ | $10^{-8}$–$10^{-5}$ | $10^{-8}$–$10^{-5}$ | $10^{-8}$–$10^{-5}$ | $10^{-6}$–$10^{-4}$ |
| **Diffusivity** | $m^2/s$ | $(5–9)\times10^{-12}$ | $(5–9)\times10^{-12}$ | $(5–9)\times10^{-12}$ | $(1–5)\times10^{-11}$ | $(5–9)\times10^{-11}$ |

### 7.2.5 Specific uncertainties

The following specific uncertainties in the description of the evolution of the properties of the slab of the concrete silo during the first 100 000 years post-closure have been identified:

- The unknown distribution and width of cracks in the slab at closure constitute a major uncertainty.
- There also remains some uncertainties regarding the evolution of the chemical properties of the slab. This is because the slab has not been included in any of the modelling efforts carried out so far and the lower amount of bentonite in the foundation is likely to give a somewhat different evolution than that of the outer wall which is surrounded by pure bentonite.
- Finally, the evolution of concrete porosity and transport properties are uncertain. Modelling suggests that the concrete pore system can be infilled by secondary minerals such as ettringite but does not consider the potential for the formation of microcracks caused by the formation of ettringite.

See also the discussion concerning the general uncertainties in Chapter 5.

## 7.3 Outer wall

### 7.3.1 Chemical properties

The most extensive studies of the evolution of the mineral composition of the outer wall over a period of up to 100 000 years post-closure were carried out by Cronstrand (2007) and Gaucher et al. (2005) and this section is therefore mainly based on these two reports. However, the pH evolution in the silo has also been modelled by Cronstrand (2014).

As a reference to the following discussion, Figure 7-1 shows the mineral composition of the various components in the silo at closure. In Figure 7-1, the white area (porosity) is unexpectedly large for the silo wall given fact that the input data for the *Silo concrete* used by Cronstrand (2007) originates from Gaucher et al. (2005) who report a total porosity of only 15 %. However, Gaucher et al. (2005) also state that 10 % of the volume is occupied by the steel structure which is not represented in the coloured fields. It is therefore assumed that the steel structure of the silo wall is included in the white area, giving a "total porosity" of 25 % even though this is not explicitly stated by either Cronstrand (2007) or Gaucher et al. (2005).

The studies by Cronstrand (2007, 2014) and Gaucher et al. (2005) show that alterations of the mineral composition as well as changes in pH and porosity in the outer wall are very slow and initially concentrated to the interface between concrete and bentonite as shown in Figure 7-2. With a thickness of 800–900 mm, alterations of the bulk chemical properties of the outer wall of the concrete silo are not expected during the first 1 000 years post-closure.

During the period 1 000 to 10 000 years post-closure, alterations of the mineral composition will proceed further into the outer wall due to continued chemical interactions between the concrete and bentonite as well as with the groundwater and species dissolved in the groundwater. However, as shown in Figure 7-3, still 10 000 years post-closure the mineral composition in the major part of the outer wall is more or less unaffected by these processes as evidenced through a comparison between Figures 7-1 and 7-3.

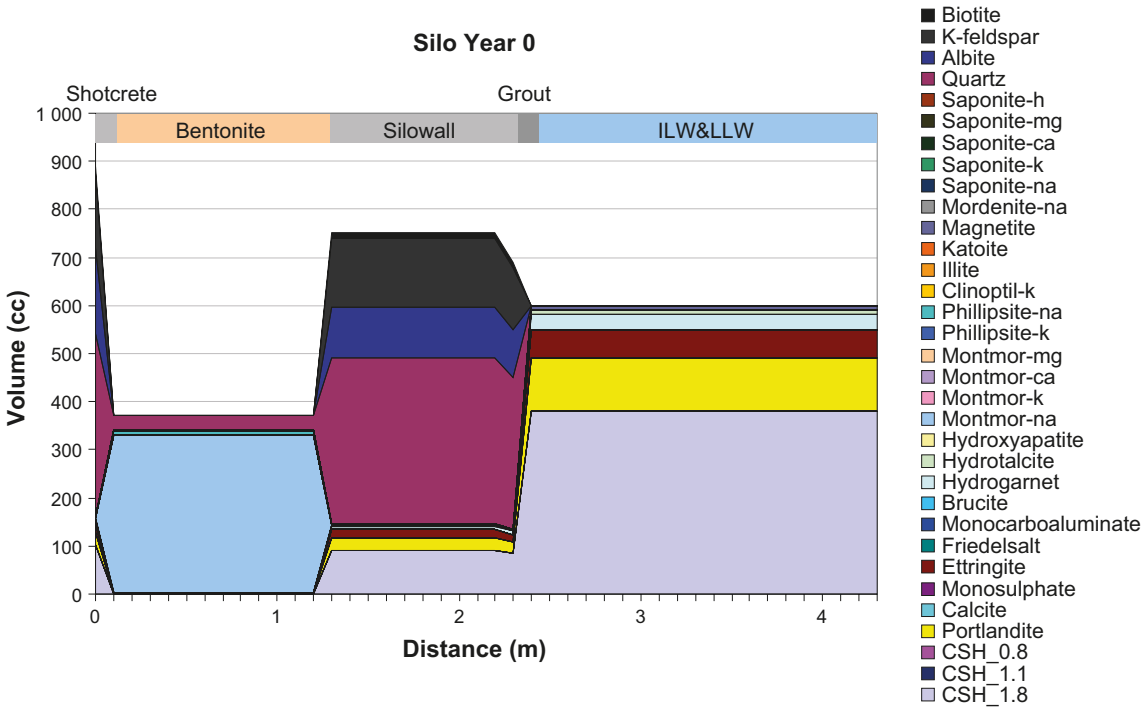


***Figure 7-1.*** *Initial mineral composition in the silo (Cronstrand 2007, Figure B-1). Note that most of the mineral volume (biotite, k-feldspar, albite and quartz) in the outer wall (silo wall) constitutes the inert aggregate material. The material in the ILW & LLW domain is the same as the shotcrete but without aggregates. The white area for the silo wall includes both the total porosity and the steel structure.*

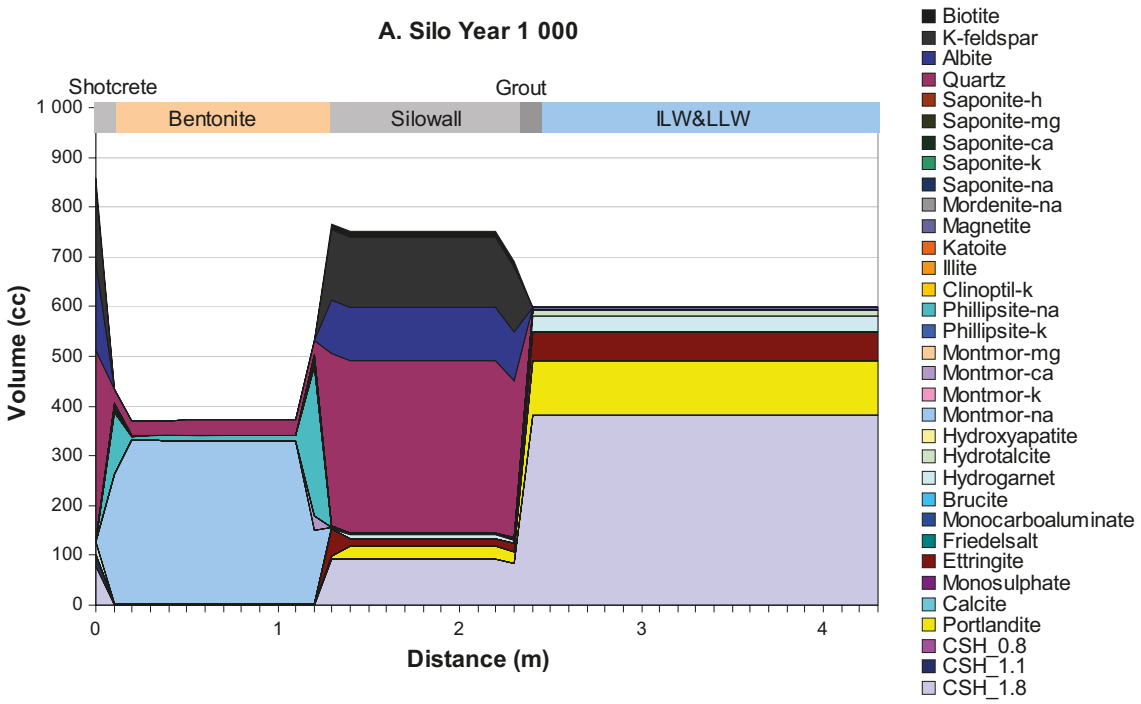


***Figure 7-2.*** *Mineral composition in the silo at 1 000 years post-closure (Cronstrand 2007, Figure B-2). Note that most of the mineral volume (biotite, k-feldspar, albite and quartz) in the outer wall (silo wall) constitutes the inert aggregate material. The white area for the silo wall includes both the total porosity and the steel structure.*

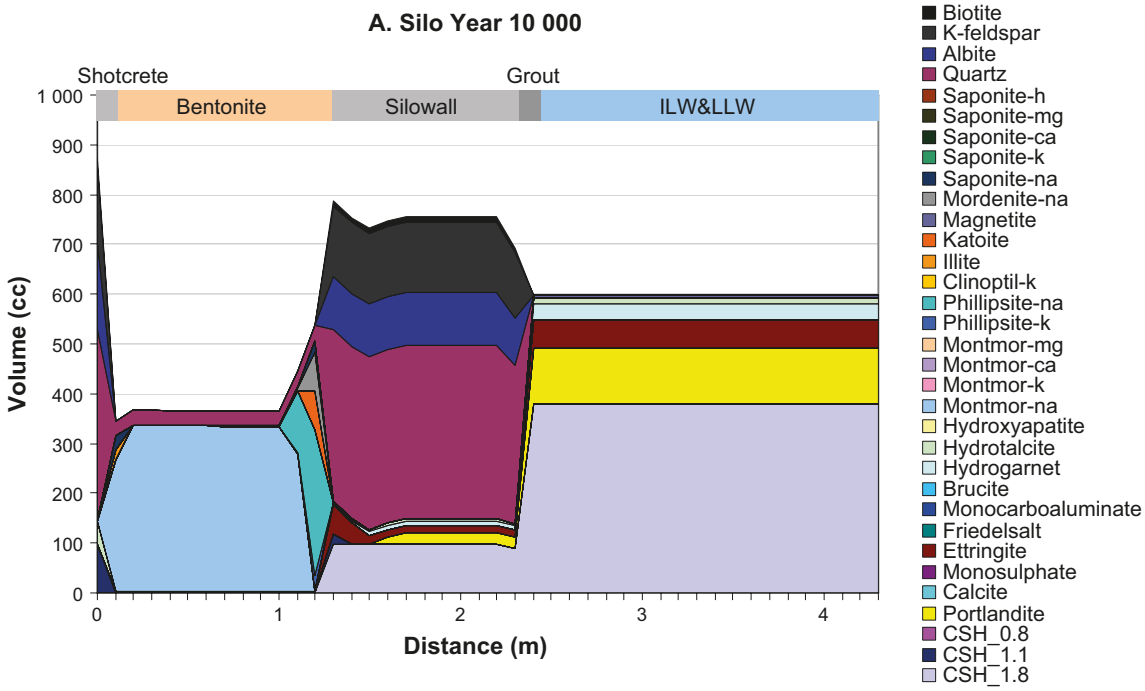


***Figure 7-3.*** *Mineral composition of the materials in the silo at 10 000 years post-closure. (Cronstrand 2007, Figure B-3). Note that most of the mineral volume (biotite, k-feldspar, albite and quartz) in the outer wall (silo wall) constitutes the inert aggregate material. The white area for the silo wall includes both the total porosity and the steel structure.*

From 10 000 years post-closure and onwards, the outer wall is slowly depleted of portlandite, Figure 7-4 and 7-5. In addition, a change from CSH_1.8 to CSH_1.1 as the dominant CSH-phase in the outer parts of the concrete wall is also observed. Finally, also increased levels of ettringite are observed in the outer wall as also reflected in the changes of the porosity distribution shown in Figure 7-7.

Even though the original concrete pore system may be infilled with secondary minerals, additional porosity may form in the shape of micro cracks caused by expansive ettringite. Because of the significant uncertainties associated with this process, porosity and transport properties recommended for the outer wall of the concrete silo, presented in Table 7-2, have a similar evolutionary trend as for e.g. 2BMA, even though porosity clogging is not expected there. See also Section 7.3.5.

The alterations of the mineral composition discussed above are also reflected in alterations of pH, pe and the concentration of different species in the porewater of the outer wall.

Both Gaucher et al. (2005) and Cronstrand (2007) show that portlandite leaching results in a drop in pH but also that there is a weak pH-gradient in the outer wall expressed by the fact that pH at 100 000 years post-closure is above 12 towards the interior of the silo whereas it is below 12 at the concrete/bentonite interface, Figure 7-6. Note that Figure 7-6 is a mirror image of the other figures in this section with the bentonite to the right instead of left as in the other figures. This agrees with Cronstrand (2014) who shows that pH in the outer wall will be about 12.5 up to 100 000 years post-closure.

Gaucher et al. (2005) also show that significant concentration gradients for Na, Mg and sulphate exist within the outer wall. The concentration of Ca is not reported but it can be expected to follow the general trend for the Ca-rich cement minerals with a lower concentration towards the bentonite and a higher towards the interior of the concrete silo.

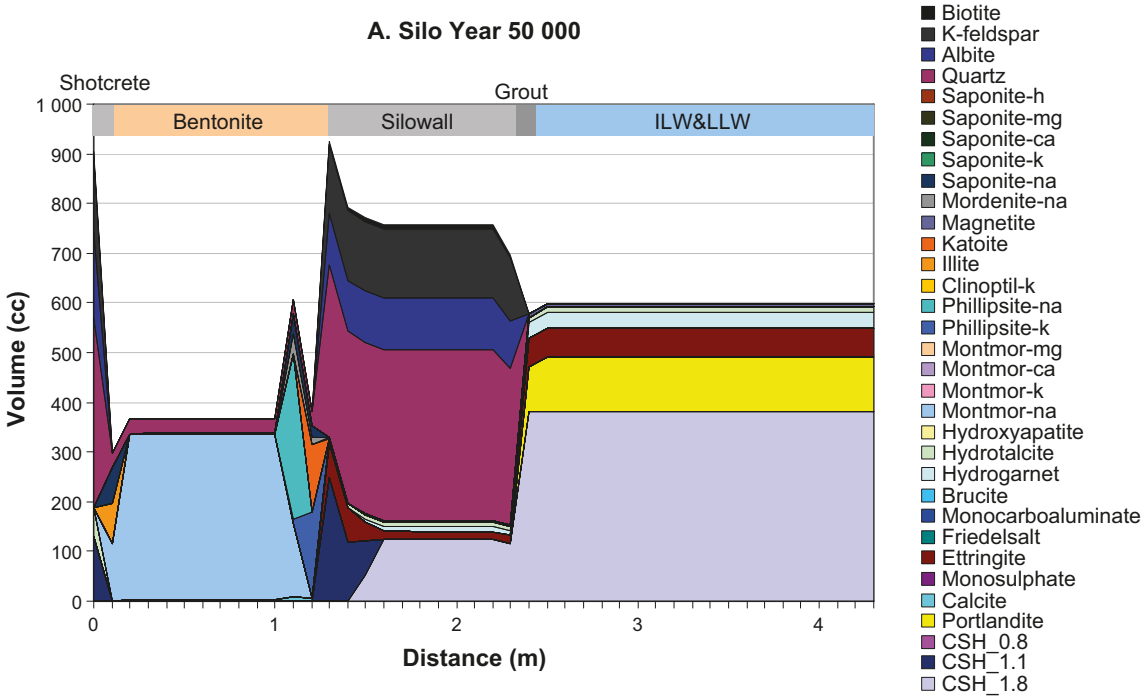


***Figure 7-4.*** *Mineral composition of the materials in the silo at 50 000 years post-closure (Cronstrand 2007, Figure B-4). Note that most of the mineral volume (biotite, k-feldspar, albite and quartz) in the outer wall (silo wall) constitutes the inert aggregate material. The white area for the silo wall includes both the total porosity and the steel structure.*

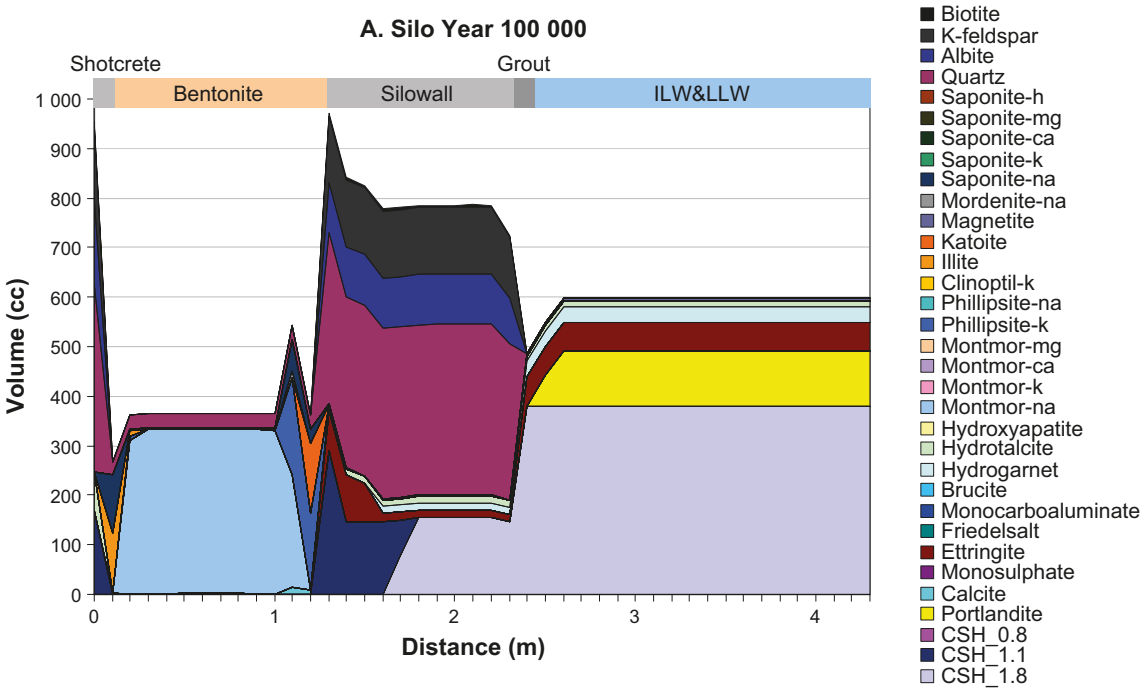


***Figure 7-5.*** *Mineral composition of the materials in the silo at 100 000 years post-closure (Cronstrand 2007, Figure B-5). Note that most of the mineral volume (biotite, k-feldspar, albite and quartz) in the outer wall (silo wall) constitutes the inert aggregate material. The white area for the silo wall includes both the total porosity and the steel structure.*

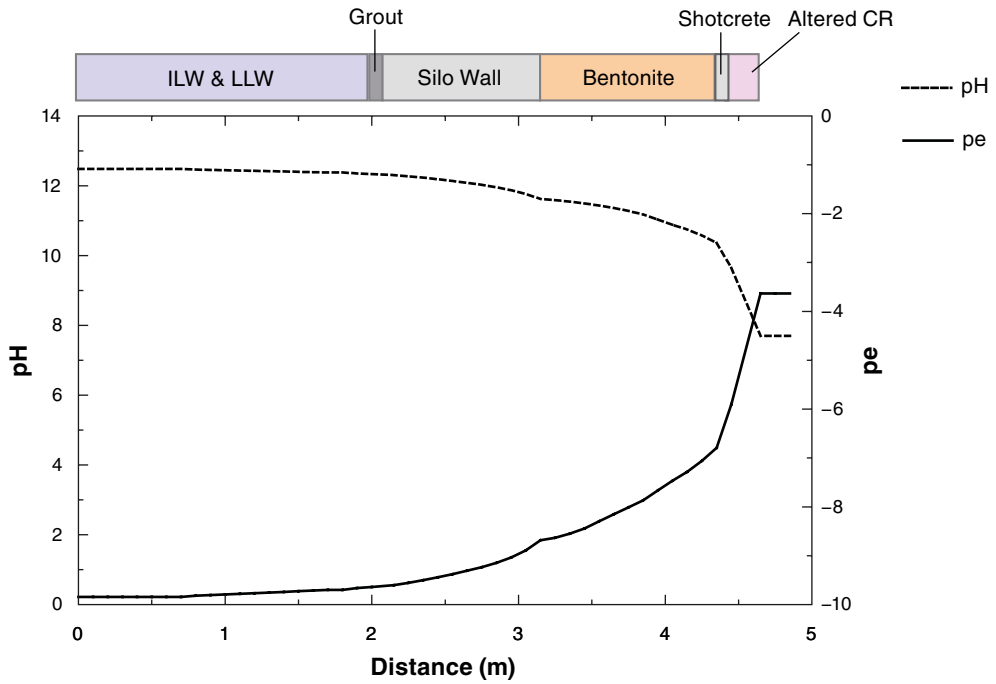


***Figure 7-6.*** *pH and pe in the silo barriers at 100 000 years post-closure (Gaucher et al. 2005). Note that this figure is a mirror image of the other figures in this section.*

### 7.3.2 Load-bearing capacity

The load-bearing capacity of the outer wall of the silo, i.e. the capacity of the outer wall to withstand external and internal loads is dependent on the mineral composition of the concrete and the status of the reinforcement bars. However, it is also influenced by the support from the inner walls and grouted waste packages as well as from the pressure from the surrounding bentonite which provides external support.

As shown in Figures 7-2 to 7-5, alterations of the mineral composition are slow and it is estimated that portlandite will remain in at least half of the cross section of the outer wall during about 20 000 years post-closure. However, the function of the reinforcement bars cannot be expected to be upheld for such a long period as indicated by the study by Höglund (2014, Appendix B).

**Impacts of external loads**

Even though the study might be overly conservative, Höglund (2014, Appendix B) reports that the time to reach a critical stress to cause spalling of the covering layer of the outer wall and therefore loss of function of the reinforcement bars is only a few years even for a corrosion rate in the range of 0.05 μm/year.

In spite of this, external loads are not expected to cause early formation of penetrating cracks in the outer wall even in the event of complete loss of function of the reinforcement bars. This is because the outer wall is supported by the grouted waste packages and inner walls and therefore expected to be able to carry the compressive load from the bentonite at least up to 50 000 years post-closure.

**Impact of internal loads**

Internal loads in the silo mainly originate from a high gas pressure or swelling of waste and can – in combination with loss of function of the reinforcement bars and (less likely) reduced swelling pressure of the surrounding bentonite – lead to the formation of cracks in the outer walls.

The impact of swelling of bituminised ion-exchange resins has been modelled by von Schenk and Bultmark (2014). In their work, the effect of swelling of ion-exchange resins on the structural integrity of the cementitious grout as well as the inner and outer walls was modelled for several different waste package emplacement scenarios with varying available expansion volume. This study showed that even though cracks can form in the interior parts of the silo, cracking of the outer concrete structure was not observed even for the worst-case scenario studied in this work.

The risk for cracking of the outer wall due to internal loads from swelling waste and gas formation has also been evaluated by Olsson (2016b). The study concluded that the resistance of the outer concrete wall to internal forces is dependent on the detailed emplacement of the different types of waste. The strategy of placing the waste with the highest potential for swelling in the central part of the silo was found to reduce the risk compared to alternative disposal strategies.

Olsson (2016b) also showed that the outer concrete structure can resist an internal pressure of 400 kPa before the first cracks would form. This can be compared with the findings by Moreno et al. (2001) who showed that a gas flow can be established in cracks with an aperture of only 10 μm already at an overpressure of 15 kPa. Assuming one crack every meter, Figure 4-3 shows that this corresponds to a hydraulic conductivity in the range of $10^{-9}$ m/s, i.e. basically the same as the required hydraulic conductivity of the *Original Silo grout* and *New silo grout*.

Also, the high hydraulic conductivity of the sand in the sand-filled channels in the lid of the concrete silo (estimated to about $10^{-2}$ to $10^{-3}$ m/s, (Kennedy et al. 1984) and reproduced by Nyblad and Wimelius (2013)) ensures that any gas reaching the lid of the silo will be effectively transported out of the concrete silo. The conclusion is therefore that the risk for formation of penetrating cracks in the outer wall due to an internal gas pressure is low.

It should finally be recognised that gas formation can pose a problem in the unlikely event that the gas evacuation system is clogged through mineral precipitations. However, as concluded by Höglund and Bengtsson (1991) the probability for this to occur is low and this process is therefore neglected.

In all the load-bearing capacity of the outer wall itself is expected to be sufficient to prevent the formation of penetrating cracks during a significant period of time but the timing of the formation of the first cracks and the following evolution are difficult to predict with accuracy.

### 7.3.3 Transport properties

The transport properties of the outer wall are influenced by the porosity of the S*ilo concrete* as well as by the existence of penetrating cracks or other permeable zones. Of these, the influence of porosity is much smaller than that of penetrating cracks or permeable zones as discussed in Section 5.1.3.

According to Section 7.3.2, the probability for the formation of penetrating cracks is low during the first 20 000 years post-closure, but this risk is low also during later periods. Further, also the risk for formation of penetrating permeable zones is low because tie rods were not used in the formwork when casting the silo but also because casting joints are absent. Finally, formation of penetrating cracks due to rebar corrosion is unlikely. This is because the reinforcement bars are placed parallel to the surface of the concrete structure and not perpendicular. The consequence of this is that surface cracks will form as a result of rebar corrosion as observed in 1BMA but that penetrating cracks are less probable.

From this discussion follows that the evolution of the transport properties of the outer wall of the concrete silo will mainly be affected by porosity changes associated with the alterations of the mineral composition of the *Silo concrete* discussed in Section 7.3.1 during at least the initial 20 000 years post-closure.

According to Cronstrand (2007), the alterations of the mineral composition in the outer wall (Section 7.3.1) lead to a decreased but varying porosity regardless of calculation model used as shown in Figure 7-7 for the time 100 000 years post-closure. Porosity clogging close to the concrete/ bentonite interface was also observed by Idiart et al. (2020) who showed that clogging of the pores in about one third of the wall occurred already at between 300 and 2 000 years post-closure depending on calculation model used.

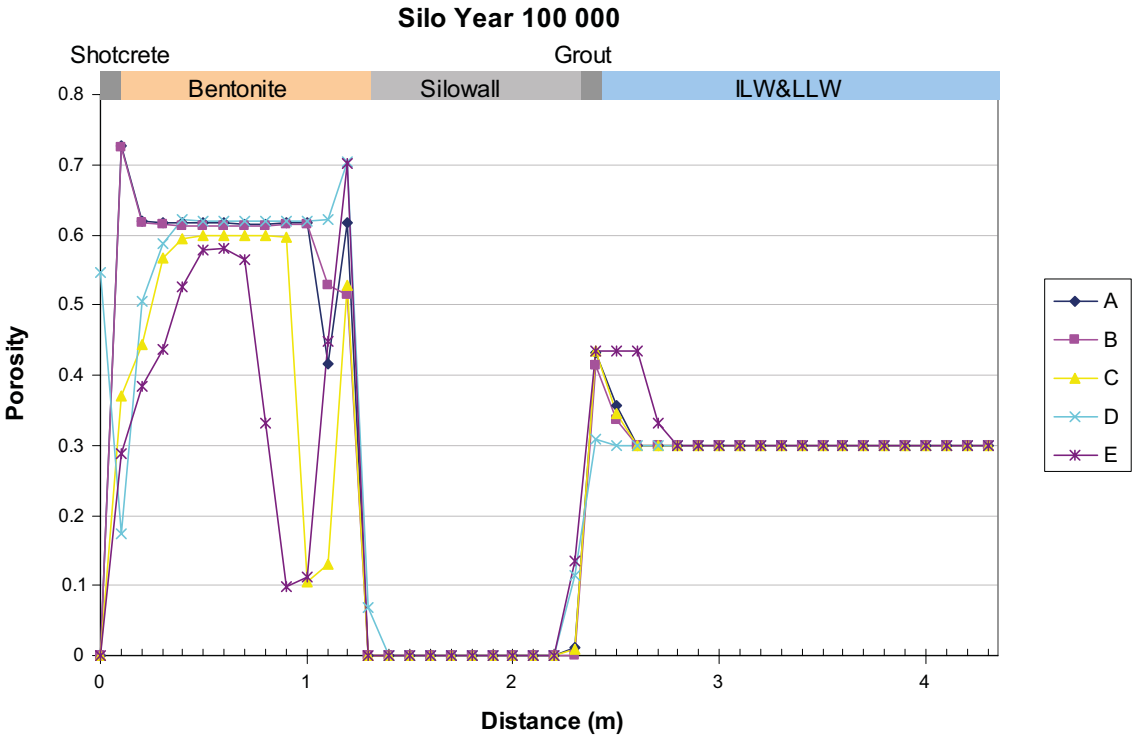


***Figure 7-7.*** *Porosity distribution in the silo at 100 000 years post-closure (Cronstrand 2007). The letters A – E represents different calculation models according to the following; A: Base case scenario, B: Varying temperature, C: Varying salinity, D: Dynamic diffusivity, E: Dynamic model. Zero porosity in the silo wall relates to the formation of ettringite as shown in Figures 7-1 to 7-5.*

However, as shown in Figures 7-1 to 7-5, clogging of the concrete pore system is associated with the formation of significant amounts of ettringite, a mineral known to be able to cause the formation of cracks in concrete. This means that even though the original concrete pore system may be infilled with secondary minerals, additional porosity may form in the shape of micro cracks caused by expansive ettringite. Due to these uncertainties, porosity and transport properties suggested for the outer wall of the concrete silo presented in Table 7-2 therefore assume a similar evolutionary trend as for e.g. 2BMA where porosity clogging is not predicted. See also Section 7.3.5.

This conclusion is in reasonable agreement with the post-closure evolution of material properties for the outer wall suggested by Höglund (2014, Appendix B) and presented in Figures 7-8 and 7-9. In these figures, both the hydraulic conductivity and the effective diffusivity indicated by the coloured lines are rather constant during the first 20 000 years post-closure even though the expected hydraulic conductivity is considerably higher than that expected for concrete without cracks suggested in this work. However, the slow evolution of the mineral composition of the outer wall of the silo presented in Section 7.3.1 and the clogging of the pore system of the outer silo wall shown in Figure 7-7, indicate that the time before significant alterations of the material properties in the outer silo wall occur is probably longer than that indicated in Figures 7-8 and 7-9.

In conclusion, the findings presented above indicate that only small alterations of the average transport properties of the outer wall are expected post-closure and that the transport properties during an extended period of time will not deviate dramatically from those at closure.

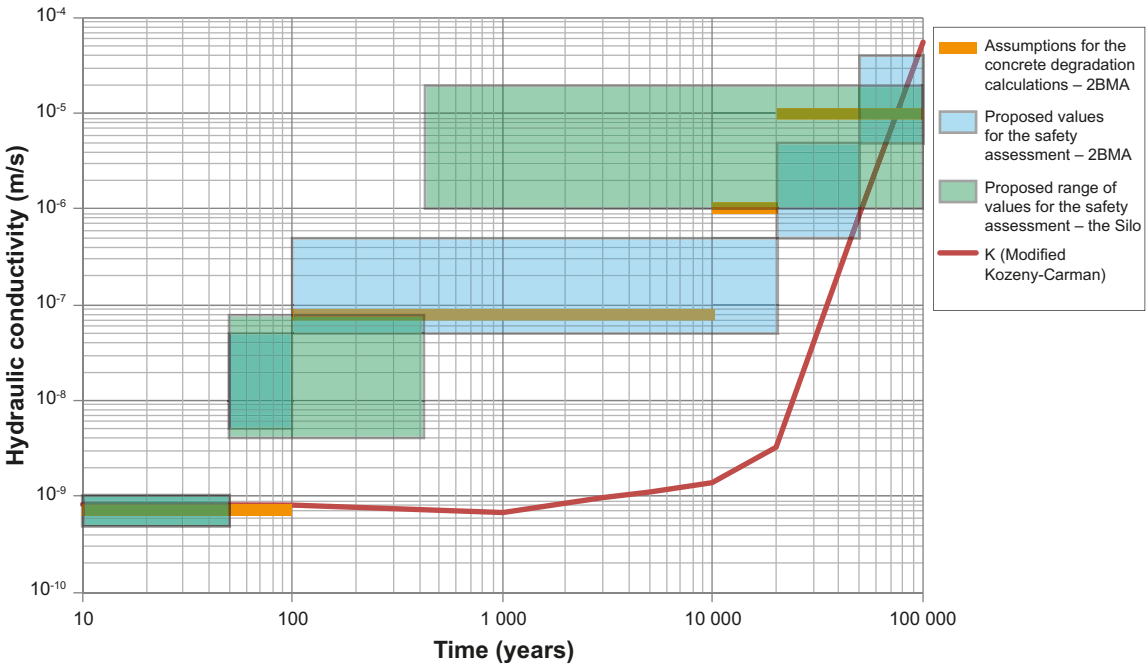


***Figure 7-8.*** *Proposed range of values for the hydraulic conductivity in structural concrete in the silo (green areas). The hydraulic conductivities calculated for 2BMA (red line) as well as the initial estimates of the gradual change of the hydraulic conductivity assumed in the PHAST modelling for 2BMA are shown as comparison. (Höglund 2014, Appendix B)*

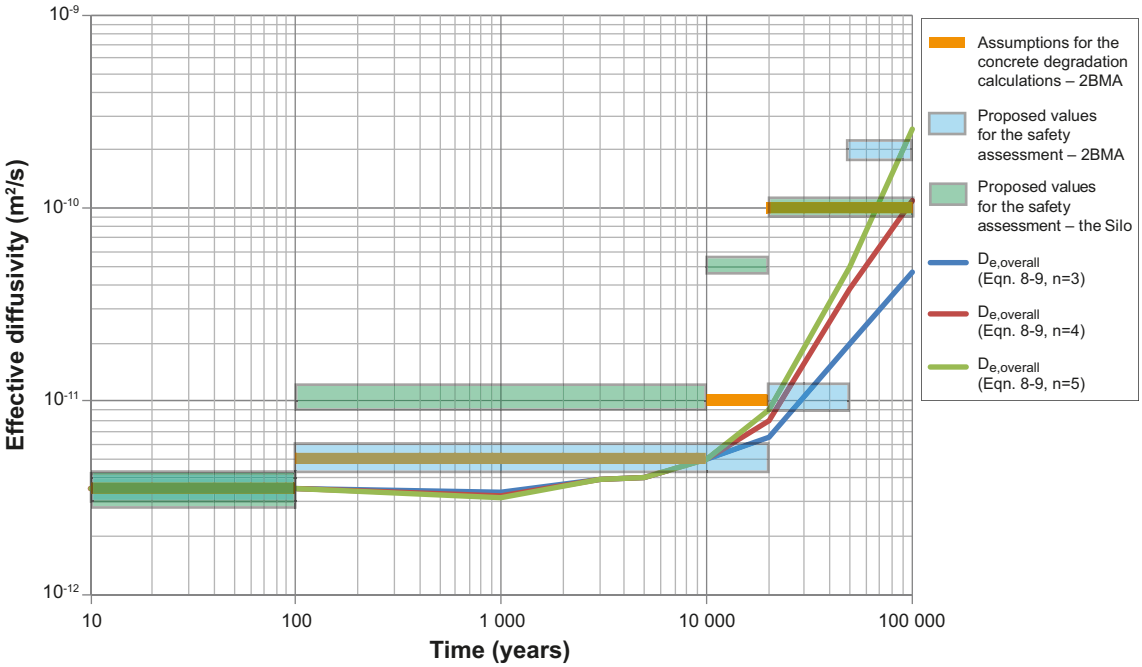


***Figure 7-9.*** *Proposed values for the effective diffusivity in structural concrete in the silo (green areas). The effective diffusivities calculated for 2BMA (blue, red and green lines) as well as the initial estimates of the gradual change of the effective diffusivity assumed in the PHAST modelling for 2BMA (orange lines) are shown as comparison (Höglund 2014 Appendix B).*

### 7.3.4 Recommended material property data

Table 7-2 presents recommended material property data for the outer wall of the silo for selected time periods up to 100 000 years post-closure. The recommendations are based on information regarding the status of the outer wall at closure presented in Section 6.1, the expected evolution of the properties of the outer wall described in the previous sections and the properties for degraded concrete given in Section 5.1.

**Table 7-2. Recommended material property data for the outer wall of silo for selected time periods up to 100 000 years post-closure.**

| | | Time period (Years post-closure) | | | | |
|---|---|---|---|---|---|---|
| **Property** | **Unit** | **At closure** | **0–1 000** | **1 000–20 000** | **20 000–50 000** | **50 000–100 000** |
| **pH** | - | ≥ 13 | ≥ 13 | 12.5–13 | 12–12.5 | 11–12 |
| **Porosity** | % | 11–13 | 11–13 | 11–14 | 12–15 | 13–16 |
| **Load-bearing capacity** | Rating (5–1) | 5 | 5 | 4–5 | 4 | 3–4 |
| **Hydraulic conductivity** | m/s | $(1–5)\times10^{-12}$ | $(1–5)\times10^{-12}$ | $(5–9)\times10^{-12}$ | $(5–9)\times10^{-12}$ | $10^{-12}–10^{-9}$ |
| **Diffusivity** | $m^2/s$ | $(2–5)\times10^{-12}$ | $(2–5)\times10^{-12}$ | $(2–5)\times10^{-12}$ | $(2–5)\times10^{-12}$ | $(5–9)\times10^{-12}$ |

### 7.3.5 Specific uncertainties

The following specific uncertainties in the description of the evolution of the properties of the outer wall of the concrete silo during the first 100 000 years post-closure have been identified:

- Despite the fact that the referred-to studies are reasonably unanimous with respect to the predicted evolution of the chemical properties of the outer wall of the concrete silo, there do remain some uncertainties concerning the evolution of – in particular – the transport properties of the outer wall. Cronstrand (2007) predicts a complete clogging of the porosity of the concrete with a reduced rate of degradation of the interior parts of the silo as a predicted consequence. However, this is in contradiction to the general trend for concrete degradation which predicts a porosity increase over time. The differences can only be explained by the concrete/ bentonite interactions. The uncertainties associated with the transport properties are also discussed by Höglund (2014, Appendix B)
- As a consequence of the uncertain evolution of the mineral composition, also the evolution of concrete porosity and transport properties are uncertain. Modelling studies indicate that the concrete pore system is infilled through the formation of secondary minerals such as ettringite but do not consider the potential for the formation of microcracks caused by ettringite formation.

See also the discussion concerning the general uncertainties in Chapter 5.

## 7.4 Lid

### 7.4.1 Chemical properties

The evolution of the mineral composition of the lid of the concrete silo and consequently also the evolution of the chemical properties are expected to roughly follow that of the outer wall presented in Section 7.3.1. However, the detailed mineral composition will be somewhat different in the lid as indicated by the study by Idiart et al. (2019a). This is because the production of *Anläggningscement Degerhamn,* which was used in the outer wall, has been terminated and another cement type must be used for construction of the lid. Additionally, the mixing proportions of the *Silo concrete* and the concrete in the lid – presumably the *2BMA concrete* – will differ further through the use of additional filler materials.

Also, concrete degradation may proceed at a slightly higher rate in the lid than in the outer walls. This is because the lid is founded on a layer of sand and covered by a mixture of different materials with expected different hydraulic and chemical properties than those of the bentonite surrounding the outer wall (Abarca et al. 2020, Appendix A). However, the differences are probably small in relation to all other uncertainties associated with predictions of the properties of the lid for a period of up to 100 000 years.

In spite of these uncertainties, the evolution of the chemical properties of the lid of the concrete silo is expected to follow that of the outer wall outlined in Section 7.3.1.

### 7.4.2 Load-bearing capacity

The load-bearing capacity of the lid is dependent on the mineral composition of the concrete as well as the status of the reinforcement bars and support from the inner walls and grouted waste packages. Of these, the status of the reinforcement bars is of lesser importance post-closure because the lid experiences only external compressive loads from the backfill materials. Instead, the load-bearing capacity (and risk for cracking) will mainly be dependent on the status of the materials in the interior of the concrete silo, i.e. the inner walls and the grouted waste packages which provide mechanical support to the lid.

As shown in Figures 7-1 to 7-5, almost no alterations of the mineral composition in the interior of the silo occur during the first 100 000 years post-closure and the materials therein will therefore be able to provide mechanical support for the lid during a very long period of time. The lid is therefore predicted to remain structurally intact during up to at least 50 000 years post-closure and formation of penetrating cracks is not expected during this period.

Further, the impact of rock fall-out or high internal pressures has to be evaluated. Here, the study for 2BMA which has a similar geometry as the silo carried out by Könönen and Olsson (2018) can serve as a representative example in lack of dedicated studies for the silo. The study concluded that the risk for formation of penetrating cracks in the lid of a concrete caisson in 2BMA is low even when considering the impact force caused by a rock piece with the dimensions 2 m × 2 m × 3 m. For the silo, the lid is also supported by the grouted waste packages and the risk for cracking therefore even lower than for 2BMA.

The impact of swelling of bituminised ion-exchange resins which was investigated by von Schenk and Bultmark (2014) and discussed in Section 7.3.2 did not include the lid.

Finally, it should be recognised that gas formation might pose a problem in the unlikely event that the gas evacuation channels in the lid are blocked through mineral precipitations. However, as concluded by Höglund and Bengtsson (1991) the probability for this to occur is low and this process therefore neglected.

In conclusion, the load-bearing capacity of the lid is expected to be sufficient to prevent cracking due to both internal and external loads up to at least 50 000 years post-closure but probably also beyond this point in time.

### 7.4.3 Transport properties

From Section 6.1.1, the transport properties of the concrete lid (not including the sand-filled channels constituting the gas evacuation system) at the time of closure will be the same as those of undegraded *Silo concrete*.

In addition, Section 7.4.2 concludes that the risk for the formation of penetrating cracks is low during the first 50 000 years post-closure and during this period the transport properties of the lid – not including the gas evacuation channels – will be controlled by the evolution of the porosity of the material.

Beyond 50 000 years post-closure, the hydraulic conductivity of the concrete increases due to some minor cracking and increased porosity caused by mineral alterations. However, as concluded in Section 7.4.2, extensive cracking of the lid is not expected.

### 7.4.4 Recommended material property data

Table 7-3 presents recommended material property data for the lid of the concrete silo for selected time periods up to 100 000 years post-closure. The recommendations are based on information regarding the status of the lid at closure presented in Section 6.1, the expected evolution of the properties of the lid described in the previous sections and the properties for degraded concrete given in Section 5.1.

**Table 7-3. Recommended material property data for the lid of the concrete silo for selected time periods up to 100 000 years post-closure.**

| | | Time period (Years post-closure) | | | | |
|---|---|---|---|---|---|---|
| **Property** | **Unit** | **At closure** | **0–1 000** | **1 000–20 000** | **20 000– 50 000** | **50 000–100 000** |
| **pH** | - | ≥ 13 | ≥ 13 | 12.5–13 | 12–12.5 | 11–12 |
| **Porosity** | % | 11–13 | 11–13 | 11–14 | 12–15 | 14–16 |
| **Load-bearing capacity** | Rating (5–1) | 5 | 5 | 4–5 | 4 | 3–4 |
| **Hydraulic* conductivity** | m/s | $(1–5) \times 10^{-12}$ | $(1–5) \times 10^{-12}$ | $(5–9) \times 10^{-12}$ | $(5–9) \times 10^{-12}$ | $10^{-12}–10^{-9}$ |
| **Diffusivity*** | $m^2/s$ | $(2–5) \times 10^{-12}$ | $(2–5) \times 10^{-12}$ | $(2–5) \times 10^{-12}$ | $(5–9) \times 10^{-12}$ | $(5–9) \times 10^{-12}$ |

* Not including the sand-filled channels.

### 7.4.5 Specific uncertainties

The following specific uncertainty in the description of the evolution of the properties of the lid of the concrete silo during the first 100 000 years post-closure has been identified:

- The main uncertainty relates to the transport properties of the lid and the influence of the gas evacuation channels. In this section, the influence of these channels was not considered, because the channels will be filled with a non-cementitious material, i.e. sand. In reality, the transport properties of the gas evacuation system will increase the average hydraulic conductivity and effective diffusivity of the lid as indicated by the findings for 2BMA by Elfwing et al. (2017).

See also the discussion concerning the general uncertainties in Chapter 5.

## 7.5 Inner walls

### 7.5.1 Chemical properties

According to the information presented in Section 7.3.1 and Figures 7-1 to 7-5, alterations of the mineral composition in the interior of the silo are considerably slower than in the outer wall. This is because the inner walls are protected by the outer concrete structure and bentonite which restrict the amount of groundwater that may come in contact with the inner walls. In addition, any water that enters the interior of the silo will be saturated with respect to cementitious degradation products.

As shown in SKB (R-18-07, Table 4-2) the waste in the silo mainly comprises ion exchange resins and filter aids which together makes up about 85 % of the total weight of the waste in the silo. The remaining part of the waste comprises iron and steel but also miscellaneous inorganic and organic material. However, no evaporator concentrates are disposed in the silo which means that the impact of high concentrations of salt can be disregarded. With a majority of the waste being conditioned in cement or concrete, a significant portion of the waste form degradation products will react with the conditioning material inside the waste packaging and not affect the properties of the inner walls.

From this follows that the main chemical degradation mechanism for the inner walls will be leaching and mineral alterations caused by the intruding groundwater. As mentioned in the first paragraph in this section, the expected amount of groundwater in contact with the inner walls will be low and therefore chemical degradation slow. As an indication, Figure 8-6 shows that the long-term portlandite leaching rate is only about 10 mm/1 000 years. This means that only a very small portion of the inner walls will be affected by chemical alterations during the first 100 000 years post-closure.

This simple model agrees with the findings by Cronstrand (2007) shown in Figures 7-1 to 7-5 which indicate that only a small part of the inner walls is chemically degraded during the first 100 000 years post-closure.

Based on these findings, the bulk chemical properties of the inner walls of the concrete silo at 100 000 years post-closure will only marginally differ from those at closure.

### 7.5.2 Load-bearing capacity

As discussed in the previous section, alterations of the mineral composition of the concrete in the inner walls are slow and will therefore have only a minor impact on the evolution of the load-bearing capacity of the inner walls post-closure. Instead, the main mechanism for loss of load-bearing capacity will be rebar corrosion and spalling of the covering layer of the inner walls which will reduce the thickness of these walls.

According to Höglund (2014, Appendix B), the time until the function of the reinforcement bars is lost is short in comparison with the 100 000-year time perspective. See also Section 7.3.2. Through rebar corrosion and spalling of the covering layer (estimated to an average of 30 mm), the thickness of the inner walls will be reduced from 200 mm (Section 2.5.2) to about 140 mm. From this follows that the load-bearing capacity of the inner walls will be similar to that of a 140 mm thick unreinforced concrete wall within 1 000 years post-closure. This, however, requires that sufficient amounts of water are available in these parts of the silo and this is somewhat uncertain during this period.

From the findings by von Schenk and Bultmark (2014), swelling of bituminised ion-exchange resins may cause cracking of the inner walls in the vicinity of bituminised waste whereas no or only minor long-range effects were found. However, even though such cracks will affect the properties of the inner walls in the direct vicinity of the waste packages in question, the load-bearing capacity of the inner walls is not expected to be affected thanks to the mechanical support provided by the grouted waste packages on both sides of the inner walls. The formation of cracks in the inner walls of some shafts in the interior of the concrete silo is therefore not expected to influence the over-all load-bearing capacity of the inner walls.

The conclusion is therefore that the load-bearing capacity of the inner walls will be sufficient to provide mechanical support to the external concrete structure during the first 100 000 years post-closure even though some cracks may form.

### 7.5.3 Transport properties

According to Sections 7.5.1 and 7.5.2, rebar corrosion may cause the formation of surface cracks in the inner walls of the silo. Such cracks will affect the transport properties in the plane of the inner walls – both vertically and horizontally – but rebar corrosion is not expected to cause the formation of penetrating cracks between adjacent shafts and thus not affect the transport properties in that direction.

However, penetrating cracks can form in the inner walls of shafts that contain bituminised ion-exchange resins, i.e. the nine central shafts. According to von Schenk and Bultmark (2014) this can occur already during the saturation period due to swelling of the ion-exchange resins upon water uptake. (For a discussion concerning the time to fully saturate the silo, please refer to Section 7.5.5.) von Schenk and Bultmark (2014) conclude that this can lead to a more heterogeneous hydraulic conductivity in the affected shafts due to the formation of channels in the axial direction of the silo.

Once the bituminised ion-exchange resins are fully saturated, additional swelling will not occur. From this point in time, further cracking is not expected. This is because of the slow rate of concrete degradation in the interior of the silo (Section 7.5.1) but also because the gas evacuation system prevents a build-up of a high gas pressure. Significant cracking in shafts that do not contain bituminised waste is therefore not expected.

### 7.5.4 Recommended material property data

Table 7-4 presents recommended material property data for the inner walls of the silo for selected time periods up to 100 000 years post-closure. The recommendations are based on information regarding the status of the inner walls at closure presented in Section 6.1, the expected evolution of the properties of the inner walls described in the previous sections and the properties for degraded concrete given in Section 5.1.

**Table 7-4. Recommended material property data for the inner walls of the silo for selected time periods up to 100 000 years post-closure.**

| | | Time period (Years post-closure) | | | | |
|---|---|---|---|---|---|---|
| **Property** | **Unit** | **At closure** | **0–1 000** | **1 000–20 000** | **20 000–50 000** | **50 000–100 000** |
| **pH** | - | ≥ 13 | ≥ 13 | 12.5–13 | 12.5 | 12.5 |
| **Porosity** | % | 11–13 | 11–13 | 11–13 | 11–13 | 11–13 |
| **Load-bearing capacity** | Rating (5–1) | 5 | 5 | 4–5 | 4 | 3–4 |
| **Hydraulic conductivity*** | m/s | $(1–5) \times 10^{-12}$ | $10^{-12}–10^{-8}$ | $10^{-8}–10^{-6}$ | $10^{-6}–10^{-5}$ | $10^{-5}–10^{-3}$ |
| **Diffusivity** | $m^2/s$ | $(2–5) \times 10^{-12}$ | $(2–5) \times 10^{-12}$ | $(2–5) \times 10^{-12}$ | $(5–9) \times 10^{-12}$ | $(5–9) \times 10^{-12}$ |

* The values presented here concerns the hydraulic conductivity in the plane of the inner walls. The hydraulic conductivity of the inner walls in the direction between adjacent shafts is considerably lower as significant formation of penetrating cracks is not expected.

### 7.5.5 Specific uncertainties

The following specific uncertainties in the description of the evolution of the properties of the inner walls of the concrete silo during the first 100 000 years post-closure have been identified:

- There remain some uncertainties concerning the time to fully saturate the silo. According to Holmén and Stigsson (2001) the time for full saturation of the silo is only 21 years. This is in reasonable accordance with the findings by Börgesson et al. (2015) who estimated the time to full saturation of the silo vault to between 13 and 53 years. However, both these studies differ considerably from the findings by Emborg et al. (2007) who conclude that the time to full saturation of the outer wall is about 2 000 years. The time to full saturation of the interior of the silo would as a consequence of this be considerably longer and possibly full saturation of the interior would not be achieved until 10 000 years post-closure.
- The uncertainties concerning the time to saturate the silo also affects the evolution of the transport properties of the silo. This is because the processes that can cause cracking of the inner walls such as metal corrosion and swelling of ion exchange resins due to water uptake require access to water. For the very slow saturation suggested by Emborg et al. (2007) the transport properties of the inner walls will be similar to those at closure for a significantly longer period of time than what is recommended in Table 7-4.
- The heterogeneous character of the transport properties of the inner walls must also be mentioned. In order to overcome the difficulties in the description of the transport properties of the inner walls, Table 7-4 only presents data for transport properties in the plane of the inner walls. The motivation for this is that the main transport path for both gases and water is expected to be in the vertical direction towards the lid of the concrete silo and not in the horizontal direction towards the outer walls or adjacent shafts.

See also the discussion concerning the general uncertainties in Chapter 5.

## 7.6 Permeable grout between waste packages

### 7.6.1 Chemical properties

The evolution of the chemical properties of the permeable grout is expected to follow that outlined for the inner walls in Section 7.5. This is because any water that enters the interior of the silo will be saturated with respect to cementitious degradation products and not able to cause any further degradation.

It is therefore judged that the average chemical properties of the permeable grout at 100 000 years post-closure will only marginally deviate from those of the grout at closure.

### 7.6.2 Load-bearing capacity

The load-bearing capacity of the permeable grout between the waste packages is poor already at closure. With a very low 28-days compressive strength, a high porosity and lack of reinforcement, the grout will be very sensitive to tensile forces whereas the resistance to purely compressive loads will be somewhat better.

von Schenk and Bultmark (2014) showed that swelling of bituminised ion-exchange resins will cause cracking of the permeable grout in the nine central shafts already during the saturation period but not in shafts where no such waste has been disposed.

However, the increased porosity observed by Cronstrand (2007) in the grout adjacent to the outer walls at 100 000 years post-closure (Figure 7-7) indicates a reduced load-bearing capacity of the grout in these sections. For the grouted waste in the interior parts, porosity increase is not observed as also shown in Figure 7-7.

The conclusion is therefore that the load-bearing capacity of the permeable grout will be poor in the entire silo already at closure but also that further reduction of the load-bearing capacity will be limited. However, in spite of this, the permeable grout will be able to provide some support to the stack of waste packages and the inner walls during a very long period post-closure.

### 7.6.3 Transport properties

With reference to the discussion in the previous sections, it is expected that the transport properties of the permeable grout between the waste packages will be affected by a significant number of cracks from the time of saturation of the interior of the silo in shafts that contains potentially swelling waste and in shafts adjacent to those.

In shafts not affected by the swelling waste, the transport properties of the grout will be basically the same as those of the *Original Silo grout* or *New silo grout* during up to 100 000 years post-closure.

### 7.6.4 Recommended material property data

Table 7-5 presents recommended material property data for the permeable grout between the waste packages for selected time periods up to 100 000 years post-closure. The recommendations are based on information regarding the status of the permeable grout between the waste packages at closure presented in Section 6.1, the expected evolution of the properties of the permeable grout between the waste packages described in the previous sections and the properties for degraded concrete given in Section 5.1.

**Table 7-5. Recommended material property data for the permeable grout between the waste packages in the silo for selected time periods up to 100 000 years post-closure.**

| | | Time period (Years post-closure) | | | | |
|---|---|---|---|---|---|---|
| **Property** | **Unit** | **At closure** | **0–1 000** | **1 000–20 000** | **20 000–50 000** | **50 000–100 000** |
| **pH** | - | ≥ 13 | ≥ 13 | 12.5–13 | 12.5 | 12.5 |
| **Porosity** | % | 30 | 30 | 30 | 30 | 30 |
| **Load-bearing capacity** | Rating (5–1) | 5 | 5 | 4–5 | 3–4 | 2–3 |
| **Hydraulic conductivity** | m/s | $(5–20)\times10^{-9}$ | $(5–20)\times10^{-9}$ | $10^{-8}$–$10^{-6}$ | $10^{-8}$–$10^{-4}$ | $10^{-8}$–$10^{-3}$ |
| **Diffusivity** | $m^2/s$ | $(1–5)\times10^{-11}$ | $(1–5)\times10^{-11}$ | $(1–5)\times10^{-11}$ | $10^{-11}$–$10^{-10}$ | $10^{-11}$–$10^{-10}$ |

### 7.6.5 Specific uncertainties

The following specific uncertainty in the description of the evolution of the properties of the permeable grout between the waste packages during the first 100 000 years post-closure has been identified:

- There remain some uncertainties concerning the influence of cracks on the transport properties of the permeable grout. However, the inherently high hydraulic conductivity of the grout itself makes the influence of additional cracks less pronounced than for less permeable construction parts.

See also the discussion concerning the general uncertainties in Chapter 5.

## 7.7 Concrete moulds

### 7.7.1 Chemical properties

Alterations of the mineral composition of the concrete moulds are expected to be very slow and in principle correspond to that outlined for the inner walls in Section 7.5.1. From Section 7.5.1 also follows that external leaching of the concrete moulds will be slow which means that degradation will mainly occur from the inside of the concrete moulds through interaction between the concrete and the waste form degradation products. However, the silo does not contain any evaporator concentrates or other easily soluble materials (SKB R-18-07) and the chemical impact of the waste is therefore expected to be limited. Interactions between the inside of the concrete moulds and the waste form degradation products is further limited by the low amount of available water inside the waste domain.

With this background, it is suggested that the evolution of the average bulk chemical properties of the concrete moulds will follow that of the inner walls of the concrete silo during up to 100 000 years post-closure. This means that leaching and mineral alterations on the outside of the concrete moulds

will be limited to the moulds closest to the outer construction parts of the silo whereas chemical interaction between the waste and the inner part of the concrete moulds will be somewhat more randomly distributed and depending of type of waste and waste matrix.

### 7.7.2 Load-bearing capacity

The dimensioning load for the concrete moulds is the total weight of the stack of waste packages experienced by the lowest mould at the time of closure. According to SKB (R-18-07) bituminised ion-exchange resins are not disposed in concrete moulds. The risk for cracking due to a high internal pressure inside the concrete moulds is therefore low.

According to Section 6.1.1, the load-bearing capacity of the concrete moulds is sufficient to ensure that even the concrete mould furthest down in the stack of moulds can carry the weight of the entire stack of concrete moulds during the initial period post-closure. In addition, following the method used by Bultmark (2017a), the concrete mould furthest down in the stack will be able to carry the weight of a stack of concrete moulds with a height of 80 meters even after spalling of the covering layer and without taking the support from the surrounding grout into account.

The same method shows that the load-bearing capacity of the lowest concrete moulds will be insufficient for a stack of waste packages when the thickness of the undegraded concrete (portlandite still present) is about 52 mm for a stack of waste packages with a height of 52 meters and disregarding any support from the surrounding grout.

However, Figures 7-1 to 7-5 show that alterations of the mineral composition in the interior of the silo are very slow and portlandite will be present in the major part during up to 100 000 years post-closure.

In all, the load-bearing capacity of the concrete moulds is expected to be sufficient to carry the load of the stack of waste packages during up to 100 000 years post-closure and external or internal loads are therefore not expected to cause cracking of the concrete moulds.

### 7.7.3 Transport properties

Section 6.1.1 states that the transport properties of the concrete moulds at closure are expected to be similar to those of the undegraded *SFR mould concrete*, characterised by a low hydraulic conductivity and a low diffusivity. In addition, Section 7.7.2 concludes that risk for formation of penetrating cracks in the concrete moulds due to external and/or internal loads is low up to 100 000 years post-closure.

However, cracking can also be caused by corrosion of the steel reinforcement in the concrete moulds. Even though rebar corrosion mainly causes spalling of the covering layer and surface cracks, it cannot be ruled out that also penetrating cracks may form even though extensive cracking is prevented by the presence of the surrounding grout.

To summarise, it is expected that the transport properties of most of the concrete moulds will be similar to those of the concrete moulds at closure during up to 100 000 years post-closure. Formation of penetrating cracks in some of the concrete moulds must, however, be anticipated because of e.g. rebar corrosion whereas the structural integrity of the concrete moulds is expected to remain rather intact also at the end of this period. This is because the moulds are enclosed in the grout-filled shafts and significant material transport is therefore prevented.

### 7.7.4 Recommended material property data

Table 7-6 presents recommended material property data for the concrete moulds for selected time periods up to 100 000 years post-closure. The recommendations are based on information regarding the status of the concrete moulds at closure presented in Section 6.1, the expected evolution of the properties of the concrete mouldsdescribed in the previous sections and the properties for degraded concrete given in Section 5.1.

**Table 7-6. Recommended material property data for the concrete moulds in the silo for selected time periods up to 100 000 years post-closure.**

| | | Time period (Years post-closure) | | | | |
|---|---|---|---|---|---|---|
| **Property** | **Unit** | **At closure** | **0–1 000** | **1 000–20 000** | **20 000–50 000** | **50 000–100 000** |
| **pH** | - | ≥ 13 | ≥ 13 | 12.5–13 | 12.5 | 12.5 |
| **Porosity** | % | 10–12 | 10–12 | 10–12 | 10–12 | 10–12 |
| **Load-bearing capacity** | Rating (5–1) | 5 | 5 | 4–5 | 3–4 | 2–3 |
| **Hydraulic conductivity** | m/s | $(1–5)\times10^{-12}$ | $(1–5)\times10^{-12}$ | $(5–9)\times10^{-12}$ | $(5–9)\times10^{-12}$ | $(1–5)\times10^{-11}$ |
| **Diffusivity** | $m^2/s$ | $(2–5)\times10^{-12}$ | $(2–5)\times10^{-12}$ | $(2–5)\times10^{-12}$ | $(5–9)\times10^{-12}$ | $(5–9)\times10^{-12}$ |

### 7.7.5 Specific uncertainties

The following specific uncertainty in the description of the evolution of the properties of the concrete moulds during the first 100 000 years post-closure has been identified:

- There remain some uncertainties concerning the cement conditioning of ion-exchange resins. Recent information indicates that insufficient amounts of water have been used when mixing ion-exchange resins, water and cement powder disposed in concrete moulds. The potential effect of this is a larger swelling (or swelling pressure) than previously assumed. The consequences of this for the post-closure evolution of the properties of the concrete moulds remain to be resolved.

See also the discussion concerning the general uncertainties in Chapter 5.

# 8 1BMA: post-closure evolution

In this chapter, the expected evolution of the properties of the cementitious components in 1BMA during the first 100 000 years post-closure is described. The starting point for the descriptions is the expected status of the cementitious components in 1BMA at closure presented in Section 6.2. The evolution of the properties of the cementitious components in 1BMA is then influenced by the processes presented in Chapter 4.

Detailed descriptions of the cementitious components in 1BMA are given in Section 2.6. In addition, Chapter 3 presents detailed specifications and properties of the cementitious materials in the various components in 1BMA.

## 8.1 Literature

The following reports form the basis for the description of the post-closure evolution of the properties of the cementitious components in 1BMA presented in this chapter:

- **Cronstrand (2007)** modelled the evolution of the mineral composition of the original concrete structure in 1BMA.
- **Cronstrand (2010)** modelled the impact of high concentrations of salts on the evolution of the mineral composition in 1BMA.
- **Cronstrand (2014)** modelled the evolution of pH the waste vaults in SFR1.
- **Elfwing et al. (2015)** presents a detailed description of the current status of the concrete structure in 1BMA.
- **Eriksson (2021)** calculated the load-bearing capacity of the new and existing outer walls in 1BMA.
- **Höglund (2014)** modelled the evolution of the repaired concrete structure in 1BMA.
- **Höglund (2019)** modelled the pH evolution in 2BMA. This study is judged to be representative also for 1BMA as the *2BMA concrete* is planned for use also in the new outer walls in 1BMA even though groundwater flow and composition may differ between 1BMA and 2BMA.
- **Idiart et al. (2019a)** modelled the influence of concrete mixing proportions for different types of concrete used in SFR on the evolution of the properties of concrete in the rock vault for core components (BHK) in SFL.
- **Lagerblad et al. (2017)** and **Mårtensson and Vogt (2019, 2020)** investigated the properties of the *2BMA concrete* currently planned for use in the lid and new outer walls in 1BMA.
- **Laviña and Idiart (**SKBdoc 1967610 ver 1.0, internal document) modelled the influence of sulphates on the properties of the 1BMA concrete barriers.
- **Mårtensson (2017)** evaluated the impact of degradation processes of the load-bearing capacity of the repaired concrete structure in 1BMA and the concrete caissons in 2BMA.
- **Nytorp Jansson (2020a)** modelled the load-bearing capacity of the slab in 1BMA.
- **Villar et al. (2019)** performed an experimental investigation of the properties of new concrete specimens with similar mixing proportions as the *1BMA concrete*.
- **von Schenck and Bultmark (2014)** calculated the load-bearing capacity of the existing outer walls against the pressure from swelling waste.
- **Westerberg (2017)** calculated the load-bearing capacity of the various structural components of the concrete structure in 1BMA.
- **Wimelius (2021)** presents details on the method of construction of the new outer walls of 1BMA that are planned to be cast at closure.

## 8.2 Slab

### 8.2.1 Chemical properties

The evolution of the chemical properties of the concrete structure in 1BMA has been modelled by e.g. Cronstrand (2007) but using the mixing proportions of the *Silo concrete* rather than the *1BMA concrete*. However, since Idiart et al. (2019a) showed that the evolution of the *Silo concrete* and the *1BMA concrete* is reasonably similar, the impact of this is judged to be minor.

As a reference to the discussions following in this chapter, Figure 8-1 shows the mineral composition in 1BMA at closure with the inert aggregate material constituting most of the mineral volume in the concrete. It must be emphasised that Cronstrand (2007) used several different calculation models of which the following discussions emanate from results obtained by the so-called "Fracture model". This model included varying temperature and groundwater composition as well as dynamic diffusivity and fracture mechanics. For explanation, see Cronstrand (2007).

From Figure 8-2, the concrete will be depleted of portlandite to a depth of about 400 mm already at 10 000 years post-closure, i.e. already at this stage exceeding the total thickness of slab. This can be compared with the findings reported by von Schenck (2017), Figure 8-6, which show that portlandite depletion progresses with a rate of about 10 millimetres per 1 000 years. Also, the findings by Höglund (2019) indicate a slower progression of portlandite depletion than that shown in Figure 8-2.

However, because groundwater may also reach the interior of the waste compartment through the cracks in the slab, degradation may occur from both sides of the slab, even though probably considerably slower on the inside due to the very slow groundwater exchange in this part. With leaching occurring on both sides, the slab will probably be depleted from portlandite somewhere between 15 000 and 20 000 years post-closure as a reasonable average.

Once the concrete is depleted from portlandite, transformation of the CSH-gel will occur. This process is slower than portlandite leaching (compare Figure 4-5) and still at 100 000 years post-closure the chemical properties of the slab will be controlled by the presence of CSH_1.8 or CSH_1.1, Figure 8-4.

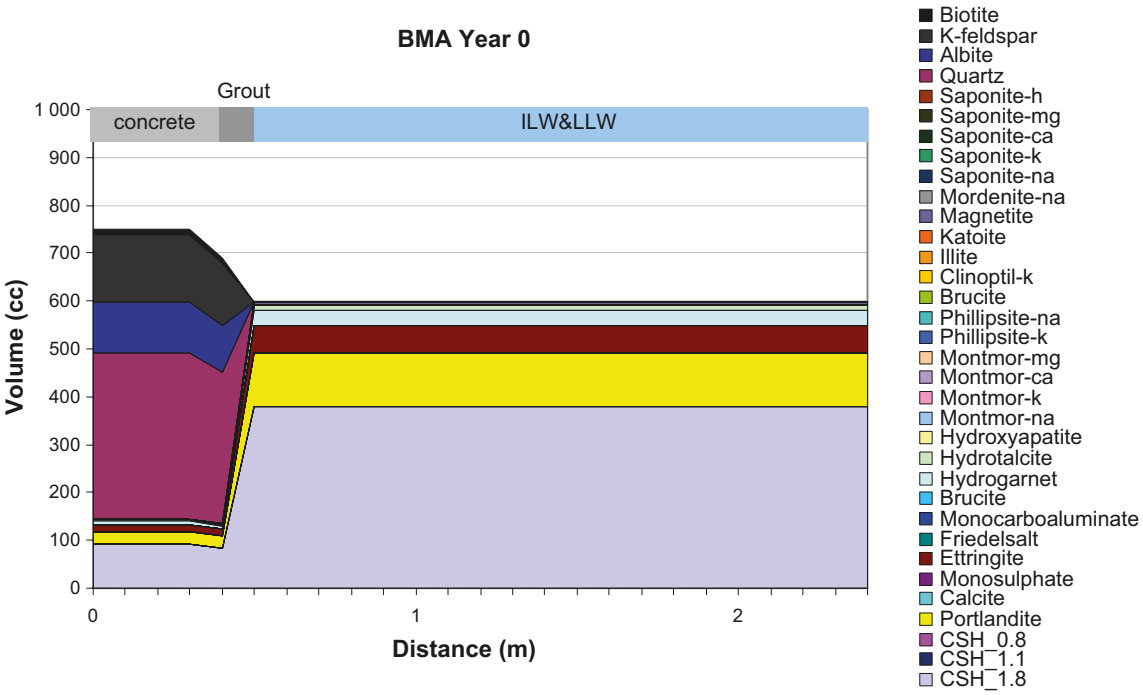


***Figure 8-1.*** *Initial mineral composition in 1BMA (Cronstrand 2007, Figure B-38). Note that the three dominant minerals in the concrete constitute the aggregate material (quartz, K-feldspar and albite) and that grouting of the waste packages in 1BMA is currently not planned. The material in the ILW & LLW domain does not contain aggregates.*

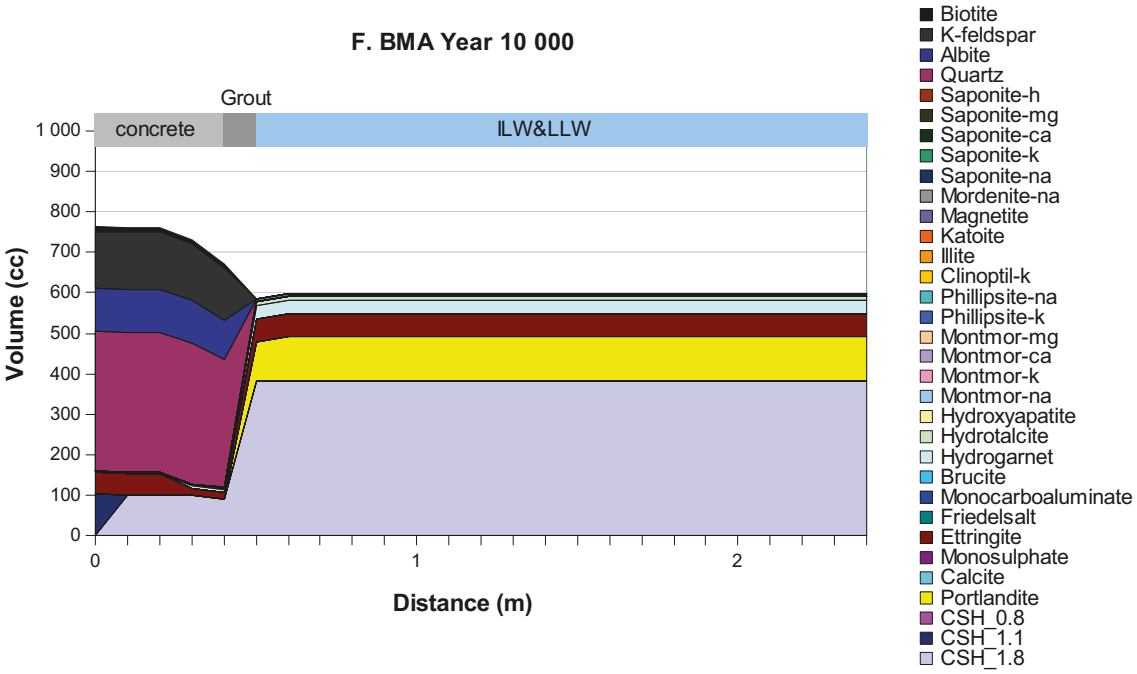


***Figure 8-2.*** *Mineral composition in 1BMA 10 000 years post-closure. (Cronstrand 2007, Figure B-60). Note that the three dominant minerals in the concrete constitute the aggregate material (quartz, K-feldspar and albite) and that grouting of the waste packages in 1BMA is currently not planned.*

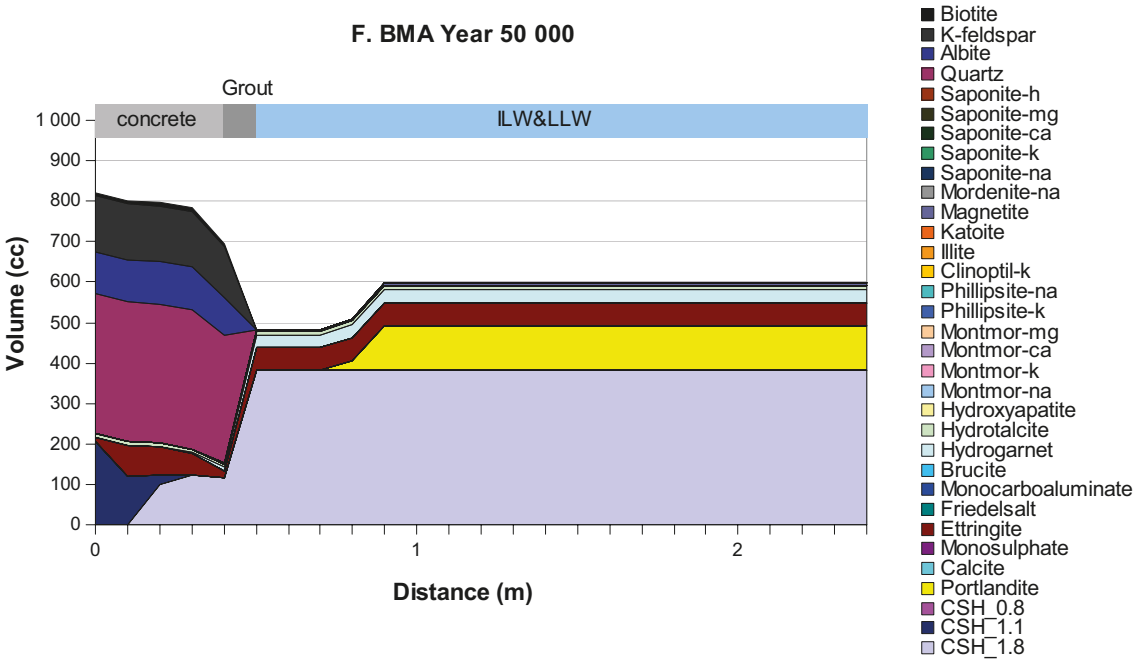


***Figure 8-3.*** *Mineral composition in 1BMA at 50 000 years post-closure (Cronstrand 2007, Figure B-61). Note that the three dominant minerals in the concrete constitute the aggregate material (quartz, K-feldspar and albite) and that grouting of the waste packages in 1BMA is currently not planned.*

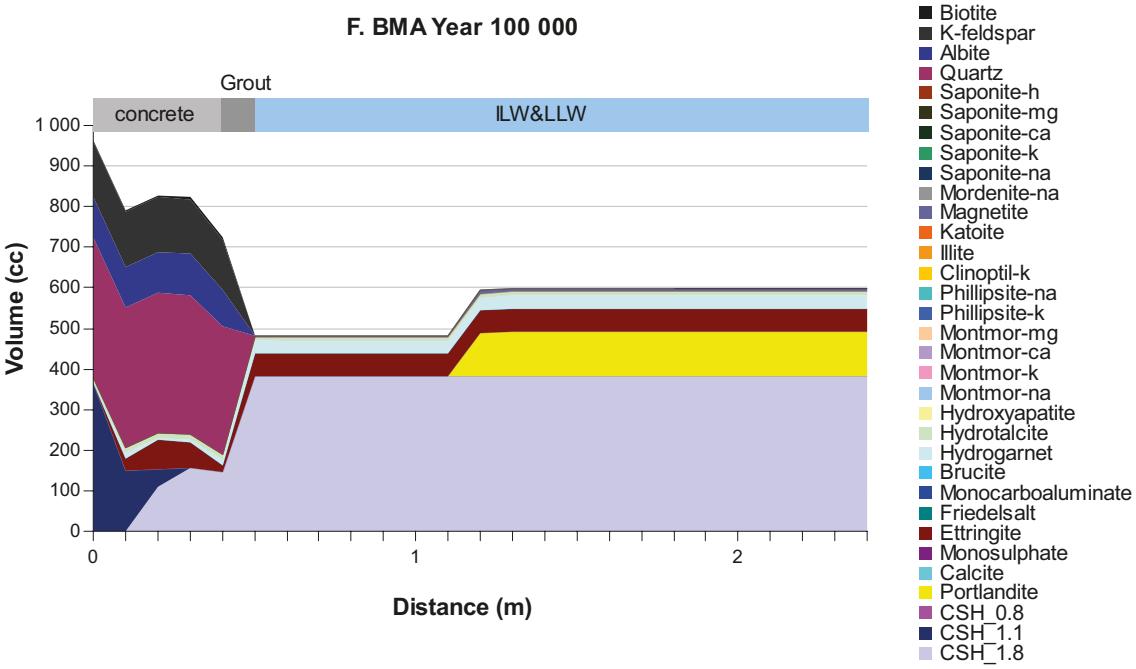


***Figure 8-4.*** *Mineral composition in 1BMA 100 000 years post-closure. (Cronstrand 2007, Figure B-62). Note that the three dominant minerals in the concrete constitute the aggregate material (quartz, K-feldspar and albite) and that grouting of the waste packages in 1BMA is currently not planned.*

Figure 4-5 shows that pH in the porewater at this stage would be 11–12 which agrees with Figure 8-5 which indicates a pH in the region of 12. This can, however, be questioned since complete degradation with pH below 10 must be expected in the surface regions at 100 000 years post-closure. Note that Figure 8-5 shows the results from five different models none of which included the impact of cracking on concrete degradation and which therefore are somewhat different from the model behind the results presented in Figures 8-1 to 8-4 which included the impact of cracking.

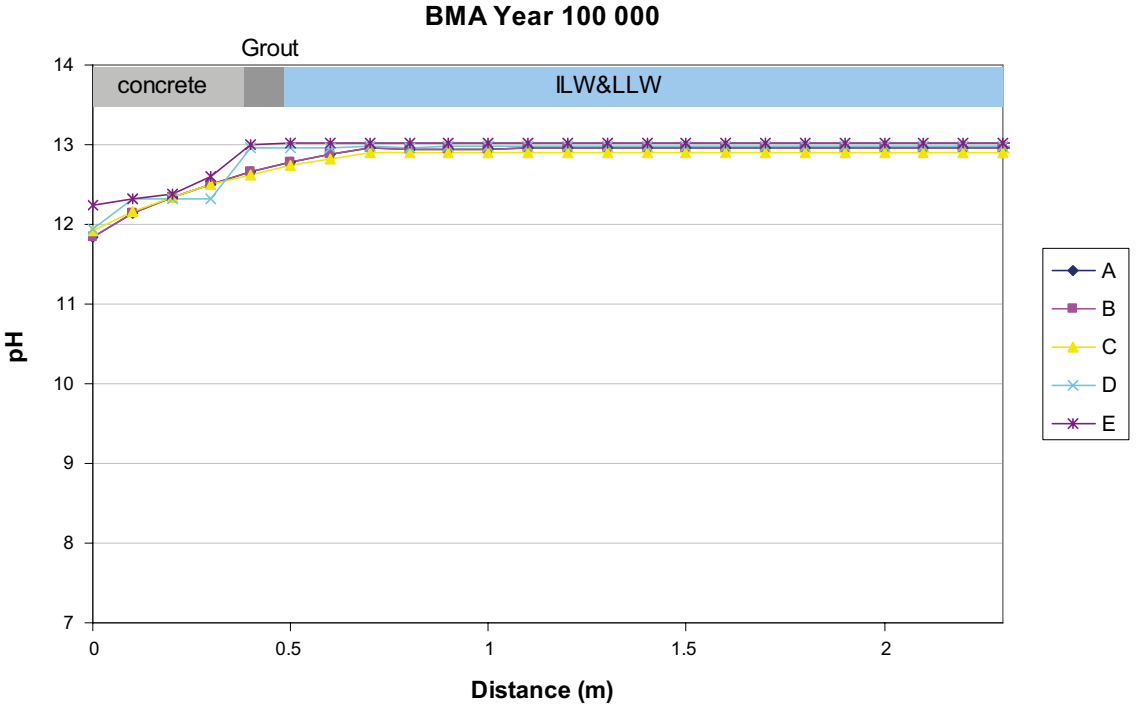


***Figure 8-5.*** *pH distribution in 1BMA at 100 000 years post-closure for five different models not including the impact of cracking on concrete degradation (Cronstrand 2007, Figure B-74).*

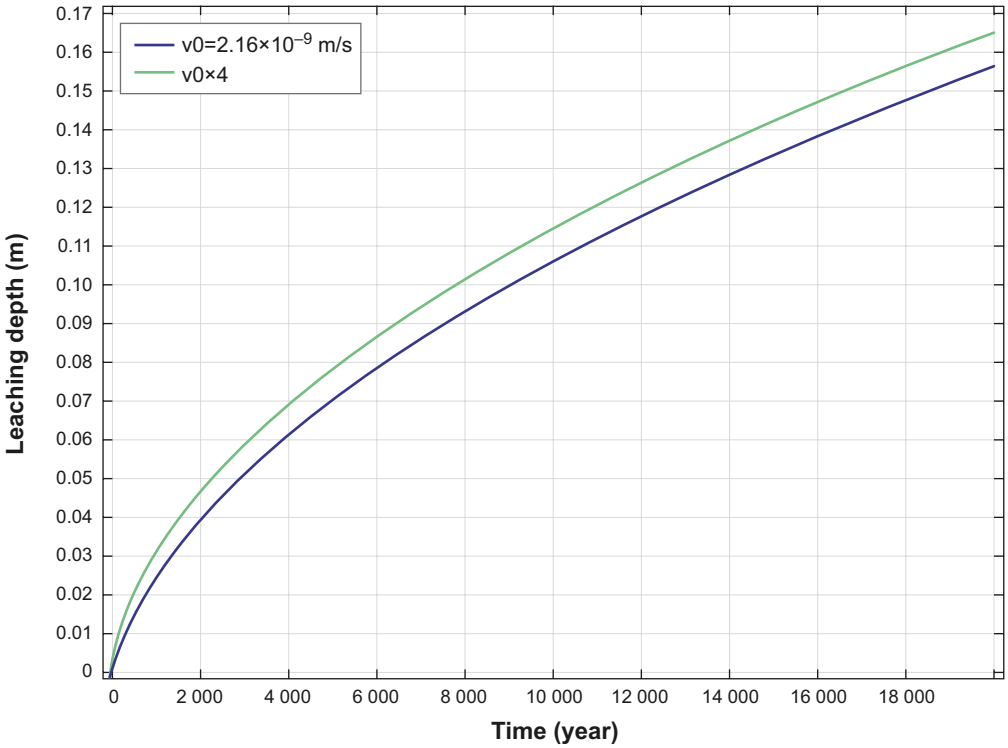


***Figure 8-6.*** *Leaching depth for portlandite as a function of time for the* ***Silo concrete*** *when studied for a case where it is used in 2BMA. Blue line represents a case with a groundwater flow as expected at 5 000 years (Abarca et al. 2013) and the green line represents a case with a four times larger groundwater flow (von Schenck 2017).*

### 8.2.2 Load-bearing capacity

With an original thickness of only 250–300 mm (Section 2.6.2), the load-bearing capacity of the slab in 1BMA is sensitive to loss of function of the reinforcement bars and the stiffness of the foundation layer.

According to Nytorp Jansson (2020a), the load-bearing capacity of already the undegraded slab is insufficient to prevent cracking if settlements in the foundation occur, and for a slab in which the function of the reinforcement has been lost, extensive cracking must be expected. The risk for extensive cracking due to settlements in the foundation layer is additionally higher since the slab is partly supported by concrete beams founded on the bedrock.

Westerberg calculated the load-bearing capacity of the slab during saturation of the repository and concluded that the slab can only resist an external pressure from the intruding groundwater of 148 kPa (14.8 meters of water) if also the counteracting weight of the waste packages but not that from the lid and backfill material was considered.[60] This means that significant cracking of the slab must be expected already during the resaturation period unless efficient groundwater transport through the concrete structure ensures a fast saturation of the waste compartments.

Through dissolution, the slab will slowly be depleted from portlandite with a subsequent reduction of the load-bearing capacity of the slab. Assuming a loss of load-bearing capacity of 15 mm/1 000 years (Mårtensson 2017) the load-bearing capacity of the slab will be more or less lost before 20 000 years post-closure.

However, from the findings by Babaahmadi (2015) also portlandite depleted concrete has some remaining cohesion and strength. A more plausible prediction is therefore that some cohesion will remain at least until 15 000 years post-closure, even though not sufficient to withstand any tensile stresses.

[60] SKBdoc 1583182 ver 1.0. (Internal document, in Swedish.)

In all, it is expected that the slab will be able to carry the load from the waste packages for an extensive period of time even though extensive cracking is expected from about 10 000 years post-closure. This is because the load is mainly compressive and material losses small.

### 8.2.3 Transport properties

With reference to Section 6.2.1 the transport properties of the slab in 1BMA will have the characteristics of *1BMA concrete* with penetrating cracks already at closure. See also Elfwing et al. (2015).

Through continued leaching and rebar corrosion, both the number and width of the cracks as well as the porosity of the slab will increase and beyond 20 000 years post-closure the transport properties of the slab in 1BMA will correspond to those of concrete with a significant number of cracks.

### 8.2.4 Recommended material property data

Table 8-1 presents recommended material property data for the slab in 1BMA for selected time periods up to 100 000 years post-closure. The recommendations are based on information regarding the status of the slab at closure presented in Section 6.2, the expected evolution of the properties of the slab described in the previous sections and the properties of degraded concrete given in Section 5.1.

**Table 8-1. Recommended material property data for the slab in 1BMA for selected time periods up to 100 000 years post-closure.**

| | | Time period (Years post-closure) | | | | |
|---|---|---|---|---|---|---|
| **Property** | **Unit** | **At closure** | **0–1 000** | **1 000–20 000** | **20 000–50 000** | **50 000–100 000** |
| **pH** | - | ≥ 13 | 12.5–13 | 12–12.5 | 11–12 | 10–11 |
| **Porosity** | % | 12–15 | 12–15 | 13–16 | 15–17 | 17–25 |
| **Load-bearing capacity** | Rating (5–1) | 5 | 5–2 | 2 | 2 | 2 |
| **Hydraulic conductivity** | m/s | $10^{-5}$–$10^{-4}$ | $10^{-4}$–$10^{-3}$ | $10^{-4}$–$10^{-3}$ | $10^{-3}$–$10^{-2}$ | $10^{-3}$–$10^{-2}$ |
| **Diffusivity** | $m^2/s$ | $(2–5)\times10^{-12}$ | $(1–5)\times10^{-11}$ | $(1–5)\times10^{-11}$ | $(5–9)\times10^{-11}$ | $(5–9)\times10^{-11}$ |

### 8.2.5 Specific uncertainties

The following specific uncertainties in the description of the evolution of the properties of the slab of the concrete structure in 1BMA during the first 100 000 years post-closure have been identified:

- There is a lack of information concerning the extent of cracking in the non-inspectable compartments. Available information originates from compartments in which no waste has been disposed and in which the slab has not been exposed to the load from the waste packages. In addition, the slab in the inspectable compartments has been exposed to dripping groundwater as manifested in the increased levels of chlorine in cores from these parts. Chlorine levels in the non-inspectable compartments are not known.
- There is also a lack of information concerning the status of the foundation layer beneath the concrete structure. This relates both to the thickness of the foundation layer and the amount of fine-grained materials that has been accumulated in this layer during the operational period.
- There is also a lack of information concerning the final design of the supporting beams beneath the slab and whether they are placed on bare rock or in “ditches” in the foundation layer itself. The design will have some impact on the consequences of settlements in the foundation layer.
- The impact of high concentrations of salt in the waste packages depends on the type of waste in each waste package as well as of the conditioning method used. The consequence of this is that the general description of the evolution of the chemical properties of the slab will be associated with some uncertainties as discussed further in Section 4.14.

See also the discussion concerning the general uncertainties in Chapter 5.

## 8.3 Existing outer walls

### 8.3.1 Chemical properties

The degradation of the chemical properties of the existing outer walls will be considerably slower than that outlined by Cronstrand (2007) and which was discussed in Section 8.2. This is because the existing outer walls will be sandwiched between the new outer walls and the waste domain and the rate of exchange of groundwater and leaching of the cement minerals therefore very slow.

Leaching and mineral alterations are therefore expected to be small during at least the first 20 000 years post-closure, i.e. the period when the lid and new outer walls are expected to be structurally intact. From this period and onwards, the rate of concrete degradation will increase somewhat but probably at a rate that will be below that indicated by Figures 8-2 to 8-4. This is because a complete loss of structural integrity of the lid and new outer walls is not expected and buffering capacity is therefore provided by these components.

### 8.3.2 Load-bearing capacity

The existing outer walls will experience only small external loads as long as the load-bearing capacity of the lid and the new outer walls is sufficient and additional cracking is therefore not expected during the first 20 000 years post-closure. However, from Sections 8.4.2 and 8.5.2, the load-bearing capacity of the lid and new outer walls will be reduced through concrete degradation and rebar corrosion and eventually insufficient to resist the weight of the backfill material. Because of material movements caused by loss of structural integrity of the lid and new outer walls, the magnitude and direction of the loads experienced by the existing outer walls will vary. The consequence of this is probably the formation of additional cracks but the timing of this is uncertain.

### 8.3.3 Transport properties

Höglund (2014, Section 6.15) estimated the hydraulic conductivity of the existing outer walls based on the description of the status of these walls presented in Elfwing et al. (2015) to about $1 \times 10^{-4}$ m/s and the effective diffusivity to just above $3 \times 10^{-12}$ m$^2$/s.

From Section 8.3.2, the load-bearing capacity of the existing outer walls is sufficient to prevent significant additional cracking during the first 20 000 years post-closure. However, from this point in time additional cracking must be expected with an increased hydraulic conductivity as a consequence.

Finally, cracking or formation of permeable zones may also be caused by corrosion of the tie rods in the existing outer walls. The magnitude of this process is somewhat uncertain but according to Höglund (2014) only limited corrosion is required for the first cracks to form around a penetrating tie rod.

### 8.3.4 Recommended material property data

Table 8-2 presents recommended material property data for the existing outer walls in 1BMA for selected time periods up to 100 000 years post-closure. The recommendations are based on information regarding the status of the existing outer walls at closure presented in Section 6.2, the expected evolution of the properties of the existing outer walls described in the previous sections and the properties for degraded concrete given in Section 5.1.

**Table 8-2. Recommended material property data for the existing outer walls in 1BMA for selected time periods up to 100 000 years post-closure.**

| | | Time period (Years post-closure) | | | | |
|---|---|---|---|---|---|---|
| **Property** | **Unit** | **At closure** | **0–1 000** | **1 000–20 000** | **20 000–50 000** | **50 000–100 000** |
| **pH** | - | ≥ 13 | 12.5–13 | 12.5 | 12–12.5 | 12–12.5 |
| **Porosity** | % | 12–15 | 12–15 | 12–15 | 12–15 | 13–16 |
| **Load-bearing capacity** | Rating (5–1) | 5 | 5 | 3–5 | 3–2 | 2–1 |
| **Hydraulic conductivity** | m/s | $10^{-5}$–$10^{-4}$ | $10^{-5}$–$10^{-4}$ | $10^{-4}$–$10^{-3}$ | $10^{-4}$–$10^{-3}$ | $10^{-4}$–$10^{-2}$ |
| **Diffusivity** | m$^2$/s | (2–5) × $10^{-12}$ | (2–5) × $10^{-12}$ | (5–9) × $10^{-12}$ | (1–5) × $10^{-11}$ | (5–9) × $10^{-11}$ |

### 8.3.5 Specific uncertainties

The following specific uncertainties in the description of the evolution of the properties of the existing outer walls of the concrete structure in 1BMA during the first 100 000 years post-closure have been identified:

- The impact of high concentrations of salt depends on the type of waste in each waste package as well as of the conditioning method used. The consequence of this is that the general description of the evolution of the chemical properties of the existing outer walls will be associated with some uncertainties as discussed further in Section 4.14.
- The evolution of the load-bearing capacity is somewhat uncertain. The main reason for this is the uncertain impact of the evolution of the load-bearing capacity of the new outer walls and lid but also of the concrete moulds which could provide some internal support.

See also the discussion concerning the general uncertainties in Chapter 5.

## 8.4 New outer walls

### 8.4.1 Chemical properties

The post-closure evolution of the chemical properties of the new outer walls of the concrete structure in 1BMA will follow that outlined for the outer walls of the concrete caissons in 2BMA reported by Höglund (2019) and presented in Section 9.4. This is because *2BMA concrete* is expected to be used also for the construction of the new outer walls in 1BMA according to the method suggested by Wimelius (2021) but also because the outer walls in 1BMA and 2BMA will be of equal thickness and in direct contact with groundwater-saturated crushed rock backfill material.

The findings presented in Section 9.4 indicate that the average chemical properties of the new outer walls in 1BMA will be controlled by the presence of portlandite during at least up to 50 000 years post-closure. From this period and onwards, pH will be controlled by the slow transformation of the CSH-phases. For more details on the evolution of the mineral composition in the new outer walls of the concrete caissons in 2BMA, please refer to Section 9.4 and Höglund (2019).

As a remark, the chemical evolution of the new outer walls in 1BMA has also been modelled by Höglund (2014). In this study, a strong bond was assumed between the existing and new outer walls and the thickness of the latter therefore only 200 mm. Also, Höglund (2014) assumed that the *Silo concrete* was used for the new outer walls. For these reasons, the study by Höglund (2014) is less relevant than that of Höglund (2019) and therefore not considered here.

### 8.4.2 Load-bearing capacity

The evolution of the load-bearing capacity of the new outer walls has been evaluated by Mårtensson (2017). The study concluded that the new outer walls will resist the groundwater pressure during the saturation period as well as the pressure from the crushed rock backfill during at least the first 20 000 years post-closure if they are restored according to the description in Section 2.6.4. From this point in time, the resistance against external loads is more uncertain and some cracking must be expected.

The resistance of the existing outer walls against internal loads from swelling waste has been calculated by von Schenck and Bultmark (2014) as well as by Olsson (2016a) who also included the effect of an internal gas pressure. However, since Olsson (2016a) included the now excluded grouting of the waste packages this study is judged not to be valid for the current conditions.

For the existing outer walls, the study by von Schenck and Bultmark (2014) included both grouted and non-grouted waste packages and concluded that there will be sufficient expansion volume to handle swelling of ion-exchange resins as long as the waste is not grouted. The conclusion is therefore that the load-bearing capacity of the new outer walls will be sufficient to resist the load from swelling of ion-exchange resins and the probability for the formation of penetrating cracks because of this process therefore low.

In all, the findings presented in this section suggest that the load-bearing capacity of the new outer walls in 1BMA will be sufficient to carry the weight from the lid and the backfill material during at least 20 000 years post-closure. From this point in time, the resistance towards external loads is more uncertain and some cracking must probably be expected.

### 8.4.3 Transport properties

From the findings presented in Sections 6.2.1 and 8.4.2 it is concluded that the transport properties of the new outer walls in 1BMA will not be affected by penetrating cracks caused by external or internal loads during the first 20 000 years post-closure.

However, post-closure, the transport properties of the new outer walls can also be affected by temperature changes or corrosion of metal objects inside the concrete structure. This will be discussed below.

The risk for formation of penetrating cracks in the new outer walls due to corrosion of embedded metal objects is limited. This is because tie rods will not be used during construction but also because reinforcement will only be placed parallel to the surface of the new outer walls. The consequence of this is that corrosion will lead to surface cracks and spalling of the covering layer but not to formation of penetrating cracks.

Höglund (2014) suggests that the low temperature of the intruding groundwater during the saturation period can cause a contraction (temperature shrinkage) of the concrete structure, the consequence of which would be the formation of cracks. Höglund (2014) estimates the shrinkage of the concrete structure in 1BMA due to this cooling effect to about $-70 \times 10^{-6}$ m/m, i.e. 70 μm/m corresponding to a total of 11 mm for the entire concrete structure.

Based on this, Höglund (2014) estimates the impact of this effect for the overall hydraulic conductivity for 2BMA whereas no such calculations were found for 1BMA. The estimate shows that the overall hydraulic conductivity is dependent on the width of and spacing between the individual cracks. For the worst-case scenario (corresponding to the formation of a few wide cracks as shown in Figure 4-3) the hydraulic conductivity due to temperature cooling will increase by several orders of magnitude. For 1BMA, the distribution of cracks will be dependent on the amount and distribution of reinforcement in the new outer walls and the consequences of temperature shrinkage during saturation is therefore uncertain.

However, in the calculations, Höglund (2014) did not consider the fact that the concrete structure is in thermal equilibrium with the bedrock beneath it and that also the bedrock will be affected by the intruding groundwater. For that reason, the conclusions made by Höglund (2014) can be partly questioned even though not disregarded. Höglund (2014) also mentions that the swelling of the concrete due to capillary suction could counteract the temperature shrinkage even though Höglund (2014) also states that this could be difficult to take credit for in a safety assessment.

Finally, the transport properties of the concrete walls will also be affected by the increased porosity of the materials caused by alterations of the mineral composition in the concrete. According to Figure 4-5, the maximum porosity of completely degraded standard concrete is about 25 %. According to Table 5-6, the hydraulic conductivity of such a material is in the range of $10^{-7}$–$10^{-5}$ m/s. Figure 4-3 shows that this corresponds to concrete with a few cracks in the range of 0.1 mm. The conclusion is therefore that the impact of cracks on the hydraulic conductivity will be considerably larger than that of increased porosity.

In all, the findings presented in this section imply that the transport properties of the new outer walls of the concrete structure in 1BMA will be similar to those of these walls at closure during the first 20 000 years post-closure. After this point in time the evolution of the transport properties is uncertain. This is because of the uncertainties associated with the description of the evolution of the load-bearing capacity of the new outer walls and the timing of the different mechanical degradation events.

The impact of chemical concrete degradation in itself is, however, expected to be limited during a very long period of time and rather insignificant in relation to the impact of the formation of penetrating cracks.

### 8.4.4 Recommended material property data

Table 8-3 presents recommended material property data for the new outer walls in 1BMA for selected time periods up to 100 000 years post-closure. The recommendations are based on information regarding the status of the new outer walls at closure presented in Section 6.2, the expected evolution of the properties of the new outer walls described in the previous sections and the properties for degraded concrete given in Section 5.1.

**Table 8-3. Recommended material property data for the new outer walls in 1BMA for selected time periods up to 100 000 years post-closure.**

| | | Time period (Years post-closure) | | | | |
|---|---|---|---|---|---|---|
| **Property** | **Unit** | **At closure** | **0–1 000** | **1 000–20 000** | **20 000–50 000** | **50 000–100 000** |
| **pH** | - | ≥ 13 | ≥ 13 | 12.5 | 12–12.5 | 12–12.5 |
| **Porosity** | % | 11–13 | 11–13 | 11–14 | 12–15 | 13–16 |
| **Load-bearing capacity** | Rating (5–1) | 5 | 5 | 4–5 | 1–4 | 1 |
| **Hydraulic conductivity** | m/s | $(1–5)\times10^{-12}$ | $(1–5)\times10^{-12}$ | $(1–5)\times10^{-12}$ | $10^{-8}–10^{-2}$ | $10^{-2}$ |
| **Diffusivity** | $m^2/s$ | $(2–5)\times10^{-12}$ | $(2–5)\times10^{-12}$ | $(2–5)\times10^{-12}$ | $10^{-12}–10^{-9}$ | $10^{-9}$ |

### 8.4.5 Specific uncertainties

The following specific uncertainty in the description of the evolution of the properties of the new outer walls of the concrete structure in 1BMA during the first 100 000 years post-closure has been identified:

- The main uncertainty relates to evolution of the load-bearing capacity of the new outer walls and the influence of this on the transport properties of these. The evolution of the load-bearing capacity depends on the rate of concrete degradation and degradation of the function of the reinforcement bars. However, the load-bearing capacity also relies on mechanical support from adjacent components. Because all these dependencies are associated with different levels of uncertainties, also the prediction of the evolution of the load-bearing capacity of the new outer walls is uncertain.

See also the discussion concerning the general uncertainties in Chapter 5.

## 8.5 Lid

### 8.5.1 Chemical properties

The concrete lid will be constructed at closure of 1BMA, preliminary using the *2BMA concrete* (Section 3.3.3). The post-closure evolution of the chemical properties of the lid will therefore follow that of the outer walls of the concrete caissons in 2BMA outlined in detail in Section 9.4. The difference in thickness between the lid of the concrete caisson in 2BMA (600 mm) and the lid of the concrete structure in 1BMA (800 mm) is too small to cause any significant difference given the general uncertainties regarding the prediction of material properties over very long time periods. A rather early reduction of the thickness of the lid in 1BMA caused by rebar corrosion and spalling of the covering layer is also expected.

### 8.5.2 Load-bearing capacity

The evolution of the load-bearing capacity of the lid will be affected by the combined effect of loss of function of the reinforcement bars and concrete degradation, but also by the evolution of the load-bearing capacity of the outer and inner walls. However, the support from the concrete moulds that supports the prefabricated concrete elements during the operational period is not accounted for when assessing the post-closure evolution of the load-bearing capacity of the lid. This is because the evolution of the load-bearing capacity of the concrete moulds for the time periods in question is associated with great uncertainties.

For the lid, the dimensioning load will be the combined load from the crushed rock backfill material and the groundwater pressure during saturation. From Section 2.6.2, Westerberg recommends that the lid should be 800 mm thick and contain significant amounts of reinforcement to withstand these loads and thus to prevent cracking.[61]

The post-closure evolution of the load-bearing capacity of the lid has been evaluated by Mårtensson (2017). Based on a number of studies, Mårtensson (2017) suggests that the loss of load-bearing capacity caused by transformation of the strength bearing minerals can be described as a reduction of the thickness of the lid by about 15 mm per 1 000 years but also loss of function of the reinforcement bars in the affected parts. However, as shown in Section 9.4, leaching occurs mainly from the outside of the concrete lid and Mårtensson (2017) therefore does not consider corrosion of the reinforcement bars on the inside of the waste compartments.

According to Mårtensson (2017) the load-bearing capacity of the concrete lid at 20 000 years post-closure corresponds to that of a 500 mm thick reinforced concrete lid, assuming an original thickness of 800 mm, Section 2.6.2. According to Westerberg, this is sufficient to carry the load from the crushed rock backfill material and the risk for cracking due to external loads up to 20 000 years post-closure is therefore low.[62]

However, no studies seem to have been carried out to investigate the required minimum thickness of the lid to withstand the load from the crushed rock backfill material. For that reason, it is assumed that the lid will not be able to carry the load from the backfill beyond 20 000 years post-closure with the formation of several penetrating cracks as a consequence. A complete collapse is however not expected at this stage This is because the waste compartments will be filled with material from the degraded waste packages and prefabricated elements even though the load-bearing capacity of these components has been lost at an earlier stage. Through continued degradation of the lid and materials in the waste compartments, loss of structural integrity can be expected before 50 000 years post-closure.

### 8.5.3 Transport properties

The transport properties of the lid are mainly affected by the formation of hydraulically conducting zones such as cracks, channels and parts with increased porosity. Of these, increased porosity due to leaching will have a minor influence during a majority of the first 100 000 years post-closure and instead the presence of penetrating cracks will be the most influential factor.

According to Section 8.5.2, the risk for formation of penetrating cracks in the lid due to external loads during the first 20 000 years post-closure is low even though it cannot be entirely excluded. However, from Section 8.5.2 the transport properties of the concrete lid will be affected by a number of cracks from about 20 000 years post-closure and onwards. Through continued degradation of the lid and materials in the waste compartments, this will be followed by loss of structural integrity before 50 000 years post-closure.

[61] SKBdoc 1583182 ver 1.0. (Internal document, in Swedish.)

[62] SKBdoc 1583182 ver 1.0. (Internal document, in Swedish.)

### 8.5.4 Recommended material property data

Table 8-4 presents recommended material property data for the lid in 1BMA for selected time periods up to 100 000 years post-closure. The recommendations are based on information regarding the status of the lid at closure presented in Section 6.2, the expected evolution of the properties of the lid described in the previous sections and the properties for degraded concrete given in Section 5.1.

**Table 8-4. Recommended material property data for the concrete lid in 1BMA for selected time periods up to 100 000 years post-closure.**

| | | Time period (Years post-closure) | | | | |
|---|---|---|---|---|---|---|
| **Property** | **Unit** | **At closure** | **0–1 000** | **1 000–20 000** | **20 000–50 000** | **50 000–100 000** |
| **pH** | - | ≥ 13 | ≥ 13 | 12.5 | 12–12.5 | 12–12.5 |
| **Porosity** | % | 11–13 | 11–13 | 11–14 | 12–15 | 13–16 |
| **Load-bearing capacity** | Rating (5–1) | 5 | 5 | 4–5 | 1–4 | 1 |
| **Hydraulic conductivity** | m/s | $(1–5)\times10^{-12}$ | $(1–5)\times10^{-12}$ | $(1–5)\times10^{-12}$ | $10^{-8}$–$10^{-2}$ | $10^{-2}$ |
| **Diffusivity** | $m^2/s$ | $(2–5)\times10^{-12}$ | $(2–5)\times10^{-12}$ | $(2–5)\times10^{-12}$ | $10^{-12}$–$10^{-9}$ | $10^{-9}$ |

### 8.5.5 Specific uncertainties

The following specific uncertainties in the description of the evolution of the properties of the lid of the concrete structure in 1BMA during the first 100 000 years post-closure have been identified:

- The main uncertainty relates to the evolution of the load-bearing capacity of the lid and the support from the concrete moulds inside the waste compartments. Also, the rate and impact of corrosion of reinforcement bars placed deep inside the lid are uncertain.
- There is also a lack of information concerning the minimum thickness of the lid and amount of reinforcement required to carry the load from the backfill material. With a better understanding of the requirements, the accuracy of the predictions of the evolution of the transport properties of the lid can be improved.

See also the discussion concerning the general uncertainties in Chapter 5.

## 8.6 Inner walls

### 8.6.1 Chemical properties

The post-closure evolution of the chemical properties of the inner walls in 1BMA is expected to follow the general trend for the waste compartments outlined by Cronstrand (2007, 2014). However, with the construction of new outer walls planned for 1BMA (Sections 2.6.4 and 8.4), additional large amounts of concrete will be added with an expected slower degradation of the chemical properties of the inner walls as a consequence.

As shown in Figure 8-3, some portlandite leaching has occurred inside the waste compartment at 50 000 years post-closure but CSH_1.8 is still the dominant CSH-phase. (In this report, the results presented in Figures 8-2 to 8-4 are interpreted such that a part of the total amount of the portlandite has been leached rather than that the portlandite leaching front has reached a certain distance into the waste compartment. This is because the slits between the concrete moulds allow for advective transport of groundwater inside the waste compartment.) Portlandite leaching continues up to 100 000 years post-closure but still then significant amounts of portlandite remain and consequently pH will be about 12.5, Figure 8-4. In addition, the new outer walls which were not considered by Cronstrand (2007) are expected to extend the period during which portlandite remains in the inner walls.

In conclusion, alterations of the mineral composition in the inner walls will be very slow and the average pH is expected to remain at about 12.5 during up to 100 000 years post-closure.

### 8.6.2 Load-bearing capacity

Section 8.2 shows that alterations of the mineral composition in the inner walls (here represented by the waste compartment, denoted *ILW & LLW*) are slow. Instead, the main process for loss of load-bearing capacity of the inner walls is loss of function of the reinforcement bars and spalling of the covering layer which has an estimated thickness of 30 mm.

With the very slow chemical degradation of the inner walls indicated in Figures 8-1 to 8-4, the inner walls are expected to have the load-bearing capacity of about 300 mm thick unreinforced concrete walls at least up to 20 000 years post-closure. As concluded by Mårtensson (2017) this is sufficient to carry the weight of the lid and the backfill material.

Figure 8-3 shows that the amount of portlandite in the waste compartment will be significant 50 000 years post-closure. Following the assumptions by Mårtensson (2017) this implies that the load-bearing capacity of the inner walls is sufficient also at this point in time.

However, once the load-bearing capacity of the lid and outer walls is lost, the magnitude and direction of the loads acting on the inner walls will change. In addition to this, the rate of chemical alterations will also increase compared to the previous stages.

As a reasonable average, it is predicted that the load-bearing capacity of the inner walls between the waste compartments will be entirely lost at about 35 000 years post-closure and that the inner walls will lose their structural integrity at this stage due to the load from the lid and the backfill material.

### 8.6.3 Transport properties

Section 6.2.1 concludes that the transport properties of the inner walls during the initial period post-closure will be controlled by cracks that have formed during construction and the operational period (Figure 6-4). Because concrete degradation will be slow inside the waste compartment (Section 8.6.1), the evolution of the transport properties will be mainly controlled by corrosion of the tie rods which is likely to cause the formation of hydraulically conducting zones through the inner walls. The impact of this process is, however, dependent on whether solid corrosion products are formed or if they dissolve in the porewater (Section 4.17).

According to Section 4.17, the corrosion rate for steel under anaerobic and alkaline conditions is 0.001 to 0.1 mm/year. For a process in which the corrosion products are dissolved, Figure 4-3 shows that the presence of a crack with a width of 1 μm will increase the average hydraulic conductivity of a concrete wall only marginally. However, as corrosion proceeds and the width of the slit increases, the impact of tie rod corrosion will increase. If instead solid corrosion products are formed, cracking in the adjacent concrete will occur as also discussed in Section 4.17. This means that regardless of other processes, the evolution of the transport properties of the inner walls will be affected by corrosion of the tie rods. For a more thorough discussion concerning the impact of corroding tie rods and the impact of formation of solid corrosion products on the surface of embedded steel components, see Höglund (2014).

The transport properties will also be affected by cracking caused by rebar corrosion and loss of load-bearing capacity caused by concrete degradation. This means that the inner walls eventually will have the transport properties of thin concrete walls with an increasing number of cracks and other permeable zones and at some point in time, also loss of structural integrity of the inner walls must be expected.

### 8.6.4 Recommended material property data

Table 8-5 presents recommended material property data for the inner walls for selected time periods up to 100 000 years post-closure. The recommendations are based on information regarding the status of the inner walls at closure presented in Section 6.2, the expected evolution of the properties of the inner walls described in the previous sections and the properties for degraded concrete given in Section 5.1.

**Table 8-5. Recommended material property data for the inner walls in 1BMA for selected time periods up to 100 000 years post-closure.**

| | | Time period (Years post-closure) | | | | |
|---|---|---|---|---|---|---|
| **Property** | **Unit** | **At closure** | **0–1 000** | **1 000–20 000** | **20 000–50 000** | **50 000–100 000** |
| **pH** | - | ≥ 13 | ≥ 13 | 12.5–13 | 12–12.5 | 12–12.5 |
| **Porosity** | % | 12–15 | 12–15 | 12–15 | 12–15 | 13–16 |
| **Load-bearing capacity** | Rating (5–1) | 5 | 5 | 4–5 | 1–4 | 1 |
| **Hydraulic conductivity** | m/s | $10^{-5}$–$10^{-4}$ | $10^{-5}$–$10^{-4}$ | $10^{-4}$–$10^{-3}$ | $10^{-4}$–$10^{-3}$ | $10^{-4}$–$10^{-2}$ |
| **Diffusivity** | $m^2/s$ | (2–5) × $10^{-12}$ | (2–5) × $10^{-12}$ | (5–9) × $10^{-12}$ | $10^{-12}$–$10^{-9}$ | $10^{-9}$ |

### 8.6.5 Specific uncertainties

The following specific uncertainties in the description of the evolution of the properties of the inner walls during the first 100 000 years post-closure have been identified:

- The main uncertainty relates to the load-bearing capacity and transport properties of the inner walls whereas the evolution of the chemical properties is less uncertain. This is because the magnitude and direction of the loads that affect the inner walls will change with time as the load-bearing capacity of the outer walls and lid is lost. It is also because of uncertainties regarding the extent of the different degradation processes during the different time periods, in particular the effects of rebar and tie rod corrosion.
- There are also some uncertainties regarding the fact that the modelling conducted by Cronstrand (2007) included the grout between the waste packages. According to current plans, the waste packages will not be grouted and the amounts of cementitious minerals in the waste compartments therefore slightly reduced.
- Also, as discussed in Section 4.14, the impact of high concentrations of salts from evaporator concentrates in the waste on the degradation of the inner walls adds some additional uncertainty to the degradation model for the inner walls.

See also the discussion concerning the general uncertainties in Chapter 5.

## 8.7 Prefabricated concrete elements

### 8.7.1 Chemical properties

The evolution of the chemical properties of the concrete elements in 1BMA is expected to follow that outlined for the inner walls; see Section 8.6 for details.

### 8.7.2 Load-bearing capacity

As concluded in Section 8.5.2, the load-bearing capacity of the lid is expected to be sufficient to withstand the load from the backfill material during at least the first 20 000 years post-closure. The consequence of this is that the prefabricated concrete elements will not have to carry any external loads during this period.

Section 8.5.2 also states that the load-bearing capacity of the lid is uncertain beyond 20 000 years post-closure. This means that from this point in time, the weight of the backfill material and the lid might have to be carried by the elements with support from the concrete moulds. However, because of the uncertain load-bearing capacity of the concrete moulds at this stage (Section 8.9.2), the load-bearing capacity of the elements will be insufficient to carry the load from the backfill material and the lid. The consequence of this is that the elements will slowly sink into the waste compartments even though extensive cracking of the individual elements is not expected.

### 8.7.3 Transport properties

The evolution of the transport properties of the prefabricated concrete elements in 1BMA are presented for the elements as a group, i.e. also including the slits between the individual elements. This means that the hydraulic conductivity and effective diffusivity will be determined by the distance between the individual elements rather than by the properties of the concrete and degree of degradation.

Because of this, the transport properties of the prefabricated concrete elements will have the characteristics of degraded concrete with wide cracks already at closure and only through a complete collapse of the concrete structure, the effective diffusivity and hydraulic conductivity will increase.

### 8.7.4 Recommended material property data

Table 8-6 presents recommended material property data for the prefabricated concrete elements in 1BMA for selected time periods up to 100 000 years post-closure. The recommendations are based on information regarding the status of the prefabricated elements at closure presented in Section 6.2, the expected evolution of the properties of the prefabricated concrete elements described in the previous sections and the properties for degraded concrete given in Section 5.1.

**Table 8-6. Recommended material property data for the prefabricated concrete elements in 1BMA during different time periods up to 100 000 years post-closure.**

| | | Time period (Years post-closure) | | | | |
|---|---|---|---|---|---|---|
| **Property** | **Unit** | **At closure** | **0–1 000** | **1 000–20 000** | **20 000–50 000** | **50 000–100 000** |
| **pH** | - | ≥ 13 | ≥ 13 | 12.5–13 | 12–12.5 | 12–12.5 |
| **Porosity** | % | 12–15 | 12–15 | 12–15 | 12–15 | 13–16 |
| **Load-bearing capacity** | Rating (5–1) | 5 | 5 | 4–5 | 1–4 | 1 |
| **Hydraulic conductivity** | m/s | $10^{-3}$ | $10^{-3}$ | $10^{-3}$ | $10^{-2}$ | $10^{-2}$ |
| **Diffusivity** | $m^2/s$ | $10^{-10}$ | $10^{-10}$ | $10^{-10}$ | $10^{-10}$–$10^{-9}$ | $10^{-9}$ |

### 8.7.5 Specific uncertainties

No important specific uncertainties in the description of the evolution of the properties of the prefabricated elements have been identified. See instead the discussion concerning the general uncertainties in Chapter 5.

## 8.8 Gas evacuation system

### 8.8.1 Chemical properties

The evolution of the chemical properties of the gas evacuation system is expected to follow that of the gas evacuation system in 2BMA outlined in Section 9.8.1.

### 8.8.2 Load-bearing capacity

The load-bearing capacity of the gas evacuation system is not relevant. This is because this system does not contribute to the over-all load-bearing capacity of the lid.

### 8.8.3 Transport properties

The evolution of the transport properties of the gas evacuation system is expected to follow that of the gas evacuation in 2BMA system outlined in Section 9.8.3.

### 8.8.4 Recommended material property data

Table 8-7 presents recommended material property data for the gas evacuation system in 1BMA for selected time periods up to 100 000 years post-closure. The recommendations are based on information regarding the status of the gas evacuation system at closure presented in Section 6.2, the expected evolution of the properties of the gas evacuation system described in the previous sections and the properties for degraded concrete given in Section 5.1.

**Table 8-7. Recommended material property data for the gas evacuation system in 1BMA for selected time periods up to 100 000 years post-closure.**

| | | Time period (Years post-closure) | | | | |
|---|---|---|---|---|---|---|
| **Property** | **Unit** | **At closure** | **0–1 000** | **1 000–5 000** | **5 000–50 000** | **50 000–100 000** |
| **pH** | - | ≥ 13 | 12.5–13 | 11–12.5 | 10–11 | ≤ 10 |
| **Porosity** | % | 30 | 30 | 30–35 | 35–40 | ≥ 40 |
| **Load-bearing capacity** | Rating (5–1) | Not relevant | Not relevant | Not relevant | Not relevant | Not relevant |
| **Hydraulic conductivity** | m/s | $(5–20) \times 10^{-9}$ | $(5–20) \times 10^{-9}$ | $10^{-9}–10^{-5}$ | $10^{-5}–10^{-2}$ | $10^{-2}$ |
| **Diffusivity** | $m^2/s$ | $(1–5) \times 10^{-11}$ | $(1–5) \times 10^{-11}$ | $10^{-11}–10^{-10}$ | $10^{-10}–10^{-9}$ | $10^{-9}$ |

### 8.8.5 Specific uncertainties

The following specific uncertainty in the description of the evolution of the properties of the gas evacuation system in 1BMA during the first 100 000 years post-closure has been identified:

- There is a general uncertainty originating from the fact that no studies have been conducted concerning the post-closure evolution of permeable grouts. Also, the impact of leaching during the saturation period where a steady flow of groundwater passes through the gas evacuation system adds additional uncertainties.

See also the discussion concerning the general uncertainties in Chapter 5.

## 8.9 Concrete moulds

### 8.9.1 Chemical properties

The post-closure evolution of the chemical properties of the vast majority of the concrete moulds is expected to follow that of the inner walls outlined in Section 8.6.1. See also Figures 8-1 to 8-4 and 4-5.

### 8.9.2 Load-bearing capacity

#### *Impact of external loads*

The load-bearing capacity of the concrete moulds in 1BMA has been calculated by Bultmark (2017a) who showed that a concrete mould can carry the weight of a 100-meter-tall stack of a material with a density of 2 500 $kg/m^3$ without cracking. Bultmark (2017a) also showed that a concrete mould can carry the weight of a stack of concrete moulds with a height of 80 meters even after spalling of the covering layer.

Once spalling of the covering layer has occurred, the evolution of the load-bearing capacity of the concrete moulds is determined by the rate of mineral alterations in the concrete walls. From Figures 8-1 to 8-4 such alterations are slow inside the waste compartments and significant amounts of portlandite will be present during up to 100 000 years post-closure. The implication of this is that post-closure degradation of the load-bearing capacity of the concrete moulds due to concrete degradation alone is limited even though the uncertainties are considerable beyond 20 000 years post-closure, see below.

Beyond 20 000 years post-closure, the load on the concrete moulds will increase because the load-bearing capacity of the lid is reduced and finally lost. However, according to Bultmark (2017a) the load-bearing capacity of the concrete moulds is sufficient to carry also the weight of the backfill material with a thickness of only 6 meters even after spalling of the covering layer. In all, though, the evolution of the load-bearing capacity of the concrete moulds will be dependent on the type of waste in each mould and the type of waste in other waste packages in the respective waste compartments. See also Section 8.9.5.

#### *Impact of internal loads*

Internal loads mainly arise from swelling of ion-exchange resins, processes related to high concentrations of salts and gas related processes. Currently, the only waste categories comprising concrete moulds with cement-conditioned ion-exchange resins which are planned for disposal in 1BMA are O.01:09 and R.01:09 (SKB R-18-07). However, according to von Schenck and Bultmark (2014), this waste is not expected to swell in contact with water. For that reason, cracking of the concrete moulds due to internal loads caused by swelling of waste is not expected in 1BMA.

For evaporator concentrates, (SKB R-18-07) informs that no concrete moulds containing evaporator concentrates have yet been disposed in 1BMA even though 43 packages of waste category R.29:00 are currently planned for disposal. However, these waste packages also each contain an inner layer of compressible polyethylene which provides expansion volume in case of expansion of the waste and thus prevents a high pressure inside the concrete mould.

In all, the impact of swelling waste on the average properties of the concrete moulds is limited and the average load-bearing capacity of the concrete moulds will be controlled by their ability to withstand the external loads discussed in the previous section.

### 8.9.3 Transport properties

As concluded in 8.9.2, general cracking of the concrete moulds due to external and/or internal loads is not expected until after significant concrete degradation. A majority of the concrete moulds are therefore expected to have the transport properties of undegraded *SFR mould concrete*, during up to about 20 000 years post-closure. However for some concrete moulds some cracking which will affect the transport properties must be expected even though not on a general scale. Beyond this point in time, cracking of all concrete moulds must be expected.

### 8.9.4 Recommended material property data

Table 8-8 presents recommended material property data for the concrete moulds in 1BMA for selected time periods up to 100 000 years post-closure. The recommendations are based on information regarding the status of the concrete moulds at closure presented in Section 6.2, the expected evolution of the properties of the concrete moulds described in the previous sections and the properties for degraded concrete given in Section 5.1.

**Table 8-8. Recommended material property data for the concrete moulds in 1BMA for selected time periods up to 100 000 years post-closure.**

| | | Time period (Years post-closure) | | | | |
|---|---|---|---|---|---|---|
| **Property** | **Unit** | **At closure** | **0–1 000** | **1 000–20 000** | **20 000–50 000** | **50 000–100 000** |
| **pH** | - | ≥ 13 | ≥ 13 | 12.5–13 | 12–12.5 | 12–12.5 |
| **Porosity** | % | 12–15 | 12–15 | 12–15 | 12–15 | 13–16 |
| **Load-bearing capacity** | Rating (5–1) | 5 | 5 | 3–5 | 2–3 | 1–2 |
| **Hydraulic conductivity** | m/s | $(1–5) \times 10^{-12}$ | $(1–5) \times 10^{-12}$ | $(1–5) \times 10^{-12}$ | $10^{-11}–10^{-5}$ | $10^{-5}–10^{-2}$ |
| **Diffusivity** | $m^2/s$ | $(2–5) \times 10^{-12}$ | $(2–5) \times 10^{-12}$ | $(5–9) \times 10^{-12}$ | $10^{-12}–10^{-11}$ | $10^{-11}–10^{-9}$ |

### 8.9.5 Specific uncertainties

The following specific uncertainty in the description of the evolution of the properties of the concrete moulds in 1BMA during the first 100 000 years post-closure has been identified:

- There are some uncertainties regarding the influence of high concentrations of salts from evaporator concentrates in the waste in 1BMA. Even though (SKB R-18-07) informs that no concrete moulds containing evaporator concentrates have yet been disposed in 1BMA, many other waste categories in 1BMA contain significant amounts of salts which can be released and influence the properties of the concrete moulds. The impact of salts is further discussed in Section 4.14.

See also the discussion concerning the general uncertainties in Chapter 5.

# 9 2BMA: post-closure evolution

In this chapter, the expected evolution of the properties of the cementitious components in 2BMA during the first 100 000 years post-closure is described. The starting point for the descriptions is the expected status of the cementitious components in 2BMA at closure, Section 6.3. The evolution of the properties of the cementitious components in 2BMA is then influenced by the processes presented in Chapter 4.

Detailed descriptions of the cementitious components in 2BMA are given in Section 2.7. In addition, Chapter 3 presents detailed specifications and properties of the cementitious materials in the various components in 2BMA.

## 9.1 Literature

The following reports form the basis for the description of the post-closure evolution of the properties of the cementitious components in 2BMA presented in this chapter:

- **Elfwing et al. (2017)** studied the influence of the properties of the material in the gas evacuation system on the over-all transport properties of the lid of a concrete caisson for different time periods.
- **Höglund (2014)** modelled the evolution of the concrete caissons in 2BMA based on the use of the *Silo concrete*.
- **Höglund (2019)** modelled the evolution of the chemical conditions in 2BMA over 100 000 years based on the use of the *2BMA concrete*.
- **Idiart et al. (2019a)** modelled the influence of concrete mix proportions for different types of concrete used in SFR on the evolution of concrete properties in BHK in SFL.
- **Könönen and Olsson (2018)** modelled the load-bearing capacity of the concrete caissons with respect to rock fall-out, groundwater pressure and distribution of waste packages.
- **Lagerblad et al. (2017)** and **Mårtensson and Vogt (2019, 2020)** presents material property data of the *2BMA concrete* expected to be used in the concrete caissons in 2BMA.
- **Mårtensson (2017)** evaluated the impact of degradation processes on the load-bearing capacity concrete caissons in 2BMA.
- **Mårtensson and Vogt (2019, 2020)** developed construction methods for the concrete caissons in 2BMA and evaluated the risk for crack formation during construction.
- **Villar et al. (2019)** performed an experimental investigation of the properties of specimens made from *2BMA concrete* manufactured by Mårtensson and Vogt (2019).
- **Westerberg (2017)** calculated the load-bearing capacity of the different structural components of the concrete caissons in 2BMA.

## 9.2 Reinforced concrete slab

### 9.2.1 Chemical properties

Leaching and mineral alterations will mainly occur from the underside of the reinforced concrete slab which is in contact with the groundwater in the drainage layer. Leaching from the top of the slab will be considerably slower or even negligible as this part is in direct contact with – and therefore protected by – the concrete caisson.

As shown in Figures 9-2 and 9-3, portlandite concentration and pH in the reinforced concrete slab (denoted “grouted crushed rock” in the model illustration shown in Höglund (2019, Figure 1-8)) is only marginally affected during the first 20 000 years post-closure. From this follows that also the bulk chemical properties are expected to remain in principle unaltered during the first 20 000 years post-closure.

Also, beyond 20 000 years post-closure the rate of alterations of the mineral composition of the reinforced concrete slab will be slow with significant remaining amounts of portlandite and pH of about 12.5 still 100 000 years post-closure, Figures 9-4 and 9-5.

### 9.2.2 Load-bearing capacity

As shown in Section 9.2.1, concrete degradation is very slow in the reinforced concrete slab. From this follows that the load-bearing capacity of the reinforced concrete slab will be sufficient to carry the compressive and homogeneous load from the concrete caisson during up to 100 000 years post-closure even if the function of the reinforcement bars may have been lost at an earlier stage.

From this also follows that the risk for formation of penetrating cracks in the reinforced concrete slab due to insufficient load-bearing capacity will be low during up to 100 000 years post-closure. Tensile loads are finally not expected because of the low risk for settlements in the foundation layer.

### 9.2.3 Transport properties

According to Section 9.2.2, the load-bearing capacity of the reinforced concrete slab will be sufficient to prevent the formation of penetrating cracks during up to 100 000 years post-closure and the transport properties will therefore remain virtually unchanged compared to those at the day of closure. Also, even though rebar corrosion may cause the formation of surface cracks and concrete spalling, penetrating cracks are not expected.

However, there is a potential for the formation of cracks or other permeable zones already during construction of the reinforced concrete slab. This is because this slab does not formally constitute a part of the engineered barrier system and cracks can therefore be accepted. A few small cracks must therefore be expected in the slab already at closure as stated in Section 6.3.1.

### 9.2.4 Recommended material property data

Table 9-1 presents recommended material property data for the reinforced concrete slab in 2BMA for selected time periods up to 100 000 years post-closure. The recommendations are based on the expected status of the reinforced concrete slab at closure presented in Section 6.3, the expected evolution of the properties of the reinforced concrete slab described in the previous sections and the properties of degraded concrete given in Section 5.1.

**Table 9-1. Recommended material property data for the reinforced concrete slab in 2BMA for selected time periods up to 100 000 years post-closure.**

| | | Time period (Years post-closure) | | | | |
|---|---|---|---|---|---|---|
| **Property** | **Unit** | **At closure** | **0–1 000** | **1 000–20 000** | **20 000–50 000** | **50 000–100 000** |
| **pH** | - | ≥ 13 | ≥ 13 | 12.5 –13 | 12.5 | 12–12.5 |
| **Porosity** | % | 11–13 | 11–13 | 11–13 | 12–13 | 13–14 |
| **Load-bearing capacity** | Rating (5–1) | 5 | 5 | 4–5 | 4–3 | 3 |
| **Hydraulic conductivity** | m/s | $10^{-9}$–$10^{-7}$ | $10^{-9}$–$10^{-7}$ | $10^{-9}$–$10^{-7}$ | $10^{-9}$–$10^{-7}$ | $10^{-7}$–$10^{-5}$ |
| **Diffusivity** | $m^2/s$ | (5–9) × $10^{-12}$ | (5–9) × $10^{-12}$ | (5–9) × $10^{-12}$ | (5–9) × $10^{-12}$ | (1–5) × $10^{-11}$ |

### 9.2.5 Specific uncertainties

The following specific uncertainty in the description of the evolution of the properties of the reinforced concrete slabs in 2BMA during the first 100 000 years post-closure has been identified:

- The main uncertainty regarding the post-closure evolution of the reinforced concrete slab in 2BMA is associated with the transport properties. This is because the reinforced concrete slab does not constitute a part of the engineered barrier system and the prevention of e.g. cracking during construction is not prescribed.

See also the discussion concerning the general uncertainties in Chapter 5.

## 9.3 Slabs

### 9.3.1 Chemical properties

The post-closure evolution of the chemical properties of the slabs will follow the general trend outlined for the outer walls discussed in Section 9.4, but the rate of the alterations will be considerably slower. This is because leaching will be negligible from the underside of the slabs which is in direct contact with the reinforced concrete slab, but also because the top of the slabs is protected by the waste packages and inner walls. As shown in Figure 9-5, portlandite depletion will only occur in a small part of the slabs at 100 000 years post-closure and pH will therefore remain at 12.5 in the major part of the slabs up to 100 000 years post-closure.

### 9.3.2 Load-bearing capacity

As concluded in Section 9.3.1, significant amounts of portlandite will remain in the slabs during up to 100 000 years post-closure, thus rendering the slabs a sufficient load-bearing capacity against the compressive loads for which it is exposed. It is therefore expected that the formation of penetrating cracks in the slabs will not occur unless extensive settlements of the foundation and severe degradation of the reinforced concrete slab occurs. However, this is unlikely as settlements can be mitigated through careful compaction of the relatively thin foundation layer during construction.

Also, cracking of the slabs due to an uneven load distribution as discussed by Könönen and Olsson (2018) is prevented since the foundation also comprises a reinforced concrete slab (Section 9.2) not considered by Könönen and Olsson (2018). The reinforced concrete slab provides additional structural stability to the slabs and mitigates the effects of an uneven load distribution.

### 9.3.3 Transport properties

From the conclusions in Section 9.3.1, porosity increase due to leaching of the cement minerals are only expected to cause minor alterations of the average transport properties of the slabs in 2BMA. In addition, significant cracking is not expected, Section 9.3.2. From this follows that the transport properties of the slabs will remain in principle unaffected during up to 100 000 years post-closure with only some minor alterations caused by increased porosity in parts of the slabs.

### 9.3.4 Recommended material property data

Table 9-2 presents recommended material property data for the slabs of the caissons in 2BMA for selected time periods up to 100 000 years post-closure. The recommendations are based on the expected status of the slabs at closure presented in Section 6.3, the expected evolution of the properties of the slabs described in the previous sections and the properties for degraded concrete given in Section 5.1.

**Table 9-2. Recommended material property data for the slabs of the concrete caissons in 2BMA for selected time periods up to 100 000 years post-closure.**

| | | Time period (Years post-closure) | | | | |
|---|---|---|---|---|---|---|
| **Property** | **Unit** | **At closure** | **0–1 000** | **1 000–20 000** | **20 000–50 000** | **50 000–100 000** |
| **pH** | - | ≥ 13 | ≥ 13 | 12.5–13 | 12.5 | 12–12.5 |
| **Porosity** | % | 11–13 | 11–13 | 11–13 | 11–14 | 11–15 |
| **Load-bearing capacity** | Rating (5–1) | 5 | 5 | 4–5 | 4 | 4 |
| **Hydraulic conductivity** | m/s | $(1–5)\times10^{-12}$ | $(1–5)\times10^{-12}$ | $(1–5)\times10^{-12}$ | $10^{-12}–10^{-11}$ | $10^{-12}–10^{-11}$ |
| **Diffusivity** | $m^2/s$ | $(2–5)\times10^{-12}$ | $(2–5)\times10^{-12}$ | $(2–5)\times10^{-12}$ | $(2–5)\times10^{-12}$ | $(2–5)\times10^{-12}$ |

### 9.3.5 Specific uncertainties

The uncertainties in the predictions of the post-closure evolution of the properties of the slabs of the caissons in 2BMA are small. This is because the slabs are well protected between the reinforced concrete slab and the waste packages and inner walls, but also because the slabs do not contain any reinforcement and the risk for cracking due to rebar corrosion can therefore be disregarded.

See also the discussion concerning the general uncertainties in Chapter 5.

## 9.4 Outer walls

### 9.4.1 Chemical properties

The evolution of the chemical properties of the concrete caissons in 2BMA has been investigated by Höglund (2019) and the discussion presented in this section is mainly based on that report. The pH and mineral composition profiles presented in Figures 9-1 to 9-7 are the results from calculations performed at 25 °C and with time-dependent transport properties. In addition, MSH- and CASH-phases were allowed to form in these calculations. Further details and results from other calculations are found in Höglund (2019).

Figure 9-1 shows a small pH reduction in parts of the outer walls already during the first 1 000 years post-closure. However, pH remains above 12.5 indicating that pH is controlled by the dissolution of portlandite and that the pH reduction is caused by leaching of the alkali hydroxides. Simultaneously, pH increases in the groundwater in the backfill material.

Between 1 000 and 20 000 years post-closure, portlandite dissolution slowly proceeds. However, Figures 9-2 and 9-3 show that there are still significant amounts of portlandite and a pH of about 12.5 in the outer walls at 20 000 years post-closure.

Beyond 20 000 years post-closure, portlandite dissolution will proceed further into the concrete structure but complete portlandite depletion is only observed in the upper left corner of the concrete caisson at 100 000 years post-closure, Figure 9-5, right illustration. Dark blue areas indicate complete portlandite leaching whereas all other colours indicate that some portlandite remains.

Once no portlandite remains, transformation of the CSH-gel starts. Figure 9-6 shows the mineral composition in the upper left-hand corner of the concrete wall (upstream side) during the first 100 000 years post-closure. According to Figure 9-6, the slow transformation of the CSH-phases will lead to a slow reduction in pH but still 100 000 years post-closure, pH will be close to 12 in the affected parts whereas pH will remain at 12.5 in the major part of the outer walls, Figure 9-4.

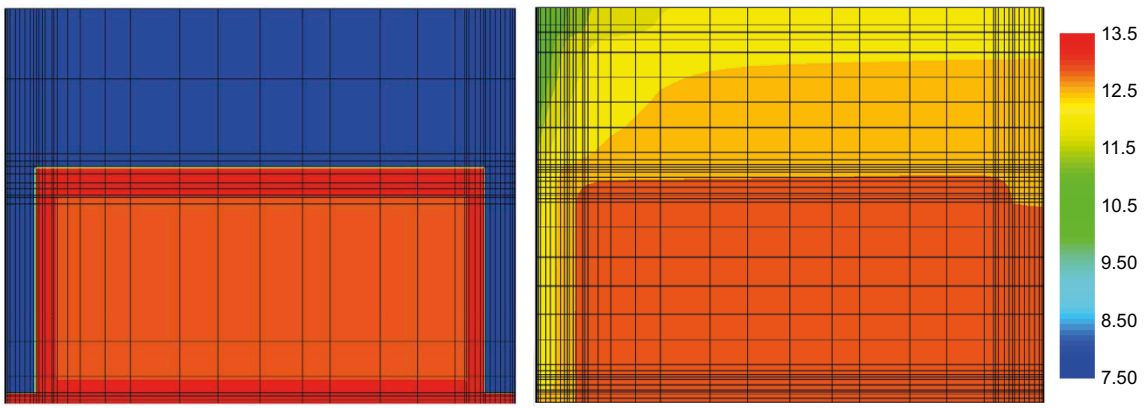


***Figure 9-1.*** *pH distribution in a concrete caisson at closure (left Höglund 2019, Figure A3-147) and 1 000 years post-closure (right Höglund 2019, Figure A3-153).*

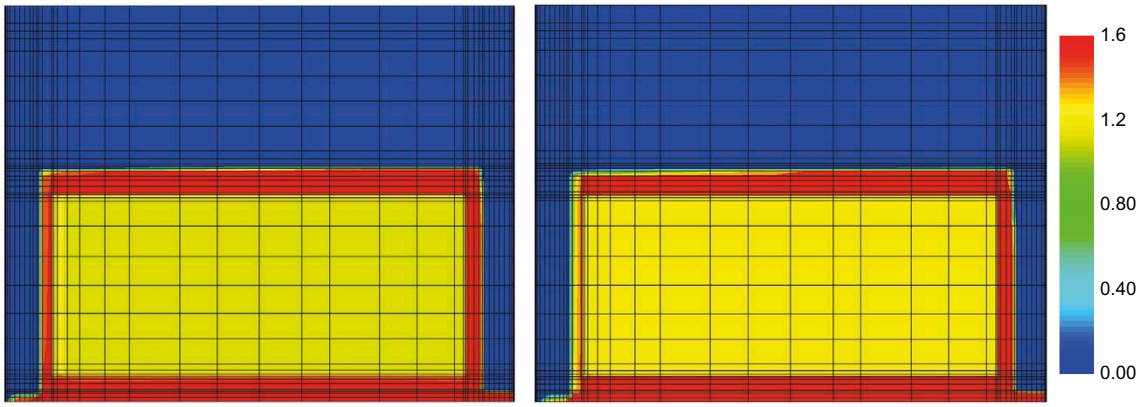


***Figure 9-2.*** *Portlandite distribution in a concrete caisson at 10 000 years (left Höglund 2019, Figure A3-156) and 20 000 years post-closure (right (Höglund 2019, Figure A3-158).*

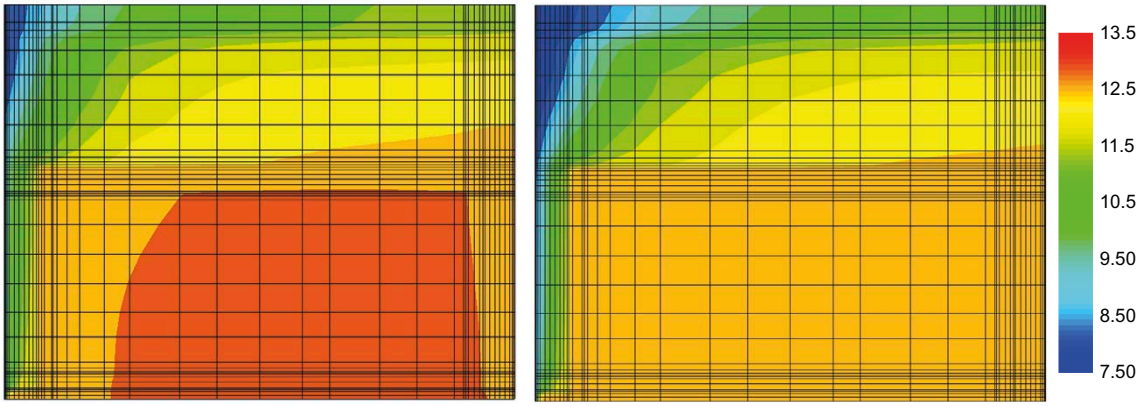


***Figure 9-3.*** *pH distribution in a concrete caisson at 10 000 (left (Höglund 2019, Figure A3-155) and 20 000 years post-closure (right Höglund 2019, Figure A3-157).*

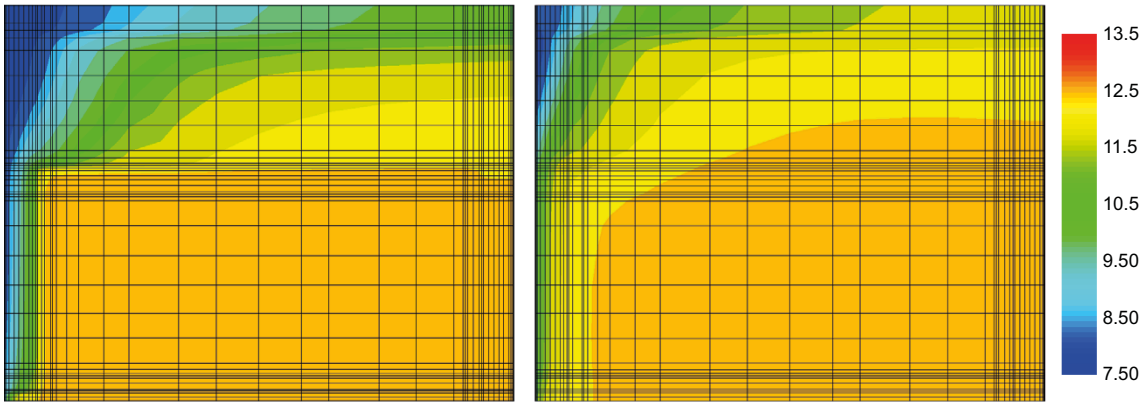


***Figure 9-4.*** *pH distribution in a concrete caisson at 50 000 (left (Höglund 2019, Figure A3-159) and 100 000 years post-closure (right (Höglund 2019, Figure A3-161).*

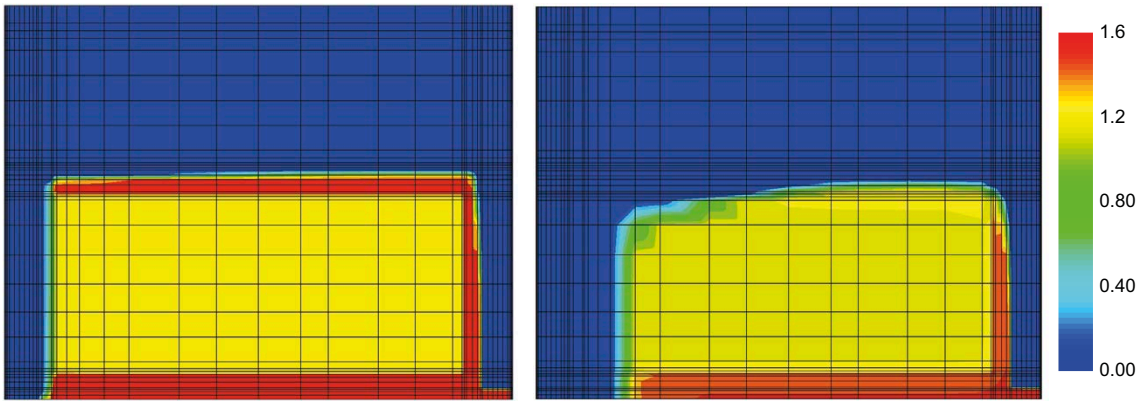


***Figure 9-5.*** *Portlandite distribution in a concrete caisson at 50 000 years (left Höglund 2019, Figure A3-160) and 100 000 years post-closure (right Höglund 2019, Figure A3-162).*

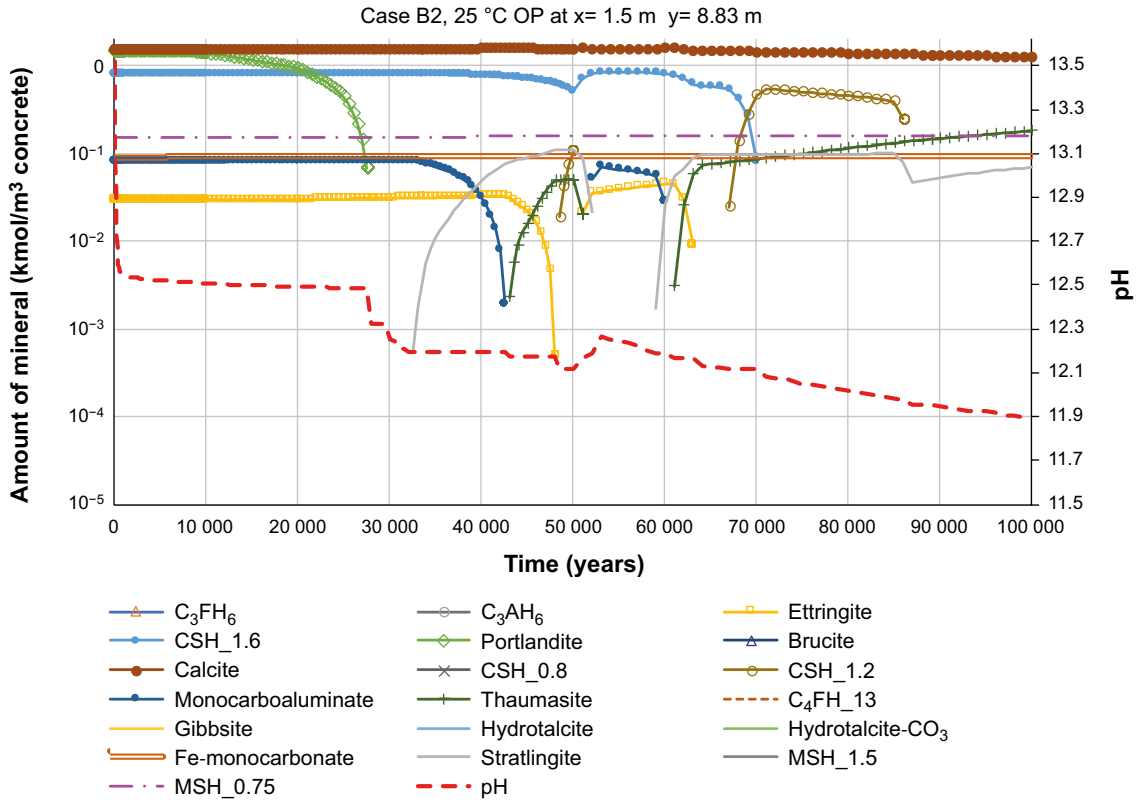


***Figure 9-6.*** *Evolution of pH and mineral composition at an observation point in the upper left-hand corner of the concrete wall (upstream side (left in the previous figures)) during 100 000 years with time-dependent transport properties (Höglund 2019, Figure A3-170).*

Finally, Höglund (2019) compiled the pH evolution for the different time periods, Figure 9-7. In Figure 9-7, a pH gradient is observed with pH at about 12.5 on the inside of the outer walls and inside the waste compartment up to about and beyond 50 000 years post-closure but with a lower value in the outside part of the outer walls.

In all, these findings show that the average chemical properties of the outer walls of the concrete caisson will be controlled by the presence of portlandite during up to about 50 000 years post-closure. From this point in time and onwards, pH will be controlled by the slow transformation of the CSH-phases. This is in accordance with the conclusions by Höglund (2019) whose final statement is that "*This shows that a significant buffering capacity is available and provides a robust pH-regulating system in the 2BMA vault*".

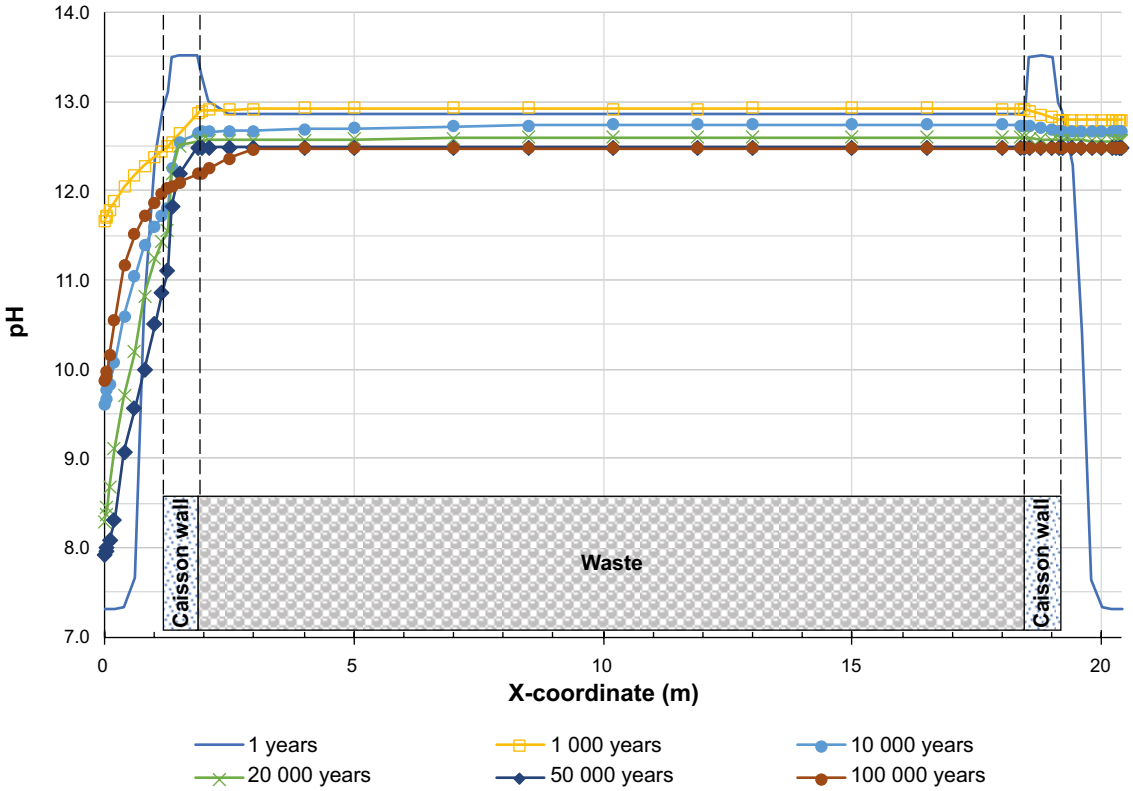


***Figure 9-7.*** *pH-profiles at selected times along a horizontal centre-line through 2BMA at height y= 4.63 m for time-dependent transport properties at 25 °C (Höglund 2019, Figure A3-146).*

### 9.4.2 Load-bearing capacity

#### *External loads*

The load-bearing capacity of the outer walls of the concrete caisson at closure is dependent on type of concrete used and thickness of the different construction parts. The dimensions of the different structural components of the caissons (Section 2.7.2) have been chosen to ensure that the concrete caissons will withstand the combined load from the crushed rock backfill and the groundwater pressure that may occur during the saturation of the repository (Westerberg 2017, Könönen and Olsson 2018).

Könönen and Olsson (2018) also calculated the risk for cracking of the undegraded concrete caisson in the event of rock fall-out. The study showed that the risk for the formation of penetrating cracks in the upper parts of the outer walls caused by rock fall-out is low even for a rock piece with the dimensions 2 m × 2 m × 3 m.

The load-bearing capacity of the outer walls during the later periods is dependent on the extent of concrete degradation as well as of the load-bearing capacity of the inner walls whereas the influence of corrosion can be disregarded since steel reinforcement is not used in the outer walls.

Westerberg (2017) showed that the thickness of the outer walls must be at least 320 mm to resist the pressure from the backfill material, as long as mechanical support from the inner walls is provided.

After evaluating several studies, Mårtensson (2017) pessimistically (See Section 5.1.2 and Höglund 2019) suggested that the degradation rate of the load-bearing capacity of concrete under repository conditions correspond to a reduction of the thickness of the concrete structure by about 15 mm/1 000 years.

With an original thickness of 680 mm for the outer walls (Section 2.7.2) and a loss of load-bearing capacity of 15 mm/1 000 years, the load-bearing capacity of the outer walls will be sufficient to withstand the load from the backfill material up to about 25 000 years post-closure. This means that from this stage and onwards, the risk for formation of penetrating cracks in the outer walls must be considered.

#### *Internal loads*

The caissons may also experience internal loads caused by the swelling of waste or waste packaging or by a gas pressure caused by the degradation of waste. The main process behind both swelling and gas formation is anaerobic corrosion of the large amounts of steel (both waste and waste packaging) disposed in 2BMA which generates $H_2$ (g) and voluminous corrosion products, see also Section 4.17.

The impact of an internal high gas pressure has been investigated by Eriksson et al. (2015) for the previous reference design of the concrete caissons (SKB TR-14-02) and the results are therefore only indicative of the load-bearing capacity of the current design. The study showed that the concrete caisson can withstand an internal gas pressure of 31 kPa without cracking. However, according to Elfwing et al. (2017) gas can be transported through the permeable grout planned for use in the gas evacuation system already at a pressure of 6 kPa. There should therefore be a sufficient margin to prevent cracking due to a high gas pressure inside the concrete caisson also for the current design which has thicker outer walls and lid.

As a remark, the potential blocking of all gas evacuation channels which could occur during very unfavourable conditions must be considered. However, as concluded in Section 9.8 the risk for clogging of the pore system of the gas evacuation system is low and therefore the risk is disregarded.

Finally, the risk for a high internal pressure due to swelling of waste is low. This is because the width of the slit between the waste packages and the inner/outer walls is expected to be sufficient to accommodate the increased material volume caused by e.g. swelling of ion exchange resins or voluminous corrosion products and that a high pressure will therefore not evolve.

In all, it is concluded that the load-bearing capacity of the outer walls of the concrete caissons will be sufficient to withstand both internal and external loads during up to at least 25 000 years post-closure. The formation of penetrating cracks in the outer walls is therefore not expected during this period. However, from this point in time, the risk for cracking in at least some parts of some of the 13 caissons must be expected.

### 9.4.3 Transport properties

The evolution of the transport properties of the outer walls of the concrete caissons in 2BMA will follow the evolution of their load-bearing capacity. No cracks or other permeable zones are expected at closure (Section 6.3.1) and the influence of the chemical processes on the transport properties is small.

In addition to the processes discussed in Section 9.4.2, penetrating cracks can also form through shrinkage of the caissons during saturation when cooler groundwater enters the waste vault as suggested by Höglund (2014). However, this is considered less likely for the free-standing caissons which are placed on a foundation that allows for unrestrained shrinkage as discussed in Section 2.7. This process is therefore not likely to affect the transport properties of the outer walls of the concrete caissons.

From this and from the findings presented in Section 9.4.2 follows that the transport properties of the outer walls of the concrete caissons will remain virtually unchanged during the initial 25 000 years post-closure. However, from this point the formation of penetrating cracks must be expected and from about 30 000–40 000 years post-closure the transport properties of the outer walls will probably be severely degraded.

Finally, the absence of reinforcement increases the risk for fall-out of concrete pieces compared to a reinforced structure. For that reason, the transport properties of the outer walls may be similar to those of the backfill material from about 40 000 years post-closure.

### 9.4.4 Recommended material property data

Table 9-3 presents recommended material property data for the outer walls of the concrete caissons in 2BMA for selected time periods up to 100 000 years post-closure. The recommendations are based on the expected status of the outer walls at closure presented in Section 6.3, the expected evolution of the properties of the outer walls described in the previous sections and the properties for degraded concrete given in Section 5.1.

**Table 9-3. Recommended material property data for the outer walls of the concrete caissons in 2BMA for selected time periods up to 100 000 years post-closure.**

| | | Time period (Years post-closure) | | | | |
|---|---|---|---|---|---|---|
| **Property** | **Unit** | **At closure** | **0–1 000** | **1 000–20 000** | **20 000–50 000** | **50 000–100 000** |
| **pH** | - | ≥ 13 | ≥ 13 | 12.5 | 12–12.5 | 12–12.5 |
| **Porosity** | % | 11–13 | 11–13 | 11–14 | 12–15 | 13–16 |
| **Load-bearing capacity** | Rating (5–1) | 5 | 5 | 4–5 | 1–4 | 1 |
| **Hydraulic conductivity** | m/s | $(1–5)\times10^{-12}$ | $(1–5)\times10^{-12}$ | $(1–5)\times10^{-12}$ | $10^{-8}$–$10^{-2}$ | $10^{-2}$ |
| **Diffusivity** | $m^2/s$ | $(2–5)\times10^{-12}$ | $(2–5)\times10^{-12}$ | $(2–5)\times10^{-12}$ | $10^{-12}$–$10^{-9}$ | $10^{-9}$ |

### 9.4.5 Specific uncertainties

The following specific uncertainties in the description of the evolution of the properties of the outer walls in 2BMA during the first 100 000 years post-closure have been identified:

- The impact of concrete degradation on the evolution of the load-bearing capacity and transport properties (both in terms of timing and consequences) is somewhat uncertain. For the unreinforced outer walls of the concrete caissons, the load-bearing capacity will after significant concrete degradation have to rely on the support from the backfill and the waste packages. If this support fails, the walls may collapse with a significant impact on the transport properties as a consequence. However, as long as the walls remain structurally intact, alterations of the transport properties will be limited. In addition, Figures 9-2 and 9-5 show that chemical degradation of the caissons is highly heterogeneous which means that the evolution of the load-bearing capacity and transport properties in terms of timing of the different events may differ considerably.
- There also remain some uncertainties regarding the post-closure evolution of the material used to seal the holes from the tie rods suggested by Mårtensson (2021a). As informed in Mårtensson (2021a), a commercial product whose detailed composition is not known was used in this work. As an alternative to this product a specifically designed material with known composition can be used instead.

See also the discussion concerning the general uncertainties in Chapter 5.

## 9.5 Lids

### 9.5.1 Chemical properties

The post-closure evolution of the chemical properties of the lids will follow the general trend outlined for the outer walls, Section 9.4. The rate of alteration will be the same in the lids as in the outer walls as these components are both in contact with the groundwater saturated backfill material.

In analogy with the outer walls, the average chemical properties of the lids will be controlled by the presence of portlandite during up to about 50 000 years post-closure. From this time onwards, pH will be controlled by the slow transformation of the CSH-phases. This is in accordance with the conclusions by Höglund (2019) whose final statement is that "*This shows that a significant buffering capacity is available and provides a robust pH-regulating system in the 2BMA vault*".

### 9.5.2 Load-bearing capacity

From Section 2.7.2, the thickness of the lids is sufficient to withstand the combined load from the crushed rock backfill and the groundwater pressure at repository depth that may occur during saturation of the repository as shown by Westerberg (2017) and Könönen and Olsson (2018).

Könönen and Olsson (2018) also modelled the load-bearing capacity of the undegraded concrete caisson against rock fall-out. The study showed that the risk for the formation of penetrating cracks in the lids caused by rock fall-out (dimensions of rock piece: 2 m × 2 m × 3 m) is low for a 6 meters thick layer of backfill material. If less backfill material is used, the risk for cracking is higher due to the higher impact force from the falling rock piece.

Through reduction of the load-bearing capacity of the lids, their load-bering capacity becomes increasingly dependent on the load-bearing capacity of the inner walls, waste packages and prefabricated concrete elements. The influence of corrosion can be neglected as steel reinforcement is not used.

Westerberg (2017) showed that a thickness and concrete compressive strength of 350 mm and 50 MPa respectively were required for the lid to resist the pressure from the backfill material if mechanical support from the inner walls was provided.

With an original thickness of 600 mm (Section 2.7.2), and a loss of load-bearing capacity of 15 mm/1 000 years (Section 5.1.2), the lids will be able to withstand the load from the backfill material up to about 20 000 years post-closure. This means that from this stage onwards, the risk for formation of penetrating cracks in the lids must be considered. However, it should be remembered that the additional support provided by the prefabricated elements and waste packages has not been included in this evaluation. Also, the findings by Höglund (2019) and von Schenck (2017) indicate a slower rate of reduction of the load-bearing capacity than the somewhat pessimistic rate suggested by Mårtensson (2017).

Finally, the discussion concerning the impact of internal loads is also valid for the lid, see Section 9.4.2.

In all, the load-bearing capacity of the lids of the concrete caissons will be sufficient to resist internal and external forces and thereby prevent cracking during at least the first 20 000 years post-closure but probably also a bit beyond this point in time. However, formation of penetrating cracks in the lids in some of the 13 caissons must be expected already from about 20 000 years post-closure.

With a continued degradation, the load-bearing capacity of the lids will eventually be insufficient to carry the load from the backfill material and severe cracking must be expected. However, the risk for a complete collapse of the lids is also dependent on the mechanical support from the outer and inner walls as well as the prefabricated concrete elements, waste packages and backfill material and the system is therefore rather complex.

### 9.5.3 Transport properties

The evolution of the transport properties of the lids of the concrete caissons in 2BMA (not including the gas evacuation system) will broadly correspond to that outlined for the outer walls, Section 9.4.3. No cracks or other permeable zones are expected at closure (Section 6.3.1) and the influence of the chemical processes on the transport properties post-closure is small.

Because of the low risk for cracking during the first 20 000 years (Section 9.5.2), the transport properties of the lids will remain virtually unchanged during this period. However, from this point in time some cracks may start to form with an expected increase of the hydraulic conductivity and effective diffusivity of the lids as a consequence. In addition, the impact of cracking can be severe because the lids lack reinforcement that prevents the fall-out of pieces of concrete with the possible formation of holes as a consequence.

From this and from the findings presented in Section 9.5.2 follow that the transport properties of the lids of the concrete caissons will remain virtually unchanged during the initial 20 000–25 000 years post-closure. However, from this point the formation of penetrating cracks must be expected and from about 30 000–40 000 years post-closure both the hydraulic conductivity and effective diffusivity will increase significantly.

### 9.5.4 Recommended material property data

Table 9-4 presents recommended material property data for the lids of the concrete caissons in 2BMA for selected time periods up to 100 000 years post-closure. The recommendations are based on the expected status of the lids at closure presented in Section 6.3, the expected evolution of the properties of the lids described in the previous sections and the properties for degraded concrete given in Section 5.1. Note that the suggested data do not include the impact of the gas evacuation system as this is handled separately in Section 9.8.

**Table 9-4. Recommended material property data for the lids in 2BMA for selected time periods up to 100 000 years post-closure.**

| | | Time period (Years post-closure) | | | | |
|---|---|---|---|---|---|---|
| **Property** | **Unit** | **At closure** | **0–1 000** | **1 000–20 000** | **20 000–50 000** | **50 000–100 000** |
| **pH** | - | ≥ 13 | ≥ 13 | 12.5 | 12–12.5 | 12–12.5 |
| **Porosity** | % | 11–13 | 11–13 | 11–14 | 12–15 | 13–16 |
| **Load-bearing capacity** | Rating (5–1) | 5 | 5 | 4–5 | 1–4 | 1 |
| **Hydraulic conductivity** | m/s | $(1–5)\times10^{-12}$ | $(1–5)\times10^{-12}$ | $(1–5)\times10^{-12}$ | $10^{-8}$–$10^{-2}$ | $10^{-2}$ |
| **Diffusivity** | $m^2/s$ | $(2–5)\times10^{-12}$ | $(2–5)\times10^{-12}$ | $(2–5)\times10^{-12}$ | $10^{-12}$–$10^{-9}$ | $10^{-9}$ |

### 9.5.5 Specific uncertainties

The following specific uncertainty in the description of the evolution of the properties of the lids in 2BMA during the first 100 000 years post-closure has been identified:

- The impact of concrete degradation on the evolution of the load-bearing capacity and transport properties of the lids (both in terms of timing and consequences) is uncertain as discussed in Section 9.5.3. For the unreinforced lid, the load-bearing capacity will after significant concrete degradation have to rely on the support from the prefabricated concrete elements and the waste packages. If this support fails, the lid may collapse with a significant impact on the transport properties as a consequence. The timing of such a collapse is uncertain given the complexity of the system even though Section 9.5.3 suggests that this will occur sometime beyond 20 000 years post-closure.

Uncertainties related to the influence of the gas evacuation system are discussed in Section 9.8. See also the discussion concerning the general uncertainties in Chapter 5.

## 9.6 Inner walls

### 9.6.1 Chemical properties

Figures 9-1 to 9-5 indicate that the evolution of the chemical properties of the inner walls of the concrete caissons will follow that of the caisson slabs outlined in Section 9.3. From these figures, the chemical properties of the inner walls will be controlled by the presence of portlandite during at least up to 50 000 years post-closure with pH of about 12.5. Beyond 50 000 years post-closure, portlandite is depleted in parts of the interior of the caisson but the average pH will still be about 12.5. The uncertainties associated with this prediction are discussed in Section 9.6.5.

### 9.6.2 Load-bearing capacity

The load-bearing capacity of the inner walls of the concrete caissons will be affected by concrete degradation and loss of function of the reinforcement (if such is used). According to Westerberg (2017), a minimum thickness of 40 mm is required for the inner walls to withstand the load from the backfill material after saturation of the waste vault and caissons.

With the very slow concrete degradation of the inner walls (Figures 9-1 to 9-5) spalling of the covering layer due to corrosion of the reinforcement bars (if such are used) will therefore be the main process for loss of load-bearing capacity. However, according to Westerberg (2017), reinforcement is not required post-closure. The reinforcement bars (if required during construction) can therefore be placed as close to the surface of the inner walls as possible to reduce the impact of spalling of the covering layer.

With this background, a thickness of the covering layer of only 10 mm is assumed. Therefore, through rebar corrosion and spalling of the covering layer, the load-bearing capacity of the inner walls will correspond to that of a 150 mm thick unreinforced concrete wall already at 1 000 years post-closure.

In Section 9.6.1 pH is predicted to remain at about 12.5 up to 100 000 years post-closure. From this follows that the compressive strength and load-bearing capacity of the inner walls should remain relatively unaltered. However, the rate of leaching may increase if significant cracking of the outer walls and lid occur as discussed in Sections 9.4 and 9.5.

If extensive cracking of the outer construction parts occurs, there is a non-negligible risk that material movements will alter the direction and magnitude of the loads on the inner walls. Extensive cracking of the outer construction parts will also increase the rate of chemical degradation of the inner walls as groundwater flow inside the caissons will increase. Because of the large uncertainties associated with predictions of the evolution of such a coupled system, it is expected that the load-bearing capacity of the inner walls is lost at about the same time as for the outer concrete structure, i.e. at between 20 000 and 40 000 years post-closure.

As discussed in Sections 9.4 and 9.5, any predictions of the evolution of the structural integrity of the external concrete structure beyond this point in time will be uncertain. Consequently, also predictions involving the inner walls will be uncertain from this point and onwards. See also Section 9.6.5.

### 9.6.3 Transport properties

For the period during which the concrete structure is structurally intact, the transport properties of the inner walls will be dominated by the holes that are made to ensure that the water that enters the interior of the caissons is evenly distributed and that no pressure gradients are developed between adjacent shafts. When the external construction parts no longer can carry the load from the backfill material, and larger cracks start to form, the transport properties of the inner walls are no longer relevant.

### 9.6.4 Recommended material property data

Table 9-5 presents recommended material property data for the inner walls of the concrete caissons in 2BMA for selected time periods up to 100 000 years post-closure. The recommendations are based on the expected status of the inner walls at closure presented in Section 6.3, the expected evolution of the properties of the inner walls described in the previous sections and the properties for degraded concrete given in Section 5.1.

**Table 9-5. Recommended material property data for the inner walls of the concrete caissons in 2BMA for selected time periods up to 100 000 years post-closure.**

| | | Time period (Years post-closure) | | | | |
|---|---|---|---|---|---|---|
| **Property** | **Unit** | **At closure** | **0–1 000** | **1 000–20 000** | **20 000–50 000** | **50 000–100 000** |
| **pH** | - | ≥ 13 | ≥ 13 | 12.5–13 | 12.5 | 12–12.5 |
| **Porosity** | % | 11–13 | 11–13 | 11–13 | 12–13 | 13–15 |
| **Load-bearing capacity** | Rating (5–1) | 5 | 5 | 4–5 | 1–4 | 1 |
| **Hydraulic conductivity** | m/s | $10^{-2}$ | $10^{-2}$ | $10^{-2}$ | $10^{-2}$ | $10^{-2}$ |
| **Diffusivity** | $m^2/s$ | $10^{-10}$ | $10^{-10}$ | $10^{-10}$ | $10^{-10}$–$10^{-9}$ | $10^{-9}$ |

### 9.6.5 Specific uncertainties

The following specific uncertainty in the description of the evolution of the properties of the inner walls in 2BMA during the first 100 000 years post-closure has been identified:

- The main source of uncertainty originates from the uncertain impact of cracking of the outer walls and lid on the structural integrity of the inner walls. Here, also the impact of the support from the waste packages adds additional uncertainties. The uncertainties are also related to the fact that design (including potential use of reinforcement) and construction method for the inner walls have not yet been decided.

See also the discussion concerning the general uncertainties in Chapter 5.

## 9.7 Prefabricated concrete elements

### 9.7.1 Chemical properties

The evolution of the chemical properties of the prefabricated concrete elements in 2BMA will follow that outlined for the inner walls, Section 9.6.1.

### 9.7.2 Load-bearing capacity

In Section 9.5.2, the load-bearing capacity of the lids was predicted to be sufficient to carry the backfill material during at least the first 20 000 years post-closure and the prefabricated concrete elements will therefore experience only limited external loads during this period.

Beyond about 20 000 years post-closure, the load-bearing capacity of the lids will eventually be insufficient to carry the load from the backfill material. The consequence of this is that the prefabricated concrete elements will instead have to carry this load. Here, even though only slow concrete degradation is expected inside the caissons, the impact of rebar corrosion cannot be ignored. For this reason, the prefabricated concrete elements at this point in time will have the load-bearing capacity of unreinforced concrete. Cracking of these elements must therefore – on the time-scale of the repository life-time – be expected to occur more or less simultaneously with the appearance of the first cracks in the lid.

### 9.7.3 Transport properties

The transport properties of the prefabricated concrete elements in 2BMA are evaluated for the elements as a group, i.e. also including the slits between the individual elements. This means that the hydraulic conductivity and effective diffusivity will be determined by the distance between the individual elements rather than by the properties of the concrete and degree of degradation.

Because of this, the transport properties of the prefabricated concrete elements will have the characteristics of severely cracked concrete already at closure and only through a collapse of the concrete structure, the effective diffusivity and hydraulic conductivity will increase further.

### 9.7.4 Recommended material property data

Table 9-6 presents recommended material property data for the prefabricated concrete elements of the concrete caissons in 2BMA for selected time periods up to 100 000 years post-closure. The recommendations are based on the expected status of the prefabricated concrete elements at closure presented in Section 6.3, the expected evolution of the properties of the prefabricated concrete elements described in the previous sections and the properties for degraded concrete given in Section 5.1.

**Table 9-6. Recommended material property data for the prefabricated concrete elements in 2BMA for selected time periods up to 100 000 years post-closure.**

| | | Time period (Years post-closure) | | | | |
|---|---|---|---|---|---|---|
| **Property** | **Unit** | **At closure** | **0–1 000** | **1 000–20 000** | **20 000–50 000** | **50 000–100 000** |
| **pH** | - | ≥ 13 | ≥ 13 | 12.5–13 | 12.5 | 12–12.5 |
| **Porosity** | % | 11–13 | 11–13 | 11–13 | 12–13 | 13–16 |
| **Load-bearing capacity** | Rating (5–1) | 5 | 5 | 4–5 | 1–4 | 1 |
| **Hydraulic conductivity** | m/s | $10^{-3}$ | $10^{-3}$ | $10^{-3}$ | $10^{-2}$ | $10^{-2}$ |
| **Diffusivity** | $m^2/s$ | $10^{-10}$ | $10^{-10}$ | $10^{-10}$ | $10^{-10}$–$10^{-9}$ | $10^{-9}$ |

### 9.7.5 Specific uncertainties

The following specific uncertainty in the description of the evolution of the properties of the prefabricated concrete elements in 2BMA during the first 100 000 years post-closure has been identified:

- The main uncertainty concerns the load-bearing capacity of the prefabricated concrete elements once the load-bearing capacity of the lid is insufficient to carry the load from the backfill material. However, as mentioned in Section 9.7.2 it cannot be expected that the prefabricated elements alone will be able to carry the weight of the backfill material over a significantly longer period than the lid even though some support from the waste packages could be accounted for.

See also the discussion concerning the general uncertainties in Chapter 5.

## 9.8 Gas evacuation system

### 9.8.1 Chemical properties

No detailed studies of the post-closure evolution of the chemical properties of the gas evacuation system in the lid of the concrete caissons in 2BMA have yet been conducted and the following discussion is therefore based on a general understanding of the involved processes.

According to Figure 8-6, the long-term portlandite leaching rate for ordinary concrete is about 10 mm/1 000 years assuming only diffusive transport and an effective diffusivity of $5 \times 10^{-12}$ $m^2/s$. For the grout, the expected effective diffusivity at closure is $(1–5) \times 10^{-11}$ $m^2/s$, i.e. 2–10 times higher than that of the concrete, Table 6-3. In addition, the hydraulic conductivity of the *2BMA grout* expected for use in the gas evacuation system is about three orders of magnitude higher than that of the *2BMA concrete* in the lid, Table 6-3.

The consequence of this is that diffusive transport of dissolved species will be higher but also that advective flow of groundwater and species dissolved in the groundwater will have a more pronounced influence on leaching of the cement minerals in the gas evacuation system compared to the other parts of the lid where slow diffusive transport will be the dominant transport mechanism.

With a 2–10 times higher effective diffusivity and also considering the contribution from advective transport of groundwater and species dissolved in the groundwater, leaching and mineral alterations of the grout in the gas evacuation will be significantly higher than in the lid even though the lack of dedicated studies introduces some uncertainties.

With this background, the rate of leaching and mineral alterations of the grout in the gas evacuation system is expected to be 5–10 times higher than that of the concrete in the lid, i.e. 50–100 mm/1 000 years. With a thickness of the lid of 600 mm this means that the gas evacuation system will be depleted from portlandite at about 6 000–12 000 years post-closure. Through continued leaching, also the CSH-phases will slowly be depleted. However, the rate of this transformation will be controlled by the cohesion of the material where disintegration will lead to a faster degradation rate than if the material remains reasonably structurally intact.

### 9.8.2 Load-bearing capacity

The load-bearing capacity of the gas evacuation system is not relevant. This is because the dimensions of this system are small and that it therefore cannot be expected to carry any external or internal loads even though the material itself has some inherent strength.

From Section 3.4.2 the 28 days compressive strength of the *New silo grout* is just above 5 MPa. Through leaching and mineral alterations, the compressive strength will decrease and from about 10 000 years post-closure the grout will have the compressive strength of that of a compacted multi-graded material.

### 9.8.3 Transport properties

The transport properties of the gas evacuation system at closure will be controlled by the properties of the material used to fill these channels. In this section it is assumed that the *New silo grout*, Section 3.4.2, with an initial hydraulic conductivity of $5 \times 10^{-9}$ m/s is used.

The evolution of porosity of the previously planned permeable grout in 1BMA studied by Cronstrand (2007) can serve as a representative example also for 2BMA. According to Cronstrand (2007, Appendix B, Figure B-70) the porosity of the permeable grout in 1BMA follows a similar trend as that of the waste compartment with a maximum porosity at the interface between these two components of about 45 %. With a 45 % porosity, the gas evacuation system at the time of complete degradation of the cement minerals is expected to have the transport properties of the aggregate material, i.e. sand with a grain size of 0–4 mm. According to Kennedy et al. (1984) the hydraulic conductivity of such a material is about $1 \times 10^{-2}$ m/s.

Finally, the potential for clogging of the grout through precipitation of secondary minerals in the pore system or through accumulation of fines from the groundwater must be considered. For the grout, clogging of the pores due to precipitation of secondary minerals is not expected and therefore not discussed further here.

The impact of fines on the transport properties of the gas evacuation system has not been studied for 2BMA. However, in order to dramatically influence the transport properties of this system, the fines must be firmly attached within the pore system of the grout, not to be expelled by the pressure from the gases or by groundwater transport.

For 2BMA, a certain amount of fines will settle on top of the lid – including the top of the gas evacuation system – with time. This is because the surface of the crushed rock backfill material is expected to be covered by a thin layer of fines (unless carefully washed prior to backfilling) which will gradually detach from the rock material and settle on top of the lid through the act of gravity. Also, the intruding groundwater may contain some fines but the amounts are expected to be considerably smaller than that originating from the crushed rock backfill. In addition to the settled material, a portion of very fine-grained material will remain suspended in the groundwater.

Also, inside the concrete caisson, fines will form with concrete degradation as the most probable source. During this process, the fines which are not small enough to remain suspended in the groundwater will slowly fall through the groundwater and collect on top of the slab. This means that the groundwater will only contain a small amount of very fine-grained material.

Whether a fine is prone to clog a pore in the grout of the gas evacuation system or not will be dependent on its dimensions. Of the material settled on the lid, the more coarse-grained fines are unlikely to clog the pores whereas the finer could enter the pore system and become stuck. The likely implication of this is that the suspended fines are more likely to cause clogging of the pore system than the settled material.

However, the risk for clogging of the gas evacuation is not only dependent on the amount and size of the fines but also on the direction of groundwater flow and impact of an internal gas pressure. Here, Elfwing et al. (2017) show that the direction of the groundwater through the gas evacuation system is dependent on the position of the holes in the lid with respect to the direction of groundwater flow in the waste vault. For a gas evacuation system with the row of holes in the lid perpendicular to the groundwater flow, groundwater flow will be inwards. For a row of holes in the same direction as the groundwater flow, the direction of flow will vary with inwards flow in some holes and outwards flow in others.

In all this means that the risk for clogging of the gas evacuation system though clogging of the pores by suspended fines in the groundwater cannot be neglected. This is because such particles will be found in the groundwater both on the outside and on the inside of the caissons and groundwater transport must proceed in either of these directions. However, in order to present a well-based conclusion, a deeper understanding of groundwater flow through the gas evacuation system and particle distribution in the groundwater is required.

### 9.8.4 Recommended material property data

Table 9-7 presents recommended material property data for the gas evacuation system in the lid of the concrete caissons in 2BMA for selected time periods up to 100 000 years post-closure. The recommendations are based on the expected status of the gas evacuation system at closure presented in Section 6.3, the expected evolution of the properties of the gas evacuation system described in the previous sections and the properties for degraded concrete given in Section 5.1.

**Table 9-7. Recommended material property data for the gas evacuation system in 2BMA for selected time periods up to 100 000 years post-closure.**

| | | Time period (Years post-closure) | | | | |
|---|---|---|---|---|---|---|
| **Property** | **Unit** | **At closure** | **0–1 000** | **1 000–5 000** | **5 000–50 000** | **50 000–100 000** |
| **pH** | - | ≥ 13 | 12.5–13 | 11–12.5 | 10–11 | ≤ 10 |
| **Porosity** | % | 30 | 30 | 30–35 | 35–40 | ≥ 40 |
| **Load-bearing capacity** | Rating (5–1) | Not relevant | Not relevant | Not relevant | Not relevant | Not relevant |
| **Hydraulic conductivity** | m/s | $(5–20) \times 10^{-9}$ | $(5–20) \times 10^{-9}$ | $10^{-9}–10^{-5}$ | $10^{-5}–10^{-2}$ | $10^{-2}$ |
| **Diffusivity** | $m^2/s$ | $(1–5) \times 10^{-11}$ | $(1–5) \times 10^{-11}$ | $10^{-11}–10^{-10}$ | $10^{-10}–10^{-9}$ | $10^{-9}$ |

### 9.8.5 Specific uncertainties

The following specific uncertainties in the description of the evolution of the properties of the gas evacuation system during the first 100 000 years post-closure have been identified:

- The main source of uncertainty originates from the lack of detailed understanding of the evolution of the mineral composition of the permeable grout and its impact on the transport properties. The model used by Cronstrand (2007) for 1BMA does not provide sufficient information to be used in an assessment of the evolution of the properties of the gas evacuation system in 2BMA with sufficient accuracy.
- Also, there do remain some uncertainties regarding the risk for clogging of the gas evacuation system through accumulation of fines in the pore system of the grout.

See also the discussion concerning the general uncertainties in Chapter 5.

## 9.9 Concrete moulds

### 9.9.1 Chemical properties

The post-closure evolution of the chemical properties of the concrete moulds in 2BMA will follow that of the inner walls outlined in Section 9.6. According to Figures 9-4 and 9-5, portlandite will be present in the interior of the caissons and pH therefore at about 12.5 up to 100 000 years post-closure. Also, according to SKB (R-18-07) none of the concrete moulds in 2BMA will contain evaporator concentrates and the influence of high concentrations of salt on the post-closure evolution of the chemical properties of the concrete moulds in 2BMA can therefore be disregarded.

However, Figures 9-4 and 9-5 does not show the impact of cracking and a possible loss of the structural integrity of the outer walls and lid (Sections 9.4 and 9.5). If also this process is included, a higher degradation rate of the concrete moulds must be expected.

### 9.9.2 Load-bearing capacity

According to SKB (R-18-07), the waste in the concrete moulds in 2BMA mainly comprise scrap, sludge and minor amounts of metals but only minor amounts of evaporator concentrate (waste category R:29:00). Because of this, loads from processes involving these waste categories are not expected to exceed the load-bearing capacity of the concrete moulds and cracking is therefore not expected. Instead, external loads will constitute the main risk for cracking of the concrete moulds.

The evolution of the load-bearing capacity of the concrete moulds will initially be affected by rebar corrosion and spalling of the covering layer. However, according to Bultmark (2017a), the load-bearing capacity of the concrete moulds will be sufficient to carry the weight of a stack of concrete moulds with a height of 80 meters even after spalling of the covering layer. See also Section 8.9.2.

Once the function of the reinforcement bars has been lost, the evolution of the load-bearing capacity of the concrete moulds will be determined by the rate of mineral alterations in the concrete. According to Figures 9-1 to 9-5, alterations of the mineral composition inside the caissons are slow and portlandite will be present up to 100 000 years post-closure.

However, with the loss of the structural integrity of the outer walls and lid (Sections 9.4 and 9.5), both the rate of degradation and the risk for mechanical damage of the concrete moulds will increase. The consequence of this is that cracking of the concrete moulds must be expected from about 20 000 years post-closure even though cracking of all concrete moulds will probably not occur, Sections 9.4 and 9.5. Beyond 50 000 years post-closure, extensive cracking of the concrete moulds must be expected.

### 9.9.3 Transport properties

The transport properties of the concrete moulds during the initial period post-closure will be basically the same as those of the concrete moulds at closure, Section 6.3.1. However, according to Section 9.9.2, cracking which will affect the transport properties of the concrete moulds must be expected from about 20 000 years post-closure. With time, the load-bearing capacity of the concrete moulds will eventually be lost and from that point in time the transport properties will correspond to those of severely cracked concrete.

### 9.9.4 Recommended material property data

Table 9-8 presents recommended material property data for the concrete moulds in 2BMA for selected time periods up to 100 000 years post-closure. The recommendations are based on information on the status of the concrete moulds at closure presented in Section 6.3, the expected evolution of the properties of the concrete moulds described in the previous sections and the properties for degraded concrete given in Section 5.1.

**Table 9-8. Recommended material property data for concrete moulds in 2BMA for selected time periods up to 100 000 years post-closure.**

| | | Time period (Years post-closure) | | | | |
|---|---|---|---|---|---|---|
| **Property** | **Unit** | **At closure** | **0–1 000** | **1 000–20 000** | **20 000–50 000** | **50 000–100 000** |
| **pH** | - | ≥ 13 | ≥ 13 | 12.5–13 | 12.5 | 12–12.5 |
| **Porosity** | % | 11–13 | 11–13 | 11–13 | 12–13 | 13–16 |
| **Load-bearing capacity** | Rating (5–1) | 5 | 5 | 3–5 | 2–3 | 1–2 |
| **Hydraulic conductivity** | m/s | $(1–5)\times10^{-12}$ | $(1–5)\times10^{-12}$ | $(1–5)\times10^{-12}$ | $10^{-12}$–$10^{-5}$ | $10^{-5}$–$10^{-2}$ |
| **Diffusivity** | $m^2/s$ | $(2–5)\times10^{-12}$ | $(2–5)\times10^{-12}$ | $(5–9)\times10^{-12}$ | $10^{-12}$–$10^{-11}$ | $10^{-11}$–$10^{-9}$ |

### 9.9.5 Specific uncertainties

The following specific uncertainties in the description of the post-closure evolution of the properties of the concrete moulds in 2BMA during the first 100 000 years post-closure have been identified:

- The main uncertainty regards the magnitude of the internal loads caused by processes in the waste on the evolution of the transport properties of the concrete moulds. Here, the presence and volume of any internal expansion volume that could accommodate the increased volume from swelling waste will be important to reduce the risk for cracking and degradation of the transport properties of the concrete moulds.
- The post-closure evolution of the chemical properties is associated with small uncertainties except for the evolution of a number of concrete moulds from Ringhals (Waste category R.29:00) which each contains up to 700 kg of evaporator concentrates (SKB R-18-07). In order to reduce the impact of high concentrations of salt on the concrete barriers, each concrete mould also contains additional 800 kg of cement as a conditioning material (SKB R-18-07). As a comparison, Figures 4-7 and 4-8 show the mineral evolution in 1BMA for a case where high-carbonate waste is conditioned in cement and bitumen respectively. These figures show that mineral alterations on the inside of the concrete barrier is more significant for bituminised waste than for cement-conditioned waste. Cronstrand (2010) concludes that "*The local acceleration of degradation mechanisms due to carbonation is predicted to be substantial for bituminized waste matrices but non-significant for cementitious waste forms of similar carbon content*".

See also the discussion concerning the general uncertainties in Chapter 5.

# 10 1BRT: post-closure evolution

In this chapter, the expected evolution of the properties of the cementitious components in 1BRT during the first 100 000 years post-closure is described. The starting point for the descriptions is the expected status of the cementitious components in 1BRT at closure presented in Section 6.4. The evolution of the properties of the cementitious components in 1BRT is then influenced by the processes presented in Chapter 4.

Detailed descriptions of the cementitious components in 1BRT are given in Section 2.8. In addition, Chapter 3 presents detailed specifications and properties of the cementitious materials in the various components in 1BRT.

## 10.1 Literature

The following reports form the basis for the description of the post-closure evolution of the properties of the cementitious components in 1BRT presented in this chapter:

- **Höglund (2014)** modelled the evolution of the concrete structures in 1BMA and 2BMA which can serve as representative examples when evaluating the post-closure evolution of the concrete structure in 1BRT.
- **Höglund (2018)** modelled the pH evolution in 1BRT.
- **Höglund (2019)** modelled the pH evolution in 2BMA.
- **Idiart et al. (2019a)** modelled the influence of concrete mixing proportions for different types of concrete used in SFR on the evolution of the properties of concrete in the rock vault for core components (BHK) in SFL.
- **Lagerblad et al. (2017)** and **Mårtensson and Vogt (2019, 2020)** presents material property data of the 2BMA concrete expected to be used in the concrete caissons in 2BMA.
- **Mårtensson (2017)** evaluated the impact of degradation processes on the load-bearing capacity of the concrete structure in 1BMA under the assumption that the concrete structure had been repaired prior to closure as well as of the concrete caissons in 2BMA.
- **Olsson (2016a)** calculated the resistance of the outer walls of 1BMA against internal loads from swelling waste and a high gas pressure which can be used as a representative example for 1BRT.
- **Rosenberg** modelled the effect of rock fall-out on the structural integrity of the concrete structure in 1BRT.[63]
- **Villar et al. (2019)** performed an experimental investigation of the properties of 2BMA concrete specimens manufactured by Mårtensson and Vogt (2019).
- **von Schenck and Bultmark (2014)** calculated the resistance of the outer walls of 1BMA against internal loads from swelling waste

[63] SKBdoc 1908329 ver 1.0. (Internal document, in Swedish.)

## 10.2 Slab

### 10.2.1 Chemical properties

The post-closure evolution of the chemical properties of the slab of the concrete structure in 1BRT will broadly follow that previously outlined for the outer walls of the concrete caissons in 2BMA, Section 9.4. This is because the slab in 1BRT – similar to the outer walls in 2BMA – is in contact with groundwater saturated crushed rock on one side and the waste compartment which contains large amounts of cementitious materials on the other side. In addition to this, *2BMA concrete* (Section 3.3.3) is expected to be used in both 1BRT and 2BMA, Sections 2.8 and 2.7.

From the information presented in Section 9.4, the average chemical properties of the slab in 1BRT are expected to be controlled by the presence of portlandite up to about 50 000 years post-closure. From this period and onwards, pH will be controlled by the slow transformation of the CSH-phases.

This is in accordance with the findings by Höglund (2018) who showed that pH in 1BRT will remain above 12 for at least 25 000 years. However, the model used by Höglund (2018) did not include the effect of diffusion and mass transport but instead consider the limit of infinite diffusivity where all of the concrete is in direct contact with all of the water in the waste vault. For that reason, this model probably overestimates the transformation rate of the cement minerals.

### 10.2.2 Load-bearing capacity

During the first 1 000 years post-closure, rebar corrosion will lead to a reduced capacity of the reinforcement bars and spalling of the covering layer on the underside of the slab, estimated to a maximum of about 50 mm of concrete. However, being founded on a bed of carefully compacted crushed rock material, this will not influence the capacity of the slab to resist the homogeneous compressive load from the grouted waste packages.

From Höglund (2018, 2019), concrete degradation is very slow in the slab, Figures 9-1 to 9-5, and some portlandite will remain even at 100 000 years post-closure (Figure 9-5). According to Babaahmadi (2015) the compressive strength of portlandite depleted concrete is just below 10 MPa. This value exceeds the compressive load from the grouted waste packages by a significant margin.

The load-bearing capacity of the slab will therefore be sufficient to resist the compressive load from the grouted waste packages up to at least 50 000 years post-closure. From this also follows that the probability for the formation of penetrating cracks in the slab due to compressive loads will be low during this period even though this requires that significant settlements in the foundation layer do not occur. The probability for such settlements is considered to be low due to expected careful compaction of the foundation layer during construction.

Eventually all portlandite will be dissolved and transformation of the CSH-phases starts. However, in spite of this, the load-bearing capacity of the slab against compressive loads should still be sufficient to prevent cracking.

In all, the load-bearing capacity of the slab in 1BRT will probably be sufficient to carry the homogeneous compressive load from the grouted waste packages up to 100 000 years post-closure. Tensile loads are not expected to affect the slab post-closure.

### 10.2.3 Transport properties

The evolution of the transport properties of the slab of the concrete structure in 1BRT is controlled by the presence of cracks whereas the influence of porosity changes due to mineral alterations is limited.

According to Section 10.2.2, the risk for cracking due to insufficient load-bearing capacity of the slab is low. The transport properties of the slab are therefore expected to be similar to those of the slab at closure up to and possibly beyond 50 000 years post-closure.

However, from Sections 2.8.2 and 6.4.1, the formation of cracks must be expected already during construction of the slab. This is because the slab does not formally constitute a significant hydraulic barrier and the use of such construction methods to prevent cracking during construction is therefore currently not prescribed.

Through continued transformation of the cement minerals, the transport properties of the slab will be affected by an increasing number of cracks from about 50 000 years post-closure.

### 10.2.4 Recommended material property data

Table 10-1 presents recommended material property data for the slab in 1BRT for selected time periods up to 100 000 years post-closure. The recommendations are based on information regarding the status of the slab at closure presented in Section 6.4, the expected evolution of the properties of the slab described in the previous sections and the properties for degraded concrete given in Section 5.1.

**Table 10-1. Recommended material property data for the slab in 1BRT for selected time periods up to 100 000 years post-closure.**

| | | Time period (Years post-closure) | | | | |
|---|---|---|---|---|---|---|
| **Property** | **Unit** | **At closure** | **0–1 000** | **1 000–20 000** | **20 000–50 000** | **50 000–100 000** |
| **pH** | - | ≥ 13 | ≥ 13 | 12.5 –13 | 12.5 | 12–12.5 |
| **Porosity** | % | 11–13 | 11–13 | 11–13 | 12–14 | 14–17 |
| **Load-bearing capacity** | Rating (5–1) | 5 | 5 | 4–5 | 3–4 | 3 |
| **Hydraulic conductivity** | m/s | $10^{-11}$–$10^{-8}$ | $10^{-11}$–$10^{-8}$ | $10^{-11}$–$10^{-8}$ | $10^{-7}$–$10^{-4}$ | $10^{-4}$–$10^{-3}$ |
| **Diffusivity** | $m^2/s$ | (2–5) × $10^{-12}$ | (2–5) × $10^{-12}$ | (2–5) × $10^{-12}$ | (5–9) × $10^{-12}$ | $10^{-11}$–$10^{-10}$ |

### 10.2.5 Specific uncertainties

The following specific uncertainty in the description of the evolution of the properties of the slab in 1BRT during the first 100 000 years post-closure has been identified:

- The main uncertainty relates to the fact that the slab does not formally constitute a significant hydraulic barrier and that the use of construction methods that prevent cracking during construction are therefore currently not prescribed. The consequence of this is that the hydraulic conductivity of the slab at closure as well as its evolution post-closure are somewhat uncertain. The consequence of these uncertainties are, however, judged to be limited because the entire waste domain constitutes a concrete monolith with an expected very slow degradation.

See also the discussion concerning the general uncertainties in Chapter 5.

## 10.3 Outer walls

### 10.3.1 Chemical properties

The post-closure evolution of the chemical properties of the outer walls of the concrete structure in 1BRT will broadly follow that of the outer walls of the concrete caissons in 2BMA, Section 9.4. This is because the outer walls in 1BRT – just like the outer walls in 2BMA – are surrounded by crushed rock backfill material and that the waste compartments contain large amounts of cementitious materials. However, for 1BRT, a somewhat slower degradation is expected since the waste domain constitutes a concrete monolith and leaching and mineral alterations on the inside of the outer walls thus prevented. In addition to this, *2BMA concrete* (Section 3.3.3) is expected to be used in both 1BRT and 2BMA, Sections 2.8 and 2.7.

With reference to Section 9.4, the average chemical properties of the outer walls in 1BRT will be controlled by the presence of portlandite up to, but probably also beyond, 50 000 years post-closure. Beyond this, pH will be controlled by the slow transformation of the CSH-phases.

This is in accordance with the findings by Höglund (2018) who showed that pH in 1BRT will remain above 12 for at least 25 000 years. However, the model used by Höglund (2018) did not include the effect of diffusion and mass transport. For that reason, this model probably overestimates the transformation rate of the cement minerals.

In all, the average chemical properties of the outer walls in 1BRT will be controlled by the presence of portlandite during at least up to 50 000 years post-closure. From this period and onwards, pH will be controlled by the slow transformation of the CSH-phases.

### 10.3.2 Load-bearing capacity

#### *External loads*

The load-bearing capacity of the outer walls against external loads will be sufficient during a considerable period of time. This is because the outer walls are mechanically supported by the waste packages and inner walls between the waste packages which together forms a concrete monolith. The large amounts of concrete inside the waste compartments also prevents degradation on the inside of the outer walls as well as reduces the risk for spalling of the concrete covering layer due to corrosion of the reinforcement bars.

As a special case, the capacity of the outer walls against rock fall-out was studied by Rosenberg.[64] The study concluded that the risk for cracking was low but that for some unfavourable conditions, the probability for the formation of a few small penetrating cracks must not be disregarded.

In all, the load-bearing capacity of the outer walls against external loads will be sufficient to prevent the formation of penetrating cracks up to at least 50 000 years post-closure. Beyond this point in time, the cohesion of the concrete will be reduced due to concrete degradation. However, the risk for fall-out of larger pieces of concrete is limited thanks to internal and external support from the materials in the waste domain and backfill material respectively.

#### *Internal loads*

The load-bearing capacity against internal loads has not been explicitly studied for 1BRT. Instead, the studies for 1BMA conducted by Olsson (2016a) and von Schenck and Bultmark (2014) can serve as representative examples. These studies – which both included grouting of the waste packages prior to closure – concluded that the risk for cracking of the external construction parts is considerable. The studies also concluded that sufficient expansion volume must be provided inside the waste packages to prevent significant expansion of these.

For 1BRT, these studies indicate that the risk for the formation of penetrating cracks in the outer concrete structure due to e.g. the formation of voluminous corrosion products in the waste must be considered. However, the effect of this process will be dependent on the conditioning method used and if expansion cassettes are installed in the waste packages as e.g. in some of the waste packages in the silo.

### 10.3.3 Transport properties

According to Section 6.4.1, the transport properties of the outer walls of the concrete structure in 1BRT at closure are difficult to determine. This is because they are dependent on the detailed method of construction and the associated risk for formation of cracks, casting joints or other permeable zones. For that reason, cracks or permeable construction joints are expected already at closure of 1BRT.

From Section 10.3.2, cracking due to external loads is not expected during the first 50 000 years post-closure thanks to the mechanical support from the waste compartment. In addition, Section 10.3.2 also notes that the impact of corroding metallic waste will be dependent on the available expansion volume within the waste packages. According to SKB (R-18-07), the waste for 1BRT (segmented reactor pressure vessels) will be placed in steel moulds which are also filled with a cementitious material (grout or concrete). However, no information concerning internal expansion volume is provided. For this reason, corrosion presents a non-negligible risk for cracking of the outer walls.

[64] SKBdoc 1908329 ver 1.0. (Internal document, in Swedish.)

The impact of tie rod corrosion has been studied by Höglund (2014). The study showed that cracks may start to form around a tie rod already at small corrosion depths but also that the length and width of these cracks are dependent on the distance from the corroding component to the concrete surface. From this follows that corrosion of tie rods (if such are used) may cause the formation of penetrating cracks in the outer walls but for tie rods at some distance from the edge of the walls, cracking will probably be limited.

In all, the findings presented above suggest that the transport properties of the outer walls during the initial period post-closure will be the same as those at closure. Through corrosion of tie rods, cracks will form in the walls but the impact of this on the transport properties of the walls is uncertain. Finally, corrosion of metallic waste may cause further cracking. However, the consequence of this is uncertain because the detailed conditioning methods have yet not been decided.

### 10.3.4 Recommended material property data

Table 10-2 presents recommended material property data for the outer walls in 1BRT for selected time periods up to 100 000 years post-closure. The recommendations are based on information regarding the status of the outer walls at closure presented in Section 6.4, the expected evolution of the properties of the outer walls described in the previous sections and the properties for degraded concrete given in Section 5.1.

**Table 10-2. Recommended material property data for the outer walls of the concrete structure in 1BRT for selected time periods up to 100 000 years post-closure.**

| | | Time period (years post-closure) | | | | |
|---|---|---|---|---|---|---|
| **Property** | **Unit** | **At closure** | **0–1 000** | **1 000–20 000** | **20 000–50 000** | **50 000–100 000** |
| **pH** | - | ≥ 13 | ≥ 13 | 12.5–13 | 12.5 | 12–12.5 |
| **Porosity** | % | 11–13 | 11–13 | 11–13 | 13–15 | 15–20 |
| **Load-bearing capacity** | Rating (5–1) | 5 | 5 | 3–5 | 2–3 | 2 |
| **Hydraulic conductivity** | m/s | $10^{-11}$–$10^{-8}$ | $10^{-11}$–$10^{-8}$ | $10^{-11}$–$10^{-8}$ | $10^{-7}$–$10^{-4}$ | $10^{-4}$–$10^{-3}$ |
| **Diffusivity** | $m^2/s$ | (2–5) × $10^{-12}$ | (2–5) × $10^{-12}$ | (2–5) × $10^{-12}$ | (5–9) × $10^{-12}$ | $10^{-11}$–$10^{-10}$ |

### 10.3.5 Specific uncertainties

The following specific uncertainties in the description of the evolution of the properties of the outer walls in 1BRT during the first 100 000 years post-closure have been identified:

- There remain significant uncertainties regarding the detailed construction method for the outer walls in 1BRT. These uncertainties originate from the fact that the outer walls do not formally constitute a hydraulic barrier and the use of construction methods that prevent the formation of cracks, joints or other permeable zones are not prescribed. In addition, tie rods may also be used during construction and there is therefore a potential risk that tie rod corrosion will influence the transport properties of the outer walls.
- Also, the impact of internal loads adds additional uncertainties. This is because the consequence of metal corrosion inside the waste packages will be dependent on the conditioning method used for the waste.

See also the discussion concerning the general uncertainties in Chapter 5.

## 10.4 Lid

### 10.4.1 Chemical properties

The post-closure evolution of the chemical properties of the lid will follow that of the outer walls described in Section 10.3.1 and is not repeated here. This is because the lid will be made from a similar type of concrete as the outer walls, but also because the lid will be exposed to the same chemical environment.

### 10.4.2 Load-bearing capacity

The load-bearing capacity of the lid against the compressive load from the backfill material will be sufficient for a very long period of time. This is because the lid rests on the prefabricated concrete elements which in turn rest on the waste packages and inner walls.

According to Section 2.8.2, the lid will be 500 mm thick even though this has not been finally settled. With portlandite leaching according to Figure 8-6, portlandite will be present in the lid for about 50 000 years. However, complete degradation of the lid is not expected until beyond 100 000 years post-closure. The consequence of this is that the compressive strength of the concrete in the lid will exceed the load from the backfill material up to 100 000 years post-closure.

However, the load-bearing capacity of the lid as such is also dependent on the support from the inner walls between the waste packages and the waste packages. At this stage though, it cannot be clearly stated that this support can be relied on up to 100 000 years post-closure. This is because of the uncertain influence of corrosion of waste and waste packaging. Even though the large amounts of material in the waste compartment will prevent loss of structural integrity of the lid, the load-bearing capacity of the lid will probably be insufficient to prevent cracking from about 50 000 years post-closure.

Finally, the potential that expanding waste will displace (lift) the lid must be considered. To prevent this, the lid must be securely fastened in the outer walls. However, the impact of this process can only be speculated upon and it is therefore not discussed further in this report.

### 10.4.3 Transport properties

The transport properties of the lid of the concrete structure in 1BRT at the time of closure are uncertain, Section 6.4.1. This is because they are dependent on the detailed method of construction and the associated risk for formation of cracks, casting joints or other permeable zones. For that reason, the presence of cracks or permeable construction joints must be expected already at closure of 1BRT.

According to Section 10.4.2, cracking due to external loads from the backfill material is not expected to cause the formation of any penetrating cracks during the first 50 000 years post-closure thanks to the support from the monolithic waste compartment. However, beyond this period in time, additional cracking must be expected.

Section 10.4.2 also notices that the impact of corroding metallic waste will be dependent on the available expansion volume within the waste packages. This is because no empty volume exists between the waste packages. However, as the conditioning method has not yet been decided the impact of corroding waste on the transport properties of the lid remains uncertain.

In all, the findings presented above suggest that the transport properties of the lid will be similar to those at closure during the first 50 000 years post-closure. Through corrosion of metallic waste, additional cracking will occur. However, as noted in Section 10.4.2, a complete collapse of the lid is not expected thanks to the large amounts of material in the waste compartments.

### 10.4.4 Recommended material property data

Table 10-3 presents recommended material property data for the lid in 1BRT for selected time periods up to 100 000 years post-closure. The recommendations are based on information regarding the status of the lid at closure presented in Section 6.4.1, the expected evolution of the properties of the lid described in the previous sections and the properties for degraded concrete given in Section 5.1.

**Table 10-3. Recommended material property data for the lid of the concrete structure in 1BRT for selected time periods up to 100 000 years post-closure.**

| | | Time period (Years post-closure) | | | | |
|---|---|---|---|---|---|---|
| **Property** | **Unit** | **At closure** | **0–1 000** | **1 000–20 000** | **20 000–50 000** | **50 000–100 000** |
| **pH** | - | ≥ 13 | ≥ 13 | 12.5–13 | 12–12.5 | 11–12 |
| **Porosity** | % | 11–13 | 11–13 | 11–14 | 12–15 | 15–20 |
| **Load-bearing capacity** | Rating (5–1) | 5 | 5 | 4–5 | 3–4 | 2–3 |
| **Hydraulic conductivity** | m/s | $10^{-11}$–$10^{-8}$ | $10^{-11}$–$10^{-8}$ | $10^{-11}$–$10^{-8}$ | $10^{-7}$–$10^{-4}$ | $10^{-4}$–$10^{-3}$ |
| **Diffusivity** | $m^2/s$ | (2–5) × $10^{-12}$ | (2–5) × $10^{-12}$ | (2–5) × $10^{-12}$ | (5–9) × $10^{-12}$ | $10^{-11}$–$10^{-10}$ |

### 10.4.5 Specific uncertainties

The following specific uncertainties in the description of the evolution of the properties of the lid of the concrete structure in 1BRT during the first 100 000 years post-closure have been identified:

- There remain some uncertainties regarding the detailed construction method for the lid in 1BRT. These uncertainties originate from the fact that the lid does not formally constitute a hydraulic barrier and the use of construction methods that prevents the formation of cracks, joints or other permeable zones are currently not prescribed.
- The impact of internal loads is also somewhat uncertain. This is because the consequence of metal corrosion inside the waste packages will be dependent on the conditioning method used for the waste.
- Because the load-bearing capacity of the lid will rely on structural support from the monolithic waste compartment, uncertainties in the evolution of the properties of the components in the waste compartment also have to be accounted for.

See also the discussion concerning the general uncertainties in Chapter 5.

## 10.5 Inner walls between the waste compartments

### 10.5.1 Chemical properties

The post-closure evolution of the chemical properties of the inner walls between the waste compartments in 1BRT will broadly follow that outlined for the inner walls of the concrete caissons in 2BMA, Section 9.6. This assumption is justified by the fact that the inner walls between the waste compartments in 1BRT – just like the inner walls in 2BMA – are enclosed in a concrete structure that buffers the groundwater that enters the waste compartment and that the waste compartment contains large amounts of cementitious materials. However, for the inner walls between the waste compartments in 1BRT, additional protection against concrete degradation is provided by the inner walls between the waste packages and the waste packages which together forms a concrete monolith.

Figures 9-4 and 9-5 indicate that the average chemical properties of the inner walls between the waste compartments in 1BRT will be controlled by the presence of portlandite during up to 100 000 years post-closure.

However, in the rather unlikely event of early extensive cracking of the external concrete structure, the alteration rate of the chemical properties of the inner walls between the waste compartments will increase. Here, the study by Höglund (2018) can serve as an illustrative example of the degradation of severely cracked concrete. Using simple mass balance calculations and therefore not including the effect of diffusion and mass transport Höglund (2018) showed that pH in 1BRT will remain above 12 for at least 25 000 years.

As a reasonable average, it is suggested that the chemical properties of the inner walls between the waste compartments will be controlled by the presence of portlandite during at least up to 60 000 years post-closure even though probably beyond this. From this point in time, pH will be

controlled by the slow transformation of the CSH-gel with an expected lowest pH in the parts of the inner walls between the waste compartments closest to the external construction parts of 12 after 100 000 years.

### 10.5.2 Load-bearing capacity

The inner walls between the waste compartments constitute one part of the internal concrete monolith, also comprising the waste packages and the inner walls between the waste packages. For that reason, the load-bearing capacity of the inner walls between the waste compartments cannot be evaluated without considering also the other components mentioned.

The load-bearing capacity of the inner walls between the waste compartments against external loads from the groundwater pressure and backfill material will be sufficient for a very long period of time. This is because these walls are enclosed between the waste compartments which provide significant mechanical support but also because concrete degradation is very slow here.

However, for the inner walls between the waste compartments also loads from swelling waste must be considered. This is because the conditioning method for the metallic have has not yet been decided and any available expansion volume inside the waste packages uncertain.

For unfavourable conditions, Section 10.3.2 informs that swelling of waste due to e.g. metal corrosion poses a significant risk for cracking of the outer walls. However, for the inner walls between the waste compartments, the risk for cracking due to internal loads is lower. This is because the inner walls between the waste compartments are sandwiched between the waste compartments which each constitutes a concrete monolith with a high compressive strength. In addition, the consequences of metal corrosion can be mitigated by the use of a suitable conditioning method for the metallic waste.

In all, the load-bearing capacity of the inner walls between the waste compartments will be sufficient to prevent cracking during at least up to 50 000 years post-closure and the formation of penetrating cracks during this period is therefore not anticipated. From this point in time, the risk for cracking will increase but the fact that the inner walls between the waste compartments are sandwiched between the waste compartments ensures slow degradation.

### 10.5.3 Transport properties

According to Section 6.4.1, the presence of cracks in the inner walls between the waste compartments must be expected already at the end of the construction period. However, according to Section 10.5.2, the load-bearing capacity of the inner walls between the waste compartments will be sufficient to prevent the formation of additional penetrating cracks during at least up to 50 000 years post-closure. From this information follows that the average transport properties of the inner walls between the waste compartments are expected to be similar to those at closure during at least up to 50 000 years post-closure.

From about 50 000 years post-closure onwards, additional penetrating cracks may start to form as a consequence of corrosion of waste and waste packaging as well as concrete degradation. The transport properties of the inner walls between the waste compartments will therefore have the characteristics of concrete with an increasing number of cracks, but which is otherwise structurally intact from this period and onwards.

### 10.5.4 Recommended material property data

Table 10-4 presents recommended material property data for the inner walls between the waste compartments in 1BRT for selected time periods up to 100 000 years post-closure. The recommendations are based on information regarding the status of the inner walls between the waste compartments at closure presented in Section 6.4, the expected evolution of the properties of these walls described in the previous sections and the properties for degraded concrete given in Section 5.1.

**Table 10-4. Recommended material property data for the inner walls between the waste compartments in the concrete structure in 1BRT for selected time periods up to 100 000 years post-closure.**

| | | Time period (years post-closure) | | | | |
|---|---|---|---|---|---|---|
| **Property** | **Unit** | **At closure** | **0–1 000** | **1 000–20 000** | **20 000–50 000** | **50 000– 100 000** |
| **pH** | - | ≥ 13 | ≥ 13 | 12.5–13 | 12.5 | 12–12.5 |
| **Porosity** | % | 11–13 | 11–13 | 11–13 | 12–13 | 13–15 |
| **Load-bearing capacity** | Rating (5–1) | 5 | 5 | 4–5 | 3–4 | 2–3 |
| **Hydraulic conductivity** | m/s | $10^{-11}$–$10^{-8}$ | $10^{-11}$–$10^{-8}$ | $10^{-11}$–$10^{-8}$ | $10^{-11}$–$10^{-6}$ | $10^{-6}$–$10^{-4}$ |
| **Diffusivity** | $m^2/s$ | (2–5) × $10^{-12}$ | (2–5) × $10^{-12}$ | (2–5) × $10^{-12}$ | (5–9) × $10^{-12}$ | (1–5) × $10^{-11}$ |

### 10.5.5 Specific uncertainties

The following specific uncertainties in the description of the evolution of the properties of the inner walls between the waste compartments of the concrete structure in 1BRT during the first 100 000 years post-closure have been identified:

- There remain some uncertainties regarding the detailed design of the waste packaging for the metallic waste and the presence of expansion volume that could prevent external swelling of the waste packages in the case of e.g. extensive metal corrosion.
- There also remains some uncertainties concerning the use of steel tie rods during construction and whether such will be left in the concrete structure or not. In the case that steel tie rods are used and left in the walls after construction, cracks or channels can form at a much earlier stage than predicted above. The influence of tie rod corrosion was also discussed in Section 10.3.3.

See also the discussion concerning the general uncertainties in Chapter 5.

## 10.6 Inner walls between the waste packages

### 10.6.1 Chemical properties

The evolution of the average chemical properties of the inner walls between the waste packages is in all major aspects expected to follow that of the inner walls between the waste compartments outlined in Section 10.5.1 and is not repeated here.

### 10.6.2 Load-bearing capacity

The inner walls between the waste packages constitute one part of the waste compartment monolith, also comprising the waste packages and the inner walls between the waste compartments. Because of this, the evolution of the load-bearing capacity of the inner walls between the waste packages cannot be evaluated without considering also the other components mentioned.

In comparison with the inner walls between the waste compartments, the tensile strength of the inner walls between the waste packages will be lower because of the lack of reinforcement. The impact of this is a lower resistance against tensile loads caused by e.g. swelling of waste.

However, the risk for cracking due to swelling waste packages can be mitigated by ensuring that sufficient internal volume is provided inside the waste packages to accommodate the increased volume caused by the formation of corrosion products. Under these circumstances, the mechanical support from the waste packages and the inner walls between the waste compartments will ensure that the load-bearing capacity of the inner walls between the waste packages is sufficient to resist also the external loads from the backfill material during a significant portion of the first 100 000 years post-closure.

According to Section 10.5.1, portlandite will be present in the waste compartment during at least up to 60 000 years post-closure, but probably considerably longer. Because of this, the compressive strength of the concrete in the inner walls between the waste packages will be significant during this

period. From the time when the structural integrity of the external concrete structure is lost, the rate of alterations will increase. However, the structural integrity of the inner walls between the waste packages is not expected to be compromised even though additional cracks may form.

From this follows that the load-bearing capacity of the inner walls between the waste packages is expected to be sufficient to prevent extensive cracking or loss of structural integrity of these walls up to 100 000 years post-closure.

### 10.6.3 Transport properties

Section 6.4.1 suggests that formation of cracks in the inner walls between the waste packages must be expected already during construction of these walls. In addition to these cracks, cracks will also form as a consequence of concrete degradation and metal corrosion post-closure.

Because of this, the transport properties of the inner walls between the waste packages will have the characteristics of concrete with a number of cracks already from the time of closure. Through concrete degradation and metal corrosion, the number and width of cracks will increase, but a complete disintegration of the inner walls between the waste packages is not foreseen.

### 10.6.4 Recommended material property data

Table 10-5 presents recommended material property data for the inner walls between the waste packages in 1BRT for selected time periods up to 100 000 years post-closure. The recommendations are based on information regarding the status of the inner walls between the waste packages at closure presented in Section 6.4, the expected evolution of the properties of these walls described in the previous sections and the properties for degraded concrete given in Section 5.1.

**Table 10-5. Recommended material property data for the inner walls between the waste packages in 1BRT for selected time periods up to 100 000 years post-closure.**

| | | Time period (years post-closure) | | | | |
|---|---|---|---|---|---|---|
| **Property** | **Unit** | **At closure** | **0–1 000** | **1 000–20 000** | **20 000–50 000** | **50 000–100 000** |
| **pH** | - | ≥ 13 | ≥ 13 | 12.5–13 | 12.5 | 12–12.5 |
| **Porosity** | % | 11–13 | 11–13 | 11–13 | 13–15 | 15–18 |
| **Load-bearing capacity** | Rating (5–1) | 5 | 5 | 4–5 | 3–4 | 2–3 |
| **Hydraulic conductivity** | m/s | $10^{-10}$–$10^{-7}$ | $10^{-10}$–$10^{-7}$ | $10^{-10}$–$10^{-7}$ | $10^{-7}$–$10^{-5}$ | $10^{-5}$–$10^{-3}$ |
| **Diffusivity** | $m^2/s$ | $(2–5)\times10^{-12}$ | $(2–5)\times10^{-12}$ | $(5–9)\times10^{-12}$ | $(5–9)\times10^{-12}$ | $(1–5)\times10^{-11}$ |

### 10.6.5 Specific uncertainties

The following specific uncertainties in the description of the evolution of the properties of the inner walls between the waste packages of the concrete structure in 1BRT during the first 100 000 years post-closure have been identified:

- There remain some uncertainties regarding the detailed design of the waste packaging for the metallic waste and the presence of expansion volume that could prevent external swelling of the waste packages in the case of e.g. extensive metal corrosion. This will influence the evolution of the transport properties of the inner walls between the waste packages.
- There are also some uncertainties concerning the properties of these walls at closure. The main reason for this is the uncertain result of the casting process which will be dependent on concrete properties and distance between the waste packages. Experience from SFR1 here indicate that the actual distance between the waste packages not always corresponds to that specified in the instructions.

See also the discussion concerning the general uncertainties in Chapter 5.

## 10.7 Prefabricated concrete elements

### 10.7.1 Chemical properties

According to Figures 9-1 to 9-5 the chemical properties of the prefabricated concrete elements will be controlled by the presence of portlandite during a majority of the first 100 000 years post-closure.

However, in the rather unlikely event of early extensive cracking of the lid, the degradation rate of the chemical properties of the prefabricated concrete elements will increase. Here, the study by Höglund (2018) can serve as an illustrative example of the degradation of severely cracked concrete. Using simple mass balance calculations and therefore not including the effect of diffusion and mass transport, Höglund (2018) showed that pH in 1BRT will remain above 12 for at least 25 000 years.

As a reasonable average, it is predicted that the chemical properties of the prefabricated concrete elements will be controlled by the presence of portlandite during at least up to 60 000 to 70 000 years post-closure. After this point in time, pH will be controlled by the slow transformation of the CSH-gel with an expected lowest pH of 12 after 100 000 years.

### 10.7.2 Load-bearing capacity

The load-bearing capacity of the prefabricated concrete elements will be sufficient to carry the compressive load from the lid and the backfill material during a significant part of the first 100 000 years post-closure. This is because these loads are strictly compressive and the prefabricated concrete elements are supported by the concrete monolith inside the waste compartment.

However, later on, this support may not be entirely accounted for. This is because of the uncertain influence of corrosion of waste and waste packaging. Even though the large amounts of material inside the waste compartment will prevent a collapse of the prefabricated elements, their load-bearing capacity may probably not be guaranteed beyond 50 000 years post-closure, i.e. the same point in time as when the load-bearing capacity of the lid is expected to be partly lost.

### 10.7.3 Transport properties

The transport properties of the prefabricated concrete elements in 1BRT are evaluated for the elements as a group, i.e. also including the slits between the individual elements. This means that the hydraulic conductivity and effective diffusivity will be determined by the distance between the individual elements rather than by the properties of the concrete and degree of degradation. The transport properties of the prefabricated concrete elements will therefore have the characteristics of concrete with wide cracks already at closure and only through a loss of the structural integrity of the concrete structure, the effective diffusivity and hydraulic conductivity of the prefabricated concrete elements will increase. However, according to Section 10.7.2, this is not expected.

### 10.7.4 Recommended material property data

Table 10-6 presents recommended material property data for the prefabricated concrete elements in 1BRT for selected time periods up to 100 000 years post-closure. The recommendations are based on information regarding the status of the prefabricated concrete elements at closure presented in Section 6.4, the expected evolution of the properties of the prefabricated concrete elements described in the previous sections and the properties for degraded concrete given in Section 5.1.

**Table 10-6. Recommended material property data for the prefabricated concrete elements in 1BRT for selected time periods up to 100 000 years post-closure.**

| | | Time period (Years post-closure) | | | | |
|---|---|---|---|---|---|---|
| **Property** | **Unit** | **At closure** | **0–1 000** | **1 000–20 000** | **20 000–50 000** | **50 000–100 000** |
| **pH** | - | ≥ 13 | ≥ 13 | 12.5–13 | 12.5 | 12–12.5 |
| **Porosity** | % | 11–13 | 11–13 | 11–13 | 13–15 | 15–18 |
| **Load-bearing capacity** | Rating (5–1) | 5 | 5 | 4–5 | 3–4 | 2–3 |
| **Hydraulic conductivity** | m/s | $10^{-3}$ | $10^{-3}$ | $10^{-3}$ | $10^{-3}$ | $10^{-3}$ |
| **Diffusivity** | $m^2/s$ | $10^{-10}$ | $10^{-10}$ | $10^{-10}$ | $10^{-10}$ | $10^{-10}$ |

### 10.7.5 Specific uncertainties

The following specific uncertainty in the description of the post-closure evolution of the properties of the prefabricated concrete elements in 1BRT during the first 100 000 years post-closure has been identified:

- There remain some minor uncertainties regarding the duration of the period during which structural support from the components that constitute the concrete monolith of the waste compartment can be accounted for. Because the load-bearing capacity of the prefabricated concrete elements relies on structural support from this monolith, uncertainties in the evolution of the properties of these components have to be accounted for.

See also the discussion concerning the general uncertainties in Chapter 5.

# 11 1–2BTF: post-closure evolution

In this chapter, the expected evolution of the properties of the cementitious components in 1–2BTF during the first 100 000 years post-closure is described. The starting point for the description is the expected status of the cementitious components in 1–2BTF at closure as presented in Section 6.5. The evolution of the properties of the cementitious components in 1–2BTF is then influenced by the processes presented in Chapter 4.

Detailed descriptions of the cementitious components in 1–2BTF are given in Section 2.9. In addition, Chapter 3 presents detailed specifications and properties of the cementitious materials in the various components in 1–2BTF.

## 11.1 Literature

The following reports form the basis for the description of the post-closure evolution of the properties of the cementitious components in 1–2BTF presented in this chapter:

- **Bultmark (2017b)** calculated the influence of corrosion of the reinforcement bars and the subsequent spalling of the layer of concrete that covers the reinforcement on the load-bearing capacity of the concrete tanks.
- **Cronstrand (2007)** modelled the evolution of the mineral composition of the original concrete structure in 1BMA.
- **Cronstrand (2014)** modelled the evolution of pH the waste vaults in SFR1.
- **Eriksson** modelled the impact of a high groundwater pressure on the transport properties of the concrete tanks.[65]
- **Höglund (2014)** modelled the evolution of the concrete structure in 1BMA, including the planned repair measures.
- **Idiart et al. (2019a, 2019b)**, **Idiart and Shafei (2019)** and **Idiart and Laviña (2019)** modelled the post-closure evolution of the rock vault for reactor pressure vessels (BHK) in SFL for different types of concrete for up to 1 million years.
- **Könönen and Malm (2021)** modelled the load-bearing capacity of the concrete tanks.
- **Lundqvist** experimentally tested the load-bearing capacity of a concrete tank towards an external water pressure.[66]
- **Mårtensson (2017)** evaluated the impact of degradation processes of the load-bearing capacity of the repaired concrete structure in 1BMA and the concrete caissons in 2BMA.
- **Mårtensson (2021b)** studied the resistance of the concrete tanks towards intrusion of water.
- **Norvatek (The manufacturer of the concrete tanks)** provided information on the mixing proportions of the concrete currently used for the production of the concrete tanks as well as drawings.
- **Nytorp Jansson (2020a, 2020b)** modelled the load-bearing capacity of concrete slabs in the waste vaults in SFR.

[65] SKBdoc 2000080 ver 1.0. (Internal document, in Swedish.)

[66] SKBdoc 2000090 ver 1.0. (Internal document, in Swedish.)

## 11.2 Slabs

### 11.2.1 Chemical properties

The evolution of the chemical properties of the slabs in 1–2BTF will broadly follow that outlined for the slab in 1BMA, Section 8.2.1, with leaching mainly occurring from the underside of the slab which is in contact with the groundwater saturated foundation layer.

According to Figure 8-2, the concrete will be depleted of portlandite to a depth of about 300 mm already after 10 000 years. As this exceeds the total thickness of the slabs in 1–2BTF, which is only 250 mm, this model indicates that no portlandite will remain in the slabs from about 12 000–15 000 years post-closure. However, as a comparison, Figure 8-6 indicates a slower leaching rate with an average portlandite depletion rate of about 10 mm/1 000 years. From this follows that complete portlandite depletion of the slabs in 1–2BTF would occur at about 25 000 years post-closure. Leaching from the top of the slab will be considerably slower thanks to the protection provided by the grouted waste packages, the lid and cementitious backfill.

Leaching of the CSH-phases is slower than portlandite leaching and Figure 8-4 indicates that CSH_1.1 will be dominant CSH-phase in the slab still 100 000 years post-closure. According to Figure 4-5, the pH of concrete in which CSH_1.1 dominates is about 12.

However, this evolution does probably not fully include the influence of a physical breakdown of the slabs caused by rebar corrosion and cracking. For this reason, a somewhat faster chemical degradation can be expected even though the exact details are difficult to determine.

### 11.2.2 Load-bearing capacity

The load-bearing capacity of the slabs in 1–2BTF has been calculated by Nytorp Jansson (2020b). The study showed that the risk for cracking is dependent on the properties of the foundation layer and the distribution of the waste packages. Post-closure, a homogeneous distribution is predicted in this report. Unfortunately, no documentation has been found in which the methods used for preparation of the foundation layer or the properties thereof are reported. For this reason, Nytorp Jansson (2020b) performed a literature survey on the properties of compacted rock material. These studies indicate that it is reasonable to assume that the stiffness modulus of the foundation layer is sufficient to prevent cracking of the undegraded slabs in 1–2BTF.

The load-bearing capacity of the slabs in 1–2BTF is therefore expected to be sufficient to carry the homogeneous compressive load from the grouted waste packages for a significant part of the first 100 000 years post-closure even in the case of loss of function of the reinforcement bars.

This statement is supported by the slow concrete degradation and the fact that the slabs will retain some cement minerals still at 100 000 years post-closure, Figure 8-4. In addition, the compressive strength of the aggregates and cement minerals exceeds the comparatively small compressive loads from the grouted waste packages and backfill material by a significant margin.

However, the resistance of the severely degraded slabs against tensile loads is negligible and cracking will certainly be observed if settlements in the foundation layer occur. However, a complete loss of the structural integrity of the slabs is not expected.

### 11.2.3 Transport properties

According to Section 6.5.1, the slabs in 1–2BTF will have the transport properties of concrete with penetrating cracks already at closure.

Through continued leaching and rebar corrosion (Section 11.2.1), both the number and width of the cracks as well as the porosity of the slabs will increase. From this follows that the slabs will have the transport properties of severely degraded concrete with some retaining cohesion from about 25 000 years post-closure.

### 11.2.4 Recommended material property data

Table 11-1 presents recommended material property data for the slabs in 1–2BTF for selected time periods up to 100 000 years post-closure. The recommendations are based on information regarding the status of the slabs at closure presented in Section 6.5, the expected evolution of the properties of the slabs described in the previous sections and the properties for degraded concrete given in Section 5.1.

**Table 11-1. Recommended material property data for the slabs in 1–2BTF for selected time periods up to 100 000 years post-closure.**

| | | Time period (Years post-closure) | | | | |
|---|---|---|---|---|---|---|
| **Property** | **Unit** | **At closure** | **0–1 000** | **1 000–20 000** | **20 000–50 000** | **50 000–100 000** |
| **pH** | - | ≥ 13 | 12.5–13 | 12–12.5 | 11–12 | 10–11 |
| **Porosity** | % | 12–15 | 12–15 | 13–16 | 15–17 | 16–25 |
| **Load-bearing capacity** | Rating (5–1) | 5 | 5 | 4–5 | 3–4 | 2–3 |
| **Hydraulic conductivity** | m/s | $10^{-8}$–$10^{-5}$ | $10^{-5}$–$10^{-4}$ | $10^{-4}$–$10^{-3}$ | $10^{-4}$–$10^{-3}$ | $10^{-3}$–$10^{-2}$ |
| **Diffusivity** | $m^2/s$ | $(2–5)\times10^{-12}$ | $(2–5)\times10^{-12}$ | $(5–9)\times10^{-12}$ | $(1–5)\times10^{-11}$ | $10^{-10}$ |

### 11.2.5 Specific uncertainties

The following specific uncertainties in the description of the evolution of the properties of the slabs in 1–2BTF during the first 100 000 years post-closure have been identified:

- The main uncertainties relate to the prediction of the load-bearing capacity and the influence of the formation of penetrating cracks already during construction and the operational period on the transport properties of the slabs. This is because the properties of the foundation layer are not fully known.
- Also, the fact that the study by Cronstrand (2007), discussed here, rely on the composition of the *Silo concrete* and not the *1BMA concrete* adds some uncertainties on the evolution of the chemical properties of the slabs. However, the findings by Idiart et al. (2019a) suggest that the difference between the evolution of the *Silo concrete* and the *1BMA concrete* is small.

See also the discussion concerning the general uncertainties in Chapter 5.

## 11.3 Lids

### 11.3.1 Chemical properties

The evolution of the chemical properties of the concrete lids in 1–2BTF will broadly follow that of the outer walls in 2BMA, Section 9.4.1 since both these construction parts will be made from *2BMA concrete*.

With reference to Figures 9-1 to 9-5, alterations of the chemical properties of the lids in 1–2BTF will be slow and portlandite is expected to be present at least until 50 000 years post-closure. This, however, requires that the lids are structurally intact and that cracking has not occurred at an earlier stage as this will increase the degradation rate. Through continued degradation, the lids will finally be depleted from portlandite and, from Figure 9-6, CSH_1.6 is likely to be the dominant cement phase in the major part of the lids at 100 000 years post-closure with a pH of just below 12.3. This statement too is dependent on structurally intact lids.

However, the information in Section 11.3.2 implies that the structural integrity of the lids becomes uncertain beyond 20 000 years post-closure unless the thickness and amount of reinforcement is considerably increased compared to present plans, Section 2.9.2. For that reason, the risk for a faster degradation of the chemical properties must be accounted for.

### 11.3.2 Load-bearing capacity

The predicted evolution of the load-bearing capacity of the concrete lids in 1–2BTF presented in this section is broadly based on that outlined for the lid in 1BMA in Section 8.5.2.

Section 8.5.2 reports that a thickness of the lid of the concrete structure in 1BMA of 500 mm is sufficient to carry the weight from the crushed rock backfill if the lid also contains sufficient amounts of reinforcement. However, no information about the minimum required thickness and amount of reinforcement was found in the referred-to background material. Even though the span of the lid in 1–2BTF is somewhat shorter and the amount of backfill a little lower than in 1BMA, the same minimum thickness is assumed to be required also for these lids.

However, with an intended thickness of only 400 mm (Section 2.9.2), the load-bearing capacity of the lids in 1–2BTF will be insufficient already from an early stage and physical support from the grouted waste packages must therefore be relied upon. According to Bultmark (2017b) the load-bearing capacity of the concrete tanks will be sufficient to provide this support as long as they are not severely degraded. The properties of the concrete tanks and the uncertainties concerning their load-bearing capacity are discussed in Section 11.7.2.

In addition, the support from the grouted concrete tanks also requires that the channels formed by the steel pallets which separates the concrete tanks are entirely filled with grout. In the case that grouting is incomplete, the load-bearing capacity of the steel pallets will soon be lost. The consequence of this is a subduction of the concrete tanks by up to 400 mm (corresponding to the total height of two pallets) and also that the mechanical support of the lids is lost.

A special case concerns the part of the lid in 1BTF that rests on top of the grouted steel drums. According to studies by Könönen (SKBdoc 1904756, ver 1.0, internal document, in Swedish) and Olsson (SKBdoc 1889700, ver 1.0, internal document, in Swedish), the load-bearing capacity of the steel drums against the load from the lid and backfill material is uncertain.

In all, the load-bearing capacity of the lids in 1–2BTF with the design that is described in Section 2.9.2 is insufficient already at an early stage post-closure and physical support from the grouted concrete tanks and drums must be relied upon. In the case this cannot be provided, an early loss of structural integrity of the lids must be expected. However, the load-bearing capacity of the lids can be significantly improved by increasing their thickness and amount of reinforcement.

### 11.3.3 Transport properties

The transport properties of the concrete lids in 1–2BTF will probably remain virtually unaltered as long as their load-bearing capacity is sufficient to withstand the load from the backfill material. According to Section 11.3.2, this is dependent on the load-bearing capacity of the concrete tanks and drums.

However, in the case of a loss of structural integrity of the concrete tanks, there is a significant risk for a loss of structural integrity of also the lids. From this point in time, the transport properties of the lids will therefore be similar to those of the crushed rock backfill. However, as noted is Section 11.3.2, the load-bearing capacity of the lids can be improved and a collapse delayed by increasing the thickness of and amount of reinforcement in the lids. The consequence of this is also a slower degradation of the transport properties.

### 11.3.4 Recommended material property data

Table 11-2 presents recommended material property data for the lids in 1–2BTF for selected time periods up to 100 000 years post-closure. The recommendations are based on information regarding the status of the lids at closure presented in Section 6.5, the expected evolution of the properties of the lids described in the previous sections and the properties for degraded concrete given in Section 5.1.

**Table 11-2. Recommended material property data for the concrete lids in 1–2BTF for selected time periods up to 100 000 years post-closure.**

| | | Time period (Years post-closure) | | | | |
|---|---|---|---|---|---|---|
| **Property** | **Unit** | **At closure** | **0–1 000** | **1 000–20 000** | **20 000–50 000** | **50 000–100 000** |
| **pH** | - | ≥ 13 | 12.5–13 | 12.5 | 12–12.5 | 10–12 |
| **Porosity** | % | 11–13 | 11–13 | 11–13 | 13–15 | 15–20 |
| **Load-bearing capacity** | Rating (5–1) | 5 | 5 | 3–5 | 1–3 | 1 |
| **Hydraulic conductivity** | m/s | $(1–5)\times10^{-12}$ | $(1–5)\times10^{-12}$ | $(5–9)\times10^{-12}$ | $10^{-8}$–$10^{-2}$ | $10^{-2}$ |
| **Diffusivity** | $m^2/s$ | $(2–5)\times10^{-12}$ | $(2–5)\times10^{-12}$ | $(5–9)\times10^{-12}$ | $10^{-12}$–$10^{-9}$ | $10^{-9}$ |

### 11.3.5 Specific uncertainties

The following specific uncertainties in the description of the evolution of the properties of the lids in 1–2BTF during the first 100 000 years post-closure have been identified:

- The main uncertainties concern the prediction of the load-bearing capacity and transport properties of the lids in 1–2BTF. This is because the dimensions of and amount of reinforcement in the lids in the current design are insufficient and physical support from the concrete tanks have to relied upon. Uncertainties regarding the evolution of the load-bearing capacity of the concrete tanks are discussed in Section 11.7.5.
- It is also uncertain if the channels formed by the steel pallets on which the concrete tanks are placed will be entirely filled during grouting of the concrete tanks. In the case of incomplete fill, there is a potential risk that the load-bearing capacity of the steel pallets will be lost through steel corrosion with a loss of mechanical support for the lids as a consequence. The strategy for grouting of the concrete tanks therefore needs to be developed and verified.

See also the discussion concerning the general uncertainties in Chapter 5.

## 11.4 Prefabricated concrete elements

### 11.4.1 Chemical properties

The evolution of the chemical properties of the prefabricated concrete elements in 1–2BTF will follow that outlined for the prefabricated concrete elements (Section 8.7.1) and inner walls (Section 8.6.1) in 1BMA and is not repeated here.

### 11.4.2 Load-bearing capacity

The load-bearing capacity of the prefabricated concrete elements is not sufficient to carry the load from the backfill material without the support from the concrete tanks. This is because these elements are simply placed on top of the tanks and therefore unable to withstand tensile loads. For this reason, the prefabricated concrete elements will fall into the waste compartment in the same moment as the stack of concrete tanks loses its structural integrity and the load-bearing capacity of these elements alone is therefore not relevant.

### 11.4.3 Transport properties

The transport properties of the prefabricated concrete elements in 1–2BTF are evaluated for the elements as a group, i.e. also including the slits between the individual elements. This means that the hydraulic conductivity and effective diffusivity will be determined by the distance between the individual elements rather than by the properties of the concrete and degree of degradation.

Because of this, the transport properties of the prefabricated concrete elements will have the characteristics of degraded concrete with wide cracks already at closure.

### 11.4.4 Recommended material property data

Table 11-3 presents recommended material property data for the prefabricated concrete elements in 1–2BTF for selected time periods up to 100 000 years post-closure. The recommendations are based on information regarding the status of the prefabricated concrete elements at closure presented in Section 6.5, the expected evolution of the properties of these elements described in the previous sections and the properties for degraded concrete given in Section 5.1.

**Table 11-3. Recommended material property data for the prefabricated concrete elements in 1–2BTF during different time periods up to 100 000 years post-closure.**

| | | Time period (Years post-closure) | | | | |
|---|---|---|---|---|---|---|
| **Property** | **Unit** | **At closure** | **0–1 000** | **1 000–10 000** | **10 000–50 000** | **50 000–100 000** |
| **pH** | - | ≥ 13 | 12.5–13 | 12.5 | 12–12.5 | 10–12 |
| **Porosity** | % | 12–15 | 12–15 | 12–15 | 13–15 | ≥ 15 |
| **Load-bearing capacity*** | Rating (5–1) | Not relevant | Not relevant | Not relevant | Not relevant | Not relevant |
| **Hydraulic conductivity** | m/s | $10^{-3}$ | $10^{-3}$ | $10^{-3}$ | $10^{-2}$ | $10^{-2}$ |
| **Diffusivity** | $m^2/s$ | $10^{-10}$ | $10^{-10}$ | $10^{-10}$ | $10^{-10}$ | $10^{-10}$ |

* The prefabricated concrete elements do not provide any additional load-bearing capacity not provided by the lid or the concrete tanks.

### 11.4.5 Specific uncertainties

No specific uncertainties of significance have been identified. See instead the discussion concerning the general uncertainties in Chapter 5.

## 11.5 Grout between waste packages

### 11.5.1 Chemical properties

No dedicated studies on the evolution of the chemical properties of the grout between the waste packages in 1–2BTF have been carried out so far and other sources of information from other representative systems will therefore have to be relied upon.

Being enclosed within a concrete structure comprising the slab, lid and cementitious backfill, leaching and mineral alterations in the grout between the waste packages will initially be slow. The low flow of groundwater through the waste vault (Öhman and Odén 2018) also ensures a slow degradation rate. However, the possible presence of voids in the grout between the waste packages already at closure may enhance the rate of degradation.

Following the formation of cracks in the surrounding structural components, mainly slab and lid, the flow of groundwater between the waste packages will increase. This can also be caused by a collapse of the steel pallets with significant cracking of the grout between the waste packages as a consequence.

However, extensive chemical degradation of this grout is not expected before 10 000 years post-closure and up to this point pH in the grout will be controlled by the presence of portlandite. This is because of the large amounts of cementitious materials in the waste vault which saturates the intruding groundwater with respect to cementitious degradation products.

However, the rate of chemical alterations will probably increase beyond 10 000 years post-closure due to cracking of the external construction parts, and from about 20 000 years post-closure the chemical properties will be controlled by the transformation of the CSH-phases. Because of significant cracking, the mineral composition of the grout between the waste packages will probably be dominated by the aggregate material and calcite from about 50 000 years post-closure even though the timing of the different degradation states will vary throughout the waste compartment because of the varying degree of cracking of the lid and concrete tanks.

### 11.5.2 Load-bearing capacity

The load-bearing capacity of the grout between the waste packages towards external and internal loads is insignificant and therefore disregarded. This is justified by the very thin layers of grout between the waste packages, the absence of reinforcement and the uncertain outcome of the grouting procedure.

### 11.5.3 Transport properties

According to Section 6.5.1, the transport properties of the grout between the waste packages will be controlled by the presence of voids and channels already at closure. This is because of the difficulties to entirely fill the narrow slits between the concrete tanks with grout. Through loss of load-bearing capacity of the concrete tanks, additional large cracks will form in the grout.

### 11.5.4 Recommended material property data

Table 11-4 presents recommended material property data for the grout between then waste packages in 1–2BTF for selected time periods up to 100 000 years post-closure. The recommendations are based on information regarding the status of the grout between the waste packages at closure presented in Section 6.5, the expected evolution of the properties of the grout described in the previous sections and the properties for degraded concrete given in Section 5.1.

**Table 11-4. Recommended material property data for the grout between the waste packages in 1–2BTF for selected time periods up to 100 000 years post-closure.**

| | | Time period (Years post-closure) | | | | |
|---|---|---|---|---|---|---|
| **Property** | **Unit** | **At closure** | **0–1 000** | **1 000–10 000** | **10 000–30 000** | **30 000–100 000** |
| **pH** | - | ≥ 13 | 12.5–13 | 12–12.5 | 10–12 | ≤ 10 |
| **Porosity** | % | 14–16 | 14–16 | 15–20 | 20–25 | ≥ 25 |
| **Load-bearing capacity*** | Rating (5–1) | Not relevant | Not relevant | Not relevant | Not relevant | Not relevant |
| **Hydraulic conductivity** | m/s | $10^{-5}$–$10^{-3}$ | $10^{-3}$ | $10^{-3}$–$10^{-2}$ | $10^{-2}$ | $10^{-2}$ |
| **Diffusivity** | $m^2/s$ | $(1–5)\times10^{-11}$ | $(5–9)\times10^{-11}$ | $10^{-11}$–$10^{-10}$ | $10^{-10}$ | $10^{-10}$ |

* The load-bearing capacity of the grout between the waste packages is insignificant and therefore not relevant.

### 11.5.5 Specific uncertainties

The following specific uncertainty in the description of the evolution of the properties of the grout between the waste packages in 1–2BTF during the first 100 000 years post-closure has been identified:

- The evolution of the transport properties of the grout is uncertain. This is because of the uncertain outcome of the grouting process and the uncertain evolution of the load bearing capacity of the lid, concrete tanks and steel pallets.

See also the discussion concerning the general uncertainties in Chapter 5.

## 11.6 Cementitious backfill

### 11.6.1 Chemical properties

Leaching and mineral transformations in concrete in direct connection to the adjacent bedrock do not differ process-wise from corresponding processes in concrete that is in contact with free groundwater. The main difference is instead the rate with which these processes take place and which is directly dependent on the limited availability of groundwater at the interface between rock and concrete. In addition to this, it can also be expected that the degradation will – at least during the early period and before extensive concrete degradation has occurred – be somewhat heterogeneous since the availability of groundwater will vary depending on the properties of the adjacent rock. Here, one can imagine a faster degradation in the vicinity of water-bearing fractures and a lower rate in the vicinity of dense rock.

For the cementitious backfill in 1–2BTF, similar evolution of the mineral composition is expected as that suggested for the cementitious backfill in the waste vault for core components (BHK) in the repository for long-lived radioactive waste, SFL, studied by Idiart et al. (2019a, 2019b), Idiart and Laviña (2019) and Idiart and Shafei (2019).

Of these, Idiart and Shafei (2019) studied the degradation of concrete and its effect on the concrete properties in a 3D-model for a period of up to 50 000 years post-closure. Figures 11-1 to 11-4 present a compilation of the results from this study for the time 50 000 years post-closure for concrete with heterogeneous properties (3D-model) compared to homogeneous concrete in a 2D-model. In these figures, the thickness of the backfill, i.e. the distance between the rock wall and the waste domain, is 2.8 meters (Idiart and Shafei 2019, Figure 5-1). In comparison, the distance between the concrete tanks and the bedrock in 1–2BTF is only 0.5 meter, Figure 2-29.

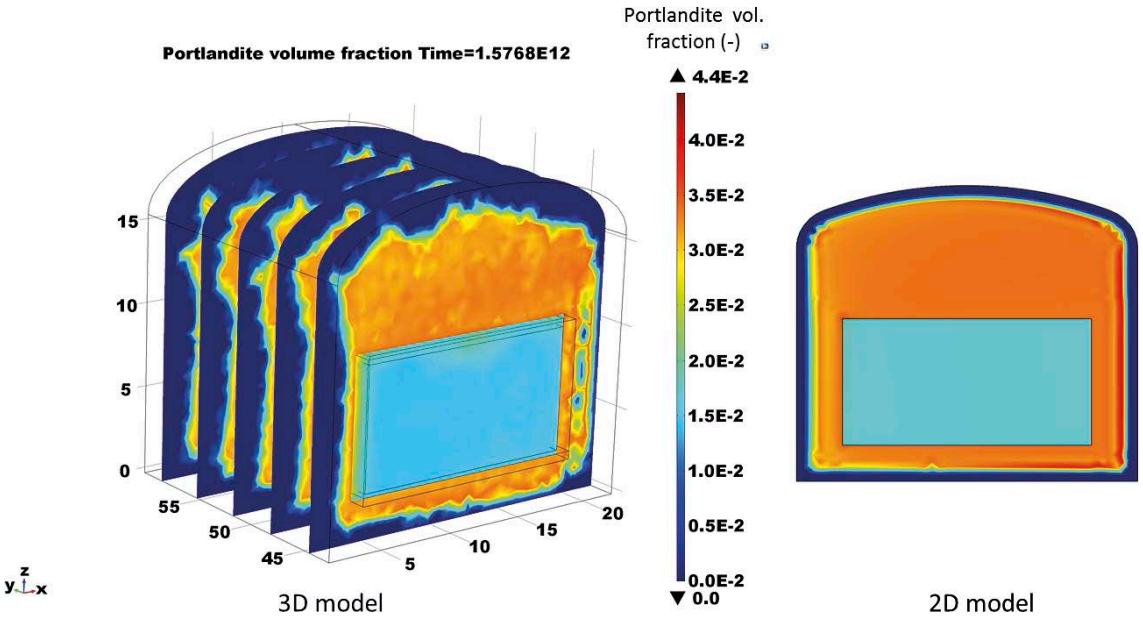


***Figure 11-1.*** *Portlandite distribution in BHK at time 50 000 years post-closure. Comparison between 3D- and 2D-model (Idiart and Shafei 2019, Figure 6-16).*

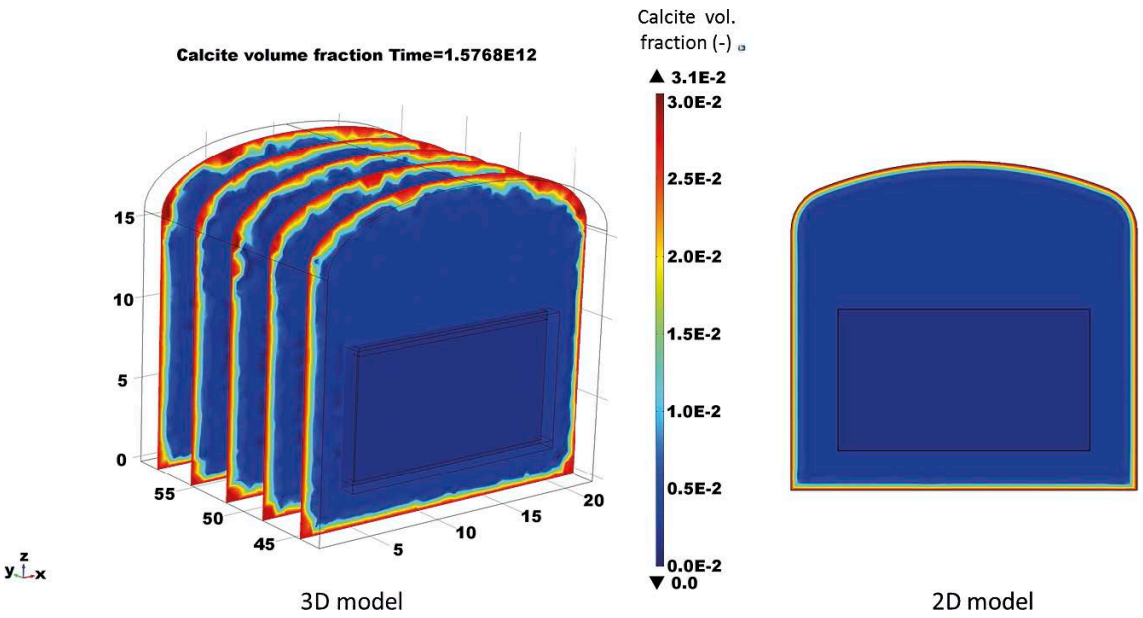


***Figure 11-2.*** *Calcite distribution in BHK at time 50 000 years post-closure. Comparison between 3D- and 2D-model (Idiart and Shafei 2019, Figure 6-23).*

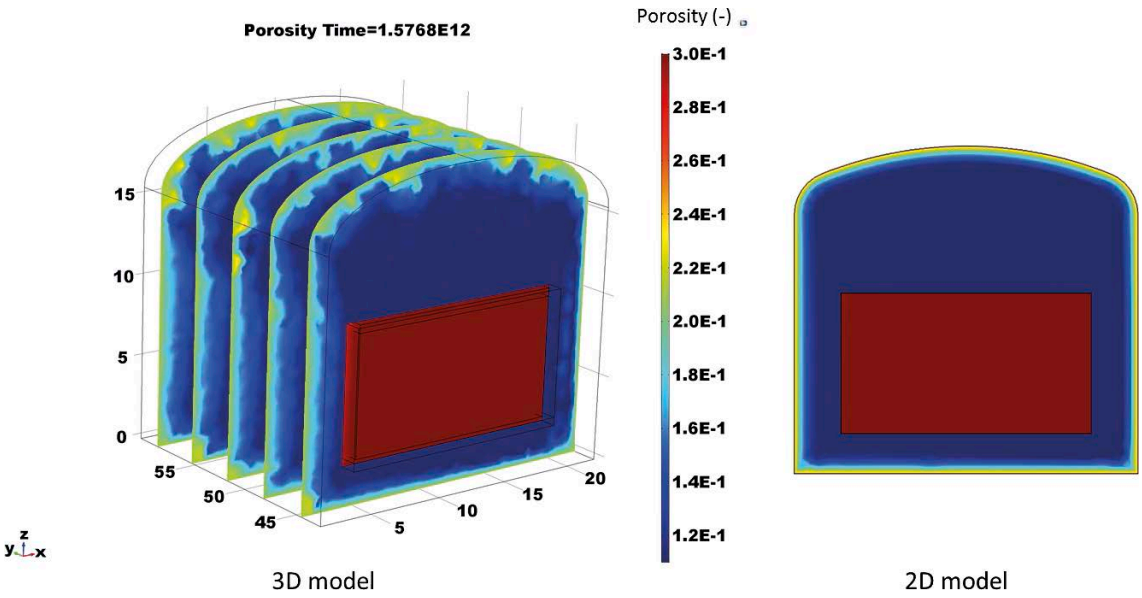


***Figur 11-3.*** *Porosity distribution in BHK at time 50 000 years post-closure. Comparison between 3D- and 2D-model (Idiart and Shafei 2019, Figure 6-25).*

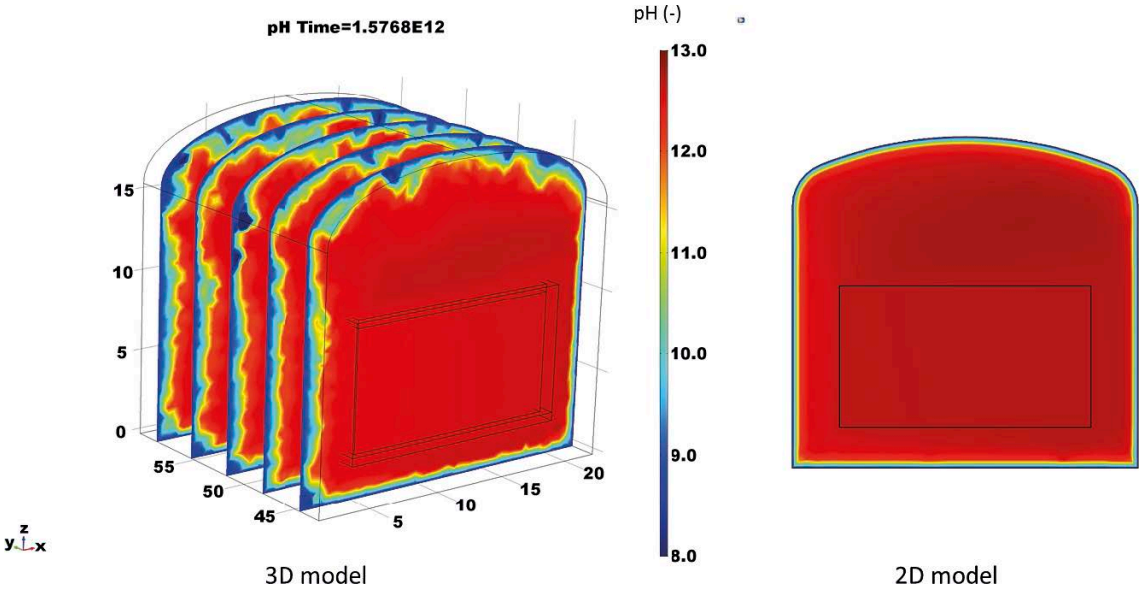


***Figur 11-4.*** *pH distribution in BHK at time 50 000 years post-closure. Comparison between 3D- and 2D-model (Idiart and Shafei 2019, Figure 6-24).*

Figures 11-1 to 11-4 show that a zone of degraded concrete is formed against the adjacent bedrock. In this zone, the portlandite is dissolved which leads to a portlandite-depleted zone in the interface with the bedrock, Figure 11-1. This is followed by transformation of the CSH-phases and finally a zone consisting mainly of calcite (Figure 11-2) with relatively high porosity (Figure 11-3) and low pH (Figure 11-4) is formed at the interface with the adjacent bedrock.

The extent of these zones is – as noted above – dependent on the hydrogeological properties of the adjacent bedrock and in relation to what is shown in Figures 11-1 to 11-4, the affected zone can likely be both larger and smaller. However, for the considerably thinner cementitious backfill in 1–2BTF compared to BHK, it is considered unlikely that the entire cross-section will remain unaffected and one or more slightly more permeable zones must therefore be expected.

The inhomogeneous structure of the degradation front highlights the difficulties in accurately predicting the evolution of the chemical properties of the cementitious material cast directly against adjacent bedrock.

In another study, Idiart et al. (2019a) modelled the influence of the mixing proportions of the concrete on the evolution of the properties of the concrete backfill in BHK for five different materials. With reference to Figures 11-5 and 11-6, the following types of concrete were studied. See also (Idiart et al. 2019a, Table 2-1).

- **Case I**: *Silo concrete* (w/c ratio: 0.47)
- **Case IIa**: *1BMA concrete* (320 kg cement/m$^3$ of concrete, w/c ratio: 0.63)
- **Case IIb**: *1BMA concrete* (280 kg cement/m$^3$ of concrete, w/c ratio: 0.63)
- **Case III**: *Silo concrete* with cement containing additional fly-ash (w/c ratio: 0.47)
- **Case IV**: *2BMA concrete* (w/c ratio: 0.49)

Of these, the *2BMA concrete* (Case IV) will be the most representative alternative to the *BTF backfill concrete* even though it is not self-compacting.

Figures 11-5 and 11-6 show portlandite and pH distribution in the concrete backfill in BHK at 100 000 years post-closure for the five different materials studied by Idiart et al. (2019a). According to these figures, the portlandite leaching front has reached between 0.9 and 1.3 meters into the backfill after 100 000 years. Also, transformation of the CSH-phases must have occurred in these parts as indicated by the fact that pH is below 12 in the outermost 0.5 meters of the backfill, Figure 11-6.

With an expected thickness of the cementitious backfill in 1–2BTF of about 0.5 meters (Figure 2-29), depletion of portlandite will occur prior to 100 000 years post-closure (Figure 11-5). At this point in time, pH in the part closest to the concrete tanks will be about 12 (Figure 11-6) indicating some remaining CSH in the cementitious backfill.

However, Figure 2-28 shows that the distance between the concrete tanks and the rock wall appears to be somewhat longer than 0.5 meters. From this follows that the time to complete portlandite depletion in the inner parts of the cementitious backfill will be somewhat longer than that indicated above. In addition, the rate of degradation indicated in these figures corresponds broadly to that of concrete in contact with free groundwater. Intuitively, this is unexpected as the rate of concrete degradation at the concrete/bedrock interface should be very low because of the limited availability of groundwater.

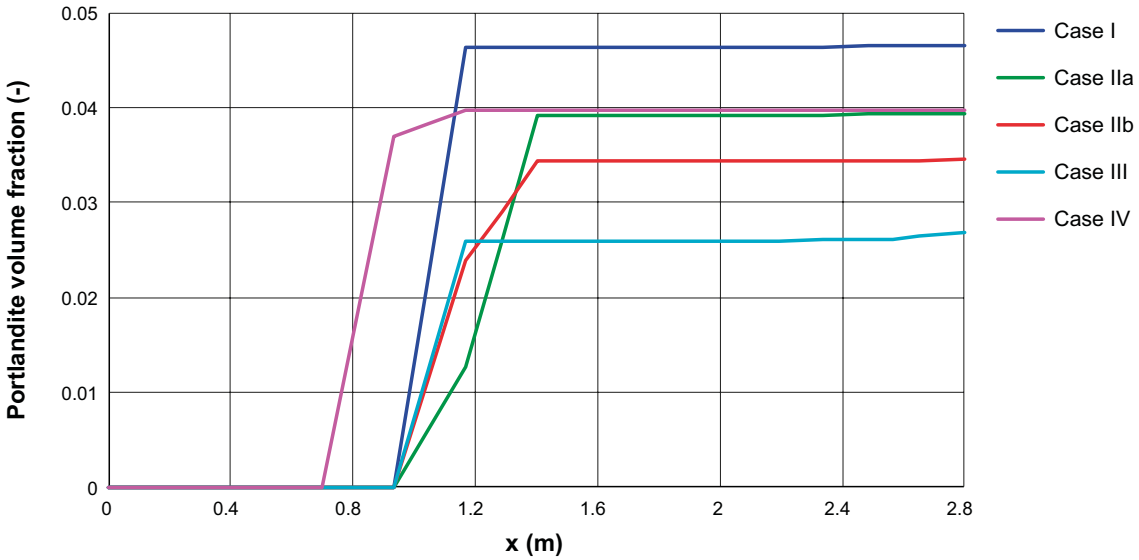


***Figure 11-5.*** *Portlandite dissolution fronts in terms of volume fraction after 100 000 years for five different simulated cases (Idiart et al. 2019a).*

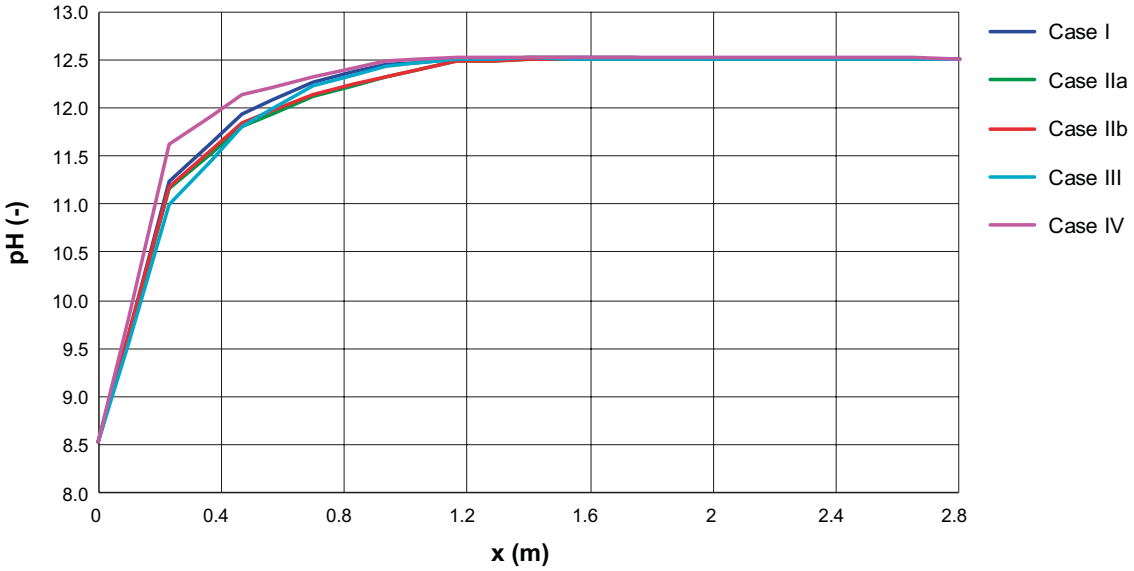


***Figure 11-6.*** *pH distribution in the concrete backfill in BHK after 100 000 years for five different simulated cases (Idiart et al. 2019a).*

### 11.6.2 Load-bearing capacity

The load-bearing capacity of the cementitious backfill in 1–2BTF against the compressive vertical load from the lid and the crushed rock backfill will in principle be dependent on the compressive strength of the *BTF backfill concrete*. Because no crushed rock backfill is installed between the cementitious backfill and the rock wall, horizontal forces will be absent until after significant degradation of the lid and concrete tanks. However, also at this stage support from the adjacent bedrock can be accounted for.

With an estimated compressive strength of 55–60 MPa at closure (Table 6-5), the load-bearing capacity of the cementitious backfill will significantly exceed the compressive load from the lid and the backfill material during the early period post-closure.

Through portlandite depletion, the thickness of remaining undegraded cementitious backfill will be reduced. However, according to Babaahmadi (2015) the compressive strength of portlandite depleted concrete is on the order of 10 MPa. The following simple calculation is therefore made.

From Figure 2-29, the estimated total load from a one-meter wide strip across the waste vault will correspond to

$$14.7 \times 1 \times 3 \times 2\,500 \times 9.82 = 1\,081 \text{ kN}$$

assuming an average thickness of the lid and backfill layer of 3 meters and a density of 2 500 kg/m$^3$. The impact of the groundwater saturation of the backfill is conservatively not considered.

For portlandite depleted concrete with a compressive strength of 10 MPa (i.e. 10 000 kN/m$^2$) a strip with a width of $\frac{1\,081}{10\,000} = 108$ mm (corresponding to 54 mm on each side of the waste vault) would provide sufficient load-bearing capacity.

From this follows that the load-bearing capacity of the cementitious backfill will be sufficient to resist the load from the lid and the backfill material up to 100 000 years post-closure. See also Section 11.6.5 for a discussion concerning the uncertainties associated with this prediction.

### 11.6.3 Transport properties

In Section 6.5.1, the transport properties of the cementitious backfill at closure was considered a bit uncertain. This is because neither the mixing proportions of the *BTF backfill concrete* nor the detailed method of backfilling have been decided.

Also, in lack of specific studies on the post-closure evolution of the transport properties of the cementitious backfill in 1–2BTF, the studies for BHK conducted by Idiart and Shafei (2019) will instead serve as a representative example.

Figure 11-7 shows the evolution of the porosity in the concrete backfill in BHK for different time periods up to 100 000 years post-closure for a calculation model using the mixing proportions of the *Silo concrete* (Table 3-10). Figure 11-7 shows that the porosity at a depth of 0.5 meters – corresponding to the assumed thickness of the cementitious backfill in 1–2BTF – is unaffected during the first 20 000 years post-closure. However, from this period onwards, the porosity in this point starts to increase but still 100 000 years post-closure the porosity in this point has only increased from 0.11 to 0.145.

In addition, Idiart et al. (2019a) calculated the spatial distribution of the effective diffusivity (Figure 11-8) and hydraulic conductivity (Figure 11-9) in the concrete backfill in BHK for five different calculation cases (See Section 11.6.1) at 100 000 years post-closure.

For a porosity increase in the region of that shown in Figure 11-7, Figures 11-8 and 11-9 show that the effective diffusivity and hydraulic conductivity increase by only about one order of magnitude respectively. See also Section 5.1.3.

From the findings above follows that mineral transformations alone will not have a significant impact on the transport properties of the cementitious backfill and instead the impact of cracking must be evaluated. However, according to Section 11.6.2, the risk for formation of penetrating cracks due to insufficient load-bearing capacity is low during a majority of the first 100 000 years post-closure.

In all, the transport properties of the cementitious backfill will remain rather unaltered during a majority of the first 100 000 years post-closure and an increase in hydraulic conductivity and effective diffusivity can be expected only during the later periods.

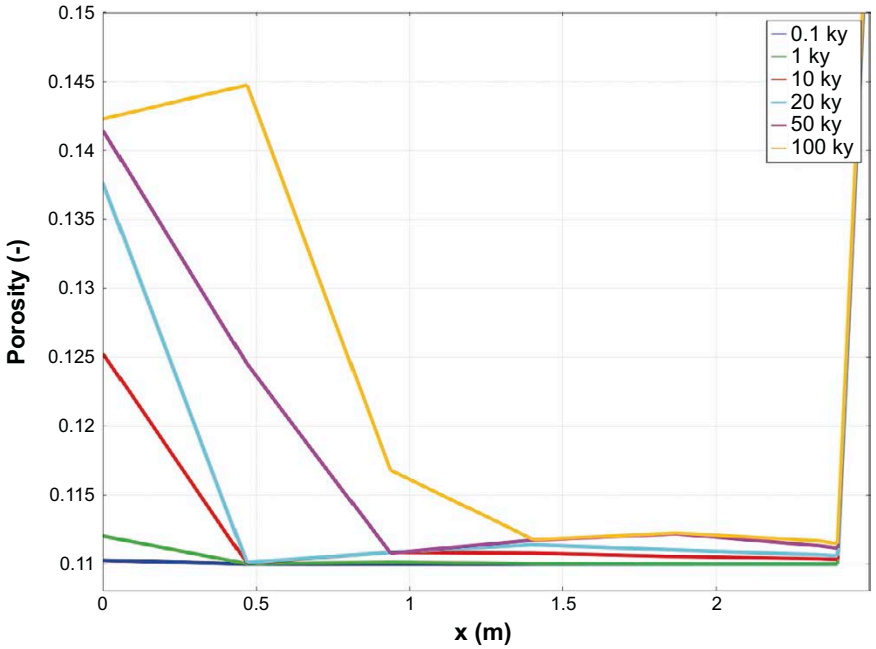


***Figure 11-7.*** *1D-profiles of porosity in the concrete backfill in BHK after 100, 10 000, 20 000, 50 000, and 100 000 years (Idiart and Shafei 2019).*

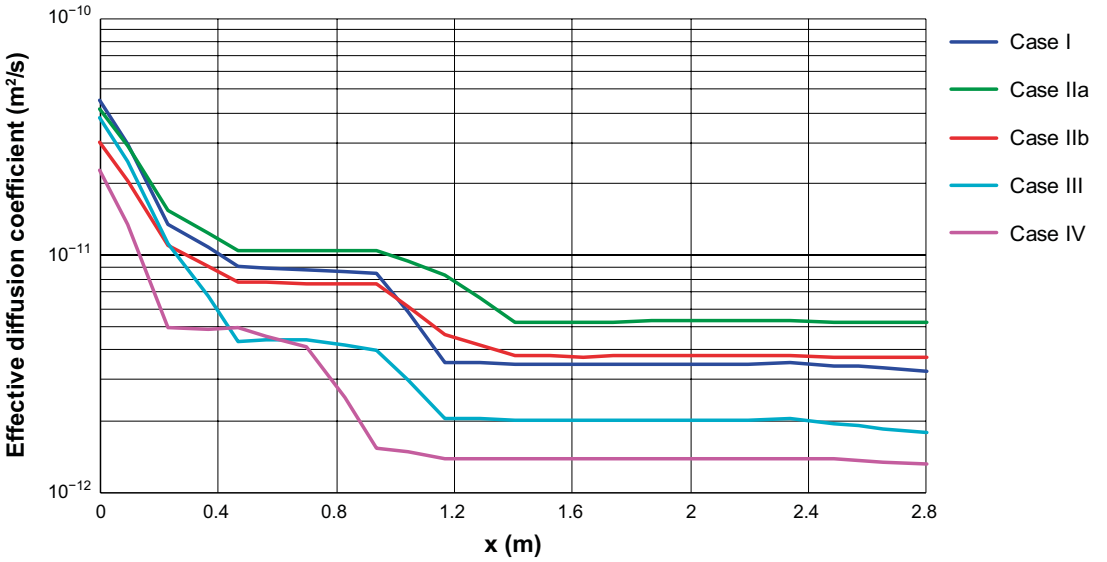


***Figure 11-8.*** *Predicted spatial distribution of the effective diffusivity in the concrete backfill in BHK for five different concrete mixing proportions at 100 000 years post-closure (Idiart et al. 2019a, Figure 5-21).*

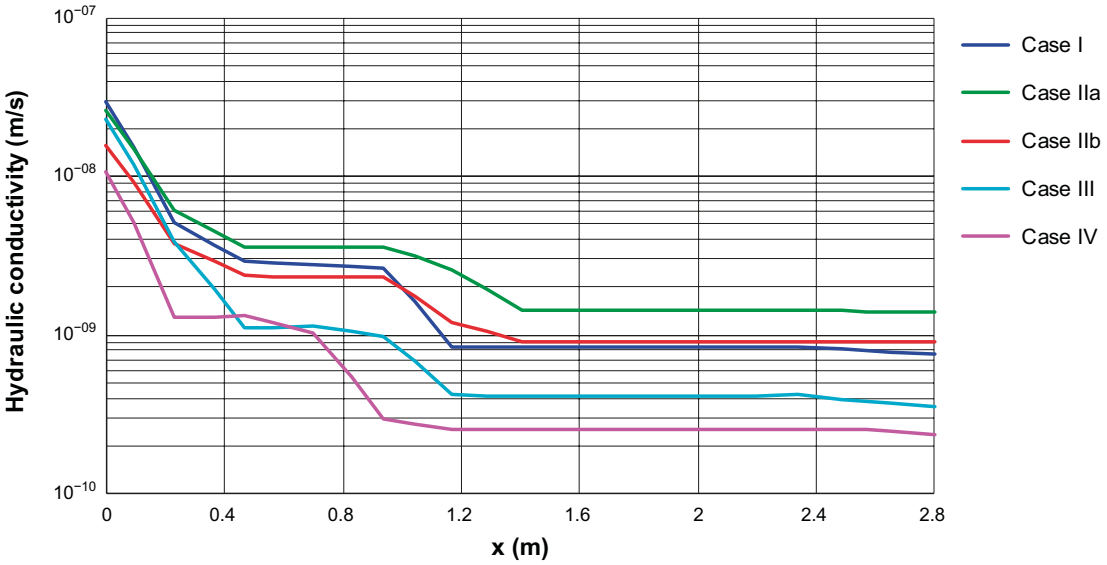


***Figure 11-9.*** *Predicted spatial distribution of the hydraulic conductivity in the concrete backfill for BHK for five different concrete mixing proportions at 100 000 years post-closure (Idiart et al. 2019a, Figure 5-22).*

### 11.6.4 Recommended material property data

Table 11-5 presents recommended material property data for the cementitious backfill in 1–2BTF for selected time periods up to 100 000 years post-closure. The recommendations are based on information regarding the status of the cementitious backfill at closure presented in Section 6.5, the expected evolution of the properties of the cementitious backfill described in the previous sections and the properties for degraded concrete given in Section 5.1.

**Table 11-5. Recommended material property data for the cementitious backfill in 1–2BTF for selected time periods up to 100 000 years post-closure.**

| | | Time period (Years post-closure) | | | | |
|---|---|---|---|---|---|---|
| **Property** | **Unit** | **At closure** | **0–1 000** | **1 000–20 000** | **20 000–50 000** | **50 000–100 000** |
| **pH** | - | ≥ 13 | ≥ 13 | 12.5–13 | 12.5 | 12–12.5 |
| **Porosity** | % | 11–13 | 11–13 | 12–13 | 13–14 | 14–16 |
| **Load-bearing capacity** | Rating (5–1) | 5 | 5 | 5 | 4–5 | 3–4 |
| **Hydraulic conductivity** | m/s | $(1–5)\times10^{-11}$ | $(1–5)\times10^{-11}$ | $(1–5)\times10^{-11}$ | $10^{-11}$–$10^{-6}$ | $10^{-6}$–$10^{-4}$ |
| **Diffusivity** | $m^2/s$ | $(3–8)\times10^{-12}$ | $(3–8)\times10^{-12}$ | $(3–8)\times10^{-12}$ | $10^{-12}$–$10^{-11}$ | $10^{-11}$ |

### 11.6.5 Specific uncertainties

The following specific uncertainties in the description of the evolution of the properties of the cementitious backfill in 1–2BTF during the first 100 000 years post-closure have been identified:

- The main uncertainty for the cementitious backfill in 1–2BTF relates to the prediction of the evolution of the transport properties which mainly originates from uncertainties concerning the status of the cementitious backfill at closure.
- The closure plan for SFR (Mårtensson et al. 2022) only specifies backfilling of the space between the concrete tanks and the adjacent rock walls but makes no mention about the short sides facing the entrance tunnels of the waste vaults.
- The impact of concrete degradation in the interior of the waste domain e.g. a collapse of the concrete tanks has not been considered here. This may be of some importance in the case the lid loses its structural integrity.

See also the discussion concerning the general uncertainties in Chapter 5.

## 11.7 Concrete tanks

### 11.7.1 Chemical properties

According to the information in Sections 6.5.3 and 11.7.2, the interior of the concrete tanks will be filled with groundwater already during saturation of the repository. During this period, water will enter the concrete tanks either through the hole in the wall shown in Figure 6-7 or through cracks formed during saturation of the waste vault. Here Lundqvist showed that significant cracking of the concrete tanks will occur already at an external pressure of about 3 bars.[67] In addition, Angele shows that the rubber seal for the small steel hatch (Figure 2-27, right image) will be displaced by the water pressure during saturation and the sealing function will therefore be lost.[68]

From this follows that the interior of all concrete tanks will be filled with groundwater already during the saturation period. Concrete degradation and rebar corrosion will therefore start from the inside of the tanks already at this stage whereas the sealing epoxy paint protects the outside of the

[67] SKBdoc 2000090 ver 1.0. (Internal document, in Swedish.)

[68] SKBdoc 2000089 ver 1.0. (Internal document, in Swedish.)

tanks from groundwater interactions. However, in case of significant cracking during the saturation period the epoxy paint will be partially lost and leaching may occur also from the outside as well as in the cracks.[69]

However, because the concrete tanks are embedded in a cementitious grout and surrounded by concrete walls, slab and cementitious backfill, leaching will be very slow regardless of the extent of cracking of the concrete tanks. This is because any water that comes in contact with the concrete tanks will be saturated with respect to cementitious degradation products and therefore not aggressive towards the concrete tanks.

With reference to the similar conditions inside the waste compartments in 1BMA and 1–2BTF, the alterations of the mineral composition of the concrete tanks in 1–2BTF will broadly follow that outlined for the inner walls in 1BMA described in Section 8.6.

Figures 8-1 to 8-4 show that leaching of portlandite in the waste compartment is slow and still at 50 000 years post-closure a significant portion of the portlandite remains. See also Figures 9-1 to 9-5 which show that the evolution of pH inside the waste compartment in 2BMA is slow and pH at about 12.5 still at 100 000 years post-closure. Finally, see also Sections 11.7.2 and 11.3 for discussions concerning the evolution of the load-bearing capacity of the concrete tanks and the influence of this of the structural integrity of the lid and – following a loss of structural integrity of the lid – an increased degradation rate of the concrete tanks.

### 11.7.2 Load-bearing capacity

Experiments conducted at the Äspö HRL (Mårtensson 2021b) showed that intrusion of water into a concrete tank is very slow. The consequence of this is that there will be a pressure difference between the outside and the inside of the tanks during the saturation period.

According to a modelling study conducted by Könönen and Malm (2021), the load-bearing capacity of the concrete tanks is insufficient to resist the groundwater pressure at repository depth, i.e. about 70 meters. This was also verified in a large-scale experiment in which a concrete tank was submerged in a water tank and exposed to an increasing external pressure. The study showed that extensive cracking of the concrete tanks occurs already at a pressure difference between the inside and outside of the concrete tank of about 3 bars.[70]

However, for tanks in which the hole shown in Figure 6-7 has not been sealed with a bolt, water will enter the tanks through this hole and cracking therefore not occur during saturation. The number of tanks with and without bolts respectively is unknown. In addition, as mentioned in Section 11.7.1 the rubber seal that seals the steel hatch in the lid of the concrete tank can be displaced during the saturation period. According to Angele this can occur already at a pressure of 1 bar.[71] The implication of this is that also tanks in which the hole is sealed with a bolt will be filled with groundwater at an external pressure which is significantly lower than that required to cause extensive cracking of the concrete tanks. The conclusion is therefore that the risk for cracking of the concrete tanks is low during the saturation period even though cracking cannot be fully excluded.

Once the tanks are filled with water, the weight of the lid and the backfill material on top of the lid will constitute the maximum vertical load. Horizontal loads are expected to be limited during the early post-closure period. This is because the cementitious backfill does not exert a horizontal pressure on the concrete tanks in the same way as crushed rock backfill materials. However, limited horizontal loads can occur through corrosion of the steel pallets beneath the concrete tanks and toppling of the concrete tanks if grouting of the tanks is not complete. In addition, severe degradation of the cementitious backfill can lead to a loss of structural integrity of this material but also this will cause only small horizontal loads the consequence of which will be small until after significant degradation of the cementitious backfill, Section 11.6.

[69] SKBdoc 2000090 ver 1.0. (Internal document, in Swedish.)

[70] SKBdoc 2000090 ver 1.0. (Internal document, in Swedish.)

[71] SKBdoc 2000089, ver 1.0. (Internal document, in Swedish.)

According to information provided in Section 11.3, the load-bearing capacity of the lid depends on its thickness and amount of reinforcement. A lid with a very high load-bearing capacity will be able to carry the weight of the backfill material without the support from the stack of concrete tanks. The lower tank will in such a case only have to carry the weight of the upper tank. As reported by Bultmark (2017b), the load-bearing capacity of the lower concrete tank against vertical loads is sufficient to carry the weight of the upper tank also in the case of rebar corrosion and a complete delamination of the covering layer. The conclusion is therefore that the load-bearing capacity of the concrete tanks will be sufficient as long as the load-bearing capacity of the lid is sufficient to carry the weight of the backfill material unless the tanks are completely degraded.

The load-bearing capacity of a cracked concrete tank has been examined by Angele et al..[72] In this experiment, the tank previously used in the test carried out by Lundqvist (SKBdoc 2000090 ver 1.0, internal document, in Swedish) and therefore significantly cracked was exposed to a vertical load of 550 kN, corresponding to 139 kN/m$^2$ given a surface area for the lid of 3.93 m$^2$ (This area corresponds to the total area of the lid but excluding the area of the steel hatch). This load is somewhat lower than the load on the bottom tank which corresponds to the combined load from the upper tank, the lid and the backfill material, i.e. a total of 236 kN/m$^2$ (Könönen and Malm 2021). However, for a fully saturated repository, the load will be reduced to 139 kN/m$^2$ (SKBdoc 2004996 ver 1.0, internal document, in Swedish), i.e. a total of 550 kN.

The test showed that the load-bearing capacity of also a cracked concrete tank is sufficient to resist these vertical loads and neither additional cracking nor a collapse of the concrete tank were reported but instead only low levels of tensile strain were observed. The conclusion is therefore that the load-bearing capacity of the concrete tanks is sufficient to carry the vertical load from the lid and the backfill material even after significant cracking. Only after severe rebar corrosion and loss of cohesion a complete loss of structural integrity of the concrete tanks is expected.

The continued post-closure evolution of the load-bearing capacity of the concrete tanks will be dependent on whether cracking has occurred or not. For an uncracked concrete tank, the rate of degradation of the load-bearing capacity will broadly follow the evolution of the chemical properties outlined in Section 11.7.1. However, for a concrete tank with a significant number of cracks, a faster degradation is expected but the uncertainties are significant.

### 11.7.3 Transport properties

According to Section 11.7.2, the hydraulic properties of the concrete tanks will be affected by the presence of cracks, joints and/or other hydraulically conducting zones already after the saturation period regardless of whether the tanks are perfectly watertight at closure or not.

The future evolution of the transport properties of the concrete tanks will be determined by the evolution of the load-bearing capacity of these tanks. However, from Section 11.7.2, there remain some uncertainties regarding the evolution of the load-bearing capacity of the tanks; see also Section 11.7.5.

### 11.7.4 Recommended material property data

Table 11-6 presents recommended material property data for the concrete tanks in 1–2BTF for selected time periods up to 100 000 years post-closure. The recommendations are based on information regarding the status of the concrete tanks at closure presented in Section 6.5, the expected evolution of the properties of the concrete tanks described in the previous sections and the properties for degraded concrete given in Section 5.1.

It should here be stressed that the data presented in Table 11-6 assumes that the tanks are watertight at closure and that significant cracking therefore has occurred already during the saturation period. However, for tanks in the which the hole shown in Figure 6-7 is not sealed with a bolt, cracking will not occur with a different evolution of the load-bearing capacity as a consequence.

[72] SKBdoc 2004996, ver 1.0. (Internal document, in Swedish.)

**Table 11-6. Recommended material property data for the concrete tanks in 1–2BTF for selected time periods up to 100 000 years post-closure.**

| | | Time period (Years post-closure) | | | | |
|---|---|---|---|---|---|---|
| **Property** | **Unit** | **At closure** | **0–1 000** | **1 000–20 000** | **20 000–50 000** | **50 000– 100 000** |
| **pH** | - | ≥ 13 | 12.5–13 | 12.5 | 12–12.5 | 11–12 |
| **Porosity** | % | 10–12 | 10–12 | 11–13 | 12–14 | 16–20 |
| **Load-bearing capacity** | Rating (5–1) | 5 | 5–2 | 2–1 | 1 | 1 |
| **Hydraulic conductivity** | m/s | $(1–5)\times10^{-12}$ | $10^{-7}$–$10^{-5}$ | $10^{-5}$–$10^{-2}$ | $10^{-2}$ | $10^{-2}$ |
| **Diffusivity** | $m^2/s$ | $(2–5)\times10^{-12}$ | $(1–5)\times10^{-11}$ | $10^{-10}$–$10^{-9}$ | $10^{-9}$ | $10^{-9}$ |

### 11.7.5 Specific uncertainties

The following specific uncertainties in the description of the evolution of the properties of the concrete tanks in 1–2BTF during the first 100 000 years post-closure have been identified:

- There remain uncertainties concerning the number of tanks for which the hole shown in Figure 6-7 has not been sealed with a bolt.
- There are also uncertainties related to the seal for the steel hatch and the pressure required to displace this seal.
- There also remain some uncertainties concerning the status of the seal between the lid and the body of the tank at closure as well as its post-closure evolution.
- The load-bearing capacity of the concrete tanks and the risk for a complete collapse of the tanks are also affected by the load-bearing capacity of the lids in 1–2BTF. At present, the dimensions of and amount of reinforcement in the lids have not been decided.
- The evolution of the chemical properties of the concrete tanks is uncertain as this is partly affected by the degree of cracking during saturation of the waste vaults.

See also the discussion concerning the general uncertainties in Chapter 5.

## 11.8 Concrete moulds

### 11.8.1 Chemical properties

The evolution of the chemical properties of the concrete moulds will broadly follow that of the concrete tanks presented in Section 11.7.1. However, for the concrete moulds, degradation will mainly occur from the outside rather than from the inside as expected for the concrete tanks.

### 11.8.2 Load-bearing capacity

The concrete moulds will experience external loads from the water pressure during saturation of the repository and from the stack of waste packages, lid and backfill material but also internal loads caused by processes in the waste. The resistance of the concrete moulds towards the groundwater pressure during saturation is dependent on the properties of the waste and has not been studied.

The study by Bultmark (2017a) for concrete moulds in 1BMA shows that a concrete mould can carry the weight from a 100-meter-tall stack of a material with a density of 2 500 $kg/m^3$ without cracking. Bultmark (2017a) also shows that a concrete mould can carry the load from a stack of concrete moulds with a height of 80 meters even after spalling of the covering layer.

Once spalling of the covering layer has occurred, the evolution of the load-bearing capacity of the concrete moulds will be determined by the rate of mineral alterations. According to Figures 8-1 to 8-4 mineral alterations are very slow in the waste compartment in 1BMA and portlandite will be present in the major part of the waste compartment up to 100 000 years post-closure; see also Section 11.7.1. The implication of this is that degradation of the load-bearing capacity of the concrete moulds due to concrete degradation alone will be limited up to about 20 000 years post-closure.

Beyond 20 000 years post-closure, the load on the concrete moulds will increase because the load-bearing capacity of the lid is reduced and finally lost. However, from the findings by Bultmark (2017a), the load-bearing capacity of the concrete moulds is sufficient to carry also the load from the lid and backfill material which has a thickness of only 3 meters also beyond 20 000 years post-closure. Eventually though, the load-bearing capacity of the concrete moulds is entirely lost but the exact timing is difficult to determine.

### 11.8.3 Transport properties

From the information provided in Sections 11.8.1 and 11.8.2, the transport properties of the concrete moulds will be similar to those of undegraded *SFR mould concrete*, during up to 20 000 years post-closure but from this point in time and onwards, cracking must be expected.

It is therefore suggested that the transport properties of the majority of the concrete moulds will be similar to those of the concrete moulds at closure during up about 20 000 years post-closure. Formation of penetrating cracks that influence the transport properties in some of the concrete moulds must, however, be expected. Beyond this point in time, cracking which affects the transport properties of all concrete moulds must be expected.

### 11.8.4 Recommended material property data

Table 11-7 presents recommended material property data for the concrete moulds in 1–2BTF for selected time periods up to 100 000 years post-closure. The recommendations are based on information regarding the status of the concrete moulds at closure presented in Section 6.5, the expected evolution of the properties of the concrete moulds described in the previous sections and the properties for degraded concrete given in Section 5.1.

**Table 11-7. Recommended material property data for the concrete moulds in 1–2BTF for selected time periods up to 100 000 years post-closure.**

| | | Time period (Years post-closure) | | | | |
|---|---|---|---|---|---|---|
| **Property** | **Unit** | **At closure** | **0–1 000** | **1 000–20 000** | **20 000–50 000** | **50 000–100 000** |
| **pH** | - | ≥ 13 | 12.5–13 | 12.5 | 12–12.5 | 12–12.5 |
| **Porosity** | % | 10–12 | 10–12 | 11–13 | 12–14 | 16–20 |
| **Load-bearing capacity** | Rating (5–1) | 5 | 5 | 3–5 | 2–3 | 1–2 |
| **Hydraulic conductivity** | m/s | $(1–5)\times10^{-12}$ | $(1–5)\times10^{-12}$ | $(1–5)\times10^{-12}$ | $10^{-12}$–$10^{-5}$ | $10^{-5}$–$10^{-2}$ |
| **Diffusivity** | $m^2/s$ | $(2–5)\times10^{-12}$ | $(2–5)\times10^{-12}$ | $(5–9)\times10^{-12}$ | $10^{-12}$–$10^{-11}$ | $10^{-11}$–$10^{-9}$ |

### 11.8.5 Specific uncertainties

The following specific uncertainties in the description of the post-closure evolution of the properties of the concrete moulds in 1–2BTF during the first 100 000 years post-closure have been identified:

- The main uncertainty concerns the impact of degradation of the load-bearing capacity of the lid on the evolution of the properties of the concrete moulds. As long as the structural integrity of the concrete lid is intact, degradation of the concrete moulds will be very slow. However, once the load-bearing capacity of the lid is lost, the rate of degradation of the moulds will increase.
- In addition, no studies covering the resistance of the concrete moulds towards the groundwater pressure have been found. However, because of their small dimensions, the risk for cracking is probably limited during the saturation period.
- There also remain some uncertainties regarding processes in the waste and the risk for a high pressure inside the concrete moulds, in particular those containing ion exchange resins, metals and sludge.

See also the discussion concerning the general uncertainties in Chapter 5.

# 12 1BLA: post-closure evolution

In this chapter, the expected evolution of the properties of the slab in 1BLA during the first 100 000 years post-closure is described. The starting point for the description is the expected status of the slab at closure presented in Section 6.6. The evolution of the properties of the slab is then influenced by the processes presented in Chapter 4.

A description of the slab is given in Section 2.10. In addition, Chapter 3 presents specifications and properties of the concrete presumably used in the slab.

## 12.1 Literature

The following reports form the basis for the description of the post-closure evolution of the properties of the slab in 1BLA presented in this chapter:

- **Cronstrand (2007)** modelled the evolution of mineral composition of the original concrete structure in 1BMA.
- **Cronstrand (2014)** modelled the evolution of pH the waste vaults in SFR1.
- **Könönen** (SKBdoc 1360313 ver 1.0, internal document, in Swedish) calculated the load bearing capacity of the concrete slab in 1BLA.
- **Lagerblad (2001)** and **Trägårdh and Lagerblad (1998)** investigated the influence of leaching in stagnant and flowing freshwater for up to 100 years exposure on the chemical composition of concrete.
- **Mårtensson (2017)** evaluated the impact of degradation processes of the load-bearing capacity of the concrete structure in 1BMA under the assumption that the concrete structure had been repaired prior to closure as well as of the concrete caissons in 2BMA.
- **Nytorp Jansson (2020a, 2020b)** modelled the load-bearing capacity of the slabs in the waste vaults in SFR.

## 12.2 Slab

### 12.2.1 Chemical properties

Cronstrand (2014) presents the post-closure evolution of the average pH in 1BLA but does not provide any details on the evolution of the mineral composition in the different parts of the slab. Cronstrand (2014) concludes that the average pH in 1BLA will drop below 12.5 already at an early stage and below 11 before 10 000 years post-closure. Through continued leaching, Cronstrand (2014) predicts that pH will be below 10 from before 10 000 years post-closure.

This is in reasonable agreement with Figure 8-6, which shows that portlandite leaching proceeds with an average rate of about 10 mm/1 000 years. With a total thickness of only 250 mm, the slab in 1BLA will be depleted of portlandite already at about 12 000 to 15 000 years post-closure if leaching from both sides is assumed. However, Figure 8-6 does not fully describe the influence of a physical breakdown of the slab caused by rebar corrosion and cracking. For this reason, a faster chemical degradation of the slab in 1BLA can be expected than that estimated from Figure 8-6.

### 12.2.2 Load-bearing capacity

According to information provided in Section 6.6, the load-bearing capacity of the slab is probably not sufficient to prevent cracking during the operational period due to the loads from the stack of waste packages and transport of these. See also Nytorp Jansson (2020b) and Könönen (SKBdoc 1360313 ver 1.0, internal document, in Swedish) for details.

Through intrusion of chlorine containing groundwater, rebar corrosion will lead to a loss of function of the reinforcement bars during the first 1 000 years post-closure. In addition, concrete degradation will reduce the cohesion and "effective thickness" of the concrete slab.

With reference to Section 12.2.1 and assuming a loss of load-bearing capacity corresponding to a reduction of the thickness of the slab of 15 mm/1 000 years (Mårtensson 2017), the load-bearing capacity of the slab in 1BLA will be more or less lost at 10 000–15 000 years post-closure. However, as the loads are strictly compressive, the remnants of the slab will still be able to carry the load from the waste packages even though extensive cracking has occurred.

### 12.2.3 Transport properties

Section 6.6.1 suggests that the transport properties of the slab in 1BLA will have the characteristics of concrete with a number of penetrating cracks already at closure. Through leaching and rebar corrosion, both the number and width of the cracks as well as the porosity of the slab will increase, Section 12.2.1 and 12.2.2. From this follows that the slab will have the transport properties of significantly degraded concrete from about 10 000 to 15 000 years post-closure up to 100 000 years post-closure.

### 12.2.4 Recommended material property data

Table 12-1 presents recommended material property data for the slab in 1BLA for selected time periods up to 100 000 years post-closure. The recommendations are based on information regarding the status of the slab at closure presented in Section 6.6, the expected evolution of the properties of the slab described in the previous sections and the properties for degraded concrete given in Section 5.1.

**Table 12-1. Recommended material property data for the slab in 1BLA for selected time periods up to 100 000 years post-closure.**

| | | Time period (Years post-closure) | | | | |
|---|---|---|---|---|---|---|
| **Property** | **Unit** | **At closure** | **0–1 000** | **1 000–20 000** | **20 000–50 000** | **50 000–100 000** |
| **pH** | - | ≥ 13 | 12.5–13 | 11–12.5 | < 10–11 | < 10 |
| **Porosity** | % | 12–15 | 12–15 | 13–16 | 15–17 | 16–25 |
| **Load-bearing capacity** | Rating (5–1) | 3-4 | 3-4 | 2–4 | 2–3 | 1–2 |
| **Hydraulic conductivity** | m/s | $10^{-8}$–$10^{-5}$ | $10^{-8}$–$10^{-5}$ | $10^{-5}$–$10^{-3}$ | $10^{-4}$–$10^{-3}$ | $10^{-3}$–$10^{-2}$ |
| **Diffusivity** | $m^2/s$ | $(2–5)\times10^{-12}$ | $(2–5)\times10^{-12}$ | $(5–9)\times10^{-12}$ | $(1–5)\times10^{-11}$ | $10^{-10}$–$10^{-9}$ |

### 12.2.5 Specific uncertainties

In general, the uncertainties associated with the prediction of the post-closure evolution of the properties of the slab in 1BLA are small. This is because of the expected poor status of the slab already at closure.

See also the discussion concerning the general uncertainties in Chapter 5.

# 13 2–5BLA: post-closure evolution

In this chapter, the expected evolution of the properties of the slabs in 2–5BLA during the first 100 000 years post-closure is described. The starting point for the description is the expected status of the slabs at closure presented in Section 6.7. The evolution of the properties of the slabs is then influenced by the processes presented in Chapter 4.

A detailed description of the slabs is given in Section 2.11. In addition, Chapter 3 presents detailed specifications and properties of the concrete expected to be used in the slabs.

## 13.1 Literature

The following reports form the basis for the description of the post-closure evolution of the properties of the slabs in 2–5BLA presented in this chapter:

- **Cronstrand (2014)** modelled the evolution of pH in 1BLA which can serve as a representative example also for the slabs in 2–5BLA.
- **Höglund (2014)** modelled the evolution of the properties of the concrete caissons in 2BMA which is expected to use the same concrete as for the slabs in 2–5BLA.
- **Höglund (2019)** modelled the evolution of pH and mineral composition of the concrete caissons in 2BMA which is expected to use the same concrete as for the slabs in 2–5BLA.
- **Idiart et al. (2019a)** modelled the influence of the original mixing proportions of different types of concrete used in SFR on the evolution of the properties of concrete in SFL.
- **Mårtensson (2017)** evaluated the impact of degradation processes of the load-bearing capacity of the repaired concrete structure in 1BMA and the concrete caissons in 2BMA.
- **Lagerblad et al. (2017)** as well as **Mårtensson and Vogt (2019, 2020)** reported material property data for the *2BMA concrete*.
- **Villar et al. (2019)** performed an experimental investigation of the properties of *2BMA concrete* specimens manufactured by Mårtensson and Vogt (2019).

## 13.2 Slabs

### 13.2.1 Chemical properties

The evolution of the average pH in the slabs in 2–5BLA will broadly follow that outlined for the slab in 1BLA (Section 12.2.1) but the greater thickness of the slabs in 2–5BLA will prolong the time to complete degradation. Following the rate of portlandite leaching presented in Figure 8-6 (average portlandite dissolution rate of about 10 mm/1 000 years) portlandite is expected to be present up to about 20 000 years post-closure, assuming leeching from both sides.

With continued degradation, also the CSH phases will be depleted and with the same average degradation rate as for 1BLA, pH is expected to fall below 10 at about 50 000 years after closure. Through continued degradation, the slabs will have the chemical properties of a mixture of the aggregate material and calcite at 100 000 years post-closure.

### 13.2.2 Load-bearing capacity

No dedicated studies of the load-bearing capacity of the concrete slabs in 2–5BLA have been found and other sources of information will therefore have to be relied upon.

According to the information provided in Section 12.2.2, a thickness of 250 mm is not sufficient to ensure the load-bearing capacity for the slab in 1BLA even with the rather homogenous loads

from the stack of waste packages. With an original thickness of 400 mm and a reduction of the load-bearing capacity corresponding to a reduction of the thickness of the slab of 15 mm/1 000 years as pessimistically suggested by Mårtensson (2017), the load-bearing capacity of the slabs in 2–5BLA is expected to be sufficient up to about 5 000–8 000 years post-closure. From that point in time, the load-bearing capacity of the slabs in 2–5BLA will probably be insufficient, also considering the expected significant rebar corrosion and cracking must therefore be expected.

Through continued degradation, the cohesion of the material will be further reduced. However, as the loads are strictly compressive, the remnants of the slabs will still be able to carry the combined load from the waste packages even after extensive cracking.

### 13.2.3 Transport properties

According to Section 6.7.1, the slabs in 2–5BLA will have the transport properties of concrete with a few penetrating cracks already at closure of the repository. Through the reduction of the load-bearing capacity indicated in Section 13.2.2, both the number and width of the cracks will increase but also the porosity, Section 13.2.1.

From this follows that the transport properties will correspond to those of significantly degraded concrete from about 20 000 to 25 000 years and up to 100 000 years post-closure.

### 13.2.4 Recommended material property data

Table 13-1 presents recommended material property data for the slabs in 2–5BLA for selected time periods up to 100 000 years post-closure. The recommendations are based on information regarding the status of the slabs at closure presented in Section 6.7, the expected evolution of the properties of the slabs described in the previous sections and the properties for degraded concrete given in Section 5.1.

**Table 13-1. Recommended material property data for the slabs in 2–5BLA for selected time periods from closure to 100 000 years post-closure.**

| | | Time period (Years post-closure) | | | | |
|---|---|---|---|---|---|---|
| **Property** | **Unit** | **At closure** | **0–1 000** | **1 000–20 000** | **20 000–50 000** | **50 000–100 000** |
| **pH** | - | ≥ 13 | 12.5–13 | 12.5 | < 10–12.5 | < 10 |
| **Porosity** | % | 11–13 | 11–13 | 11–14 | 13–15 | 15–20 |
| **Load-bearing capacity** | Rating (5–1) | 5 | 5 | 4–5 | 3–4 | 2–3 |
| **Hydraulic conductivity** | m/s | $10^{-8}$–$10^{-5}$ | $10^{-8}$–$10^{-5}$ | $10^{-8}$–$10^{-5}$ | $10^{-8}$–$10^{-4}$ | $10^{-4}$–$10^{-3}$ |
| **Diffusivity** | $m^2/s$ | $(2–5)\times10^{-12}$ | $(2–5)\times10^{-12}$ | $(5–9)\times10^{-12}$ | $(1–5)\times10^{-11}$ | $(5–9)\times10^{-11}$ |

### 13.2.5 Specific uncertainties

The following specific uncertainty in the description of the evolution of the properties of the slabs in 2–5BLA during the first 100 000 years post-closure has been identified:

- The evolution of the load-bearing capacity and the transport properties of the slabs are a bit uncertain. This is because neither the amount of reinforcement not detailed concrete mixing proportions and method of construction have yet been decided.

See also the discussion concerning the general uncertainties in Chapter 5.

# 14 Common cementitious components in SFR: post-closure evolution

In this chapter, the expected evolution of the properties of the plugs and other closure components and the common cementitious components during the first 100 000 years post-closure is described. The starting point for the descriptions is the expected status of these components at closure as presented in Section 6.8. The evolution of the properties of these components is then influenced by the processes presented in Chapter 4.

Detailed descriptions of the common cementitious components are given in Section 2.12. In addition, Chapter 3 presents detailed specifications and properties of the cementitious materials in the common cementitious components.

## 14.1 Literature

The following reports form the basis for the description of the post-closure evolution of the properties of the common cementitious components presented in this chapter:

- **Bogdanoff (2013)** describes degradation of rock reinforcement and rock injection in tunnels.
- **Cronstrand (2007)** modelled the evolution of the chemical properties of the engineered barriers in 1BMA which serve as a representative example of the evolution of the shotcrete.
- **Eriksson and Malm (2013)** calculated the load-bearing capacity of the concrete plugs for tunnels under different conditions.
- **Gaucher et al. (2005)** and **Cronstrand (2007)** modelled the post-closure evolution of the properties of the engineered barriers in the silo which here serves as a representative example of the interaction between the concrete plugs in the tunnels and the adjacent bentonite sections.
- **Grandia et al. 2010a** modelled the degradation of concrete plugs in boreholes.
- **Holmberg (2021)** investigated the properties of the shotcrete in SFR.[73]
- **Höglund (2019)** modelled the chemical evolution of the concrete caissons in 2BMA which serves as a representative example for the part of the concrete plugs in the tunnels which are in direct contact with the groundwater saturated crushed rock backfill material.
- **Idiart et al. (2019a, 2019b), Idiart and Shafei (2019) and Idiart and Laviña (2019)** modelled the degradation of different types of concrete in direct contact with the bedrock which here serves as a representative example of degradation of the part of the concrete plugs in the tunnels in direct contact with the bedrock.
- **Idiart et al. (2020)** modelled concrete/bentonite interactions in the bentonite barrier in the rock vault for legacy waste (BHA) in SFL. Even though the focus of this study was on montmorillonite dissolution, some parts of the report also included concrete degradation.
- **Lundin** investigated the properties of the shotcrete in SFR.[74]
- **Malm et al. (2017)** studied the load-bearing capacity of grouted rock bolts as a function of degradation.
- **Mårtensson (2019)** studied the properties of concrete plugs which had been cast in a water-filled borehole at a depth of about 220 meters in the Äspö HRL.
- **Sainz-Garcia et al. (2018)** modelled the influence of degradation of massive concrete plugs in SFR on the evolution of the transport properties of these plugs as well as the influence on groundwater flow in and in the vicinity of the repository.
- **Windelhed et al. (2002)** studied the stability of grouted rock bolts and describes different degradation mechanisms of importance for degradation of rock bolts and grout for rock bolts.

[73] SKBdoc 1991682 ver 1.0. (Internal document, in Swedish.)

[74] SKBdoc 1390675 ver 1.0. (Internal document, in Swedish.)

## 14.2 Concrete plugs in tunnels

### 14.2.1 Chemical properties

For the concrete plugs in tunnels, heterogeneous evolution of the chemical properties is expected. This is because the plugs will interact with the bentonite section on one side and with the groundwater saturated crushed rock backfill material on the other side. The periphery of the concrete plugs will be in direct contact with the surrounding bedrock and thus have low access to groundwater.

According to the studies of concrete/bentonite interactions by Cronstrand (2007) and Gaucher et al. (2005) discussed in Chapter 7, alterations of the chemical properties of concrete in contact with low-permeability bentonite are slow. Figure 7-3 shows that portlandite depletion stretches only about 300 mm into the concrete wall after 10 000 years and still after 100 000 years CSH_1.8 is the dominant CSH-phase in the major part of the outer wall of the silo, Figure 7-5. With a total thickness of at least 2 500 mm (Eriksson and Malm 2013), this means that only a small part of the concrete plug will be affected by interactions with the bentonite.

According to Cronstrand (2007), the alterations of the mineral composition in the outer wall of the silo (Section 7.3.1) leads to a decreased but varying porosity regardless of calculation model used as shown in Figure 7-7 for the time 100 000 years post-closure. Porosity clogging close to the concrete bentonite interface is also observed by Idiart et al. (2020) who show that clogging of the pores in about one third of the silo wall occurred already at 300 and 2 000 years post-closure depending on calculation model used.

The study by Höglund (2019) shows that also alterations of the concrete in contact with the groundwater saturated crushed rock backfill material are slow, Figures 9-1 to 9-5. Figure 9-5 shows that pH in the inner parts of the outer concrete wall – i.e. 680 mm from the interaction zone – varies between 12 and 12.5 at 100 000 years post-closure, indicating the presence of portlandite in at least some parts of the outer walls.

Finally, the studies by Idiart et al. (2019a) and Idiart and Shafei (2019) show that also degradation of concrete in direct contact with the bedrock is slow. However, as shown in Figure 11-1, a portlandite depleted zone can be formed at the plug/bedrock interface. Even if this zone does not dramatically affect the average chemical properties of the concrete plug, it can instead influence its transport properties by increasing the porosity in this zone as shown in Figure 11-3. However, the width of this zone and the extent of portlandite leaching are dependent on the local hydrogeological conditions at the position of the plug and for a bedrock with very few cracks only minor degradation is expected in the interface zone.

In all, the findings presented above indicate that portlandite will be present in the central parts of the concrete plugs up to 100 000 years post-closure.

### 14.2.2 Load-bearing capacity

The load-bearing capacity of the concrete plugs in the tunnels will be affected by the combined influence of concrete degradation and loss of function of the (optional) reinforcement bars. However, at present, the detailed design of the concrete plugs in the tunnels has not been decided and the use of reinforcement bars is therefore uncertain. For that reason, the discussion in this section assumes that reinforcement is not used as in the study by Eriksson and Malm (2013).

With an expected swelling pressure of the bentonite in the hydraulically tight sections of 2–4 MPa (Mårtensson et al. 2022), the load-bearing capacity of the concrete plugs can be estimated using e.g. structural mechanical calculations. In a study by Eriksson and Malm (2013), the impact of groundwater pressure, bentonite swelling pressure and temperature changes due to the annual temperature variations on the structural integrity of the concrete plugs were modelled.

Eriksson and Malm (2013) conclude that a thickness of the different concrete plugs in SFR of between 2.5 and 3 meters is required to withstand the analysed loads. However, in this study, the assumed annual temperature variations are exaggerated compared to those observed in SFR today and any results from these calculations probably on the cautious side.

In the case also concrete degradation is considered, the thickness has to be increased according to the desired life span of the concrete plugs. Assuming a loss of load-bearing capacity corresponding to a thickness reduction of 15 mm/1 000 years as pessimistically suggested by Mårtensson (2017), the thickness of the plugs needs to be increased by a total of 600 mm in order to ensure that the load-bearing capacity will be sufficient during the first 20 000 years post-closure. To ensure the load-bearing capacity over a longer period of time, the thickness of the plugs will have to be increased further.

### 14.2.3 Transport properties

As shown in Sections 5.1.3 and 11.6.3, alterations of the mineral composition of the concrete alone is not sufficient to dramatically alter the transport properties of the concrete plugs. Instead significant alterations can only be caused by the formation of penetrating cracks.

As mentioned in Section 14.2.2, the dimensions of the different concrete plugs in the tunnels in SFR have yet not been decided. However, based on the discussion in Section 14.2.2, the concrete plugs can be dimensioned to ensure that the load-bearing capacity will be sufficient over the required period of time. For that reason, it is not expected that cracks will form in the bulk of the concrete plugs during the first 20 000 years post-closure. Beyond this point in time, some cracks can form in parts of the plug but the impact of this on the transport properties of the concrete plugs is uncertain.

Finally, it should be noted that the influence of alterations of the mineral composition and increased porosity at the concrete/bedrock interface has not been considered. This is motivated by the expected slow concrete degradation in this area in combination with the small impact of increased porosity on the transport properties compared to that of the formation of penetrating cracks. See e.g. Idiart et al. (2019a) and Idiart and Shafei (2019) but also Section 5.1.3.

### 14.2.4 Recommended material property data

Table 14-1 presents recommended material property data for the concrete plugs in tunnels for selected time periods up to 100 000 years post-closure. The recommendations are based on information regarding the status of the concrete plugs in tunnels at closure presented in Section 6.8, the expected evolution of the properties of these plugs described in the previous sections and the properties for degraded concrete given in Section 5.1.

**Table 14-1. Recommended material property data for concrete plugs in the tunnels for selected time periods up to 100 000 years post-closure.**

| | | Time period (Years post-closure) | | | | |
|---|---|---|---|---|---|---|
| **Property** | **Unit** | **At closure** | **0–1 000** | **1 000–20 000** | **20 000–50 000** | **50 000–100 000** |
| **pH** | - | ≥ 13 | ≥ 13 | 12.5–13 | 12.5 | 12–12.5 |
| **Porosity** | % | 11–13 | 11–13 | 11–13 | 12–14 | 14–15 |
| **Load-bearing capacity** | Rating (5–1) | 5 | 5 | 4–5 | 3–4 | 2–3 |
| **Hydraulic conductivity** | m/s | $(1–5)\times10^{-12}$ | $(1–5)\times10^{-12}$ | $(1–5)\times10^{-12}$ | $10^{-11}–10^{-8}$ | $10^{-8}–10^{-5}$ |
| **Diffusivity** | $m^2/s$ | $(2–5)\times10^{-12}$ | $(2–5)\times10^{-12}$ | $(2–5)\times10^{-12}$ | $(5–9)\times10^{-12}$ | $(5–9)\times10^{-12}$ |

### 14.2.5 Specific uncertainties

The following specific uncertainties in the description of the evolution of the properties of the concrete plugs in tunnels during the first 100 000 years post-closure have been identified:

- The main uncertainties relate to the evolution of the properties at the concrete/bedrock interface. This is because this is dependent on the local conditions for each individual plug. This also includes bedrock movements which can induce the formation of small penetrating cracks or a permeable zone containing many such cracks.

- Also, the evolution of the load-bearing capacity is uncertain as the design and dimensions of the concrete plugs have not yet been decided. However, these can be adjusted in order to fulfil the required properties over time and are therefore not considered a major problem.
- Finally, the description of the evolution of the chemical properties of the concrete plugs is somewhat uncertain due to the large dimensions of the plugs which results in completely different chemical properties in different parts of the concrete plugs. This has been handled by assuming that the expected average chemical properties are controlled by the properties in the central parts of the plugs.

See also the discussion concerning the general uncertainties in Chapter 5.

## 14.3 Concrete plugs in investigation boreholes

### 14.3.1 Chemical properties

From the information presented in Section 3.4, three alternative materials for the concrete plugs in the investigation boreholes with considerably different mixing proportions and chemical properties exist, i.e. *SFR borehole concrete*, *Alternative SFR borehole concrete* and *Cement paste for boreholes*. From Section 2.12.2, the *Alternative SFR borehole concrete* has been envisioned for use in the concrete plugs for boreholes and the following evaluation is based on this prerequisite.

The post-closure evolution of the chemical properties of the concrete plugs in the investigation boreholes will be dependent on the success of the installation (Section 6.8.1) as well as on the flow of groundwater in the borehole in the zones adjacent to those where the concrete plugs have been installed. The consequence of this is that the evolution of the chemical properties will be unique for each individual concrete plug.

According to Grandia et al. (2010a), concrete degradation in boreholes is slow with an expected degradation rate of about 10 mm per 1 000 years. It should be noted though, that the grout used in this study contained significant amounts of silica fume which at least today is not expected to be present in the *Alternative SFR borehole concrete*.

An indication of the impact of concrete mixing proportions on degradation of concrete in direct contact with the adjacent bedrock (illustrative of the situation for a borehole plug enclosed by the tight bedrock and bentonite sections with very low hydraulic conductivity) can be found in Section 11.6. Here, portlandite depletion reaches about 1 meter in 100 000 years regardless of initial mixing proportions. If degradation is assumed to proceed only in the direction of the borehole, a plug with a length of about 2 meters is required to ensure that portlandite will be present up to about 100 000 years post-closure if degradation occurs from both sides of the plug. However, in the case of leaching in the direction perpendicular to the borehole, the concrete plug will be depleted of portlandite already at an early stage.

### 14.3.2 Load-bearing capacity

As shown in Figure 2-38, the concrete plugs enclose the bentonite section and will therefore only experience compressive loads corresponding to a maximum swelling pressure of the bentonite of about 4 MPa (Sandén et al. 2017).

As shown in Section 3.4.1 and 3.4.2 as well as by Babaahmadi (2015) both originally very porous grout as well as severely leached concrete have a compressive strength exceeding 4 MPa. For that reason, the risk for compression of the concrete plugs is low unless leaching is very extensive and a large amount of material is removed from the concrete plugs. However, this is considered unlikely.

Also, the risk for displacement of the concrete plugs in the boreholes is small even in the case of poor adhesion between the concrete plug and the bedrock. This is because the concrete plugs will also be enclosed by copper expanders and long sections of sand which will provide additional support and prevent displacement of the concrete plug.

In all, it is concluded that the ability of the concrete plug to prevent expansion of the bentonite section will be sufficient up to 100 000 years post-closure.

### 14.3.3 Transport properties

The evolution of the transport properties of the concrete plugs in the boreholes post-closure is uncertain and depend on the success of the installation as discussed in Section 6.8.1.

With an assumed status at closure corresponding to that shown in Figure 6-9, the low flow of water in the investigation borehole will ensure that leaching and alterations of the mineral composition in the concrete plugs in the investigation boreholes will be slow. Also, the formation of permeable cracks in the direction of the borehole is not expected even though rock movements can cause cracking of the concrete plugs in the direction perpendicular to the direction of the borehole.

It is therefore expected that the concrete plugs in the investigation boreholes will retain their original transport properties up to at least 20 000 years post-closure unless the flow of groundwater suddenly increases through the concrete zone. However, this is less probable as the concrete plugs will be placed in positions with few water bearing fractures and be surrounded by copper expanders and sections of sand and bentonite.

The transport properties of the concrete plugs in the investigation boreholes beyond 20 000 years post-closure is more difficult to predict but the main influencing factor will probably be the formation of cracks due to rock movements rather than mineral alterations. The consequence of this is that the timing of the different degradation states is uncertain.

### 14.3.4 Recommended material property data

Table 14-2 presents recommended material property data for the concrete plugs in boreholes for selected time periods up to 100 000 years post-closure. The recommendations are based on information regarding the status of the concrete plugs in boreholes at closure presented in Section 6.8, the expected evolution of the properties of these plugs described in the previous sections and the properties for degraded concrete given in Section 5.1.

**Table 14-2. Recommended material property data for concrete plugs in investigation boreholes for selected time periods up to 100 000 years post-closure.**

| | | Time period (Years post-closure) | | | | |
|---|---|---|---|---|---|---|
| **Property** | **Unit** | **At closure** | **0–1 000** | **1 000–20 000** | **20 000–50 000** | **50 000–100 000** |
| **pH** | - | ≥ 13 | 12.5–13 | 12–12.5 | 11–12 | 10–11 |
| **Porosity** | % | 11–13 | 11–13 | 11–13 | 12–16 | 16–20 |
| **Load-bearing capacity** | Rating (5–1) | 5 | 5 | 4–5 | 3–4 | 2–3 |
| **Hydraulic conductivity** | m/s | $10^{-12}$–$10^{-11}$ | $10^{-11}$–$10^{-10}$ | $10^{-11}$–$10^{-10}$ | $10^{-11}$–$10^{-10}$ | $10^{-10}$–$10^{-5}$ |
| **Diffusivity** | $m^2/s$ | $(2–5)\times10^{-12}$ | $(2–5)\times10^{-12}$ | $(2–5)\times10^{-12}$ | $(1–5)\times10^{-11}$ | $(5–9)\times10^{-11}$ |

### 14.3.5 Specific uncertainties

The following specific uncertainties in the description of the evolution of the properties of the concrete plugs in boreholes during the first 100 000 years post-closure have been identified:

- The dominant uncertainty regarding the evolution of the properties of the concrete plugs in the boreholes originates from the fact that the outcome of the installation of these plugs cannot be verified after casting.
- In addition, also the degradation rate of these plugs is somewhat uncertain as it is dependent on the local hydrogeological conditions in each borehole.

See also the discussion concerning the general uncertainties in Chapter 5.

## 14.4 Shotcrete on rock walls

### 14.4.1 Chemical properties

In the work by Cronstrand (2007) and Gaucher et al. (2005), the shotcrete used in SFR was assumed to have the same porosity and a similar mineral composition as the concrete (*Silo concrete*) used in the concrete structures in the silo and 1BMA. If the same assumption is made also here, the evolution of the chemical properties of the shotcrete on the rock walls of non-backfilled vaults (1-5BLA) or vaults backfilled with crushed rock (1–2BMA, 1BRT, upper parts of 1–2BTF) will follow that of the slab in 1BMA (Section 8.2) whereas the evolution of the shotcrete in the silo will follow that of the outer walls of the silo (Section 7.3) and the shotcrete in the lower parts of 1–2BTF will follow that of the cementitious backfill in 1–2BTF (Section 11.6) .

However, even though these scenarios indicate an intact shotcrete over many years, the most likely scenario is that leaching and mineral alterations in the contact zone between the shotcrete and the rock wall will cause the shotcrete to crack and detach from the rock wall with an increased rate of chemical alterations as a consequence. This will primarily occur in non-backfilled vaults but probably also near the roof in backfilled waste vaults. However, in backfilled areas, the pressure from the backfill material will prevent the shotcrete from completely detaching from the rock wall and thus reduce the rate of alterations of the chemical properties of the shotcrete.

In all, a reasonable estimate is that the “average evolution” of the chemical properties of the shotcrete involves a complete portlandite depletion before 5 000 years post-closure. Through continued degradation, the shotcrete is expected to be completely degraded with the chemical characteristics of a mixture of calcite and the aggregate material from about 10 000 to 20 000 years post-closure.

### 14.4.2 Load-bearing capacity

The load-bearing capacity of the shotcrete is basically determined by the adhesion between the rock wall and the shotcrete whereas the degradation of the concrete and steel fibre reinforcement has a smaller influence.

According to Section 14.4.1, the shotcrete will most probably detach from the rock wall and therefore lose its load-bearing capacity already at an early stage, probably before 1 000 years post-closure. However, for backfilled waste vaults, the backfill material will keep the shotcrete more or less in place even after a complete detachment and only in 1-5BLA, the shotcrete will become completely separated from the rock wall.

### 14.4.3 Transport properties

The evolution of the transport properties of the shotcrete on the rock walls is dependent on the evolution of the load-bearing capacity, Section 14.4.2. The transport properties of the shotcrete will therefore be affected by the presence of a large number of cracks already before 1 000 years post-closure. Through continued degradation and detachment from the rock wall, the shotcrete will have similar transport properties as the crushed rock backfill from before 5 000 years post-closure.

### 14.4.4 Recommended material property data

Table 14-3 presents recommended material property data for the shotcrete on the rock walls for selected time periods up to 100 000 years post-closure. The recommendations are based on information regarding the status of the shotcrete on the rock walls at closure presented in Section 6.8, the expected evolution of the properties of the shotcrete described in the previous sections and the properties for degraded concrete given in Section 5.1.

**Table 14-3. Recommended material property data for the shotcrete on the rock walls for selected time periods up to 100 000 years post-closure.**

| | | Time period (Years post-closure) | | | | |
|---|---|---|---|---|---|---|
| **Property** | **Unit** | **At closure** | **0–1 000** | **1 000–5 000** | **5 000–10 000** | **10 000–100 000** |
| **pH** | - | 12.5 | 13–12.5 | 12–12.5 | 10–12 | ≤ 10 |
| **Porosity** | % | 12–15 | 12–15 | 15–18 | 18–20 | ≥ 20 |
| **Load-bearing capacity** | Rating (5–1) | 5 | 1–5 | 1 | 1 | 1 |
| **Hydraulic conductivity** | m/s | $10^{-10}$ | $10^{-10}$–$10^{-4}$ | Not relevant* | Not relevant* | Not relevant* |
| **Diffusivity** | $m^2/s$ | $(3–7) \times 10^{-12}$ | $10^{-12}$–$10^{-11}$ | Not relevant* | Not relevant* | Not relevant* |

* The shotcrete will detach from the rock wall before 1 000 years post-closure and these properties are therefore not relevant for these time periods.

### 14.4.5 Specific uncertainties

The following specific uncertainty in the description of the evolution of the properties of the shotcrete on the rock walls during the first 100 000 years post-closure has been identified:

- The main uncertainty relates to the expected different short-term (up to 5 000 years post-closure) evolution of the properties of the shotcrete in backfilled and non-backfilled waste vaults. However, in the long-term perspective, the impact of this can be disregarded.

See also the discussion concerning the general uncertainties in Chapter 5.

## 14.5 Grout for rock bolts

### 14.5.1 Chemical properties

The post-closure evolution of the chemical properties of the grout for rock bolts will be dependent on the detailed conditions in the installation hole. This is because the rate of leaching and mineral alterations will be dependent on e.g. the width of the fractures intersecting the installation holes, the flow of groundwater as well as of the quality if the injection work. For an introduction to the impact of cement degradation processes on the properties of grout for rock bolts, see Windelhed et al. (2002).

For dry holes, leaching will occur only from the surface of the bedrock in a process similar to that described for leaching of concrete plugs for boreholes as discussed in Section 14.3.1 with an expected degradation rate of about 10 mm/1 000 years.

However, for grout for rock bolts, also the impact of corrosion of the rock bolts must be considered. This is because corrosion can cause the formation of hydraulically conducting channels in the grout that allows the groundwater to penetrate deeper into the hole. The rate and impact of these processes are associated with significant uncertainties.

In all, portlandite depletion must be expected before 5 000 years post-closure in “average” holes with complete degradation beyond 10 000 years post-closure. However, for bolts installed in very dry holes, leaching will be extremely slow as shown by Windelhed et al. (2002) and Malm et al. (2017).

### 14.5.2 Load-bearing capacity

The load-bearing capacity of the grout for rock bolts is defined as the ability to prevent rock fall-out. The tensile strength and the properties of the grout/bedrock interface as well as the interface between the grout and the bolt are therefore the most critical parameters. However, also the length of the grouted zone will influence on the load-bearing capacity.

In analogy to the shotcrete, the most important degradation mechanism will be loss of adhesion and increased porosity in the rock/grout interface. However, also corrosion of the rock bolts will affect the adhesion and load-bearing capacity even though this is not strictly related to the properties of the grout.

According to Windelhed et al. (2002) degradation of grout in boreholes that are not intersected by water bearing fractures is very slow. However, in spite of this, it is very difficult to argue that the load-bearing capacity of the grout for rock bolts will be sufficient to prevent rock fall-out beyond 5 000 years post-closure, i.e. the time for complete portlandite depletion.

### 14.5.3 Transport properties

The prediction of the evolution of the transport properties of the grout for rock bolts suffers from the same uncertainties as the prediction of the evolution of the chemical properties. For that reason, no well-based general timeline for the evolution of the transport properties of the grout for rock bolts can be presented. Following the information provided in Section 14.5.2, the transport properties of the grout for rock bolts in an average hole will correspond to those of a material with cracks and other hydraulically conducting zones from not later than 5 000 years post-closure. However, as shown by Windelhed et al. (2002) the function of the grout can be upheld for a very long time under favourable conditions.

### 14.5.4 Recommended material property data

Table 14-4 presents recommended material property data for the grout for rock bolts for selected time periods up to 100 000 years post-closure. The recommendations are based on information regarding the status of the grout for rock bolts at closure presented in Section 6.8, the expected evolution of the properties of this grout described in the previous sections and the properties for degraded concrete given in Section 5.1.

**Table 14-4. Recommended material property data for the grout for rock bolts for selected time periods up to 100 000 years post-closure.**

| | | Time period (Years post-closure) | | | | |
|---|---|---|---|---|---|---|
| **Property** | **Unit** | **At closure** | **0–1 000** | **1 000–5 000** | **5 000–10 000** | **10 000–100 000** |
| **pH** | - | 12.5 | 12.5 | 12–12.5 | 10–12 | ≤ 10 |
| **Porosity** | % | 15–20 | 15–20 | 20–25 | 25–30 | ≥ 30 |
| **Load-bearing capacity** | Rating (5–1) | 5 | 3–5 | 1–3 | 1 | 1 |
| **Hydraulic conductivity** | m/s | $10^{-8}$–$10^{-4}$ | $10^{-6}$–$10^{-4}$ | $10^{-4}$–$10^{-2}$ | $10^{-2}$ | $10^{-2}$ |
| **Diffusivity** | $m^2/s$ | $(2–5)\times10^{-12}$ | $(5–9)\times10^{-12}$ | $10^{-11}$–$10^{-9}$ | $10^{-9}$ | $10^{-9}$ |

### 14.5.5 Specific uncertainties

The following specific uncertainty in the description of the evolution of the properties of the grout for rock bolts during the first 100 000 years post-closure has been identified:

- The main uncertainties originate from the uncertain outcome of the filling of the borehole and the varying properties of the bedrock. However, in the long perspective, there exist few uncertainties on the evolution of the properties of this grout. This is because the grout is expected to be severely degraded already at an early stage post-closure.

See also the discussion concerning the general uncertainties in Chapter 5.

## 14.6 Injection grout in the fractures in the surrounding bedrock

### 14.6.1 Chemical properties

The post-closure evolution of the chemical properties of the injection grout in the fractures in the surrounding bedrock will be more or less unique for each individual fracture and for that reason no general timeline for the post-closure evolution can be presented. This is because the rate of leaching will be dependent on e.g. the width of the fracture, the flow of groundwater adjacent to the injected part as well as of the quality of the injection work.

However, from the low amount of injection grout in each fracture and the rather large uncertainties, it is expected that portlandite will be depleted already at between 3 000 and 10 000 years post-closure and the grout completely degraded at between 10 000 and 20 000 years post-closure.

For an introduction to degradation processes for injection grouts, see e.g. (Bogdanoff 2013) and references therein.

### 14.6.2 Load-bearing capacity

The load-bearing capacity is not relevant for the injection grout in the surrounding bedrock.

### 14.6.3 Transport properties

The prediction of the evolution of the transport properties of the injection grout in the surrounding bedrock suffers from the same uncertainties as the prediction of the evolution of the chemical properties. The low amount of materials in combination with scarce information on the homogeneity of the injection grout in the fractures and lack of information on the quality of the grout/bedrock interface make any predictions very uncertain.

For that reason, no well-based general timeline for the post-closure evolution of the transport properties of the injection grout in the fractures in the surrounding bedrock can be presented. However, it must be expected that the transport properties will be representative of a rather porous material already from about 1 000 years post-closure. This is mainly because injection grouts do not contain any aggregates and leaching will therefore affect the entire material volume.

### 14.6.4 Recommended material property data

Table 14-5 presents recommended material property data for the injection grout in the fractures in the surrounding bedrock for selected time periods up to 100 000 years post-closure. The recommendations are based on information regarding the status of the injection grout in the fractures in the surrounding bedrock at closure presented in Section 6.8, the expected evolution of the properties of this grout described in the previous sections and the properties for degraded concrete given in Section 5.1.

**Table 14-5. Recommended material property data for injection grout in the fractures in the surrounding bedrock for selected time periods up to 100 000 years post-closure.**

| | | Time period (Years post-closure) | | | | |
|---|---|---|---|---|---|---|
| **Property** | **Unit** | **At closure** | **0–1 000** | **1 000–3 000** | **3 000–10 000** | **10 000–100 000** |
| **pH** | - | 12.5 | 12.5 | 12–12.5 | 10–12 | ≤ 10 |
| **Porosity** | % | 15–20 | 15–20 | 20–25 | 25–30 | ≥ 30 |
| **Load-bearing capacity** | Rating (5–1) | Not relevant | Not relevant | Not relevant | Not relevant | Not relevant |
| **Hydraulic conductivity** | m/s | $10^{-8}$–$10^{-4}$ | $10^{-6}$–$10^{-4}$ | $10^{-4}$–$10^{-3}$ | $10^{-3}$–$10^{-2}$ | $10^{-2}$ |
| **Diffusivity** | $m^2/s$ | (1–5) × $10^{-11}$ | $10^{-11}$–$10^{-10}$ | $10^{-11}$–$10^{-10}$ | $10^{-11}$–$10^{-10}$ | $10^{-10}$ |

### 14.6.5 Specific uncertainties

The following specific uncertainty in the description of the evolution of the properties of the injection grout in the fractures in the surrounding bedrock during the first 100 000 years post-closure has been identified:

- The main uncertainties regarding the evolution of the properties of the injection grout in the surrounding bedrock originate in the uncertain outcome of the injection and the varying properties of the different fractures. However, in the long perspective, there exist few uncertainties on the evolution of the properties of this grout. This is because the grout is expected to be severely degraded already at an early stage post-closure.

See also the discussion concerning the general uncertainties in Chapter 5.

# 15 Summary and future work

In this report, SKB's current understanding of the post-closure evolution of the properties of the cementitious materials and components used in SFR during the first 100 000 years post-closure has been presented.

The report presents detailed information on cement types used and planned for use in the cementitious materials, mixing proportions of the cementitious materials and finally also information concerning the properties of the cementitious components in SFR1 and planned for SFR1 and SFR3.

In this work, information from the construction of SFR1 as well as from recent inspections of the cementitious components have been used. However, for SFR1, some information from the construction of the facility has been lost over the years, the consequence of which is that a full and detailed description of all cementitious materials and components in SFR1 has not been presented in this report. As an example, protocols and photographs from a final inspection just before the facility was taken into operation have not been found.

For SFR3 and the remaining parts of SFR1, detailed information on the status of the facility prior to start of operation is lacking and the analyses presented in this report have therefore been based on planned dimensions, materials and construction methods for the different cementitious components. First when the facility has been constructed, all details concerning e.g. dimensions and concrete mixing proportions will be known.

Because of this partial lack of information, the descriptions of the post-closure evolution of the cementitious components in SFR are associated with some uncertainties. For some cementitious components, in particular those which do not constitute significant parts of the engineered barrier systems, the consequence of these uncertainties is of limited importance. However, for other parts, lack of information may impose uncertainties in the assessment of the post-closure safety of the repository.

In the following sections, a short summary of the report is presented including the most important remaining uncertainties for the different waste vaults along with identified needs for future work aiming at reducing these uncertainties.

## 15.1 Silo

### *Description of the cementitious components*

The silo comprises the following cementitious components which are described in detail in Section 2.5.2:

- Slab.
- Outer walls.
- Lid.
- Inner walls.
- Permeable grout between waste packages and inner walls.
- Concrete moulds.

### *Status at closure and post-closure evolution*

The status at closure and the expected post-closure evolution of the cementitious components in the silo are presented in Section 6.1 and Chapter 7 respectively.

According to Section 6.1, only very small alterations of the properties of the cementitious components are expected during the operational period. This is because the concrete structure is surrounded by bentonite and other materials which limit groundwater interactions but also because the waste packages are grouted after disposal.

Also post-closure, the layers of bentonite or sand/bentonite will limit concrete degradation of the outer structural components even though this can of course never be entirely avoided. For the interior parts, the outer concrete structure and surrounding materials will ensure that concrete degradation will be slow during a significant period of time as shown in Chapter 7.

Finally, chemical interactions with the waste or with waste degradation products are expected to be small, Section 7.5.1. However, the impact of swelling waste is somewhat uncertain as discussed below.

#### *Uncertainties and future work*

For the silo, the main uncertainties originate from a lack of information on the current status of the different cementitious components, the main concern being the potential presence of cracks in the slab and outer walls formed during construction. For the outer walls, some information can be obtained by lowering a camera into the small shafts and recording the inside of the outer wall. Recording can also be used to obtain information regarding the status of the inner walls, at least for the upper parts in which waste has not yet been disposed and grouted. For the slab this is not possible.

There also remain some uncertainties regarding the closure of the silo. The current version of the closure plan for SFR (Mårtensson et al. 2022) does not include a description of the handling of the small shafts in direct proximity to the outer walls. Currently, there are no plans to use these shafts for disposal of waste which means that they could simply be filled with concrete to further improve the barrier properties of the outer walls. The strategy for these shafts must be described in a coming update of the closure plan for SFR (Mårtensson et al. 2022).

Finally, there remain some uncertainties concerning the cement conditioning of ion-exchange resins. Recent information indicates that insufficient amounts of water may have been used when mixing ion-exchange resins, water and cement powder disposed in concrete moulds. The potential effect of this is a larger swelling (or swelling pressure) than previously assumed. The consequences of this for the post-closure evolution of the properties of the concrete moulds remain to be resolved.

## 15.2 1BMA

#### *Description of the cementitious components*

1BMA comprises the following cementitious components which are described in detail in Section 2.6.2:

- Slab.
- Existing outer walls.
- New outer walls.
- Lid.
- Inner walls.
- Prefabricated concrete elements.
- Gas evacuation system.
- Concrete moulds.

#### *Status at closure and post-closure evolution*

The status at closure and the expected post-closure evolution of the cementitious components in 1BMA are presented in Section 6.2 and Chapter 8 respectively.

The status of the different cementitious components at closure will differ widely. Whereas the status of the slab and existing outer walls will be affected by up to 90 years of operation with observed increased level of chlorine, significant rebar corrosion and cracking as a consequence, the lid and new outer walls which are constructed at closure will instead be unaffected by the conditions in the repository. For the concrete moulds and prefabricated concrete elements, the status at closure will be dependent on the year of disposal or installation and their properties therefore vary from those of up to 90 years-old to those of younger concrete structures.

Post-closure, degradation of the chemical properties of the slab is expected to be faster than degradation of the lid and new outer walls because of its rather poor current condition. Also, a majority of the groundwater transport between the rock vault and the interior of the concrete structure will occur through the cracks in the slab, thus further increasing the rate of degradation of the slab.

The load-bearing capacity of the outer structural components is expected to be sufficient to resist the groundwater pressure during saturation as well as the pressure from the backfill material until when significant concrete degradation and rebar corrosion have occurred. At that point in time, cracks will start to appear in the outer concrete structure and eventually the structural integrity of the concrete structure may be lost. According to Chapter 8, the load-bearing capacity will be sufficient for at least up to 20 000 years post-closure but the detailed evolution of the load-bearing capacity and transport properties and the timing of the different events beyond this point in time cannot be determined with accuracy.

#### *Uncertainties and future work*

For 1BMA, a significant body of information on the current status of the existing concrete structure exists. However, for the slab, such information is lacking for a majority of the waste compartments which have already been filled with waste and in which inspections cannot be carried out. In addition, also detailed information on the mixing proportions of the *1BMA concrete* is scarce even though some information has been found. The prospect for obtaining additional information on the current status of the concrete structure in 1BMA is small and no plans have currently been made.

Instead, the main focus for 1BMA must be aimed at increasing the level of understanding of the status at closure and evolution of the properties of the new outer walls and lid which will be constructed at closure. As a first step, the detailed design – including dimensions, type and amount of reinforcement and required concrete properties – of these structural components must be determined. In addition, also a decision on the installation of a gas evacuation system is required as this will affect the over-all transport properties of the lid.

## 15.3 2BMA

#### *Description of the cementitious components*

2BMA comprises the following cementitious components which are described in detail in Section 2.7.2:

- Reinforced concrete slab.
- Slabs (bottom of concrete caissons).
- Outer walls.
- Lid.
- Inner walls.
- Prefabricated concrete elements.
- Gas evacuation system.
- Concrete moulds.

#### *Status at closure and post-closure evolution*

The expected status at closure and the expected post-closure evolution of the cementitious components in 2BMA are presented in Section 6.3 and Chapter 9 respectively.

The status of the cementitious components in 2BMA at closure are expected to show only minor differences. This is because none of the cementitious components will be older than about 45 years but more importantly because a waterproofing membrane will be installed in the waste vault during construction which will protect the cementitious components from intruding groundwater and therefore prevent both leaching and chlorine intrusion. In addition, corrosion is not expected to affect the cementitious components during the operational period. This is because steel reinforcement will not

be used but also because tie rods (if used during casting of the outer walls) will be removed and the holes sealed with a cementitious material. The exceptions are the concrete slab and the inner walls in which reinforcement can be used.

Also, post-closure, the impact of corrosion can probably be entirely ignored. For the outer construction parts which do not contain steel components, this is obvious. In addition, for the waste sufficient space around the waste packages will be provided to prevent that the formation of voluminous corrosion products or other expansive waste degradation products will cause cracking of the inner walls which in turn could affect the structural integrity of the external construction parts.

The consequence of this is that concrete degradation will be the sole cause of alterations of the properties of the cementitious components in 2BMA and diffusion will be the main transport mechanism during a long period of time. However, with time concrete degradation will render the load-bearing capacity of the concrete structure insufficient to prevent cracking or eventually loss of structural integrity. From this stage onwards, the properties of the cementitious components will have the characteristics of severely degraded concrete with an increasing contribution of advection as the dominant transport mechanism and accelerated concrete degradation as a consequence.

#### *Uncertainties and future work*

For 2BMA, the main uncertainties are associated with the method for construction of the inner walls and the evolution of their load-bearing capacity. This is because no efforts have yet been aimed at developing concrete mixing proportions and method of construction for the inner walls. This is expected to be carried out within the design phase for SFR3 and no separate programme for this is judged to be required.

Besides the uncertainties associated with the inner walls, there remain only a few uncertainties regarding the initial state of the concrete caissons as well as their post-closure evolution. This is because significant amounts of information can be collected from the programme for development of concrete mixing proportions and method of construction discussed in Sections 3.3.3 and 2.7.2 respectively. However, as long as the concrete caissons have not yet been constructed some uncertainties will of course remain.

In addition, there remain some uncertainties regarding the load-bearing capacity of the caissons in general and the impact of formation of penetrating cracks in the unreinforced structure. Here, the main concern is the possible loss of the structural integrity of the entire caisson once the load-bearing capacity of one of the structural components has become insufficient due to concrete degradation. Additional work to further clarify the coupling of the load-bearing capacity between the different structural components could be carried out.

## 15.4 1BRT

#### *Description of the cementitious components*

1BRT comprises the following cementitious components which are described in detail in Section 2.8.2:

- Slab.
- Outer walls.
- Lid.
- Inner walls between waste compartments.
- Inner walls between waste packages.
- Prefabricated concrete elements.

It is worth to stress that these components together will create a concrete monolith which will be surrounded by the groundwater saturated gravel backfill. Because of this design, the structural stability of the combined structure will be significant and only limited cracking therefore expected over long periods of time. The consequence of this is that degradation of the cementitious components will mainly be controlled by diffusion and therefore slow or even insignificant in the internal parts of the waste domain.

### *Status at closure and post-closure evolution*

The expected status of the cementitious components at closure and the expected post-closure evolution of the cementitious components in 1BRT are presented in Section 6.4 and Chapter 10 respectively.

At closure, all cementitious components in 1BRT are expected to have the properties of no more than 45 years old undegraded concrete. This is because a waterproofing membrane will be installed in the waste vault during construction and protect the cementitious components from intruding groundwater. By this means, both leaching and chlorine intrusion as well as rebar corrosion during the operational period are prevented.

The post-closure evolution of the properties of the cementitious components in 1BRT is expected to be controlled by diffusion through the concrete monolith for a significant part of the post-closure period. The consequence of this is that leaching and mineral alterations will occur on the outside of the lid and outer walls at an early stage post-closure whereas such alterations will occur at a much later stage in the interior of the waste domain. The impact of processes in the waste will be limited because the waste only comprises steel components and corrosion is very slow.

### *Uncertainties and future work*

For 1BRT, there remain some uncertainties regarding the methods of construction in general. This is because the outer concrete structure does not formally constitute a significant hydraulic barrier and any requirements concerning concrete mixing proportions or methods of construction for 1BRT to prevent cracking have not been prescribed. Because of this, there remain some uncertainties regarding the risk for formation of cracks during construction or the impact of corrosion of (potential) tie rods used during casting of the outer walls and inner walls between the waste compartments. This is expected to be clarified during the design of SFR3.

## 15.5 1–2BTF

Description of the cementitious components

1–2BTF comprise the following cementitious components which are described in detail in Section 2.9.2:

- Slabs.
- Lids.
- Prefabricated concrete elements.
- Grout between waste packages.
- Cementitious backfill.
- Concrete tanks.
- Concrete moulds.

### *Status at closure and post-closure evolution*

The expected status at closure and the expected post-closure evolution of the cementitious components in 1–2BTF are presented in Section 6.5 and Chapter 11 respectively and only shortly summarised here.

The status of the different cementitious components at closure will differ widely. Whereas that status of the slabs will be affected by up to 90 years of operation with increased level of chlorine and probably significant rebar corrosion and cracking as a consequence, the lids and cementitious backfill which are constructed at closure will instead be unaffected by the conditions in the repository. For the concrete tanks, concrete moulds and prefabricated concrete elements, the status at closure will be dependent on the year of disposal or installation and their properties therefore vary from those of up to 90 years-old to very young concrete structures.

Also, the post-closure evolution of the cementitious components will vary significantly. For the unreinforced cementitious backfill, chemical degradation will be slow and the load-bearing capacity sufficient for a very long period of time. The concrete tanks will on the other hand be affected by both concrete degradation and rebar corrosion and the risk for a loss of structural integrity already at an early stage is therefore significant as discussed in Section 11.7. With a loss of structural integrity of the concrete tanks follows the possible collapse of the lids and the prefabricated elements. This will have a significant impact on the transport properties of these components as discussed in Section 11.3 and 11.4.

#### *Uncertainties and future work*

For 1–2BTF, the main uncertainties relate to the post-closure evolution of the load-bearing capacity of the concrete tanks and the coupling between this and the risk for an early collapse of the lid.

According to Section 11.7, the ability of the concrete tanks to resist the groundwater pressure at repository depth during saturation is insufficient and significant cracking must therefore be expected for tanks which are not filled with groundwater during the early part of the saturation period. The consequence of early cracking will be an increase of both the rate of concrete degradation and rebar corrosion.

For the concrete tanks, also a number of uncertainties related to the different structural components have been identified. See Section 11.7.5 for details. The handling of these uncertainties requires that the tanks are made available for inspection which in turn requires that a significant portion of the tanks are transferred to a temporary storage facility.

Finally, there also exist significant uncertainties concerning the properties of the grout between the waste packages. Here, there is a lack of information on the properties of the grout itself but also of the outcome of grouting of both steel drums and the concrete tanks. A need for studies of both material properties and the grouting process has therefore been identified.

## 15.6 1BLA

#### *Description of the cementitious components*

A short description of the slab in 1BLA is given in Section 2.10.2.

#### *Status at closure and post-closure evolution*

The expected status of the slab in 1BLA at closure and the expected post-closure evolution are presented in Section 6.6 and Chapter 12 respectively.

According to Section 6.6, at closure the chemical properties of the slab in 1BLA will have the characteristics of about 90 years old reinforced *1BMA concrete*. Major alterations of the mineral composition are not expected during the operational period, although some carbonation of the upper few millimetres of the slabs may occur.

However, Section 6.6 also notes that the slab has been partly exposed to groundwater up until the year 2021 when a waterproofing membrane which diverts the intruding groundwater was installed. The consequences of the groundwater interactions are increased levels of chlorine, carbonate and sulphate in the affected parts of the slab as well as an increased rate of rebar corrosion.

Concerning the load-bearing capacity of the slab, Section 6.6. raises some concern that cracks may have formed already during construction and the operational period and refers to two separate studies, both of which indicate that penetrating cracks may have formed in the slab of 1BLA due to external loads from the stack of waste packages during the operational period.

The risk for cracking is further increased since corrosion of the reinforcement bars during the up 90 years of operation will reduce the load-bearing capacity of the slab compared to at the time of construction.

Finally, Section 12.2.3 concludes that leaching and rebar corrosion post-closure will increase the number and width of the cracks as well as the porosity of the slab. From this it is concluded that the transport properties of the slab in 1BLA will have the characteristics of a significantly degraded concrete slab from about 10 000 to 15 000 years post-closure.

#### *Uncertainties and future work*

For the slab in 1BLA, no significant uncertainties are identified. The current status of the slab is reasonably well known and the current understanding on concrete evolution over long periods of time is sufficient to predict the post-closure evolution of the properties of the slab. The impact of uncertainties concerning concrete mixing proportions for the slab in 1BLA on the evolution of the chemical properties are small as indicated by the findings by Idiart et al. (2019a). Efforts to further decrease remaining uncertainties on concrete mixing proportions for the slab are thus not prioritised.

## 15.7 2–5BLA

#### *Description of the cementitious components*

A short description of the slabs in 2–5BLA is given in Section 2.11.2.

#### *Status at closure and post-closure evolution*

The expected status at closure and the expected post-closure evolution of the slabs in 2–5BLA are presented in Section 6.7 and Chapter 13 respectively.

According to Section 6.7, at closure the chemical properties of the slabs in 2–5BLA will have the characteristics of 40–45 years old reinforced *2BMA concrete*. Alterations of the mineral composition are not expected during the operational period, although some carbonation of the upper few millimetres of the slabs could occur. This is because a waterproofing membrane will be installed in the waste vault that diverts intruding groundwater to the drainage system and prevents concrete/groundwater interactions.

In addition, the load-bearing capacity of the slabs are expected to be sufficient to carry the load from the stack of waste packages as well as the dynamic load from the transport truck with waste. Cracking due to insufficient load bearing capacity is therefore not expected during the operational period.

However, because the slabs in 2–5BLA do not formally constitute hydraulic barriers Section 6.7 states that the use of such construction methods that prevent cracking or formation of joints or other permeable zones during construction will probably not be prescribed. For that reason, it is expected that the slabs at closure will contain a few small cracks and/or somewhat permeable construction joints which may affect the transport properties of the slabs.

Post-closure, the properties of the slabs will slowly degrade through concrete degradation and rebar corrosion. As both sides of the slabs will be in contact with the groundwater, concrete degradation will be comparatively fast which in turn will lead to a reduction of the load-bearing capacity and eventually also to significant cracking which will affect the transport properties of the slabs. Section 13.2 therefore predicts that the slabs in 2–5BLA will be severely degraded from about 20 000–25 000 years post-closure.

#### *Uncertainties and future work*

There remain some uncertainties concerning the mixing proportions of the concrete as well as thickness of and amount of reinforcement in the slabs and the impact of this on the load-bearing capacity and transport properties of the slabs in 2–5BLA. However, for the chemical properties, the impact of uncertainties concerning concrete mixing proportions is small as indicated by the findings by Idiart et al. (2019a).

Uncertainties concerning the design of the slabs are expected to be clarified during the upcoming design phase for SFR3.

## 15.8 Concrete plugs in tunnels

### *Description of the cementitious components*

A description of the concrete plugs in the tunnels is given in Section 2.12.3.

### *Status at closure and post-closure evolution*

The expected status at closure and the expected post-closure evolution of the concrete plugs in the tunnels are presented in Section 6.8.1 and Section 14.2 respectively.

The concrete plugs will be constructed at closure and their chemical properties and load bearing capacity at closure will therefore be the same as those of undegraded plugs made of *SFR plug concrete*.

For the transport properties, these are mainly controlled by the presence of cracks or permeable zones at the rock/plug interface or by cracks in the plug itself. Because of the risk for cracking during casting, Section 6.8.1 expects that the transport properties of the concrete plugs in the tunnels at closure will correspond to those of undegraded plugs made from *SFR plug concrete* with a few small penetrating cracks. However, for the thick concrete plugs, it is uncertain if all cracks will penetrate the entire plug.

Post-closure, Section 14.2.1 expects a heterogeneous evolution of the chemical properties. This is because the plugs will interact with the bentonite section on one side and with the groundwater saturated crushed rock backfill material on the other side. The periphery of the concrete plugs will be in direct contact with the surrounding bedrock and thus have low access to groundwater. Because of their great thickness, Section 14.2.1 predicts that portlandite will be present in the central parts of the concrete plugs during the first 100 000 years post-closure.

Sections 14.2.2 and 14.2.3 discuss the post-closure evolution of the load-bearing capacity and transport properties respectively. In these sections, it is again noted that the design of the concrete plugs has not yet been decided and that any prediction of the post-closure evolution and recommendations of material property data at present will have to rely on assumptions based on experiences rather than known data. However, from experiences and information in studies on concrete degradation the concrete plugs in the tunnels are expected to remain structurally intact (even though cracked) during the first 100 000 years post-closure as evident from the recommended material property data in Table 14-1.

### *Uncertainties and future work*

At present, neither the dimensions and concrete mixing proportions nor amount and type of reinforcement of any of the future concrete plugs in the tunnels in SFR are decided. The consequence of this is that the status of these plugs at closure is not yet known but also that recommendations of material property data for these plugs can only be based on assumptions.

In order to overcome the remaining uncertainties, the dimensions, concrete mixing proportions as well as type and amount of reinforcement of the concrete plugs in SFR should be decided.

In this work, experiences from casting of large concrete plugs within the DOMPLU (Grahm et al. 2015) and PROTOTYPE (Dahlström 2009) projects will provide valuable input.

## 15.9 Concrete plugs in investigation boreholes

### *Description of the cementitious components*

A description of the concrete plugs in investigation boreholes is given in Section 2.12.3.

### *Status at closure and post-closure evolution*

The expected status at closure and the expected post-closure evolution of the concrete plugs in investigation boreholes are presented in Section 6.8.1 and Section 14.3 respectively.

According to Section 6.8.1, the properties of the concrete plugs in the investigation boreholes will correspond to those of up to 90 years-old concrete. However, significant leaching during the operational period is not expected as the concrete plugs are confined between other borehole sealing components and the bedrock and groundwater flow therefore limited.

According to Section 14.3, the post-closure evolution of the chemical properties of the concrete plugs in the investigation boreholes will be dependent on the success of the installation as well as on the flow of water in the borehole in the zones adjacent to those where the concrete plugs have been installed. The consequence of this is that the evolution of the chemical properties will be unique for each individual concrete plug.

Concerning the load-bearing capacity, Section 14.3 expects that the concrete plugs will be able to prevent expansion of the bentonite section up to 100 000 years post-closure. This conclusion is based on the fact that the concrete plugs will only experience compressive loads corresponding to a maximum swelling pressure of the bentonite of about 4 MPa (Sandén et al. 2017). In addition, Section 14.3 concludes that the compressive strength of the plug concrete will be sufficient to avoid compression but also that the risk for displacement of the plug is low. This is further motivated in Section 14.3.

The evolution of the transport properties of the concrete plugs in the boreholes post-closure is uncertain and depend on the success of the installation as discussed in Section 6.8.1. See also below.

#### *Uncertainties and future work*

For concrete plugs in investigation boreholes, the main uncertainties originate from the fact that the properties of the concrete plugs cannot be tested and verified after casting. Further, there is a scarcity of results from material studies of concrete plugs from experiments focused on casting of concrete plugs at great depth. This means that both the status at closure of these plugs and the post-closure evolution are uncertain. In order to reduce these uncertainties, additional experiments – also including over-coring of concrete plugs at great depth – are required.

## 15.10 Shotcrete on the rock walls

#### *Description of the cementitious components*

A description of the shotcrete on the rock walls is given in Section 2.12.3.

#### *Status at closure and post-closure evolution*

The expected status at closure and the expected post-closure evolution of the shotcrete on the rock walls are presented in Section 6.8.1 and Section 14.4 respectively.

Section 6.8.1 states that the properties of the shotcrete at closure will be representative of up to 90 years old *SFR shotcrete* which has been exposed to a marine environment. This means that both leaching, carbonation and intrusion of species from the groundwater such as sulphate and chlorine must be expected.

The suggested post-closure evolution presented in Section 14.4 expects that the shotcrete will detach from the rock wall and lose its load-bearing capacity already at an early stage, probably before 1 000 years post-closure. However, it is also expected that the backfill material installed in some vaults will keep the shotcrete more or less in place even after a complete detachment and only in 1–5BLA, the shotcrete will become completely separated from the rock wall.

Through leaching of the detached shotcrete, Section 14.4 expects a complete portlandite depletion before 5 000 years post-closure.

The load-bearing capacity of the shotcrete, i.e. its ability to prevent rock fall-out is basically determined by the adhesion between the rock wall and the shotcrete whereas the degradation of the concrete and steel fibre reinforcement has a smaller influence. This means that the load-bearing capacity will be lost early post-closure.

The transport properties of the shotcrete on the rock walls will follow the evolution of the load-bearing capacity. The transport properties of the shotcrete will therefore be affected by the presence of a large number of cracks already from about 1 000 years post-closure. Through continued degradation and detachment from the rock wall, the shotcrete on the rock walls will have similar transport properties as the crushed rock backfill from before 5 000 years post-closure.

#### *Uncertainties and future work*

The uncertainties regarding the status of shotcrete in SFR at closure are small. This is because the periodic controls of the properties of the shotcrete in SFR1 provide detailed information during the operational period. Further, the shotcrete in SFR3 can be based on a standard concept for shotcrete with well-known mixing proportions and properties.

Section 14.4.5 identifies the main uncertainty as being the short-term (up to 5 000 years post-closure) evolution of the properties of the shotcrete in backfilled and non-backfilled waste vaults. After this point in time the shotcrete is expected to be completely degraded and uncertainties therefore small.

However, as the function of the shotcrete must only be upheld during the operational period, these uncertainties are deemed not critical as long as the shotcrete prevents rock fall-out during the operational period.

For this reason, additional work related to assignment of material property data for the shotcrete on the rock walls is not foreseen.

## 15.11 Grout for rock bolts

#### *Description of the cementitious components*

A description of the grout for rock bolts is given in Section 2.12.3.

#### *Status at closure and post-closure evolution*

The expected status at closure and the expected post-closure evolution of the grout for rock bolts are presented in Section 6.8.1 and Section 14.5 respectively.

In summary, the status of the grout for rock bolts at closure can be reasonably well described whereas the post-closure evolution is more uncertain. This is because the properties depend on the properties of the grout itself but also of the presence of fractures and groundwater flow in the surrounding bedrock as well the outcome of the installation work.

#### *Uncertainties and future work*

The main uncertainties associated with the assessment of material property data for grout for rock bolts concern the properties of the bedrock and in particular the presence of water conducting fractures that intersect the grouted borehole. On the other hand, uncertainties in the status of the grout for rock bolts at closure are small. This is because grouting of rock bolts is a standardised process and that the properties of the grout are well-known.

However, as the function of the grout for rock bolts must only be upheld during the operational period, these uncertainties are deemed not critical as long as the grout ensures that the rock bolts are securely fastened in the bedrock during the operational period.

For this reason, additional work related to assignment of material property data for the grout for rock bolts is not foreseen.

## 15.12 Injection grout in the surrounding bedrock

### *Description of the cementitious components*

A description of the injection grout in the surrounding bedrock is given in Section 2.12.3.

### *Status at closure and post-closure evolution*

The expected status at closure and the expected post-closure evolution of the injection grout in the surrounding bedrock are presented in Section 6.8.1 and Section 14.6 respectively.

In summary, no unambiguous description of the status of the injection grout in the fractures in the surrounding bedrock at closure or of its post-closure evolution can be presented. This is because the properties depend on the properties of the grout itself but also of the properties of the fracture system and the outcome of the injection work.

### *Uncertainties and future work*

The main uncertainties associated with the assessment of material property data for the injection grouts in the surrounding bedrock concern the fact that the properties will be unique for each individual fracture as mentioned above.

However, as the function of the injection grout must only be upheld during the operational period, these uncertainties are deemed not critical as long as the injection grout limits the amount of intruding groundwater into the tunnels during the operational period.

For this reason, additional work related to assignment of material property data for the injection grout in the surrounding bedrock is not foreseen.

# References

SKB's (Svensk Kärnbränslehantering AB) publications can be found at www.skb.com/publications. SKBdoc documents will be submitted upon request to document@skb.se.


**Abarca E, Idiart A, de Vries L M, Silva O, Molinero J, von Schenck H, 2013.** Flow modelling on the repository scale for the safety assessment SR-PSU. SKB TR-13-08, Svensk Kärnbränslehantering AB.

**Abarca E, Sampietro D, Sanglas J, Molinero J, 2020.** Modelling of the near-field hydrogeology. Report for the safety assessment SR-PSU (PSAR). SKB R-19-20, Svensk Kärnbränslehantering AB.

**Babaahmadi A, 2015.** Durability of cementitious materials in long-term contact with water. PhD thesis. Chalmers Institute of Technology, Sweden.

**Björkenstam E, 1997.** Utveckling av SFR-bruket. UC 97:4Ö, Vattenfall Utveckling AB. SKBdoc 1439832 ver 1.0, Svensk Kärnbränslehantering AB. (In Swedish.)

**Bogdanoff I, 2013.** Degradering av berg, förstärkningar och injektering i tunnlar. SSM 2013:26, Strålsäkerhetsmyndigheten (Swedish Radiation Protection Authority). (In Swedish.)

**Brantberger M, Jansson T, 2009.** Underground design Forsmark, Layout D2, Grouting. SKB R-08-114, Svensk Kärnbränslehantering AB.

**Bultmark F, 2017a.** Stapling av betongkokiller. SKBdoc 1561909 ver 1.0, Svensk Kärnbränslehantering AB. (In Swedish.)

**Bultmark F, 2017b.** Korrosion av armeringsjärn i betongtankar i 1–2BTF. SKBdoc 1577565 ver 1.0. Svensk Kärnbränslehantering AB. (In Swedish.)

**Börgesson L, Åkesson M, Kristensson O, Malmberg D, Birgersson M, Hernelind J, 2015.** Modelling of critical H-M processes in the engineered barriers of SFR. SKB TR-14-27, Svensk Kärnbränslehantering AB.

**Cementa AB, 2023.** Injektering 30. CEM I 52,5 N – SR 3 LA, Cementa AB, Sweden. (In Swedish.)

**Christiansson R, 1987.** Byggnadsgeologisk uppföljning, sammanställning av delrapport 1–6. SKB SFR 87-06, Svensk Kärnbränslehantering AB. (In Swedish.)

**Cronstrand P, 2007.** Modelling the long-time stability of the engineered barriers of SFR with respect to climate changes. SKB R-07-51, Svensk Kärnbränslehantering AB.

**Cronstrand P, 2010.** Consequences of increased concentrations of carbonates for the engineered barriers in SFR. T-CNV 2010-013, Vattenfall AB. SKBdoc 1281370 ver 1.0, Svensk Kärnbränslehantering AB.

**Cronstrand P, 2014.** Evolution of pH in SFR 1. SKB R-14-01, Svensk Kärnbränslehantering AB.

**Cronstrand P, Hassanzadeh M, Hed G, 2011.** Metodik för bedömning av långsiktig funktion hos betongbarriärer, SFR. AE-NCC 11-113, Vattenfall AB. SKBdoc 1326418 ver 0.1, Svensk Kärnbränslehantering AB. (In Swedish.)

**Dahlström L-O, 2009.** Experiences from the design and construction of plug II in the Prototype Repository. SKB R-09-49, Svensk Kärnbränslehantering AB.

**Duro L, Grivé M, Domènesh C, Roman-Ross G, Bruno J, 2012.** Assessment of the evolution of the rdox conditions in SFR1. SKB TR-12-12, Svensk Kärnbränslehantering AB.

**Elfwing M, Mårtensson P, Pettersson A, 2015.** Rapport över aktuell status för 1BMA i SFR. SKBdoc 1440875 ver 2.0, Svensk Kärnbränslehantering AB. (In Swedish.)

**Elfwing M, Mårtensson P, Pettersson A, von Schenck H, 2016.** Fördjupad redovisning av förstärkningsmetod för betongkonstruktionen i 1BMA i SFR1. SKBdoc 1534701 ver 2.0, Svensk Kärnbränslehantering AB. (In Swedish.)

**Elfwing M, Lundin M, von Schenck H, 2017.** Vidareutvecklad utformning av förvarsutrymmet 2BMA i utbyggd del av SFR. SKBdoc 1569813 ver 1.0, Svensk Kärnbränslehantering AB. (In Swedish.)

**Elfwing M, von Schenk H, Åstrand P-G, 2018.** Uppdaterad analys av strålsäkerheten efter förslutning för 1BMA i SFR1. SKBdoc 1686798 ver 1.0, Svensk Kärnbränslehantering AB. (In Swedish.)

**Emborg M, Jonasson J-E, Knutsson S, 2007.** Långtidsstabilitet till följd av frysning och tining av betong och bentonit vid förvaring av låg- och medelaktivt kärnavfall i SFR 1. SKB R-07-60, Svensk Kärnbränslehantering AB. (In Swedish.)

**Eriksson D, 2021.** Hållfasthetsutredning av ytterväggar i 1BMA belastade av återfyllnadstryck. DMG1009682, Vattenfall AB. SKBdoc 1954971 ver 1.0, Svensk Kärnbränslehantering AB. (In Swedish.)

**Eriksson D, Malm R, 2013.** Geometrioptimering av pluggar för förslutning av SFR – projekt SFR-utbyggnad. SKBdoc 1346127 ver 1.0, Svensk Kärnbränslehantering AB. (In Swedish.)

**Eriksson M, Petersson J, Danielsson P, Leander M, 2009.** Underground design Forsmark, Layout D2, Rock mechanics and rock support. SKB R-08-115, Svensk Kärnbränslehantering AB. (In Swedish.)

**Eriksson D, Gasch T, Malm R, 2012.** Konceptuell utformning av pluggar för SFR. SKBdoc 1334119 ver 1.0, Svensk Kärnbränslehantering AB. (In Swedish.)

**Eriksson D, Bultmark F, Andersson H, 2015.** Gasevakuering genom betongbarriär i 2BMA. SKBdoc 1409731 ver 1.0, Svensk Kärnbränslehantering AB. (In Swedish.)

**Grahm P, Malm R, Eriksson D, 2015.** System design and full-scale testing of the Dome Plug for KBS-3V deposition tunnels – Main report. SKB TR-14-23, Svensk Kärnbränslehantering AB.

**Gaucher E, Tournassat C, Nowak C, 2005.** Modelling the geochemical evolution of the multi-barrier system of the silo of the SFR repository, Final report. SKB R-05-80, Svensk Kärnbränslehantering AB.

**Grandia F, Galindez J-M, Arcos D, Molienero J, 2010a.** Quantitative modelling of the degradation processes of cement grout, Project CEMMOD. SKB TR-10-25, Svensk Kärnbränslehantering AB.

**Grandia F, Galindez J-M, Molienero J, Arcos D, 2010b.** Evaluation of low-pH cement degradation in tunnel plugs and bottom plate systems in the frame of SR-Site. SKB TR-10-62, Svensk Kärnbränslehantering AB.

**Holmberg H, 2021.** Nytt kringgjutningsbruk till silon i SFR – Spaltgjutningsförsök. VRD-R48:2021, Vattenfall AB. SKBdoc 1953607 ver 1.0, Svensk Kärnbränslehantering AB. (In Swedish.)

**Holmberg H, Lagerlund J, 2021.** Provning av kringgjutningsbruk till silo/SFR, Fältförsök betongstation. VRD-R12:2021, Vattenfall AB. SKBdoc 1933732 ver 1.0, Svensk Kärnbränslehantering AB. (In Swedish.)

**Holmén J G, Stigsson M, 2001.** Modelling of the future hydrogeological conditions at SFR. SKB R-01-02, Svensk Kärnbränslehantering AB.

**Höglund L O, 2001.** Project SAFE, Modelling of the long-term concrete degradation processes in the Swedish SFR repository. SKB R-01-08, Svensk Kärnbränslehantering AB.

**Höglund L O, 2014.** The impact of concrete degradation on the BMA barrier functions. SKB R-13-40, Svensk Kärnbränslehantering AB.

**Höglund L O, 2018.** pH-utveckling i bergssal BRT. SKBdoc 1608409 ver 2.0, Svensk Kärnbränslehantering AB. (In Swedish.)

**Höglund L-O, 2019.** pH evolution in 2BMA – assumptions, data and modelling results. SKBdoc 1698794 ver 1.0, Svensk Kärnbränslehantering AB.

**Höglund L O, Bengtsson A, 1991.** Some chemical and physical processes related to the long-term performance of the SFR repository. SKB SFR 91-06, Svensk Kärnbränslehantering AB.

**Höglund L O, Pers K, 2000.** Översiktlig bedömning av konsekvenser för omgivande barriärer i BMA (SFR) till följd av ny behandling och förpackning av indunstarkoncentrat i Forsmark. AR 2000-12, Kemakta. SKBdoc 1417785 ver 1.0, Svensk Kärnbränslehantering AB. (In Swedish.)

**Idiart A, Laviña M, 2019.** Modelling of concrete degradation in a one-million-year perspective – Hydro – chemical processes. Report for the safety evaluation SE-SFL. SKB R-19-13, Svensk Kärnbränslehantering AB.

**Idiart A, Shafei B, 2019.** Modelling of concrete degradation – Hydro – chemical processes. Report for the safety evaluation SE-SFL. SKB R-19-11, Svensk Kärnbränslehantering AB.

**Idiart A, Olmeda J, Laviña M, 2019a.** Modelling of concrete degradation – influence of concrete mix design. Report for the safety evaluation SE-SFL. SKB R-19-14, Svensk Kärnbränslehantering AB.

**Idiart A, Laviña M, Coene E, 2019b.** Modelling of concrete degradation – Hydro – chemo – mechanical processes. Report for the safety evaluation SE-SFL. SKB R-19-12, Svensk Kärnbränslehantering AB.

**Idiart A, Laviña M, Grandia F, Pont A, 2020.** Reactive transport modelling of montmorillonite dissolution. Report for the safety evaluation SE-SFL. SKB R-19-15, Svensk Kärnbränslehantering AB.

**Jacobsen S, Gjörv O, 1987.** Hydraulisk konduktivitet i SFR silobetong. SKB Teknisk PM 45, Svensk Kärnbränslehantering AB. (In Swedish.)

**Kennedy T C, Lau D, Ofoegbu G I, 1984.** Permeability of compacted granular materials. Canadian Geotechnical Journal, volume 21, 726–729.

**Könönen M, Olsson D, 2018.** 2BMA – Analys av konstruktionsstyrande lastfall och olyckslaster. SKBdoc 1609765 ver 1.0, Svensk Kärnbränslehantering AB. (In Swedish.)

**Könönen M, Malm R, 2021.** Hållfasthetsutredning betongtankar BTF (SFR-SKB) Dokument ID DMG1008901, Vattenfall AB. SKBdoc 1942553 ver 1.0, Svensk Kärnbränslehantering AB. (In Swedish.)

**Lagerblad B, 2001.** Leaching performance of concrete based on studies of samples from cold concrete constructions. SKB TR-01-27, Svensk Kärnbränslehantering AB.

**Lagerblad B, Rogers P, Vogt C, Mårtensson P, 2017.** Utveckling av konstruktionsbetong till kassunerna i 2BMA. SKB R-17-21, Svensk Kärnbränslehantering AB. (In Swedish.)

**Lagerlund J, 2022.** Hydraulisk konduktivitet i grovkorniga jordmaterial. Rapport 2022:849, Energiforsk, Sweden. (In Swedish.)

**Lagerlund J, Holmberg H, 2021.** Silobruk: undersökning av bruk med bentonit. VRD-R12:2021, Vattenfall AB. SKBdoc 1933732 ver 1.0, Svensk Kärnbränslehantering AB. (In Swedish.)

**Magnusson J, Mathern A, 2015.** System design of Dome plug, Experience of low-pH concrete mix B200, Material properties from laboratory tests and full-scale castings. SKB P-14-26, Svensk Kärnbränslehantering AB.

**Malm R, Johansson F, Hellgren R, Rios Bayona F, 2017.** Load capacity of grouted rock bolts due to degradation. Report 2017:374, Energiforsk, Sweden.

**Malmström K, 1990.** Cementsortens inverkan på betongs frostbeständighet. Report 1990:07, Byggnadsteknik, Sweden. (In Swedish.)

**Mårtensson P, 2017.** Hållfasthetsegenskaper hos betongkonstruktionerna i 1–2BMA under de första 20 000 åren efter förslutning. SKBdoc 1577237 ver 1.0, Svensk Kärnbränslehantering AB. (In Swedish.)

**Mårtensson P, 2019.** Borrhålsförslutning: Överborrning av betongfylld del av KAS13 på 220 meters djup. SKBdoc 1869976 ver 1.0, Svensk Kärnbränslehantering AB. (In Swedish.)

**Mårtensson P, 2021a.** PSU-17: Undersökning av formstagslösning samt material och metod för fyllning av hål i skyddsrör för formstag i 2BMA. SKBdoc 1921349 ver 1.0, Svensk Kärnbränslehantering AB. (In Swedish.)

**Mårtensson P, 2021b.** Undersökning av betongtanks vattengenomsläpplighet: Rapport. SKBdoc 1932575 ver 1.0, Svensk Kärnbränslehantering AB. (In Swedish.)

**Mårtensson P, Kalinowski M, 2019.** Äspö Hard Rock Laboratory, Concrete and Clay, Retrieval and analysis of experiment package #20. SKB P-19-18, Svensk Kärnbränslehantering AB.

**Mårtensson P, Vogt C, 2019.** Concrete caissons for 2BMA: Large scale test of design and material. SKB TR-18-12, Svensk Kärnbränslehantering AB.

**Mårtensson P, Vogt C, 2020.** Concrete caissons for 2BMA: Large scale test of design, material and construction method. SKB TR-20-09, Svensk Kärnbränslehantering AB.

**Mårtensson P, Elfwing M, Millqvist M, 2014.** He-läcksökniing av sprickor i betongkonstruktionen i 1BMA. SKBdoc 1452199 ver 1.0, Svensk Kärnbränslehantering AB. (In Swedish.)

**Mårtensson P, Luterkort D, Nyblad B, Wimelius H, Pettersson A, Aghili B, Andolfsson T, 2022.** SFR förslutningsplan. SKBdoc 1358612 ver 4.0, Svensk Kärnbränslehantering AB. (In Swedish.)

**Moreno L, Neretnieks I, 2013.** Impact of gas generation on radionuclide release – comparison between results for new and old data. SKB P-13-40, Svensk Kärnbränslehantering AB.

**Moreno L, Skagius K, Södergren S, Wiborgh M, 2001.** Project SAFE, Gas related processes in SFR. SKB R-01-11, Svensk Kärnbränslehantering AB.

**Neretnieks I, Ernstson M-L, 1997.** A note on radionuclide transport by gas bubbles. MRS Online Proceedings Library 465, 855–862.

**Neretnieks I, Moreno L, 2013.** Flow and transport in fractures in concrete walls in BMA – problem formulation and scoping calculations. SKB R-13-51, Svensk Kärnbränslehantering AB.

**Neville A, 2004.** The confused world of sulfate attack on concrete. Cement and Concrete Research 34:8, 1275–1296.

**Nyblad B, Wimelius H, 2013.** Återfyllning med makadam: Förslutning av SFR. SKB P-13-05, Svensk Kärnbränslehantering AB. (In Swedish.)

**Nytorp Jansson M, 2020a.** Hållfasthetsanalyser för bottenplattor och fat i SFR. Produkt-575-2, Vattenfall AB. SKBdoc 1897930 ver 1.0, Svensk Kärnbränslehantering AB. (In Swedish.)

**Nytorp Jansson M, 2020b.** Hållfasthetsanalyser för bottenplattor och fat i SFR. Produkt-575-001, Vattenfall AB. SKBdoc 1897931 ver 1.0, Svensk Kärnbränslehantering AB. (In Swedish.)

**Näslund J-O, Mårtensson P, Lindgren M, Åstrand P-G, 2017.** Information om klimat och effekter på SFR till följd av frysning av betong. SKBdoc 1572377 ver 1.0, Svensk Kärnbränslehantering AB. (In Swedish.)

**Olsson D, 2016a.** 1BMA – utredning kring gas och svällning. SKBdoc 1535025 ver 1.0, Svensk Kärnbränslehantering AB. (In Swedish.)

**Olsson D, 2016b.** Silo – utredning kring gas och svällning. SKBdoc 1535026 ver 1.0, Svensk Kärnbränslehantering AB. (In Swedish.)

**Pålbrink L, Rydman O, 2013.** Frysning av betong under inverkan av tvång: en experimentell studie av frostens inverkan på betongkonstruktionerna i slutförvaret för kortlivat radioaktivt avfall efter en permafrost. TVBM-5091, Lunds Tekniska Högskola. (In Swedish.)

**Pettersson A, 2017.** Redovisning av teknisk barriär vid övergång till segmenterade reaktortankar. SKBdoc 1580414 ver 1.0, Svensk Kärnbränslehantering AB. (In Swedish.)

**Pettersson A, Thunberg S, 2012.** Kringgjutning av medelaktivt kärnavfall – En experimentell studie av kringgjutning med betongbruk i 1BMA med fokus på arbetbarhet och reologi. TVBM 5087, Lunds tekniska högskola, Sweden. (In Swedish.)

**Pusch R, Ramqvist G, 2004.** Borehole sealing, preparative steps, design and function of plugs – basic concept. SKB IPR-04-57, Svensk Kärnbränslehantering AB.

**Pusch R, Ramqvist G, 2007.** Borehole project – Final report of phase 3. SKB R-07-58, Svensk Kärnbränslehantering AB.

**Sainz-Garcia A, Sampietro D, Abarca E, Molinero J, 2018.** Potential effects of concrete plugs on the near-field flow in SFR. SKB R-21-18, Svensk Kärnbränslehantering AB.

**Sandén T, Dueck A, Åkesson M, Börgesson L, Nilsson U, Goudarzi R, Jensen V, Karnland O, Johannesson L-E, 2017.** Sealing of investigation boreholes. Laboratory investigations of sealing components. SKB P-17-10, Svensk Kärnbränslehantering AB.

**Sandén T, Nilsson U, Johannesson L-E, Hagman P, Nilsson G, 2018.** Sealing of investigation boreholes. Full scale test and large-scale laboratory tests. SKB TR-18-18, Svensk Kärnbränslehantering AB.

**SIS, 2000.** SS 137215: Betongprovning – hårdnad betong – krympning. Stockholm: Swedish Standards Institute. (In Swedish.)

**SIS, 2011a.** SS-EN 197-1:2011. Cement – del 1: Sammansättning och fordringar för ordinära cement. (Cement – part 1: Composition, specifications and conformity criteria for common cements) Swedish Standards Institute. (In Swedish.)

**SIS, 2011b.** SS-EN 12390-3:2009: Provning av hårdnad betong. Del 3: Spräckhållfasthet hos provkroppar (Testing of hardened concrete – Part 3: Tensile splitting strength of test specimens). Stockholm: Swedish Standards Institute. (In Swedish.)

**SIS, 2012a.** SS-EN 12390-6:2009: Provning av hårdnad betong. Del 3: Tryckhållfasthet hos provkroppar (Testing of hardened concrete – Part 3: Compressive strength of test specimens). Stockholm: Swedish Standards Institute. (In Swedish.)

**SIS, 2012b.** SS-EN 21390-1:2009. Provning av betong i färdiga konstruktioner – Del 1: Borrkärnor – Uttag, undersökning och tryckprovning. Stockholm: Swedish Standards Institute. (In Swedish.)

**Skalny J, Marchand J, Odler I, 2002.** Sulphate attack on concrete. London: Spon Press.

**SKB, 1983.** Geologiska undersökningar och utvärderingar för förvarsutrymmen i berg. SFR-83-05, Svensk Kärnbränslehantering AB. (In Swedish.)

**SKB, TR-14-02.** SKB 2014. Initial state report for the safety assessment SR-PSU. Svensk Kärnbränslehantering AB.

**SKB, TR-14-07.** SKB 2014. FEP report for the safety assessment SR-PSU. Svensk Kärnbränslehantering AB.

**SKB, TR-14-10.** SKB 2014. Data report for the safety assessment SR-PSU. Svensk Kärnbränslehantering AB.

**SKB, R-18-07.** SKB 2019. Låg och medelaktivt avfall i SFR. Referensinventarium för avfall 2016. Svensk Kärnbränslehantering AB. (In Swedish.)

**SKB, TR-23-01.** SKB 2023. Post-closure safety for SFR, the final repository for short-lived radioactive waste at Forsmark. Main report, PSAR version. Svensk Kärnbränslehantering AB.

**SKB, TR-23-02.** SKB 2023. Post-closure safety for SFR, the final repository for short-lived radioactive waste at Forsmark. Initial state of the repository, PSAR version. Svensk Kärnbränslehantering AB.

**SKB, TR-23-03.** SKB 2023. Post-closure safety for SFR, the final repository for short-lived radioactive waste at Forsmark. Waste form and packaging process report, PSAR version. Svensk Kärnbränslehantering AB.

**SKB, TR-23-04.** SKB 2023. Post-closure safety for SFR, the final repository for short-lived radioactive waste at Forsmark. Engineered barrier process report, PSAR version. Svensk Kärnbränslehantering AB.

**SKB, TR-23-05.** SKB 2023. Post-closure safety for SFR, the final repository for short-lived radioactive waste at Forsmark. Climate and climate-related issues, PSAR version. Svensk Kärnbränslehantering AB.

**SKB, TR-23-10.** SKB 2023. Post-closure safety for SFR, the final repository for short-lived radioactive waste at Forsmark. Data report, PSAR version. Svensk Kärnbränslehantering AB.

**Soler J M, Watson C, Bultmark F, Chaparro M C, Manette M, Salltink M W, Savage D, Wilson J, 2020.** Long-Term Cement Studies (LCS) at the Grimsel Test Site – Modelling of the in-situ Experiment 2. Nagra NTB-17-03, National Cooperative for the Disposal of Radioactive Waste, Switzerland.

**Svensk Byggtjänst, 2000.** Betonghandboken, 2000. Högpresterande betong – Material och utförande, 2000. Stockholm: AB Svensk Byggtjänst. (In Swedish.)

**Svensk Byggtjänst, 2017.** Betonghandbok material, delmaterial samt färsk och hårdnande betong. Stockholm: Svensk Byggtjänst AB. (In Swedish.)

**Tang L, Bager D, 2013.** A study of consequences of freezing of concrete structures for storage of nuclear waste due to permafrost. SKB TR-12-13, Svensk Kärnbränslehantering AB.

**Thorsell P-E, 2013.** Studier av frysningsegenskaper hos betong från 1 BMA. SKB P-13-07, Svensk Kärnbränslehantering AB. (In Swedish.)

**Trägårdh J, Lagerblad B, 1998.** Leaching of 90-year old concrete mortar in contact with stagnant water. SKB TR-98-11, Svensk Kärnbränslehantering AB.

**Villar M V, Gutiérrez M G, Barrios B C, Álvarez C G, Martínez R I, Martín P L, Missana T, Mingarro M, Morejón J, Olmeda J, Idiart A, 2019.** Experimental study of the transport properties of different concrete mixes. SKB P-19-10, Svensk Kärnbränslehantering AB.

**Vogt C, 2019.** Full-scale test of the Dome Plug for KBS-3V deposition tunnels – concrete properties. Sampling, testing and properties of low-pH concrete in the KBP1016 dome plug. SKB P-18-16, Svensk Kärnbränslehantering AB.

**Vogt C, Lagerblad B, Wallin K, Baldy F, Jonasson J–E, 2009.** Low-pH self-compacting concrete for deposition tunnel plugs. SKB R-09-07, Svensk Kärnbränslehantering AB.

**von Schenck H, 2017.** Vattenflöde genom 2BMA – känslighet för parametrisering av bergets egenskaper. SKBdoc 1564134 ver 1.0, Svensk Kärnbränslehantering AB. (In Swedish.)

**von Schenck H, Bultmark F, 2014.** Effekt av bitumensvällning i silo och BMA. SKB R-13-12, Svensk Kärnbränslehantering AB. (In Swedish.)

**von Schenck H, Åstrand P-G, Abarca E, Sampietro D, 2015.** Analys av föreslagna åtgärder för 1BMA genom modellering av närzonshydrologi och radionuklidtransport. SKBdoc 1480977 ver 2.0, Svensk Kärnbränslehantering AB. (In Swedish.)

**Westerberg B, 2017.** 2BMA – fristående kassun med lastbärande innerväggar. SKBdoc 1587450 ver 1.0, Svensk Kärnbränslehantering AB. (In Swedish.)

**Wiborgh M, Lindgren M, 1987.** Database for the radionuclide transport calculations for SFR. SKB SFR 87-09, Svensk Kärnbränslehantering AB.

**Wimelius H, 2021.** Beräkning av kostnad och personalbehov för reparation av 1BMA. Report from NCC infra structure. SKBdoc 1953615 ver 1.0, Svensk Kärnbränslehantering AB. (In Swedish.)

**Windelhed K, Lagerblad B, Sandberg B, 2002.** Cementingjutna bultars beständighet. SveBeFo-Rapport 58, Stiftelsen Bergteknisk Forskning, Sweden. (In Swedish.)

**Öhman J, Odén M, 2018.** SR-PSU (PSAR), Bedrock hydrogeology. TD18 – Temperate climate conditions. SKB P-18-02, Svensk Kärnbränslehantering AB.

Arkitektkopia AB, Bromma, 2024

SKB is responsible for managing spent nuclear fuel and radioactive waste produced by the Swedish nuclear power plants such that man and the environment are protected in the near and distant future.

**skb.se**